

Dipartimento di / Department of
Department of Earth and Environmental Sciences
Dottorato di Ricerca in / PhD program Scienze Chimiche, Geologiche e Ambientali
Ciclo / Cycle XXXI
Curriculum in Scienze Chimiche

Towards the development of sustainable materials for organic electronics

Cognome / Surname Sanzone Nome / Name Alessandro

Matricola / Registration number 735234

Tutore / Tutor: Prof. Luca Beverina

Coordinatore / Coordinator: Prof.ssa. Maria Luce Frezzotti

ANNO ACCADEMICO / ACADEMIC YEAR 2017-2018

Contents

1	Organic printed electronics and its Red Brick Walls	1
	Bibliography	4
2	The chemistry of BTBT derivatives: challenges and new derivatives	5
2.1	Introduction	5
2.1.1	Organic Thin Film Transistors for Large Area Electronics	5
2.1.2	Organic Field Effect Transistor	6
2.1.2.1	Materials , basic operating principles, device configuration	6
2.1.2.2	Current voltage characteristics of OFETs	8
2.1.2.3	Processing Technique for OFETs	10
2.1.2.4	Factors Influencing the Performance of OFETs	11
2.1.3	[1]benzothieno[3,2-b][1]benzothiophene derivatives	15
2.1.3.1	[1]benzothieno[3,2-b][1]benzothiophene derivatives promising materials for OFET	15
2.1.3.2	Synthesis of BTBT and derivatives reported in literature .	18
2.2	Aims	19
2.3	Synthesis of conjugated BTBT derivatives	20
2.3.1	Synthesis of [1]benzothieno[3,2-b][1]benzothiophene dimer double bond-linked	20
2.3.2	Synthesis of [1]benzothieno[3,2-b][1]benzothiophene dimer heterocycle-linked derivatives	21
2.3.2.1	Friedel-Crafts acylation reaction with Dicarboxylic acid chloride	21
2.3.2.2	Friedel-Crafts acylation reaction with carboxylic anhydride	22
2.4	Direct arylation cross coupling for [1]benzothieno[3,2-b][1]benzothiophene derivatives	24
2.4.1	Direct arylation cross-coupling a greener alternative	24
2.4.2	Direct arylation cross coupling reaction for BTBT derivatives . . .	26
2.4.3	[1]benzothieno[3,2-b][1]benzothiophene bromides synthesis	27

CONTENTS

2.4.4	Synthesis of 2 and 2,7-thienyl-[1]benzothieno[3,2-b][1]benzothiophene (BTBT) derivatives by direct arylation	29
2.4.5	Synthesis of [1]benzothieno[3,2-b][1]benzothiophene dimer heterocycle-linked derivatives by direct arylation reaction	30
2.4.5.1	Synthesis of heterocycle-linker	30
2.4.5.2	Synthesis of [1]benzothieno[3,2-b][1]benzothiophene dimer heterocycle-linked derivatives	32
2.5	Synthesis of [1]benzothieno[3,2-b][1]benzothiophene with functionlized side chain derivatives	33
2.5.1	Synthesis of [1]benzothieno[3,2-b][1]benzothiophene with doublebond-fuctionalized side chain derivatives	33
2.5.2	Synthesis of [1]benzothieno[3,2-b][1]benzothiophene with hydroxy-fuctionalized side chain derivatives	34
2.5.3	Synthesis of [1]benzothieno[3,2-b][1]benzothiophene-peptide-based supramolecular nanostructures	35
2.6	Conclusion	39
2.7	Experimental part	40
2.7.1	Synthesis of [1]benzothieno[3,2-b][1]benzothiophene (1)	40
2.7.2	Synthesis of [1]benzothieno[3,2-b][1]benzothiophene-2-octan-1-one (2)	41
2.7.3	Synthesis of [1]benzothieno[3,2-b][1]benzothiophene-2-octan-1-hydroxy (3)	42
2.7.4	Synthesis of (E)-2-(oct-1-en-1-yl)benzo[b]benzo[4,5]thieno[2,3-d]thiophene (4)	45
2.7.5	Synthesis of 2-octyl-[1]benzothieno[3,2-b][1]benzothiophene (5)	48
2.7.6	Synthesis of dimethyl 6,6'-([1]benzothieno[3,2-b]-[1]benzothiophene-2,7-diyl)bis(6-oxohexanoate) (6)	49
2.7.7	Synthesis of 6,6'-([1]benzothieno[3,2-b]-[1]benzothiophene-2,7-diyl)-bis(hexan-1-ol) (7)	52
2.7.8	Synthesis of methyl 6-(benzo[b]benzo[4,5]thieno[2,3-d]thiophen-2-yl)-6-oxohexanoate (8)	53
2.7.9	Synthesis of 6-(benzo[b]benzo[4,5]thieno[2,3-d]thiophen-2-yl)hexan-1-ol (9)	56
2.7.10	Synthesis of 4-oxo-4-([1]benzothieno[3,2-b][1]benzothienyl)-butyric acid (10)	59
2.7.11	Synthesis of decanyl 4-oxo-4-([1]benzothieno[3,2-b][1]benzothienyl)butyrate (11)	62
2.7.12	Synthesis of 2,7-di-bromo-[1]benzothieno[3,2-b][1]benzothiophene (12)	65
2.7.13	Synthesis of 2-octyl-7-bromo-[1]benzothieno[3,2-b][1]benzothiophene (13)	66

2.7.14	Synthesis of 2-(5-hexyl-2-thienyl)-[1]benzothieno[3,2-b][1]benzothiophene (14)	67
2.7.15	Synthesis of 2,7-di-(5-hexyl-2-thienyl)-[1]benzothieno[3,2-b][1]benzothiophene (15)	68
2.7.16	Synthesis 7,7'-(4,5-bis(octyloxy) of benzo[1,2-b:6,5-b']dithiophene-2,7-diyl)bis(2-octylbenzo[b]benzo[4,5]thieno[2,3-d]thiophene) and 2-(4,5-bis(octyloxy)benzo[1,2-b:6,5-b']dithiophen-2-yl)-7-octylbenzo[b]benzo[4,5]thieno[2,3-d]thiophene (16 end 17)	71
2.7.17	Synthesis of 7,7'-(4,4-dioctyl-4H-cyclopenta[1,2-b:5,4-b']dithiophene-2,6-diyl)bis(2-octylbenzo[b]benzo[4,5]thieno[2,3-d]thiophene) (18) .	77
2.7.18	Synthesis of [1]benzothieno[3,2-b][1]benzothiophene-peptide (19) . .	80
	Bibliography	83
3	Green synthesis for molecular organic semiconductors	93
3.1	General introduction	93
3.1.1	Water the green solvent par excellence	95
3.1.2	Surfactants and their characterization	96
3.1.3	Micellar catalysis	97
3.1.4	Organic reaction in micellar media	98
3.2	General Aims: Micellar catalysis for organic semiconductors	99
3.3	Previous work and the discovering of the New Rules	100
3.3.1	Surfactant choice	100
3.3.2	Synthesis of organic semiconductors in micellar conditions, first examples	102
3.3.3	Synthesis of latent pigment in emulsion conditions	104
3.3.4	Kolliphor® EL-catalyzed Buchwald–Hartwig amination	108
3.4	Synthesis of benzothiadiazole derivatives in micellar condition	111
3.4.1	Introduction	111
3.4.2	Results	113
3.4.2.1	Micellar synthesis of DTBF	113
3.4.2.2	Influence of the surfactant concentration	115
3.4.2.3	Influence of the reagents formal concentration	117
3.4.2.4	Influence of the Surfactant	117
3.4.2.5	Influence of the catalyst	118
3.4.2.6	Computational analysis	120
3.4.3	Discussion	122
3.4.3.1	One pot synthesis of nonsymmetric derivatives	125

CONTENTS

3.4.4	Conclusion	127
3.4.5	Experimental part	128
3.4.5.1	Synthesis of 4,7-diphenyl-2,1,3-benzothiadiazole (20) . . .	128
3.4.5.2	Synthesis of 4,7-di(thien-2-yl)-2,1,3-benzothiadiazole (21)	129
3.4.5.3	Synthesis of symmetrical 4,7-Diaryl-5,6-difluoro-2,1,3-benzothiadiazole derivatives	130
3.4.5.3.1	Synthesis of 4,7-di(thien-2-yl)-5,6-difluoro-2,1,3-benzothiadiazole (DTBF)	130
3.4.5.3.2	Synthesis of 4,7-di(thien-3-yl)-5,6-difluoro-2,1,3-benzothiadiazole (22)	131
3.4.5.3.3	Synthesis of 4,7-diphenyl-5,6-difluoro-2,1,3-benzothiadiazole (23)	134
3.4.5.4	Synthesis of unsymmetrical 4,7-Diaryl-5,6-difluoro-2,1,3-benzothiadiazole (24, 25,26,27,28,29,30 and 31)	135
3.4.5.4.1	General synthetic procedure for unsymmetrically substituted derivatives	135
3.4.5.4.2	NMR spectra of unsymmetrically substituted derivatives	155
3.4.5.5	Synthesis of 4-bromo-7-(thien-2-yl)-5,6-difluoro-2,1,3-benzothiadiazole (TBF)	155
3.4.6	Appendix	158
3.4.6.1	Details on The Gc-Ms response factor calibration	158
3.4.6.2	Theoretical details	158
3.5	Synthesis of 2(,7)-aryl-[1]benzothieno[3,2-b][1]benzothiophene (BTBT) derivatives in micellar condition	159
3.5.1	Introduction	159
3.5.2	Results and discussion	163
3.5.2.1	2(,7)-aryl-[1]benzothieno[3,2-b]benzothiophene's synthesis in emulsion condition	163
3.5.2.2	Kolliphor® EL-catalyzed Buchwald–Hartwig amination on [1]benzothieno[3,2-b][1]benzothiophene derivatives	166
3.5.2.3	Designer π -surfactant for BTBT's derivatives synthesis . .	166
3.5.2.3.1	Pi-BTBT-750M synthesis and testing	167
3.5.2.3.2	Pi-Nap-550M synthesis and testing	169
3.5.2.3.3	Pi-Nap-750M synthesis and testing	172
3.5.3	Conclusion	173
3.5.4	Experimental part	174
3.5.4.1	Synthesis of 2-phenyl-[1]benzothieno[3,2-b][1]benzothiophene (32)	174

3.5.4.2	Synthesis of 2-decyl-7-bromo-[1]benzothieno[3,2-b][1]benzothiophene (33)	175
3.5.4.3	Synthesis of 2-decyl-7-phenyl-[1]benzothieno[3,2-b][1]benzothiophene (34)	176
3.5.4.4	Synthesis of 2-(5-hexyl-2-thienyl)-[1]benzothieno[3,2-b]-[1]benzothiophene(14)	177
3.5.4.5	Synthesis of 2-(4-hexyl-2-thienyl)-[1]benzothieno[3,2-b][1]benzothiophene(35)	178
3.5.4.6	Synthesis of 2,7-di-(5-hexyl-2-thienyl)-[1]benzothieno[3,2-b][1]benzothiophene (15)	181
3.5.4.7	Synthesis of 2,7-di-(4-hexyl-2-thienyl)-[1]benzothieno[3,2-b][1]benzothiophene (36)	182
3.5.4.8	Synthesis of 5-(7-decylbenzo[b]benzo[4,5]thieno[2,3-d]thiophen-2-yl)-5H-dibenzo[b,f]azepine (37)	185
3.5.4.9	Synthesis of 4-(7-decylbenzo[b]benzo[4,5]thieno[2,3-d]thiophen-2-yl)-4-oxobutanoic acid (38)	188
3.5.4.10	Synthesis of Pi-BTBT-750M (39)	191
3.5.4.11	Synthesis of 2-(2-hydroxyethyl)-7-nonylbenzo[lmn][3,8]phenanthroline-1,3,6,8(2H,7H)-tetraone (40)	194
3.5.4.12	Synthesis of 4-(2-(7-nonyl-1,3,6,8-tetraoxo-7,8-dihydrobenzo[lmn][3,8]phenanthroline-2(1H,3H,6H)-yl)ethoxy)-4-oxobutanoic acid (41)	197
3.5.4.13	Synthesis of Pi-Nap-550M (42)	200
3.5.4.14	Synthesis of 2-dodecyl-7-(2-hydroxyethyl)benzo[lmn][3,8]phenanthroline-1,3,6,8(2H,7H)-tetraone (43)	203
3.5.4.15	Synthesis of 2-dodecyl-7-(2-hydroxyethyl)benzo[lmn][3,8]phenanthroline-1,3,6,8(2H,7H)-tetraone (43)	206
3.5.4.16	Synthesis of Pi-Nap-750M (44)	209
3.6	General conclusion and future development	212
	Bibliography	214
4	Green approaches to the preparation of organic polymeric semiconductors	223
4.1	Introduction	223
4.2	F8BT synthesis in emulsion/micellar conditions	224
4.2.1	Why F8BT?	224
4.2.2	Results and discussion	224
4.2.3	Conclusion	231
4.2.4	Experimental part	232

CONTENTS

4.2.5	Appendix	235
4.3	Development of direct arylation polycondensation condition for innovative NDA-based materials for OFTF applications	238
4.3.1	Latent pigment approach a clever solution for OS polymers	238
4.3.2	Results and discussion	240
4.3.2.1	Monomers synthesis and preliminary data	240
4.3.2.2	Optimization of the polymerization conditions	244
4.3.3	Conclusion	247
4.3.4	Experimental part	249
4.3.4.1	Synthesis of tetradodecyl 2,6-dibromonaphthalene-1,4,5,8-tetracarboxylate (45)	249
4.3.4.2	Synthesis of tetrakis(2-ethylhexyl) 2,6-dibromonaphthalene-1,4,5,8-tetracarboxylate (46)	249
4.3.4.3	Synthesis of Copolymer Poly[tetrakis(2-dodecyl-2-([2,2'-bithiophen]-5-yl)naphthalene-1,4,5,8-tetracarboxylate] (47)	253
4.3.4.4	Synthesis of Copolymer Poly[tetrakis(2-dodecyl-2-([2,2'-bithiophen]-5-yl)naphthalene-1,4,5,8-tetracarboxylate] (48)	254
	Bibliography	257
	List of acronyms	261
	List of chemicals names	263

Chapter 1

Organic printed electronics and its Red Brick Walls

The use of materials in order to enhance our quality of living always has been a key component of the human experience. Improved materials and/or new materials have had such a dramatic impact on human life that we often describe and name periods of history by the predominate material used at the time, for example: Stone Age, Bronze Age, Iron Age, etc. The work in quantum physics carried out in the early 1900s paved the way for the silicon age, where a host of new materials, besides silicon, enabled technologies that have brought us a whole new way of life.¹ Silicon-based Electronics, and more specifically Integrated Circuits (IC), have dramatically changed our lives and the way we interact with the world. Following the so-called Moore's law,² IC complexity has been growing exponentially in the last decades. The commercial success of integrated electronics is based on a symbiotic development of technology and applications, where technical progress and economic growth nurture each other. The main strength of integrated electronics is in the low-cost-per-function enabled by an ever-growing miniaturization: mono-crystalline silicon real estate is very expensive, but the number of transistors that can be integrated per area grows according to Moore's law, bringing down the cost to realize a given function.³ Since the second half of the seventies, a completely different electronic paradigm, the so-called large-area electronics, has been developing. In this field the major aim is to decrease the cost per area (instead of the cost per function), enabling large surfaces covered with electronic devices. The main application of this kind of technology, typically based on amorphous or polycrystalline silicon transistors, is in active-matrix addressing of flat displays. The success of this technology has become evident in the last decade, when flat-panel LCD displays have swiftly replaced traditional cathode ray tubes in television sets. Amorphous and polycrystalline silicon technology typically require high-temperature vacuum-based processing, with the consequence that glass substrates are used and that the technology throughput is limited. In the nineties a new technology approach has been proposed, based on materials that enable low-temperature processing and the use of very high throughput patterning technologies, borrowed from the graphic printing field: organic and printed electronics were born. Organic electronics enables a wide range of electrical components that can be produced and directly integrated in low-cost reel-to-reel processes.⁴ Organic Printed Electronics (OPE) is based on the combination of new materials and cost-effective, large area production processes that open up new fields of application. Thinness, light weight, flexibility and environmental sustainability are key potential advantages of organic electronics. In fact, several high-tech companies have

significantly invested in cheap and high-performance organic-electronic devices, a billion-dollar market that is expected to grow rapidly. IDTechEx find that the total market for printed, flexible and organic electronics will grow from \$29.28 billion in 2017 to \$73.43 billion in 2027.⁵ Especially in fields where technology development and applications are changing, like OPE, it is important to gain an understanding of the past and present situation and to apply this to make some predictions of future developments and challenges in the field. Since the result of this process is a kind of map for where the field is going and critical work that needs to be done, this process is referred to as road mapping. Gave a look to the OE-A Roadmap for Organic and Printed Electronics, 7th Edition, (Table 1.1): Intelligent packaging, low-cost Radio-Frequency IDentification tags (RFID), rollable displays, flexible solar cells, disposable diagnostic devices or games, and printed batteries are just a few examples of promising fields of application for OPE. Organic Light-Emitting Diode (OLED) are in production and have gained market share as active displays for cellular telephones and other small devices but in large-area displays in price has kept OLED technology out of mass consumption. Organic Thin-Film Transistor (OTFT) and Organic Solar Cell (OSC) are expected gain their part in the market to the near future provided that some key challenges are won. Based on an analysis of the application and technology parameters, the recent progress in materials and process technology and the expected future technology development, the experts were able to identified that key challenges called “Red Brick Walls”, for which major breakthroughs are needed.⁶

- Cost: Capital expenditure for manufacturing equipment as well as materials
- Processes: Resolution, registration, uniformity and characterization
- Encapsulation: Not only lower cost but also stretchable encapsulation materials are needed
- Scalability: From lab to production and from small to large areas while keeping performance high
- Inspection/yield: Progress in both yield improvement and in-line inspection and recognition of defects is needed to improve competitiveness
- Standards and regulations for organic and printed electronics are under discussion, but not yet implemented

Identification of these red brick walls is particularly important because it points out the areas in which effort in new research and technology development is urgently needed.¹ It is notable that the key challenges of this 7th edition are more focused on production than the past edition roadmap, use and cost than on basic technology, which reflects the growing market orientation of OPE. Academic research has done big effort to increase devices performances, indeed for example if we look charge carrier mobility for OFET or power efficiency conversion for OSC reported in literature by years we can see that have been increase of different order of magnitude during the last decades but often overlooked the other features required for the OPE industrial development. It is desirable that also the academic research increase efforts on possible solutions and compromises to break down this Red Brick Walls in order to express the enormous potentially of OPE on all-day life of the people. As a final consideration, last but not least, only if these challenges will be won I can afford to buy big size rollable OLED TV for my living room.

	Existing 2017	Short Term 2018-2020	Medium Term 2021-2023	Long Term 2024+
OLED LIGHTING	Rigid white OLED modules; rigid red OLEDs for automotive applications	Flexible OLEDs (color); flexible OLEDs (white)	Transparent OLEDs; flexible red OLED for automotive applications	3D OLEDs; dynamic OLED signage (segmented); long stripes; OLED in general lighting
OPV	Portable OPV chargers; personal electronics power supply	Large area OPV foil; OPV objects; opaque OPV for building	OPV integrated in building products	OPV in packaging; energy harvesting combined with storage
Flexible & OLED Displays	Curved OLED displays, EPD shelf-edge labels, EPD secondary displays on phones; displays for wearables	EPD wrist band; transparent displays; conformable OLCD; enhanced display integration in wearables	Curved displays for automotive interior; integration into clothing; white goods displays	Wallpaper displays; displays in everyday objects; foldable displays
Electronics & components	Printed devices: memory, RFID antenna, primary battery, active backplane; sensors: glucose, touch, temperature, humidity	Printed mobile communication devices based on antennas, light sensor; stretchable conductors / resistors; 3D touch sensors	Printed lithium ion battery; printed super caps; active touch & gesture sensors	Printed complex logic; 3D & large area flexible electronics
Integrated smart systems	Glucose in-body sensing; pressure sensor arrays; NFC labels; hybrid RFID; HMIs (sensors)	Smart labels (discrete); HMI (embedded electronics & displays)	Human monitoring patches (single parameter, point of care, on-skin); disposable & quantitative sensors for food safety; biomedical sensors	Fully printed RFID / NFC label; ambient intelligence (connected); sensors for security (explosives)

Table 1.1 The OE-A Roadmap for organic and printed electronics applications, with a forecast for the market entry in large volumes (general availability) for the different applications

Bibliography

- [1] Nisato, G., Lupo, D., and Ganz, S. *Organic and Printed Electronics*. Pan Stanford, **2016**. ISBN 978-981-4669-74-0.
- [2] Moore, G. *No exponential is forever: but "Forever" can be delayed! [semiconductor industry]*, vol. 1. pp. 20–23. ISBN 0-7803-7707-9.
- [3] Heremans, P., Verlaak, S., and McLean, T. *Applications*. **2004**, p. 695. ISBN 978-1-4020-7707-4. doi: 10.1007/978-1-4419-9074-7.
- [4] Kymissis, I. *Organic Field Effect Transistors Theory , Fabrication and*. **2009**. ISBN 9780387921334.
- [5] Das, Raghu , Ghaffarzadeh, Khasha, and He, X. *Printed, Organic & Flexible Electronics Forecasts, Players & Opportunities 2017-2027: IDTechEx*, **2017**.
- [6] Organic Electronics Association. *OE-A Roadmap for Organic and Printed Electronics Applications 2017*, **2017**.

Chapter 2

The chemistry of BTBT derivatives: challenges and new derivatives

2.1 Introduction

2.1.1 Organic Thin Film Transistors for Large Area Electronics

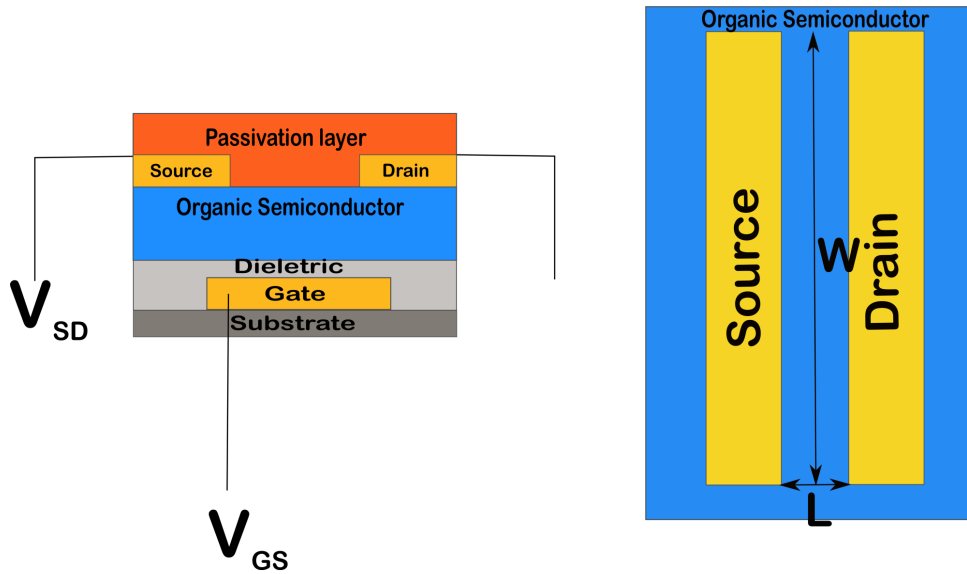
A transistor is the fundamental building block in all modern electronic devices. Transistors are semiconductor devices generally used to amplify or switch electronic signals. They are made of semiconductor material with at least three terminals for connection to an external circuit. A voltage applied to one pair of terminals controls the current through the another. Julius Edgar Lilienfeld patented a field-effect transistor in 1926¹ but it was not possible to actually construct a working device at that time. The first practically implemented device was invented in 1947 by American physicists John Bardeen, Walter Brattain, and William Shockley at Bell's laboratories. Bardeen, Brattain, and Shockley shared the 1956 Nobel Prize in Physics for their achievement.² Transistors are usually integrated in circuits with other components such as diodes, capacitors, resistances and inductors. Simple circuits have a small number of transistors meanwhile modern microprocessors have several billions. In order to have more and more powerful processors (and portable) devices, transistors are getting smaller and smaller every year: IC complexity has been growing exponentially in the last decades following Moore's law,³ Traditionally inorganic semiconductors are deposited or patterned by energy-expensive methods including high-temperature and high-vacuum processes involving post deposition lithographic steps for patterning. Mainly we can divide the Transistor in two categories Bipolar Junction Transistor (BJT) and Field Effect Transistor (FET). Metal-oxide-semiconductor field-effect transistor (MOSFET) is a silicon-base device and belong to the second transistor's category mentioned before. The growth of digital technologies like the microprocessor has provided the motivation to advance MOSFET technology faster than any other type of silicon-based transistor.⁴ A big advantage of MOSFETs for digital switching is that the oxide layer between the gate and the channel prevents DC current from flowing through the gate, further reducing power consumption. This device provides considerable energy savings and prevents overheating of the circuit, one of the main problems of integrated circuits. In the early 1970s the need for large-area applications in flat-panel displays motivated the search for alternatives to crystalline silicon and the thin-film transistor (TFT) found its application. In 1979, hydrated amorphous

silicon (a-Si:H) became a forerunner as a semiconductor to fabricate TFTs. Since the mid-1980s, silicon-based TFTs have successfully dominated the large-area liquid crystal display (LCD) technology and have become the most important devices for active matrix liquid crystal and organic light-emitting diode (OLED) applications.⁵ The success of this technology has become evident in the last decades, when flat-panel LCD displays have swiftly replaced traditional cathode ray tubes in television sets. Historically, much of the Initial work in large area electronics has centered on displays and photovoltaics however, over the last three decades, the scope of applications envisioned for large area electronics has expanded dramatically (see Roadmap chap. 1). a-Si:H and in general others inorganic semiconductors materials show limitation like high deposition and processing temperature and deposition process that which makes them incompatible with flexible plastic substrates and with low cost applications. OTFTs based on organic polymers and small molecules semiconductors have been envisioned as a viable alternative TFT based on inorganic materials. Organic semiconductors-based electronics has several advantages such as lightweight,⁶ large-area coverage,⁷ flexibility, integration with plastic substrates⁸ and most importantly potentially low costs. Because of the relatively low mobility of organic semiconductors, OTFTs cannot rival the performance of field-effect transistors based on crystallin or polycrystalline silica, which have charge carrier mobilities of three or more orders of magnitude higher. Consequently, OTFTs are not suitable for use in applications requiring very high switching speeds. However, the unique processing characteristics and demonstrated performance of OTFTs suggest that they can be competitive candidates for existing or novel thin film transistor applications. .

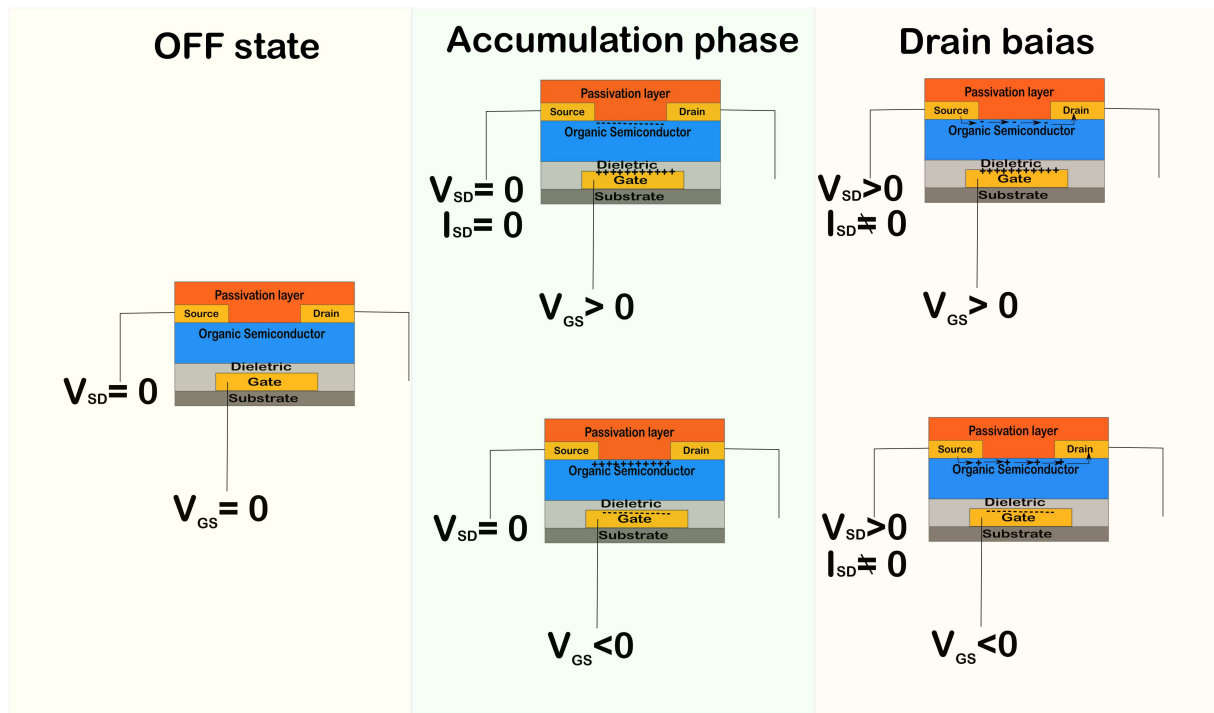
2.1.2 Organic Field Effect Transistor

2.1.2.1 Materials , basic operating principles, device configuration

An OFET, called organic thin-film transistor (OTFT), is composed of different components: a conducting material functioning as the gate, source, and drain electrodes ; a dielectric material insulating the gate ; and an organic semiconducting material acting as a variable conductance element.⁹ Figure 2.1a shows the OTFT the basic operating principles. The source electrode is grounded, and all other voltages are relative to this electrode. The drain–source current (I_d) in the conducting channel is controlled by the gate voltage. If no gate voltage ($V_{GS}=0V$) is applied there are no free charge carriers in the conducting channel and therefore the source–drain current is zero ($I_d=0$) (Figure 2.1b). After the application of a voltage $V_{DS}\neq 0$ between source and the drain electrodes, I_d will increase as a consequence of V_{DS} . Particularly, if $V_{GS} < 0V$, positive charges (p-type) will be created in the conducting channel, otherwise, if $V_{GS} > 0V$, negative charges (n-type) will be generated.⁹ Charge carrier polarity (h+or e-) in the conducting channel defines whether the semiconductor is p-type or n-type.



(a) Schematic representation of an OTFT in BGTC structure



(b) Schematic of n-type and p-type OTFT operation in BGTC structure

Figure 2.1 V_{GS} = voltage applied between gate and source electrodes; V_{DS} = voltage applied between gate and drain electrodes ; L = channel length; W = channel width; + = hole; - = electron

OTFT can have different device configuration. The configuration of a thin film transistor is distinguished on the basis of the gate position that can be either on the top or at the bottom, accordingly named as top gate (TG) and bottom gate (BG) structures, respectively. However, the majority of OTFTs are built as the bottom gate structure due to an ease in deposition of active material on the insulator instead of at the bottom. In these structures, the methods pertaining to thermal treatment can be safely employed to produce the insulating layer without creating any impairment in the OS layer.¹⁰ On the other hand, the performance of OTFT in the top gate structure severely degrades, if the underlying OS layer is contaminated during the deposition of a metal gate at high

temperature.¹¹ Therefore, bottom gate structures are preferred over the top gate. The position of a source and drain contact with respect to the active layer further classifies them into the top contact (TC) and bottom contact (BC) structures, while keeping gate electrode at the same position. Figure 2.2 shows the different device configuration schemes. . The device configuration has an important influence on the performance of OFETs. For thin film transistors, bottom contact devices typically exhibit less than half the effective drive current of top contact devices, although bottom contact devices are more easily integrated into low-cost manufacturing processes, and smaller device feature sizes can be obtained through photolithographic techniques.

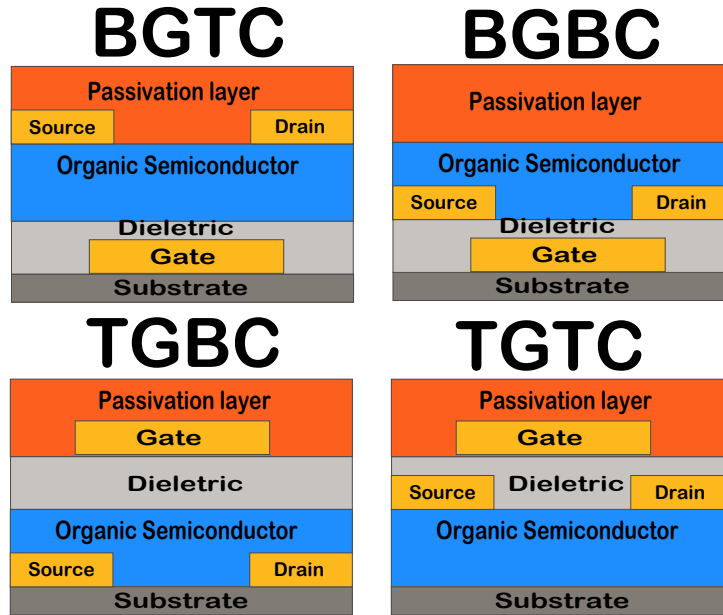


Figure 2.2 OFET Structure: Bottom-Gate/Top-Contact (BGTC) Bottom-Gate/Bottom-Contact (BGBC) Top-Gate/Bottom-Contact (TGBC) TOP-GATE/Top-Contact (TGTC)

2.1.2.2 Current voltage characteristics of OFETs

Several analytical models have been proposed to describe the current voltage characteristics of OTFTs. Most are charge control models that attempt to account for non-linear effects that cause the current-voltage characteristics of OTFTs to deviate from ideal behavior.⁵ However, in practice, OTFT parameters are frequently extracted using the expressions derived for the drain current of crystalline MOSFETs based on the gradual channel approximation developed by Shockley.¹² In Shockley's model, the drain current (I_d) in the OTFT from linear to saturation regime can be expressed as.

Algorithm 2.1 Shockley's equation model V_{GS} = Voltage applied between gate and source electrodes; V_{DS} = Voltage applied between gate and drain electrodes ; L = Channel length; W = Channel width; C_i = Dielectric capacitance per unit area; μ_{lin} = Charge-carrier mobility in linear regime μ_{sat} = Charge-carrier mobility in saturation regime

$$I_d = \frac{W\mu_{lin}C_i}{L}(V_{GS} - V_T)V_{DS} \text{ for linear regime } |V_{DS}| \ll |V_{GS} - V_T|$$

$$I_d = \frac{W\mu_{sat}C_i}{2L}(V_{GS} - V_T)^2 \text{ for saturation regime } |V| \geq |V_{GS} - V_T|$$

Three critical OTFT performance parameters are charge carrier mobility (μ), current modulation ratio (I_{on}/I_{off} , and threshold voltage (V_t).¹³

- Threshold voltage (V_t) is the critical voltage required to have the field effect operative. It is linked to the number of traps at the semiconductor/dielectric interface. These traps must be totally filled before charge carriers can flow between source and drain electrodes; therefore, high materials purity is fundamental for OTFT applications.¹⁴
- Current modulation ratio (I_{on}/I_{off}) is defined as the ratio of the source–drain current when the gate voltage is maximal (“on” state) and there is no gate voltage (“off” state). Ion/Ioff is an indicator of material purity and its susceptibility to doping by its surroundings.
- Charge-carrier mobility (μ) characterizes the critical voltage at which the field effect is operative. It can also serve as a measurement of the number of charge carrier traps at the semiconductor/dielectric interface. These traps must be filled before charge carriers can flow between the source and the drain;¹³ therefore, high materials purity is a necessity for OTFT applications. Usually charge-carrier mobility in saturation regime is reported in literature (μ_{sat})

The performance parameters can be derived from the OTFT output and transfer characteristics (Figure 2.3).

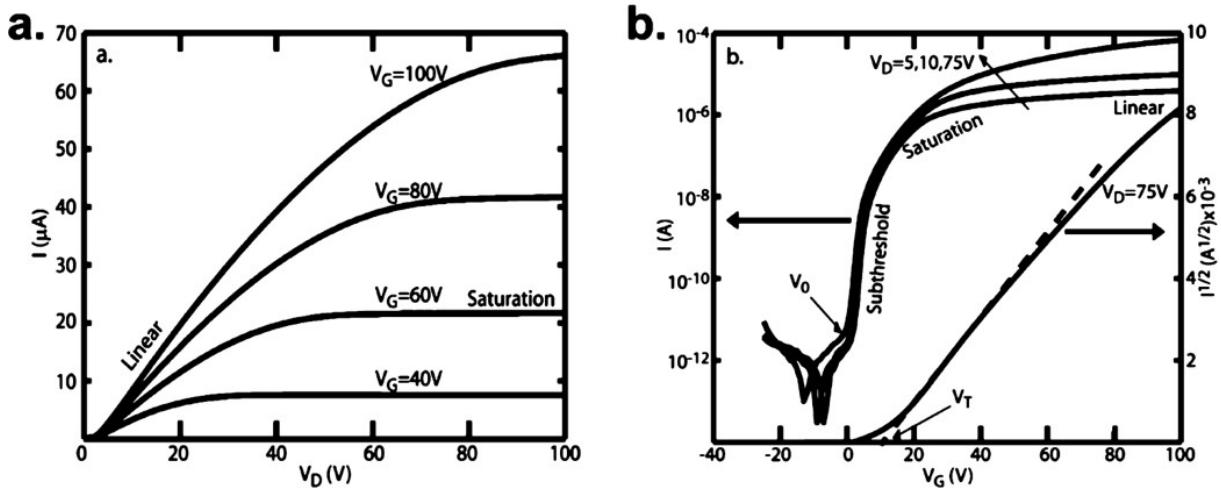


Figure 2.3 (a) Example I_d vs V_{DS} curves for OTFT for various values of V_{GS} . (b) Example $I_D - V_G$ curves plotted on semilogarithmic axes for the same device for various values of V_{DS} . The $\sqrt{I_d}$ vs V_{GS} various values of V_{DS} , 75V is shown on the right-hand axis. Reprinted with permission from ref¹³ Copyright American Chemical Society

In the output characteristics, two operation regions can be differentiated: a linear region at low drain voltage and a saturation region at high drain voltage. Charge carrier mobility (μ_{sat}) and threshold voltage (V_t) in the saturation region can be calculated from the transfer characteristic using the equation given above. The current modulation (I_{on}/I_{off}) can be derived from the quotient of “on” current divided by “off” current.

The performance of an OTFT usually deviates from the conventional transistor due to key parameters, such as the bulk leakage current, contact resistance, contact-OS interface, OS-insulator interface, morphological disorders, device configuration, channel length modulation, trap states, gate bias dependent mobility, and many more that raises difficulty in proposing a unified OTFT model.¹⁵ Over the past three decades, significant

research efforts have focused on improving the charge carrier mobility of organic thin-film transistors (OTFTs). In recent years, a commonly observed nonlinearity in OTFT current–voltage characteristics, known as the “kink” or “double slope,” has led to widespread mobility overestimations, contaminating the relevant literature. In very recent Paterson review, published data from the past 30 years is reviewed to uncover the extent of the field-effect mobility hype and identify the progress that has actually been achieved in the field of OTFTs. Present carrier-mobility-related challenges are identified, finding that reliable hole and electron mobility values of 20 and 10 $\text{cm}^2\text{V}^{-1}\text{s}^{-1}$, respectively, have yet to be achieved.¹⁶

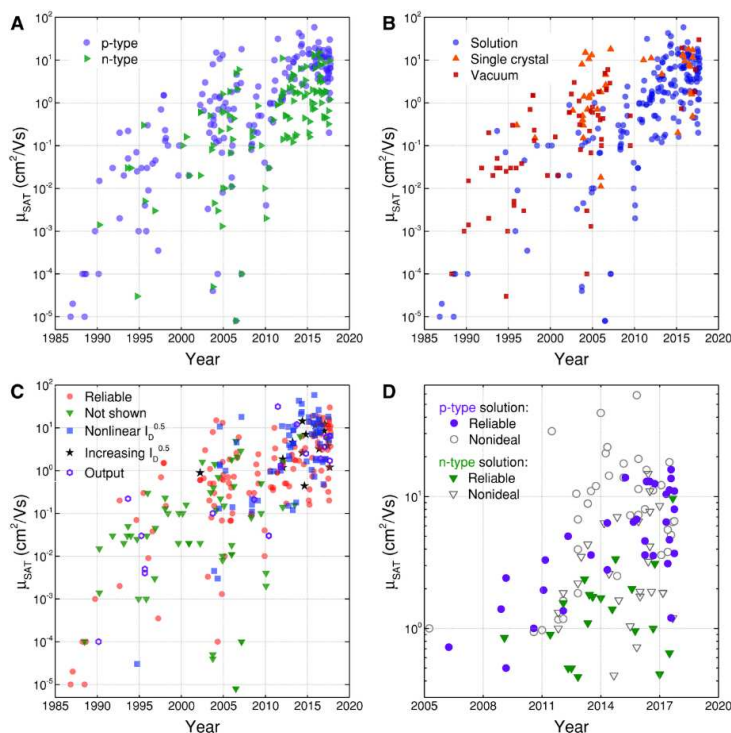


Figure 2.4 Plots of field-effect carrier mobility values over time. The data has been separated into the following categories: a) Charge carrier type: p-type and n-type. b) Processing technique: solution processed, single crystal, and vacuum. c) Features in the experimental data to determine which data sets do not comply with the classical FET model: reliable (from the data sets shown, there are no obvious nonidealities), not shown (do not show the plot of μ vs V_{GS} or $\sqrt{I_d}$ vs V_G), nonlinear $\sqrt{I_d}$ (the kink or any s-shaped or nonlinear features in $\sqrt{I_d}$ vs V_{GS}), increasing $\sqrt{I_d}$ (the gradient of $\sqrt{I_d}$ gets steeper with V_{GS}), and output (nonsaturated output characteristics). d) Solution-processed data with mobilities approaching 1 $\text{cm}^2\text{V}^{-1}\text{s}^{-1}$, by carrier type and data quality, suggesting that 55% of this data set either does not show the data that the mobility was extracted from, or has some sort of nonideality. Reprinted with permission from ref¹⁶ Copyright x American Chemical Society

2.1.2.3 Processing Technique for OFETs

A wide diversity of methods has been adopted to prepare organic thin films for the fabrication of OFET devices since the first OFET was reported.^{17, 18} The vacuum deposition technique may result in high-quality thin films, and has been widely adopted for the preparation of small-molecule semiconductor OFETs. Because of its freedom from solvents, the vacuum deposition method usually results in high-quality thin films. To avoid decomposition and degradation of small molecule semiconductors during the sublimation process, a high-vacuum environment, typically lower than 10^{-4} Pa, should be adopted. In

addition, deposition conditions, including sublimation rate, substrate temperature, etc., have an important influence on thin film morphology. Solution-processed techniques are widely used to deposit organic thin films mainly because of the low cost of such processes and the facility of obtaining large-area films by printing techniques. Moreover, when either decomposition or degradation happens during the sublimation process, it is necessary to adopt solution-processed techniques. Many elements such as solvent, concentration, evaporation temperature and rate, and substrate properties as well as the organic semiconductor itself can also affect the quality of the thin films. Solution-processed techniques for the preparation of organic thin films include spincoating, dip-coating, drop-casting, zone-casting, the Lagmuir-Blodgett (LB) technique, printing, and solution-shearing. Of these, spin-coating is the most commonly used solution-processed technique.¹⁹ The technique can provide uniform thin films of both the polymers and small molecules. The rotation speed adopted has a great influence on the thickness and morphology of thin films. Dip-coating, dropcasting, and zone-casting are three very convenient methods without the requirement of complex and/or expensive equipment. The techniques relate to self-assembled processes and can afford high orientation thin films. The LB technique is mainly used for amphiphilic molecules. Among the diverse methods used to fabricate organic thin films, the most exciting is the printing technique. Among the types of printing technique available, microcontact printing and ink-jet printing are considered to show the most promise. Solution-shearing is a new technique for organic semiconductors in which lattice strain is used to increase charge carrier mobilities by introducing greater electron orbital overlap between organic molecules. Using solution processing to modify molecular packing through lattice strain should aid the development of high-performance, low-cost organic semiconductor devices.²⁰

2.1.2.4 Factors Influencing the Performance of OFETs

OFET's performance are related to all devices and not only to OS material employed, therefore it is not entirely correct to compare different organic semiconductors comparing charge carriers mobility shown in different devices with different geometry, deposition method, purity of the material OS and so on, indeed the device performance are influenced by a lot of factors. The main factors influencing the performance of OFET can be divided into two categories: factors related to device physics and factors related to OS material.

The factors related to device physics are:

- **Device Configuration:** as mentioned before. Generally, the less the contact resistance, caused by intimate contact between the semiconductor and the electrodes, the higher the charge transport mobility tends to be.²¹
- **Interfaces and Their Modification:** The two major processes, carrier injection and carrier transport, occur at the electrode/ organic layer interface and the dielectric/organic layer interface, respectively. Therefore, the properties of these interfaces influence the device characteristics dramatically. The electrode/organic layer interface has a key influence on carrier injection. Many methods are used to modify the electrode/organic interface to improve the carrier injection, Introduction of a buffer layer between the source-drain electrode and organic layer for examples very thin layer of MoO₃,²² copper phthalocyanine (CuPc) layer for Au electrode,²³ graphene layer for copper and silver electrodes²⁴ or chemical modification

of the electrodes surface with Self assembled monolayer (SAM) usually are employed thiol for gold electrodes 3,4,5-Trimethoxythiophenol (TMP-SH)²⁵ 3,4,5-trimethoxybenzylthiol (TMP-CH₂-SH),²⁵ 1H,1H,2H,2H-perfluorodecanethiol (PFDT).²⁶ The dielectric/organic semiconductor interface implies an important influence on device stability: for examples Polymethylmetacrylate (PMMA)²⁷ and polystyrene PS-modified dielectrics.²⁸

Factors related to OS material are:

- HOMO and LUMO Energy Level: The energy levels of the highest occupied molecular orbital (HOMO) and the lowest unoccupied molecular orbitals (LUMO) have a large influence on charge carrier injection in order to obtain effective charge injection, p-type, n-type, and ambipolar semiconductors should have suitable HOMO, LUMO, and HOMO/LUMO energy levels to match with the work functions of source and drain electrodes. This is because the mismatch between the HOMO or LUMO energy level and work function of the electrodes may cause the reduction of the measured mobility, though not affect the intrinsic mobility directly. HOMO and LUMO energy levels also have an important influence on the device stability. Nowadays, there are fewer accounts of n-type than p-type organic semiconductors, primarily because of the inherent instability of organic anions in the presence of air and water^{14, 29} and problems with oxygen trapping within these materials.^{29, 30} In most cases, the mobilities of the n-type OFETs can be one or even several orders of magnitude higher when taking precautionary measures to exclude atmospheric oxygen and water in vacuum or inert atmosphere.
- Packing Mode in Solid State: The packing mode of organic semiconductors in the solid state also have an important influence on their FET properties. Besides the transfer integral, reorganization energy can also affect intrinsic mobility of organic semiconductors.³¹ The packing mode of organic small-molecule semiconductors in the solid state can be divided into four types as shown in figure 2.5: (1) herringbone packing without π - π overlap between adjacent molecules; (2) slipped π -stacking between adjacent molecules; (3) one-dimensional lamellar packing, and (4) two-dimensional lamellar packing. Of the four kinds of packing modes, one-dimensional and twodimensional lamellar packing mean main one-dimensional and two-dimensional charge carrier hopping pathways, respectively. Of these, the two-dimensional charge carrier hopping pathway is believed to be the most efficient for charge transport because it can increase the transfer integrals to the maximum and transport the charge carriers through the shortest route.³²⁻³⁴ For polymer semiconductors, the packing modes include face-on and edge-on orientation of the polymer molecules on the substrates (Fig. 3.6). The possible charge transport pathways of polymer films can be subdivided into intrachain transport, along the π -conjugation direction, interchain transport, along the π -stacking direction or alkyl stacking direction. Although high performance FET devices usually adopt an edge-on orientation, face-on orientation can also afford high performance.

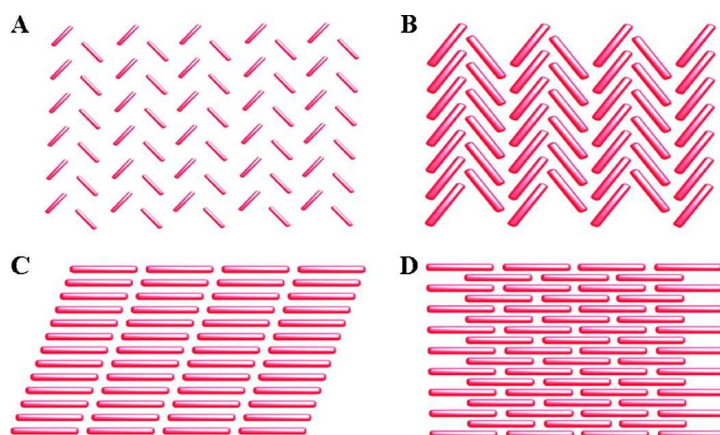


Figure 2.5 Molecular packing motifs in crystals. (A) Herringbone packing (face-to-edge) without π - π overlap (face-to-face) between adjacent molecules (example: pentacene); (B) herringbone packing with π - π overlap between adjacent molecules (example: rubrene); (C) lamellar motif, 1-D π -stacking (example: hexyl substituted naphthalene diimide); (D) lamellar motif, 2-D π -stacking (example: TIPS-PEN). Adapted with permission from refs.³⁵ Copyright 2008b Wiley-VCH Verlag GmbH & Co. KGaA and Copyright 2010 Royal Society Chemistry

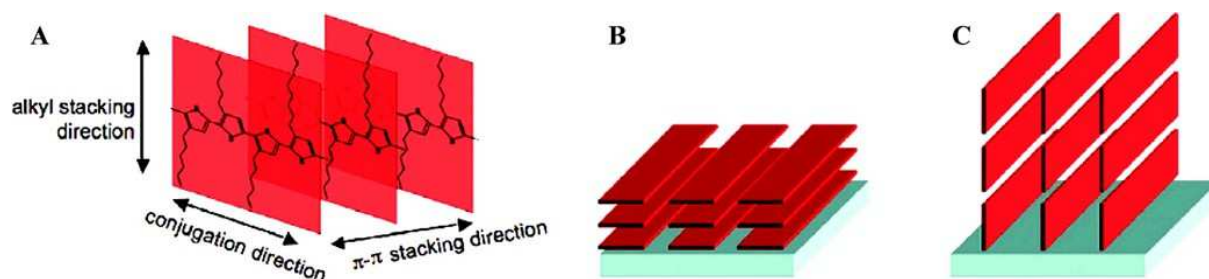


Figure 2.6 (A) Possible charge transport mechanisms in crystalline polymer films (using P3HT for illustration): Intrachain transport, along the π -conjugation direction and interchain transport, along the π -stacking direction or alkyl stacking direction. (B) Face-on and (C) edge-on orientation of the polymer molecules on the substrates. Reprinted with permission from ref.³⁶ Copyright 2007 Elsevier B.V.

- Size/Molecular weight related to polymers: the influence of molecular weight on the electronic properties of donor-acceptor conjugated copolymers has been examined, with field-effect mobilities improving significantly with increasing molecular weight.³⁷ The increased performances are accompanied by important changes in the thin film morphology: systems with high molecular weight often exhibit reduced crystallinity and more isotropic films, potentially leading to larger values for charge-carrier mobility.³⁸
- Impurities of organic semiconductors: The presence of impurities can have a serious negative impact on the function of organic semiconductors because impurities can introduce charge carriers or traps within the material. Thus, from a synthetic perspective, preparative routes that minimize difficult-to-remove by-products are growing in importance.²¹
- Doping of organic semiconductors: Recent breakthroughs in organic semiconductors and doping techniques demonstrated that doping can also be a key enabler for high-performance OFETs. OFET doping can be used for a variety of purposes,

CHAPTER 2. THE CHEMISTRY OF BTBT DERIVATIVES: CHALLENGES AND NEW DERIVATIVES

including: mobility enhancement, charge transport polarity modulation, trap passivation, threshold voltage adjustment, Ohmic contacts, ambipolar charge injection suppression, short channel effect suppression, and stability improvement.³⁹

a wide variety of organic semiconductor classes were used to produce OFET and there are many reviews dedicated to this topic,^{7, 16, 40, 41} so I decided to simply list some of the relevant structures and refer the reader to the reviews indicated for a more in-depth analysis.

Relevant structures for molecular p-Type Semiconductors are: polycyclic aromatic hydrocarbons and derivatives (Acenes, Pyrenes, Perylenes), Chalcogen-Containing Heterocyclic Aromatic Hydrocarbons and Derivatives (Thienoacenes, Thienoacene-Based Oligomers and Oligothiophenes, Tetrathiafulvalene and Derivatives); for polymer p-Type Semiconductors are: Polythiophene-Based Semiconductors, p-Type Donor–Acceptor Copolymer Semiconductors.

Relevant structures for molecular n-Type semiconductors are: Fullerenes, Diimides (Naphthalene Diimide and derivatives, Perylene Diimide and derivatives); or polymer n-Type semiconductors are: Diimide-Based n-Type polymer semiconductors,

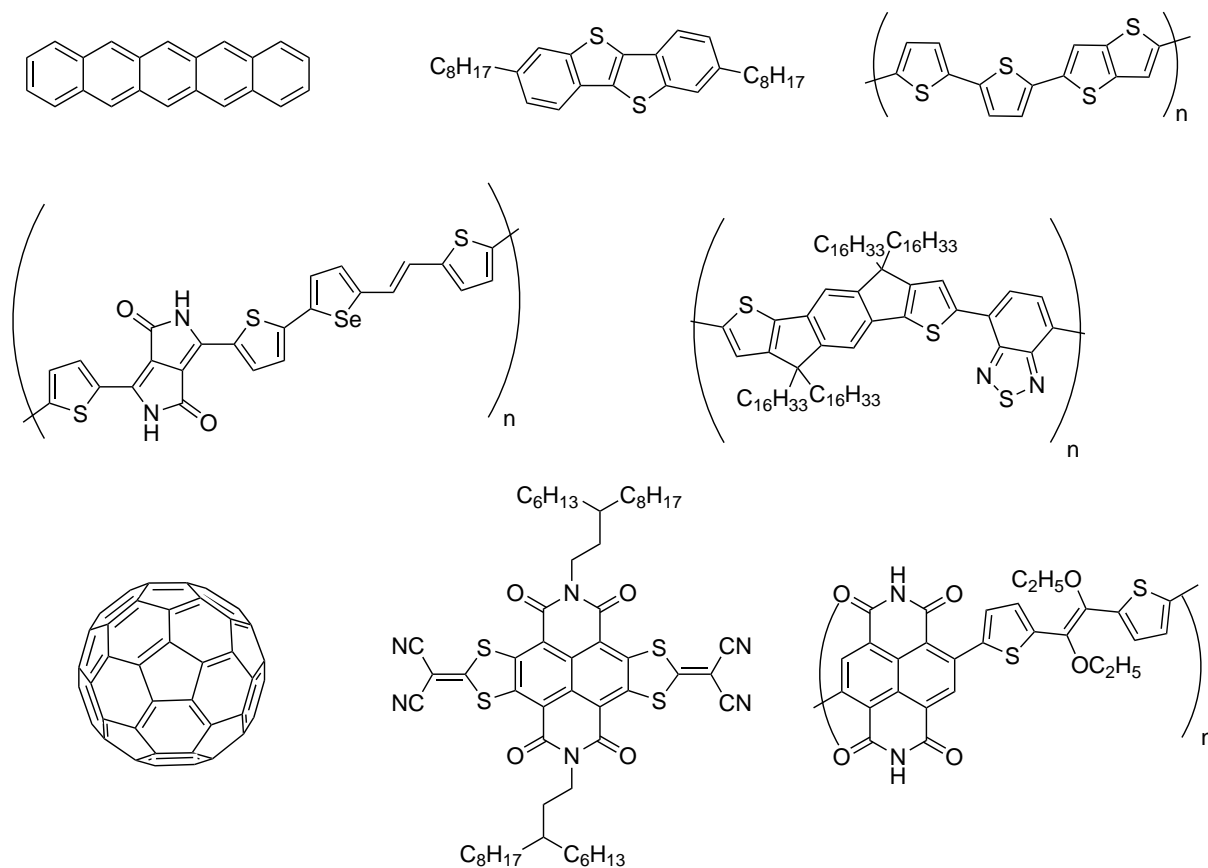


Figure 2.7 Organic semiconductors examples

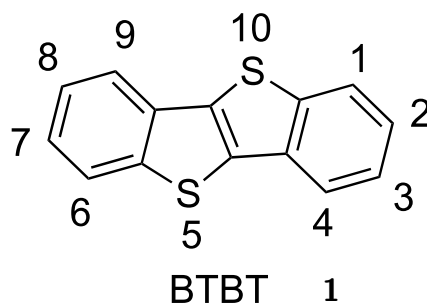
In particular in the work exposed in this chapter we focused on a promising molecular p-semiconductor materials based on the [1]benzothieno[3,2-b][1]benzothiophene (BTBT) scaffold. BTBT belongs to the Thienoacenes class: fused-thiophene compounds, several example are reported in figure 2.7. Thioacenes can exhibit high hole mobility in OFET

indeed sulfur has a larger atomic radius than carbon and then can bring to facilitate intermolecular nonbonded interaction and therefore orbital overlaps. Another important aspects is the greater stability to oxidation of thioacenes compounds indeed they are characterized by lower HOMO levels respect the corrispective Acenes. For the development of air-stable p-channel organic semiconductors, lowering the HOMO energy level while keeping it suitable to hole injection from an electrode is a feasible strategy.⁴²

2.1.3 [1]benzothieno[3,2-b][1]benzothiophene derivatives

2.1.3.1 [1]benzothieno[3,2-b][1]benzothiophene derivatives promising materials for OFET

[1]benzothieno[3,2-b]benzothiophene (BTBT) derivatives have gained a considerable interest as active, p-dopable molecular materials in the preparation of OFETs. Figure 2.8 shows the increasing numbers of papers reported in the literature and referring to BTBT derivatives. More than 25% of the hits are patents, highlighting the strong industrial interest for these materials.



Scheme 2.1 BTBT structure

From 2006 the numbers of papers started to grow considerably, indeed Takimiya et al. reported the synthesis of 2,7-Diphenyl[1]benzothieno[3,2-b]benzothiophene (**49**) and the fabrication of its evaporated thin-film-based OFET, with excellent FET characteristics in air: an average mobility of $1 \text{ cm}^2 \text{ V}^{-1} \text{ s}^{-1}$ and $I_{on}/I_{off} = 10^7$.⁴³ In 2007, the same research group reported the synthesis of different symmetric 2,7-alkyl-BTBT (DiCn-BTBT),⁴⁴ with different saturated linear carbon chains: length from 5 to 14 carbons. Compounds with the side chain up to 9 carbon atoms show good solubility in chloroform at room temperature (in the range of 60-90 g/L) while compounds with a longer chain are less soluble. The compounds DiCn-BTBT were synthesized via two reaction steps, Friedel-Crafts acylation and Wolff-Kishner reduction, using BTBT as starting material, following the condition developed for BTBT by Svoboda works some years before.^{45,46} DiCn-BTBT were used to fabricate solution-Processed OFET, the compounds were deposited by spin coating and films showed a crystalline order in the in-plane direction, indeed all devices show very good hole mobility up to $2.75 \text{ cm}^2 \text{ V}^{-1} \text{ s}^{-1}$ for n=13. Films structure consists of alternately stacked aliphatic layers and BTBT core layers. In the BTBT core layer, the molecules take herringbone packing, facilitate 2D carrier transport property. These structural aspects can be related to the high mobility of DiCn-BTBT-based FET devices, since the existence of 2D semiconducting layers with strong intermolecular overlap is considered to be one of the prerequisites to realize high-performance OFET devices.⁴⁷⁻⁴⁹

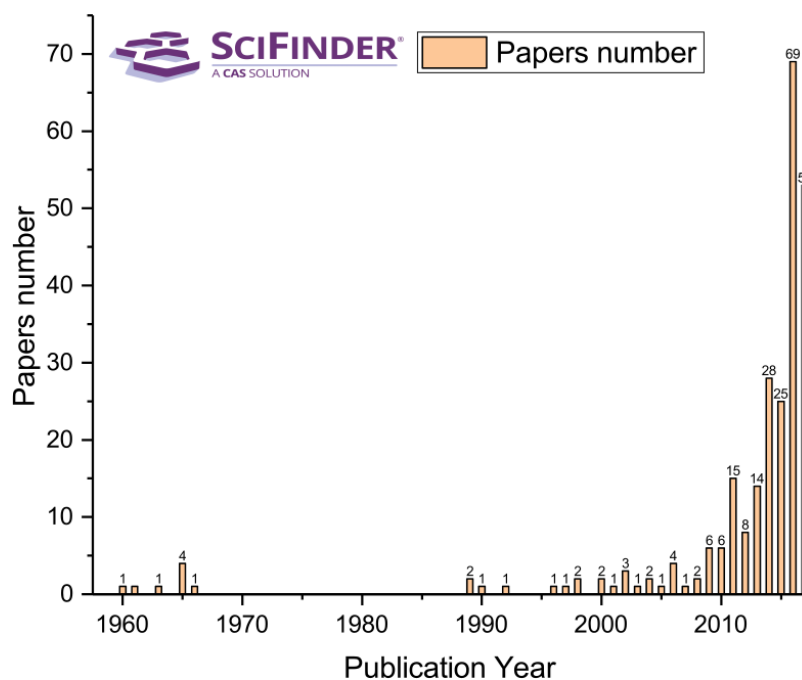
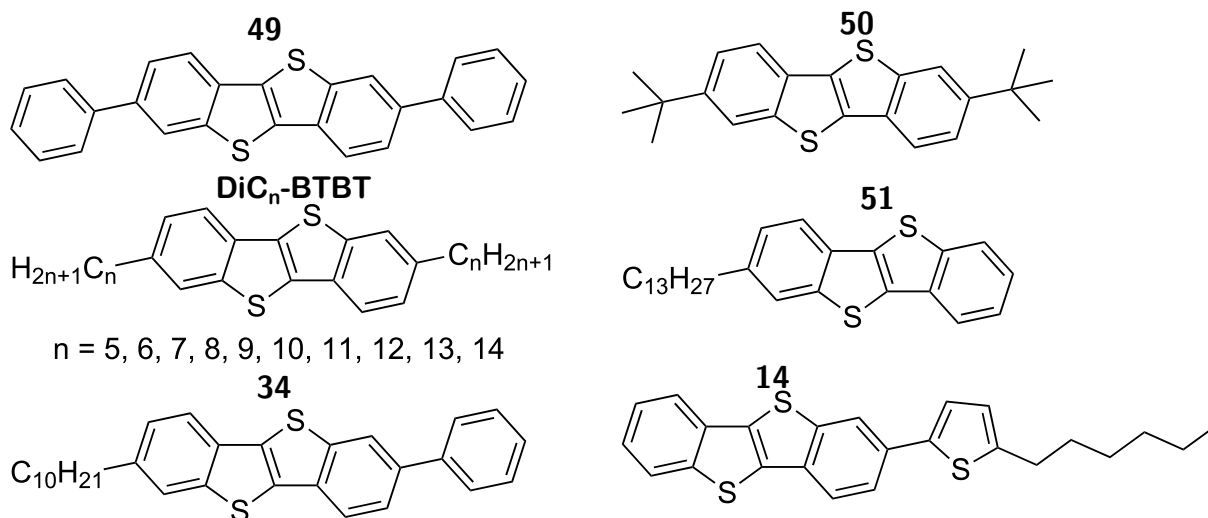


Figure 2.8 Number of hits per year for papers containing the key word “[1]benzothieno[3,2-b][1]benzothiophene” either as such or as a portion of a more complex structure. Extraction of data done on March 19th 2018, source:SciFinder



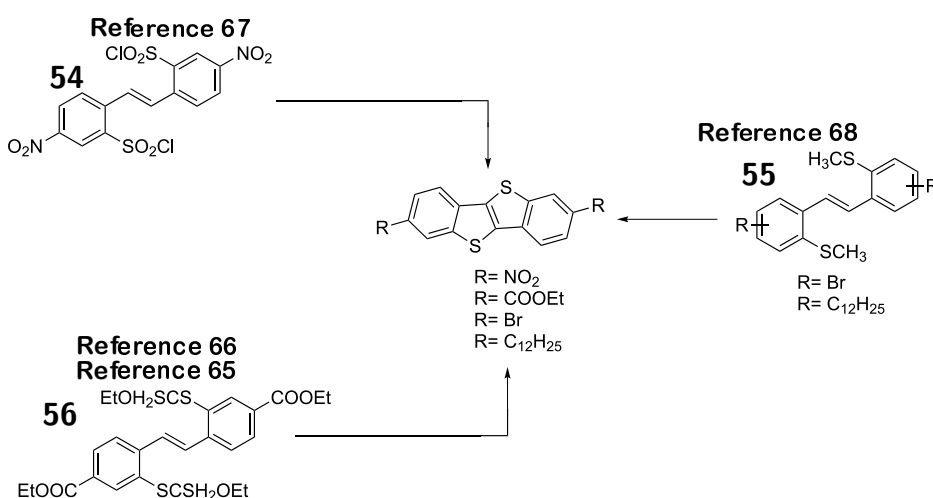
Scheme 2.2 Selection of BTBT derivatives reported in the literature

In 2011 Takimiya et al. reported that high-mobility ($\mu_{sat} = 3.5 - 6.0 \text{ cm}^2 \text{V}^{-1} \text{s}^{-1}$) solution-processed OFETs are developed using solution-crystallized 2,7-dioctyl[1]benzothieno[3,2-b][1]benzothiophene (DiC8-BTBT) main semiconductor channels combined with strong acceptor layers of 2,3,5,6-Tetrafluoro-7,7,8,8-tetracyanoquinodimethane (F4-TCNQ). The construction results in inducing moderate oxidation in the DiC8-BTBT channel to achieve device operation with low threshold voltage and high on-off ratio in air. The X-ray diffraction experiment revealed that the whole channel consists of a complete single-crystal domain with the dimension of submillimeters. The combination of low-HOMO air-stable main-channel semiconductors and low-LUMO strong acceptors turned out to be effective to reduce the threshold voltage that can be often a drawback of air-stable devices.⁵⁰ In

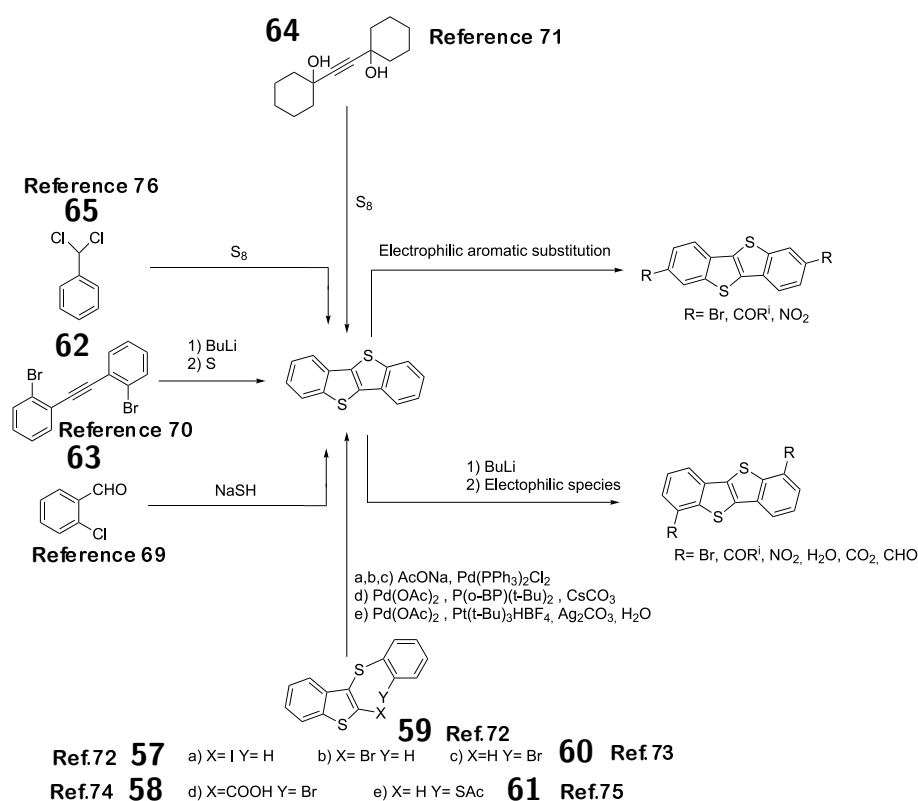
the same year Minemawari et al.⁵¹ developed a method that combines the technique of antisolvent crystallization⁵² with inkjet printing to produce organic semiconducting thin films of high crystallinity. They demonstrated that mixing fine droplets of an antisolvent and a solution of an active semiconducting component within a confined area on an amorphous substrate can trigger the controlled formation of exceptionally uniform single-crystal or polycrystalline thin films growing at the liquid–air interfaces. Using this approach, they printed single crystals of 2,7-dioctyl[1]benzothieno[3,2-b][1] benzothiophene (DiC8-BTBT), yielding thin-film transistors with average carrier mobilities as high as $16.4 \text{ cm}^2\text{V}^{-1}\text{s}^{-1}$. Always employing DiC8-BTBT it has been shown that it is possible to obtain excellent OFET devices with single crystal-spray coating⁵³ and vacuum-and-solvent-free fabrication.⁵⁴ Bulky end-capped **50** was identified as a high-performance solution processable BTBT derivatives with large and well-balanced transfer integrals. The relevant substitution by two *t*-Butyl group improves the orbital overlap of the molecules within their crystalline architecture.⁵⁵ Also the asymmetric *n*-alkyl substitution pattern employed in 2-tridecyl[1]benzothieno[3,2-b][1]-benzothiophene (**51**) leads to improved charge transport properties in organic thin-film transistors, with large hole mobilities up to $17.2 \text{ cm}^2\text{V}^{-1}\text{s}^{-1}$ in low-voltage operating devices. The large mobility was related to densely packed layers of the BTBT π -systems at the channel interface due to the substitution motif and was confirmed by X-ray reflectivity measurements.⁵⁶ Another approach for improving the OFET mobility on BTBT derivatives is blending. This simple approach is to combine the high charge carrier mobilities typically associated with the small molecule materials and the film capabilities traits of polymers in a system that offers the best of both worlds. DiC8-BTBT/C16IDT-BT polymer(**52**)^{57–59} and DiC8-BTBT/ Polystyrene sulfonates (PSS)⁶⁰ blend systems are very promising OFET materials. Additionally, these blend systems seem to have shown limited nonideal characteristics, giving a clearer idea about the mobility values that can be achieved with these systems.¹⁶ A limit for this type of systems or practical application to integrated electronic devices, such as driving circuits for displays or biomedical sensors, is the thermal stability at the device stage. BTBT derivatives having long alkyl groups may not be promising owing to their thermal phase transition into the liquid crystalline phase at relatively low temperatures.⁶¹ Different are the strategy in order to overcome this limit, the most promising is the synthesis of liquid crystal compounds like **34** and **14** that show excellent mobility in OFET and can show highly ordered liquid crystalline phases that can provide an easy fabrication of quality polycrystalline thin films and high thermal stability of the polycrystalline thin films by solvent deposition,⁶² but they will be introduced in more details in section 3.5 of this thesis. Various π -extended BTBT analogues, such as dinaphtho[2,3-b:2',3'-f]thieno[3,2-b]thiophene (DNTT,**53**) have been synthesized and evaluated as organic semiconductors for OFET devices,⁶³ and DNTT turned out to be organic semiconductor, affording OFETs with high mobilities.

2.1.3.2 Synthesis of BTBT and derivatives reported in literature

Historically [1]benzothieno[3,2-b][1]benzothiophene was reported for the first times in 1889 as a reaction's product between toluene and elemental sulfur at high temperatures and, only in 1949 it was assigned the right structure by Horton.⁶⁴ Thereafter, several BTBT derivatives were synthesized mainly motivated by their potential use as liquid crystalline materials and afterwards as OFET materials.^{45, 46, 61, 65-70} There are two principals synthetic strategies for BTBT synthesis: the first (see figure 2.3 is the direct synthesis of BTBT derivatives, starting from stilbenes with o-sulfur functional groups⁶⁵⁻⁶⁸ (compounds **54**, **55**, **56**), the second is the synthesis of the parent BTBT⁶⁹⁻⁷⁶ followed by functionalization by electrophilic aromatic substitution in position 2 and 7 or go through the lithium salt intermediate for the functionalization of the positions 1 and 6.⁴⁶ Stilbenes with o-sulfur functional groups can be converted into corresponding BTBT derivatives with a range of substituents, such as nitro,⁶⁷ ester,⁶⁶ bromo,⁶⁸ and alkyl groups⁶⁸. 2,7-dinitro-BTBT can be reduced into the corresponding diamino-BTBT, which, via the Sandmeyer route, is converted into the diiodo-BTBT, a versatile intermediate for BTBT derivatives synthesis.⁴⁴ The limits of the first synthetic strategy is that stilbenes precursor are not commercially available and are prepared with multi step synthesis and it is a linear synthesis which limits the possibility of obtaining different derivatives in a short time. Conversely the second synthetic strategy diverges from BTBT thus several different derivatives can be prepared starting by the same precursor. The most recently BTBT reported syntheses start from functionalized 3-phenylbenzothiophenes (compounds **57**, **58**, **59**, **60**, **61**) and can afford BTBT in good/high yield⁷²⁻⁷⁵ but however the 3-benzothiophenes are not readily available. Differently bis(2-bromophenyl)acetylene⁷⁰ (compound **62**) and o-chlorobenzaldehyde⁶⁹ (**63**) are commodity synthetic reagents and in particular the BTBT synthesis starting from o-chlorobenzaldehyde don't required a chromatographic purification but the product is just filtered and washed to afford highly pure BTBT. The BTBT synthesis that start from o-chlorobenzaldehyde reported by Saito at al. in 2011 was our choice, indeed the authors reported also a large-scale preparation of BTBT.



Scheme 2.3 Reported synthesis of BTBT derivatives, starting from stilbenes with o-sulfur functional groups⁶⁵⁻⁶⁸



Scheme 2.4 Reported synthesis^{69–76} of the parent BTBT followed by functionalization by electrophilic aromatic substitution in position 2 and 7 or go through the lithium salt intermediate for the functionalization of the positions 1 and 6

2.2 Aims

Motivated by promising performance in OFET shown by BTBT derivatives, we have decided to synthesize new BTBT derivatives. In particular, we focused our efforts on two different classes: a) extended conjugated BTBT derivatives and b) functionalized side chains BTBT derivatives. In details, for the first type we aimed at the synthesis of new BTBT derivatives that present conjugated moieties like hetero-aromatic substituents (or simple double bond) in the structure, since they are supposed to facilitate molecular packing in the solid state and consequently improve the electron transport properties of the molecule. General target-structures are shown in figure 2.9. Generally, this kind of structures are synthesized by Stille, Suzuki-Miyaura and Kumada cross coupling reaction for BTBT derivatives. We tried to synthesize the target-structures employing different synthetic strategies like Pall-Knorr, McMurry and direct arylation reactions. For the second type, we aimed at functionalizing BTBT with side chains with particular end groups in order to tune the packing in solid state thanks to non-covalent interactions. Functionalization of the BTBT core by side chains is likely to introduce stronger interactions such as hydrogen bonds. Examples developed simultaneously with our work are already documented.^{77–79} In particular our idea was to use hydrogen bond in order to modify BTBT packing in the solid state.

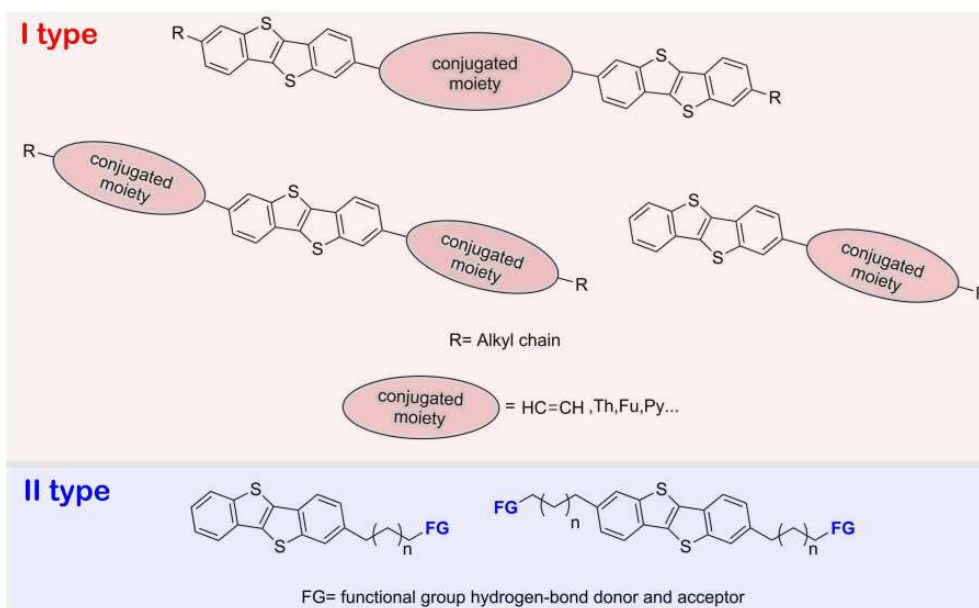


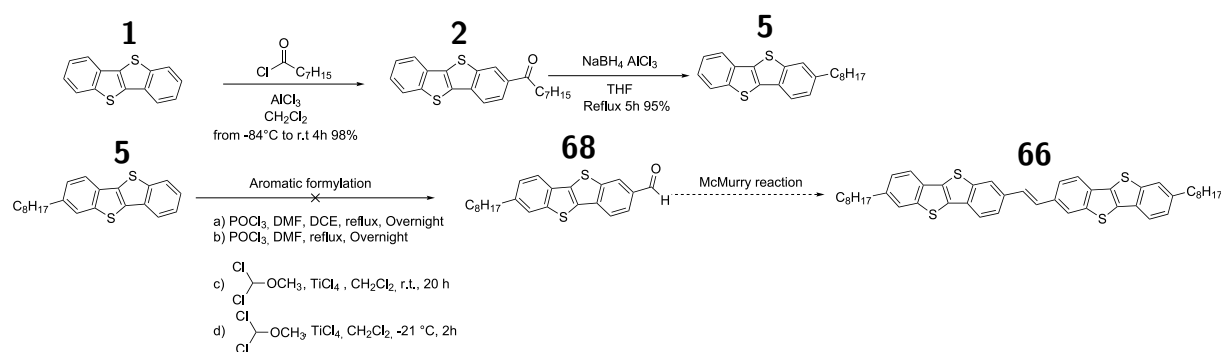
Figure 2.9 Target compounds general formula

2.3 Synthesis of conjugated BTBT derivatives

2.3.1 Synthesis of [1]benzothieno[3,2-b][1]benzothiophene dimer double bond-linked

Our first target was the extended conjugation derivative **66** (see scheme 2.5) in principle accessible through aldehyde **67** via the McMurry reaction. Soluble precursor **5** was synthesized via two reaction steps, Friedel-Crafts acylation and carbonyl reduction, using BTBT as the starting material. The condition of Friedel-Crafts acylation were taken from the literature: BTBT was reacted with octanoyl chloride activated by aluminium chloride (AlCl_3) in dichloromethane at low temperature (-84°C) in order to control the regioselectivity of the electrophilic attack. For the reduction of the carbonyl to methylene group, literatures reports a Wolff-Kishner reduction condition. Aiming at avoiding the use of hydrazine, we turned to aluminium hydride (AlH_3) generated in situ by reacting sodium borohydride (NaBH_4) with aluminium chloride (AlCl_3) in tetrahydrofuran at reflux. The reaction's yield is high and comparable with Wolff-Kishner reduction reported in literature. We intended to prepare the intermediates **67** thanks an aromatic formylation reaction, because in several examples reported in literature BTBT shows very good reactivity in terms of regioselectivity and conversion in Friedel-Crafts acylation, another aromatic electrophilic substitution. Our first attempt was the Vilsmeier-Haack reaction. Thus compound **5** was reacted with the Vilsmeier-Haack reagent in reflux dichloroethane (DCE) for 5 hours under nitrogen atmosphere (condition a in scheme 2.5). Vilsmeier-Haack reagent was previously prepared by reacting dimethylformamide (DMF) with phosphorus oxychloride (POCl_3) at 0°C . Unfortunately, the reaction was checked with TLC analysis and after acid work up by NMR spectroscopy but in both case no traces of aldehyde were observed, mostly starting material **5** was recovered. Even the use of N,N-dimethylformamide (DMF) as the solvent gave no conversion of the starting materials **5** (condition b in scheme 2.5). Probably the lack of reactivity of the BTBT was due to the

weakness of the electrophile used so we decided to use the conditions of Rieche formylation. In Rieche formylation dichloromethyl methyl ether acts as the formyl source upon activation by titanium chloride. Compound **5** was reacted with dichloromethyl methyl ether and titanium chloride in dichloromethane at 0°C, followed by room temperature stirring for 20 h (condition c in scheme 2.5). The reaction's conversion was complete as assessed by TLC analysis. Unfortunately, formation affords 4 different regioisomers (as confirmed by NMR spectroscopy) that can not be separated by chromatographic purification. We tried to run the reaction at lower temperature (-21°C) but also under such conditions the formation of the 4 different regioisomers was observed (condition d in scheme 2.5). In conclusion we could not isolate the intermediates **67**, consequently we dropped the target compound **66**.



Scheme 2.5 Planned synthesis of compound **66**

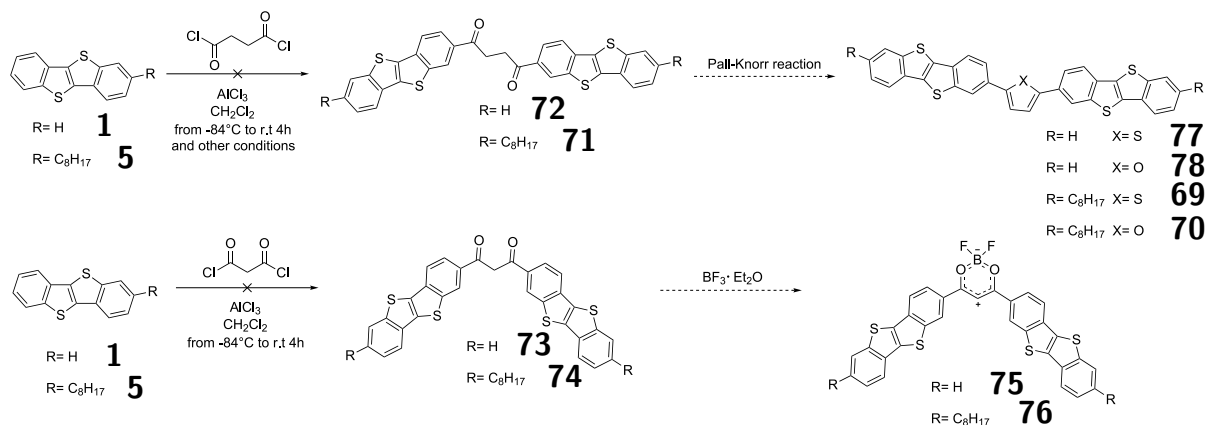
2.3.2 Synthesis of [1]benzothieno[3,2-b][1]benzothiophene dimer heterocycle-liked derivatives

2.3.2.1 Friedel-Crafts acylation reaction with Dicarboxylic acid chloride

As simple double bond bridged derivatives proved to be inaccessible we turned to heteroaromatic (thiophene and pyrrole) bridged derivatives. Our first synthetic strategy in order to obtain compounds **69** and **70**, were based on Pall-Knorr reaction of the key intermediate **71**. The idea was to synthesize the intermediates **71** with a double Friedel-Craft acylation of succinic acid dichloride in the same condition of BTBT acylation exploiting for the synthesis of the compound **2**: in dichloromethane at -84°C . Reaction's conversion was complete but surprisingly it was not possible to isolate the desired product. In both cases we observed the formation of a complex mixture of decomposition structures. Neither crude product's NMR analysis nor GC-MS analysis allowed us to identify the structures obtained. We suspect that we obtained a mixture of non-separable compounds due to inter and intramolecular electrophilic attacks. In order to understand if the problem could be the activation of the aromatic ring due to the introduction of the electron donating octyl chain group, we tried the same reaction with BTBT in order to obtain intermediate **72** but we obtained similar results. We tried to change the carboxylic diacid chloride in order to test if the BTBT derivatives reactivity in double Friedel-Craft acylation was peculiar of the succinic derivative or more general, we decided to use malonic acid dichloride. Moreover the intermediates **73** and **74** are β -diketones useful for the synthesis of the difluoro-dioxaborine derivatives **75** and **76**. Unfortunately, for BTBT and

CHAPTER 2. THE CHEMISTRY OF BTBT DERIVATIVES: CHALLENGES AND NEW DERIVATIVES

compound **5** both behaviour was the same as that observed with succinic acid dichloride. We dropped this approach as well.

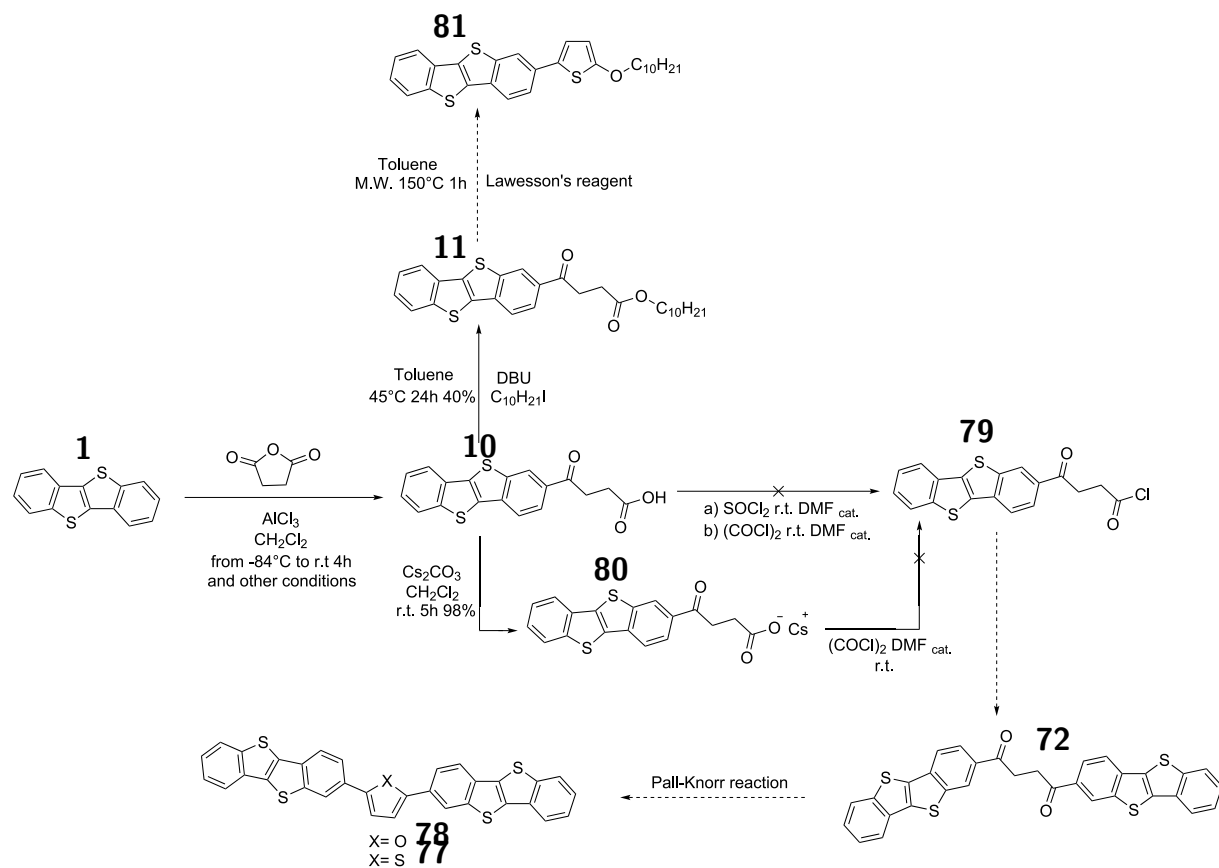


Scheme 2.6 Planned syntheses of compounds **77-70** and **75,76**

2.3.2.2 Friedel-Crafts acylation reaction with carboxylic anhydride

Derivative **72** could not be made by double Friedel-Crafts acylation reaction, but other approaches are possible, that involves more synthetic steps. We started with Friedel-Crafts acylation of BTBT with succinic anhydride in order to obtain the compound **10**. This time we were able to isolate the carboxylic acid **10** in moderate yield (60%). We still observed the formation of a regioisomers, but thanks a hot washing in toluene and extractive crystallization in THF, we managed to isolate pure **10**. The second step of our synthetic strategy was the synthesis of the acyl chloride **79**, we tried two different chlorinating reagent: the first was Thionyl chloride (SOCl_2) in presence of catalytic amount of DMF but we obtained the decomposition of the reagent. Indeed in the NMR of crude product we observed a lot of new aromatic signal, not coherent with the BTBT scaffold. We thought the problems could be linked with the aggressive reaction's byproduct like hydrogen chloride and sulfur dioxide so tried also with Oxalyl chloride ($(\text{COCl})_2$) in presence of DMF like catalyst, because the byproduct of the chlorination with this second reagent are the carbon monoxide and carbon dioxide, but also in this case we were unable to isolate the target **79**. We tried to run the chlorination on the activate acid carboxylic acid as cesium salt (**80**) prepared by the reaction of compound **10** with cesium carbonate in Toluene, but yet again we could not isolate the compound **79**. Nonetheless the development of the condition for the synthesis of compound **10** proved useful for different synthetic schemes (section 2.5.3 and 3.5.2.3). In particular the compound **10** opened the way to the synthesis of target compound **81**, still to be optimized. The esterification of compound **10** with decanoyl iodide in the presence of 1,8-diazabicyclo[5.4.0]undec-7-ene (DBU) as activating base affords ester **11** in moderate yield (40%), due to the poor solubility of the reagent in toluene at 45°C (temperature was not raised further to avoid elimination of the iodide). Finally we made only a first attempt of Pall-Knorr reaction of the compound **11** with Lawesson's reagent in Toluene under pressure and microwave irradiation. The crude product's NMR analysis confirm the formation of the product, along with other byproduct, the purification still to optimize.

2.3. SYNTHESIS OF CONJUGATED BTBT DERIVATIVES

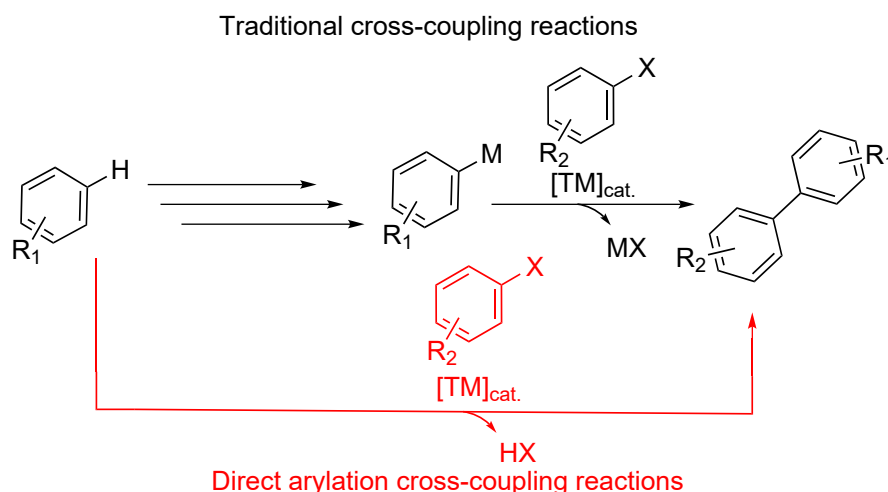


Scheme 2.7 Planned alternative syntheses for compounds **78** and **77** and synthesis of compound **81**

2.4 Direct arylation cross coupling for [1]benzothieno-[3,2-b][1]benzothiophene derivatives

2.4.1 Direct arylation cross-coupling a greener alternative

Compounds the like of **11** and **81** could be prepared via cross coupling reactions: the like of Stille,^{80, 81} Suzuki,^{82, 83} (palladium-catalyzed)⁸⁴ and Kumada⁸⁵ (nickel-catalyzed)⁸⁶ more in general, transition-metal(TM)-catalyzed cross-coupling methodologies, in particular Pd-catalyzed reaction have evolved over the past four decades into one of the most powerful and versatile methods for C(sp²)-C(sp²) bond formation, enabling the construction of a diverse and sophisticated range of π -conjugated molecules and polymers.⁸⁷ However, this traditional cross coupling reactions require organometallic nucleophilic reagents, particularly when being functionalized, are often not commercially available or are relatively expensive and their synthesis provides the use flammable (e.g. butyl lithium), unstable and/or highly toxic (e.g. organo tin derivatives) reagents. Therefore, direct arylation reactions based on the activation of the C-H bonds represent an environmentally and economically more attractive strategy⁸⁸⁻⁹¹ (Scheme 2.8) very promising for the development of organic semiconductors that can be prepared in large scale and sustainably , one of the key challenge for Organic printed electronics as mentioned in chapter 1.

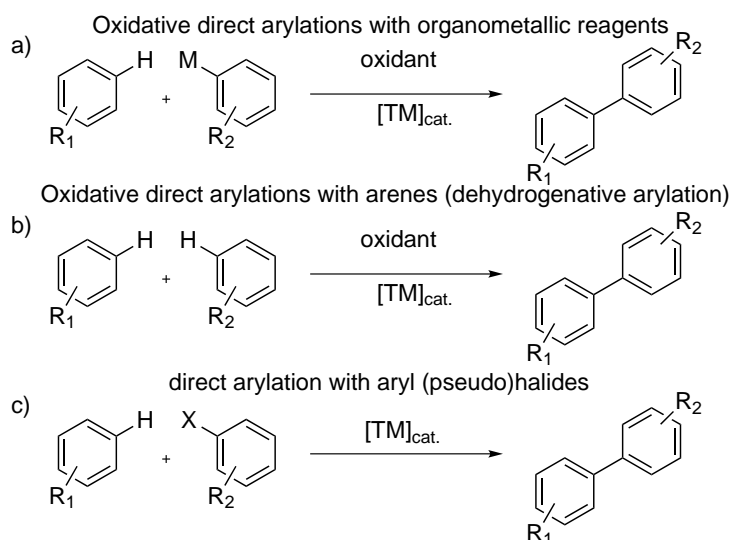


Scheme 2.8 Comparison between classical cross-coupling and direct arylation reactions

TM-catalyzed direct arylation reaction through cleavage of C-H bonds has undergone rapid development in recent years and is becoming an increasingly viable alternative to traditional cross-coupling reactions with organometallics. In particular, palladium and ruthenium catalysts have been described that enable the direct arylation of (hetero)arenes with challenging coupling partners including electrophilic aryl chlorides and tosylates.⁸⁸ Catalytic direct arylations by cleavage of C-H bonds can be differentiated on the basis of the nature of the coupling partners into 1) oxidative arylations (Scheme 2.9 a, b) and 2) reactions with aryl (pseudo)halides as electrophilic coupling partners (Scheme 2.9 c). Oxidative arylations inherently require the presence of sacrificial oxidants, and can be achieved with either stoichiometric amounts of organometallic reagents (Scheme 2.9 a) or (hetero)arenes⁹² (Scheme 2.9 b) as arylating reagents. Since the use of organometal-

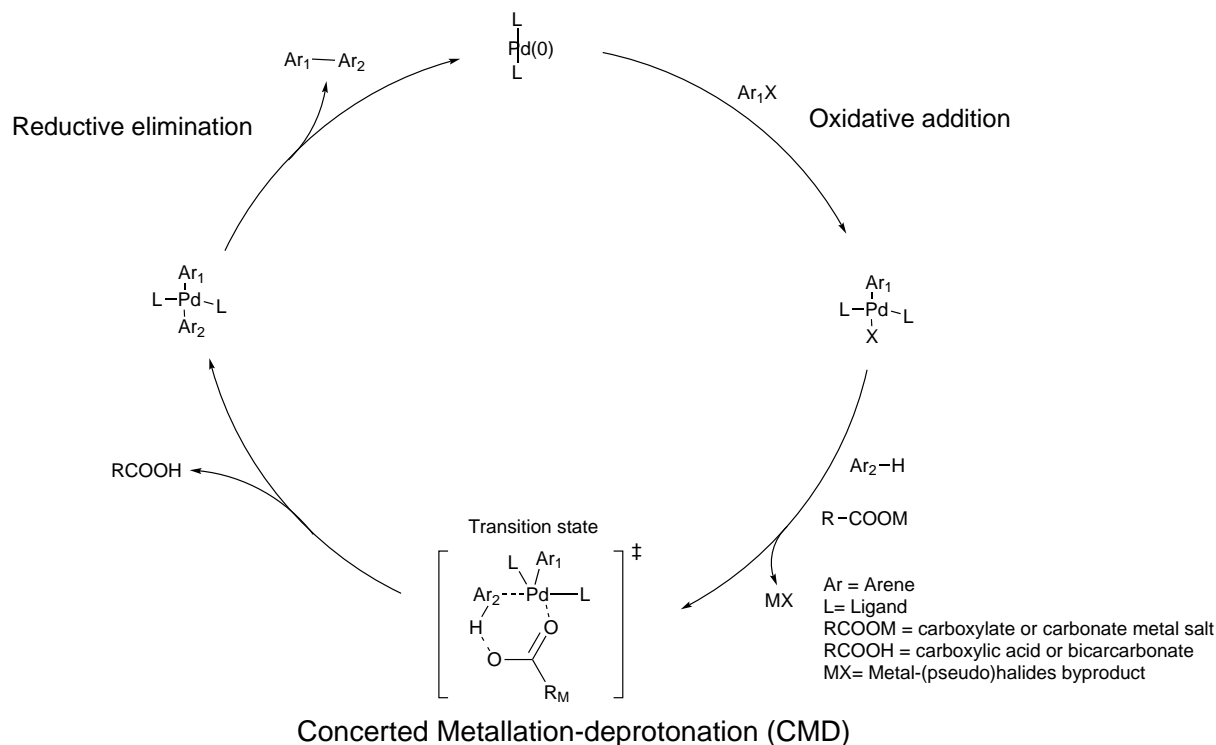
2.4. DIRECT ARYLATION CROSS COUPLING FOR [1]BENZOTHIENO[3,2-B][1]BENZOTHIOPHENE DERIVATIVES

lic reagents is associated with the formation of stoichiometric amounts of undesired by-products, dehydrogenative arylation is significantly more appealing.



Scheme 2.9 Strategies for catalytic direct arylation for the synthesis of biaryls. TM=transition-metal catalyst M= metallic group X= (pseudo)halide

The mechanism of direct arylation coupling has been the subject of several experimental^{93, 94} and computational reports^{95, 96} in the past two decades. Two pathways that have been widely studied are the electrophilic aromatic substitution and concerted metalation deprotonation (CMD). In 2000, Sakaki and coworkers reported⁹⁷ a computational study of the C–H activation of benzene by palladium that report a CMD pathway and afterwards Fagnou^{98, 99} and coworkers works demonstrated the applicability of the CMD pathway to a wide range of heteroarenes. Scheme 2.10 describes the common mechanism of direct heteroarylation by the CMD pathway for carboxylate-mediated models.^{100, 101} The reaction begins with the oxidative addition of the aryl halide bond ($\text{Ar}_1\text{--X}$) to the Pd(0) complex (Scheme 2.10) with ligands (L) to form an aryl–halo complex. Depending on the catalytic model, a carboxylate or carbonate ion coordinates with the aryl–halo complex to deprotonate Ar_2 while simultaneously forming the $\text{Ar}_2\text{--Pd}$ bond, hence leading to the formation of the transition state. The concerted-metalation and deprotonation step distinguishes direct C–H arylation from convention C–C coupling. It should be noted that while most arenes follow the CMD pathway, the exact mechanism depends on the nature of substrates, ligands and solvents involved.^{102–104} The product is formed by the reductive elimination of $\text{Ar}_1\text{--Ar}_2$ from palladium.



Scheme 2.10 General mechanism of direct arylation via the concerted metalation-deprotonation (CMD) pathway

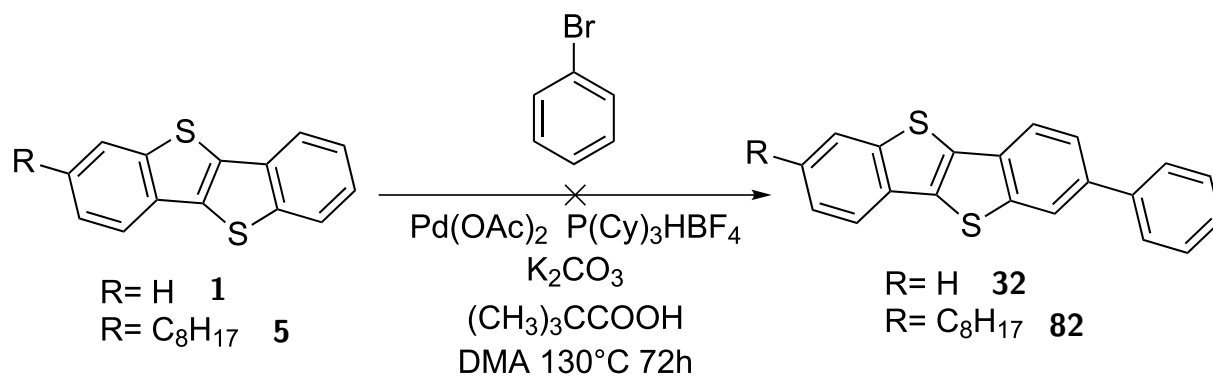
Several examples of direct arylation with aryl (pseudo)halides as electrophilic coupling partners are reported for OS small-molecules indeed OS synthesized by direct arylation belong to different classes: Benzothiadiazole (BT),^{105–111} Diketopyrrolopyrrole (DPP),^{112–117} Naphthalenediimide (NDI),^{107, 118, 119} Isoindigo (IG),¹²⁰ Thienothiadiazole (TTD)^{119, 121} and Thienoisindigo (TIIG).¹²² Reported BTBT derivatives synthesis by direct arylation are limited to their synthesis via 3-phenylbenzothiophene intermediate that are mentioned before in section 2.1.3.2^{72–75} and examples of late stage functionalization of BTBT scaffold by direct arylation are not yet reported. This reason prompted us to study the reactivity of BTBT in conditions of direct arylations and verify if it was possible to obtain the conjugate extension derivatives under these conditions.

2.4.2 Direct arylation cross coupling reaction for BTBT derivatives

We started to test the BTBT's reactivity in direct arylation with simple model reactions. We chose bromobenzene as the model substrate for test reactions on BTBT C-H bonds in direct arylation condition. This strategy for the functionalization of the BTBT scaffold would avoid the synthesis of BTBT bromides, which as explained in section 2.4.3 presents several limitations in the purification. The first trials of BTBT derivatives synthesis by direct arylation reaction was the synthesis of compounds **32** and **82**. We reacted BTBT with: bromobenzene as coupling partner, palladium(II) acetate ($\text{Pd}(\text{OAc})_2$) as palladium source, tricyclohexylphosphine tetrafluoroborate ($\text{P}(\text{Cy})_3\cdot\text{HBF}_4$) as precursor of the catalyst ligand, pivalic acid ($((\text{CH}_3)_3\text{COOH})$) as protonic shuttle and potassium carbonate (K_2CO_3) as base; in dimethylacetamide (DMA) at 130°C for 72h. We choose

2.4. DIRECT ARYLATION CROSS COUPLING FOR [1]BENZOTHIENO[3,2-B][1]BENZOTHIOPHENE DERIVATIVES

these condition as they are already reported for the functionalization of several others OS system^{113–115, 120, 121}. The crude product's analysis by GC-MS analysis reveals a low conversion and the formation of two mono-arylated regioisomers and two di-arylated regioisomers. Similar results were obtained when we reacted compounds **82** under the same condition. Unfortunately the reactivity of the BTBT C-H bonds in direct arylation is poor and with lack of regioselectivity for the different C-H bonds, so we decided to reverse the functionality, thus developing mono and di bromination protocols for BTBT.

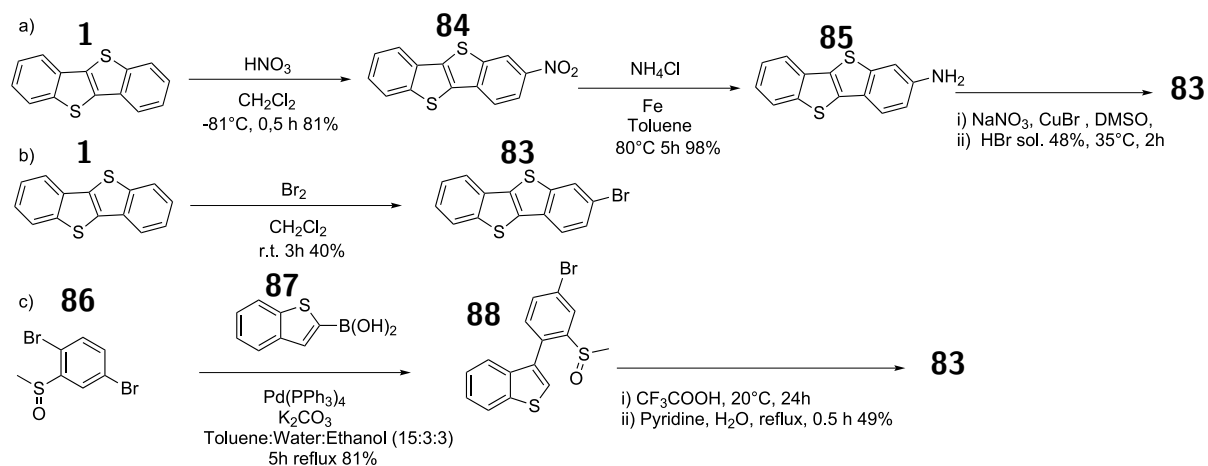


Scheme 2.11 Attempt of BTBT's phenylation by direct arylation

2.4.3 [1]benzothieno[3,2-b][1]benzothiophene bromides synthesis

In order to test the reactivity of BTBT's bromide we synthesized different bromides. We started with the compound 2-bromo-[1]benzothieno[3,2-b][1]benzothiophene (**83**) synthesis, scheme 2.12 shows the three literature synthesis. The route **a**¹²³ is 3 steps synthesis, it starts with the nitration of BTBT with fuming nitric acid (HNO_3 in dichloromethane at -81°C in order to control the regioselectivity). Compound **84** was obtained in good yield (81%). In the second step the nitro group of the compound **84** is reduced to amino group with ammonium chloride and iron catalysis in toluene at 80°C to afford compound **85** in high yield (98%). Last step is a bromination under Sandmeyer conditions with the preparation in situ of the corresponding diazonium salt, in dimethyl sulfoxide (DMSO) at 35°C . Compound **83** was obtained in moderate yield. The route **c**¹²⁴ starts from Suzuki-Miyaura cross coupling of the compounds **86** and **87** to afford the phenyl-benzothiophene derivative **88**. The final step is a two step cyclization affording the compound **83** in moderate yield (48%). In summary the route **a** and **c** are multi step synthesis with a overall yield of 38% and 40% respectively moreover compound **86** is not commercially available. For this reason we prefer the route **b**¹²⁵ because is only one synthetic step: bromination of BTBT in dichloromethane at room temperature, the conversion of the reaction is complete but the compound **83** was obtained in moderate yield (40%), the problem is the formation of a regioisomer that is removed with a crystallization in chloroform.

CHAPTER 2. THE CHEMISTRY OF BTBT DERIVATIVES: CHALLENGES AND NEW DERIVATIVES

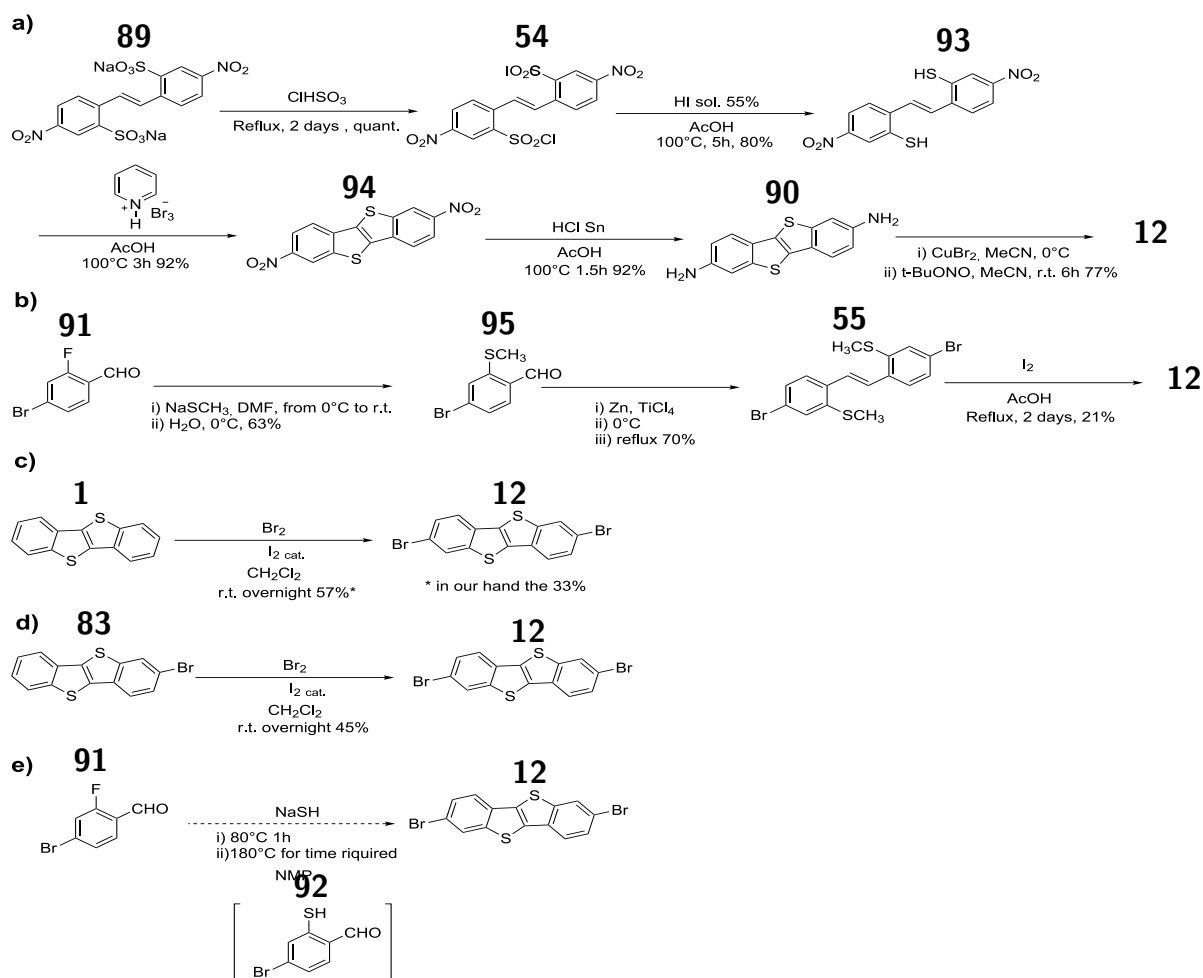


Scheme 2.12 Reported syntheses a¹²³ b¹²⁴ c¹²⁵ of compound **83**

Our second target bromide was 2,7-di-bromo-[1]benzothieno[3,2-b][1]benzothiophene (**12**), Scheme 2.13 shows the literature syntheses (**a**, **b**, **c**). The route **a**⁶⁷ is the first synthesis reported for this compound already in the 1980, is 5 steps synthesis starting with the commercial stilbene **89** and after several functional group interconversion under harsh conditions it gives BTBT functionalized **90** that is converted in the corresponding bromide (**12**) in the last step, with an overall yield of 52%. More recently the synthesis of the intermediate **90** was proposed directly starting with a nitration of the deactivated compound **84** but the second nitration is inefficient leading to a 17% yield. The route **b**⁶⁸ starts from the commercially available aldehyde **91**, the first step is aromatic nucleophilic substitution of the fluoride group with methylsulfur group to afford the compound **55**. The second step is a McMurry reaction giving stilbene derivatives **55** that is cyclised to afford compound **12** with an overall synthesis of 9%. The direct bromination of BTBT was another time our choice (route **c**¹²⁶), with bromide in dichloromethane at room temperature in presence of a catalytic amount of iodide. The conversion is almost complete but the formation of three regioisomers make the purification troublesome. The author reported a yield of 57% after a chromatographic column and crystallization in chloroform, but in our hands the purification wasn't reproducible particularly regarding chromatographic separation and for the crystallization a big amount of solvent is required due the very poor solubility of the product **12**. We thus developed a non-chromatographic purification: a crude product's hot washing with boiling dichloromethane. The yield is 33% and little regioisomer impurities remain confirmed by GC-MS, but is more scalable technique. In order to obtain more pure product we tried the bromination of the compound **83** and we could isolate clean **12** with a yield of 45%, , an overall yield from BTBT of 18%. In order to increase the bromination regioselectivity we tried to exchange the brominating agent: N-bromosuccinimide (NBS) and tribromoisocyanuric acid, but with the first reagent in dark condition in various solvent (CH₂Cl₂, CHCl₃, CCl₄, DMF, THF, Dioxane) no bromination was observed and with tribromoisocyanuric acid in sulphuric acid as the solvent the bromination doesn't show better regioselectivity. We plan to try a route **e**, starting from commercially aldehyde **91** and under the same condition employed for the one-pot synthesis of BTBT condition: Sodium hydrosulfide hydrate (NaSH) in N-Methyl-2-pyrrolidone (NMP). We think we could obtain the desired product **83** in good yield in only one synthetic step. Indeed if the aromatic substitution on aldehyde **91** follow a classical addition-elimination mechanism the hydrosulfide anion will react predominantly with the fluoride to give the intermediate thiol intermediate **92** that be condensed and

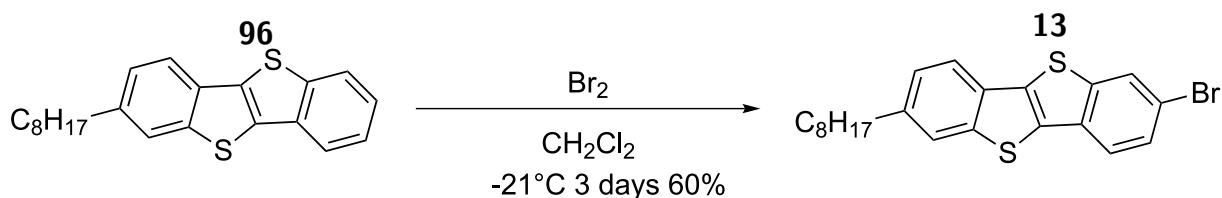
2.4. DIRECT ARYLATION CROSS COUPLING FOR [1]BENZOTHIENO[3,2-B][1]BENZOTHIOPHENE DERIVATIVES

dehydrated to gave the product **12**, the route is under evaluation.



Scheme 2.13 Syntheses of compound **12**: Reported in literature a,^{67b},⁶⁸ c¹²⁶ and not reported d and e

Finally we prepared a more soluble BTBT bromide, 2-octyl-7-bromo-[1]benzothieno[3,2-b][1]benzothiophene follow reported condition,¹²³ (see scheme 2.14) but we performed the reaction at low temperature, - 21°C instead of r.t. in order to try to control better the regioselectivity. Our result were compatible with those of the literature (60%).

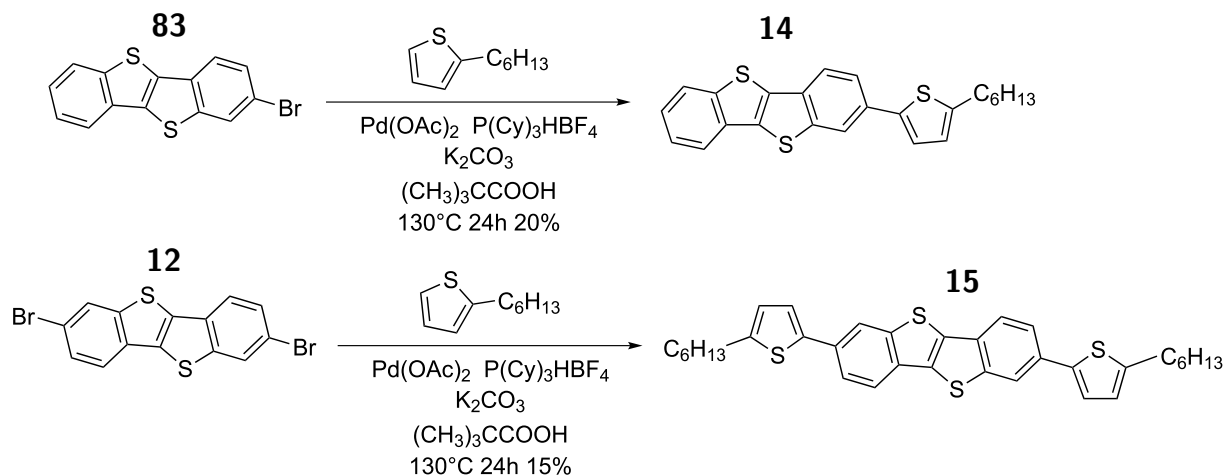


Scheme 2.14 Synthesis of compound **13**

2.4.4 Synthesis of **2** and 2,7-thienyl-[1]benzothieno[3,2-b][1]benzothiophene (BTBT) derivatives by direct arylation

Once we got the bromides, we decided to test their reactivity in direct arylation reactions with 2-hexylthiophene like coupling partner. The reason for the 2-hexylthiophene

as the coupling partner is that 2-hexylthiophene has only one activate position for direct arylation, the position 5 and moreover **14** is a very promising OFET materials, more details about that can be found in the section 3.5. Bromides **83** was reacted with: 2-hexylthiophene as coupling partner, palladium(II) acetate ($\text{Pd}(\text{OAc})_2$) as palladium source, tricyclohexylphosphine tetrafluoroborate ($\text{P}(\text{Cy})_3\text{HBF}_4$) as precursor of the catalyst ligand, pivalic acid as protonic shuttle and potassium carbonate (K_2CO_3) as base; in dimethylacetamide (DMA) at 130°C for 24h. The product was observed in TLC analysis, but also several other not well indicated byproduct were formed. The crude product was purified by chromatography and crystallization to afford 2-(5-hexyl-2-thienyl)-[1]benzothieno[3,2-b][1]benzothiophene (**14**) with 20% yield. Under the same conditions we tried the synthesis of compound **15** and we could isolate the target in 15% yield starting from bromide **12**.



Scheme 2.15 Synthesis of compounds **14** and **15** by direct arylation starting from BTBT bromides (**83** and **12**). stoichiometry = BTBT's bromide (**83** and **12**) 1 eq., 5-Hexyl-2-thiopheneboronic 1 eq, $\text{Pd}(\text{OAc})_2$ 0.04 eq, $\text{P}(\text{Cy})_3\text{HBF}_4$ 0.08 eq, K_2CO_3 0.6 eq, Pivalic acid 0.6 eq. Solvent = dimethylacetamide

Although the reaction yields are not high, these were the first examples of BTBT derivatives synthesized by direct arylation starting from BTBT, so we decided to try the synthesis of more complex [1]benzothieno[3,2-b][1]benzothiophene dimer heterocycle-linked derivatives under such conditions.

2.4.5 Synthesis of [1]benzothieno[3,2-b][1]benzothiophene dimer heterocycle-linked derivatives by direct arylation reaction

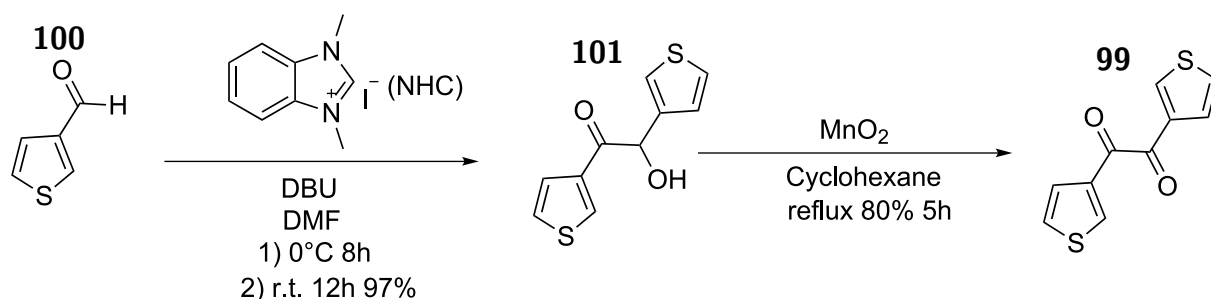
2.4.5.1 Synthesis of heterocycle-linker

We decided to synthesize more complex heteroaromatic linkers, other than simple thiophene rings. Among the emerging classes of electroactive conjugated materials, fused ring bithiophene derivatives, such as dithienothiophene oligomers, have attracted considerable attention for their semiconducting properties.^{127, 128} Fused ring derivatives of aromatic or heteroaromatic molecules (e.g. fluorene vs. biphenylene) lead to: more extended conjugation in the ground state, more planar molecular geometries and more rigid structures. These tend to increase the degree of conjugation, lower the HOMO–LUMO separation and enable closer intermolecular interactions. The rigid fused ring structure also lowers

2.4. DIRECT ARYLATION CROSS COUPLING FOR [1]BENZOTHIENO[3,2-B][1]BENZOTHIOPHENE DERIVATIVES

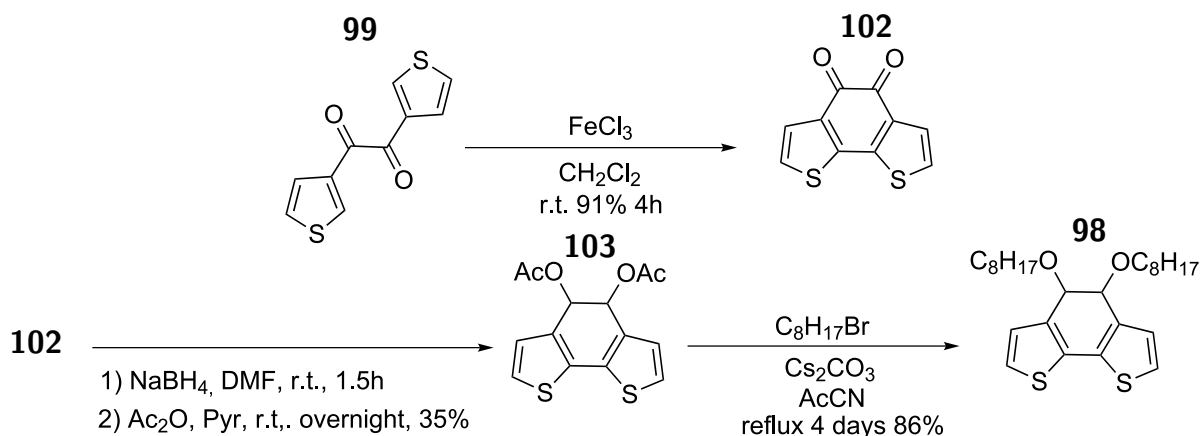
the reorganization energy, a factor that has been shown to strongly affect the rate of intermolecular hopping and hence the mobility of charges in organic semiconductors.¹²⁷ For these reasons, we decided to synthesize 4,4-bis(octyl)-cyclopentadithiophene (compounds **97**, see scheme 2.18) and 4,5-bis(octyloxy)benzo[1,2-b:6,5-b']dithiophene (compound **98**, see scheme 2.17) as linkers also designed in order to improve solubility in common organic solvents.

Compounds **97** and **98** were prepared following literature reported syntheses.^{129, 130} Compound **99** (see figure 2.16) is a common precursor for both bithiophene derivatives. Derivative **99** can be prepared in two steps, starting from a commercially available aldehyde **100**. The NHC-catalyzed benzoin condensation of **100** affords the alcohol **101** in excellent yield under very mild conditions. The latter can be converted to **99** by manganese(IV) oxide (MnO_2) promoted, heterogeneous phase oxidation in cyclohexane. Both steps are exceedingly simple and can be readily scaled up to hundreds of grams scale with minimum amount of organic solvents employed.



Scheme 2.16 Synthesis of compound **99** starting from commercial aldehyde **100**

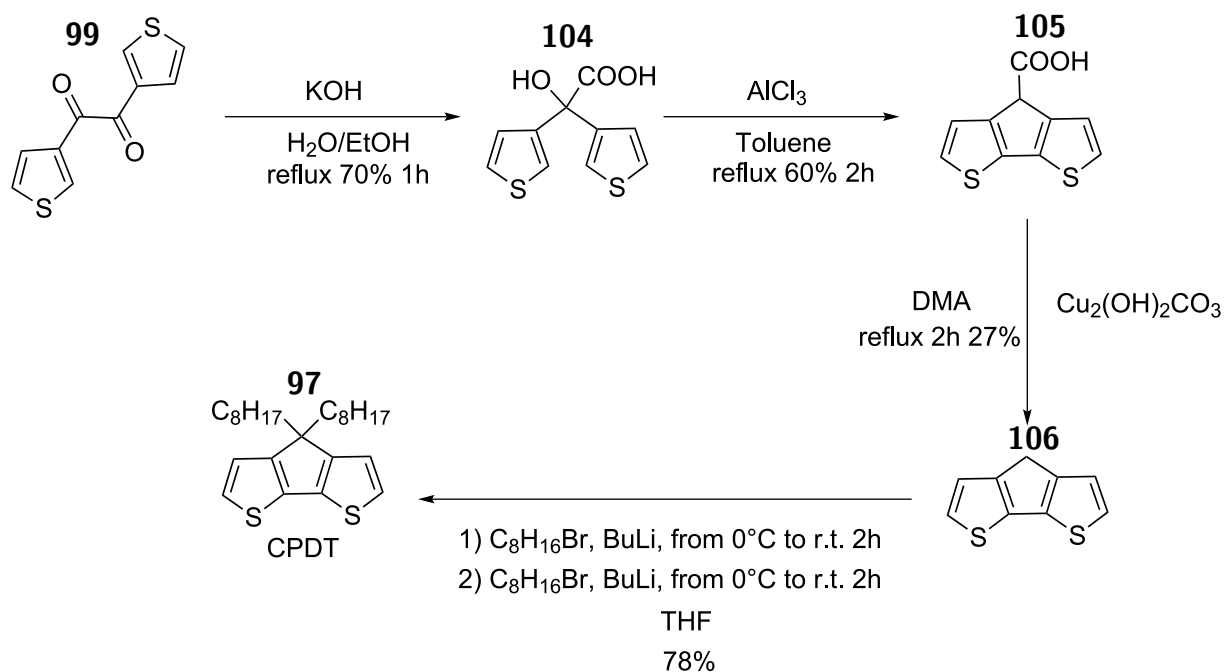
Cyclized product **102** (see scheme 2.17) was obtained under oxidative ring-closing conditions.¹³¹ In the last step, compound **98** is prepared by oxygen alkylation from the acylated intermediate **103**.¹²⁹



Scheme 2.17 Synthesis of compound **98** starting from the precursor **99**

Compound **97** was prepared with a 4 step synthesis starting from compound **99**. The first step is a transposition base catalyzed reaction to give compound **104**. Cyclized product **105** was obtained under oxidative ring-closing conditions. Copper-Catalyzed decarboxylation of carboxylic acids **105** gives cyclopentadithiophene **106**. In the last step,

compound **106** is alkylated with two subsequent nucleophilic substitutions on octyl bromide by lithium salt intermediates to afford product **97**.

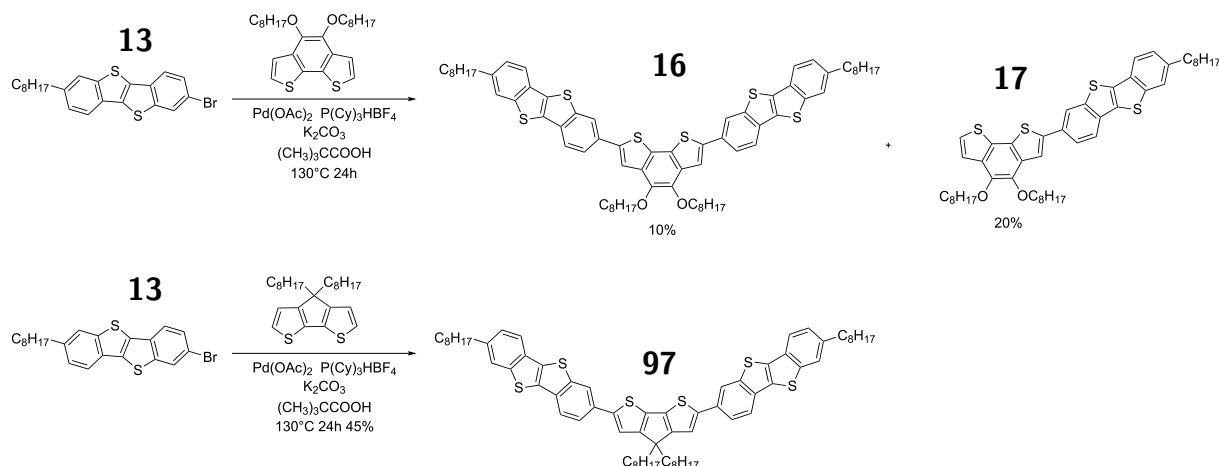


Scheme 2.18 Synthesis of compound **97** starting from the precursor **99**

2.4.5.2 Synthesis of [1]benzothieno[3,2-b][1]benzothiophene dimer heterocycle-linked derivatives

We reacted two equivalent of bromide **13** with 1 equivalent of the heterocycle-linker **98** in order to prepare the compound **16**. Direct arylation condition were the same tested in the synthesis of **14** and **15** : Pd(OAc)₂ (0.04eq), P(Cy)₃HBF₄ (0.08eq), (CH₃)₃CCOOH (0.60 eq) and K₂CO₃ (3.00 eq), in dimethylacetamide (DMA) at 130°C for 24h. Raw materials was a mixture of disubstituted compound **16** and monosubstituted **17** and other byproducts. The purification was not trivial cause instability of compound **16** when it is deposited on the silica, indeed only **17** was obtained in pure form. Compound **16** contains some impurity that could not be eliminated. Finally, two equivalent of bromide **13** was reacted with 1 equivalent of the heterocycle-linker **97**, better results were obtained when we reacted two equivalent of bromide **13** with 1 equivalent of the heterocycle-linker **97** in the same conditions, thanks to a greater stability of the compound **18**, it was possible to purify it by chromatography column and crystallization.

2.5. SYNTHESIS OF [1]BENZOTHIENO[3,2-B][1]BENZOTHIOPHENE WITH FUNCTIONLIZATED SIDE CHAIN DERIVATIVES

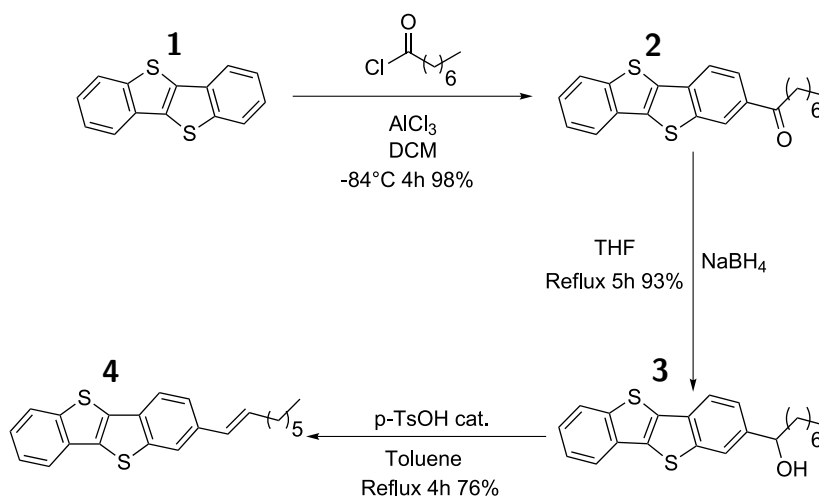


Scheme 2.19 Synthesis of compounds **16**, **17** and **18** by direct arylation starting from BTBT bromide **13**. stoichiometry = 2-octyl-7-bromo-[1]benzothieno[3,2-b][1]benzothiophene **13** 2 eq., heterocycle (**98** and **97**) 1 eq, Pd(OAc)₂ 0.04 eq, P(Cy)₃HBF₄ 0.08 eq, K₂CO₃ 0.6 eq, Pivalic acid 0.6 eq. Solvent = dimethylacetamide

2.5 Synthesis of [1]benzothieno[3,2-b][1]benzothiophene with functionlized side chain derivatives

2.5.1 Synthesis of [1]benzothieno[3,2-b][1]benzothiophene with doublebond-fuctionalized side chain derivatives

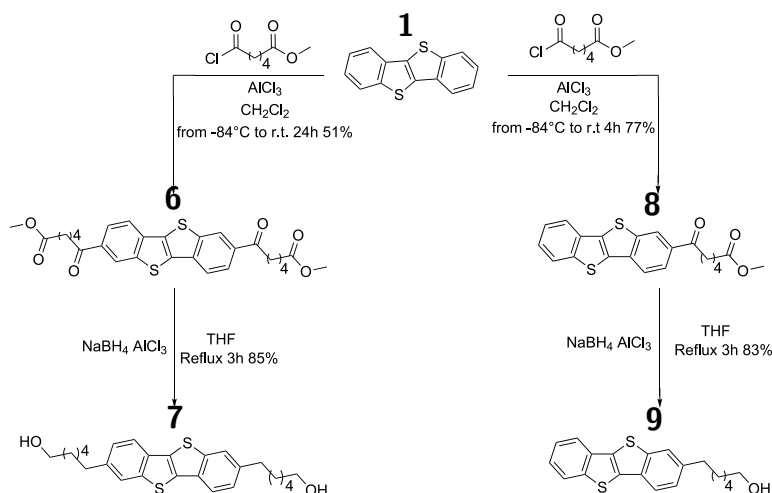
The first simple functionality that we inserted in a BTBT's sidechain was a double bond. The synthesis of alkene **4** start with a Friedel-Crafts acylation of BTBT with octanoyl chloride followed by reduction with sodium borohydride in THF to afford the alcohol **3** in high yield. The last step is a acid-catalyzed dehydration of the secondary alcohol **3** to afford alkene **4**.



Scheme 2.20 Synthesis of compound **4**

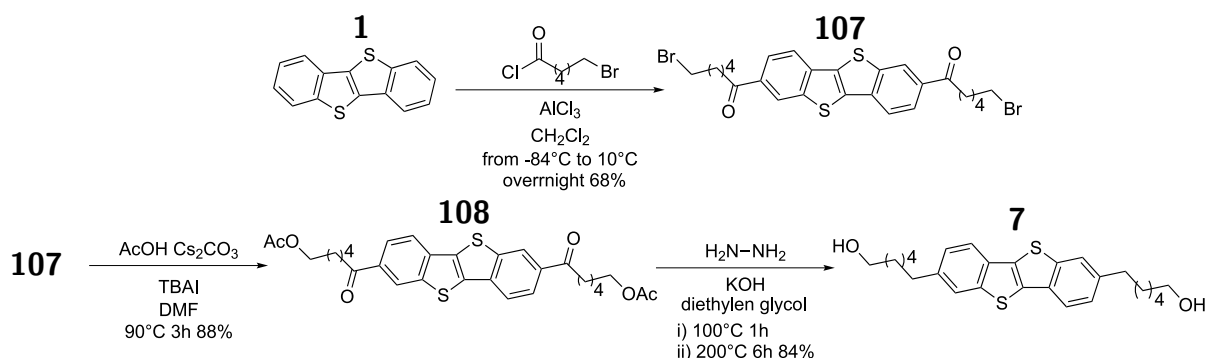
2.5.2 Synthesis of [1]benzothieno[3,2-b][1]benzothiophene with hydroxy-fuctionalized side chain derivatives

In order to tune the packing in the solid state of BTBT derivatives thanks to hydrogen bonds, we synthetized the alcohol **9** and the diol **7**. First steps from BTBT is mono and diacylation with methyl adipoyl chloride respectively to afford compounds **8** and **6**. The last steps are the reduction of the carbonyl groups to methylene groups and contemporaneously the reduction of methyl ester groups to hydroxy group with aluminium hydride to afford alcohols **9** and **7**.



Scheme 2.21 Synthesis of compounds **7** and **9**

The diol **7** have been reported recently.⁷⁹ The reported synthesis is different from ours and its shown in scheme 2.22. The first step is a double Friedel-Crafts acylation on BTBT, with 6-bromohexanoyl chloride to give compound **107**. The second step is nucleophilic substitution of bromo with acetate in order to form the C-O terminal bond. The last step is a reduction in Wolff-Kishner condition to afford the diol **7**. Our synthetic strategy is similar but the use of methyl adipoyl chloride insted of 6-bromohexanoyl allows us to skip a synthetic step: the introduction of the C-O terminal bond.



Scheme 2.22 Reported synthesis of compound **7**⁷⁹

Roche at al. proved that compound **7** is able to self-organize into a lamellar structure through ϑ - π stacking and van der Waals interactions but also through hydrogen bonding

2.5. SYNTHESIS OF [1]BENZOTHIENO[3,2-B][1]BENZOTHIOPHENE WITH FUNCTIONLIZATED SIDE CHAIN DERIVATIVES

interactions. The hydrogen-bonded network controls the interlamellar region in terms of organization and stability. According to thermogravimetric analysis (TGA) and Differential Scanning Calorimetry (DSC) measurements reported in the article, **7** is stable up to 333 °C with less than 5% of weight loss (figure 2.10). Interestingly, the weight loss reaches 100% slightly above 400 °C. This indicates that the compound sublimes easily before it degrades because no graphitization was observed and the crystal-liquid phase transition is around 180°C. The authors reported evaporated **7** based OFETs exhibited very good mobilities of $\mu_{sat} = 0.19 \pm 0.01 \text{ cm}^2\text{V}^{-1}\text{s}^{-1}$ under air, confirming that compound **7** have potential use as OFET chemical sensors device. Indeed these materials must show good carrier mobility and the possibility of differential interaction with analyte, and for this purpose the hydrogen bonding can be employed. The same paper reports also on the impossibility to obtain good film quality by solution deposition due to its high propensity to self-organize and to crystallize. The authors reported also a comparison of mobility values of OFET based on well know 2,7-dioctyl[1]benzothieno[3,2-b][1] benzothiophene (DiC8-BTBT). Diol **7** showed a hole mobility about one order of magnitude lower than DiC8-BTBT, the authors impute this difference to the two different supramolecular organizations of the materials in the thin films. Indeed thanks to crystal structure studies they show that the bi-dimensional character of the interaction network formed by the DiC8-BTBT while the intermolecular network formed by the diol **7** actually is more likely one-dimensional. We speculate that such an effect could be overcome, by the use of the more soluble and mono-functionalized asymmetric derivative **9**, our hypothesis will be verified or not in future device's characterization.

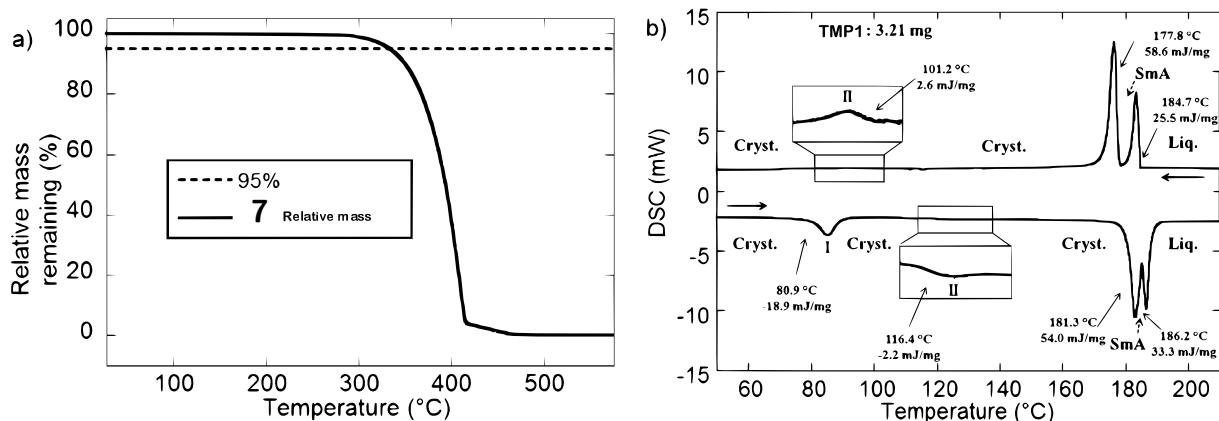


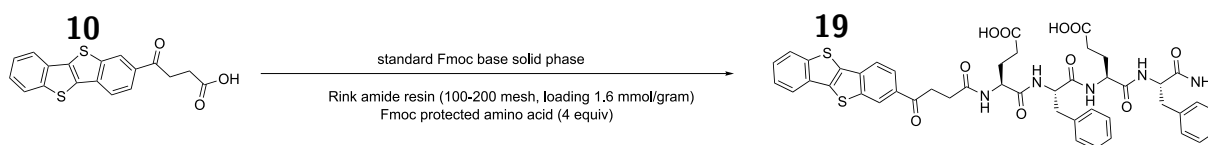
Figure 2.10 (a) compound **7** TGA. (b) compound **7** DSC profile of the first heating and cooling cycle (heating rate: 10 K/min). Four events are observables: three phase transitions at 80.9 °C, 116.4 °C, 181.3 °C (smectic A phase), and 186.2 °C isotropization (onset determination). Reprinted with permission from ref⁷⁹ Copyright American Chemical Society

2.5.3 Synthesis of [1]benzothieno[3,2-b][1]benzothiophene-peptide-based supramolecular nanostructures

Peptide-based supramolecular nanostructures are particularly of great interest due to their biocompatibility, biofunctionality, stimuli responsiveness, and rich functionality.^{132, 133} As a result of structural versatility and facile synthesis, numerous peptide-based supramolecular nanostructures with various chemical compositions have previously been developed and extensively studied for tissue engineering, drug delivery, sensing, catalysis, optoelectronic and biomedical applications.^{133–135} Recently, there is also a growing research interest to

employ semiconductor-peptide-based self-assembly process in the bottom-up fabrication of supramolecularly nanostructured (opto)electronic materials.^{133, 135} In a typical approach a π -conjugated organic semiconductor small molecule is covalently attached to a short self-assembling peptide sequence, and these peptidic organic π -structure amphiphiles self-assemble into well-defined 1D nanostructures under aqueous conditions. This type of electroactive nanostructures formed in aqueous media hold great promise in a variety of applications in (opto)electronics, organic chromophore arrays and bioelectronics.^{136, 137} Several are the examples of π -conjugated systems such as oligothiophene, naphthalenediimide, pyrene, phenylenevinylene oligomers and very recently was reported the first example on BTBT derivatives.^{77, 136, 138, 139} In collaboration with Professor Miriam Mba Blázquez of the University of Padova, we develop a second example of BTBT π -core one-dimensional (1D) nanowire that is self-assembled in aqueous media for potential use in bioelectronics and sensors.

The BTBT-peptide conjugate **19** was synthesized using standard Fmoc base solid phase peptide synthesis protocols (Scheme 2.23). We selected the tetrapeptide glutamic acid-phenylalanine-glutamic acid-phenylalanine (in amino acid's one letter code: EFEF), containing alternating polar and apolar residues, because low molecular weight gelators (LMWG) containing this sequence have been shown to form pH tunable supramolecular hydrogels rich in β -sheet structures. We predicted that compound **19** would be soluble in water at basic pH due to the electrostatic repulsions between the negatively charged glutamic acids. Decreasing the pH, protonation of the glutamic acids should allow the self-assembly of **19**. As expected, **19** was insoluble in milliQ water (pH 5) at room temperature. We found that addition of small amounts of NaOH 1M lead to homogeneous solutions of **19**, which after addition of HCl 1M became a gels. Experimentally, we found that excess of NaOH 1M was also able to trigger gel formation. Thus, self-assembly of the negatively charged **19** also occurred when the ionic strength of the solution was enough to screen the negative charges. The study on the effect of the cation is ongoing. Different salts were added to a solution of **19** in water at basic pH. MgCl₂, CaCl₂, Li(OH), K(OH), NH₄Cl. The gelation ability of **19** in organic solvents was also tested. In these studies, a stock solution of **1** in DMSO (70 mg/mL) was prepared. Then a known amount of the stock solution was added to a vial containing 1 mL of the appropriate solvent. Results are reported in Table 2.1 formed transparent gels in chloroform and opaque gels in acetonitrile at concentrations as low as 0.3 wt%. Weak gels formed also in ethyl acetate (AcOEt) and toluene.



Scheme 2.23 Fmoc base solid phase peptide synthesis of compound **19**

2.5. SYNTHESIS OF [1]BENZOTHIENO[3,2-B][1]BENZOTHIOPHENE WITH FUNCTIONLIZED SIDE CHAIN DERIVATIVES

Entry	solvent	Result ^a	mgc ^b (wt%)	notes
1	Et ₂ O	I	–	
2	MeOH	I	–	
3	THF	S	–	
4	CH ₃ CN	G	0.3	opaque
5	CHCl ₃	G	0.3	transparent
6	Toluene	WG	–	
7	AcOEt	WG	–	

Table 2.1 Gelation ability of **19** in organic solvents. a) I = insoluble, S = solution, G = gel. b) minimum gelator concentration (mgc)

Morphologies of the hydrogels were studied by Transmission electron microscopy (TEM). Samples were not diluted, but gels were directly deposited on the carbon grid and no staining was used. Hydrogels obtained at acidic pH at 0.1 wt% concentration (Figures 2.11 A, B) showed the formation of helical fibrils several microns long with diameters ranging from 5 to x nm, whereas at 0.5 wt % concentration the formation of structures with a high aspect ratio was observed (Figures 2.11 C, D).

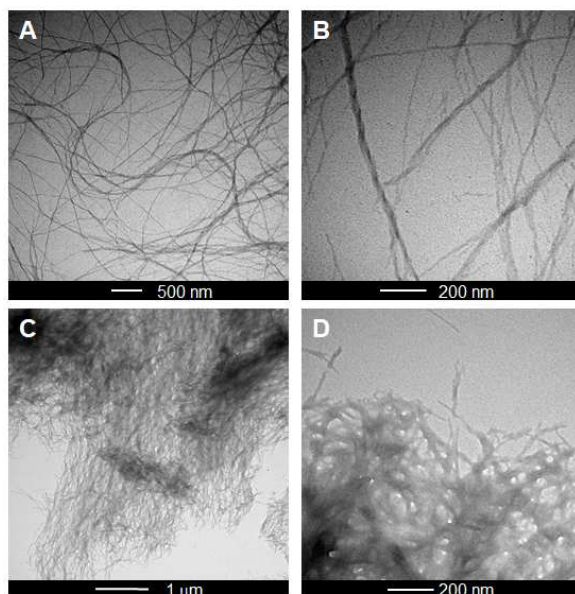


Figure 2.11 TEM images of hydrogels formed by **19** by addition of HCl at 0.1 (A, B) and 0.5 wt% (C, D).

TEM images of the hydrogels of anionic **19** at high salt concentration (NaOH) shows also the formation of fibrils up to 10 μm long at 0.1 wt% concentration (Figure 2.12 A), with an average diameter of 5 nm, corresponding to the length of the extended conformation of **19**. At 0.5 wt% concentration fibrils are found to run parallel for several microns, they seem to be in close proximity but not fused (Figures 2.12 B, C).

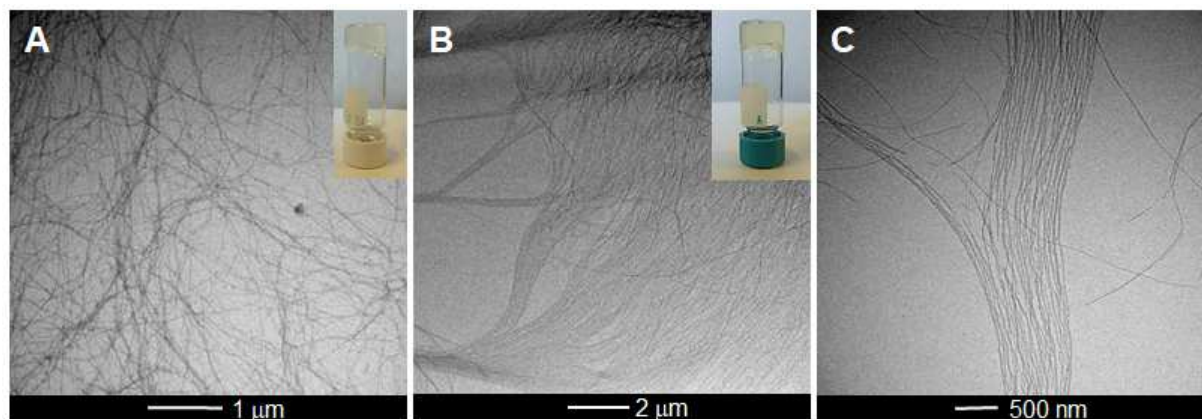


Figure 2.12 TEM images of hydrogels formed by **19** at high NaOH content at concentrations 0.1 (A) and 0.5 wt% (B, C). The inserts show photographs of the corresponding hydrogels

UV-Vis spectra of the hydrogels (Figure 2) show a small hypsochromic shift of the main absorption band from 326 nm in the solution to 323 nm in the weak gels obtained by addition of both HCl or NaOH at 0.1 wt% concentration. At 0.5 wt% concentration the absorption profiles observed for the salt- and pH triggered gels show significant differences. For the NaOH triggered gel the main absorption band shifts to 321 nm, while new shoulders appear at 339, 357 and 372 nm. On the other side, the HCl triggered gel showed a very broad absorption band ranging from 290 nm to 500 nm. Emission spectra of the 0.1 wt% solution at basic pH show a maxima at 503 nm while it is blue-shifted for both the pH- and the salt (NaOH)-triggered hydrogels to 465 nm (figure 2.13). We are currently exploring the transport properties of such structures.

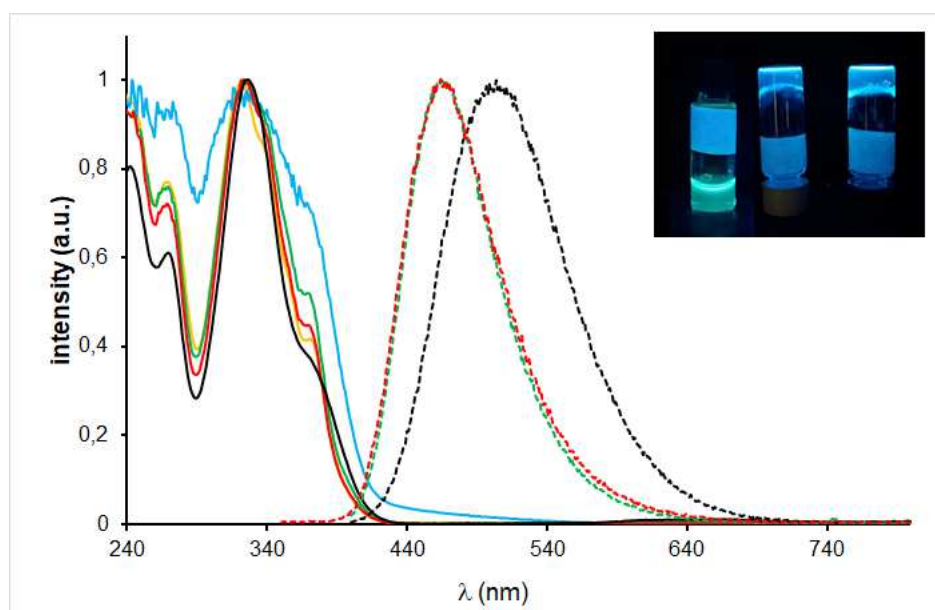


Figure 2.13 Absorption (solid lines) and emission (dotted lines) spectra of a 0.1 wt% water solution of **19**(black), hydrogels at 0.1 wt% in HCl sol. (green) and NaOH sol. (red), and 0.5 wt% hydrogels in HCl sol. (blue) and NaOH sol. (yellow). Insert: From left to right the photograph shows under UV irradiation a solution of **19**, hydrogel at 0.5 wt% in HCl sol. and hydrogel at 0.5 wt% in NaOH sol.

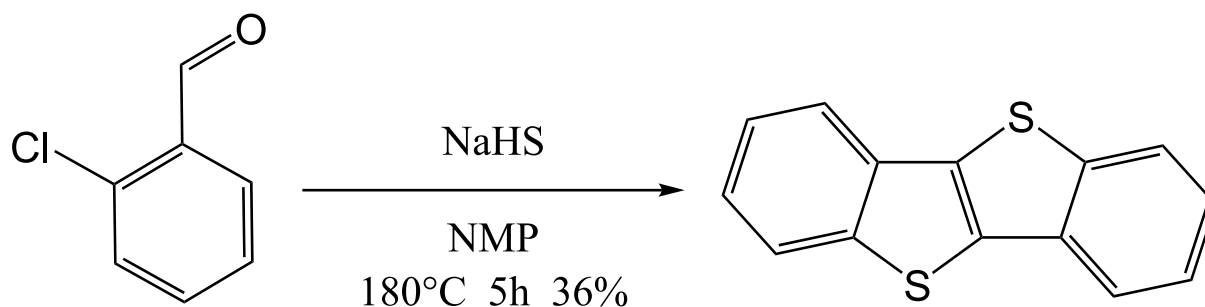
2.6 Conclusion

In order to synthesize extended conjugated BTBT derivatives, we tried different synthetic approach. In the first approaches we tried to react BTBT or 2-octyl-[1]benzothieno[3,2-b][1]benzothiophene by Friedel-Crafts acylation reaction with dicarboxylic acid chloride, in particular with succinic acid dichloride and malonic acid dichloride with the purpose of obtaining key intermediates that they would have allowed us to get different extended conjugated BTBT derivatives starting from the same intermediates. Unfortunately, it was not possible isolate a product. Neither crude product's NMR analysis or GC-MS analysis allow us to identify the structures obtained, we suspect that we obtained a mixture of non-separable compounds due to inter and intramolecular electrophilic attacks. If one of the dicarboxylic acids remain unactivated like acid or ester the isolation of the acylation product is possible as verified by the reaction of BTBT with succinic anhydride in order to obtain γ -keto-carboxylic acid (**10**) and recently Khalily and coworkers⁷⁷ reported the acylation of BTBT with methyl succinyl chloride. The subsequent activation of the carboxylic acid group of the compound **10** in acyl chloride was not possible but we have preliminary data that after its esterification, the γ -diketones portion can be cyclized to thiophene by Pall-Knorr reaction and potentially allow the synthesis of a series of 2-thienyl-[1]benzothieno[3,2-b][1]benzothiophene with ether side chain of different length starting from the same intermediate. We tried aromatic electrophilic substitution on BTBT, different from the well documented Friedel-Crafts acylation, we tried aromatic formylation reactions: Vilsmeier-Haak and Rieche formylations. In Vilsmeier-Haak reaction condition was not observed the formation of formylated BTBT derivatives, probably due to the weakness of the generated electrophile instead in Rieche reaction condition the conversion was complete but the low regioselectivity of the electrophile's attack led to a mixture of 4 formylated regioisomers that could not be separated and purified. We have verified that also in the bromination reaction of the BTBT the regioselection is low, in fact despite the reaction conversions are complete the formation of the regioisomers leads to moderate yields, also in this case the use of weak brominating agents like NBS does not lead to product formation. We therefore decided to change our synthetic approach and test the BTBT and BTBT's bromide reactivity in direct arylation cross coupling reaction. The direct arylation on BTBT scaffold it turned out not to be an efficient synthetic way indeed were observed low reaction's conversion and the formation of different regioisomers. When we reacted BTBT's bromides in direct arylation condition with several heterocycles: 2-hexylthiophene, 4,5-bis(octyloxy)benzo[1,2-b:6,5-b']dithiophene and 4,4-bis(octyl)cyclopentadithiophene we could isolate the corresponding products: compounds **14** and **15** for 2-hexylthiophene, compound **17** for 4,5-bis(octyloxy)benzo[1,2-b:6,5-b']dithiophene and compound **18** for 4,4-bis(octyl)cyclopentadithiophene. The reasons for the low/moderate conversion yields are different: from troublesome purification caused by the incomplete diarylation and the low stability of the products and probably an optimization of the reaction conditions would lead to an increase in them. Nevertheless, these are the first examples of post functionalization of BTBT by direct arylation. Exploiting also the previous results we have developed the synthesis of several promising [1]benzothieno[3,2-b][1]benzothiophene with functionalized side chain derivatives, indeed starting with the mono- or di-acylation of BTBT with methyl adipoyl chloride is it possible to obtain the terminal alcohols compounds **9** and **7** after reduction with aluminium hydride of the acylated intermediates (**8** and **6**). Starting from γ -keto-carboxylic acid (**10**) is possible obtain BTBT-peptide

conjugate **19** by standard Fmoc base solid phase peptide synthesis protocols. BTBT π -core one-dimensional (1D) nanowires that are self-assembled in aqueous media for potential use in bioelectronics and tissue engineering are obtained by self-assembling of **19** in water solution in different pH and ionic strength range. In particular the TEM images of supramolecular structures obtained in high NaOH concentration water solution of **19** at 0.5 wt% are very interesting, indeed are fibrils with an average diameter of 5 nm up to 10 μm long that run parallel for several microns, this behavior could lead to particular anisotropic OFET conduction characteristics.

2.7 Experimental part

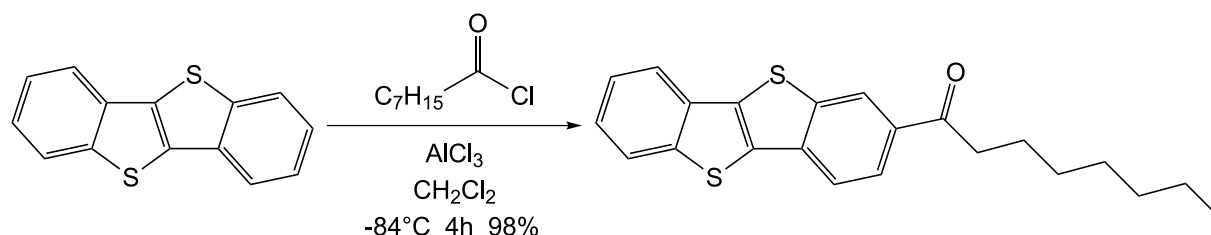
2.7.1 Synthesis of [1]benzothieno[3,2-b][1]benzothiophene (1)



Sodium hydrosulfide hydrate (267.0g, 3.56 mol) was added to a solution of o-chlorobenzaldehyde (250.0 g, 1.78 mol) in NMP (500 mL) at 80 °C and stirred for 1 h. Then, mixture was heated to 180 °C and stirred for 5 h at the same temperature. The resulting mixture was cooled with an ice-bath and the resulting precipitate was collected by filtration and washed with methanol and water. Pure [1]benzothieno[3,2-b][1]benzothiophene was obtained as a white crystallin solid (77.00 g, 0.3204 mol, 36% yield).

$^1\text{H NMR}$ (500.13 MHz, CDCl_3) 7.93 (d, 2H, $J=7.90$ Hz), 7.89 (d, 2H, $J=8.10$ Hz), 7.47 (dd, 2H, $J_1=7.63$ Hz $J_2=7.33$ Hz), 7.41 (dd, 2H, $J_1=7.95$ Hz $J_2=7.29$ Hz); $^{13}\text{CNMR}$ (125.70 MHz, CDCl_3) 143.13, 134.31, 133.98, 125.88, 125.76, 124.92 (d, $J=10.41$ Hz), 122.99 (d, $J=10.60$ Hz);

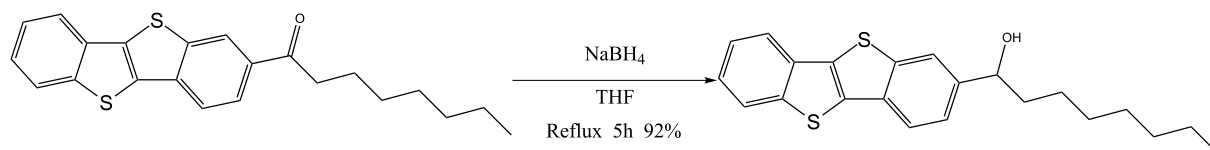
2.7.2 Synthesis of [1]benzothieno[3,2-b][1]benzothiophene-2-octan-1-one (2)



[1]Benzothieno[3,2- b][1]benzothiophene (4.000 g, 16.64 mmol) was dissolved in dry dichloromethane (200 mL), under nitrogen, followed by the addition of aluminum chloride (5.55 g, 41.6 mmol) at - 10 °C. The solution was cooled to -84 °C and octyl acid chloride (3.04 ml, 18.31 mmol) was added dropwise, and the mixture was stirred for 1h at the same temperature. The reaction mixture was allowed to stand without cooling and stirred for 3 h at rt. The reaction mixture was cooled to 0 °C, quenched with ice water (10 mL), and diluted with methanol to give a precipitate. The precipitate was filtered and washed with water (2 x 50 mL) and methanol (2 x 50 mL), then dried in vacuo to give [1]benzothieno[3,2- b][1]benzothiophene -2- octan -1- one (6.031 g, 16.37 mmol, 98 % yield) as white solid.

¹H NMR (400 MHz, CDCl₃) δ 8.56 (d, J = 0.8 Hz, 1H), 8.06 (dd, J = 8.3, 1.4 Hz, 1H), 7.99 - 7.87 (m, 3H), 7.49 (pd, J = 7.1, 1.2 Hz, 2H), 3.08 (t, J = 7.4 Hz, 2H), 1.88 - 1.76 (q, J = 7.4 Hz, 2H), 1.51 - 1.26 (m, 8H), 0.93 (t, J = 6.8 Hz, 3H). ¹³C NMR (101 MHz, CDCl₃) δ 199.60, 142.81, 142.24, 136.93, 136.24, 133.63, 132.98, 132.77, 125.84, 125.14, 124.71, 124.53, 124.16, 122.07, 121.37, 38.83, 31.76, 29.41, 29.21, 24.56, 22.67, 14.13.

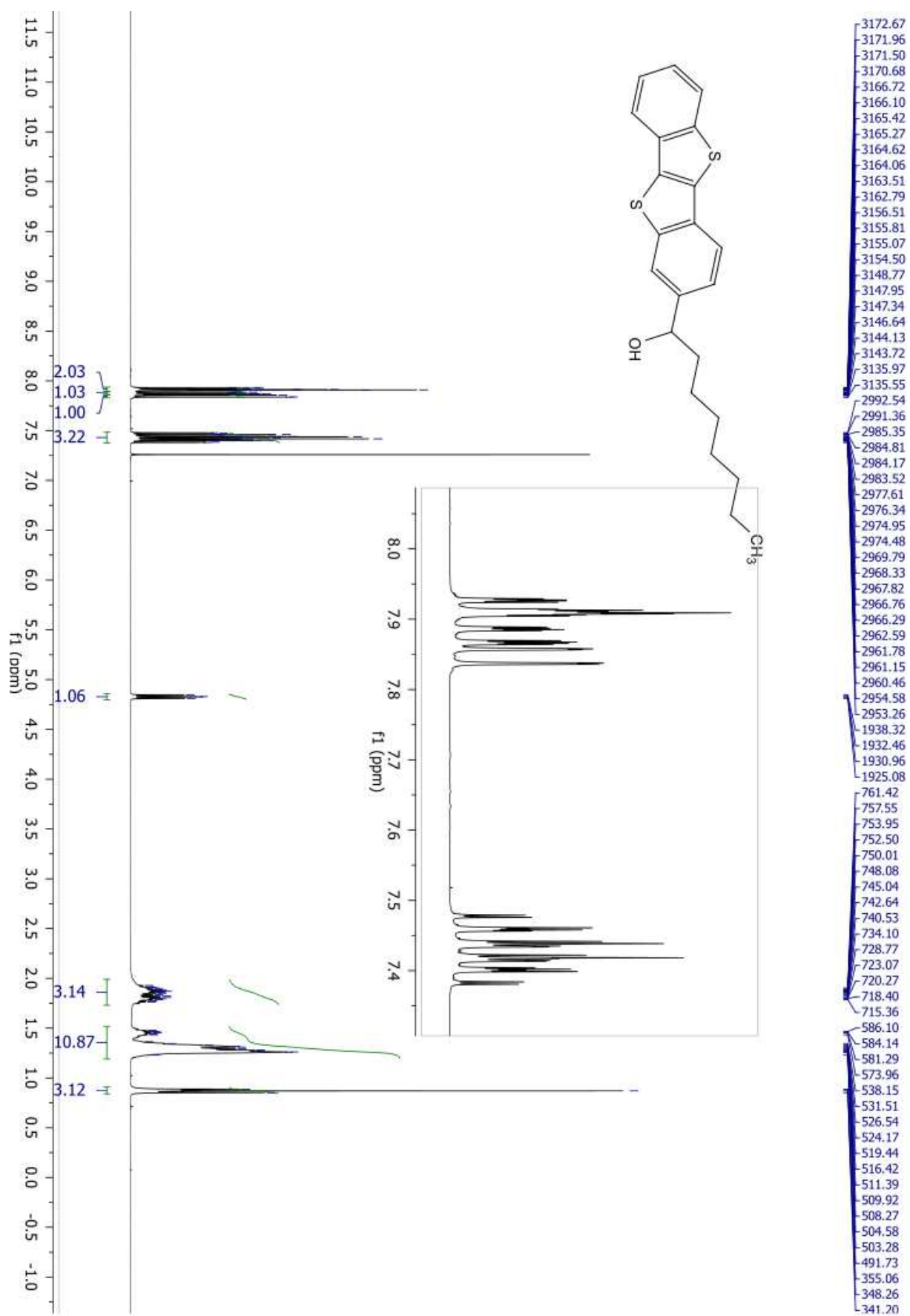
2.7.3 Synthesis of [1]benzothieno[3,2-b][1]benzothiophene-2-octan-1-hydroxy (3)



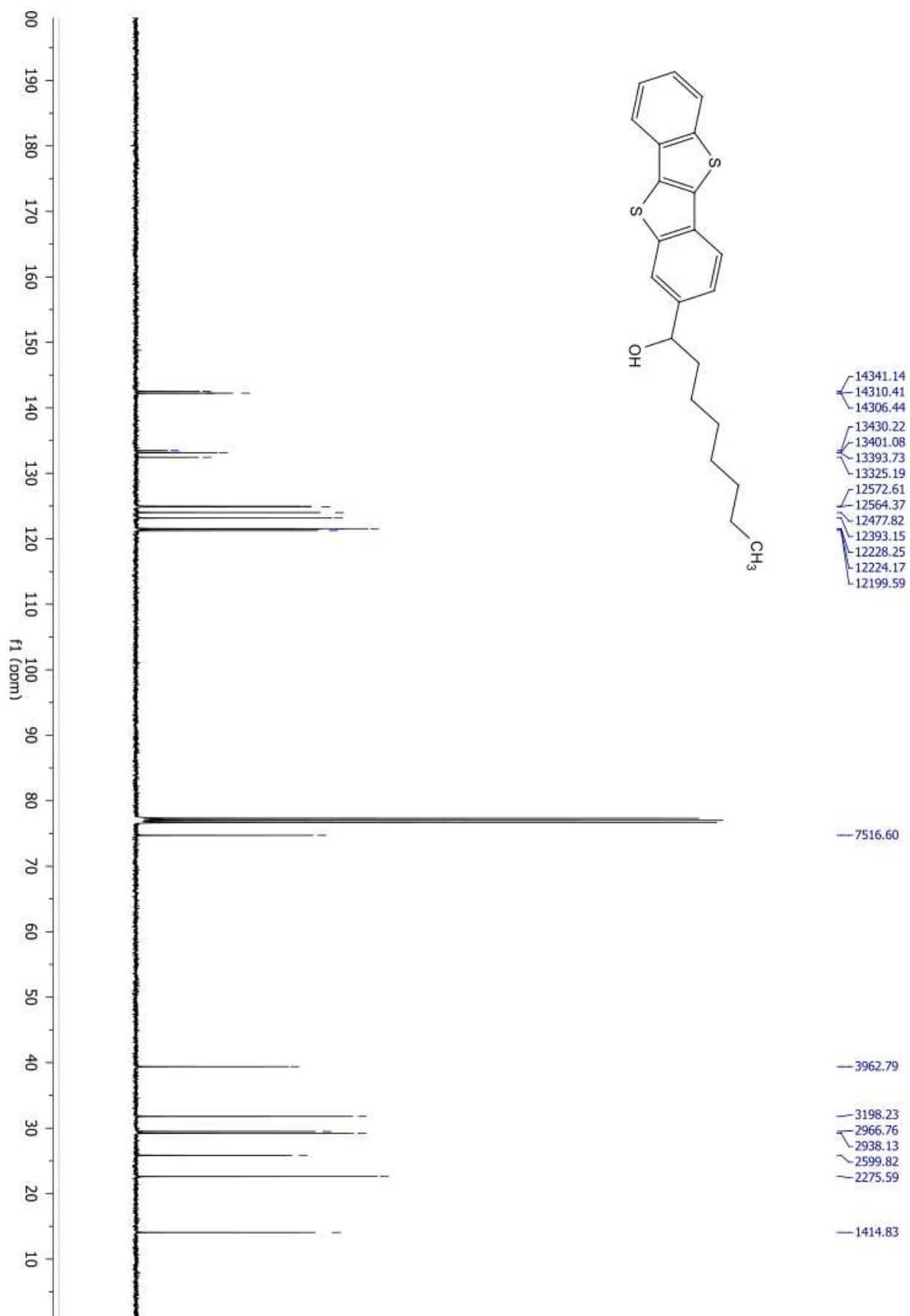
[1]Benzothieno[3,2-b][1]benzothiophene-2-octan-1-one (1.658 g, 4.523 mmol) was dissolved in dry tetrahydrofuran (100 mL), under nitrogen, followed by the addition of sodium borohydride (2.453 g, 65.36 mmol) at room temperature. The solution was stirred for 11 h at reflux. The reaction was cooled to 0°C, quenched with ice water (50 mL), the resulting white precipitate was filtered and washed with water (2 x 50 mL) and methanol (2 x 50 mL), then dried in vacuo to give [1]benzothieno[3,2-b][1]benzothiophene-2-octan-1-ol (1.583 g, 4.295 mmol, 95% yield) as white solid. The product was used without further purification for the next synthetic step, but it is possible to obtain pure with purification in toluene.

¹H NMR (400 MHz, CDCl₃) δ 7.94 – 7.90 (m, 2H), 7.88 (ddd, J = 7.9, 1.4, 0.7 Hz, 1H), 7.85 (dd, J = 8.2, 0.4 Hz, 1H), 7.48 – 7.38 (m, 3H), 4.83 (dd, J = 7.4, 5.9 Hz, 1H), 1.99 – 1.73 (m, 3H), 1.52 – 1.19 (m, 10H), 0.91 – 0.84 (m, 3H). ¹³C NMR (101 MHz, CDCl₃) δ 142.54, 142.23, 142.19, 133.48, 133.19, 133.12, 132.44, 124.96, 124.88, 124.02, 123.18, 121.54, 121.50, 121.25, 74.71, 39.39, 31.79, 29.49, 29.20, 25.84, 22.62, 14.06.

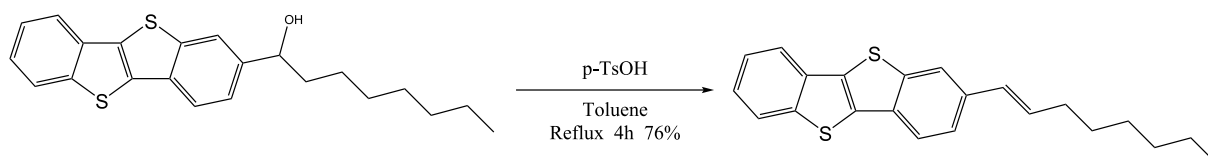
2.7. EXPERIMENTAL PART



CHAPTER 2. THE CHEMISTRY OF BTBT DERIVATIVES: CHALLENGES AND NEW DERIVATIVES



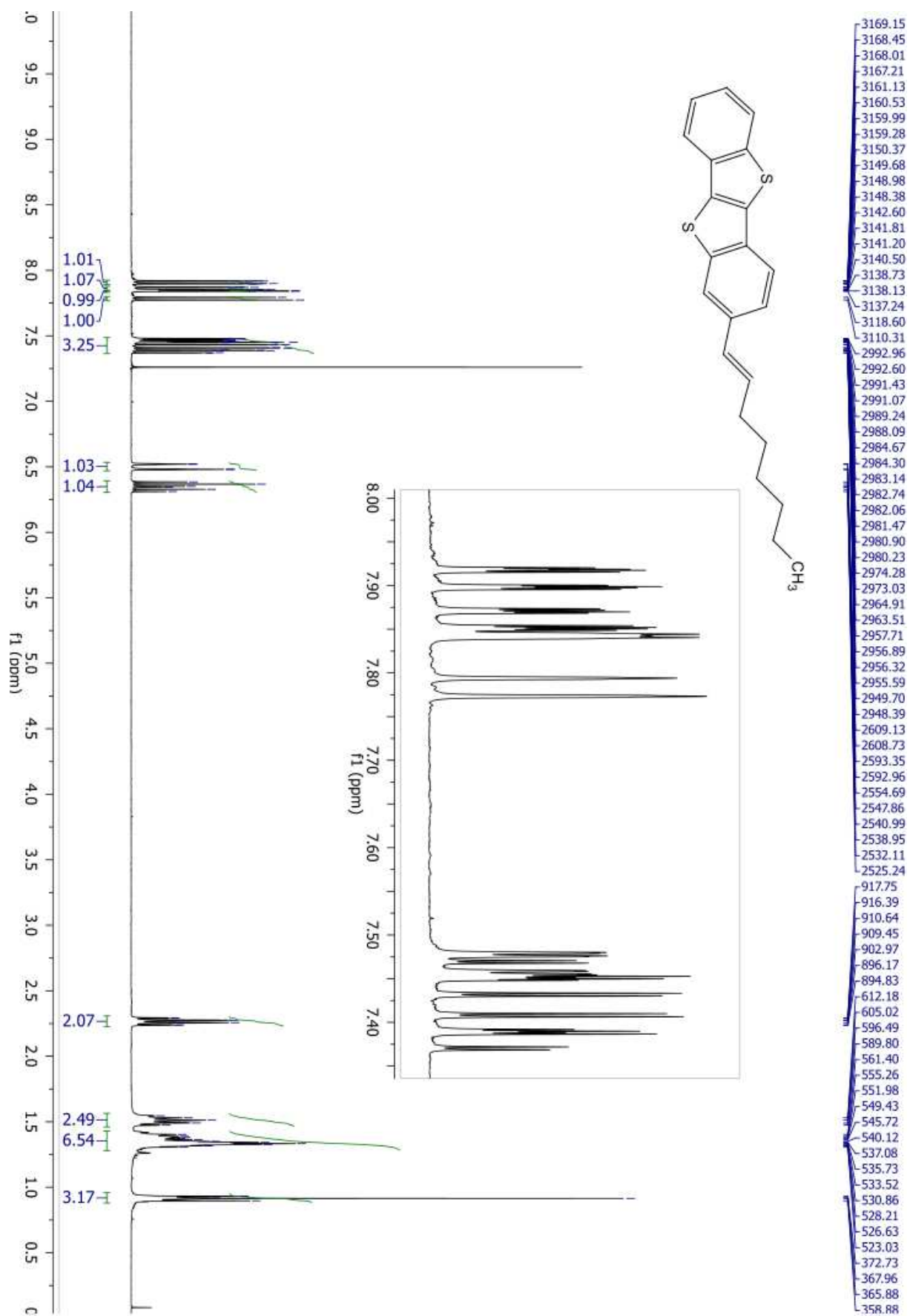
2.7.4 Synthesis of (E)-2-(oct-1-en-1-yl)benzo[b]benzo[4,5]thieno[2,3-d]thiophene (4)



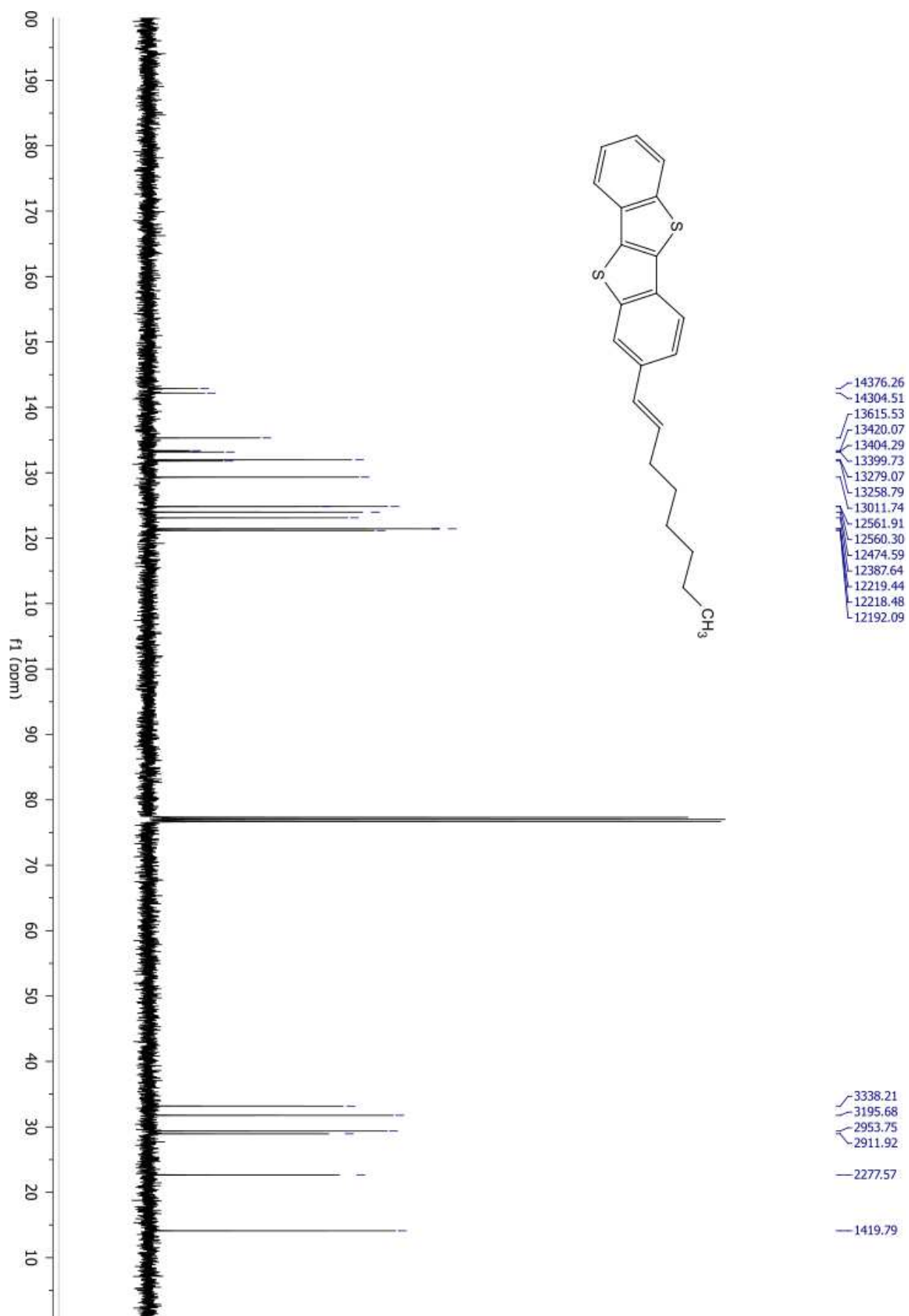
[1]Benzothieno[3,2-b][1]benzothiophene-2-octan-1-hydroxy (3.140g, 8.520 mmol) and p-toluenesulfonic acid monohydrate (0.210g, 1.11 mmol) were dissolved in toluene (175 mL). The reaction was stirred at reflux for 4h. The reaction was cooled to room temperature. Toluene was evaporated at reduce pressure to obtain a yellow solid. Crude product was dissolved in dichloromethane (200 mL) and washed with a saturated solution of sodium bicarbonate (4 x 20 mL) and brine (1 x 20 mL). The organic fraction was dried over magnesium sulfate. dichloromethane was evaporated at reduced pressure. Crude product was dispersed in methanol and filtered, washed with water and methanol. product was dried overnight at 60°C overnight, to obtain (E)-2-(oct-1-en-1-yl)benzo[b]benzo[4,5]thieno[2,3-d]thiophene as yellow solid (2.260 g , 6.457 mmol, 76% yield).

¹H NMR (400 MHz, CDCl₃) δ 7.91 (ddd, J = 7.9, 1.2, 0.7 Hz, 1H), 7.86 (ddd, J = 7.9, 1.3, 0.7 Hz, 1H), 7.85 – 7.83 (m, 1H), 7.78 (d, J = 8.3 Hz, 1H), 7.49 – 7.36 (m, 3H), 6.53 – 6.47 (m, 1H), 6.35 (dt, J = 15.8, 6.9 Hz, 1H), 2.31 – 2.23 (m, 2H), 1.56 – 1.46 (m, 2H), 1.43 – 1.28 (m, 6H), 0.96 – 0.88 (m, 3H). ¹³C NMR (101 MHz, CDCl₃) δ 142.89, 142.17, 135.33, 133.38, 133.23, 133.18, 131.98, 131.78, 129.32, 124.85, 124.84, 123.99, 123.12, 121.45, 121.44, 121.18, 33.18, 31.76, 29.36, 28.94, 22.64, 14.11.

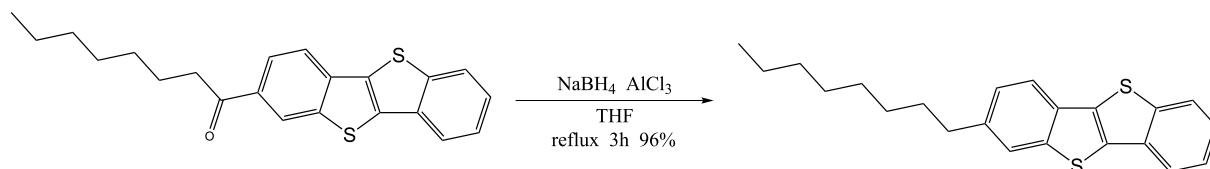
CHAPTER 2. THE CHEMISTRY OF BTBT DERIVATIVES: CHALLENGES AND NEW DERIVATIVES



2.7. EXPERIMENTAL PART



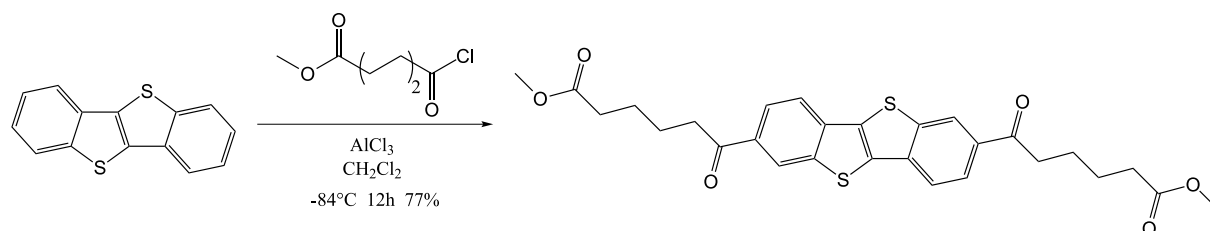
2.7.5 Synthesis of 2-octyl-[1]benzothieno[3,2-b][1]benzothiophene (5)



To a solution of [1]benzothieno[3,2-b][1]benzothiophene-2-octan-1-one (7.005 g, 19.11 mmol) in tetrahydrofuran (160 mL), was added of aluminium chloride (12.756 g, 95.67 mmol) at -10°C . The reaction mixture was stirred for 10 minutes at the same temperature and after sodium borohydride was added stepwise (7.400 g, 195.61 mmol). The reaction mixture was stirred 20 minutes at the same temperature and then for 4h at reflux. The reaction was cooled down to 0°C and a mixture of methanol and ice was added stepwise very slowly in order to obtain a precipitate. The white precipitate was filtered and disperse in dichloromethane (200 mL) and aqueous sodium hydroxide solution (15% w/w , 100 mL) was added dropwise and the mixture was stirred until the form of two liquid phase. The organic phase was washed with aqueous sodium hydroxide solution (3 x 50 mL), brine (50 mL) and dried over magnesium sulfate. The magnesium sulfate was removed by filtration over celite. Dichloromethane was evaporated at reduced pressure. The product was crystallized and washed with toluene to afford 2-octyl-[1]benzothieno[3,2-b][1]benzothiophene was obtained as yellow solid (7.915g , 18,35 mmol, 96% yield).

$^1\text{H NMR}$ (500 MHz, CDCl_3) δ 7.91 (d, $J = 7.9$ Hz, 1H), 7.87 (d, $J = 7.8$ Hz, 1H), 7.79 (d, $J = 8.1$ Hz, 1H), 7.72 (s, 1H), 7.48 – 7.42 (m, 1H), 7.42 – 7.36 (m, 1H), 7.28 (dd, $J = 8.1, 1.3$ Hz, 1H), 2.81 – 2.73 (m, 2H), 1.75 – 1.66 (m, 2H), 1.32 (ddd, $J = 13.9, 10.2, 4.4$ Hz, 11H), 0.89 (t, $J = 6.9$ Hz, 3H).

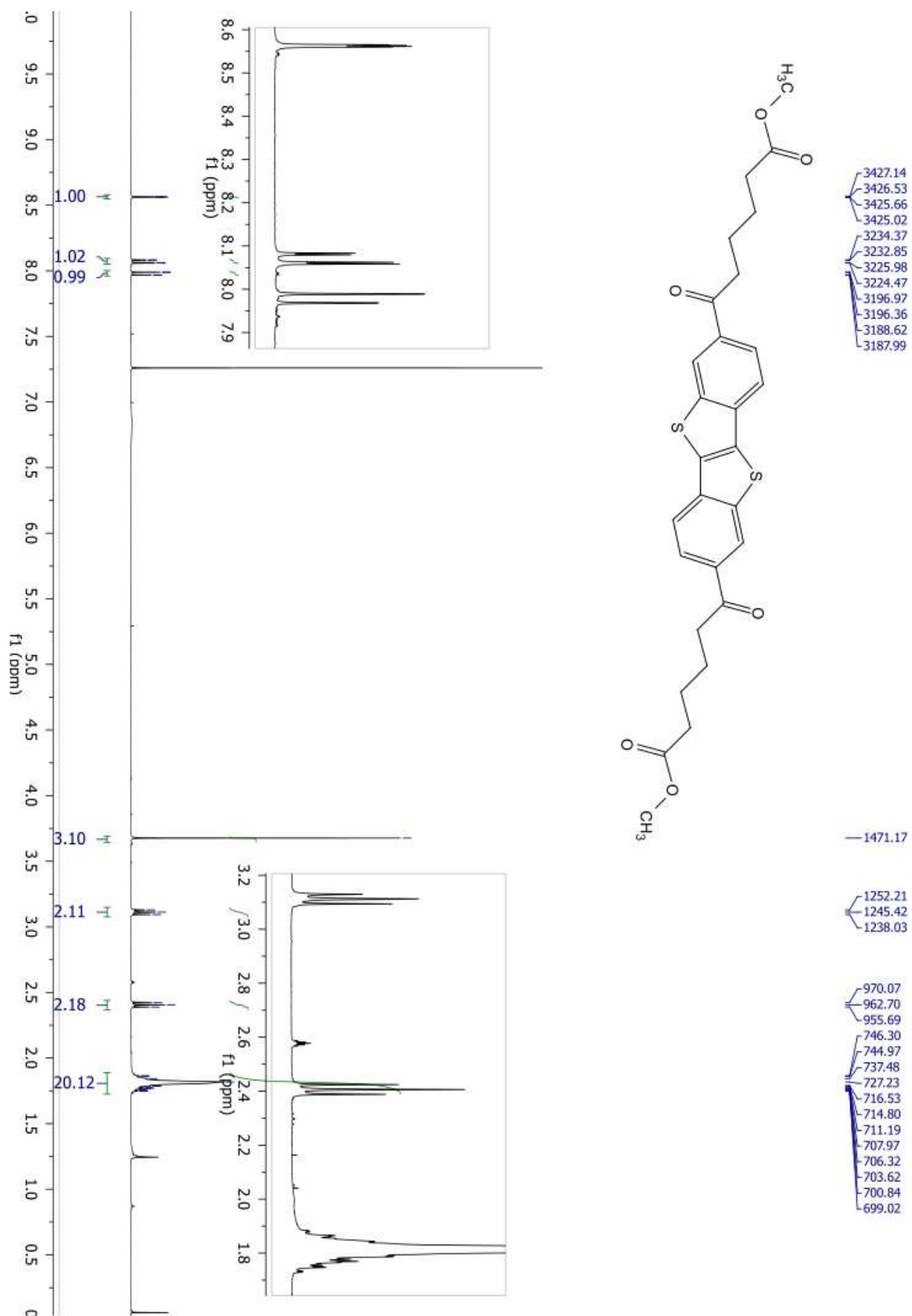
2.7.6 Synthesis of dimethyl 6,6'-([1]benzothieno[3,2-b]-[1]benzothiophene-2,7-diyl)bis(6-oxohexanoate) (6)



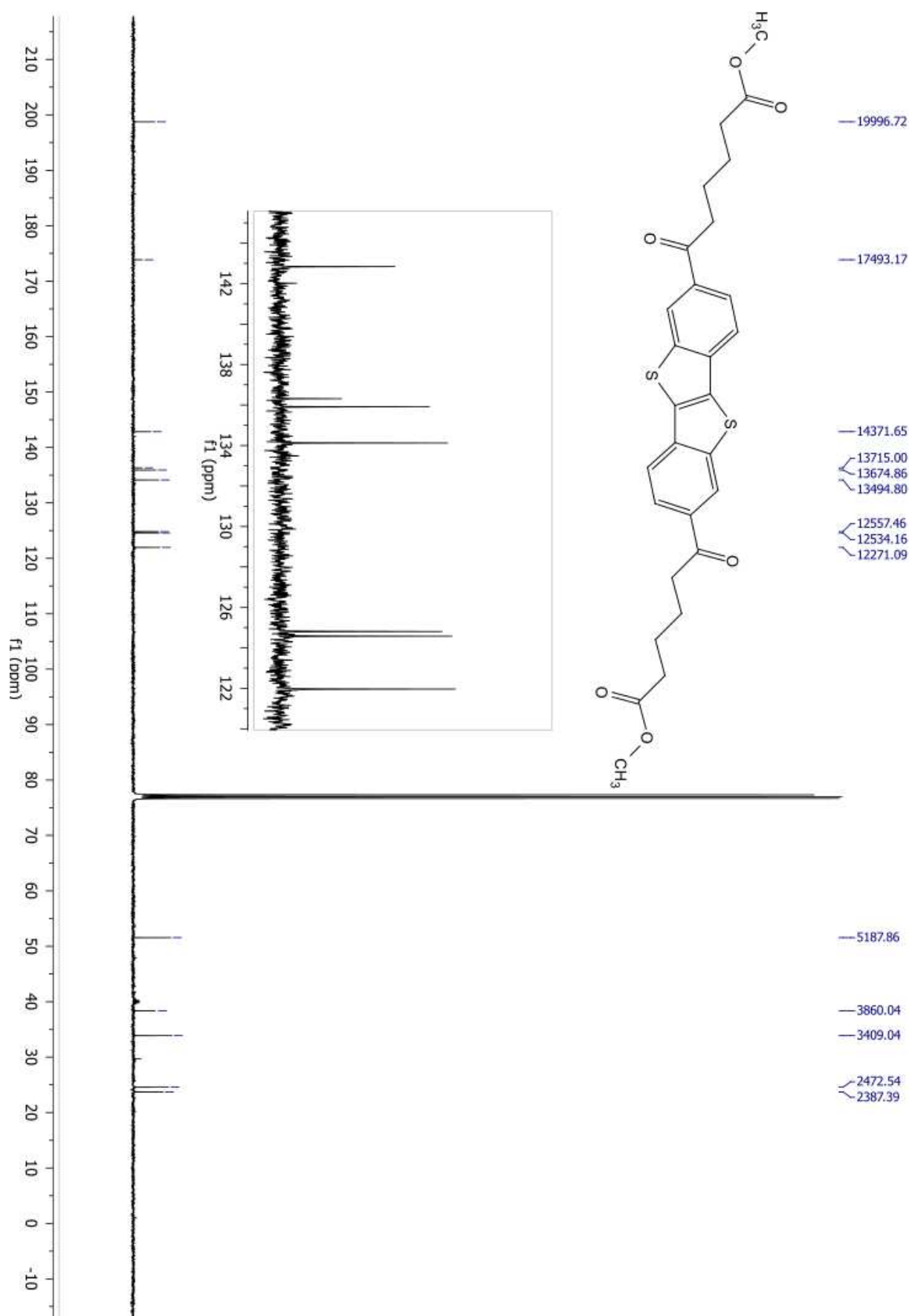
[1]Benzothieno[3,2- b][1]benzothiophene (1.903 g, 7.918 mmol) was dissolved in dry dichloromethane (200 mL), under nitrogen, followed by the addition of aluminum chloride (6.450 g, 48.37 mmol) at - 10 °C. The solution was cooled to -84 °C and methyl adipoylchloride (3.536 g, 19.80 mmol) was added dropwise, and the mixture was stirred for 1h at the same temperature. The reaction mixture was allowed to stand without cooling and stirred for 72 h at rt. The reaction mixture was cooled to 0 °C, quenched with ice water (10 mL), and diluted with methanol to give a precipitate. The precipitate was filtered and washed with water (2 x 50 mL)and methanol (2 x 50 mL). The crude product was hot filtered in toluene and allowed crystallized upon cooling of the solvent to give 6,6'-([1]benzothieno[3,2-b]-[1]benzothiophene-2,7-diyl)bis(6-oxohexanoate) (3.199 g, 6.097 mmol, 77 % yield) as white solid.

¹H NMR (400 MHz, CDCl₃) δ 8.56 (dd, J = 1.5, 0.6 Hz, 1H), 8.07 (dd, J = 8.4, 1.5 Hz, 1H), 7.98 (dd, J = 8.4, 0.6 Hz, 1H), 3.68 (s, 3H), 3.15 – 3.08 (m, 2H), 2.41 (t, J = 7.2 Hz, 2H), 1.89 – 1.73 (m, 19H). ¹³C NMR (101 MHz, CDCl₃) δ 198.75, 173.87, 142.84, 136.31, 135.92, 134.13, 124.81, 124.58, 121.96, 51.56, 38.37, 33.88, 24.57, 23.73.

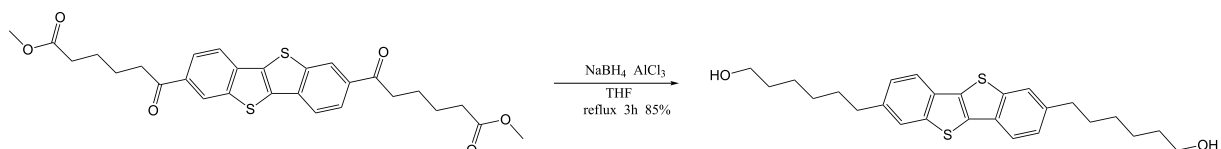
CHAPTER 2. THE CHEMISTRY OF BTBT DERIVATIVES: CHALLENGES AND NEW DERIVATIVES



2.7. EXPERIMENTAL PART



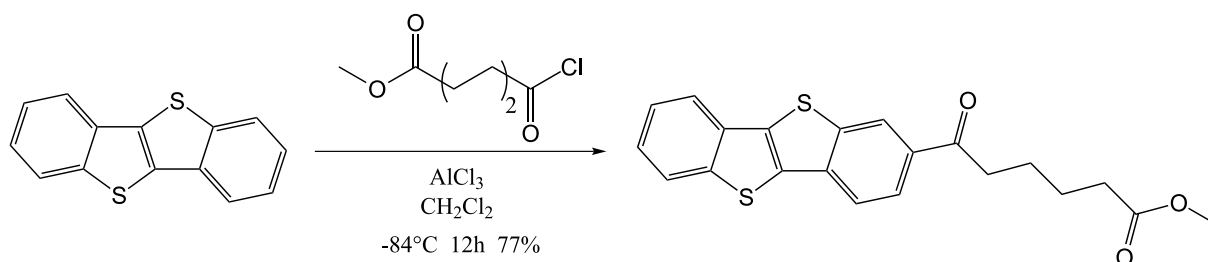
2.7.7 Synthesis of 6,6 -([1]benzothieno[3,2-b]-[1]benzothiophene-2,7-diyl)bis(hexan-1-ol) (7)



Methyl 6-(benzo[b]benzo[4,5]thieno[2,3-d]thiophen-2-yl)-6-oxohexanoate (2.03g, 3.87 mmol) was dissolved in dry tetrahydrofuran (75 mL), under nitrogen, followed by the addition of aluminum chloride (9.790 g, 73.43 mmol) at - 10 °C. The reaction mixture was stirred 10 min at the same temperature then sodium borohydride (5.623g, 148.6 mmol) was added slowly. The reaction mixture was stirred at reflux for 3 h. The reaction was cooled down at 0 °C with an ice bath. An aqueous sodium hydroxide solution (15% w/w , 200 mL) was added dropwise and the mixture stirred until the formation of two liquid phase. The organic phase was washed with aqueous sodium hydroxide solution (3 x 50 mL), brine (50 mL) and dried over magnesium sulfate. The magnesium sulfate was removed by filtration over celite. Tetrahydrofuran was evaporated at reduced pressure. The crude product was crystallized and washed with toluene. 6,6 -([1]benzothieno[3,2 - b]-[1]benzothiophene-2,7-diyl)bis(hexan-1-ol) was obtained like white solid (1.450 g , 3.290 mmol, 85% yield).

¹ H NMR (400 MHz, CDCl₃) δ : 7.76 (d, J = 8.1 Hz, 2H), 7.70 (s, 2H), 7.27 (d, J = 8.2 Hz, 2H), 3.65 (td, J = 6.6 Hz, J = 5.4 Hz, 4H), 2.77 (t, J = 7.4 Hz, 4H), 1.72 (m, 4H), 1.57 (m, 4H), 1.42 (m, 8H), 1.21 (t, J = 5.4 Hz, 2H) ; ¹³ H NMR (400 MHz, CDCl₃) δ : 142.43, 139.85, 132.57, 131.23, 36.02, 63.01, 125.81, 123.33, 121.12, 32.71, 31.63, 29.04, 25.63

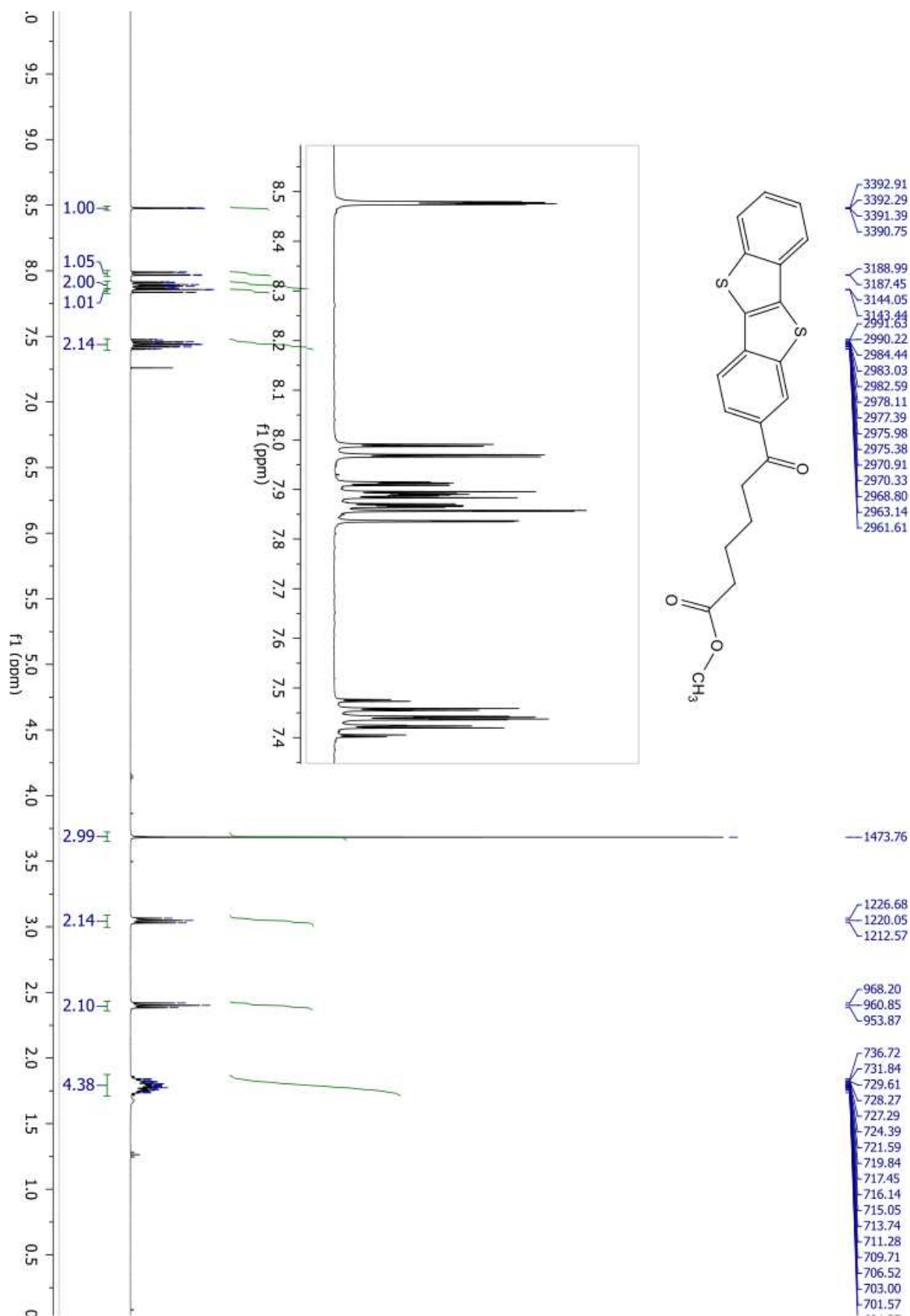
2.7.8 Synthesis of methyl 6-(benzo[b]benzo[4,5]thieno[2,3-d]thiophen-2-yl)-6-oxohexanoate (8)



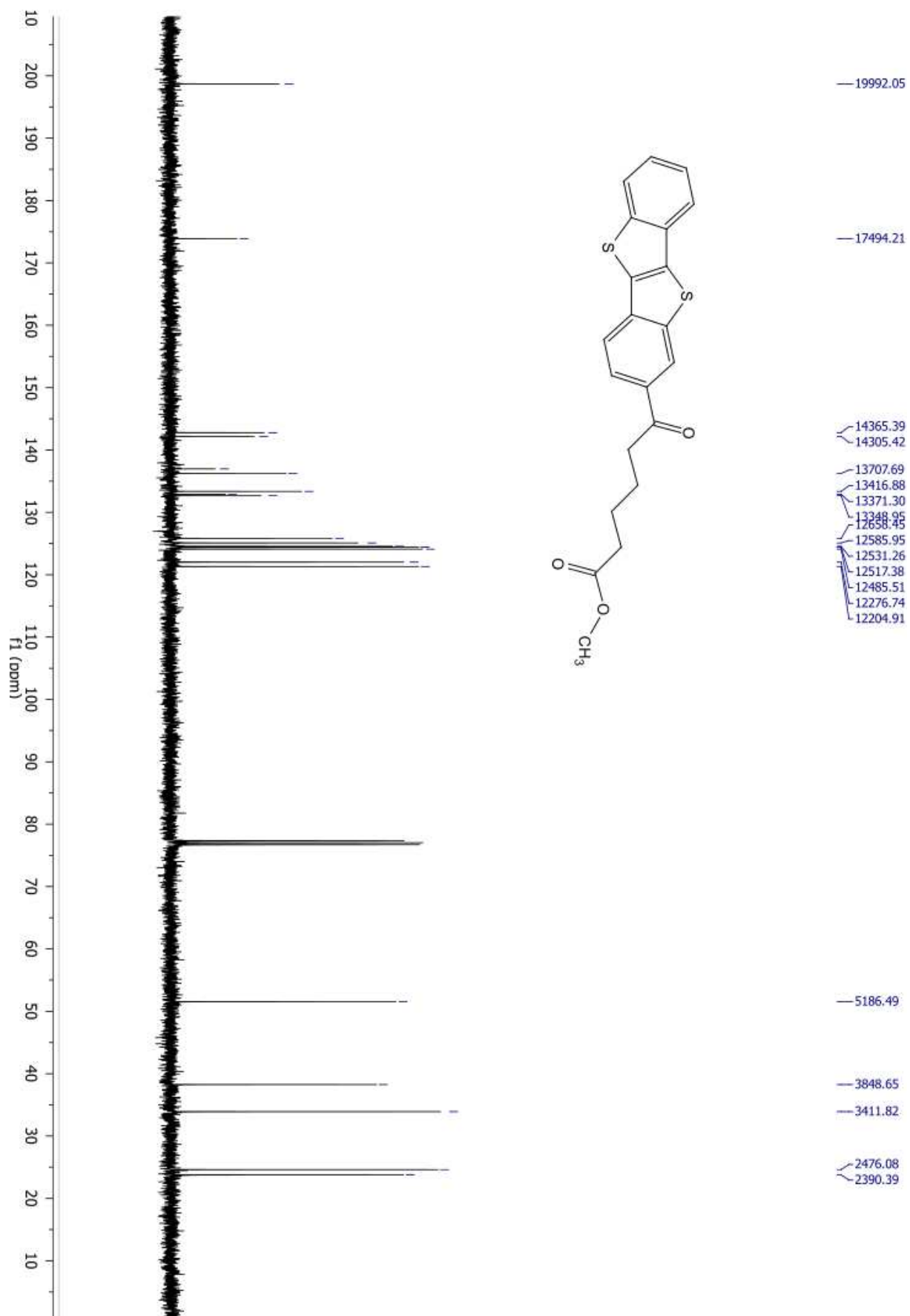
[1]Benzothieno[3,2- b][1]benzothiophene (6.569 g, 27.33 mmol) was dissolved in dry dichloromethane (150 mL), under nitrogen, followed by the addition of aluminum chloride (11.170 g, 83.77 mmol) at -10°C . The solution was cooled to -84°C and methyl adipoyl chloride (7.873 g, 44.08 mmol) was added dropwise, and the mixture was stirred for 1 h at the same temperature. The reaction mixture was allowed to stand without cooling and stirred for 12 h at rt. The reaction mixture was cooled to 0°C , quenched with ice water (10 mL), and diluted with methanol to give a precipitate. The precipitate was filtered and washed with water (2 x 50 mL) and methanol (2 x 50 mL). The crude product was hot filtered in toluene and allowed crystallized upon cooling of the solvent to give [1]benzothieno[3,2- b][1]benzothiophene -2- octan -1- one (8.080 g, 16.37 mmol, 77 % yield) as white solid.

$^1\text{H NMR}$ (400 MHz, CDCl_3) δ 8.48 (dd, $J = 1.5, 0.6$ Hz, 1H), 7.98 (dd, $J = 8.4, 1.5$ Hz, 1H), 7.92 – 7.86 (m, 2H), 7.85 (dd, $J = 8.3, 0.6$ Hz, 1H), 7.48 – 7.39 (m, 2H), 3.68 (s, 3H), 3.09 – 3.00 (m, 2H), 2.40 (t, $J = 7.2$ Hz, 2H), 1.87 – 1.71 (m, 4H).

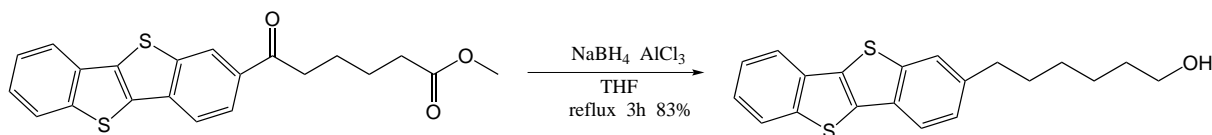
CHAPTER 2. THE CHEMISTRY OF BTBT DERIVATIVES: CHALLENGES AND NEW DERIVATIVES



2.7. EXPERIMENTAL PART



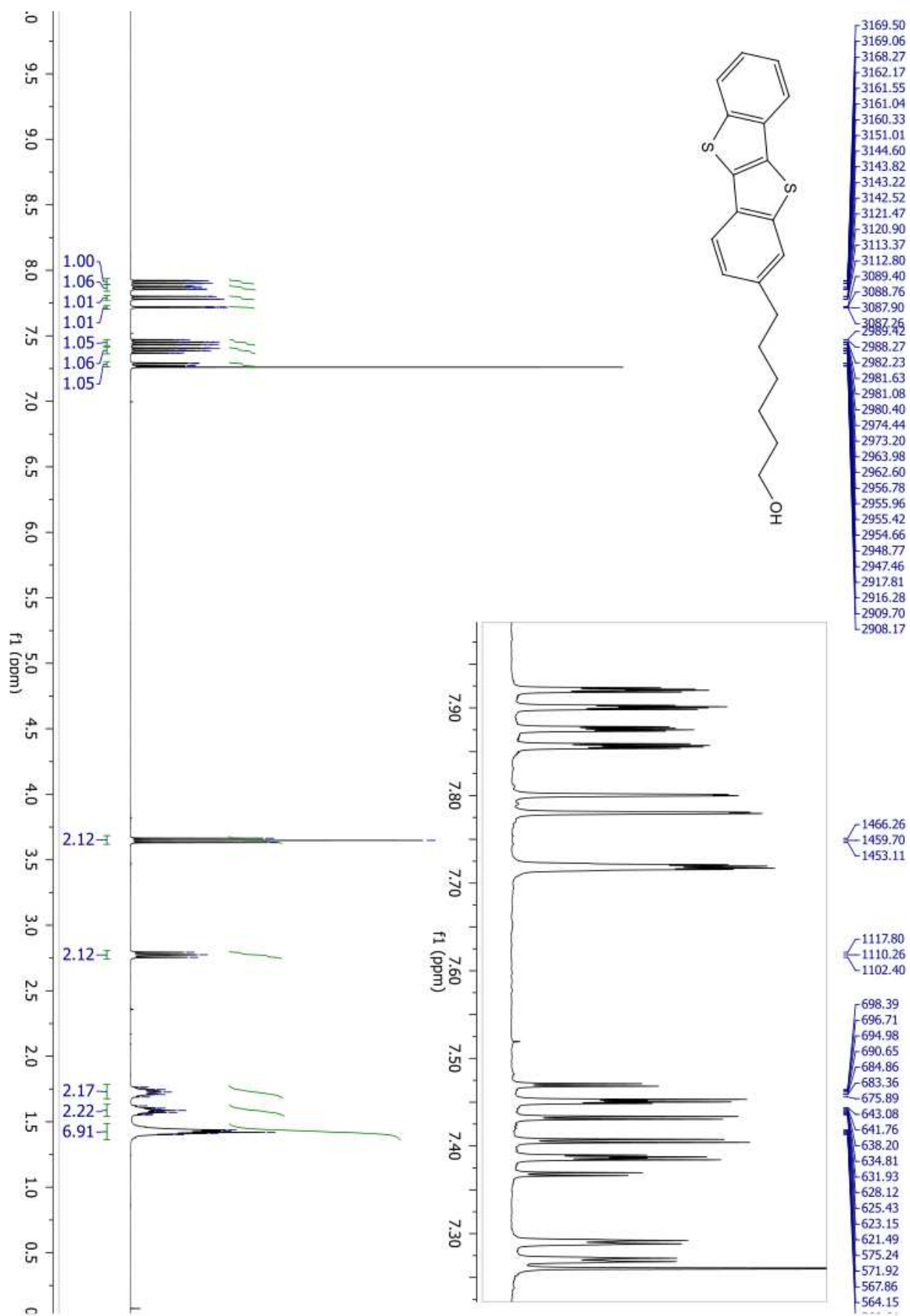
2.7.9 Synthesis of 6-(benzo[b]benzo[4,5]thieno[2,3-d]thiophen-2-yl)hexan-1-ol (9)



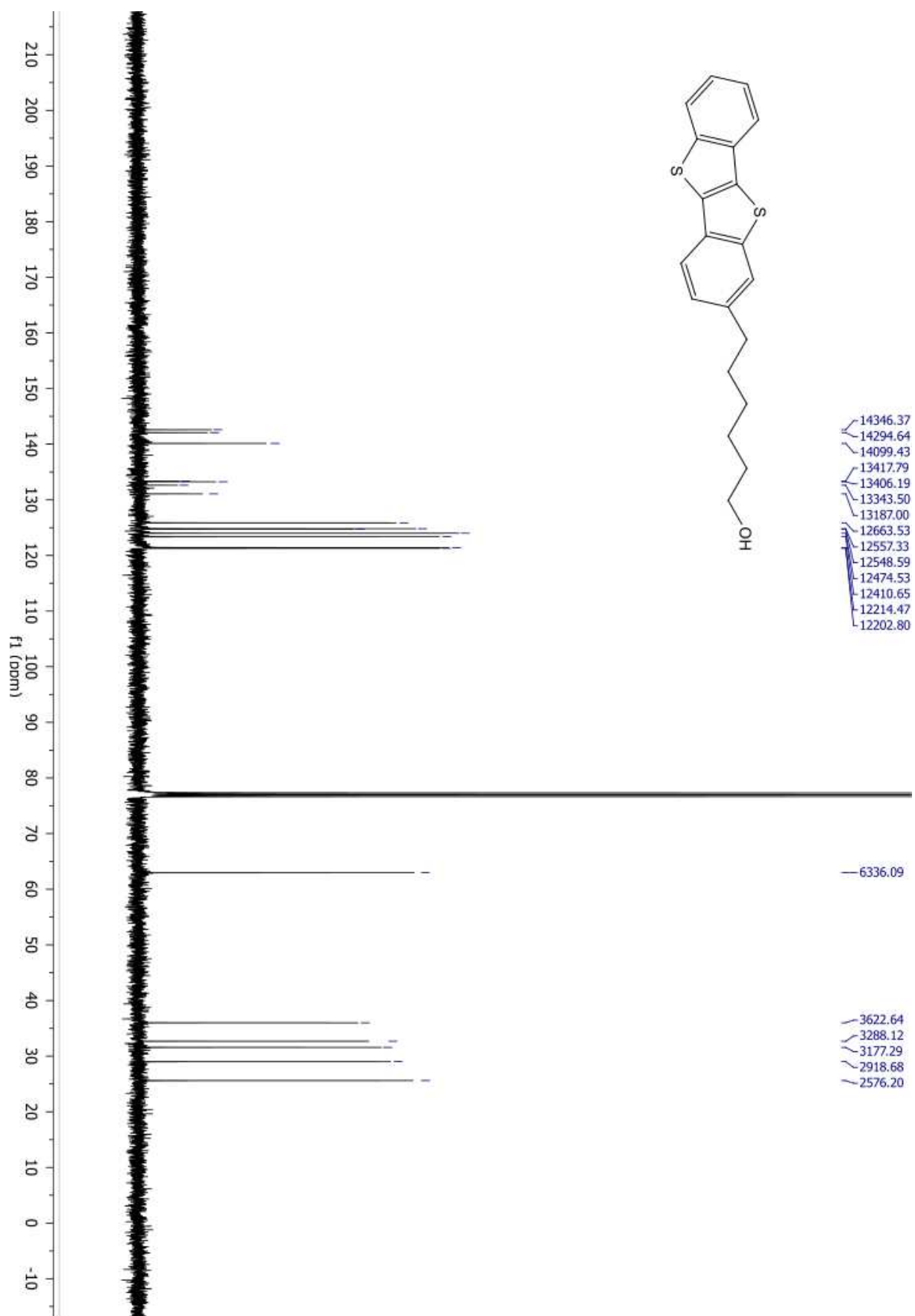
Methyl 6-(benzo[b]benzo[4,5]thieno[2,3-d]thiophen-2-yl)-6-oxohexanoate (4.011g, 10.48 mmol) was dissolved in dry tetrahydrofuran (150 mL), under nitrogen, followed by the addition of aluminum chloride (9.800 g, 73.49 mmol) at -10 °C. The reaction mixture was stirred 10 min at the same temperature then sodium borohydride (5.600g, 148.03 mmol) was added slowly. The reaction mixture was stirred at reflux for 3 h. The reaction was cooled down at 0 °C with an ice bath. An aqueous sodium hydroxide solution (15% w/w, 200 mL) was added dropwise and the mixture stirred until the formation of two liquid phases. The organic phase was washed with aqueous sodium hydroxide solution (3 x 50 mL), brine (50 mL) and dried over magnesium sulfate. The magnesium sulfate was removed by filtration over celite. Tetrahydrofuran was evaporated at reduced pressure. The crude product was crystallized and washed with toluene. 6-(benzo[b]benzo[4,5]thieno[2,3-d]thiophen-2-yl)hexan-1-ol was obtained like white solid (2.963g, 8.70 mmol, 83% yield).

¹H NMR (400 MHz, CDCl₃) δ 7.91 (ddd, J = 7.9, 1.2, 0.7 Hz, 2H), 7.87 (ddd, J = 7.9, 1.3, 0.7 Hz, 2H), 7.79 (dd, J = 8.1, 0.6 Hz, 2H), 7.72 (dd, J = 1.5, 0.6 Hz, 2H), 7.45 (ddd, J = 7.9, 7.2, 1.2 Hz, 2H), 7.39 (ddd, J = 8.0, 7.2, 1.3 Hz, 2H), 7.28 (dd, J = 8.1, 1.5 Hz, 2H), 3.65 (t, J = 6.6 Hz, 4H), 2.81 – 2.74 (m, 4H), 1.78 – 1.68 (m, 4H), 1.63 – 1.54 (m, 4H), 1.49 – 1.36 (m, 13H). ¹³C NMR (101 MHz, CDCl₃) δ 142.59, 142.08, 140.14, 133.36, 133.25, 132.62, 131.07, 125.86, 124.81, 124.72, 123.99, 123.35, 121.40, 121.28, 62.97, 36.01, 32.68, 31.58, 29.01, 25.61.

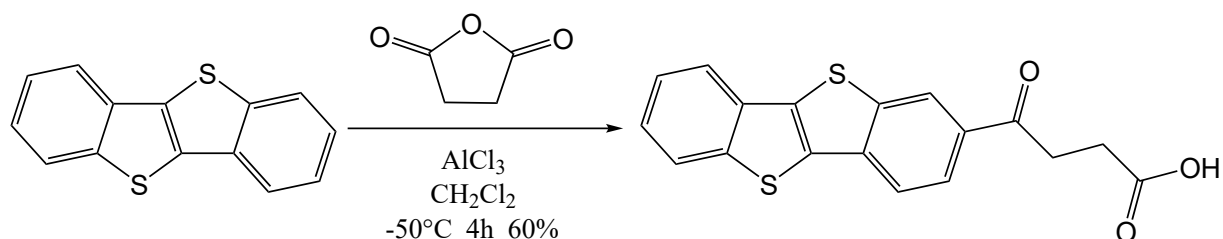
2.7. EXPERIMENTAL PART



CHAPTER 2. THE CHEMISTRY OF BTBT DERIVATIVES: CHALLENGES AND NEW DERIVATIVES



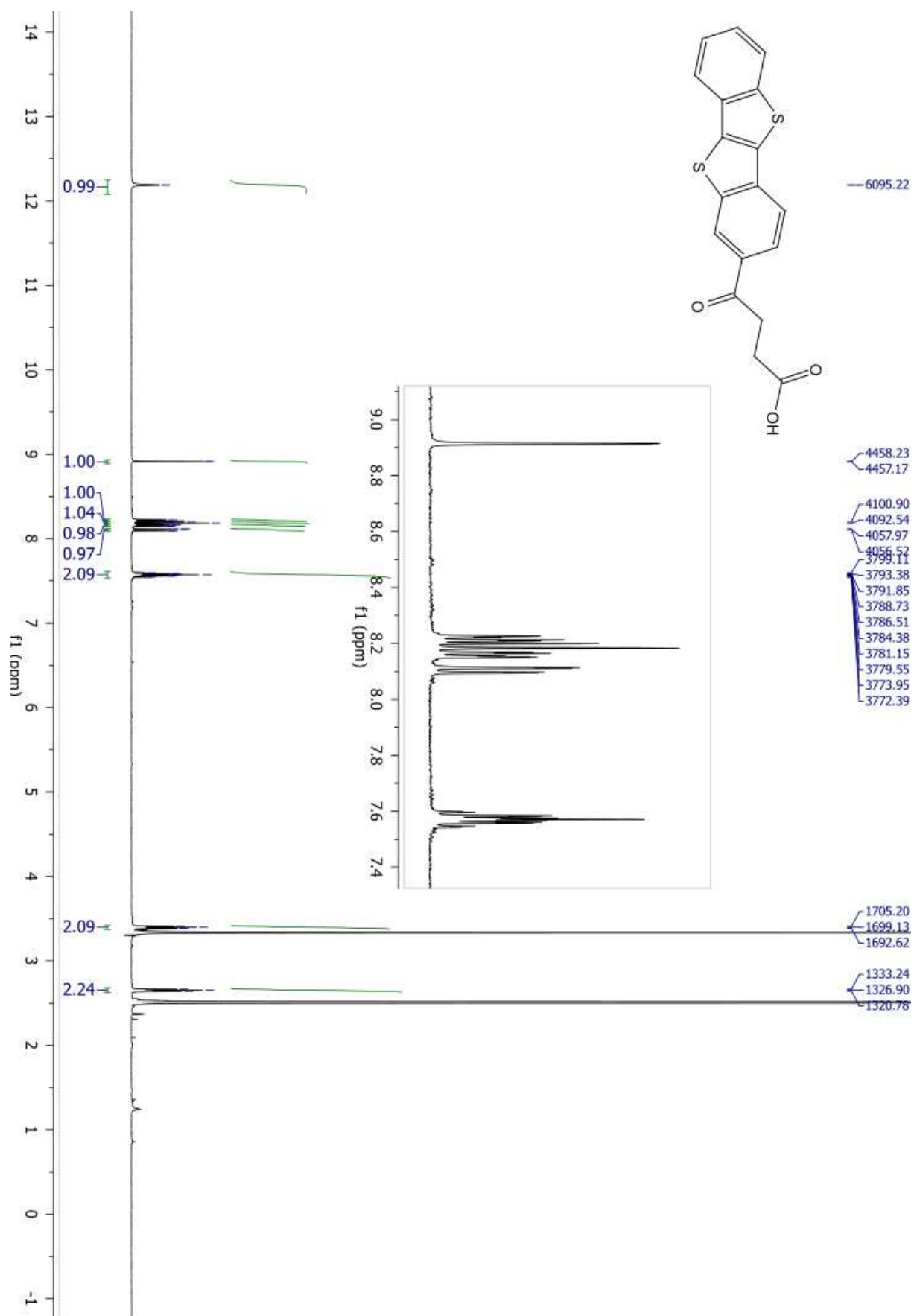
2.7.10 Synthesis of 4-oxo-4-([1]benzothieno[3,2-b][1]benzothienyl)-butyric acid (10)



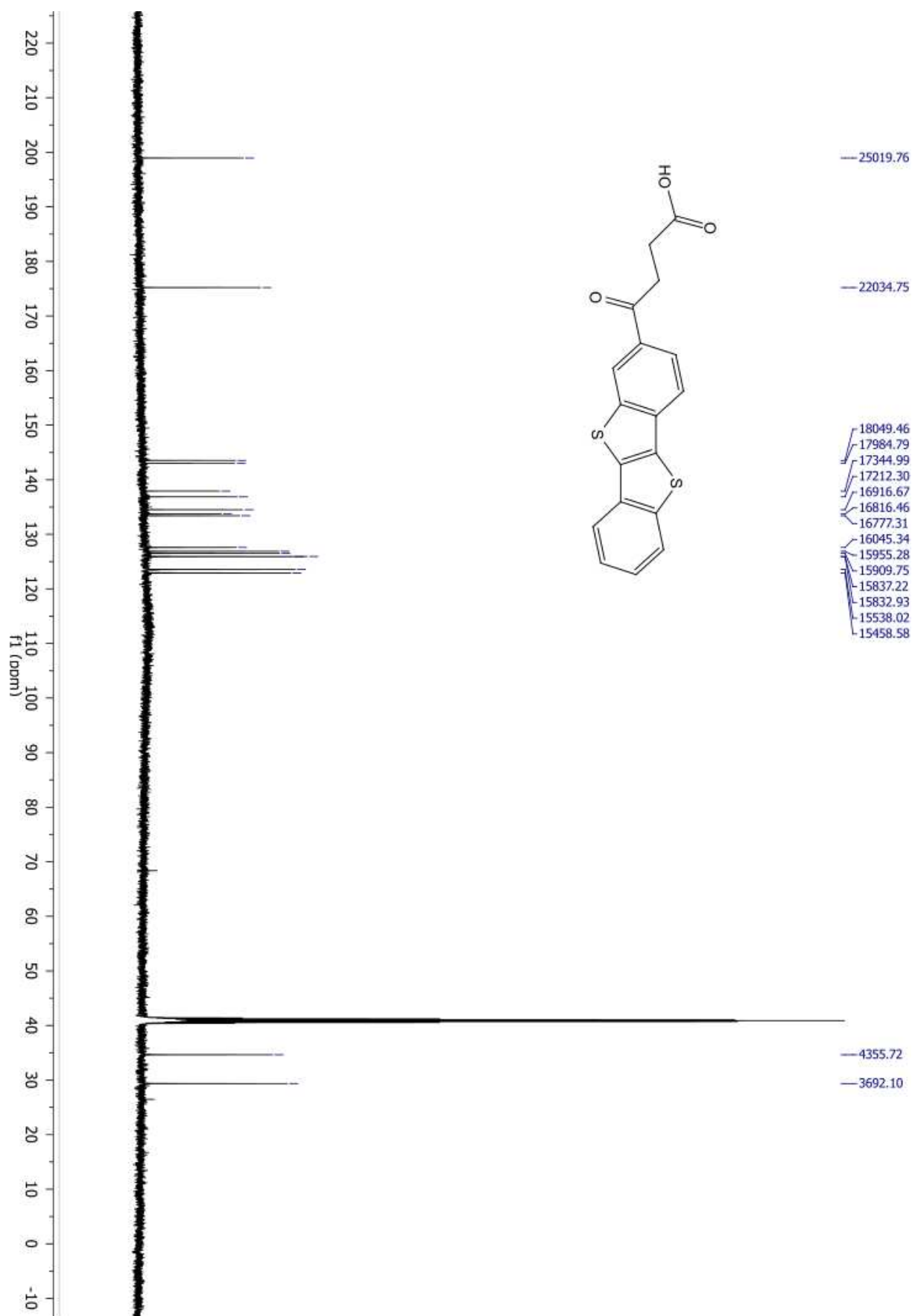
[1]Benzothieno[3,2- b][1]benzothiophene (5 g, 20.08 mmol) was dissolved in dry dichloromethane (500 mL), under nitrogen, followed by the addition of aluminum chloride 8.03, 60.22 mmol) at - 50 °C. The reaction mixture was stirred for 45 min, until the reaction mixture become dark red. succinic anhydride (8.030 g, 60.22 mmol) was added dropwise (2.3g, 22.98 mmol), and the mixture was stirred for 4 h at -20°C. The reaction mixture was quenched with ice water (50 mL) and methanol (100 mL). The white precipitate was filtered and disperse in 200 mL of a solution of chloridric acid in water (0,1 M) and stirred for 4h at room temperature. The white solid was filtered and dry at 100°C under vacuum overnight. The crude product was washed with hot toluene until the toluene was clear. The solid was the ricrystallized in tetrahydrofuran with extractive crystallization in tetrahydrofuran to afford 4-oxo-([1]benzothieno[3,2-b][1]benzothienyl)-butyric acid (4.100g, 12.04 mmol, 60 % yield) as crystallin white solid.

¹H NMR (500 MHz, DMSO) δ 12.19 (s, 1H), 8.91 (d, J = 1.1 Hz, 1H), 8.22 (dd, J = 6.7, 2.2 Hz, 1H), 8.19 (d, J = 8.4 Hz, 1H), 8.17 – 8.15 (m, 1H), 8.10 (dd, J = 8.3, 1.4 Hz, 1H), 7.61 – 7.53 (m, 2H), 3.42 – 3.37 (m, 2H), 2.68 – 2.63 (m, 2H). ¹³C NMR (126 MHz, DMSO) δ 198.95, 175.22, 143.53, 143.01, 137.92, 136.87, 134.52, 133.72, 133.41, 127.59, 126.87, 126.51, 125.93, 125.90, 123.56, 122.92, 34.64, 29.36.

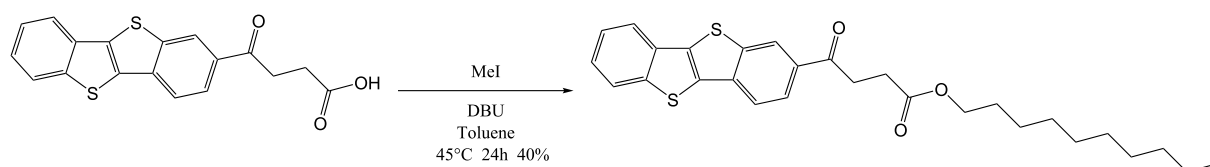
CHAPTER 2. THE CHEMISTRY OF BTBT DERIVATIVES: CHALLENGES AND NEW DERIVATIVES



2.7. EXPERIMENTAL PART



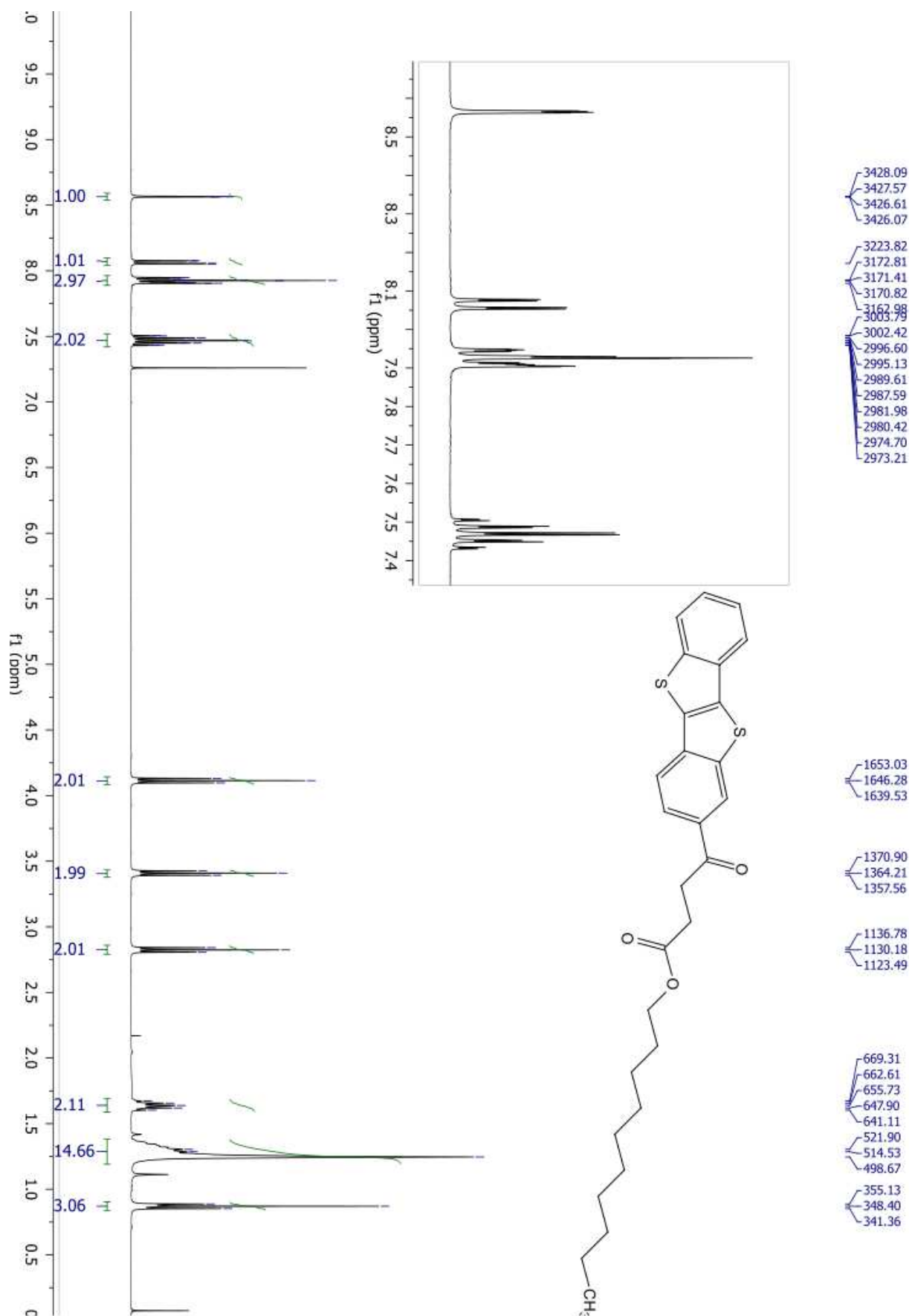
2.7.11 Synthesis of decanyl 4-oxo-4-([1]benzothieno[3,2-b][1]benzothienyl)butyrate (11)



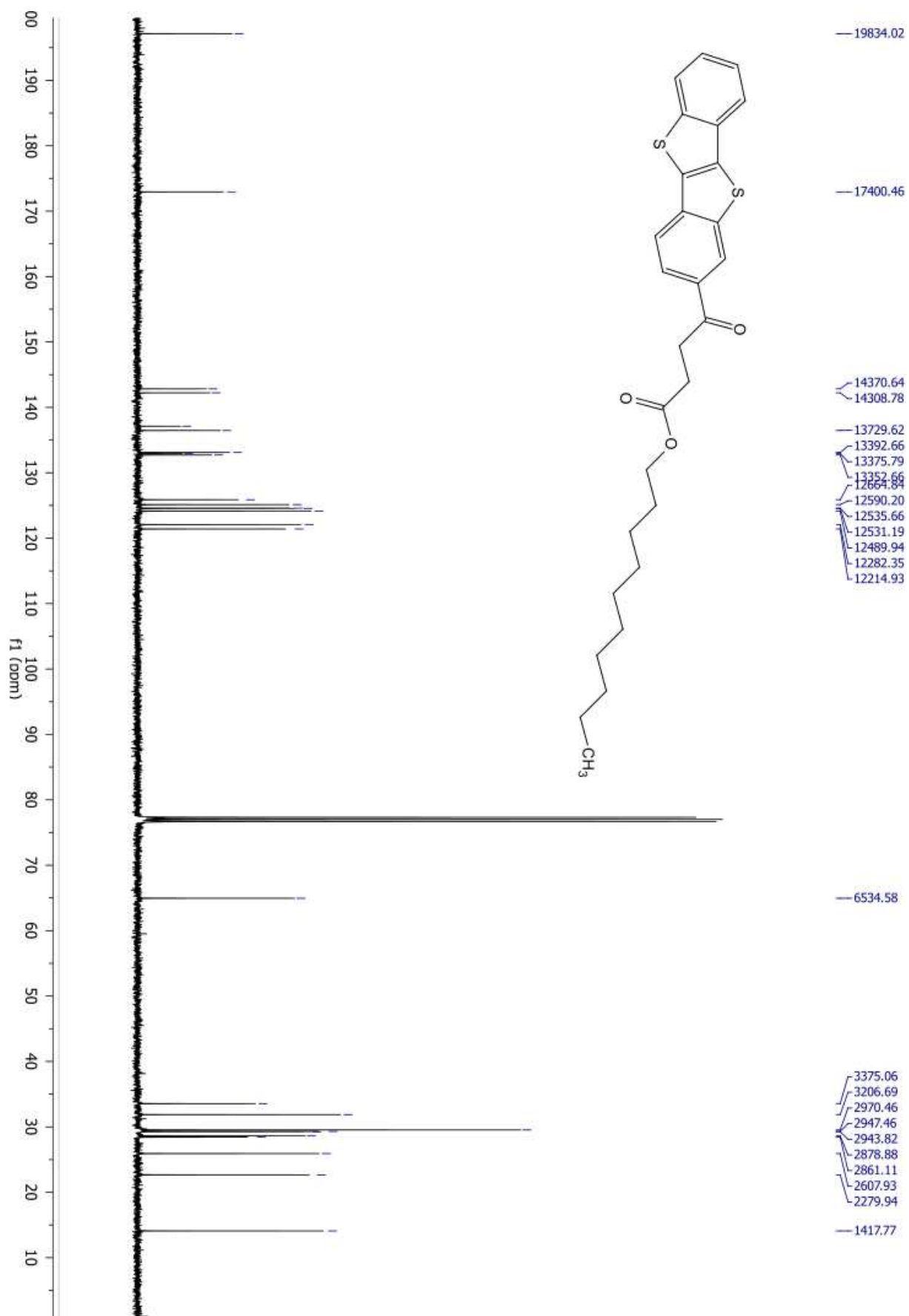
A suspension of 4-oxo-4-([1]benzothieno[3,2-b][1]benzothienyl)-butyric acid (0.5033 g, 1.48 mmol), 1,5-diazabicyclo[5.4.0]undec-5-ene (0.228 g, 1.49 mmol) and iododecane (0.396 g, 1.48 mmol) in toluene (100 mL) was stirred at 45°C for 68 h. The precipitate was removed by filtration and toluene was evaporated under reduce pressure. The solid was dispersed in dichloromethane (10 mL) the white solid was removed by filtration. dichloromethane was removed under reduce pressure to obtain decanyl 4-oxo-4-([1]benzothieno[3,2-b][1]benzothienyl)butyrate (0.268 g, 0.537 mmol, 40% yield).

¹H NMR (400 MHz, CDCl₃) δ 8.56 (dd, J = 1.5, 0.5 Hz, 1H), 8.07 (dd, J = 8.4, 1.5 Hz, 1H), 7.98 – 7.85 (m, 3H), 7.47 (pd, J = 7.2, 1.4 Hz, 2H), 4.11 (t, J = 6.7 Hz, 2H), 3.41 (t, J = 6.7 Hz, 2H), 2.82 (t, J = 6.6 Hz, 2H), 1.70 – 1.57 (m, 2H), 1.39 – 1.18 (m, 14H), 0.87 (t, J = 6.9 Hz, 3H). ¹³C NMR (101 MHz, CDCl₃) δ 197.13, 172.94, 142.83, 142.22, 137.12, 136.46, 133.11, 132.94, 132.71, 125.88, 125.14, 124.59, 124.55, 124.14, 122.08, 121.41, 64.95, 33.55, 31.87, 29.52, 29.30, 29.26, 28.61, 28.44, 25.92, 22.66, 14.09.

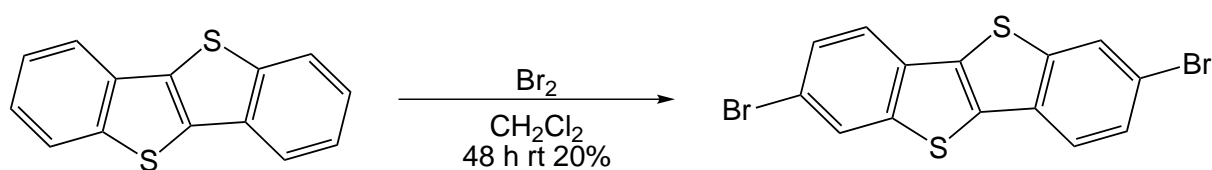
2.7. EXPERIMENTAL PART



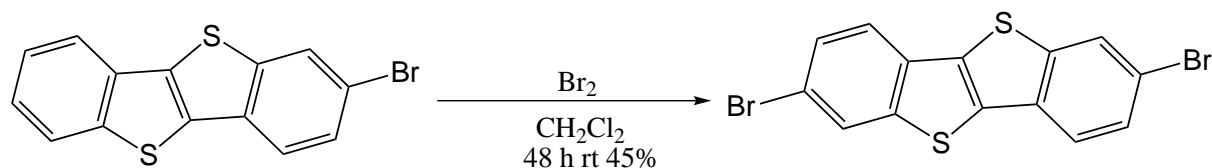
CHAPTER 2. THE CHEMISTRY OF BTBT DERIVATIVES: CHALLENGES AND NEW DERIVATIVES



2.7.12 Synthesis of 2,7-di-bromo-[1]benzothieno[3,2-b][1]benzothiophene (12)



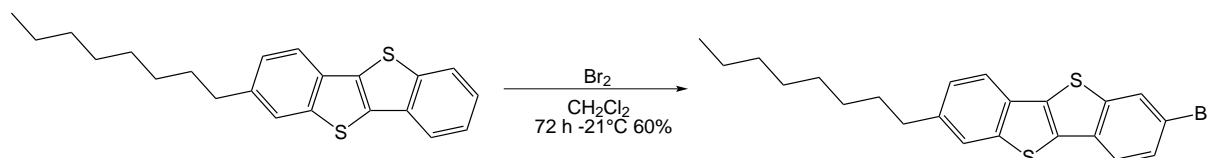
To an ice cold solution of [1]benzothieno[3,2-b]benzothiophene (1.024 g, 4.261 mmol) in dichloromethane (60 mL) was added a solution of bromine (1.47 g, 9.17 mmol) in dichloromethane (29 mL) using a dropping funnel. The solution was stirred for 2 hour at 0° C and then warmed to room temperature. The contents were stirred at room temperature for 46 hours. The precipitate was filtered and washed with aqueous sodium bisulfite solution (10% w/w, 20 mL x 3) followed by water (20 mL x 2), ethanol (20 mL x 2) and dichloromethane (20 mL x 2). Crude product was dried under vacuum at 70°C for 12h. The crude product was hot filtered in dichloromethane (330 mL) and the hot dichloromethane soluble fraction was allowed to crystallized upon cooling of the solvent to afford 2,7-di-bromo-[1]benzothieno[3,2-b][1]benzothiophene (254 mg, 0.639 mmol, 15% partial yield) as shiny colorless solid. The hot dichloromethane insoluble fraction was dried under vacuum at 70°C for 2h to afford a second fraction of 2,7-di-bromo-[1]benzothieno[3,2-b][1]benzothiophene as shiny colorless solid (85 mg, 0.21 mmol, 5% partial yield), (339 mg, 0.849 mmol, 20% yield).



To an ice cold solution of 2-bromo-[1]benzothieno[3,2-b]benzothiophene (0.320 g, 1.000 mmol) in dichloromethane (18 mL) was added a solution of bromine (0.176 g, 1.10 mmol) in dichloromethane (3.6 mL) using a dropping funnel. The solution was stirred for 2 hour at 0° C and then warmed to room temperature. The contents were stirred at room temperature for 46 hours. The precipitate was filtered and washed with aqueous sodium bisulfite solution (10% w/w, 20 mL x 3) followed by water (20 mL x 2), ethanol (20 mL x 2) and dichloromethane (20 mL x 2). Crude product was dried under vacuum at 70°C for 12h. The crude product was hot filtered in dichloromethane (80 mL) and the hot dichloromethane soluble fraction was allowed to crystallized upon cooling of the solvent to afford 2,7-di-bromo-[1]benzothieno[3,2-b][1]benzothiophene (136 mg, 0.342 mmol, 34% partial yield) as shiny colorless solid. The hot dichloromethane insoluble fraction was dried under vacuum at 70°C for 2h to afford a second fraction of 2,7-di-bromo-[1]benzothieno[3,2-b][1]benzothiophene as shiny colorless solid (45 mg, 0.21 mmol, 5% partial yield), (339 mg, 0.113 mmol, 45% yield).

¹H NMR (500 MHz, CDCl₃) δ 8.06 (d, J = 1.5 Hz, 1H), 7.74 (d, J = 8.6 Hz, 1H), 7.58 (dd, J = 8.6, 1.5 Hz, 1H). ¹³C NMR 75 MHz (CD₂D₂Cl₄, 70° C) : δ 143.70, 133.29, 131.57, 128.46, 126.51, 122.45, 118.91

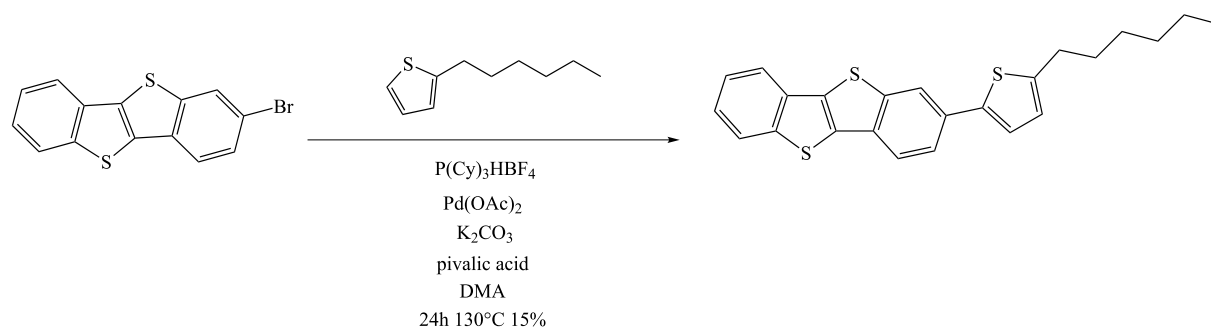
2.7.13 Synthesis of 2-octyl-7-bromo-[1]benzothieno[3,2-b][1]benzothiophene (13)



To a solution of 2-octyl-[1]benzothieno[3,2-b]benzothiophene (4.020g, 11.40 mmol) in dichloromethane (160 mL) was added a solution of bromine (2.010g, 12.50 mmol) in dichloromethane (30 mL) using a dropping funnel at -21°C . The solution was stirred for 6 h at the same temperature. The contents were stored at -21°C for 64 h in freezer to form pure 2-octyl-7-bromo-[1]benzothieno[3,2-b][1]benzothiophene as white precipitate (1.402 g, 32.45 mmol, 28% partial yield). Filtered dichloromethane solution was washed with an aqueous sodium bisulfite solution (10% w/w) and brine (50 mL x 2). Dichloromethane was removed under reduce pressure to obtain crude product. Crude product was crisyallized in heptane to afford a second fraction of 2-octyl-7-bromo-[1]benzothieno[3,2-b][1]benzothiophene(1.600 g, 37.08 mmol, 32% partial yield) (3.002 g , 69.53 mmol, 60% total yield).

¹ H NMR (CDCl₃ , 500 MHz) δ : 8.03 (d, J =1.7 Hz, 1H), 7.76 (d, J = 8.1 Hz, 1H), 7.71 (1H, s, H 6), 7.69 (d, J = 8.3 Hz,1H), 7.54 (dd, J = 8.5, 1.7 Hz, 1H), 7.28 (dd, J = 8.2, 1.4 Hz, 1H), 2.76 (t, J = 7.7 Hz, 2H), 1.76 – 1.63 (m, 2H), 1.42 – 1.21 (m, 10H), 0.89 (t, J = 6.7 Hz,3H); ¹³ C NMR (CDCl₃ , 125.7 MHz) δ : 143.63, 142.80, 140.92, 133.89, 132.23, 132.21, 130.88, 128.33, 126.59, 126.22, 123.51, 122.48, 121.42, 118.34, 36.30, 32.04, 31.81, 29.64, 29.46, 29.41, 22.82, 14.26;

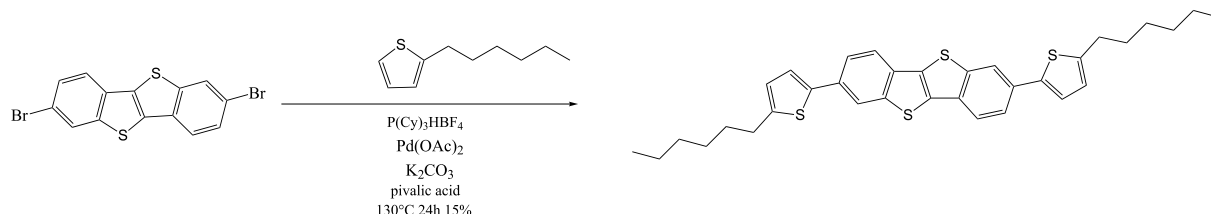
2.7.14 Synthesis of 2-(5-hexyl-2-thienyl)-[1]benzothieno[3,2-b]-[1]benzothiophene (14)



2-Bromo-benzo[b]benzo[4,5]thieno[2,3-d]thiophene (3.220 g, 10.05 mmol) potassium carbonate (2.120g, 15.34 mmol), Pd(OAc)₂ (55.01 mg, 0.246 mmol), PCy₃ · HBF₄ (148.13 mg, 0.40225 mmol), and pivalic acid (0.309 g, 3.03 mmol) were weighed to air and placed in a screw-cap pressure tube with a magnetic stir bar. The vial was purged with argon, and N,N-Dimethylacetamide (34 mL) was added. deoxygenated 2-Hexylthiophene (1.750 g, 10.40 mmol) were added under argon atmosphere. The reaction mixture was then vigorously stirred at 130 °C for 24h. The reaction mixture was then cooled to rt, diluted with dichloromethane. Inorganic salts were removed by filtration. The solution was washed with water (3x100 mL) and brine (2 x 50 mL), dried over magnesium sulfate, filtered, and evaporated under reduced pressure. The most part of residue N,N-Dimethylacetamide was removed by distillation with Claisen apparatus. The crude product was suspended in water, filtered and dried under vacuum at 70°C for 12h. The product was purified by silica gel column chromatography (eluent cyclohexane) and crystallized in toluene to afford 2-(5-hexyl-2-thienyl)-[1]benzothieno[3,2-b][1]benzothiophene (0.596 g, 1.46 mmol, 15% yield).

¹H NMR (500 MHz, CDCl₃) δ 8.08 (d, J = 1.3 Hz, 1H), 7.90 (dd, J = 20.4, 7.9 Hz, 2H), 7.83 (d, J = 8.3 Hz, 1H), 7.66 (dd, J = 8.3, 1.6 Hz, 1H), 7.44 (ddd, J = 15.2, 10.9, 3.9 Hz, 2H), 7.22 (d, J = 3.5 Hz, 1H), 6.79 (d, J = 3.5 Hz, 1H), 2.85 (t, J = 7.6 Hz, 2H), 1.78 – 1.67 (m, 2H), 1.37 (tt, J = 7.0, 5.3 Hz, 6H), 0.91 (t, J = 7.0 Hz, 3H). ¹³C NMR (126 MHz, CDCl₃) δ 147.10, 143.97, 143.13, 142.04, 134.37, 134.20, 133.99, 132.89, 132.72, 126.11, 125.85, 125.80, 124.90, 123.98, 123.82, 122.61, 122.41, 121.26, 32.50, 32.47, 31.19, 29.67, 23.47, 14.97.

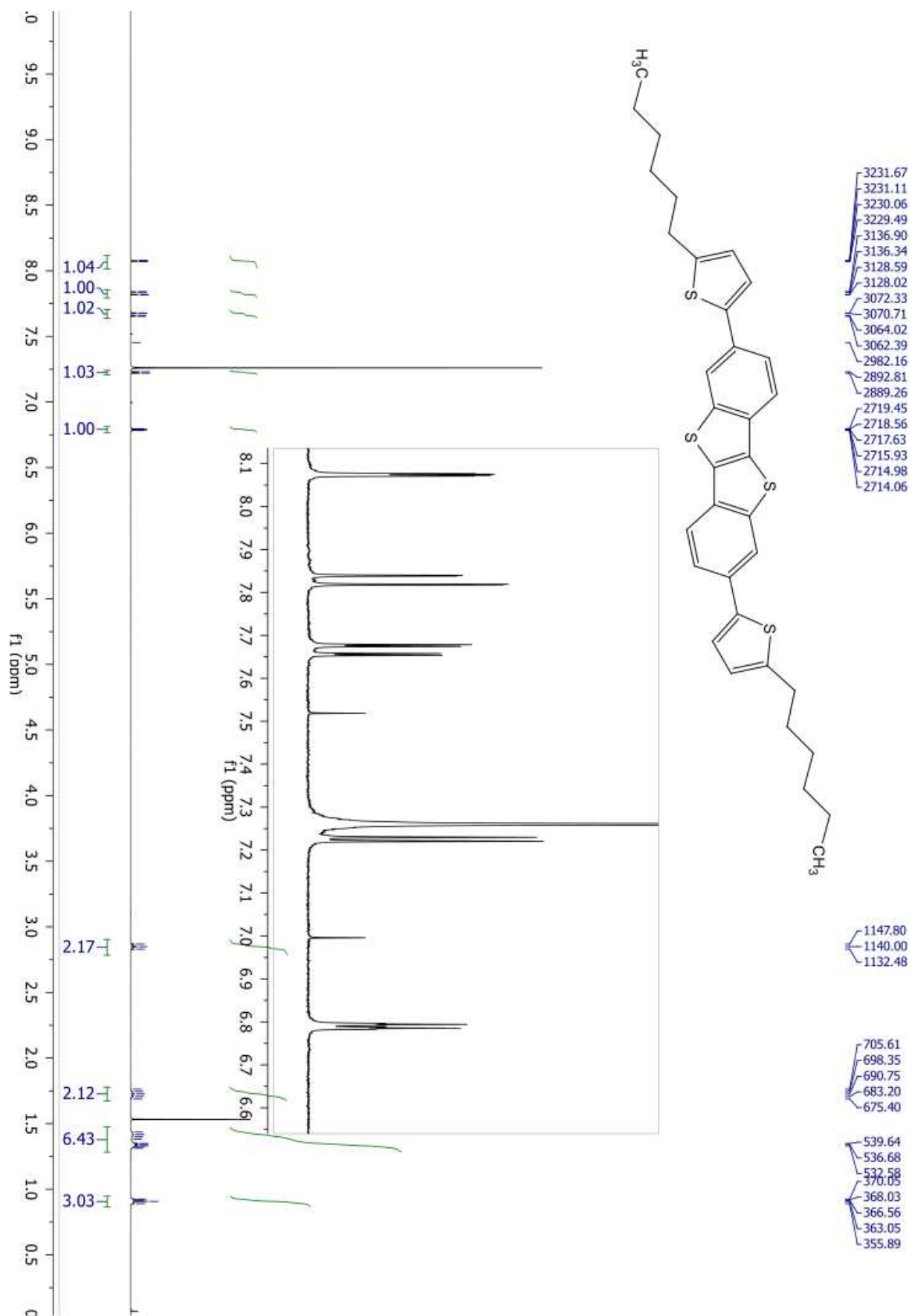
2.7.15 Synthesis of 2,7-di-(5-hexyl-2-thienyl)-[1]benzothieno[3,2-b][1]benzothiophene (15)



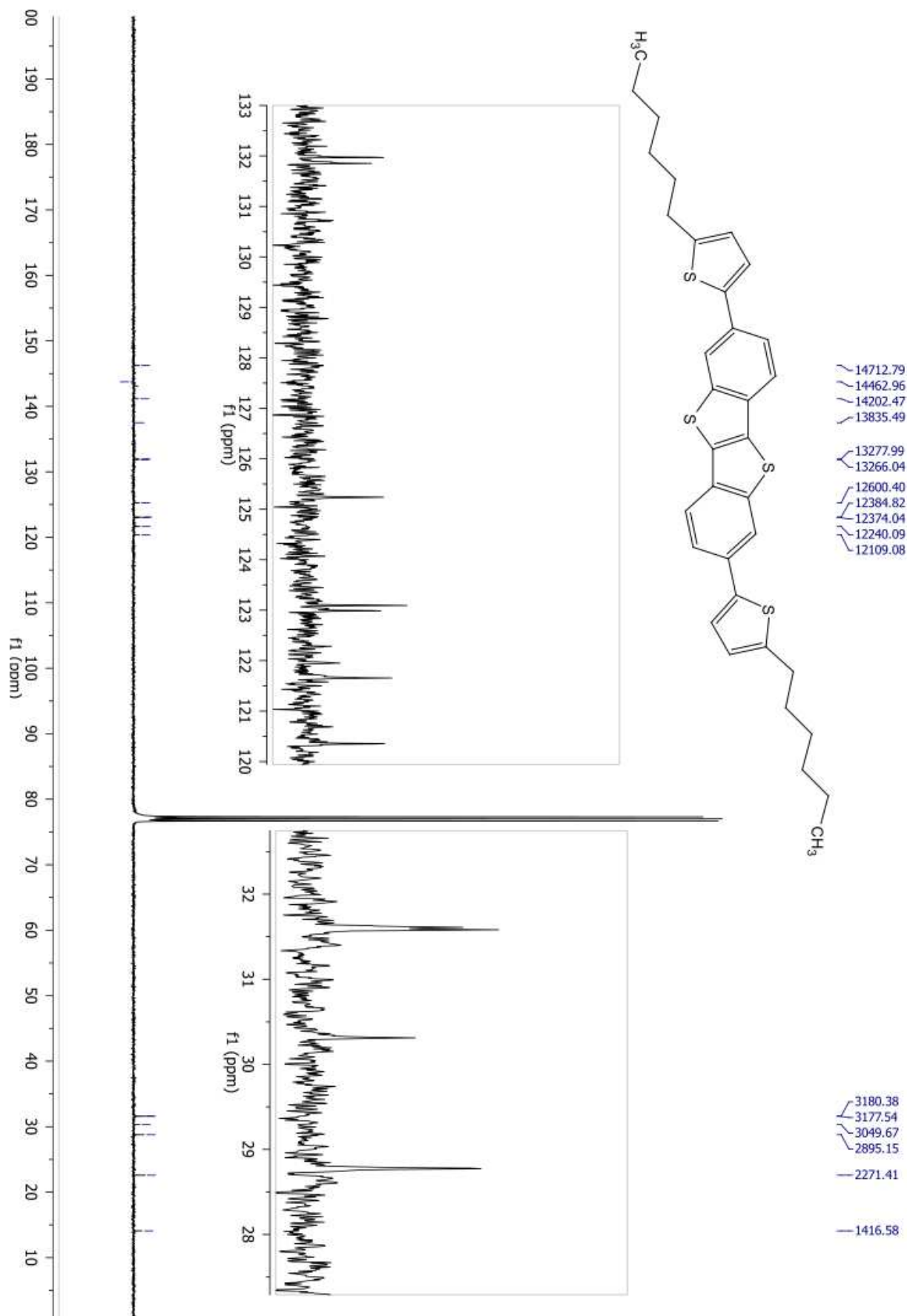
2,7-Dibromo-benzo[b]benzo[4,5]thieno[2,3-d]thiophene (0.500g, 1.26 mmol), potassium carbonate (0.521g, 3.77 mmol), $Pd(OAc)_2$ (11.0 mg, 0.0500 mmol), $PCy_3 \cdot HBF_4$ (37.1 mg, 0.100 mmol), and pivalic acid (77.0 mg, 0.754 mmol) were weighed to air and placed in a screw-cap pressure tube with a magnetic stir bar. The tube was placed in glovebox under argon atmosphere, and N,N-Dimethylacetamide (4.3 ml) and 2-Hexylthiophene (0.440 g, 2.612 mmol) were added. The tube was sealed in glovebox and extracted from the box. The reaction mixture was then vigorously stirred at 130 °C for 24h. The reaction mixture was then cooled to rt, diluted with dichloromethane. Inorganic salts were removed by filtration. The solution was washed with water (3x100 mL) and brine (2 x 50 mL), dried over magnesium sulfate, filtered, and evaporated under reduced pressure. The most part of residue N,N-Dimethylacetamide was removed by distillation with Claisen apparatus. The crude product was suspended in water, filtered and dried under vacuum at 70°C for 24h. The product was purified by silica gel column chromatography (eluent heptane) and crystallized in toluene to afford 2,7-di-(5-hexyl-2-thienyl)-[1]benzothieno[3,2-b][1]benzothiophene (0.100 g, 0.174 mmol, 15 %).

1H NMR (400 MHz, $CDCl_3$) δ 8.07 (dd, $J = 1.6, 0.6$ Hz, 1H), 7.83 (dd, $J = 8.3, 0.6$ Hz, 1H), 7.67 (dd, $J = 8.3, 1.6$ Hz, 1H), 7.23 (d, $J = 3.6$ Hz, 1H), 6.79 (dt, $J = 3.6, 0.9$ Hz, 1H), 2.85 (t, $J = 7.7$ Hz, 2H), 1.73 (dt, $J = 15.4, 7.5$ Hz, 2H), 1.37 (tt, $J = 7.2, 5.5$ Hz, 6H), 0.95 – 0.86 (m, 3H). ^{13}C NMR (101 MHz, $CDCl_3$) δ 146.23, 143.75, 141.16, 137.51, 131.97, 131.85, 125.24, 123.09, 122.99, 121.66, 120.35, 31.61, 31.58, 30.31, 28.78, 22.58, 14.08.

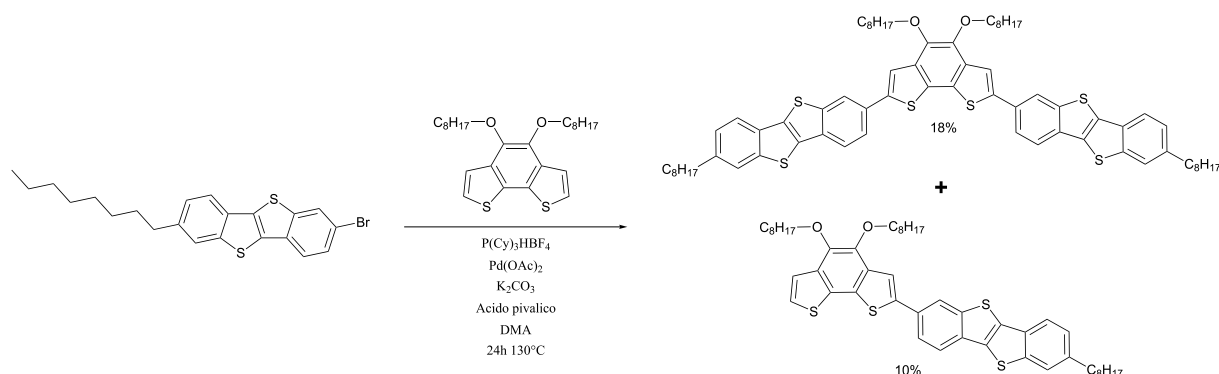
2.7. EXPERIMENTAL PART



CHAPTER 2. THE CHEMISTRY OF BTBT DERIVATIVES: CHALLENGES AND NEW DERIVATIVES



2.7.16 Synthesis 7,7'-(4,5-bis(octyloxy) of benzo[1,2-b:6,5-b']dithiophene-2,7-diyl)bis(2-octylbenzo[b]benzo[4,5]thieno[2,3-d]thiophene) and 2-(4,5-bis(octyloxy)benzo[1,2-b:6,5-b']dithiophen-2-yl)-7-octylbenzo[b]benzo[4,5]thieno[2,3-d]thiophene (16 end 17)



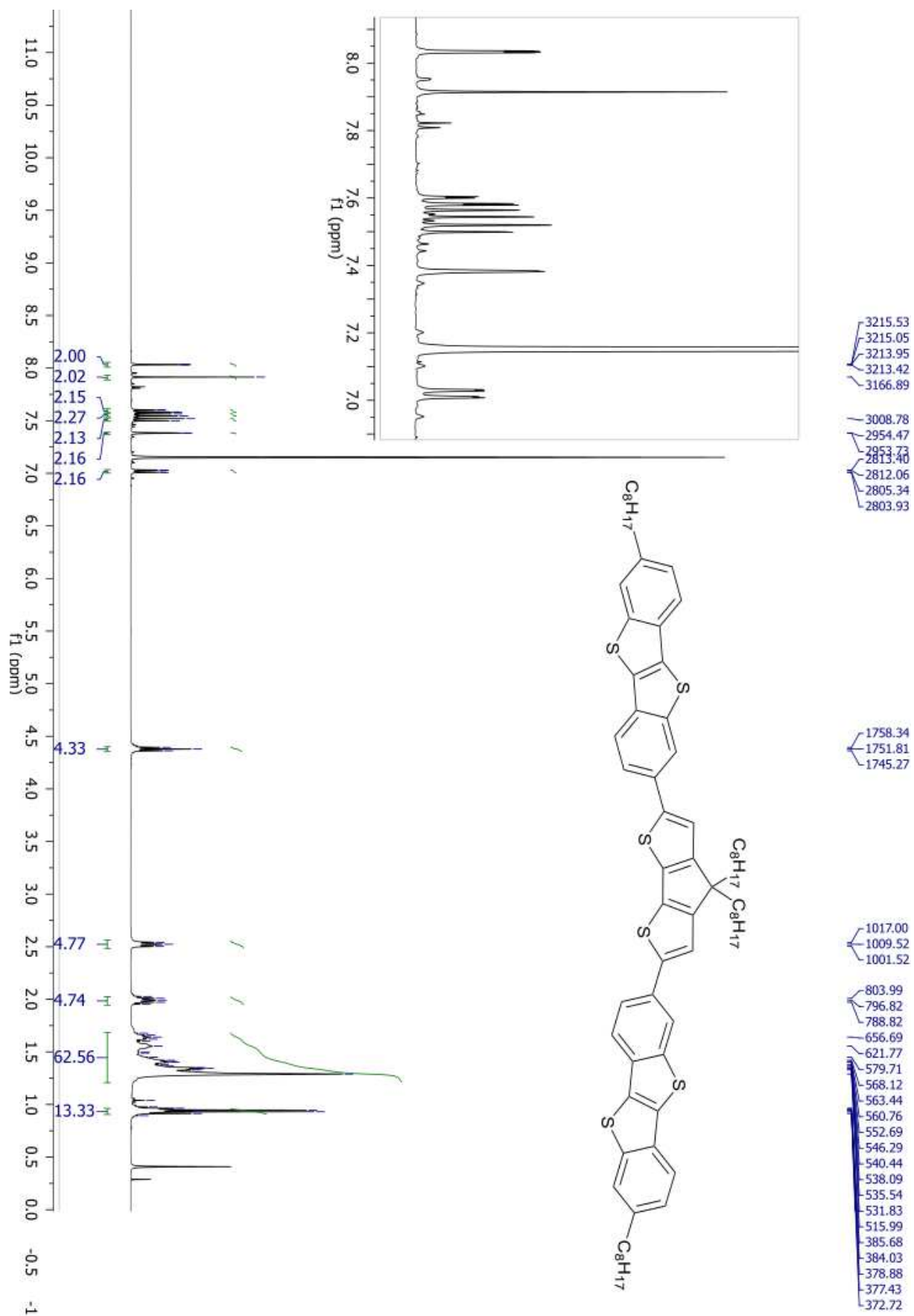
7-Octyl-2-bromo-benzo[b]benzo[4,5]thieno[2,3-d]thiophene (0.862 g, 2.00 mmol), potassium carbonate (0.400g, 2.83 mmol), Pd(OAc)_2 (9.12 mg, 0.041 mmol), $\text{PCy}_3 \cdot \text{HBF}_4$ (28.15 mg, 0.07644 mmol), and pivalic acid (60 mg, 0.59 mmol) were weighed to air and placed in a screw-cap pressure tube with a magnetic stir bar. The tube was placed in glovebox under argon atmosphere, *N,N*-Dimethylacetamide (34 mL) and 4,5-Bis(Octyloxy)Benzo[2,1-B;3,4-B']dithiophene (0.430 g, 0.963 mmol) were added. The tube was sealed in glovebox and extracted from the box. The reaction mixture was then vigorously stirred at 130 °C for 24h. The reaction mixture was then cooled to rt, diluted with dichloromethane. Inorganic salts were removed by filtration. The solution was washed with water (3x100 mL) and brine (2 x 50 mL), dried over magnesium sulfate, filtered, and evaporated under reduced pressure. The most part of residue *N,N*-Dimethylacetamide was removed by distillation with Claisen apparatus. The crude product was suspended in water, filtered and dried under vacuum at 70°C for 12h. Solid was filtered through a pad of silica with cyclohexane as eluent. Crude product was suspended in boiling isopropanol (100 mL) and filtered. The fraction soluble in hot isopropanol was left to crystallized to afford 2-(4,5-bis(octyloxy)benzo[1,2-b:6,5-b']dithiophen-2-yl)-7-octylbenzo[b]benzo[4,5]thieno[2,3-d]thiophene (80 mg, 0.10 mmol, 10%) as light green solid. The insoluble fraction in isopropanol was crystallized in heptane to afford 7,7'-(4,5-bis(octyloxy)benzo[1,2-b:6,5-b']dithiophene-2,7-diyl)bis(2-octylbenzo[b]benzo[4,5]thieno[2,3-d]thiophene) (200 mg, 0.175 mmol, 18%) as brown solid.

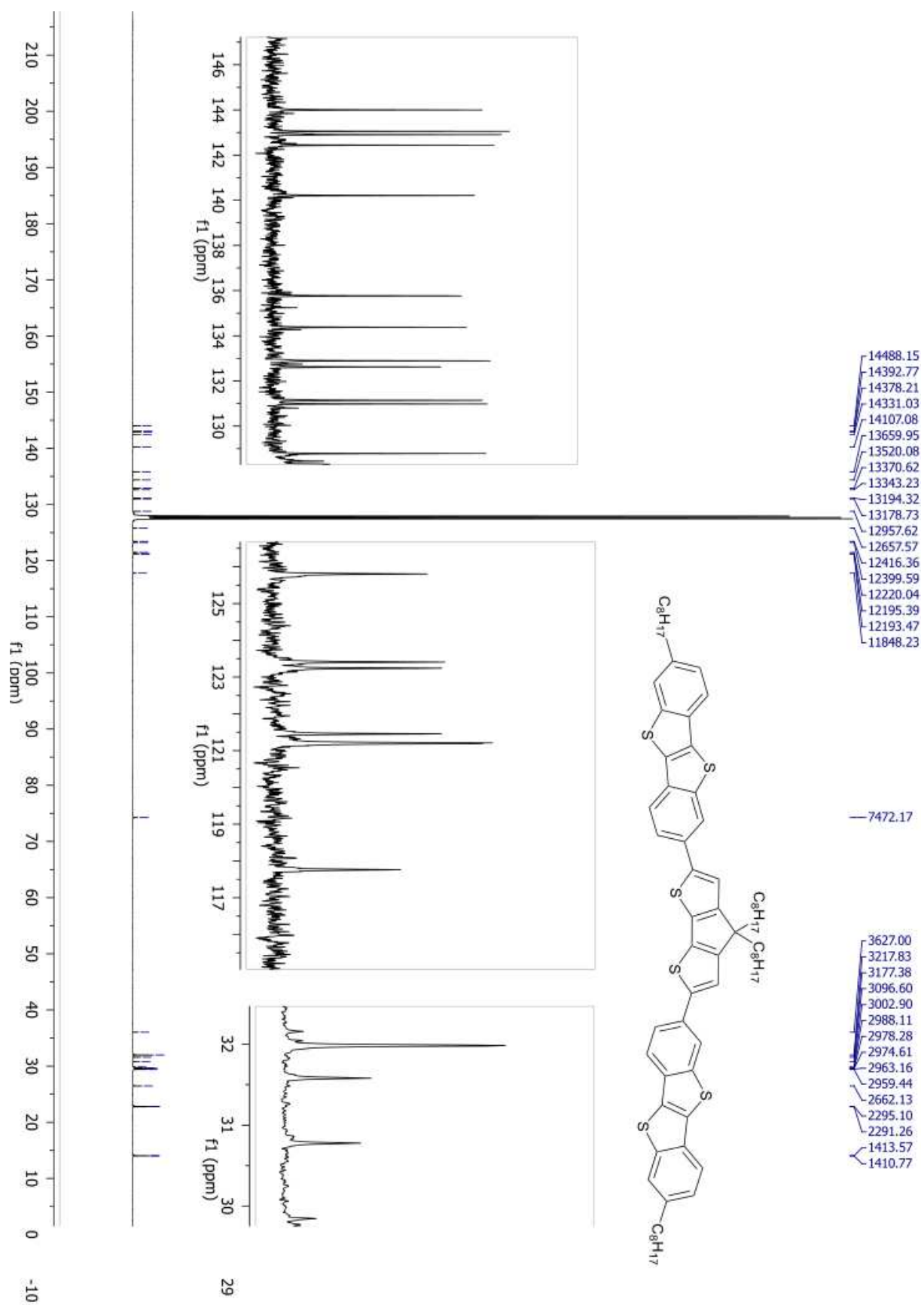
$^1\text{H NMR}$ (400 MHz, C_6D_6) δ 8.05 (d, $J = 1.1$ Hz, 1H), 7.95 (s, 1H), 7.62 (dd, $J = 8.3, 1.6$ Hz, 1H), 7.57 (d, $J = 8.1$ Hz, 1H), 7.53 (d, $J = 8.2$ Hz, 1H), 7.39 (d, $J = 0.5$ Hz, 1H), 7.03 (dd, $J = 8.1, 1.2$ Hz, 1H), 4.38 (t, $J = 6.6$ Hz, 3H), 2.58 – 2.46 (m, 2H), 2.05 – 1.92 (m, 3H), 1.66 – 1.60 (m, 2H), 1.58 – 1.53 (m, 2H), 1.47 – 1.24 (m, 24H), 0.99 – 0.89 (m, 7H), 0.39 (s, 2H). $^{13}\text{C NMR}$ (101 MHz, C_6D_6) δ 144.00, 143.05, 142.91, 142.44, 140.21, 135.77, 134.38, 132.89, 132.62, 131.14, 130.98, 128.79, 127.92, 127.68, 127.57, 127.44, 125.80, 123.41, 123.24, 121.46, 121.21, 117.76, 74.27, 36.05, 31.98, 31.58, 30.78, 29.85, 29.70, 29.60, 29.56, 29.45, 29.41, 26.46, 22.81, 22.77, 14.05, 14.02.

CHAPTER 2. THE CHEMISTRY OF BTBT DERIVATIVES: CHALLENGES AND NEW DERIVATIVES

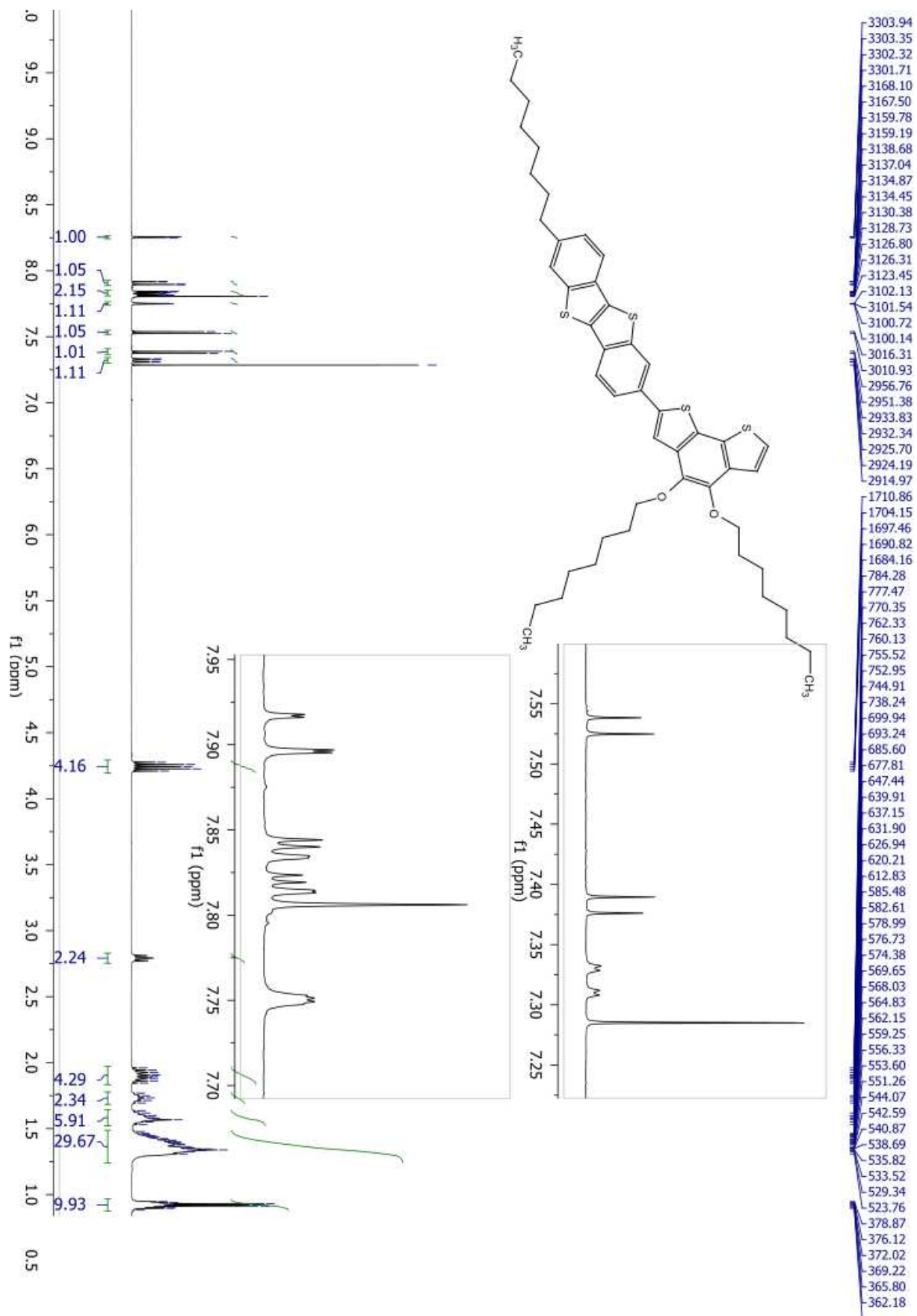
¹H NMR (400 MHz, CDCl₃) δ 8.25 (dd, J = 1.6, 0.6 Hz, 1H), 7.91 (dd, J = 8.3, 0.6 Hz, 1H), 7.83 (ddd, J = 8.1, 3.1, 1.1 Hz, 2H), 7.81 (s, 1H), 7.75 (dd, J = 1.4, 0.6 Hz, 1H), 7.53 (d, J = 5.4 Hz, 1H), 7.38 (d, J = 5.4 Hz, 1H), 7.32 (dd, J = 8.1, 1.5 Hz, 1H), 4.24 (dt, J = 13.3, 6.7 Hz, 4H), 2.88 – 2.74 (m, 2H), 1.99 – 1.81 (m, 4H), 1.77 – 1.69 (m, 2H), 1.64 – 1.52 (m, 6H), 1.49 – 1.27 (m, 30H), 0.96 – 0.89 (m, 10H). ¹³C NMR (101 MHz, CDCl₃) δ 143.75, 143.33, 142.98, 142.77, 142.03, 140.69, 135.34, 134.55, 134.24, 132.93, 132.45, 131.04, 130.96, 128.96, 128.66, 126.06, 124.35, 123.50, 123.39, 122.09, 121.69, 121.45, 121.34, 117.68, 74.42, 74.39, 36.17, 31.90, 31.87, 31.69, 30.50, 29.50, 29.39, 29.33, 29.27, 26.24, 22.68, 14.12.

2.7. EXPERIMENTAL PART

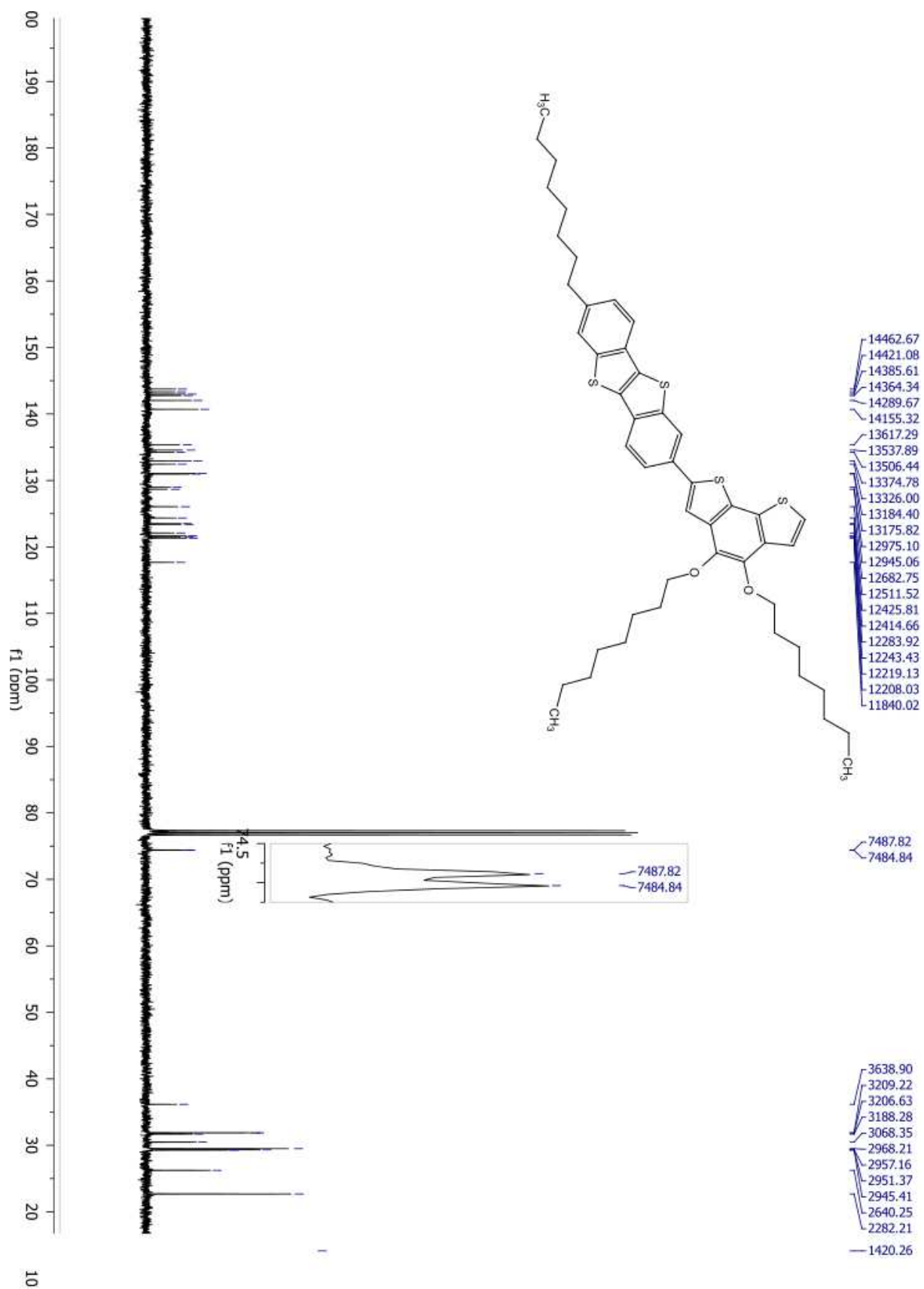




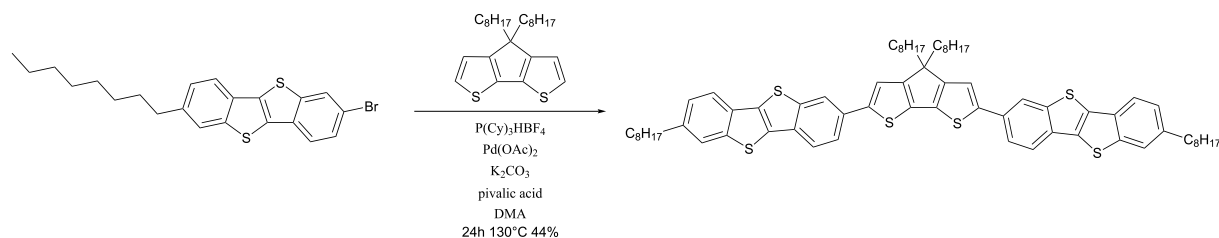
2.7. EXPERIMENTAL PART



CHAPTER 2. THE CHEMISTRY OF BTBT DERIVATIVES: CHALLENGES AND NEW DERIVATIVES



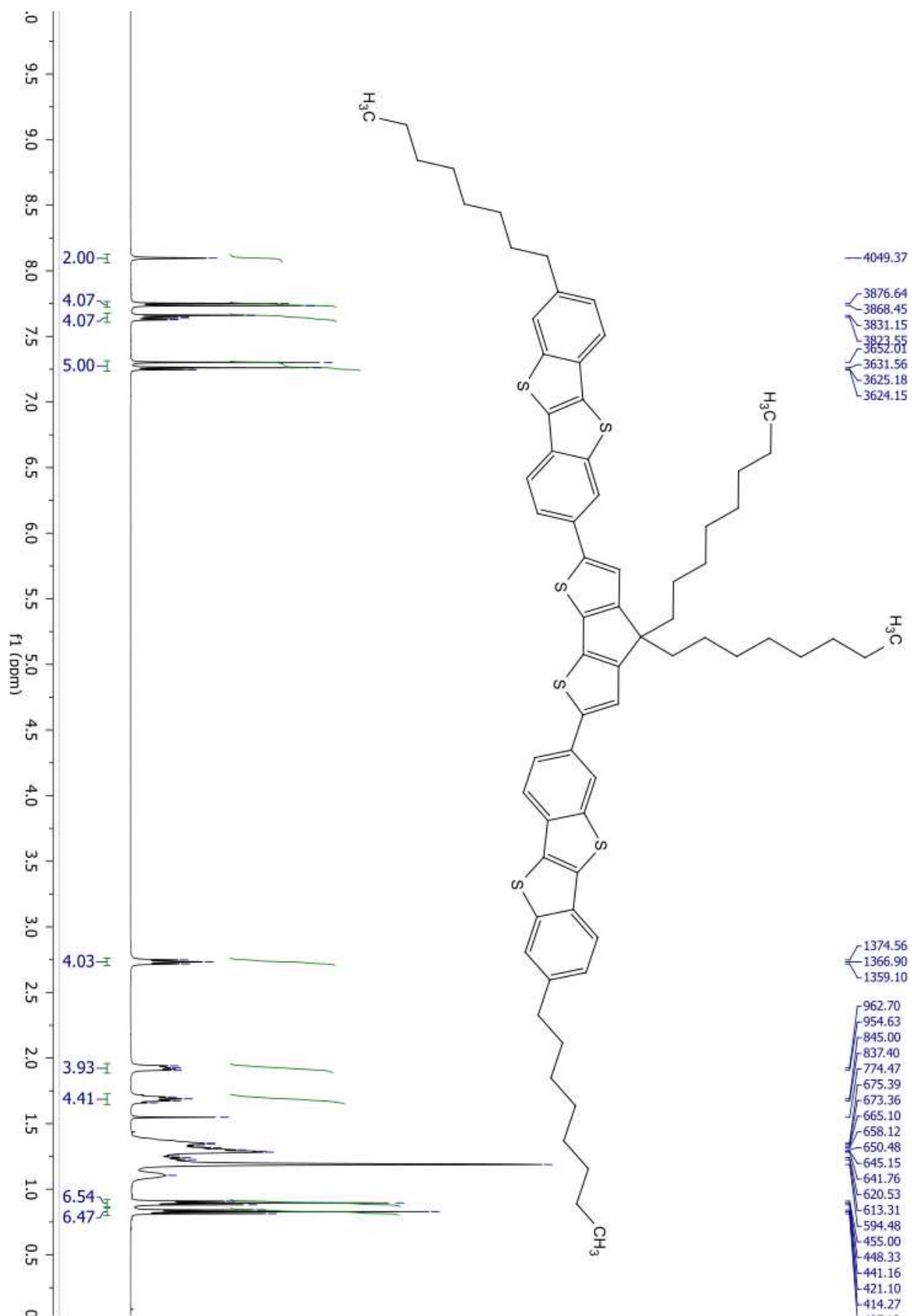
2.7.17 Synthesis of 7,7'-(4,4-dioctyl-4H-cyclopenta[1,2-b:5,4-b']dithiophene-2,6-diyl)bis(2-octylbenzo[b]benzo[4,5]thieno[2,3-d]thiophene) (18)



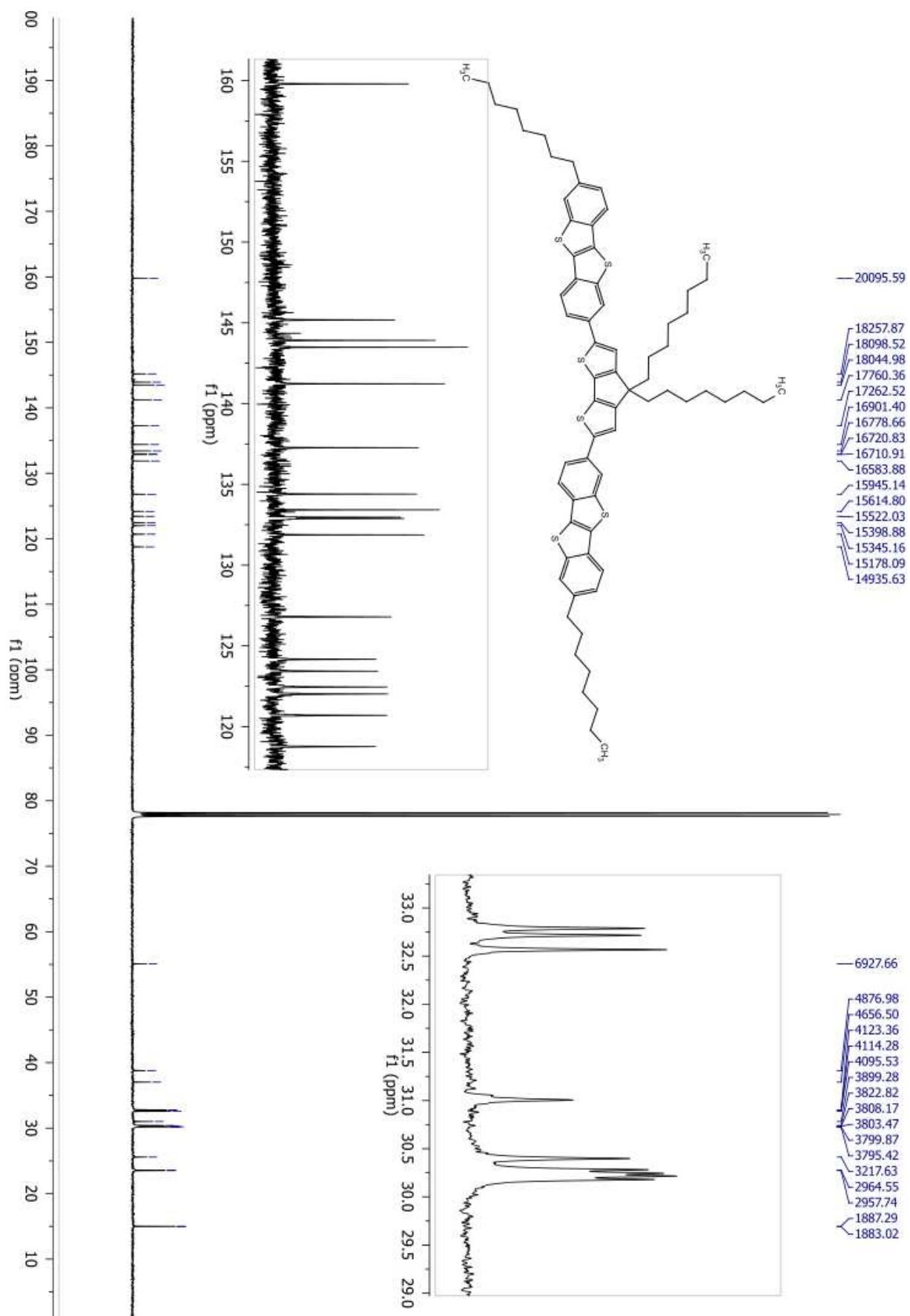
7-Octyl-2-bromo-benzo[b]benzo[4,5]thieno[2,3-d]thiophene (1.154 g, 2.677 mmol), K₂CO₃ (0.515g, 3.725 mmol), Pd(OAc)₂ (11.20 mg, 0.04988 mmol), PCy₃ · HBF₄ (37.02 mg, 0.1005 mmol), and pivalic acid (76.34 mg, 0.7475 mmol) were weighed to air and placed in a screw-cap pressure tube with a magnetic stir bar. The tube was placed in glovebox under argon atmosphere, N,N-Dimethylacetamide (8.8 ml) and 4,5-Bis(Octyloxy)Benzo[2,1-B;3,4-B']dithiophene were added (0.430 g, 0.963 mmol). The tube was sealed in glovebox and extracted from the box. The reaction mixture was then vigorously stirred at 130 °C for 24h. The reaction mixture was then cooled to rt, diluted with dichloromethane. Inorganic salts were removed by filtration. The solution was washed with water (3x100 ml) and brine (2 x 50 ml), dried over magnesium sulfate, filtered, and evaporated under reduced pressure. The most part of residue N,N-Dimethylacetamide was removed by distillation with Claisen apparatus. The crude product was suspended in water, filtered and dried under vacuum at 70°C for 12h. The product was purified by two silica gel column chromatography as eluent a mixture of cyclohexane and chloroform (8:2) for the first column and only cyclohexane for the second column to afford 7,7'-(4,4-dioctyl-4H-cyclopenta[1,2-b:5,4-b']dithiophene-2,6-diyl)bis(2-octylbenzo[b]benzo[4,5]thieno[2,3-d]thiophene) as red solid (605.15 mg, 0.5482 mmol, 44%).

¹H NMR (500 MHz, CDCl₃) δ 8.10 (s, 1H), 7.74 (d, J = 8.2 Hz, 2H), 7.67 – 7.62 (m, 2H), 7.30 (s, 1H), 7.28 – 7.23 (m, 2H), 2.73 (t, J = 7.7 Hz, 2H), 1.96 – 1.89 (m, 2H), 1.69 (dt, J = 15.4, 7.7 Hz, 2H), 1.55 (s, 1H), 1.41 – 1.06 (m, 26H), 0.90 (t, J = 6.9 Hz, 4H), 0.83 (t, J = 7.0 Hz, 3H). ¹³C NMR (126 MHz, CDCl₃) δ 159.80, 145.18, 144.35, 143.92, 143.49, 141.23, 137.27, 134.40, 133.42, 132.96, 132.88, 131.87, 126.79, 124.17, 123.43, 122.45, 122.02, 120.69, 118.77, 55.09, 38.78, 37.03, 32.79, 32.72, 32.57, 31.01, 30.40, 30.28, 30.24, 30.22, 30.18, 25.59, 23.57, 23.52, 15.01, 14.97.

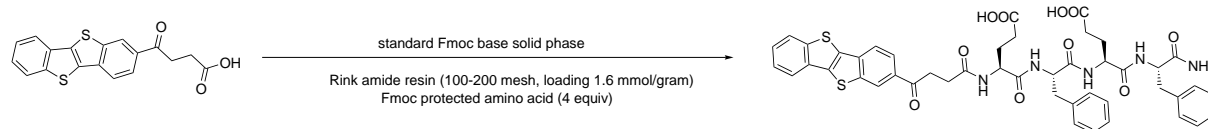
CHAPTER 2. THE CHEMISTRY OF BTBT DERIVATIVES: CHALLENGES AND NEW DERIVATIVES



2.7. EXPERIMENTAL PART

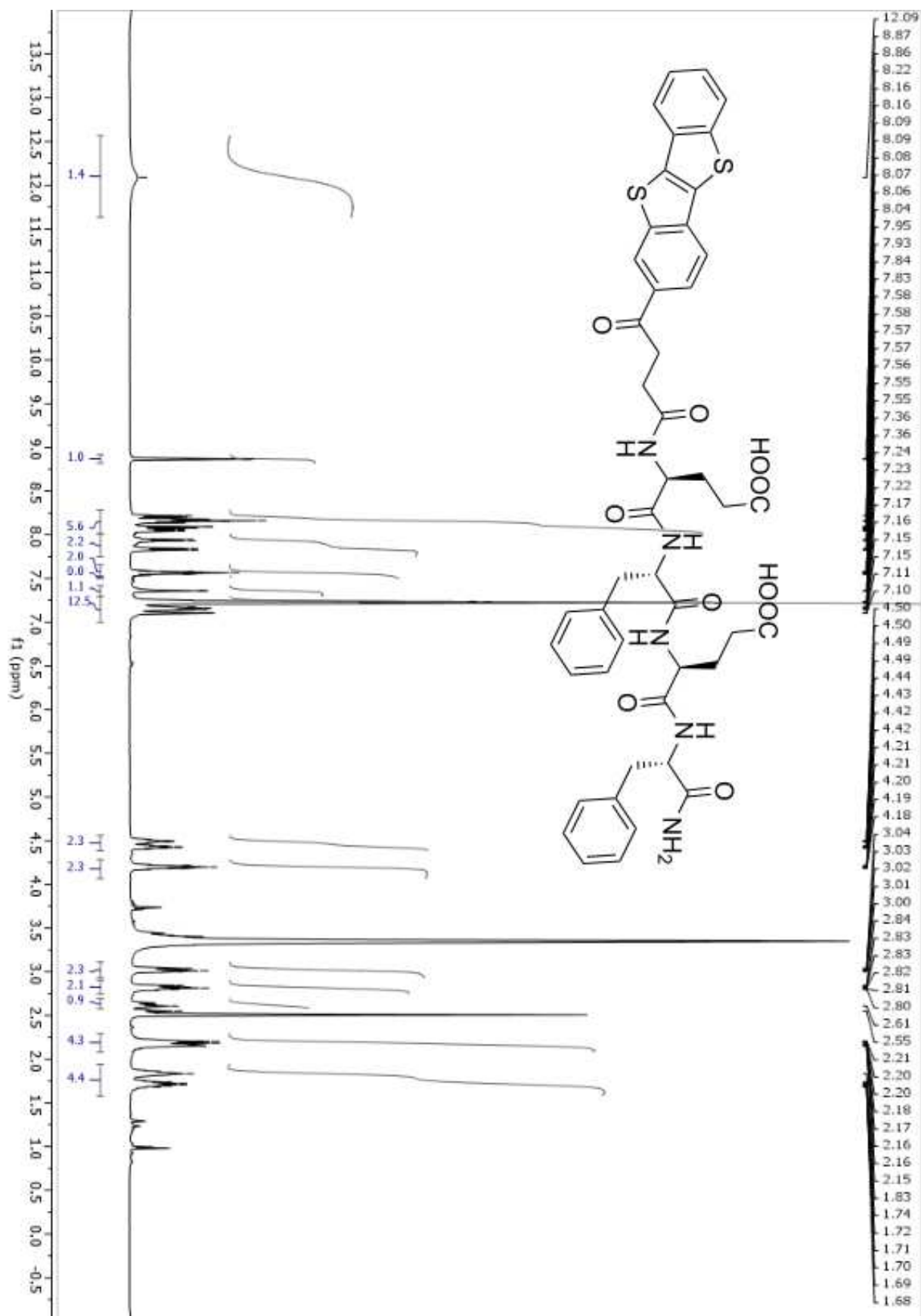


2.7.18 Synthesis of [1]benzothieno[3,2-b][1]benzothiophene-peptide (19)

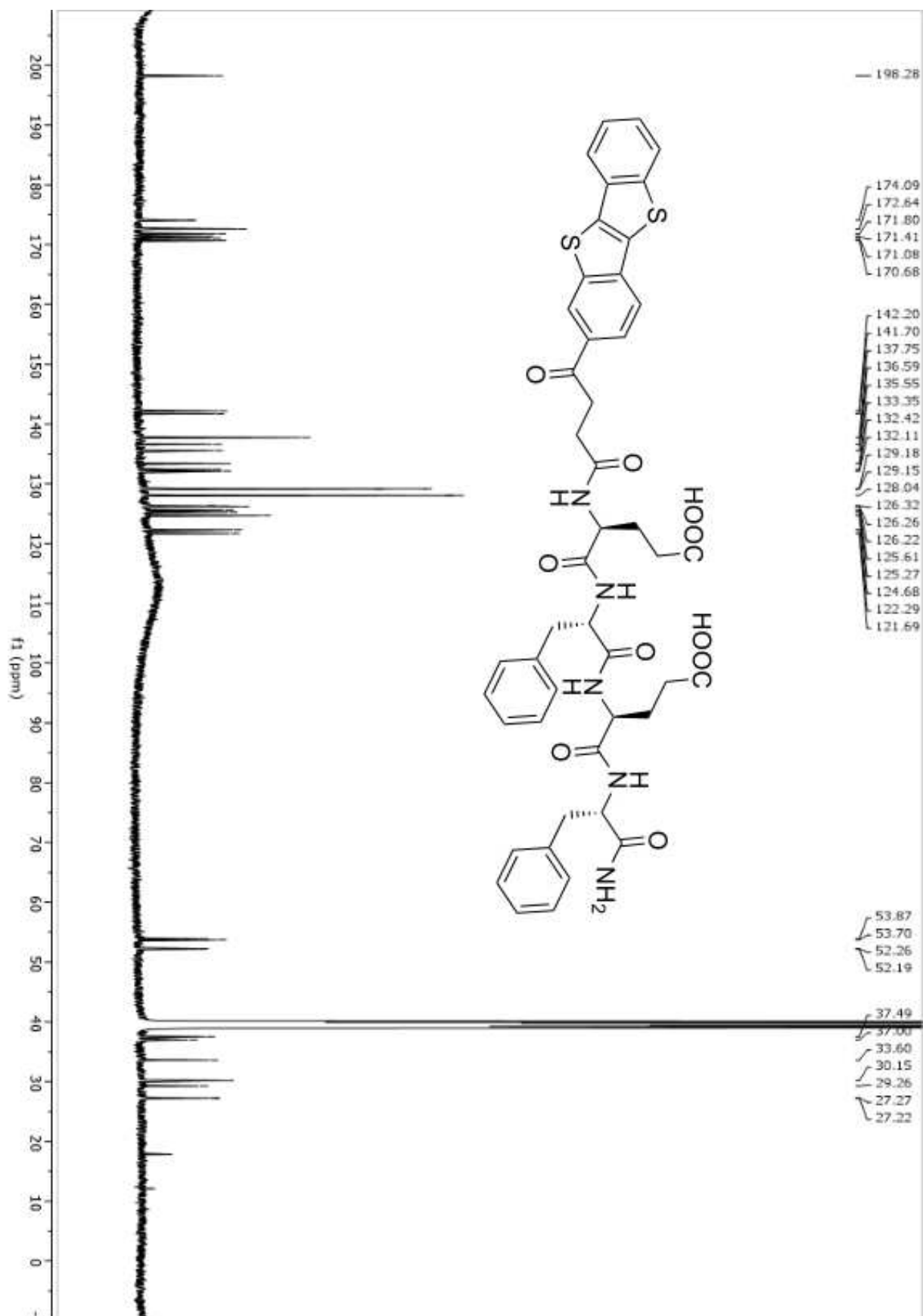


SPPS-General procedure Peptides were synthesized using standard solid phase 9-fluorenylmethoxycarbonyl (Fmoc) chemistry on Rink amide resin. When not in use the resin was dried and stored at 0 °C. Equipment SPPS was performed manually in a standard vessel for manual SPPS equipped with a glass frit (G2) and two outlets. Stirring was achieved by bubbling nitrogen from below. A washing step implies 1 min of stirring and then removal of solvent. In general, 10 mL of solvent must be used for 1 gram of resin. Preparation of the resin 1. 2 gram of resin was dump into a reaction vessel for SPPS 2. 30 mL of DMF were added for resin swelling and stirred gently for 30 min. 3. The solvent was removed and the resin was washed with DCM (2 x 20 mL) Attachment of the first Amino Acid 4. A solution of the Fmoc protected amino acid (4 equiv) in DCM (10 mL) was prepared in a vial. Then, DIPEA (12 equiv) was added and the resulting solution was added to the resin and stirred for 3 hours. 5. The solvent was removed and a mixture of DCM: methanol: DIPEA 17:2:1 (10 mL) was added to the resin and stirred for 10 min. The process was repeated twice. 6. The solvent was removed and the resin was washed with DCM (3 x 20 mL), DMF (2 x 20 mL) Fmoc deprotection and coupling 7. A 20% solution of piperidine in DMF (10 mL per gram of resin) was added to the resin and stirred for 20 min. 8. The solvent was removed and step 7 was repeated 9. The solvent was removed and the resin was washed with DMF (3 x 20 mL), DCM (3 x 20 mL) and DMF (2 x 20 mL) 10. A solution of the corresponding Fmoc-protected amino acid (4 equiv), HOBT (3.9 equiv) and HBTU (3.9 equiv) in DMF (final concentration 0.3-0.5 M) was prepared in a vial. Then, DIPEA (12 equiv) was added and the resulting solution was added to the resin and stirred for 2 hours. When BTBT was used the coupling was performed using 1.5 equiv of BTBT, 1.45 equiv of HBTU and HOBT and 4.5 equiv of DIPEA. 11. The solvent was removed and the resin was washed with DMF (3 x 20 mL), DCM (3 x 20 mL) and DMF (2 x 20 mL). 13. At this point the success of the reaction can be checked using the Kaiser test. If necessary, the coupling (step 10) was repeated. 14. At this point a stop in the synthesis may be done. In this case the resin should be washed with DCM, dried under nitrogen flow and stored at 0°C. The resin should be brought to room temperature and swelled again prior to use. Cleavage with TFA/ DCM 15. The resin was swelled with DCM 16. A solution of 3% TFA in dry DCM was added to the resin and stirred for 5 minutes. The solvents were collected in a flask and the process was repeated 5 times. 17. Solvents collected were concentrated in rotavapor (a potassium hydroxide trap was used) to the half. DCM was added and the volatiles were evaporated again. The process was repeated 3 times, after which the solvents were evaporated to dryness. 18. The product was precipitated from diethyl ether and lyophilized .

2.7. EXPERIMENTAL PART



CHAPTER 2. THE CHEMISTRY OF BTBT DERIVATIVES: CHALLENGES AND NEW DERIVATIVES



Bibliography

- [1] Lilienfeld, J. E. *METHOD AND APPARATUS FOR CONTROLLING ELECTRIC CURRENTS*, **1930**.
- [2] *The Nobel Prize in Physics 1956*. NobelPrize.org.
- [3] Moore, G. *No exponential is forever: but "Forever" can be delayed! [semiconductor industry]*, vol. 1. pp. 20–23. ISBN 0-7803-7707-9.
- [4] Hall, S., Nazarov, A., and Lysenko, V. *Nanoscaled Semiconductor-on-Insulator Structures and Devices*. **2006**. ISBN 9781402063787.
- [5] Nisato, G., Lupo, D., and Ganz, S. *Organic and Printed Electronics*. Pan Stanford, **2016**. ISBN 978-981-4669-74-0.
- [6] Kaltenbrunner, M., Sekitani, T., Reeder, J., Yokota, T., Kuribara, K., Tokuhara, T., Drack, M., Schwödiauer, R., Graz, I., Bauer-Gogonea, S., Bauer, S., and Someya, T. *Nature* **2013**, *499*, 458–463. doi: 10.1038/nature12314.
- [7] Arias, A. C., MacKenzie, J. D., McCulloch, I., Rivnay, J., and Salleo, A. *Chemical Reviews* **2010**, *110*, 3–24. doi: 10.1021/cr900150b.
- [8] Forrest, J. and Thompson, M. *Chemical Reviews* **2007**, *107*, 923–925. doi: 10.4324/9780203830734.
- [9] Guo, X., Facchetti, A., and Marks, T. J. *Chemical Reviews* **2014**, *114*, 8943–9012. doi: 10.1021/cr500225d.
- [10] Klauk, H. *Device Research Conference - Conference Digest, DRC* **2012**, , 237–238doi: 10.1109/DRC.2012.6256946.
- [11] Zhang, X., Zhang, J., Zhang, W., and Hou, X. *Journal of Materials Science: Materials in Electronics* **2010**, *21*, 671–675. doi: 10.1007/s10854-009-9975-3.
- [12] Shockley, W. **1952**, , 1365–1376.
- [13] Newman, C. R., Frisbie, C. D., Da Silva Filho, D. A., Brédas, J. L., Ewbank, P. C., and Mann, K. R. *Chemistry of Materials* **2004**, *16*, 4436–4451. doi: 10.1021/cm049391x.
- [14] Dimitrakopoulos, C. D. and Malenfant, P. R. *Advanced Materials* **2002**, *14*, 99–117. doi: 10.1002/1521-4095(20020116)14:2;99::AID-ADMA99;3.0.CO;2-9.
- [15] Deen, M. J., Kazemeini, M. H., and Holdcroft, S. *Journal of Applied Physics* **2008**, *103*. doi: 10.1063/1.2942400.
- [16] Paterson, A. F., Singh, S., Fallon, K. J., Hodsdon, T., Han, Y., Schroeder, B. C., Bronstein, H., Heeney, M., McCulloch, I., and Anthopoulos, T. D. *Advanced Materials* **2018**, *1801079*, 1–33. doi: 10.1002/adma.201801079.
- [17] Tsumura, A., Koezuka, H., and Ando, T. *Applied Physics Letters* **1986**, *49*, 1210–1212. doi: 10.1063/1.97417.

BIBLIOGRAPHY

- [18] Assadi, A., Svensson, C., Willander, M., and Inganäs, O. *Applied Physics Letters* **1988**, *53*, 195–197. doi: 10.1063/1.100171.
- [19] Zhang, W. and Yu, G. *Organic Optoelectronic Materials*, vol. 91. **2015**. ISBN 978-3-319-16861-6.
- [20] Giri, G., Verploegen, E., Mannsfeld, S. C. B., Atahan-Evrenk, S., Kim, D. H., Lee, S. Y., Becerril, H. A., Aspuru-Guzik, A., Toney, M. F., and Bao, Z. *Nature* **2011**, *480*, 504–508. doi: 10.1038/nature10683.
- [21] Berrouard, P., Najari, A., Pron, A., Gendron, D., Morin, P. O., Pouliot, J. R., Veilleux, J., and Leclerc, M. *Angewandte Chemie - International Edition* **2012**, *51*, 2068–2071. doi: 10.1002/anie.201106411.
- [22] Chu, C. W., Li, S. H., Chen, C. W., Shrotriya, V., and Yang, Y. *Applied Physics Letters* **2005**, *87*, 1–3. doi: 10.1063/1.2126140.
- [23] Chen, F.-C., Kung, L.-J., Chen, T.-H., and Lin, Y.-S. *Applied Physics Letters* **2007**, *90*, 073504. doi: 10.1063/1.2535741.
- [24] Pang, S., Tsao, H. N., Feng, X., and Mullen, K. *Advanced Materials* **2009**, *21*, 3488–3491. doi: 10.1002/adma.200803812.
- [25] Jesper, M., Alt, M., Schinke, J., Hillebrandt, S., Angelova, I., Rohnacher, V., Pucci, A., Lemmer, U., Jaegermann, W., Kowalsky, W., Glaser, T., Mankel, E., Lovrincic, R., Golling, F., Hamburger, M., and Bunz, U. H. F. *Langmuir* **2015**, *31*, 10303–10309. doi: 10.1021/acs.langmuir.5b02316.
- [26] Cheng, X., Noh, Y. Y., Wang, J., Tello, M., Frisch, J., Blum, R. P., Vollmer, A., Rabe, J. P., Koch, N., and Sirringhaus, H. *Advanced Functional Materials* **2009**, *19*, 2407–2415. doi: 10.1002/adfm.200900315.
- [27] Chen, F. C. and Liao, C. H. *Applied Physics Letters* **2008**, *93*, 2006–2009. doi: 10.1063/1.2980421.
- [28] Kumaki, D., Yahiro, M., Inoue, Y., and Tokito, S. *Applied Physics Letters* **2007**, *90*, 2005–2008. doi: 10.1063/1.2717552.
- [29] de Leeuw, D., Simenon, M., Brown, A., and Einerhand, R. *Synthetic Metals* **1997**, *87*, 53–59. doi: 10.1016/S0379-6779(97)80097-5.
- [30] Brown, A. R., de Leeuw, D. M., Lous, E. J., and Havinga, E. E. *Synthetic Metals* **1994**, *66*, 257–261. doi: 10.1016/0379-6779(94)90075-2.
- [31] Bromley, S. T., Mas-Torrent, M., Hadley, P., and Rovira, C. *Journal of the American Chemical Society* **2004**, *126*, 6544–6545. doi: 10.1021/ja049762a.
- [32] Würthner, F. and Schmidt, R. *ChemPhysChem* **2006**, *7*, 793–797. doi: 10.1002/cphc.200600078.
- [33] Dong, H., Wang, C., and Hu, W. *Chemical Communications* **2010**, *46*, 5211–5222. doi: 10.1039/c0cc00947d.

- [34] Moon, H., Zeis, R., Borkent, E. J., Besnard, C., Lovinger, A. J., Siegrist, T., Kloc, C., and Bao, Z. *Journal of the American Chemical Society* **2004**, *126*, 15322–15323. doi: 10.1021/ja045208p.
- [35] Wang, C., Dong, H., Hu, W., Liu, Y., and Zhu, D. *Chemical Reviews* **2012**, *112*, 2208–2267. doi: 10.1021/cr100380z.
- [36] Salleo, A. *Materials Today* **2007**, *10*, 38–45. doi: 10.1016/S1369-7021(07)70018-4.
- [37] Henson, Z. B., Müllen, K., and Bazan, G. C. *Nature Chemistry* **2012**, *4*, 699–704. doi: 10.1038/nchem.1422.
- [38] Kline, R. J., McGehee, M. D., Kadnikova, E. N., Liu, J., and Fréchet, J. M. J. *Advanced Materials* **2003**, *15*, 1519–1522. doi: 10.1002/adma.200305275.
- [39] Xu, Y., Sun, H., Liu, A., Zhu, H.-H., Li, W., Lin, Y.-F., and Noh, Y.-Y. *Advanced Materials* **2018**, *1801830*, 1801830. doi: 10.1002/adma.201801830.
- [40] Facchetti, A. *Materials Today* **2007**, *10*, 28–37. doi: 10.1016/S1369-7021(07)70017-2.
- [41] Mei, J., Diao, Y., Appleton, A. L., Fang, L., and Bao, Z. **2013**, *18*, 6724–6746.
- [42] Meng, H., Bao, Z., Lovinger, A. J., Wang, B. C., and Muzicek, A. M. *Journal of the American Chemical Society* **2001**, *123*, 9214–9215. doi: 10.1021/ja016525o.
- [43] Takimiya, K., Ebata, H., Sakamoto, K., Izawa, T., Otsubo, T., and Kunugi, Y. *Journal of the American Chemical Society* **2006**, *128*, 12604–12605. doi: 10.1021/ja064052l.
- [44] Ebata, H., Izawa, T., Miyazaki, E., Takimiya, K., Ikeda, M., Kuwabara, H., and Yui, T. *Journal of the American Chemical Society* **2007**, *129*, 15732–15733. doi: 10.1021/ja074841i.
- [45] Kosata, B., Kozmik;Vaclav, Svoboda;Jiri, Novotna;Vladimira, Vanek;Premysl, and Glogarova;milada. *Liquid Crystals* **2003**, *30*, 603–610. doi: 10.1080/0267829031000097484.
- [46] Košata, B., Kozmík, V., and Svoboda, J. *Collection of Czechoslovak Chemical Communications* **2002**, *67*, 645–664. doi: 10.1135/cccc20020645.
- [47] Cornil, J., Calbert, J. P., Beljonne, D., Silbey, R., and Brédas, J. L. *Advanced Materials* **2000**, *12*, 978–983. doi: 10.1002/1521-4095(200006)12:13;978::AID-ADMA978;3.0.CO;2-S.
- [48] Cornil, J., Calbert, J. P., and Brédas, J. L. *Journal of the American Chemical Society* **2001**, *123*, 1250–1251. doi: 10.1021/ja005700i.
- [49] Cornil, B. J., Beljonne, D., Calbert, J.-p., Brødas, J.-l., Cornil, J., Beljonne, D., Calbert, J.-p., and Brédas, J.-L. *Advanced Materials* **2001**, *13*, 1053–1067. doi: 10.1002/1521-4095(200107)13:14;1053::AID-ADMA1053;3.0.CO;2-7.

BIBLIOGRAPHY

- [50] Soeda, J., Hirose, Y., Yamagishi, M., Nakao, A., Uemura, T., Nakayama, K., Uno, M., Nakazawa, Y., Takimiya, K., and Takeya, J. *Advanced Materials* **2011**, *23*, 3309–3314. doi: 10.1002/adma.201101027.
- [51] Minemawari, H., Yamada, T., Matsui, H., Tsutsumi, J. Y., Haas, S., Chiba, R., Kumai, R., and Hasegawa, T. *Nature* **2011**, *475*, 364–367. doi: 10.1038/nature10313.
- [52] Tung, H. H., Paul, E. L., Midler, M., and McCauley, J. A. *Crystallization of Organic Compounds: An Industrial Perspective*. **2008**. ISBN 9780471467809.
- [53] Rigas, G. P., Payne, M. M., Anthony, J. E., Horton, P. N., Castro, F. A., and Shkunov, M. *Nature Communications* **2016**, *7*, 1–8. doi: 10.1038/ncomms13531.
- [54] Matsushima, T., Sandanayaka, A. S. D., Esaki, Y., and Adachi, C. *Scientific Reports* **2015**, *5*, 1–9. doi: 10.1038/srep14547.
- [55] Schweicher, G., Lemaire, V., Niebel, C., Ruzié, C., Diao, Y., Goto, O., Lee, W. Y., Kim, Y., Arlin, J. B., Karpinska, J., Kennedy, A. R., Parkin, S. R., Olivier, Y., Mannsfeld, S. C., Cornil, J., Geerts, Y. H., and Bao, Z. *Advanced Materials* **2015**, *27*, 3066–3072. doi: 10.1002/adma.201500322.
- [56] Amin, A. Y., Khassanov, A., Reuter, K., Meyer-Friedrichsen, T., and Halik, M. *Journal of the American Chemical Society* **2012**, *134*, 16548–16550. doi: 10.1021/ja307802q.
- [57] Panidi, J., Paterson, A. F., Khim, D., Fei, Z., Han, Y., Tsetseris, L., Vourlias, G., Patsalas, P. A., Heeney, M., and Anthopoulos, T. D. *Advanced Science* **2018**, *5*, 1–10. doi: 10.1002/advs.201700290.
- [58] Paterson, A. F., Treat, N. D., Zhang, W., Fei, Z., Wyatt-Moon, G., Faber, H., Vourlias, G., Patsalas, P. A., Solomeshch, O., Tessler, N., Heeney, M., and Anthopoulos, T. D. *Advanced Materials* **2016**, *28*, 7791–7798. doi: 10.1002/adma.201601075.
- [59] Paterson, A. F., Lin, Y.-H., Mottram, A. D., Fei, Z., Niazi, M. R., Kirmani, A. R., Amassian, A., Solomeshch, O., Tessler, N., Heeney, M., and Anthopoulos, T. D. *Advanced Electronic Materials* **2017**, *1700464*, 1700464. doi: 10.1002/aelm.201700464.
- [60] Kwon, S., Kim, J., Kim, G., Yu, K., Jo, Y. R., Kim, B. J., Kim, J., Kang, H., Park, B., and Lee, K. *Advanced Materials* **2015**, *27*, 6870–6877. doi: 10.1002/adma.201502980.
- [61] Takimiya, K., Osaka, I., Mori, T., and Nakano, M. *Accounts of Chemical Research* **2014**, *47*, 1493–1502. doi: 10.1021/ar400282g.
- [62] Lino, H., Usui, T., Kobori, T., and Hanna, J.-I. *SID Symposium Digest of Technical Papers* **2012**, *43*, 497–500. doi: 10.1002/j.2168-0159.2012.tb05826.x.
- [63] Yamamoto, T. and Takimiya, K. *Journal of the American Chemical Society* **2007**, *129*, 2224–2225. doi: 10.1021/ja068429z.
- [64] Horton, A. W. **1949**, , 1946–1948.

- [65] Haristoy, D., Mery, S., Heinrich, B., Mager, L., Nicoud, J. F., and Guillon, D. *Liquid Crystals* **2000**, *27*, 321–328. doi: 10.1080/026782900202769.
- [66] Kaszynski, P. and Dougherty, D. A. **1993**, , 5209–5220.
- [67] Zherdeva, S. Y., Zheltov, A. Y., Kozik, T., and Stepanov, B. I. *Zhurnal Organicheskoi Khimii* **1980**, *16*, 425 – 429.
- [68] Ruzie, C., Karpinska, J., Kennedy, A. R., and Geerts, Y. H. *Journal of Organic Chemistry* **2013**, *78*, 7741–7748. doi: 10.1021/jo401134c.
- [69] Saito, M., Osaka, I., Miyazaki, E., Takimiya, K., Kuwabara, H., and Ikeda, M. *Tetrahedron Letters* **2011**, *52*, 285–288. doi: 10.1016/j.tetlet.2010.11.021.
- [70] Sashida, H. and Yasuike, S. *Journal of Heterocyclic Chemistry* **1998**, *35*, 725–726. doi: 10.1002/jhet.5570350337.
- [71] Choi, K. S., Sawada, K., Dong, H., Hoshino, M., and Nakayama, J. **1994**, *38*, 143–149.
- [72] Mori, T., Nishimura, T., Yamamoto, T., Doi, I., Miyazaki, E., Osaka, I., and Takimiya, K. *Journal of the American Chemical Society* **2013**, *135*, 13900–13913. doi: 10.1021/ja406257u.
- [73] Vásquez-Céspedes, S., Ferry, A., Candish, L., and Glorius, F. *Angewandte Chemie - International Edition* **2015**, *54*, 5772–5776. doi: 10.1002/anie.201411997.
- [74] Minami, S., Hirano, K., Satoh, T., and Miura, M. *Tetrahedron Letters* **2014**, *55*, 4175–4177. doi: 10.1016/j.tetlet.2014.05.084.
- [75] Chen, S., Wang, M., and Jiang, X. *Chinese Journal of Chemistry* **2018**, *36*, 921–924. doi: 10.1002/cjoc.201800242.
- [76] Varonkov, M. and Undre, V. *Khim.Gaterosikl. Seodin.* **1966**, , 4791.
- [77] Khalily, M. A., Usta, H., Ozdemir, M., Bakan, G., Dikecoglu, F. B., Edwards-Gayle, C., Hutchinson, J. A., Hamley, I. W., Dana, A., and Guler, M. O. *Nanoscale* **2018**, *10*, 9987–9995. doi: 10.1039/c8nr01604f.
- [78] Higashino, T., Ueda, A., Yoshida, J., and Mori, H. *Chemical Communications* **2017**, *53*, 3426–3429. doi: 10.1039/c7cc00784a.
- [79] Roche, G. H., Tsai, Y. T., Clevers, S., Thuau, D., Castet, F., Geerts, Y. H., Moreau, J. J., Wantz, G., and Dautel, O. J. *Journal of Materials Chemistry C* **2016**, *4*, 6742–6749. doi: 10.1039/c6tc01814a.
- [80] Milstein, D. and Stille, J. K. *Journal of Organic Chemistry* **1978**, *44*, 1613–1618. doi: 10.1021/jo01324a006.
- [81] Carsten, B., He, F., Son, H. J., Xu, T., and Yu, L. *Chemical Reviews* **2011**, *111*, 1493–1528. doi: 10.1021/cr100320w.
- [82] Miyaura, N. A. S. *J. Chem. Soc., Chem. Comm.* **1979**, , 866–867doi: 10.1039/C39790000866.

BIBLIOGRAPHY

- [83] Sakamoto, J., Rehahn, M., Wegner, G., and Schlüter, A. D. *Macromolecular Rapid Communications* **2009**, *30*, 653–687. doi: 10.1002/marc.200900063.
- [84] Johansson Seechurn, C. C., Kitching, M. O., Colacot, T. J., and Snieckus, V. *Angewandte Chemie - International Edition* **2012**, *51*, 5062–5085. doi: 10.1002/anie.201107017.
- [85] Tamao, K., Sumitani, K., and Kumada, M. *Journal of the American Chemical Society* **1972**, *94*, 4374–4376. doi: 10.1021/ja00767a075.
- [86] Tasker, S. Z., Standley, E. A., and Jamison, T. F. *Nature* **2014**, *509*, 299–309. doi: 10.1038/nature13274.
- [87] Xu, S., Kim, E. H., Wei, A., and Negishi, E.-i. *Science and Technology of Advanced Materials* **2014**, *15*, 044201. doi: 10.1088/1468-6996/15/4/044201.
- [88] Ackermann, L., Vicente, R., and Kapdi, A. R. *Angewandte Chemie - International Edition* **2009**, *48*, 9792–9826. doi: 10.1002/anie.200902996.
- [89] Nitti, A., Signorile, M., Boiocchi, M., Bianchi, G., Po, R., and Pasini, D. *Journal of Organic Chemistry* **2016**, *81*, 11035–11042. doi: 10.1021/acs.joc.6b01922.
- [90] Nitti, A., Po, R., Bianchi, G., and Pasini, D. *Molecules* **2017**, *22*. doi: 10.3390/molecules22010021.
- [91] Nitti, A., Debattista, F., Abbondanza, L., Bianchi, G., Po, R., and Pasini, D. *Journal of Polymer Science, Part A: Polymer Chemistry* **2017**, *55*, 1601–1610. doi: 10.1002/pola.28532.
- [92] Lessene, G. and Feldman, K. S. *Oxidative Aryl-Coupling Reactions in Synthesis*, chap. 14. **2002**, pp. 479–535. ISBN 3527304894.
- [93] Gorelsky, S. I. *Organometallics* **2012**, *31*, 4631–4634. doi: 10.1021/om300230b.
- [94] Wakioka, M., Nakamura, Y., Wang, Q., and Ozawa, F. **2012**, .
- [95] Lapointe, D. and Fagnou, K. *Chemistry Letters* **2010**, *39*, 1118–1126. doi: 10.1246/cl.2010.1118.
- [96] Balcells, D., Clot, E., and Eisenstein, O. *Chemical Reviews* **2010**, *110*, 749–823. doi: 10.1021/cr900315k.
- [97] Sakaki, S., Kai, S., and Sugimoto, M. *Organometallics* **1999**, *18*, 4825–4837. doi: 10.1021/om990461x.
- [98] Gorelsky, S. I., Lapointe, D., and Fagnou, K. *Journal of the American Chemical Society* **2008**, *130*, 10848–10849.
- [99] Gorelsky, S. I., Lapointe, D., and Fagnou, K. *The Journal of organic chemistry* **2011**, *77*, 658–668.
- [100] Lafrance, M. and Fagnou, K. *Journal of the American Chemical Society* **2006**, *128*, 16496–16497.

- [101] Ackermann, L. and Metalation, I. **2011**, , 1315–1345.
- [102] Alberico, D., Scott, M. E., and Lautens, M. *Chemical Reviews* **2007**, *107*, 174–238. doi: 10.1021/cr0509760.
- [103] Colletto, C., Islam, S., Juliá-Hernández, F., and Larrosa, I. *Journal of the American Chemical Society* **2016**, *138*, 1677–1683. doi: 10.1021/jacs.5b12242.
- [104] Ueda, K., Yanagisawa, S., Yamaguchi, J., and Itami, K. *Angewandte Chemie - International Edition* **2010**, *49*, 8946–8949. doi: 10.1002/anie.201005082.
- [105] Wang, X., Wang, K., and Wang, M. *Polymer Chemistry* **2015**, *6*, 1846–1855. doi: 10.1039/c4py01627k.
- [106] Chang, S. W., Waters, H., Kettle, J., and Horie, M. *Organic Electronics: physics, materials, applications* **2012**, *13*, 2967–2974. doi: 10.1016/j.orgel.2012.08.023.
- [107] Matsidik, R., Martin, J., Schmidt, S., Obermayer, J., Lombeck, F., Nübling, F., Komber, H., Fazzi, D., and Sommer, M. *Journal of Organic Chemistry* **2015**, *80*, 980–987. doi: 10.1021/jo502432e.
- [108] Lombeck, F., Matsidik, R., Komber, H., and Sommer, M. *Macromolecular Rapid Communications* **2015**, *36*, 231–237. doi: 10.1002/marc.201400437.
- [109] Zhang, J., Chen, W., Rojas, A. J., Jucov, E. V., Timofeeva, T. V., Parker, T. C., Barlow, S., and Marder, S. R. *Journal of the American Chemical Society* **2013**, *135*, 16376–16379. doi: 10.1021/ja4095878.
- [110] He, C. Y., Wu, C. Z., Qing, F. L., and Zhang, X. *Journal of Organic Chemistry* **2014**, *79*, 1712–1718. doi: 10.1021/jo402675v.
- [111] Zhang, J., Parker, T. C., Chen, W., Williams, L. R., Khrustalev, V. N., Jucov, E. V., Barlow, S., Timofeeva, T. V., and Marder, S. R. *Journal of Organic Chemistry* **2016**, *81*, 360–370. doi: 10.1021/acs.joc.5b02551.
- [112] Kudrjasova, J., Kesters, J., Verstappen, P., Brebels, J., Vangerven, T., Cardinaletti, I., Drijkoningen, J., Penxten, H., Manca, J., Lutsen, L., Vanderzande, D., and Maes, W. *Journal of Materials Chemistry A* **2016**, *4*, 791–795. doi: 10.1039/c5ta09023g.
- [113] Liu, S. Y., Liu, W. Q., Xu, J. Q., Fan, C. C., Fu, W. F., Ling, J., Wu, J. Y., Shi, M. M., Jen, A. K. Y., and Chen, H. Z. *ACS Applied Materials and Interfaces* **2014**, *6*, 6765–6775. doi: 10.1021/am500522x.
- [114] Wang, S., Yang, J., Broch, K., Novák, J., Cao, X., Shaw, J., Tao, Y., Hu, Y., and Huang, W. *RSC Advances* **2016**, *6*, 57163–57173. doi: 10.1039/c6ra10832f.
- [115] Palai, A. K., Kumar, A., Sim, K., Kwon, J., Shin, T. J., Jang, S., Cho, S., Park, S. U., and Pyo, S. *New Journal of Chemistry* **2016**, *40*, 385–392. doi: 10.1039/c5nj02631h.
- [116] Liu, S. Y., Fu, W. F., Xu, J. Q., Fan, C. C., Jiang, H., Shi, M., Li, H. Y., Chen, J. W., Cao, Y., and Chen, H. Z. *Nanotechnology* **2014**, *25*. doi: 10.1088/0957-4484/25/1/014006.

BIBLIOGRAPHY

- [117] Lucarelli, J., Lessi, M., Manzini, C., Minei, P., Bellina, F., and Pucci, A. *Dyes and Pigments* **2016**, *135*, 154–162. doi: 10.1016/j.dyepig.2016.03.036.
- [118] Li, C. H., Kettle, J., and Horie, M. *Materials Chemistry and Physics* **2014**, *144*, 519–528. doi: 10.1016/j.matchemphys.2014.01.029.
- [119] Bohra, H., Shao, J., Huang, S., and Wang, M. *Tetrahedron Letters* **2016**, *57*, 1497–1501. doi: 10.1016/j.tetlet.2016.02.081.
- [120] McAfee, S. M., Topple, J. M., Payne, A. J., Sun, J. P., Hill, I. G., and Welch, G. C. *ChemPhysChem* **2015**, *16*, 1190–1202. doi: 10.1002/cphc.201402662.
- [121] Wang, X. and Wang, M. *Polymer Chemistry* **2014**, *5*, 5784–5792. doi: 10.1039/c4py00565a.
- [122] Huang, J., Wang, K., Gupta, S., Wang, G., Yang, C., Mushrif, S. H., and Wang, M. *Journal of Polymer Science, Part A: Polymer Chemistry* **2016**, *54*, 2015–2031. doi: 10.1002/pola.28068.
- [123] Niebel, C., Kim, Y., Ruzí, C., Karpinska, J., Chattopadhyay, B., Schweicher, G., Richard, A., Lemaure, V., Olivier, Y., Ome Cornil, E., Kennedy, A. R., Diao, Y., Lee, W.-Y., Mannsfeld, S., Bao, Z., and Geerts, Y. H. *J. Mater. Chem. C* **2015**, *3*, 674–685. doi: 10.1039/c4tc02158d.
- [124] Sun, K. and Cai, H. *Metaposition phosphinoxygen group substituted carbazole derivative and organic light emitting device with the derivative*, **2017**.
- [125] Minemawari, H., Inoue, S., Yamada, J., Tanaka, M., Hasegawa, T., and Sadamitsu, Y. *NOVEL CONDENSED POLYCYCLIC AROMATIC COMPOUND AND USE THEREFOR*, **2016**.
- [126] Vyas, V. S., Gutzler, R., Nuss, J., Kern, K., and Lotsch, B. V. *CrystEngComm* **2014**, *16*, 7389–7392. doi: 10.1039/c4ce00752b.
- [127] Bré Das, J. L., Calbert, J. P., Da, D. A., Filho, S., Cornil, J., and Heeger, A. J. **2002**, *99*, 5804–5809.
- [128] Sirringhaus, H., Friend, R. H., Li, X. C., Moratti, S. C., Holmes, A. B., and Feeder, N. *Applied Physics Letters* **1997**, *71*, 3871–3873. doi: 10.1063/1.120529.
- [129] Arroyave, F. a., Richard, C. a., and Reynolds, J. R. *Organic Letters* **2012**, *14*, 6138–6141. doi: 10.1021/ol302704v.
- [130] Lange, A., Krueger, H., Ecker, B., Tunc, A. V., Von Hauff, E., and Morana, M. *Journal of Polymer Science, Part A: Polymer Chemistry* **2012**, *50*, 1622–1635. doi: 10.1002/pola.25933.
- [131] Bianchi, G., Po, R., Sassi, M., Beverina, L., Chiaberge, S., Spera, S., and Cominetti, A. *ACS Omega* **2017**, *2*, 4347–4355. doi: 10.1021/acsomega.7b00987.
- [132] Arslan, E., Garip, I. C., Gulseren, G., Tekinay, A. B., and Guler, M. O. *Advanced healthcare materials* **2014**, *3*, 1357–1376.

- [133] Ekiz, M. S., Cinar, G., Khalily, M. A., and Guler, M. O. *Nanotechnology* **2016**, *27*, 402002.
- [134] Hosseinkhani, H., Hong, P.-D., and Yu, D.-S. *Chemical reviews* **2013**, *113*, 4837–4861.
- [135] Wei, G., Su, Z., Reynolds, N. P., Arosio, P., Hamley, I. W., Gazit, E., and Mezzenga, R. *Chemical Society Reviews* **2017**, *46*, 4661–4708.
- [136] Tovar, J. D. *Accounts of chemical research* **2013**, *46*, 1527–1537.
- [137] Ardon, H. A. M. and Tovar, J. D. *Bioconjugate chemistry* **2015**, *26*, 2290–2302.
- [138] Eakins, G. L., Pandey, R., Wojciechowski, J. P., Zheng, H. Y., Webb, J. E., Valéry, C., Thordarson, P., Plank, N. O., Gerrard, J. A., and Hodgkiss, J. M. *Advanced Functional Materials* **2015**, *25*, 5640–5649.
- [139] Khalily, M. A., Bakan, G., Kucukoz, B., Topal, A. E., Karatay, A., Yaglioglu, H. G., Dana, A., and Guler, M. O. *ACS nano* **2017**, *11*, 6881–6892.

Chapter 3

Green synthesis for molecular organic semiconductors

3.1 General introduction

Among the key challenge for Organic Printed Electronics (cap. 1), identified by OE-A, there are the cost and the scalability. OPE does not aim at substituting existing products but at creating different one's, yet costs have to be low in most cases. For some applications, such as rollable displays, a cost premium over conventional rigid displays may be accepted, while for other applications, for example, in packaging, low cost will be a major driving factor.¹ These challenges are linked also with the active materials: films deposition technique and their synthesis. In particular the development scalable and sustainable synthesis of organic semiconductors remain a key challenge. When moving from the Lab to the Fab environment, high performance is not enough to ensure successful technology transfer.² Active materials have to become available at the large scale and through sustainable processes. All hazards have to be minimized thus leaving little room for toxic and/or flammable solvents.³ Current state of the art printable materials are far from optimal on this respect.⁴ The processes leading to their synthesis are expensive and do not take into account established sustainability indexes like the E factor (kg of organic waste/kg of product).⁵ In general in order to achieve the development of more sustainable and scalable Organic Semiconductor synthesis the 12 principles⁶ of green chemistry listed below must be taken into account. The concept of Green Chemistry was born in 1991 with the launch of the Green Chemistry Program by the United States Environmental Protection Agency (EPA). Aim of the program was “to promote the research, development, and implementation of innovative chemical technologies that accomplish pollution prevention in both a scientifically sound and cost-effective manner”.⁷

1. **Prevention** : It is better to prevent waste than to treat or clean up waste after it has been created.
2. **Atom Economy**: Synthetic methods should be designed to maximize the incorporation of all materials used in the process into the final product.
3. **Less Hazardous Chemical**: Syntheses Wherever practicable, synthetic methods should be designed to use and generate substances that possess little or no toxicity to human health and the environment.

4. **Designing Safer Chemicals:** Chemical products should be designed to affect their desired function while minimizing their toxicity.
5. **Safer Solvents and Auxiliaries:** The use of auxiliary substances (e.g., solvents, separation agents, etc.) should be made unnecessary wherever possible and innocuous when used.
6. **Design for Energy Efficiency:** Energy requirements of chemical processes should be recognized for their environmental and economic impacts and should be minimized. If possible, synthetic methods should be conducted at ambient temperature and pressure.
7. **Use of Renewable Feedstocks:** A raw material or feedstock should be renewable rather than depleting whenever technically and economically practicable.
8. **Reduce Derivatives:** Unnecessary derivatization (use of blocking groups, protection/ deprotection, temporary modification of physical/chemical processes) should be minimized or avoided if possible, because such steps require additional reagents and can generate waste.
9. **Catalysis:** Catalytic reagents (as selective as possible) are superior to stoichiometric reagents.
10. **Design for Degradation:** Chemical products should be designed so that at the end of their function they break down into innocuous degradation products and do not persist in the environment.
11. **Real-time analysis for Pollution Prevention:** Analytical methodologies need to be further developed to allow for real-time, in-process monitoring and control prior to the formation of hazardous substances.
12. **Inherently Safer Chemistry for Accident Prevention:** Substances and the form of a substance used in a chemical process should be chosen to minimize the potential for chemical accidents, including releases, explosions, and fires.

Among the twelve principles of green chemistry, proper solvent selection to minimize toxicity, energy demand, pollution and so on is a key issue that has spurred great efforts in the development of alternative green solvents. Enormous amount of organic waste generated each year from reactions run in organic media is mainly attributable to solvents.^{8, 9} Likewise, the waste water streams contaminated by miscible solvents further exacerbate this major environmental problem.^{10, 11} In chemical reactions, solvents account for about 80% of the total mass handled¹² and in 70% of the cases they are incinerated to recover heat.¹³ Therefore their substitution with more environmentally friendly ones can directly have a positive effect on both emissions and safety issues.¹⁴ Replacement of the use of organic solvents in the synthesis of organic semiconductors with water would provide more economically and environmentally sustainable process. In the next sections of this introduction I explain the reason for the water choice as alternative reaction medium (section 3.1.1) and our strategy (section 3.2) in order to develop more sustainable and scalable syntheses compared to literature protocols giving access to popular OS. In pharmaceutical chemistry there are several academic and industrial examples following this strategy but for the organic semiconductor field, only a few pioneering papers are published.¹⁵⁻¹⁷

Potential low cost of devices is one of the driving forces behind the development of OPE technologies for this reason the development of more sustainable and scalable synthesis is an important challenge for the Organic Semiconductor chemist.

3.1.1 Water the green solvent par excellence

Solvents play several roles at the same time, e.g. to ensure contacts between substrates of different polarity, to control heat transfer, and to favor the interaction that leads to the final transformation.¹⁸ Historically organic chemistry has embraced volatile organic solvents as the reaction media of choice.⁹ Over the previous decades, organic solvents have been associated with a series of environmental and health issues (environmental damage, toxicity, hazards in handling). A huge research effort has been directed towards alternatives to chlorinated solvents and volatile Volatile Organic Compounds (VOCs) in general. The different approaches taken into consideration are reviewed in Clark work⁸, alternative reaction solvents are reviewed in terms of life cycle. Supercritical CO₂ (scCO₂), Ionic Liquid (IL), fluorinated solvents, water, and renewable organics are compared on the basis of their solvency, ease of use, reusability, health and safety, environmental impact, and economic cost. Designer IL solvents and scCO₂, are recognized as useful solvents for a range of applications, but they suffer from several drawbacks limiting their applicability. The authors believe that water and no-solvent approaches (mechanochemistry) to the problem deserve greater attention; the advantages of these will be even greater as a life cycle approach to solvent assessment, including transportation, becomes more widely adopted. Among all possible liquids, water is certainly the one with the smallest impact on the environment. Water as a solvent has been selected by Nature to carry out all kinds of chemical transformations unregarding to the substrates hydrophilic or hydrophobic nature.^{18, 19} Water as a solvent is extremely economical, non-toxic, non-flammable, it does not contribute to greenhouse emissions, it does not require synthesis, the energy necessary for its isolation in the pure form is modest. Additional properties are tuneable acidity, a large heat capacity and heat of evaporation which allow easy control of exothermic reactions, high polarity, and the coexistence of hydrogen bond donor and acceptor functionalities that often make catalysis easier. In one word it is the green solvent par excellence. Despite these excellent properties, it is among the least used solvents simply because it is highly polar and its strong hydrogen bonds give rise to the hydrophobic effect, i.e. the property of water to segregate apolar species rather than provide single molecule solvation.¹⁸ Historically, it has been known since the 1980s that the hydrophobic effect can greatly accelerate reactions between poorly water soluble substrates²⁰ but water has been routinely used at times in combination with organic solvents; that is, reactions run “with water”.²¹ More recently the concept of water as the only medium has been put forward; that is, reactions “on water”.²² Performing reactions truly “in water”, however, is especially challenging, requiring the substrate to be water-soluble. But for most cases, substrate and catalyst solubility issues exist, and therefore, water tends to be overlooked unless high temperatures are applied.²³ However, the need for product extraction from aqueous phases poses some critical issues about the green character of catalysis in water, such as (i) the volume of organic solvent used in the workup often exceeds the total volume of water used in the reaction by factors of up to 30-fold and this operation is of major concern for the overall green character of the system and (ii) the resulting water solution is essentially a water stream contaminated by organics that is subject to strict regulations and purified usually by stripping under vacuum or adsorption of activated carbon.²¹ From

this point of view the green character of aqueous media in replacing organic solvents while using an organic solvent to extract products from water is questionable, but as long as water provides extra performance in terms of activity and selectivity, the concerns about the use of limited amounts of traditional solvents at the end of the reaction are at least mitigated and in the cases of successful recycling, reduced to a minimum.¹⁸ In order to provides extra performance in terms of activity and selectivity by reactions run in water we must take inspiration from Nature indeed doing chemistry in water is very old news also with lipophilic substrates, for example they react in enzymatic hydrophobic pockets formed in water.¹⁹ Another important aspects is that, Nature runs reactions under very mild conditions, near room temperature reaction and heating reaction mixtures is oftentimes the prime source of byproduct formation. Development of artificial enzyme models mimicking natural enzymes is a promising and active field that has been pursued by researchers for several decades²⁴ a second simplest option for doing chemistry in water is the micellar catalysis. The use of surfactants under micellar conditions represents one of the simplest methods to achieve catalysis in water since surfactants are in most cases very economical thanks to their extensive everyday use in detergency and formulation in general.¹⁸

3.1.2 Surfactants and their characterization

Surfactants is the short name for surface active agents. Surfactants are amphiphilic molecules, composed by hydrophilic and lipophilic parts. Generally the polar part is called head and nonpolar group is called tail.²⁵ head and tail can have different nature (see Figure 3.1) for example the head can be feature the presence or absence of electric charge (cationic, anionic, zwitterionic, non-ionic) whilst the tale can have different composition (hydrocarbon, fluorocarbon, siloxane). The tail length ranges from small molecule to polymer, with linear or branched chains, or containing insaturations and rings. Particular classes of surfactants possess two heads (“bola surfactants”), or both a double head and tail (they are called “gemini”).^{25, 26} When a surfactant is in the presence of water and immiscible organic species tend to mediate between the two phases. If water is present in a large amount the hydrophobic effect drives the formation of spontaneous micellar aggregates in solution when the surfactant is present above a certain minimum concentration called critical micellar concentration (cmc). The nanoscale assemblies, micelle, formed by aggregation of about 50–100 monomers are in thermodynamic equilibrium with monomers rapidly exchanging in solution. For example, the typical lifetime of a surfactant micelle is on the order of 10^{-3} – 10^{-2} s.²⁶ The type of aggregate formed is a function of several variables: (i) the molecular structure of the amphiphile, (ii) the proportion between hydrophilic and hydrophobic parts, (iii) the geometry of the molecule and (iv) the experimental conditions in which they are used such as temperature, pH and ionic strength of the dispersing phase.²⁷ The effect of concentration is extremely important since possible aggregates are initially typically spherical micelles, but as soon as the concentration increases also ellipsoidal micelles, rods, hexagonal liquid crystal phase (LC, hexagonal arrangement of long cylinders), lamellar LC phase and, eventually, reverse phases are possible.²⁶ The first information needed in order to be sure to work under micellar conditions is the value of the cmc of the surfactant employed. Several methods are available, all based on the observation that the properties of the solution drastically change crossing the cmc value. The most common methods for the determination of the cmc are based on surface tension measurements, UV-VIS, fluorescence analysis, conductometry²³ and

NMR spectroscopy,²⁸ The average size of micellar aggregates can be easily determined Dynamic Light Scattering (DLS) analyses²⁹ providing information concerning the hydrodynamic radius of the aggregates and the distribution of the different structures present in solution even if the measurement is an average of the contribution from all different kinds of aggregates. Complementary to this, Transmission electron cryomicroscopy (cryo-TEM) analysis allows achieving real pictures of the aggregates formed by the surfactant.³⁰

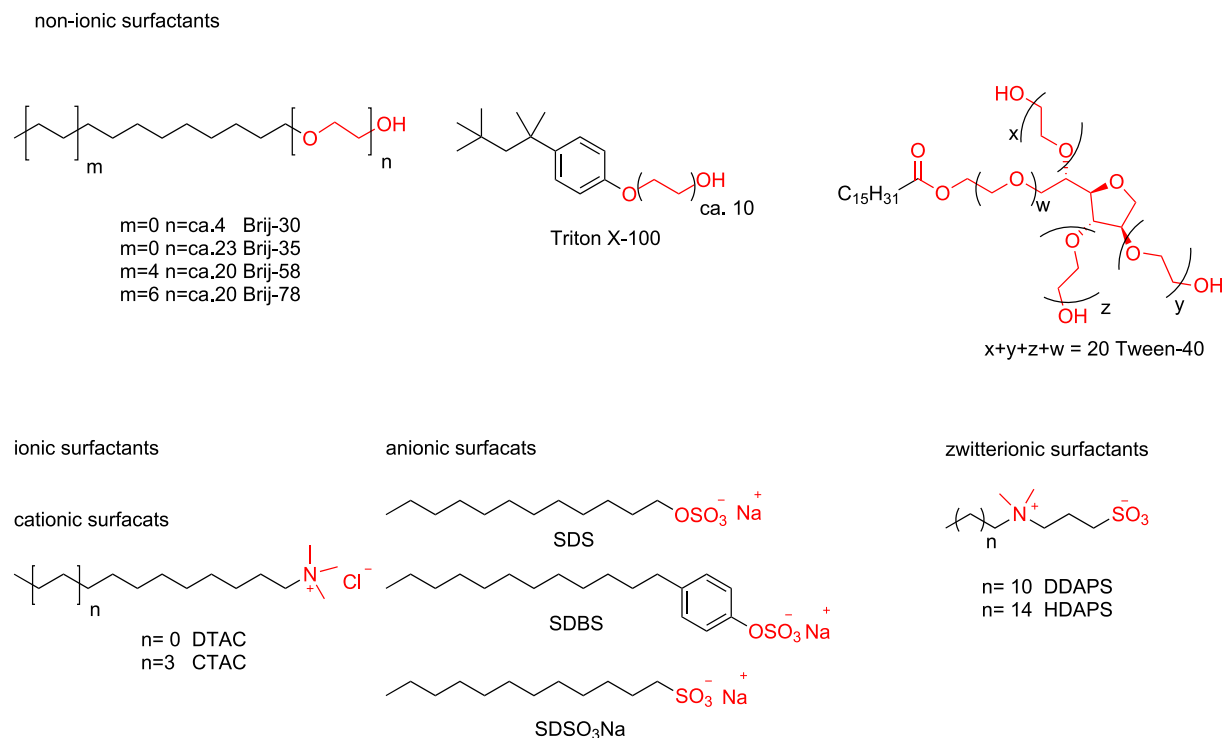


Figure 3.1 Structures of commercially available surfactants. The Red part is the head group and the black part is the tail group.

3.1.3 Micellar catalysis

A micellar solution appears completely homogeneous to the eye inspection due to the small dimensions of micellar associating colloids; however, in reality the absorbed reactants are in a microheterogeneous two-phase system.³¹ In the presence of large amounts of substrates, usually liquids, to favor their intimate contact with water and the surfactant, microemulsions are obtained and also under these conditions, enhancement of catalytic activity and selectivity has been observed.¹⁸ Organic species added to micellar media are distributed between bulk water and micelles depending on their polarity, charge and dimension. It has been established, by spectroscopic measurement, that nonpolar compounds such as hydrocarbons are generally to be found in the hydrophobic core while semipolar and polar compounds such as alcohols, carboxylic acids, and amines are located in the palisade layer. Aromatic compounds are often found to be present in both the head-group region and the core and they can be described using equilibria.³² The effect of micelles, according to Brown et al,²⁷ be ascribed to a combination of the following factors :

1. The dielectric constant in the micelle is lower than in water, which causes a solvent effect.

2. The transition state of the reaction can be stabilized by interaction with the polar head groups.
3. The reactants are concentrated relative to the surrounding water phase through interactions with the micelle surface or through insertion into the micelle itself, thus leading to an increased rate of bimolecular reactions.

The concentration effect (N^3) can be considered as dominant in many cases. In general, the micellar effect is referred to as “micellar catalysis” when it refers to the alteration of the rate of a reaction. One of the simplest kinetic model of reactions in micellar systems can be accomplished by considering them as microheterogeneous two-phase systems²⁷. From a certain point of view micelles behave like enzymes, isolating species from the bulk solvent, playing several roles at a time like improving solubilization of organic reagents in water, helping compartmentalization of reagents with enhancement of the local concentration and reactivity, imparting unique chemo-, regio- and stereoselectivities.¹⁸ The rules of micellar chemistry are still not completely clear, for examples is not know which and why surfactant is best for a given reaction type, if micellar shape and size play a role in successfully enabling a desired transformation or what is the role of co-solvents in the documented examples where they are required.¹⁹

3.1.4 Organic reaction in micellar media

Micellar reactions are a well established topic in modern organic synthesis, indeed the numbers of reactions reported in literature to date in micellar condition is quite impressive. I report some examples: Oxidation,³³⁻³⁹ reduction,⁴⁰⁻⁴⁴ dehydration,⁴⁵ C-C or C-heteroatom Bondig former reaction. Reactions leading to the formation of C-C or C-N bonds can be sorted in two classes: TM catalyzed and not. They are part of the first group: Michael additions,⁴⁶ aldol addition,^{47, 48} Friedel-Crafts alkylation⁴⁹ and Diels-Alder cycloaddition.⁵⁰ Copper,⁵¹⁻⁵⁶ Rhodium,⁵⁷ Gold^{58, 59} and Palladium-catalyzed reactions belong instead to the second group. In particular we can find several of Pd-catalyzed cross-coupling reactions reported like Buchwald-Hartwig, Sonogashira, Negishi, Heck, Stille, Olefin metathesis, Suzuki-Miyaura, direct arylation reaction. These last examples are very relevant for OS synthesis. Indeed TM-catalyzed cross-coupling methodologies, in particular Pd-catalyzed reaction have evolved over the past four decades into one of the most powerful and versatile methods for C-C bond formation, enabling the construction of a diverse and sophisticated range of π -conjugated molecules and polymers.⁶⁰ Nearly all organic electronic materials consist of π -conjugated backbones. Most of these are comprised of polyaromatic or heteroaromatic units. For this reason micellar Pd-catalyzed cross-coupling are very interesting for the development of green OS synthesis. Literature reports a large number of surfactants suitable to carry out SM coupling in high yield and at room temperature under micellar conditions.⁶¹ Some of them are well established industrial surfactants (eg Triton X 100, brij) originally developed for the needs of formulation chemistry.¹⁸ Others specifically designed for micellar reactions (PTS, TPGS, NOK) have been shown to feature superior performances in terms of yield and/or reduction of the reaction time.^{59, 62-65} Despite the seminal value of these observations, there are no general structure-property relationships clearly correlating performances in micellar reactions with the surfactant chemical nature. Mostly, the difference in performances

are ascribed to the aspect ratio (spherical vs worm like) and/or dimensions of the micelles obtained in water solution. Recently, a seminal computational investigation of the association behaviour of micelles was also reported.⁶⁶ The use of micellar Pd-catalyzed cross-coupling in the field of organic semiconductors is still limited and only a few examples of conjugated molecular materials have been reported.^{5, 15-17, 67} Our research group in the last three years have been focusing on the development of micellar condition for the synthesis of OS materials. In particular we have developed SM couplings on different OS classes, along with an example on Buchwald-Hartwig reaction.

3.2 General Aims: Micellar catalysis for organic semiconductors

Within my PhD I helped working on the scaling up of an OS to 100g batches. This experience made it clear that sustainability is not a priority in the field. Indeed according to the literature the synthesis of that compound is a multi step synthesis requiring the use of several liters of toxic and flammable organic solvents both as a reaction medium and for different chromatographic purification. Also, the protocol was based on Stille coupling a notoriously troublesome reaction involving the use of toxic organotin compounds. Partially to address this specific issue and more in to promote a change in the general approach to the preparation of OS, we focused on the development of micellar synthetic protocol for OS molecular materials. Micellar strategy is already giving excellent results in the industrial pharmaceutical synthesis.⁶⁸ We focused first on the reaction of Suzuki-Miyaura cross coupling reaction like greener alternative to Stille reaction, but we have begun to extend the work also to different reactions such as Buchwald-Hartwig Reaction. The use of micellar catalysis for OS material in not trivial indeed organic semiconductors are usually heavily functionalized molecules, highly crystalline and they can interfere with surfactant micellization these lead to low conversion, consequently long purification steps and low yield. The major issue is that the coupling partner and the catalyst must be localized in the same micellar compartment in order to perform the coupling of instead of parasitic reaction as dehalogenation and homo-coupling or incomplete conversion.

3.3 Previous work and the discovering of the New Rules

The results reported in this section are already published. more relevant findings are summarized. For the details is refer to published works (coauthorated within PhD).

3.3.1 Surfactant choice

The first big difference between the literature works and ours works is the surfactant choice. In the last decade, thanks to the intuition of Lipshutz and co-workers, the nature of the surfactant started to become the subject of in depth investigations. This led to the design, synthesis, development and application of new surfactants in catalysis application, these new surfactants covers several aspects of palladium-catalyzed cross-coupling reactions specifically carried out under mild room temperature conditions in water. These surfactants are specifically designed to boost the nanoreactor properties of micelles, for this reason are called designer surfacatant (see figure 3.2). This is the case of PTS that is a non-ionic surfactant composed of racemic vitamin E as the apolar portion, sebacic acid, and PEG-600 as the hydrophilic portion. An evolution of PTS is polyoxyethanyl- α -tocopheryl succinate TPGS that represents a second example of a designer green surfactant. It is composed of a lipophilic α -tocopherol moiety, a succinic spacer and a hydrophilic poly(ethylene-glycol) methyl ether chain (PEG-750-M) with the average mole of 750 u.m.a. These two designer surfactants, even if sharing similar lipophilic structures, lead to different outcomes in several catalyzed reactions. This is likely due to the different kinds and shapes of micellar aggregates formed. While PTS forms both 8–10 nm spheres and larger worm- or rod-like particles with the overall average size of 25 nm, TPGS in water provides very sharp 12–13 nm spherical micelles. The same group developed the latest designer surfactant SPGS-550-M called “Nok” based on a β -sitosterol methoxypolyethyleneglycol succinate structure, prepared in only two steps from β -sitosterol with succinic anhydride and PEG-550-M. Despite the existence of these designed surfactants we focused on the use a large-scale, commercially available surfactant, called Kolliphor® EL(see figure 3.2). Kolliphor® EL is BASF’s non-ionic solubilizer and emulsifier for the production of semi-solid and liquid formulations of water-insoluble drugs and other hydrophobic compounds. Kolliphor® EL is a complex mixture, the main component of Kolliphor® EL is glycerol polyethylene glycol ricinoleate. Together with fatty acid esters of polyethylene glycol, this forms the hydrophobic part of the product. The smaller hydrophylic part consists of free polyethylene glycols and ethoxylated glycerol. The main reason for our choice is that,a previous PhD thesis demonstrated that the core of Kolliphor’s nanomicelles is oxygen free, this offering advantages in oxygen sensitive reactions such as SM reaction. Other Kolliphor advantages are the low cost, indeed for example his prices for grams is around 0.23 €/g against Nok price of 17.23 €/g from the same supplier (Sigma-Aldrich), and the cost is a important factor to consider for a scalable synthesis. Kolliphor EL is a low-toxic product for human health, in fact it is approved by the competent administrations (e.g. Food and Drugs Administration) for the formulation of several drugs (Taxol and its derivatives.⁶⁹). Kolliphor® EL is made from a natural precursor in fact is made by reacting castor oil with ethylene oxide in a molar ratio of 1 : 35.

3.3. PREVIOUS WORK AND THE DISCOVERING OF THE NEW RULES

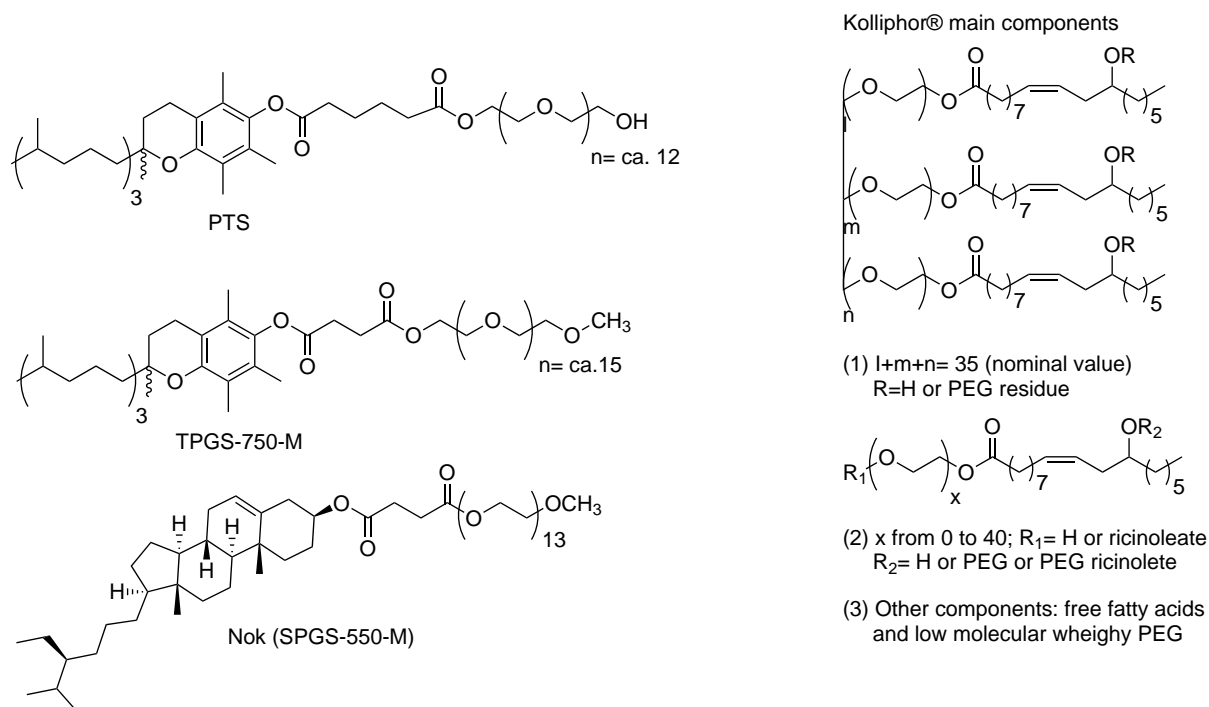
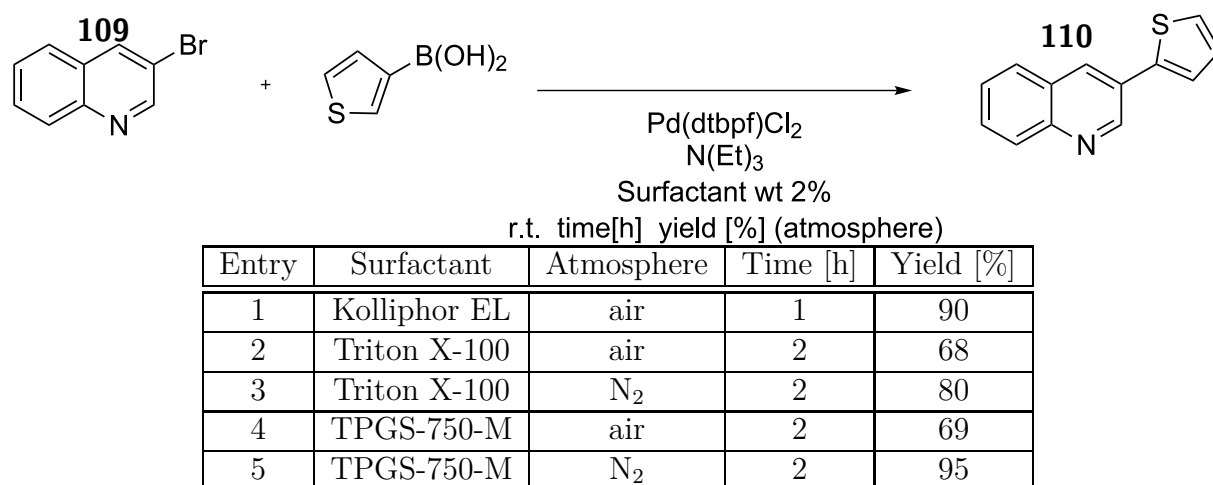


Figure 3.2 Designer surfactants on the Left and Kolliphor® EL on the right

In the first work titled “ Suzuki–Miyaura Micellar Cross-Coupling in Water, at Room Temperature, and under Aerobic Atmosphere” published on Organic letters (DOI: 10.1021/acs.orglett.6b03817) we compared the yield of SM reaction between 3-Bromoisoquinoline (**109**) and 3-thienylboronic acid (**110**) in different 2 wt% surfactant solution in water (scheme 3.1). We compared Kolliphor® EL with two other established coupling promoting surfactants like Triton X-100 and TPGS-750-M. We tested the method under a set of experimental conditions generally accepted as appropriate in the dedicated literature: room temperature, a 2 wt % solution of the surfactant in distilled water, 0.5 M concentration of the halide (bromide in all our reactions), [1,1'-bis(di-tert-butylphosphino)ferrocene]dichloropalladium(II) ($\text{Pd}(\text{dtbpf})\text{Cl}_2$) 2 mol % with respect to the bromide as the catalyst, and triethylamine ($\text{N}(\text{Et})_3$) as the base. The result are shown in the table of scheme 3.1.

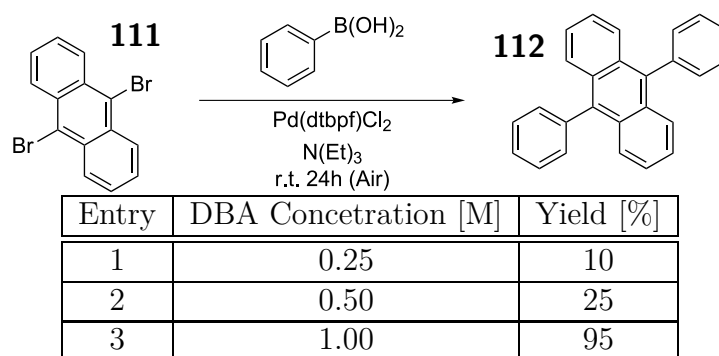


Scheme 3.1 Reaction of 3-bromoisoquinoline with 3-thienylboronic acid in different surfactant dispersions.

For the entry 1,2,4 of table of scheme 3.1 the reactions were carried under air (without the use of inert atmosphere or degassed water), the comparison of the yields is demonstrates that the Kolliphor Oxygen barrier effect allows running reactions without special precaution in high yield (90%). In order to confirm our hypothesis we perform the same reactions under nitrogen atmosphere and with degassed water for Triton X-100 (entry 3) and TPGS-750-M (entry 5). The yields increase from 68% to 80% for Triton X-100 and from 69% to 95% for TPGS-750-M. Triton X-100 result less performant in both condition (under air or nitrogen atmosphere) in stead of TPGS-750-M that resulted more performing than Kolliphor® EL. The absolute higher yields of TPGS-750-M, under nitrogen, respect Kolliphor® EL being a designer surfactant it is not surprising but the Kolliphor-catalyzed yied was only little lower (90% against 95%), and the possibility of work without particular precaution is a great advantage from the stand point of scalability of the reaction. We made several examples on model small molecoules and the conclusions were that Kolliphor® EL-catalyzed reaction were comparable in terms of yield with TPGS-750-catalyzed reaction but with the advantage of oxygen insensitivity.

3.3.2 Synthesis of organic semiconductors in micellar conditions, first examples

After choosing surfactant we started finally to make some OS derivatives. We used the standard micelle-condition that we developed with the model small molecoules: 0.5 M Ar-Br, 1.5 M 2- Ar-boronic acid, 3 M N(Et)₃ and 2 mol% with respect to the bromide of Pd(dppf)Cl₂, at room temperatue under air atmosphere. We started with the optimization of 9,10-dibromoanthracene (DBA, **111**) phenylation reaction (scheme 3.2, and we started to observe that the exploitation of micellar catalysis for OS synthesis is not trivial as shown in Entry 2 of table of the scheme 3.2 that standard micelle-condition bring to low yield (25%) despite a reaction's time of 24h. We decided of study the influence of DBA concetration, as shown in table of the scheme 3.2 we observed that the reaction yield increased (from 10% to 95%) as the bromide concentration increased (from 0.25M to 1M).

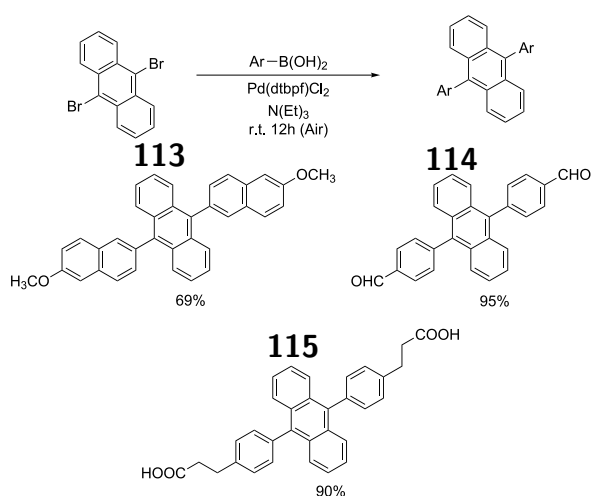


Scheme 3.2 Micellar phenylation reaction of **111**

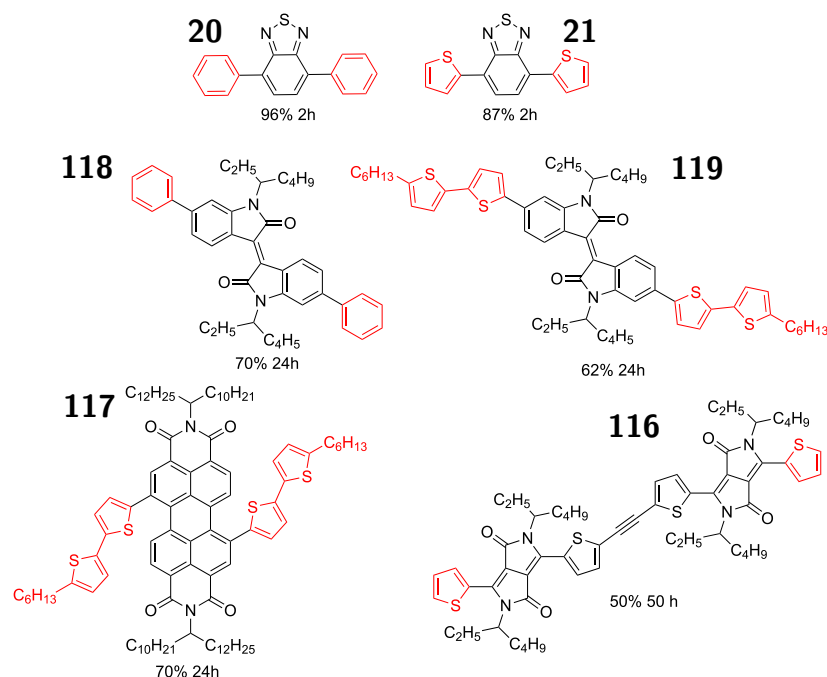
We think this behaviour is connected with a problem of localization of the coupling partners in the different micelle's compartments, indeed a similar effect was observed in a previous work while focusing on phosphorescent compounds.⁷⁰ The use of Oxigen-free Kolliphormicelle-core enviroment aimed at observing an oxygen sensitive nonlinear optical

3.3. PREVIOUS WORK AND THE DISCOVERING OF THE NEW RULES

phenomena called Up-Conversion (UC) gave best result only at increasing concentration of the hydrophobic molecules involved in the process. In short; the capability to successfully carry out a micellar coupling is connected with the colocalization of reactive species within the compartment of the micelle where the Pd(0) catalyst is localized. The increase of concentration of bromide (the most hydrophobic components) favors saturation of all the pockets of the micelle, including those that are O₂ free and catalyst loaded, thus favoring the oxidative insertion of palladium kick starting the reaction. In the same article we reported also the synthesis of others 9,10-diarylanthracene derivatives (**113**, **114** and **115**) with different aryl groups and the synthesis of others OS compounds belonging to the classes of: diarylbenzothiadiazoles (**20,21**), diketopyrrolopyrroles (**116**), perylene diimides (**117**) and isoindigos (**118**, **119**). The products structure are shown in scheme 3.4.



Scheme 3.3 Synthesis of 9,10-diarylanthracene derivatives



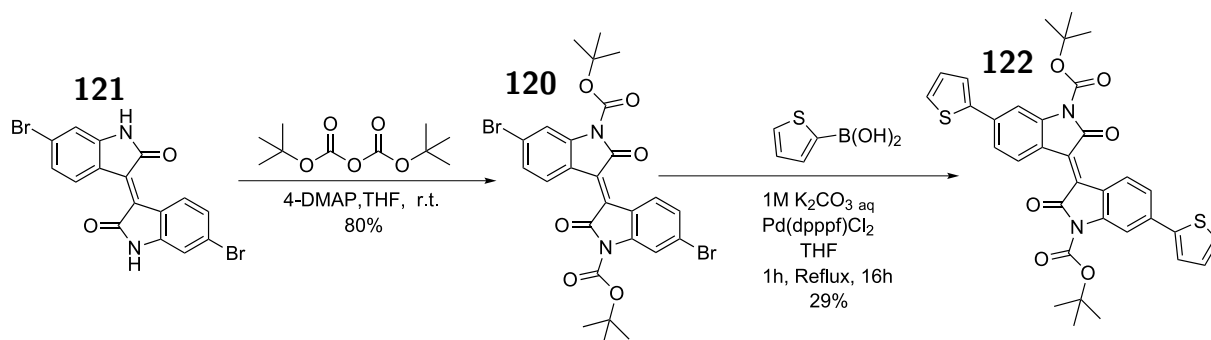
Scheme 3.4 Couplings of brominated precursors (in red) and arylboronic acids or esters (in black) performed in a 2 wt% Kolliphor EL solution in deionized water. Isolated yields and reaction times are given.

Using the same protocol we isolated the OS compounds with yields between the 50% to 96% (scheme 3.4). In the case of highly crystalline compounds like **112**, **113**, **114** and **115** they can be directly filtered from the reaction medium and purified by crystallization. Derivatives **118** and **117** are examples of heavily functionalized compounds that could interfere with the micellar structure of Kolliphor EL in solution. Characteristics of such isoindigo derivatives made the reaction mixture difficult to efficiently stir, as most of the material formed an oily and sticky residue on the walls of the reaction flask. To deal with the problem, we mechanically shook the reaction mixture and increased the reaction time to 24 h. Derivatives **117** and **116** are examples of a coupling reaction involving a boronic ester instead of an acid. The reactions proved to be significantly slower, again mostly due to the high viscosity of the reaction mixture, all other products could, in any case, be isolated after chromatographic purification in moderate to good yields. Further optimization of our method will likely require the devising of improved mixing procedures. For benzothiadiazole derivatives like **20** and **21** we have developed a more sustainable non-chromatographic purification which will be discussed later in the section 3.4.

3.3.3 Synthesis of latent pigment in emulsion conditions

The results reported in this section are published in the article “Suzuki-Miyaura Cross-Coupling of latent pigments in water/toluene emulsion under aerobic atmosphere” (DOI:10.1016/j.dyepig.2017.11.044).

Aiming at extending the generality of the approach, we focused our attention on the elaboration of latent pigments, a very peculiar class of organic semiconductors recently singled out when a tradeoff between performances and sustainability is paramount. The latent pigments strategy was originally developed as a tool to process organic pigments from solution by reversibly turning them into dyes.⁷¹ Latent pigments are thermosensitive dyes that can be reverted to insoluble pigments via thermal treatment, are a well-established component of high performance inks which find uses in OLEDs and OPVs. Latent pigment strategy are discussed in greater detail in chapter 3. Latent pigments derivatives synthesis is challenging due to the thermal sensitivity of the protecting group, indeed Boc group is often present in that compounds. SM cross-coupling reactions involving latent pigments have been reported yet, yields are generally poor. This is particularly true when a thiophene ring is present in one or both the reactions partners.⁷² We chose as a representative example of a troublesome SM reaction, the coupling shown in scheme 3.5 involving the latent isoindigo pigment **120** and 2-thienylboronic acid.



Scheme 3.5 Literature approach for the couplings of thiophene-2-boronic acid and the latent pigment **120**

3.3. PREVIOUS WORK AND THE DISCOVERING OF THE NEW RULES

We tested this reaction under micellar conditions both with Kolliphor EL and TPGS-750-M. In both cases the reaction medium was a 2% by weight solution of the surfactant in deionized water. We used $N(Et)_3$ as the base and a number of different palladium catalysts (including $Pd(dtbpf)Cl_2$) and palladium precatalyst/phosphine mixtures, all of which have documented use in the SM couplings. Rather surprisingly, none of the attempts resulted in the target compound. We tested a wide range of different reaction conditions, namely: the nature and stoichiometry of the catalyst, the concentration of the reaction medium, the temperature, the reaction time and the reaction atmosphere (air vs N_2). In all cases, we recovered some of the starting material along with a dark, insoluble residue. The result was particularly surprising because we did not expect this behavior as we were able to synthesize the very similar compounds **118** and **117** with these conditions. Likewise this wasn't a problem of reactivity but was a problem of unsuitable localization of the coupling partner within the micelle's compartment, in some way BOC protecting group altered the correct partitioning of the reagent in the micelle's compartments. According to formulation chemistry guidelines, such issue requires either a change in the surfactant or the introduction of a co-surfactant and/or a co-solvent capable of tuning the Hydrophilic-Lipophilic Balance (HLB factor) of the reaction medium, indeed As we started to isolate some product (**122**) only when we start to add small amount of co-solvent in the reaction medium. Prof. Lipshutz described the benefits of using small amounts of an organic co-solvents in improving micellar couplings.⁷² The effect was rationalized in terms of a swelling effect of the micelles's core. This results in a larger effective volume for the reactions to take place. The use of a co-solvent was found particularly beneficial with highly crystalline or poorly soluble starting materials, but is not our case, indeed compound **120** is soluble in low polarity organic solvents and not particularly prone to crystallization, yet the use of a co-solvent proved successful. 0.5 M dibromide **120**, 1.5 M 2-thiethylboronic acid, 3 M $N(Et)_3$, 2 mol% with respect to the bromide of $Pd(dppf)Cl_2$ at room temperature under air atmosphere and used a mixture of Kolliphor 2% solution in water mixed with a co-solvent add at 10% in volume respect the Kolliphor solution. We tested different co-solvent: THF, Acetone and Toluene. When we employed the water-soluble solvents THF and Acetone we remain in the micellar regime like is possible to see in the DLS analysis (line red and green in figure 3.3), the swelling of the micelle lead to an average bigger micelle size from 10 nm without co-solvent to 21 nm for THF and 16 nm for Acetone. In 2 h and with a mild heating of 60 °C, we were able to isolate derivative **122** after chromatographic purification in around 40% yield using $Pd(dtbpf)Cl_2$ as the catalyst and $N(Et)_3$ as the base.

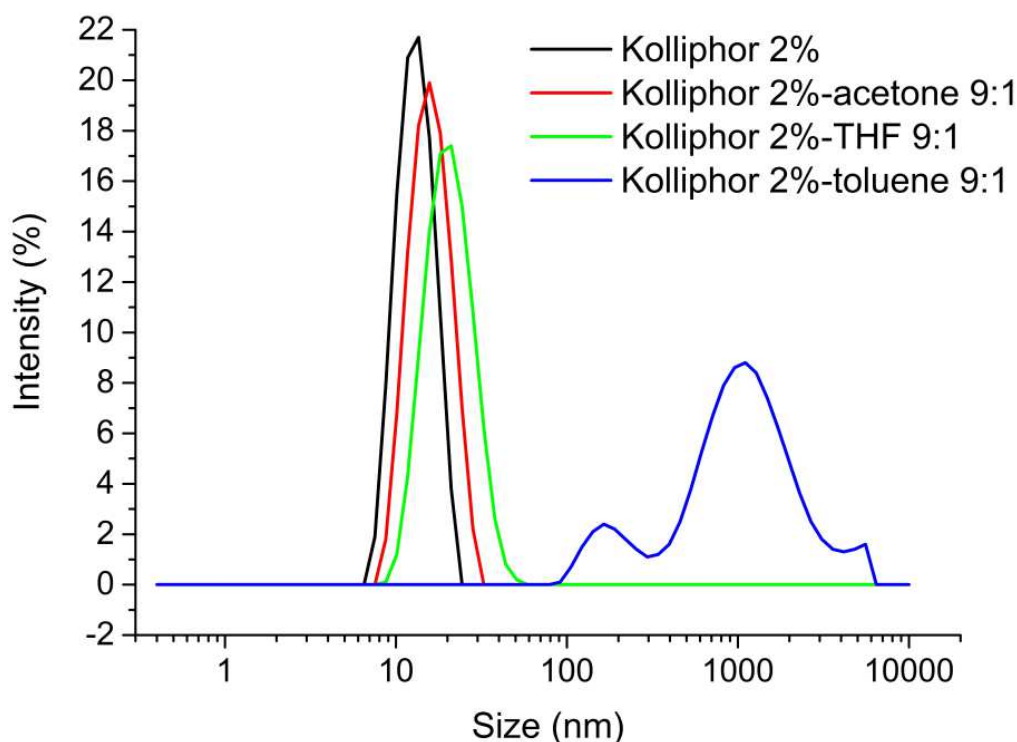
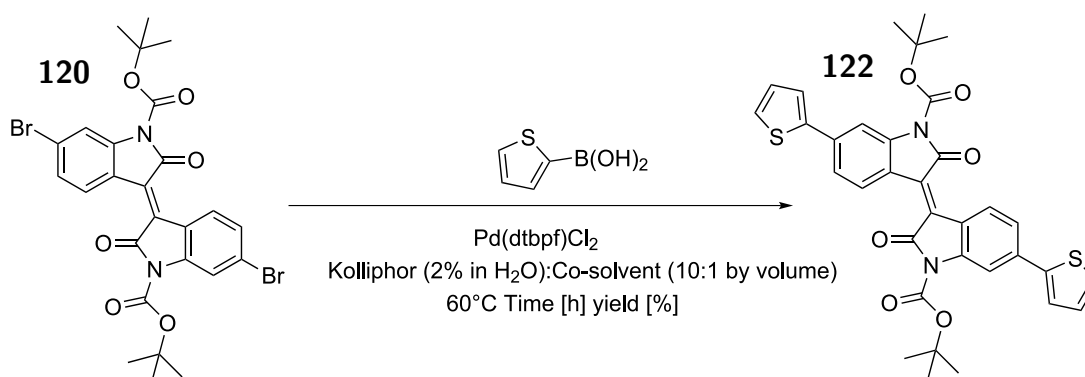


Figure 3.3 DLS spectra of Kolliphor EL 2 % by weight in water (black) and of the corresponding 10 % by volume mixtures with acetone (red), THF (green) and toluene (blue)

Remarkably, we did not observe any difference in the reaction yield when working under nitrogen or under standard laboratory atmosphere. In all cases, we still observed formation of sizeable amounts of compound **121**. This indicates a continuing issue of localization of **120** within the swollen micelles. When Toluene was tested, a solvent in which compound **120** is particularly soluble, we observed a remarkably different behavior. Firstly, a 10% by volume mixture of toluene in 2% by weight Kolliphor EL in water no longer forms a micellar solution but rather an emulsion (see blue line in figure 3.3). In an emulsion the reaction medium is biphasic, the surfactant constitutes the separation layer between phases, instead of being the reaction medium itself like in standard micellar couplings. Emulsion conditions proved to be definitively more efficient than micellar ones for this set of reaction substrates. The use of toluene as a co-solvent gave the expected product quantitatively, as evaluated by TLC. Isolated yield was limited to 80% due to the pronounced tendency of **120** to deprotect over the silica employed during purification. We did not observe any change in the reaction behavior when working under inert instead of oxygenated atmosphere. This is surprising: the solubility of oxygen in toluene is far greater than in water, yet the peculiar effect of Kolliphor, in this case only acting as a barrier layer rather than being the reaction medium, was preserved.

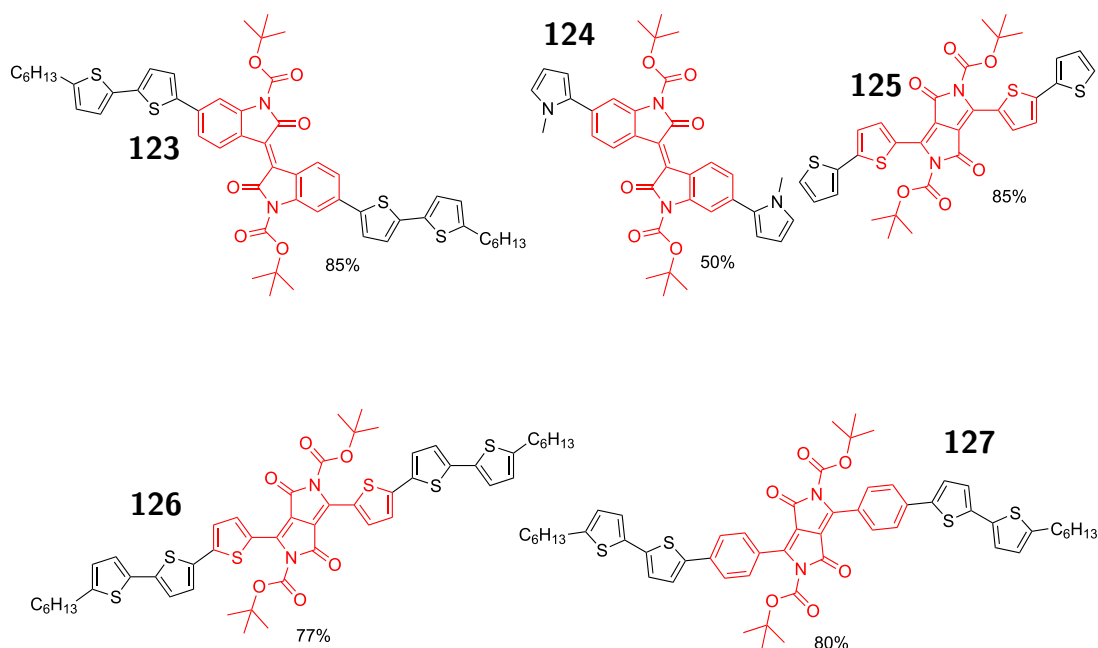
3.3. PREVIOUS WORK AND THE DISCOVERING OF THE NEW RULES



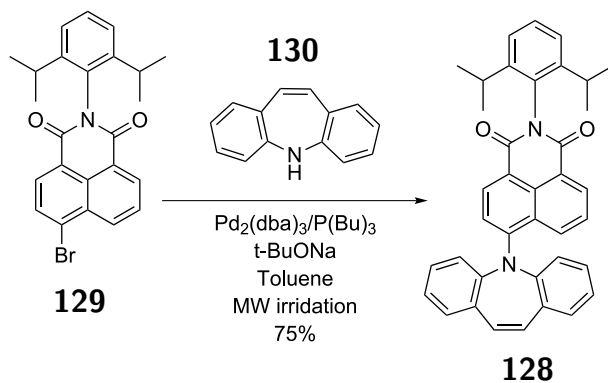
Entry	reaction medium (Volume ratio)	Atmosphere	Time [h]	yield [%]
1	Kolliphor EL /acetone (10:1)	Air	2	42
2	Kolliphor EL /acetone(10:1)	N ₂	2	40
3	Kolliphor EL /THF (10:1)	Air	2	38
4	Kolliphor EL /THF (10:1)	N ₂	2	39
5	Kolliphor EL /toluene(10:1)	Air	1	80
6	Kolliphor EL /toluene(10:1)	N ₂	1	79

Scheme 3.6 Cosolvent optimization for the couplings of thiophene-2-boronic acid and the latent pigment **120**

The table of scheme 3.6 summarizes the results of the co-solvent experiments. We tested the method's scope and generality by carrying out several reactions involving both isoindigos and diketopyrrolopyrroles as latent pigment precursors. The boronic counterparts included: thiophene-2-boronic acid, 5'-N-hexyl- 2,2'-bithiophene-5-boronic acid pinacol ester, phenylboronic acid, 6-methoxynaphthalene-2-boronic acid and 1- methylpyrrole-2-boronic acid pinacol ester. Scheme 3.7 summarizes the results.



Scheme 3.7 Cosolvent approach for the couplings of thiophene-2-boronic acid and the latent pigment **120**



Scheme 3.8 Test reaction selected to optimize the BHA protocol

3.3.4 Kolliphor® EL-catalyzed Buchwald–Hartwig amination

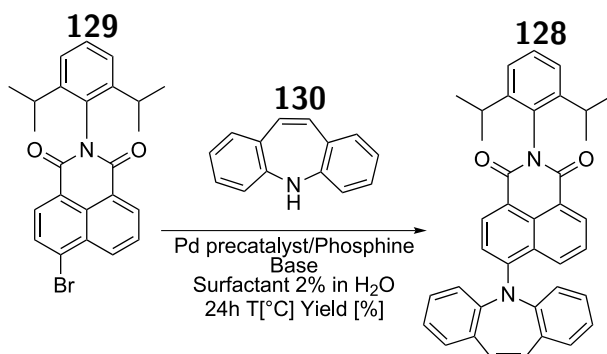
The results reported in this section are published in the article “Synthesis of Fluorinated Acridines via Sequential Micellar Buchwald–Hartwig Amination/Cyclization of Aryl Bromides” (DOI:10.1055/s-0036-1591937).

Aiming at extending the Kolliphor-micellar catalysis also to other cross-coupling reactions, we focused on the palladium-catalyzed Buchwald–Hartwig amination (BHA). BHA is a palladium-catalyzed cross-coupling reaction of amines and aryl halides that results in formation of C–N bonds and widely utilized in medicinal chemistry and material chemistry.^{73–81} Recently, the compounds having 9H-carbazole-9-yl group have attracted much attention in organic electronic materials^{82–88} and have been synthesized through the Buchwald–Hartwig amination. In addition to BHA, the Cu-catalyzed Ullmann reaction^{89–93} or Ni-catalyzed amination^{94, 95} are known for the syntheses of the compounds having 9H-carbazole-9-yl group from (hetero)aryl halides with 9H-carbazole derivatives. However, they have some disadvantage; the use of large amount of catalyst or peculiar apparatus, harsh condition and limitation of a substrate. In order to optimize the micellar B-H protocol, we selected the test reaction shown in Scheme 3.8. Derivative **128** was previously prepared by our group via the reaction of bromide **129** and azepine **130** according to a microwave-enhanced protocol, with toluene as the solvent and working under a nitrogen atmosphere. This molecule behaves as a fluorescent molecular rotor and finds application in the monitoring of the self-assembly process of relevant block copolymers in water.⁹⁶

Micellar B-H amination has a relevant track record in the dedicated literature, TPGS-750-M is the surfactant of choice, several studies have highlighted the critical role of both the precatalyst/phosphine system and the base employed in the reaction kinetics and yield. Restricting to readily available materials, Takesago’s cBRIDP phosphine and (allyl)PdCl₂ are generally considered a good starting point while optimizing a method.^{97, 98} It is also important to note that the role of the employed base is crucial. In fact, the group of Lipshutz pointed out that in order to achieve co-localization of all reaction partners within the micelle core, the lipophilicity of the base is crucial. As such, the addition of commercially available triisopropylsilanol (TIPS-OH) to the standard t-BuOK (obviously corresponding to a KOH/t-BuOH mixture while working in water) greatly reduces reaction times due to the formation in situ of lipophilic TIPS-OK.⁹⁷ We tested this reaction under micellar conditions both with Kolliphor EL and TPGS-750-M (see scheme 3.9). In both cases the reaction medium was a 2% by weight solution of the

3.3. PREVIOUS WORK AND THE DISCOVERING OF THE NEW RULES

surfactant in deionized water. We tried different bases and base mixtures (t-BuOK,t-BuONa,t-BuOK/TIPS-OH and KOH/TIPS-OH) and a number of different palladium catalysts and palladium precatalyst/phosphine mixtures, all of which have documented use in the BHA couplings (see table in scheme 3.9).

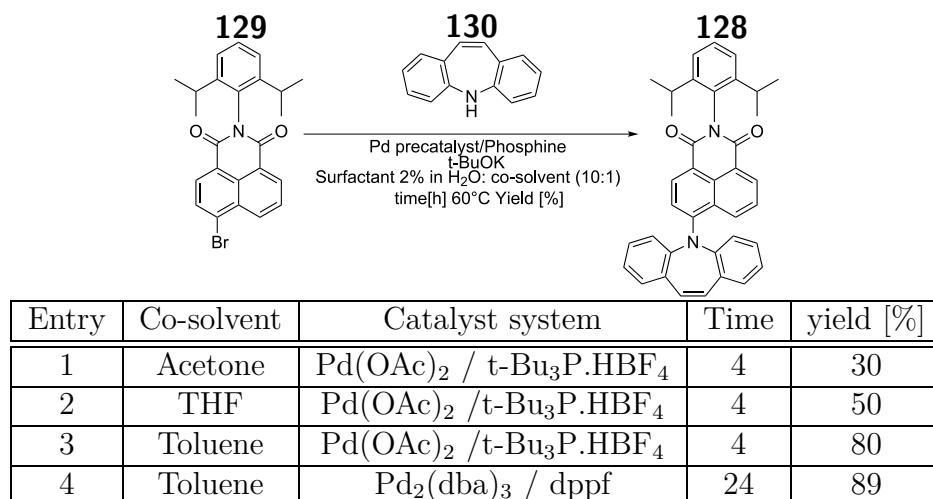


Entry	Surfactant	Catalyst	Base	Temp.	Yield [%]
1	Kolliphor	(allyl)PdCl ₂ / cBRIDP	t-BuOK /TIPS- OH	r.t.	-
2	Kolliphor	(allyl)PdCl ₂ /cBRIDP	t-BuOK /TIPS- OH	50 °C	-
3	Kolliphor	(allyl)PdCl ₂ / t-Bu ₃ P.HBF ₄	KOH/TIPS- OH	r.t.	-
4	Kolliphor	(allyl)PdCl ₂ / t-Bu ₃ P.HBF ₄	KOH/TIPS- OH	50 °C	-
5	Kolliphor	Pd(OAc) ₂ / t-Bu ₃ P.HBF ₄	KOH/TIPS- OH	50 °C	-
6	Kolliphor	Pd(OAc) ₂ / t-Bu ₃ P.HBF ₄	t-BuONa	50 °C	2
7	Kolliphor	(allyl)PdCl ₂ / cBRIDP	t-BuOK	r.t.	-
8	Kolliphor	(allyl)PdCl ₂ / cBRIDP	t-BuOK	50 °C	3
9	TPGS-750M	Pd(OAc) ₂ / t-Bu ₃ P.HBF ₄	t-BuOK /TIPS- OH	r.t.	4
10	TPGS-750M	Pd(OAc) ₂ / t-Bu ₃ P.HBF ₄	t-BuOK /TIPS- OH	50 °C	23

Scheme 3.9 BHA under Micellar Conditions

Conditions tested in the solution of Kolliphor (entry from 1 to 8) give traces or very

low yield (max 4%), better result with TPGS-750M but anyway only 23% yield despite 50°C and lipophilic base TIPSOK generated in situ. once again the micellar conditions reported in the literature did not give satisfactory results on OS systems. We think that the problem was always the same, a correct micellar partitioning of the reagents and not a reactivity problem. Indeed in the entry 6 we use the same catalytic system and the same base that were used in literature solution condition and the reaction yield was only of 2%. In order to tune the micellar environments we decided to use the co-solvent strategy: a 10% by volume mixture of co-solvent in 2% by weight Kolliphor EL, we tested different co-solvents: THF, Acetone and Toluene, the result are summired in table 3.10



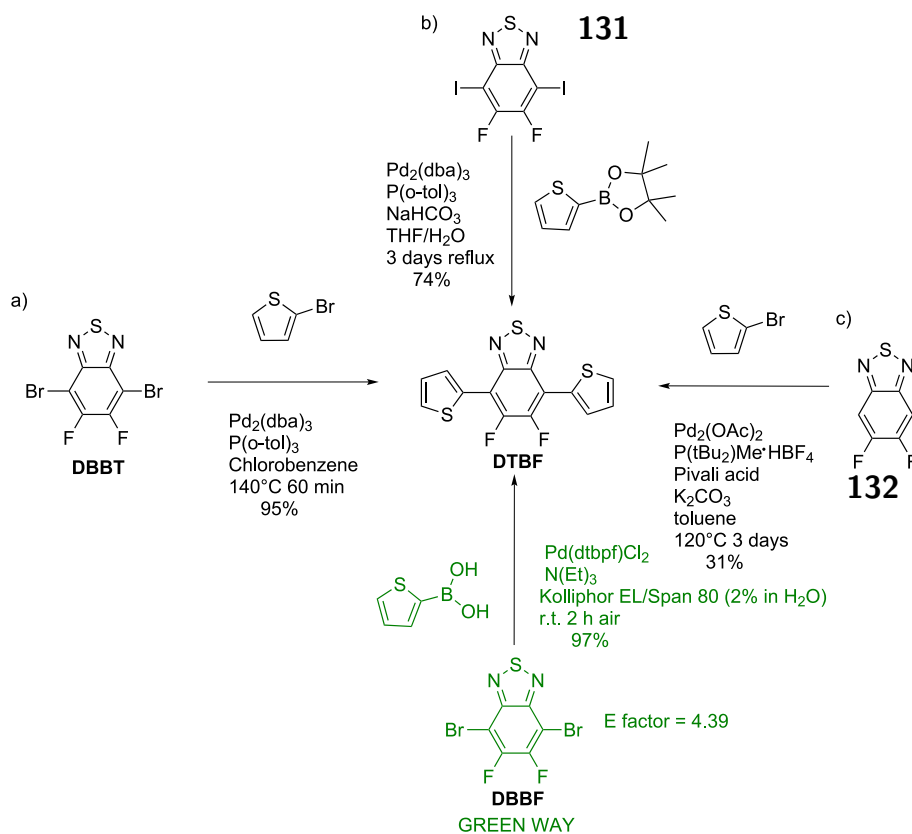
Scheme 3.10 BHAunder Micellar/Emulsion Conditions Aided by a Cosolvent

With the co-solvent adding, the polarity of the micelle core is tuned. In other words, the hydrophilic-lipophilic balance (HLB) of the micellar nano-reactor is changed. When we worked with a 10% by volume of toluene within a 2% by weight Kolliphor EL solution, we were able to go from no reaction at all to 80% isolated yield in just 4 hours at 60 °C while using the very simple and affordable Pd(OAc)₂/t-Bu₃P catalytic system. The yield increased to 89% when the well-established Buchwald-Hartwig Pd₂(dba)₃/dppf catalytic system was used (Table in scheme 3.10). Even more interestingly, the reaction could be performed directly in air, confirming the peculiar resistance to oxygen of Kolliphor EL/Toluene reaction medium even in we worked in emulsion rather than micellar solution. In the article is possible to find synthesis of fluorinated acridines via amination/cyclization that exploit the conditions developed by us for the first step of BHA.

3.4 Synthesis of benzothiadiazole derivatives in micellar condition

3.4.1 Introduction

4,7-Di(thiophene-2-yl)-5,6-difluoro-2,1,3-benzothiadiazole DTBF (scheme 3.11) is a commercially available, rather expensive, building block that is gaining a relevant momentum in the dedicated literature.^{99–102} In the last 8 years DTBF was reported, directly as it is or as a part of more complex polymer or molecule, in nearly 300 papers, with a steady increase in the number of hits per year (See 3.4).



Scheme 3.11 Scheme 1 Literature vs micellar approach for the preparation of DTBF

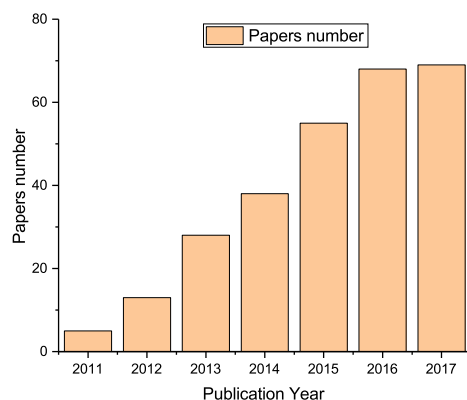


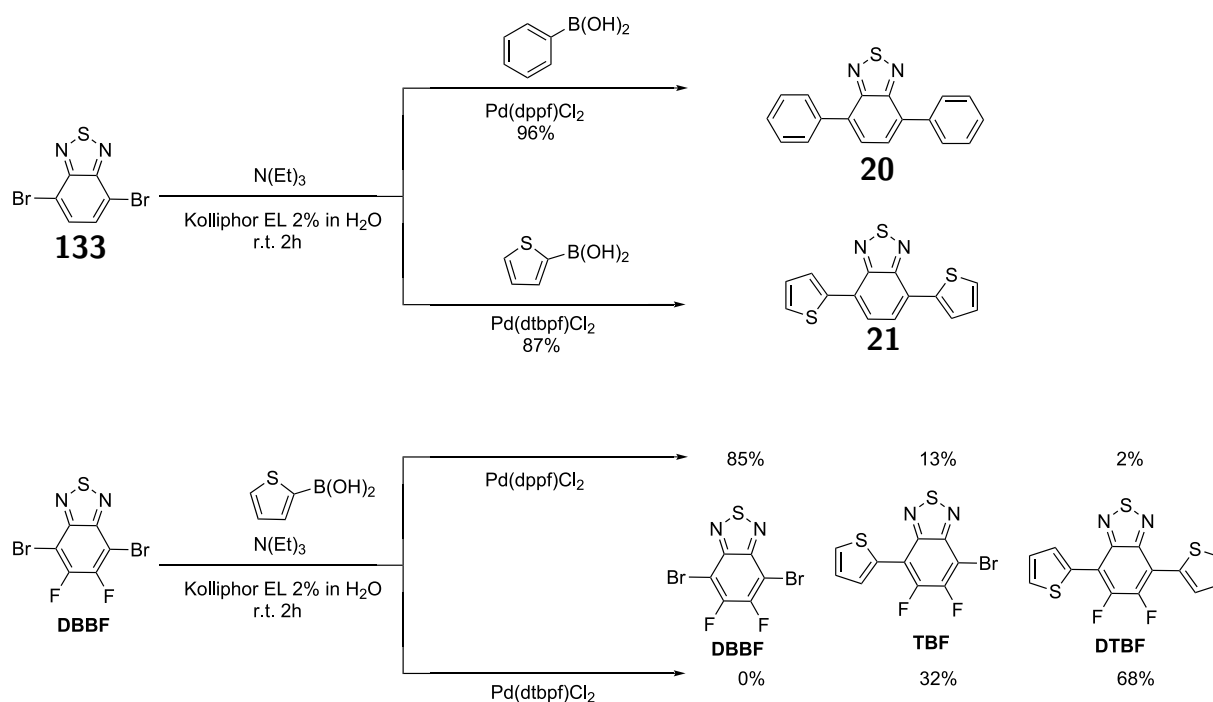
Figure 3.4 Number of hits per year for papers containing DTBF either as such or as a portion of a more complex structure. Extraction of data done on march 24th 2018, source:SciFinder

As shown in scheme 3.11, DTBF can be prepared according to three routes: a) from 4,7-dibromo-5,6-difluoro-2,1,3-benzothiadiazole (DBBF) and 2-tributylstannyl thiophene with various Stille coupling protocols,^{103, 104} for example in chlorobenzene and under microwave irradiation¹⁰⁵ b) from 4,7- diiodo-5,6-difluoro-2,1,3-benzothiadiazole (**131**) and 2-thienylboronic acid pinacol ester via SM coupling in water/THF mixture in moderate to good yield,¹⁰⁶ c) directly from 5,6-difluoro-2,1,3-benzothiadiazole (**132**) and 2- bromothiophene via C-H activation, in modest yield.¹⁰⁷ None of such methods can be considered sustainable. The Stille route is efficient but involves both the use of organic solvents and of tin compounds. The Suzuki coupling is generally inefficient in the case of thiophene containing derivatives as the poor reactivity of the thienyl-boronic acid is connected with a pronounced tendency to protodeborylation, particularly at high temperature.¹⁰⁸ Finally, the C-H activation is attractive, as it does not require activation of 5,6-difluoro-2,1,3-benzothiadiazole. However, the need for prolonged heating in an organic solvent in combination with a poor yield limit convenience. Micellar synthesis has demonstrated strong potential to improve sustainability,⁶¹ as discussed extensively in the introduction of this chapter. In this section we show that the careful tuning of reaction conditions - in this case particularly referring to the definition of the micellar environment through a formulation chemistry approach - enables the preparation in quantitative yield of DTBF in water as the only solvent, at room temperature and under standard laboratory environment by means of the SM coupling of DBBF and 2-thienylboronic acid. We also show that conditions can be tuned in order to prepare unsymmetrical derivatives bearing two different aryl residues in a one pot procedure not requiring the isolation of the monoarylated intermediate. Results are relevant both as they provide a simple and sustainable access to valuable intermediates and because they shed some light on the peculiar characteristic of microheterogeneous micellar reactions over homogeneous phase approaches.

3.4.2 Results

3.4.2.1 Micellar synthesis of DTBF

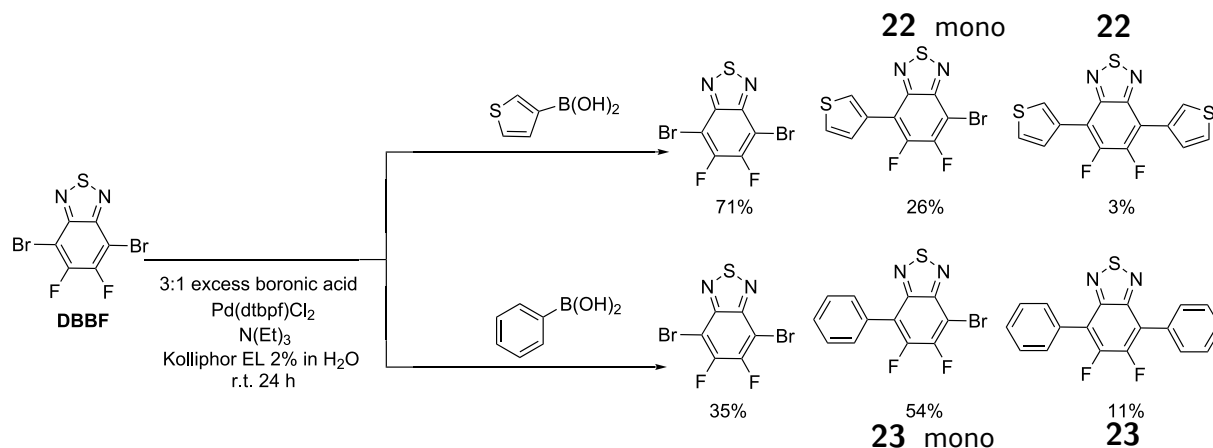
We recently prepared the two 4,7-diaryl-2,1,3-benzothiadiazole derivatives (**20,21**) shown in 3.12 by means of an efficient room temperature micellar SM reaction, carried out in a 2 wt% water solution of Kolliphor EL.¹⁷ Whilst the phenyl end-capped derivative **20** can be prepared in quantitative yield using 2 mol% Pd(dppf)Cl₂ as the catalysts, the synthesis of **21** requires the use of the more efficient Pd(dtbpf)Cl₂ in analogous stoichiometry. No doubt, this is connected with the poor reactivity of 2-thienylboronic acid. However, in both reactions we did not observe the formation of the monoarylated species. Reactions were selective towards the formation of the diarylated compounds, even in the case of excess of 4,7-dibromo-2,1,3-benzothiadiazole (**133**) over the boronic acid employed (scheme 3.12).



Scheme 3.12 Difference in the mono vs diarylation selectivity in SM reactions carried out on 4,7-dibromo-2,1,3-benzothiadiazole (**133**) vs DBBF.

When moving from compound **133** to DBBF, the reaction behaviour changes completely. As it is shown in scheme 3.12, the reaction carried out with Pd(dppf)Cl₂ gives very little conversion, mostly leading to the monoarylated species. The only byproducts we observed by GC-MS of the reaction mixture were bithiophene (the homocoupling product of the boronic acid) and 4-(thiophene-2-yl)-5,6-difluoro-2,1,3-benzothiadiazole, both of them in concentration below 0.5%. TLC inspection and NMR analysis confirmed that the 2-thienylboronic acid was still present, so that protodeborylation can be ruled out as the reason for the reaction not reaching full conversion. When switching to Pd(dtbpf)Cl₂, the conversion increases substantially yet the reaction does not go to completion. Further extension of the reaction time does not influence the composition of the reaction mixture. As in the previous case, the homocoupling and debromination byproducts are barely distinguishable from the background noise in the GC-MS chromatograms.

In order to evaluate the generality of the effect, we also tested the coupling of DBBF with two additional boronic acids: 3-thienylboronic acid and phenylboronic acid. Reactions were performed in 2 wt% Kolliphor EL under standardized conditions: 0.5 M DBBF, 1.5 M boronic acid, 3 M $N(Et)_3$ and 2 mol% with respect to the bromide of $Pd(dppf)Cl_2$. Scheme 3.13 shows the results we obtained.



Scheme 3.13 Examples of SM reactions carried out on DBBF and leading to limited conversion.

None of the reaction gave complete conversion and the monocoupling product was the dominating component. Results also reflect the different reactivity of the boronic acids employed: the reaction performed with phenylboronic acid was sizeably more effective.

As discussed before in the section 3.3.3, we observed a similar behaviour in the SM coupling of both thiophene and phenyl boronic acid with di-bromides pertaining to the family of the latent pigments. Such species give essentially no conversion with a variety of surfactants (including the popular designer surfactant TPGS-750-M⁶³) and catalysts. The reaction becomes very efficient in the presence of a small amount of a water immiscible co-solvent of suitable polarity.¹⁶ Such observation hinted at a problem of unsuitable localization of the reactive species within the micelles, thus requiring evolution from micellar to an emulsion approach. The use of a co-solvent is a known and resourceful tool.¹⁰⁹ Although efficient, it remains unsatisfactory from the stand point of sustainability and E-factor reduction, as the use of organic solvents should be limited as much as possible. In this work we aim both at finding a satisfactory protocol leading to DTBF in high yield and without the use of organic solvents and at the elucidation of the factors limiting the conversion in schemes 3.12 and 3.13 reactions. We thus decided to use the SM coupling of DBBF and 2-thienylboronic acid as a relevant case study and we evaluated the product distribution as a function of key reaction parameters: the concentration and nature of the surfactant(s), the concentration of the reagents, and the nature of the catalyst. The computationally aided rationalization of the results was finally exploited for the identification of conditions preferentially giving mono vs double SM coupling in order to prepare unsymmetrically substituted derivatives in a one pot procedure.

3.4.2.2 Influence of the surfactant concentration

The first parameter we investigated was the concentration of the surfactant. Literature data mostly refer to a 2 wt% as the best trade-off between efficiency and cost. The latter factor is not that relevant in the case of Kolliphor EL, we thus examined 2, 5, 10 and 20 wt% solutions (see figure 3.5).

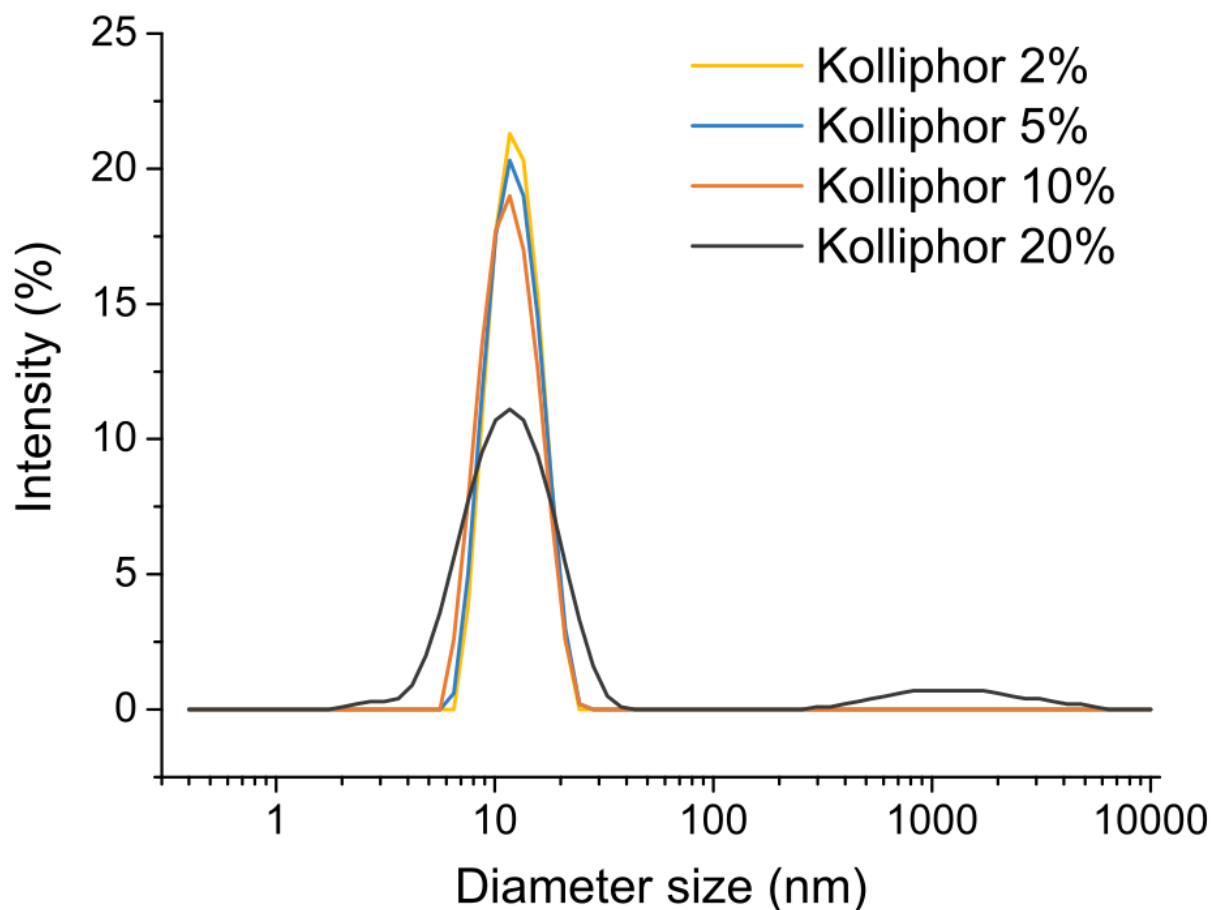


Figure 3.5 DLS measurements of Kolliphor EL solutions in water as the function of the surfactant concentration.

Dispersion	Size peak 1 (Integrated % intensity)	Size peak 2 (Integrated % intensity)
Kolliphor EL 2%	12.7 nm (100%)	-
Kolliphor EL 5%	12.6 nm (100%)	-
Kolliphor EL 10%	12.5 nm (100%)	-
Kolliphor EL 20%	12.6 nm (91%)	1600 nm (9%)

Table 3.1 peak peaks of micellar layer distributions and their relative intensities

The DLS analysis of the surfactant solution (see figures 3.5 and table 3.1) shows that while there is little difference between 2, 5 and 10 wt% solutions in terms of the dimensions

of the micelles obtained, the 20 wt% one also contains aggregates of larger dimensions. We carried out all reactions under standardized conditions: 0.5 M DBBF, 1.5 M 2-thienylboronic acid, 3 M N(Et)₃ and 2 mol% with respect to the bromide of Pd(dppf)Cl₂. Initially, we purposefully decided to use Pd(dppf)Cl₂ over the more reactive Pd(dtbpf)Cl₂ in order to magnify the differences between the various reaction conditions employed. All reactions were quenched after 12 h stirring at room temperature, extracted with CH₂Cl₂, filtered over a pad of silica gel and submitted to GC-MS characterization. Table 3.2 shows the product distributions we obtained, corrected for the instrument response factor for the three different analytes (See Appendix 3.4.6.1 for details).

Entry	Surfactant concentration (wt%)	DBBF (mol%)	TBF (mol%)	DTBF (mol%)
1	2	85	13	2
2	5	64	33	3
3	10	28	65	7
4	20	61	34	5

Table 3.2 Influence of the Surfactant concentration in the SM coupling reaction between DBBF and 2-thienylboronic acid. Conditions: 0.5 M DBBF, 1.5 M 2-thienylboronic acid, 3 M N(Et)₃ and 2 mol% with respect to the bromide of Pd(dppf)Cl₂. Room temperature, 12 h.

With the exclusion of the data relative to the 20 wt% solution – where in any case the mixture is out of the micellar regime as evidenced by the DLS data - the reaction becomes increasingly more efficient at higher surfactant concentration. The reaction is somewhat selective to the monoarylated product even in the presence of a large excess of boronic acid. Running the reaction for a longer time and/or under nitrogen atmosphere did not influence the conversion nor changed in any way the product distribution.

3.4.2.3 Influence of the reagents formal concentration

At a fixed surfactant concentration of 2 wt%, we varied the formal concentration of the reagents, while leaving fixed the respective stoichiometry ratio of 1:3:6:0.02 for DBBF:boronic acid: $\text{N}(\text{Et})_3$:catalyst respectively. It should be noted that in a micellar reaction, in our concentration range, most of the reagents and products are just suspended in water, only a fraction of them being incorporated into the micelles where the coupling reaction takes place. As such, the nominal concentration may not be correlated with the stoichiometric ratio within the micelle. Table 3.3 shows the results we obtained. The reaction shows very little sensitivity to the concentration of the reagents, coherently with the fact that in all of the cases the reaction mixture contains way more lipophilic molecules than those that can be simultaneously accommodated by the micelles. Within the 0.5 -1.0 M nominal concentration the reaction gives best results. It should be noted that at 1.0 M concentration the reaction mixture is very viscous and mechanical stirring is recommended.

Entry	DBBF (M)	DBBF (mol%)	TBF (mol%)	DTBF (mol%)
1	0.3	84	15	1
2	0.5	85	13	2
3	1.0	77	21	2
4	1.5	92	8	0

Table 3.3 Influence of the reagents molarity at 2 wt% Kolliphor concentration in the SM coupling reaction between DBBF and 2-thienylboronic acid. Reaction carried out at room temperature, 12 h.

3.4.2.4 Influence of the Surfactant

An alternative solution to the development of a new surfactant is the use of a mixture of existing and readily available ones, aimed at tuning the interaction of the micelles with either the reagents or the products of a given reaction. In such an approach, the synthetic chemist resorts to the formulation chemist's toolbox to tailor the reaction microenvironment as needed. Commercial surfactants are complex molecules possessing functional groups of different polarity. In the case of polyethoxylated species, like Kolliphor EL, they are also intrinsically polydisperse. In order to be able to qualitatively describe the affinity of a given surfactant with respect to a phase to be dispersed/emulsified, formulation chemists developed the concept of the Hydrophilic-Lipophilic Balance (HLB). This is a completely empirical parameter, not necessarily linearly correlated for example with the dielectric constant, that gives a qualitative idea of the affinity of a surfactant for water ($\text{HLB} > 10$) or for oil ($\text{HLB} < 10$).¹¹⁰The HLB of Kolliphor EL is 13.5, which identifies it as water soluble and appropriate for the preparation of oil in water emulsions. Aiming at tuning the interaction of Kolliphor EL with the components of the reaction mixture, we decided to mix it with two other neutral and polyethoxylated industrial surfactants, Tween 80 and Span 80, featuring an HLB of 15 and 4.3, respectively. In both cases we mixed the surfactants in a 7:3 ratio Kolliphor/co-surfactant. As it is discussed below, this proportion is dictated by the limited solubility in water of Span 80. The HLB values of the two mixtures can be calculated as the weighted average of the HLB of the pure constituents, thus the Kolliphor EL/Span 80 mixture has an HLB value of 10.7 and the Kolliphor EL/Tween 80 mixture of 14.0. As we have previously stressed, the HLB cannot

be directly related to the dielectric constant or the partition coefficient of the surfactants, yet it is safe to assume that at higher HLB values more polar derivatives will be preferentially dispersed. Table 3.4 shows the results we obtained while running the reaction at a 2 wt% surfactant concentration and at a nominal concentration of 0.5 M for the bromide. The decision to work at 2 wt% was dictated by the very limited solubility of Span 80 in water.

Entry	Surfactant (HLB)	DBBF (mol %)	TBF (mol %)	DTBF (mol %)
1	Kolliphor EL (13.5)	85	13	2
2	70% Kolliphor EL 30% Span 80 (10.7)	76	22	2
3	70% Kolliphor EL 30% Tween 80 (14.0)	95	5	0

Table 3.4 Influence of the Surfactants nature at 2 wt% concentration in the SM coupling reaction between DBBF and 2-thienylboronic acid. Conditions: 0.5 M DBBF, 1.5 M 2- thienylboronic acid, 3 M N(Et)₃ and 2 mol% with respect to the bromide of Pd(dppf)Cl₂. Room temperature, 12 h.

The conversion degree is poor in all three cases, yet sizeably improving when working at low HLB values. In principle, it could be interesting to explore even lower HLB values, yet this is technically difficult as surfactants approaching an HLB value of 10 are perfectly balanced between lipophilic and hydrophilic behaviour and are only partially soluble in water. Span 80 in particular is not water soluble and can be homogeneously dispersed in water only in the employed 7:3 mixture with Kolliphor EL and even then, requiring the use of an high shear mixer. Simple stirring does not provide a homogeneous formulation.

3.4.2.5 Influence of the catalyst

Having assessed that the reaction is favoured by higher surfactant concentration and, at least to some extent by lower HLB values, we tested under selected formulation conditions the use of the way more reactive catalysts Pd(dtbpf)Cl₂ instead of Pd(dppf)Cl₂. Table 3.5 shows the results. The use of Pd(dtbpf)Cl₂ greatly improves the conversion under all conditions explored, we however managed to push reaction to completion, with nearly quantitative formation of the diarylation product, only in the case of the Kolliphor EL/Span 80 mixture, corresponding to the lowest HLB mixture we explored. The mono Vs diarylation ratio can be controlled by tuning the stoichiometry of the 2-thienylboronic acid. Entry 8 of table 3.5, corresponding to a reaction where the boronic acid was used in 1.5 to 1 stoichiometric ratio over DBBF instead of the larger excess of 3:1 we employed in all other trials, shows that is it possible to prepare the monoarylated species at 83% yield without appreciable unreacted DBBF and in the presence of only 17% of DTBF.

3.4. SYNTHESIS OF BENZOTHIADIAZOLE DERIVATIVES IN MICELLAR CONDITION

As it is discussed below, this result opens the way to the preparation of unsymmetrical derivatives

Entry	Surfactant	Catalyst	DBBF (mol %)	TBF (mol %)	DTBF (mol %)
1	Kolliphor EL	Pd(dppf)Cl ₂	85	13	2
2	Kolliphor EL	Pd(dtbpf)Cl ₂	0	32	68
3	70% Kolliphor EL 30% Span 80	Pd(dppf)Cl ₂	76	22	2
4	70% Kolliphor EL 30% Span 80	Pd(dtbpf)Cl ₂	0	3	97
5	70% Kolliphor EL 30% Tween 80	Pd(dppf)Cl ₂	95	5	0
6	70% Kolliphor EL 30% Tween 80	Pd(dtbpf)Cl ₂	0	25	75
7	70% Kolliphor EL a 30% Span 80	Pd(dtbpf)Cl ₂	0	75	25
8	70% Kolliphor EL a 30% Tween 80	Pd(dtbpf)Cl ₂	0	83	17
9	70% Kolliphor EL b 30% Span 80	Pd(dtbpf)Cl ₂	48	44	8

Table 3.5 Influence of the catalyst as the function of reaction formulation in the SM coupling reaction between DBBF and 2-thienylboronic acid. Conditions: 0.5 M DBBF, 1.5 M 2-thienylboronic acid, 3 M N(Et)₃ and 2 mol% with respect to the bromide of the catalyst. Room temperature, 12 h. a) Reaction conditions: 0.5 M DFBT, 0.75 M 2-thienylboronic acid, 1.5 M N(Et)₃ and 2 mol% with respect to the bromide of Pd(dtbpf)Cl₂. b) Conditions: 0.5 M DBBF, 1.5 M 2-thienylboronic acid, 3 M N(Et)₃ and 0.05 mol% with respect to the bromide of the catalyst. Room temperature, 12 h.

3.4.2.6 Computational analysis

The datasets described in tables 3.2,3.3,3.4 and 3.5 demonstrates that the nature of the micellar environment where reactions take place has a strong influence on the product distributions and overall conversion. It remains however an open question the reason why reactions performed on 4,7-dibromo-2,1,3- benzothiadiazole (**133**) are selective towards double SM coupling whilst the opposite is true for DBBF. We carried out a computational analysis of the various aryl halides and corresponding products of mono- and di-arylation in order to get relevant parameters, such as the dipole moment, to be used as a guide in the elucidation of surfactant/molecules interaction within the micelles. A quantitative correlation of the dipole moment of the chemical species involved and the HLB of the surfactant(s) employed would be an overstretching of an empirical parameter introduced to describe the stability of industrial formulations. Nonetheless the comparison of the calculated dipole moments in water and toluene of DBBF, 4,7-dibromo- 2,1,3-benzothiadiazole (**133**) and the corresponding mono and diarylation products with the various boronic acids we employed, table 3.6 could show relevant trends.

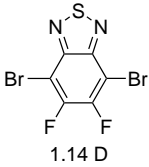
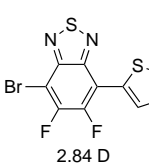
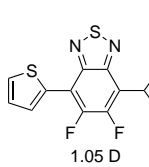
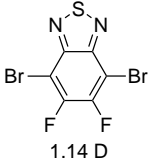
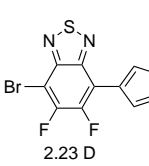
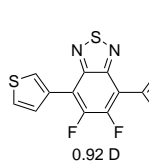
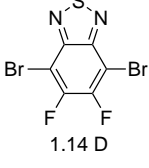
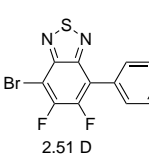
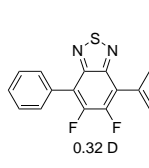
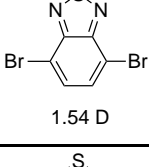
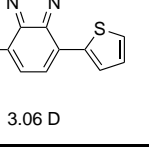
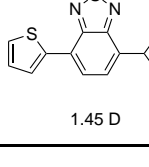
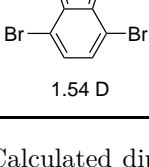
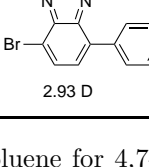
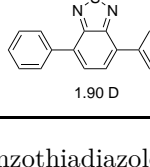
 1.14 D	 2.84 D	 1.05 D
 1.14 D	 2.23 D	 0.92 D
 1.14 D	 2.51 D	 0.32 D
 1.54 D	 3.06 D	 1.45 D
 1.54 D	 2.93 D	 1.90 D

Table 3.6 Calculated dipole moments in toluene for 4,7- dibromo-2,1,3-benzothiadiazole(**133**), DBBF and the corresponding mono and diarylation products with 2-thienylboronic acid, 3- thienylboronic acid and phenylboronic acid. Values are averaged amongst the two (for monoarylation products) and three (for diarylation products) almost degenerate rotamers available (see Appendix 3.4.6.2).

We thus carried out a series of ab initio simulations based on density functional theory (DFT), performed by using the ORCA suite of programs.¹¹¹ We report first that all the

3.4. SYNTHESIS OF BENZOTHIADIAZOLE DERIVATIVES IN MICELLAR CONDITION

mono- and diarylated compounds are characterized by the occurrence of almost degenerate (energy difference never larger than 0.013 eV) stable rotamers. In 2- and 3-thienyl adducts, the solid angle between the DBBF and thienyl planes generally approaches 0° or 180° values, corresponding to two nonequivalent isomers in the case of monoarylated compounds. Such isomers are characterized by similar molecular dipoles, always higher than that calculated for the unsubstituted DBBF and 4,7-dibromo-2,1,3- benzothiadiazole (**133**). The two equivalent monosubstituted phenyl rotamers (solid angle of 40°) are also characterized by a similar increase in the molecular dipole. Such increase is due to the strong component of the dipole moment rotated astray from the C2 symmetry axis of DBBF (4,7-dibromo-2,1,3- benzothiadiazole) in all monoarylated compounds. The addition of a second aryl group generally leads to the formation of three possible and again almost-degenerate isomers, and, in turn, to the symmetrization of the molecule, with the dipole of monoarylated compounds counterbalanced by the presence of a second thienyl or phenyl group. The resultant dipole vector is far shorter in diarylated molecules than in monoarylated, and also shorter than that calculated for DBBF, while is it longer in the case of 4,7-dibromo-2,1,3benzothiadiazole, having a dipole vector collinear but inverted with respect to DBBF. Without loss of generality, dipole values reported in table 3.6 are averaged on rotational isomers; a detailed description of all the investigated isomers, including relative energies and interconversion barriers, has been reported in the appendix. Even if the calculated values of the dipole moments in water and toluene are different, the same trend is reproduced in both datasets. Only derivatives **20** and **21** shows a polarity similar or higher than that of the starting dibromide. In all other cases, the diarylation product is sizeably less polar than both the starting bromide and the monoarylated intermediate.

3.4.3 Discussion

Most micellar reactions described in the literature require the use of a 2 to 5 wt% solution of surfactant in the presence of 0.5 to 1.0 M solutions of the reagents. As it is also quite clear from the various pictures that can be found in the published papers or from figure 3.6, reaction vessels contain way more water insoluble material than the maximum amount that can be incorporated within the micelles at a given time. Actually, micellar synthesis is not a completely appropriate term as the reaction mixture is a suspension. Achievement of complete conversion in such kind of reactions requires that a single micelle takes up reagents, localizes them in the same compartment where the catalyst is also present, assists to their transformation in the product and eventually releases the latter to replace it with a fresh aliquot of the former. This cycle has to be repeated several times, depending on the concentration of the surfactant. In the absence of a selective affinity for products vs reagents, within the normal uptake/release equilibria involving all micelles, products and reagents will have a probability of being incorporated that will depend on their relative concentration. The reaction will eventually slow down but go to complete conversion anyway. If, however the aryl halide and the corresponding arylation product have a sizeably different affinity for the micelle compartment where the reactions take place, one of the two will be preferentially incorporated. If micelles preferentially take up the halide, the reaction will be particularly efficient. On the opposite, in the case of preferential uptake of the product, the reaction will be severely slowed down by saturation of the active sites. The latter effect appears to be affecting the coupling of DBBF and 2-thienylboronic acid. Indeed, the conversion degree depends linearly upon the amount of surfactant employed. The dependency of the mono vs diarylation ratio with the surfactant concentration is less pronounced. Within the experimental error connected with the small amount of DTBF obtained, the ratio can be assumed to be almost independent from the surfactant concentration. The data suggest that a saturation effect prevents the micelles from performing the coupling reactions multiple times, opposite to what is happening in the case of, for example, the preparation of **134** and **135**. To gain further evidence that reactions do not proceed above a certain conversion degree due to selective affinity towards the products, we carried out 3.14 reaction working at 0.5 M nominal concentration of bromide in a 2 wt% Kolliphor EL solution. We let the formulation equilibrate for 24 h under stirring, prior to add the catalyst and the base. The formation of the diarylated species was barely detectable. Actually, at least half of the DTBF detected by the GC-MS after 24 h was already present at the beginning of the reaction as a contaminant of the monoarylated specie, whose chromatographic purification from DTBF is troublesome.

3.4. SYNTHESIS OF BENZOTHIADIAZOLE DERIVATIVES IN MICELLAR CONDITION

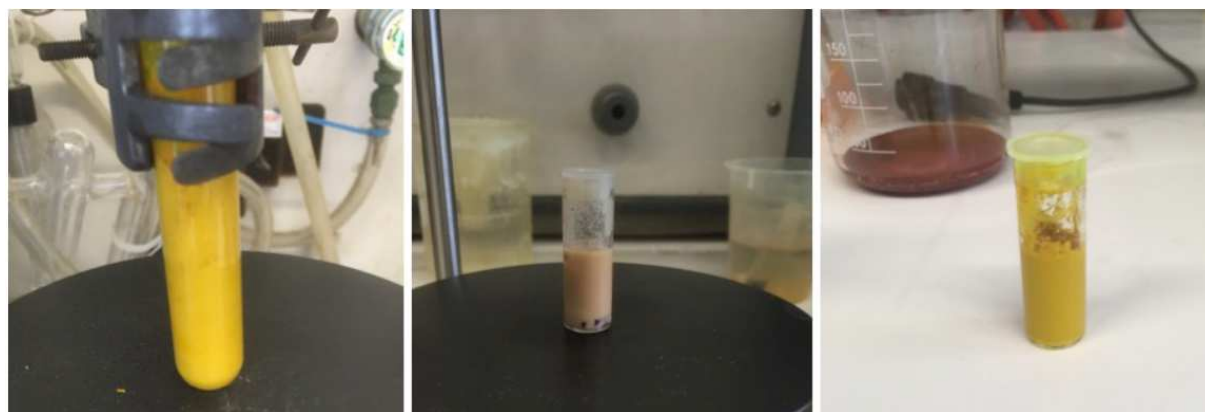
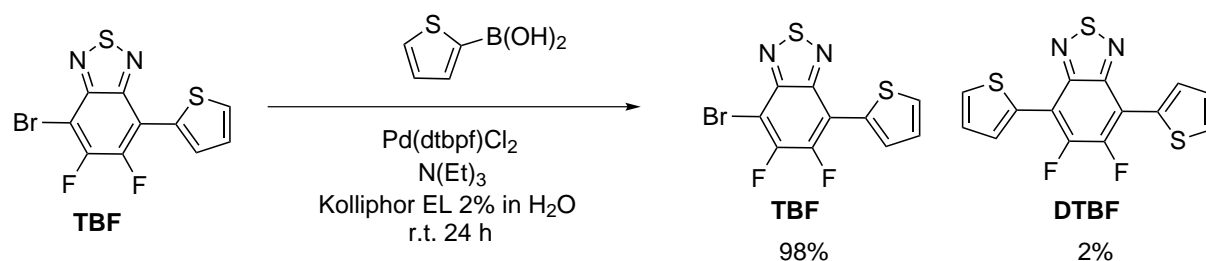


Figure 3.6 Pictures of typical micellar reactions taken at various times. Dispersing medium: from left to right Kolliphor, Kolliphor/span 80 and Kolliphore/Tween 80 mixtures.



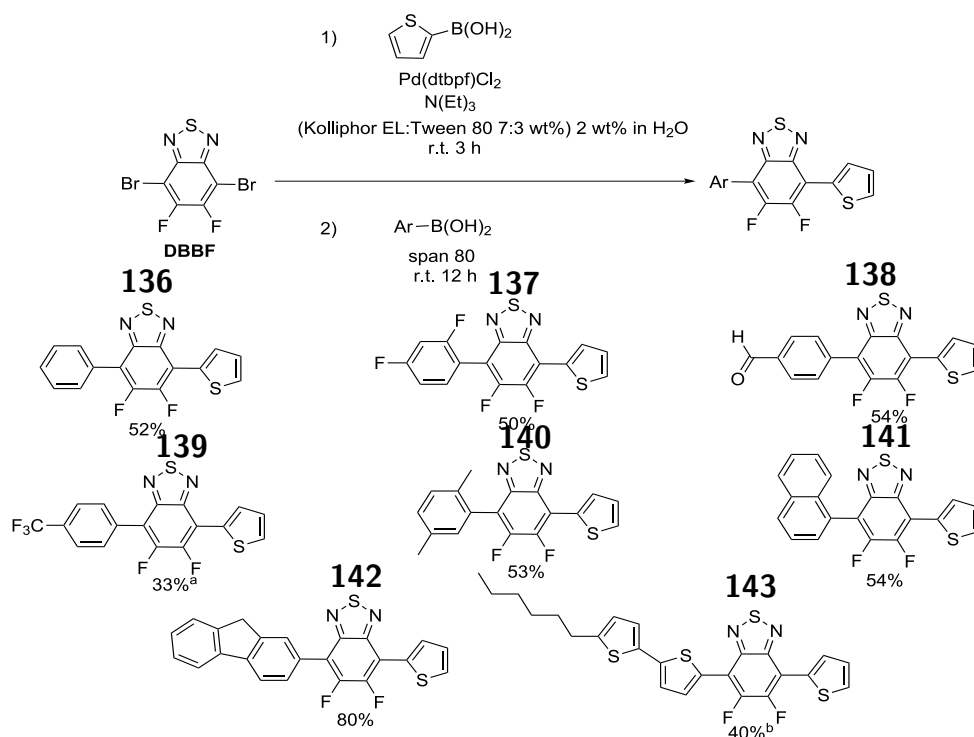
Scheme 3.14 SM reaction of TBF and 2-thienylboronic acid in 2 wt% Kolliphor EL demonstrating the micelles saturation effect.

It is accepted that in a micellar protocol, chemical transformations happen preferentially within the apolar core, where the catalyst is localized (this is in particular demonstrated in the case of Kolliphor EL according to our previous experience).¹⁷ The computational results summarized in table 3.6 differentiate fluorinated from nonfluorinated derivatives on the basis of the polarity of both precursors and reagents. In both cases the polarity is increased by the first coupling and decreased by the second one, essentially due to geometrical reasons. Fluorinated derivatives remain however in all of the cases less polar than the nonfluorinated ones. When we carried out reactions in Kolliphor EL, at the relatively high HLB values of 13.5, we privileged the emulsification of polar over nonpolar substances. In the nonfluorinated series, likewise generally better matched with Kolliphor EL HLB, dibromide and diarylated derivatives possess similar and relatively high polarity. The micelles do not preferentially stabilize neither of them and the reaction goes to completion. The most polar species, the monoarylated intermediate, is never observed as it reacts directly prior to leave the micelle. In the fluorinated series the polarity of all involved species is smaller so that the emulsification of DBBF in the first place is sluggish (indeed even by eye inspection it takes several minutes to observe the formation of a homogeneous dispersion). Moreover, reaction leads to a further reduction of polarity on going from DBBF to the diarylated species. At high HLB values the reaction does not perform for lack of compatibility. At low HLB values the situation improves yet the conversion remains limited by the preferential accumulation of diarylation product (the less polar species) over reagent within the micelles. Due to the aforementioned slow homogenization of the reaction mixture, the saturation effect takes some time to happen. When Pd(dppf)Cl₂ is used the reaction is very slow and the micelles saturation effect is

dominating over conversion. The opposite is true when Pd(dtbpf)Cl₂ is used, the reaction is very fast (GC-MS traces after 30 min and 12 h are identical) and proceeds smoothly, in the low HLB mixture (Table 4 entry 4) and somewhat less performingly at higher HLB factors (Table 4, Entries 2 and 6). Interestingly, at catalyst loading of 0.05 mol%, when the reaction is in any case slow, even with Pd(dtbpf)Cl₂ and in the low HLB surfactant mixture, we obtained results fully comparable with those obtained with Pd(dppf)Cl₂ (Table 4, entry 9). The Entry 4 of Table 4 shows that the use of 2 mol% of Pd(dtbpf)Cl₂ in combination with a Kolliphor EL/Span 80 7:3 mixture gives access, in quantitative yield, at room temperature and without the use of any cosolvent, to DTBF. The reaction is so efficient that the product can be isolated at analytical purity directly by filtration of the reaction mixture over a sintered silica filter followed by washing with water and MeOH. The reaction was scaled up to 20 g of starting DBBF in order to precisely evaluate the E-factor. As the only organic waste produced was the MeOH employed for the final washing step (performed in a Soxhlet continuous extractor), we were able to get an E-factor as low as 4.4, to be compared with the values spanning from a minimum of 9.9 to a maximum of 48.8, excluding purifications as no suitable data are available. Tuning the reaction stoichiometry enables the control of mono vs diarylation, thus opening the way for the preparation of unsymmetrically substituted derivatives in a one pot procedure.

3.4.3.1 One pot synthesis of nonsymmetric derivatives

The entry 8 of table 3.5 shows that when the reaction is carried out with a 1.5 to 1 stoichiometric ratio of 2-thienylboronic acid over DBBF and in a Kolliphor EL/Tween 80 mixture, the product distribution is 83% monoarylated and 17% diarylated. In principle this result could open the way for the one pot synthesis of unsymmetrically substituted derivatives. According to the same Table however, the only way to drive the reaction to completion is to use a Kolliphor EL/Span 80 mixture. As such, we devised a two-step, but still one pot as no isolation of the intermediate monoarylation product is necessary, procedure. Firstly, we carried out the reaction according to the conditions reported in table 3.5, entry 8. Once verified that no DBBF was left, we added a second aliquot of another arylboronic acid and as much Span 80 as it is required to reach the HLB value of 10.7, necessary to drive the reaction to completion, thus giving access to unsymmetrically substituted derivatives. Scheme 6 shows the general reactions scheme as well as the examples we obtained of original 4,7-diaryl-5,6-difluoro-2,1,3- benzothiadiazole derivatives. In details, DBBF:2-thienylboronic acid: $N(Et)_3Pd(dtbpf)Cl_2$ are mixed in the 1:1.5:6:0.02 proportion working at 0.5 M concentration of DBBF. The reaction is stirred at room temperature for 3 h. At this stage the GC-MS analysis of the reaction mixture only shows traces of unreacted DBBF. 1.5 equivalents of a different boronic acid (or pinacol ester) are added along with Span 80, and mixture is stirred at r.t. overnight. The final unsymmetrically substituted derivatives are isolated by chromatographical purification of the reaction mixture. All reactions proceed till complete conversion of the TBF remained after the first step. We did not observe the formation of byproducts, other than the DTBF formed in the first step.



Scheme 3.15 a) Low yield due to troublesome chromatographic separation. b) From the pinacol ester of the corresponding boronic acid.

The moderate to good isolated yields shown in scheme 3.15 are limited by the sometimes

troublesome (particularly in the case of derivatives **139** and **143**) chromatographic purification of the target product from DTBF. All unsymmetrically substituted derivatives we made are original and could have direct applications as luminescent compounds in applications the like of Luminescent Solar Collectors, imaging or OLEDs. Indeed, they all share a good separation between absorption and emission spectra (Stokes Shifts) connected with a moderate to good emission efficiency, figure 3.7 shows the absorption and emission spectra for all asymmetric compounds.

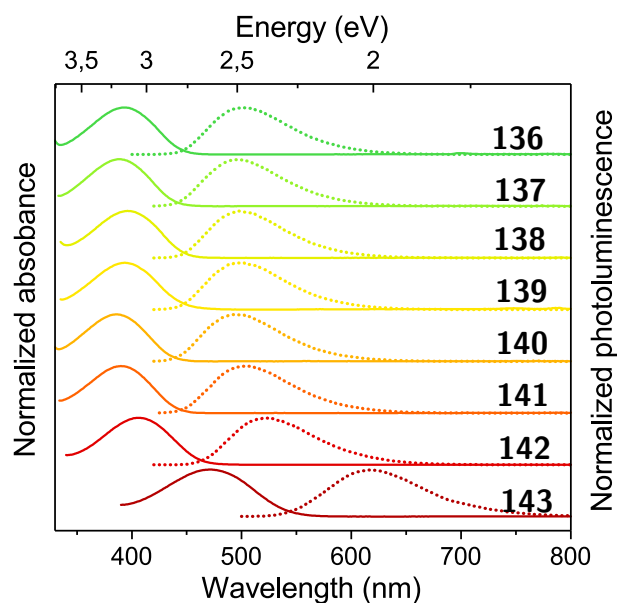


Figure 3.7 Normalized absorption (solid line) and emission (dotted line) spectra for derivatives **136-143** in CH_2Cl_2 solution.

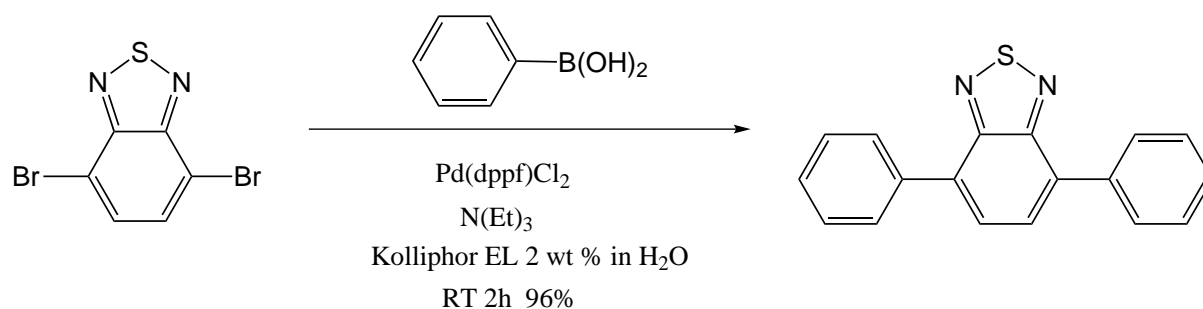
3.4.4 Conclusion

Micellar reactions are rapidly revolutionising established synthetic methods. In particular, the micellar Suzuki-Miyaura coupling represents one of the most successful examples of the capability of such techniques to dramatically improve sustainability while maintaining performances. When not immediately satisfactory, particular reactions might require tuning of conditions while moving from standard organic solvent to micellar environment. The peculiar characteristic of micro-heterogeneous micellar reactions requires a specifically devised approach where tuning of common reaction parameters (concentration, temperature, time, catalyst) has to go hand in hand with the toolbox of the formulation chemist. In the case of the synthesis of the popular conjugated building block DTBF and of several unsymmetrically substituted derivatives of the same family, reactions can be driven to completion only when the characteristics of the employed micellar environment are appropriate. The dedicated literature so far approached the problem of underperforming reactions by the introduction of new, improved surfactants. We show that the careful selection and mixing of readily available and fully sustainable commercial surfactants can lead to compete conversion where single component micellar solutions fail. We particularly focused on Kolliphor EL as the main micellar forming surfactants and on Tween 80 and Span 80 as hydrophilic and lipophilic co-surfactants respectively. We offer an interpretation of the data based on the preferential interaction of reagents vs products with micelles assembled with one or more surfactants, hampering or speeding up the reaction depending on the micelles dominating lipophilic over hydrophilic character. In particular we have found an empirical correlation between the surfactant mixture HLB value and the performance of the reaction in all cases when the polarity of reagents and products is remarkably different. Within such optimized micellar environment, it is possible to control the degree of mono vs diarylation to the point of being able to prepare unsymmetrically substituted derivatives by the sequential reaction of DBBF with two different arylboronic acids. Obviously, the generality of our results is limited to the case of the peculiar halides/boronic acids we investigated. The extension of such model to a general interpretation of the results of micellar couplings remains a tantalizing task, so far only partially undergirded by the available evidences.

3.4.5 Experimental part

Reactions were carried in a Biotage microwave vial (12 mm inner diameter) equipped with two piled round stirring bars (VWR 442-0411, crosshead, double 8x10mm) and closed with a Suba-Seal septum

3.4.5.1 Synthesis of 4,7-diphenyl-2,1,3-benzothiadiazole (20)

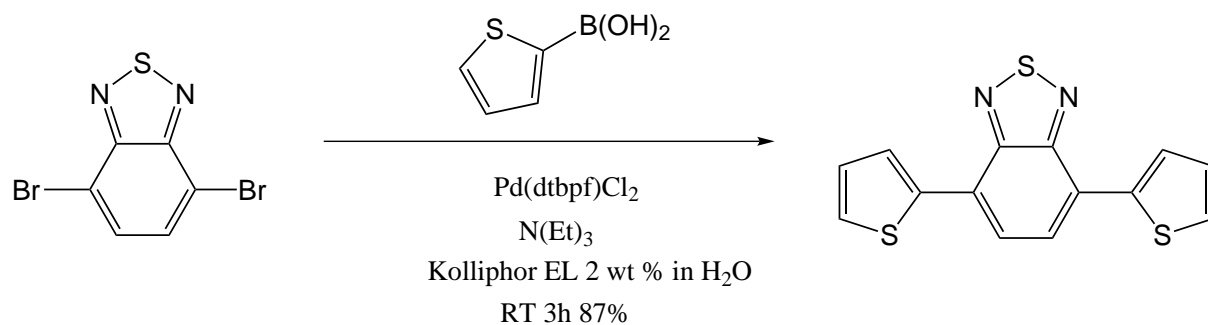


4,7-Dibromo-2,1,3-benzothiadiazole (147 mg, 0.5 mmol) and phenylboronic acid (183 mg, 1.5 mmol) are weighted in the vessel, then 1 mL of Kolliphor 2% dispersion in water is added. The mixture is stirred, then N(Et)₃ (303 mg, 3.0 mmol) is added. The mixture is allowed to homogenize for 5 minutes before addition of Pd(dppf)Cl₂ (7.3 mg, 0.01 mmol). The mixture was diluted with 10 mL of CH₂Cl₂ and filtered through a pad of silica. The filtrate was evaporated under reduced pressure and purified by chromatography with CH₂Cl₂. 4,7-diphenyl-2,1,3-benzothiadiazole was obtained as bright yellow solid (138 mg, 0.48 mmol, 96%).

¹H NMR (CDCl₃, 500 MHz): δ 7.97 (d, J = 7.78 Hz, 4H), 7.80 (s, 2H), 7.56 (t, J = 7.44 Hz, 4H), 7.47 (t, J = 7.44 Hz, 2H); ¹³C (CDCl₃, 125.7 MHz): δ 129.0, 129.3, 129.5, 130.1, 134.3, 138.3, 155.0.

3.4. SYNTHESIS OF BENZOTHIADIAZOLE DERIVATIVES IN MICELLAR CONDITION

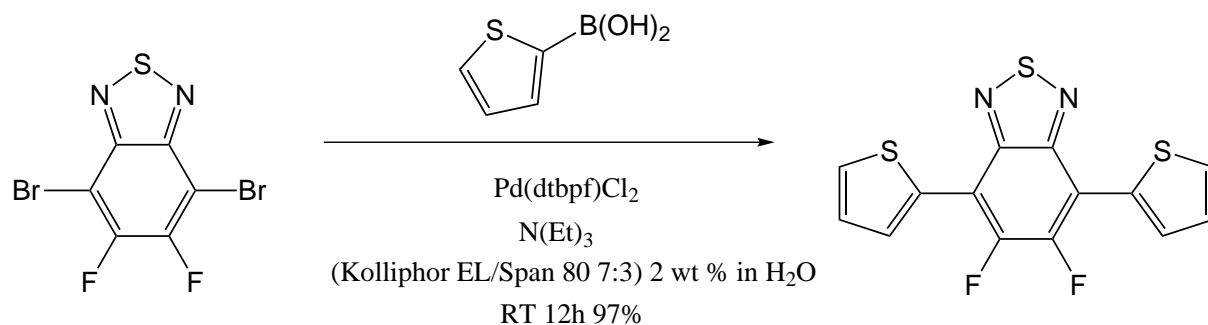
3.4.5.2 Synthesis of 4,7-di(thien-2-yl)-2,1,3-benzothiadiazole (21)



4,7-Dibromo-2,1,3-benzothiadiazole (144 mg, 0.5 mmol) and 2-thienylboronic acid (193 mg, 1.5 mmol) are weighted in the vessel, then 1 mL of Kolliphor 2% dispersion in water is added. The mixture is stirred, then N(Et)₃ (305 mg, 3.0 mmol) is added. The mixture is allowed to homogenize for 5 minutes before addition of Pd(dtbpf)Cl₂ (6.5 mg, 0.01 mmol). After 2 h, the reaction is diluted with 10 mL of water and filtered. The crude is crystallized from heptane to afford 125 mg of the pure product (87% yield).

¹H NMR (400 MHz, CDCl₃): δ 7.22–7.24 (dd, J = 5.2, 4 Hz, 2H), 7.47–7.48 (dd, J = 5.2, 1.2 Hz, 2H), 7.88 (s, 2H), 8.13–8.14 (dd, J = 3.6, 1.2 Hz, 2H). ¹³C (400 MHz, CDCl₃): δ 125.8, 126.0, 126.8, 127.5, 128.0, 139.3, 152.6.

3.4.5.3 Synthesis of symmetrical 4,7-Diaryl-5,6-difluoro-2,1,3- benzothiadiazole derivatives

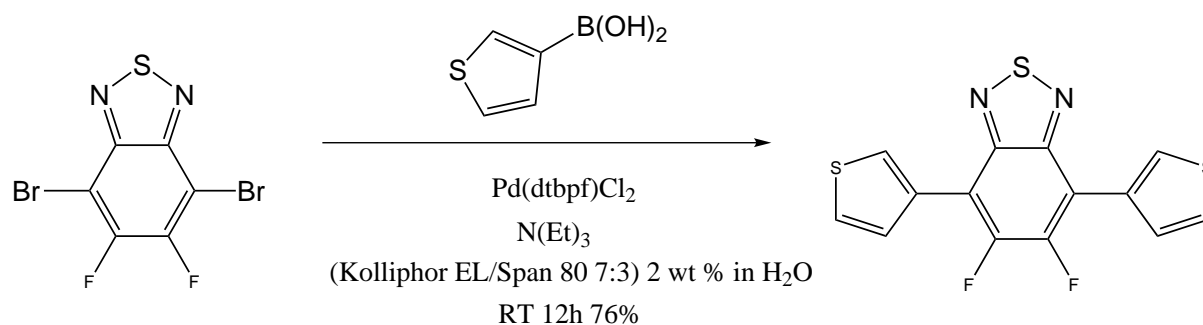


3.4.5.3.1 Synthesis of 4,7-di(thien-2-yl)-5,6-difluoro-2,1,3- benzothiadiazole (DTBF) Scaled up synthesis of DTBF

DBBF (20.0 g, 60.6 mmol) and 2-thienylboronic acid (23.3 g, 182 mmol) are weighted in a 500 mL round bottom flask, then 121 mL of 2% (Kolliphor EL/Span 80 7:3) dispersion in water are added. The mixture is stirred with a mechanical stirrer, then N(Et)₃ (36.7 g, 364 mmol) is added. The mixture is allowed to homogenize before addition of Pd(dtbbpf)Cl₂ (790 mg, 1.21 mmol). After 12 h stirring at room temperature, the reaction mixture is filtered over a sintered silica filter and the filtering cake is repeatedly washed with deionized water. The crude solid (25 g) was continuously extracted with MeOH in a Soxhlet extractor until colorless extract. A total volume of 50 ml of MeOH was employed. The pure product was recovered from the thimble as analytically pure sample. The product was recovered as a bright yellow solid. (19.8 g, 97%).

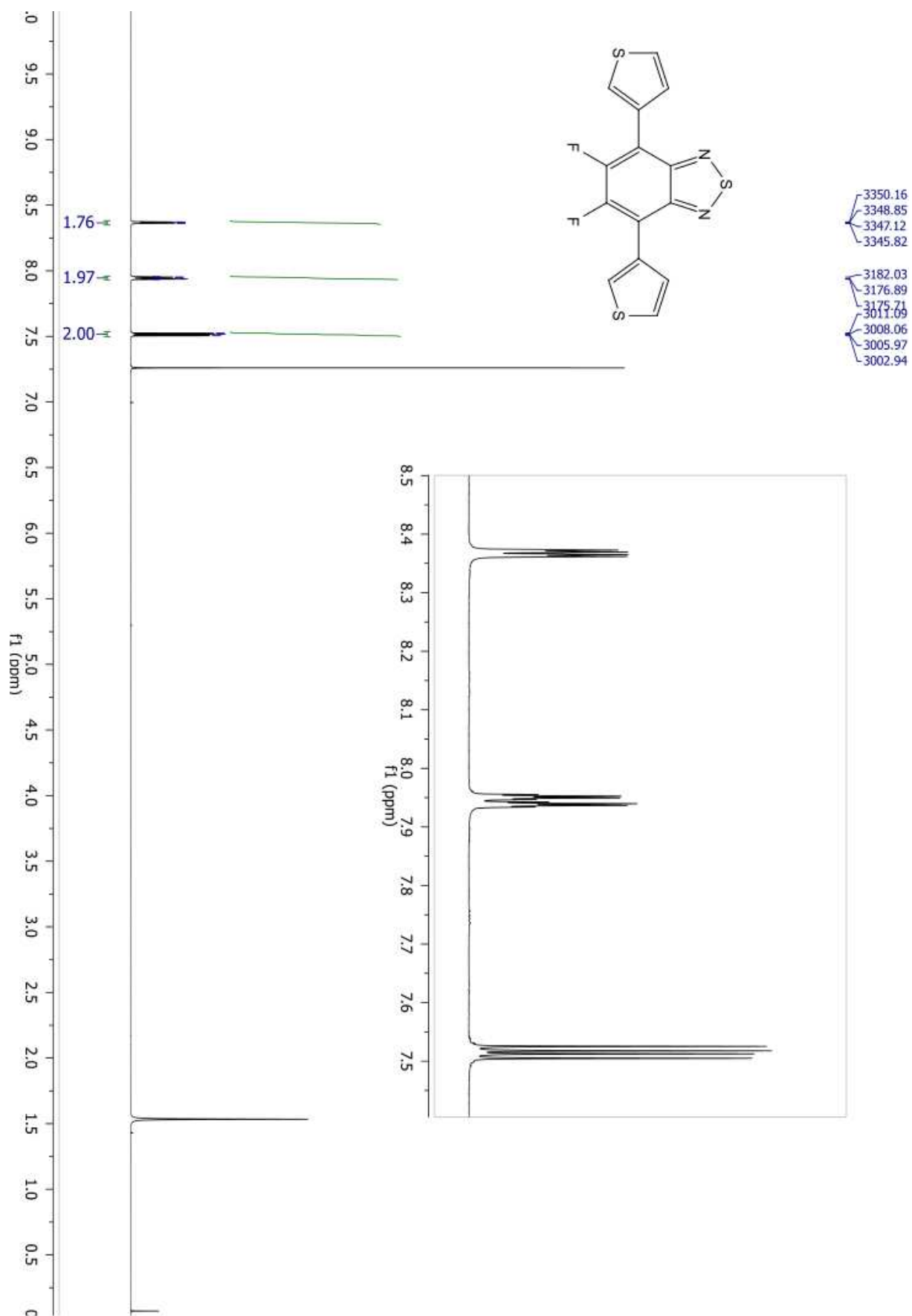
¹H (CDCl₃, 400 MHz): δ 8.30 (dd, J=3.9, 1.1 Hz, 2H), 7.62 (dd, J=5.2, 1.1 Hz, 2H), 7.27 (m, 2H). ¹³C (CDCl₃, 400 MHz): δ 149.7 (dd, J=260.0, 20.4 Hz), 148.9 (t, J=4.4 Hz), 131.5, 130.9 (t, J=3.9 Hz), 128.9 (t, J=3.1 Hz), 127.4, 111.8 (d, J=9.4 Hz).

3.4. SYNTHESIS OF BENZOTHIADIAZOLE DERIVATIVES IN MICELLAR CONDITION

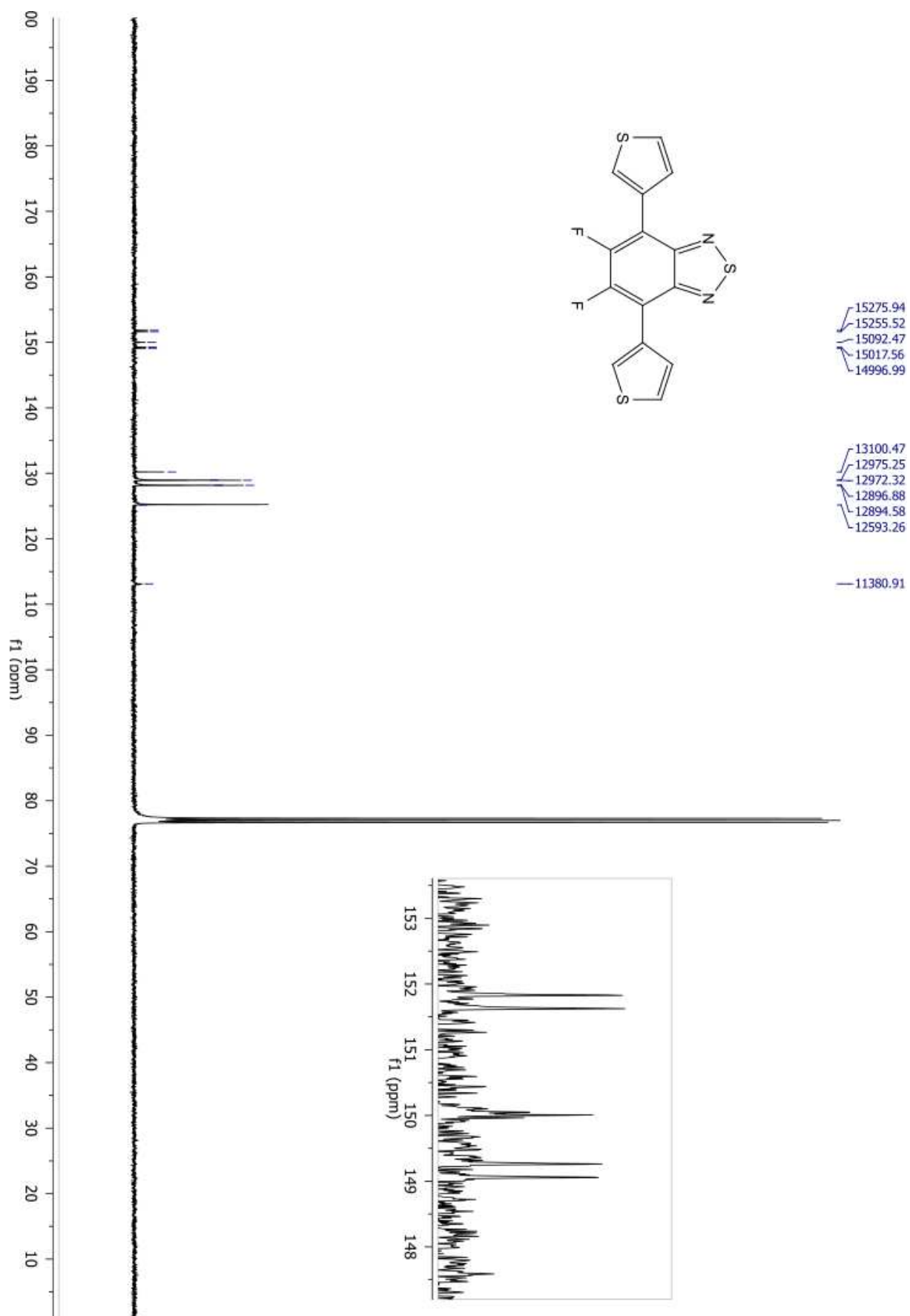


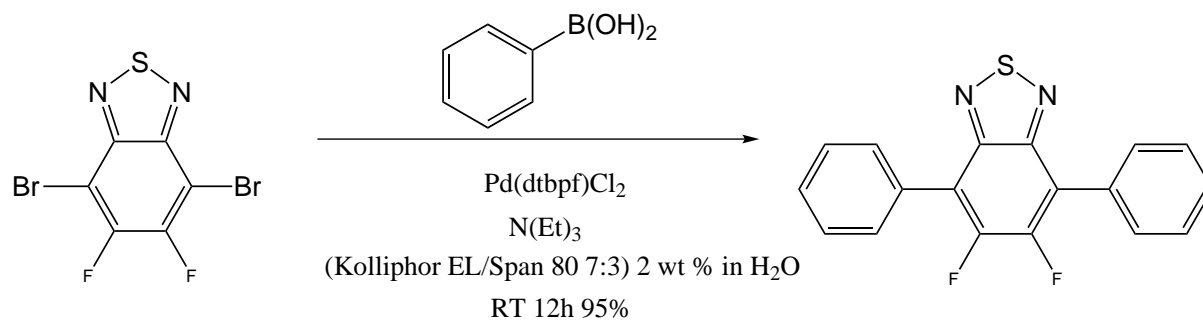
3.4.5.3.2 Synthesis of 4,7-di(thien-3-yl)-5,6-difluoro-2,1,3-benzothiadiazole (22) DBBF (165 mg, 0.5 mmol) and 3-thienylboronic acid (192 mg, 1.5 mmol) are weighed in the vessel, then 1 mL of 2% (Kolliphor EL/Span 80 7:3) dispersion in water is added. The mixture is stirred, then N(Et)₃ (303 mg, 3.0 mmol) is added. The mixture is allowed to homogenize for 5 minutes before addition of Pd(dtbpf)Cl₂ (6.5 mg, 0.01 mmol). After 12 h, the reaction is diluted with 10 mL of water and filtered. The crude is washed with cold methanol, and then crystallized from methanol to afford 128 mg of the pure product (76% yield). Anal calcd for {, 49.98; H, 1.80; N, 8.33. Found: C, 49.35; H, 1.46; N, 8.06.

¹H (CDCl₃, 400 MHz): δ 8.37 (dd, J=3.0, 1.3 Hz, 2H), 7.94 (dq, J=5.1, 1.1 Hz, 2H), 7.51 (dd, J=5.1, 3.0 Hz, 2H). ¹³C (CDCl₃, 400 MHz): δ 150.5 (dd, J=258.6, 20.4 Hz), 150.0, 130.2, 128.9 (t, J=2.9 Hz), 128.2, 125.2, 113.1.



3.4. SYNTHESIS OF BENZOTHIADIAZOLE DERIVATIVES IN MICELLAR CONDITION





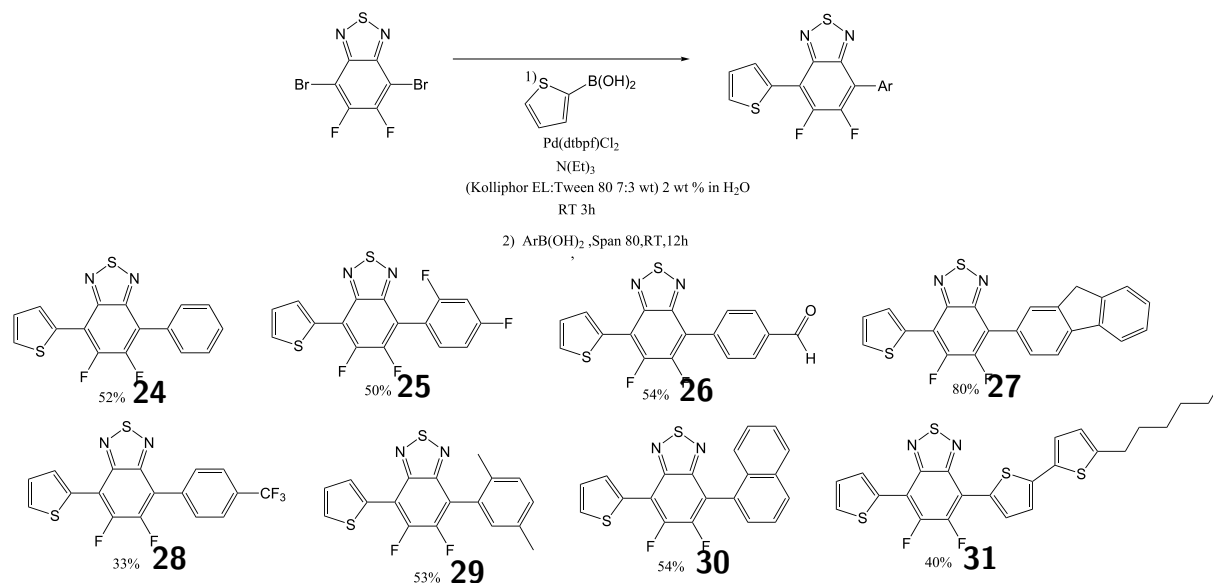
3.4.5.3.3 Synthesis of 4,7-diphenyl-5,6-difluoro-2,1,3-benzothiadiazole (23)

DBBF (165 mg, 0.5 mmol) and phenylboronic acid (183 mg, 1.5 mmol) are weighted in the vessel, then 1 mL of Kolliphor 10% dispersion in water is added. The mixture is stirred, then N(Et)₃ (303 mg, 3.0 mmol) is added. The mixture is allowed to homogenize for 5 minutes before addition of Pd(dtbpf)Cl₂ (6.5 mg, 0.01 mmol). After 12 h, the reaction is diluted with 10 mL of water and filtered. The crude is crystallized from heptane to afford 153 mg of the pure product (95% yield). Anal calcd for C₁₈H₁₀F₂N₂S: C, 66.65; H, 3.11; N, 8.64. Found: C, 66.26; H, 2.76; N, 8.54.

¹H (CDCl₃, 400 MHz): δ 7.83 (d, J=7.4 Hz, 4H), 7.59 (t, J=7.5 Hz, 4H), 7.52 (t, J=7.4 Hz, 2H). ¹³C (CDCl₃, 400 MHz): δ 151.4 (t, J=3.9 Hz), 151.3 (dd, J=258.6, 20.4 Hz), 131.4, 131.1, 130.0, 129.4, 119.7 (dd, J=10.5, 4.4 Hz).

3.4. SYNTHESIS OF BENZOTHIADIAZOLE DERIVATIVES IN MICELLAR CONDITION

3.4.5.4 Synthesis of unsymmetrical 4,7-Diaryl-5,6-difluoro-2,1,3- benzothiadiazole (24, 25,26,27,28,29,30 and 31)



3.4.5.4.1 General synthetic procedure for unsymmetrically substituted derivatives Reactions were carried in a Biotage microwave vial (12 mm inner diameter) equipped with a cylindrical stirring bar (VWR 442-4525, 6x30mm) in vertical position and closed with a Suba-Seal septum. DBBF (330 mg, 1.0 mmol), 2-thienylboronic acid (192 mg, 1.5 mmol) and Pd(dtbbpf)Cl₂ (13.2 mg, 0.02 mmol) are weighted in the vessel, then 2 mL of 2% (Kolliphor/Tween 7:3) dispersion in water are added. The mixture is allowed to homogenize for 5 minutes before addition of N(Et)₃ (607 mg, 6.0 mmol). The reaction is stirred for 3 h, then 1.5 mmol of the 2nd boronic acid/ester are added in the vessel. 20 mg of Span 80 are added as well. The reaction is stirred overnight, and subsequently diluted with 10 mL of water and filtered. The crude was finally purified by column chromatography or crystallization.

Purification of 4-phenyl-7-(thien-2-yl)-5,6-difluoro-2,1,3- benzothiadiazole (136)

The crude is purified by column chromatography using heptane:DCM=8:2 as eluent. Isolated product: 172 mg (52%).

Anal calcd for C₁₆H₈F₂N₂S₂: C, 58.17; H, 2.44; N, 8.48. Found: C, 57.82; H, 2.12; N, 8.45.

¹H (CDCl₃, 400 MHz): δ 8.31 (d, J = 3.9 Hz, 1H), 7.82 (d, J = 8.3 Hz, 2H), 7.63 (dd, J = 5.3, 0.9 Hz, 1H), 7.58 (t, J = 7.4, 0.9 Hz, 2H), 7.49-7.52 (m, 1H), 7.29 (m, 1H). ¹³C (CDCl₃, 400 MHz): δ 151.33 (d, 8.6 Hz), 151.32 (dd, J = 255.9, 19.0 Hz), 150.6 (dd, J = 259.8, 20.0 Hz), 149.9 (d, J = 8.8 Hz), 132.4 (dd, J = 5.4, 3.4 Hz), 131.9 (d, J = 8.3 Hz), 131.4 (d, J = 2.6 Hz), 131.1, 130.0, 129.8 (d, J = 6.4 Hz), 129.4, 128.3, 118.7 (d, J = 14.2 Hz), 113.6 (dd, J = 12.2, 1.2 Hz).

Purification of 4-(2,4-difluoro-phenyl)-7-(thien-2-yl)-5,6-difluoro-2,1,3- benzothiadiazole (137)

The crude is purified by column chromatography using heptane:toluene=7:3 as eluent. Isolated product: 183 mg (50%).

Anal calcd for $C_{16}H_6F_4N_2S_2$: C, 52.45; H, 1.65; N, 7.65. Found: C, 52.07; H, 1.31; N, 7.59.

1H (CDCl₃, 400 MHz): δ 8.35 (ddd, $J=3.8, 1.2, 0.6$ Hz, 1H), 7.62-7.68 (m, 2H), 7.31 (ddd, $J=5.2, 3.8, 1.4$ Hz, 1H), 7.05-7.15 (m, 2H). ^{13}C (CDCl₃, 400 MHz): δ 163.8 (dd, $J=252.1, 11.6$ Hz), 160.5 (dd, $J=253.4, 12.3$ Hz), 151.2 (dd, $J=260.7, 21.1$ Hz), 150.3 (d, $J=8.8$ Hz), 149.4 (dd, $J=265.1, 23.2$ Hz), 148.8 (d, $J=8.7$ Hz), 133.2 (dd, $J=9.9, 3.7$ Hz), 131.4 (d, $J=8.3$ Hz), 131.2, 129.3 (d, $J=6.5$ Hz), 127.5, 114.1 (d, $J=16.1$), 113.8 (d, $J=11.7$ Hz), 111.8 (dd, $J=21.7, 3.6$ Hz), 111.2 (d, $J=16.0$ Hz), 104.7 (t, $J=25.5$ Hz).

Purification of 4-(4-formyl-phenyl)-7-(thien-2-yl)-5,6-difluoro-2,1,3-benzothiadiazole (138)

The crude is purified by column chromatography using heptane:DCM=8:2 as eluent. Isolated product: 194 mg (54%).

Anal calcd for $C_{17}H_8F_2N_2OS_2$: C, 56.97; H, 2.25; N, 7.82. Found: C, 54.64; H, 1.94; N, 7.77.

1H (CDCl₃, 400 MHz): δ 10.17 (s, 1H), 8.38 (ddd, $J=3.8, 1.1, 0.7$ Hz, 1H), 8.09-8.12 (m, 2H), 8.03-8.06 (m, 2H), 7.69 (dd, $J=5.1, 1.1$ Hz, 1H), 7.33 (ddd, $J=5.3, 3.9, 1.4$ Hz, 1H). ^{13}C (CDCl₃, 400 MHz): δ 191.7, 150.9 (dd, $J=259.3, 19.6$ Hz), 149.9 (d, $J=8.0$ Hz), 149.4 (dd, $J=260.6, 19.6$ Hz), 149.0 (d, $J=8.7$ Hz), 136.3, 136.2 (m), 131.5 (d, $J=8.7$ Hz), 131.3 (d, $J=2.9$ Hz), 131.2, 129.7, 129.5 (d, $J=6.5$ Hz), 127.5, 116.2 (d, $J=13.8$ Hz), 113.8 (dd, $J=12.5, 2.1$ Hz)

Purification of 4-(4-(trifluoromethyl)-phenyl)-7-(thien-2-yl)-5,6-difluoro-2,1,3-benzothiadiazole (139)

No eluent combination allowed to separate chromatographically the product from DTBF. Therefore, the crude was refluxed in methanol and hot filtered twice to remove the symmetrical DTBF derivative. The obtained solid was then crystallized three times from heptane. Isolated product: 131 mg (33%).

Anal calcd for $C_{17}H_7F_5N_2S_2$: C, 51.25; H, 1.77; N, 7.03. Found: C, 50.90; H, 1.42; N, 6.99.

1H (CDCl₃, 400 MHz): δ 8.37 (ddd, $J=3.8, 1.0, 0.7$ Hz, 1H), 7.97-8.00 (m, 2H), 7.84-7.87 (m, 2H), 7.69 (dd, $J=5.1, 1.1$ Hz, 1H), 7.33 (ddd, $J=5.2, 3.9, 1.4$ Hz, 1H). ^{13}C (CDCl₃, 400 MHz): δ 150.8 (dd, $J=257.9, 18.9$ Hz), 150.0 (d, $J=8.7$ Hz), 149.3 (dd, $J=260.7, 19.6$ Hz), 149.0 (d, $J=8.7$ Hz), 133.8 (m), 131.4 (d, $J=8.7$ Hz), 131.3 (m), 131.01 (q, $J=32.7$ Hz), 130.95 (d, $J=2.9$ Hz), 129.4 (d, $J=6.5$ Hz), 127.5, 125.5 (q, $J=3.6$ Hz), 124.0 (q, $J=272.5$ Hz), 116.1 (d, $J=13.8$ Hz), 113.7 (dd, $J=12.3, 2.1$ Hz)

Purification of 4-(2,5-dimethyl-phenyl)-7-(thien-2-yl)-5,6-difluoro-2,1,3-benzothiadiazole (140)

The crude is purified by column chromatography using petroleum ether:toluene=8:2 as eluent. Isolated product: 190 mg (53%).

Anal calcd for $C_{18}H_{12}F_2N_2S_2$: C, 60.32; H, 3.37; N, 7.82. Found: C, 60.46; H, 3.41; N, 7.56.

3.4. SYNTHESIS OF BENZOTHIADIAZOLE DERIVATIVES IN MICELLAR CONDITION

¹H (CDCl₃, 400 MHz): δ 8.33 (ddd, J=3.8, 1.1, 0.6 Hz, 1H), 7.64 (dd, J=5.1, 1.1 Hz, 1H), 7.28-7.32 (m, 2H), 7.24-7.26 (m, 1H), 7.20 (br, 1H), 2.41 (s, 3H), 2.15 (s, 3H). ¹³C (CDCl₃, 400 MHz): δ 150.9 (d, J=8.7 Hz), 150.4 (dd, J=255.0, 18.9 Hz), 149.7 (dd, J=260.9, 19.7 Hz), 148.8 (d, J=8.7 Hz), 135.4, 134.2, 131.5 (dd, J=5.8, 3.6 Hz), 131.02, 131.00 (d, J=8.7 Hz), 130.5, 130.3, 129.4 (d, J=1.1 Hz), 128.9 (d, J=6.5 Hz), 127.4, 118.2 (d, J=16.4 Hz), 112.9 (dd, J=12.4, 1.4 Hz), 21.0, 19.6 (d, J=1.5 Hz)

Purification of 4-(naphthalen-1-yl)-7-(thien-2-yl)-5,6-difluoro-2,1,3- benzothiadiazole (144)

The crude is purified by column chromatography using heptane:DCM=8:2 as eluent. Isolated product: 207 mg (54%).

Anal calcd for C₂₀H₁₀F₂N₂S₂: C, 63.14; H, 2.65; N, 7.36. Found: C, 63.58; H, 2.85; N, 6.98.

¹H (CDCl₃, 400 MHz): δ 8.38 (ddd, J=3.8, 1.1, 0.6 Hz, 1H), 8.05 (dd, J=7.0, 2.4 Hz, 1H), 7.98 (d, J=8.2 Hz, 1H), 7.64-7.69 (m, 3H), 7.54 (ddd, J=8.3, 6.6, 1.4 Hz, 1H), 7.48-7.51 (m, 1H), 7.43 (ddd, J=8.5, 6.6, 1.3 Hz, 1H), 7.32 (ddd, J=5.2, 3.8, 1.3 Hz, 1H). ¹³C (CDCl₃, 400 MHz): δ 151.4 (d, J=8.4 Hz), 151.2 (dd, J=256.8, 20.1 Hz), 149.4 (dd, J=262.1, 21.4 Hz), 148.8 (d, J=8.3 Hz), 133.8, 131.6, 131.5 (m), 131.1 (d, J=8.0 Hz), 129.9, 129.0 (m), 128.7, 127.7 (d, J=2.5 Hz), 127.4, 126.7, 126.2, 125.30, 125.27, 116.8 (d, J=16.7 Hz), 113.4 (d, J=12.0 Hz).

Purification of 4-(9H-fluoren-2-yl)-7-(thien-2-yl)-5,6-difluoro-2,1,3- benzothiadiazole (142)

The crude is purified by column chromatography using petroleum ether:toluene=7:3 as eluent. Isolated product: 335 mg (80%).

Anal calcd for C₂₃H₁₂F₂N₂S₂: C, 66.01; H, 2.89; N, 6.69. Found: C, 65.60; H, 2.67; N, 6.67.

¹H (CDCl₃, 400 MHz): δ 8.34 (ddd, J= 3.8, 1.1, 0.6 Hz, 1H), 8.02 (m, 1H), 7.99 (dd, J= 7.9, 0.6 Hz, 1H), 7.85-7.90 (m, 2H), 7.66 (dd, J=5.2, 1.1 Hz, 1H), 7.61 (d, J=7.3 Hz, 1H), 7.45 (t, J=7.5 Hz, 1H), 7.38 (td, J=7.4, 1.3 Hz), 7.31 (ddd, J=5.2, 3.9, 1.3 Hz, 1H), 4.05 (s, 2H). ¹³C (CDCl₃, 400 MHz): δ 150.6 (d, J=8.7 Hz), 150.4 (dd, J=255.5, 18.9 Hz), 149.8 (dd, J=260.7, 20.3 Hz), 149.0 (d, J=8.7 Hz), 143.8, 143.4, 142.7, 141.1, 131.6 (dd, J=5.8, 3.6 Hz), 131.0 (d, J=8.7 Hz), 129.4 (d, J=2.9 Hz), 128.9 (d, J=6.5 Hz), 128.4, 127.4, 127.3, 127.1 (d, J=2.9 Hz), 126.9, 125.1, 120.3, 119.9, 118.2 (d, J=14.1 Hz), 112.5 (dd, J=12.4, 1.4 Hz), 37.1.

Purification of 4-(5'-hexyl-2',3'-dihydro-[2,2'-bithiophen]-5-yl)-7-(thien-2-yl)-5,6-difluoro-2,1,3- benzothiadiazole (143)

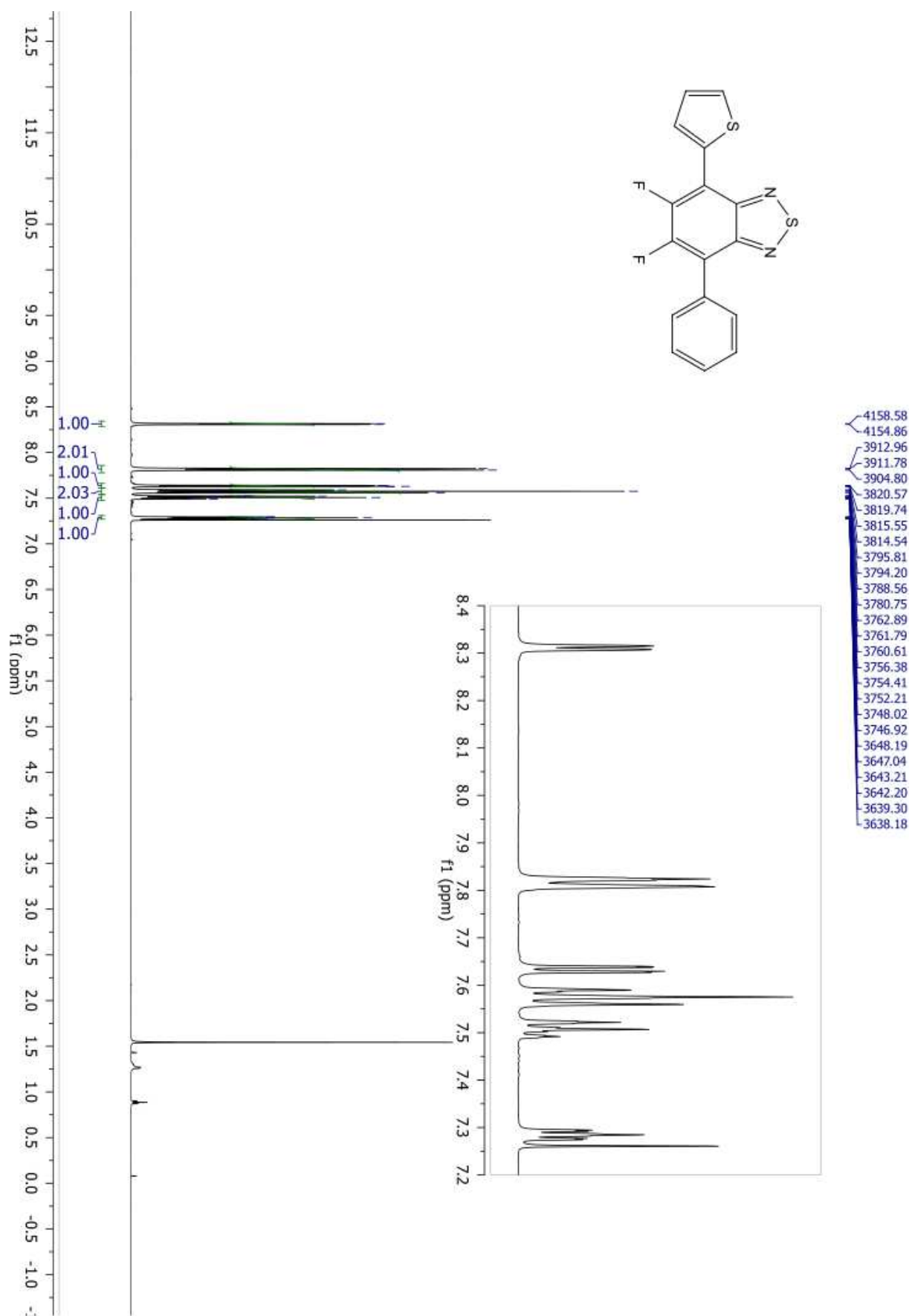
The crude is purified by column chromatography using petroleum ether:toluene=6:4 as eluent. Isolated product: 201 mg (40%).

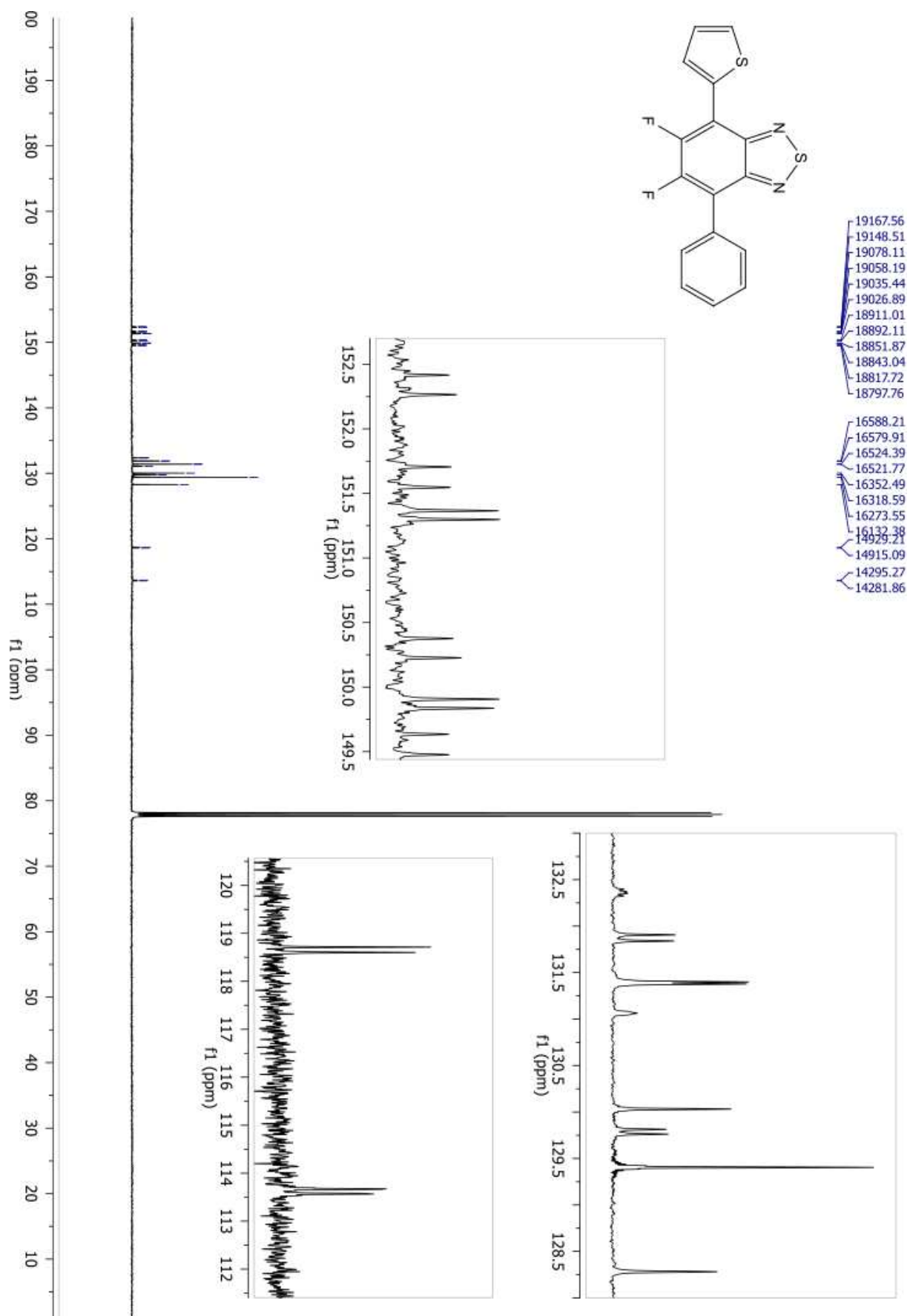
Anal calcd for C₂₄H₂₀F₂N₂S₄: C, 57.34; H, 4.01; N, 5.57. Found: C, 56.86; H, 3.79; N, 5.49.

¹H (CDCl₃, 400 MHz): δ 8.28 (dd, J=3.8, 1.1 Hz, 1H), 8.19 (d, J=4.0 Hz, 1H), 7.60 (dd, J=5.2, 1.2 Hz, 1H), 7.25-7.27 (m, 1H), 7.22 (d, J=4.1 Hz, 1H), 7.73 (dt, J=3.6, 1.0 Hz, 1H), 2.82 (t, J=7.6 Hz, 2H), 1.71 (m, 2H), 1.31-1.43 (m, 6H), 0.91 (t, J=7.1, 3H). ¹³C

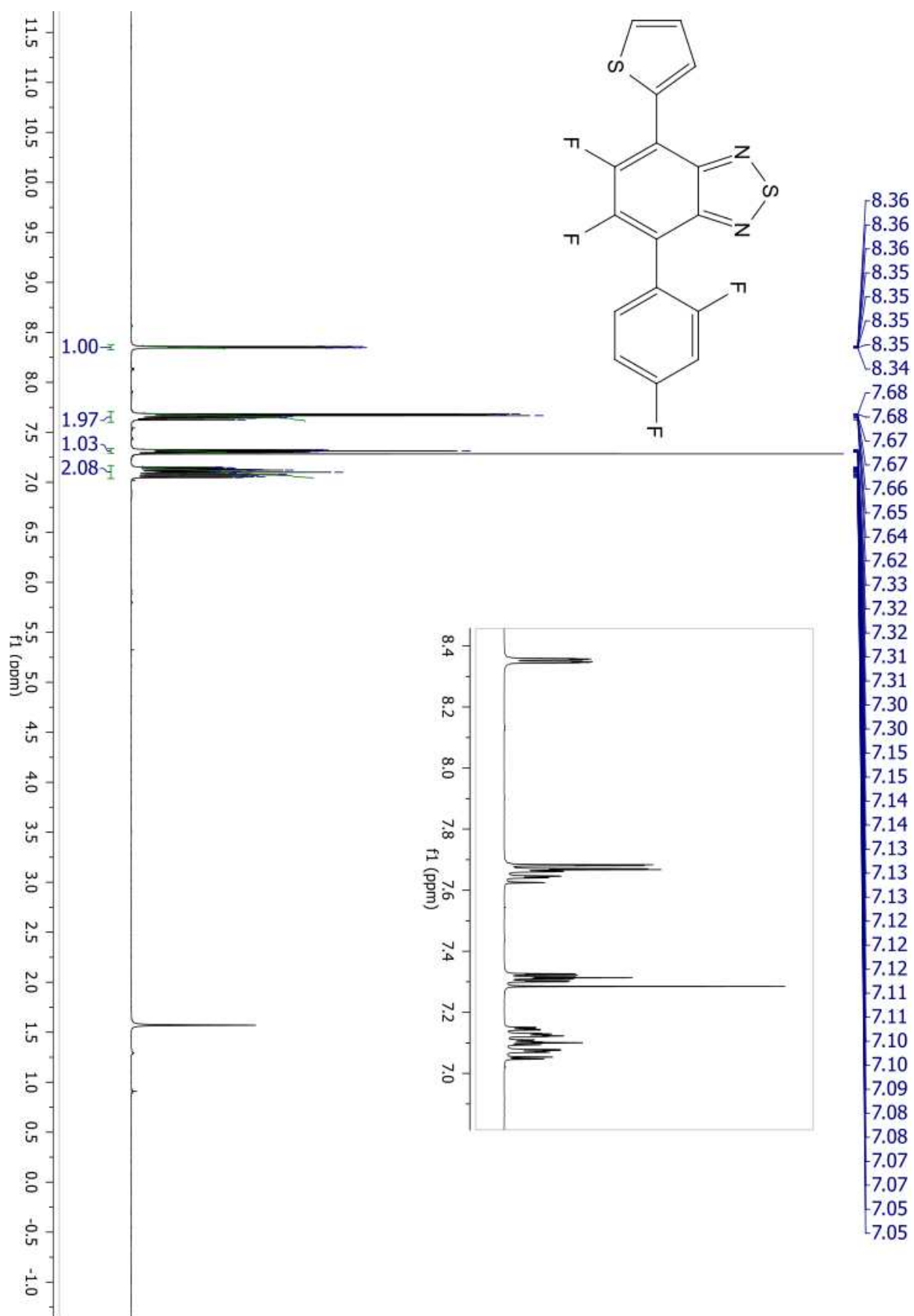
(CDCl₃, 400 MHz): δ 149.9 (dd, J=260.0, 20.4 Hz), 149.6 (dd, J=259.4, 20.8 Hz), 148.9, 148.7, 146.6, 141.5 (t, J=2.9 Hz), 134.2, 131.9 (dd, J=5.7, 3.6 Hz), 131.7, 130.8 (t, J=3.6 Hz), 129.7 (d, J=2.2 Hz), 128.8 (t, J=2.9 Hz), 127.4, 125.1, 124.2, 123.2, 111.7 (dd, J=9.5, 3.6 Hz), 111.3 (dd, J=8.9, 5.1 Hz), 31.6, 31.5, 30.3, 28.8, 22.6, 14.1.

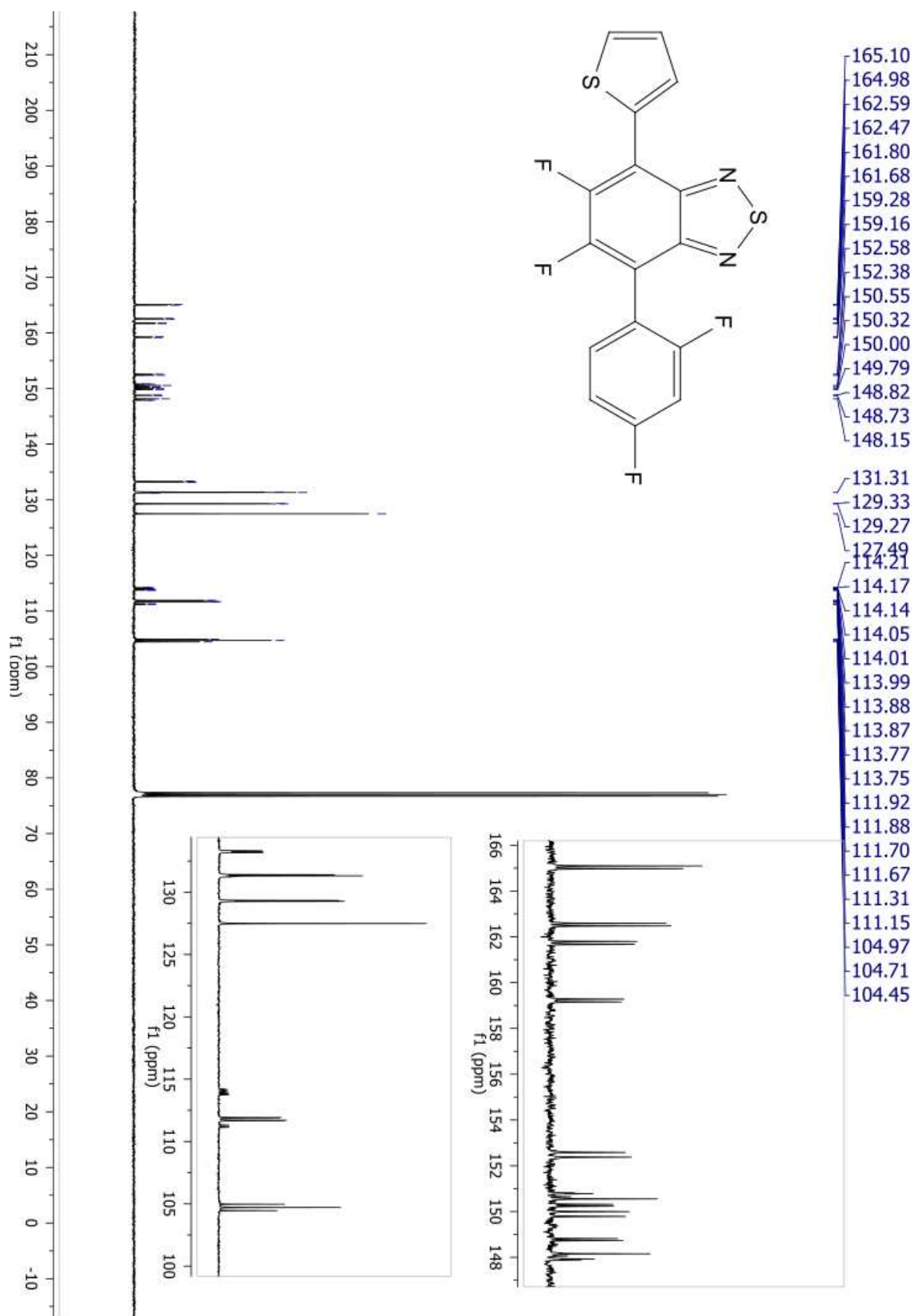
3.4. SYNTHESIS OF BENZOTHIADIAZOLE DERIVATIVES IN MICELLAR CONDITION



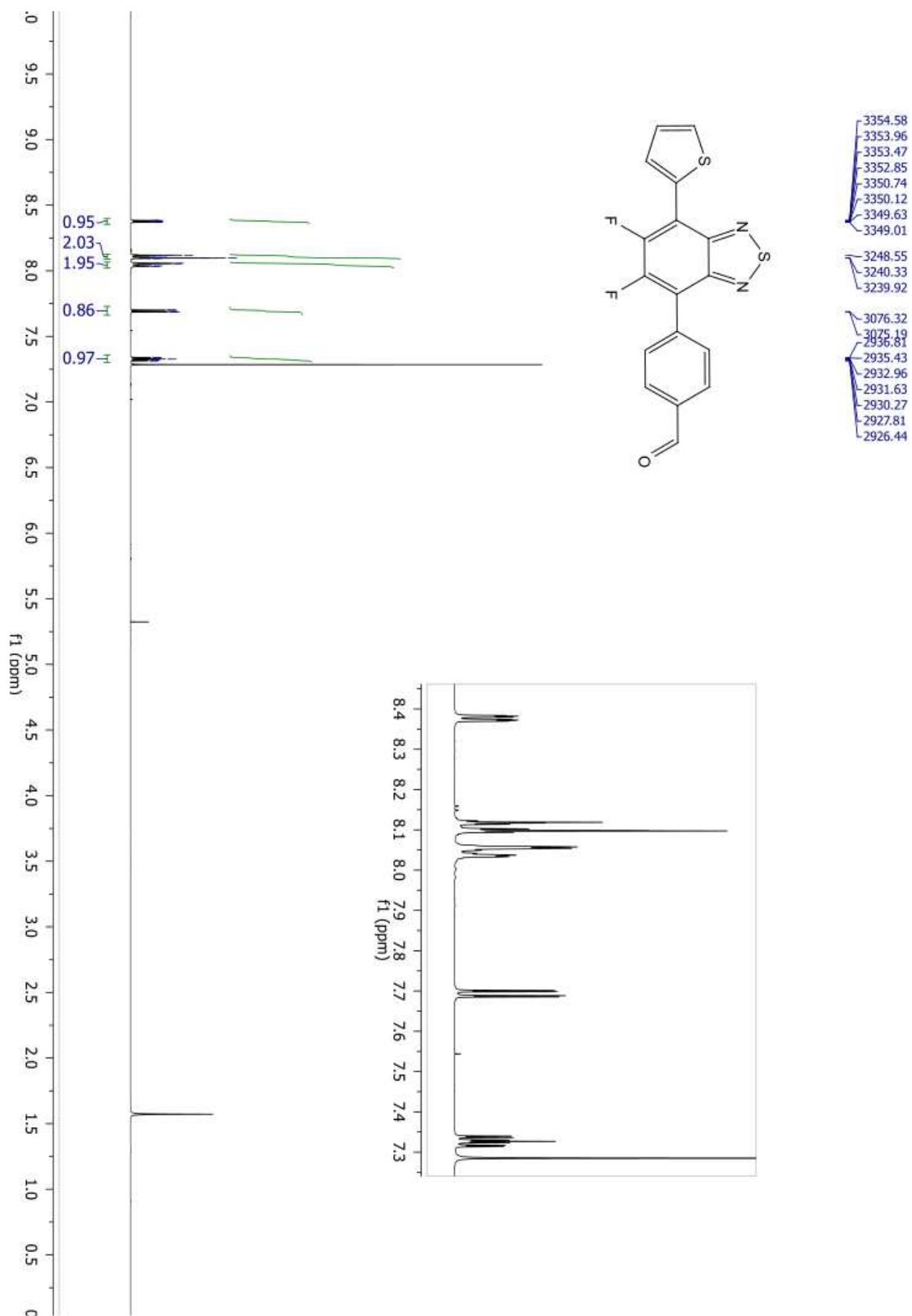


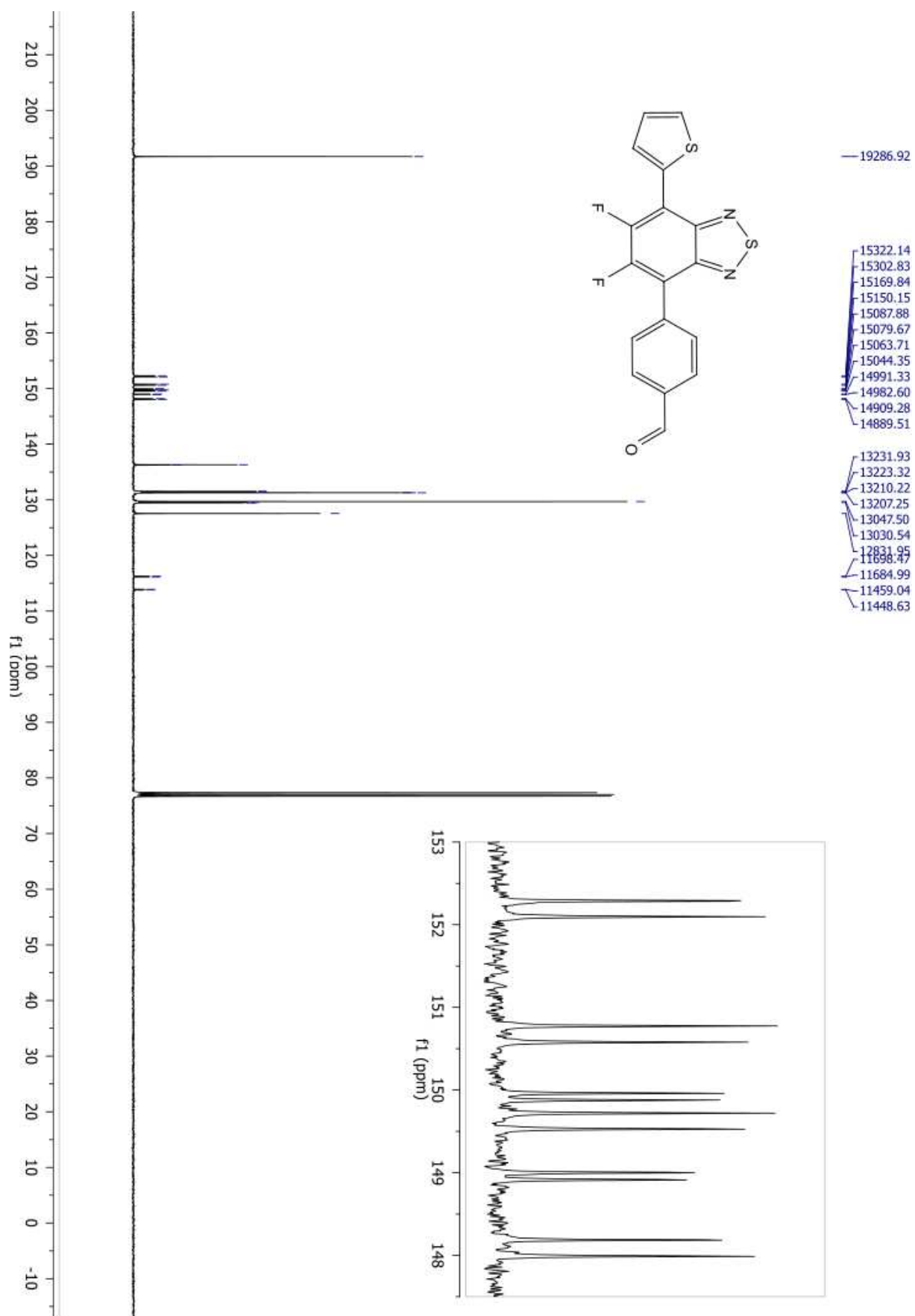
3.4. SYNTHESIS OF BENZOTHIADIAZOLE DERIVATIVES IN MICELLAR CONDITION



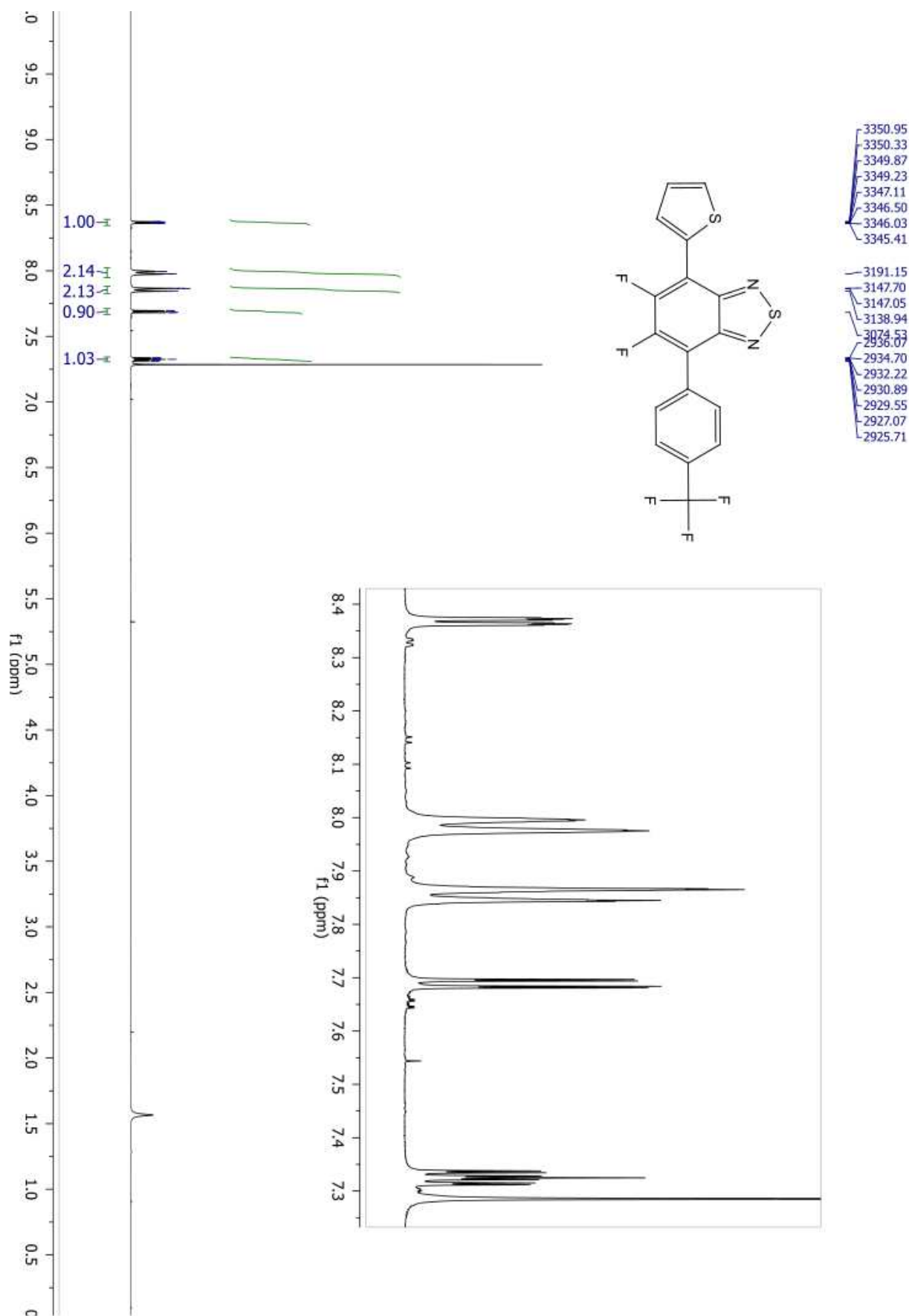


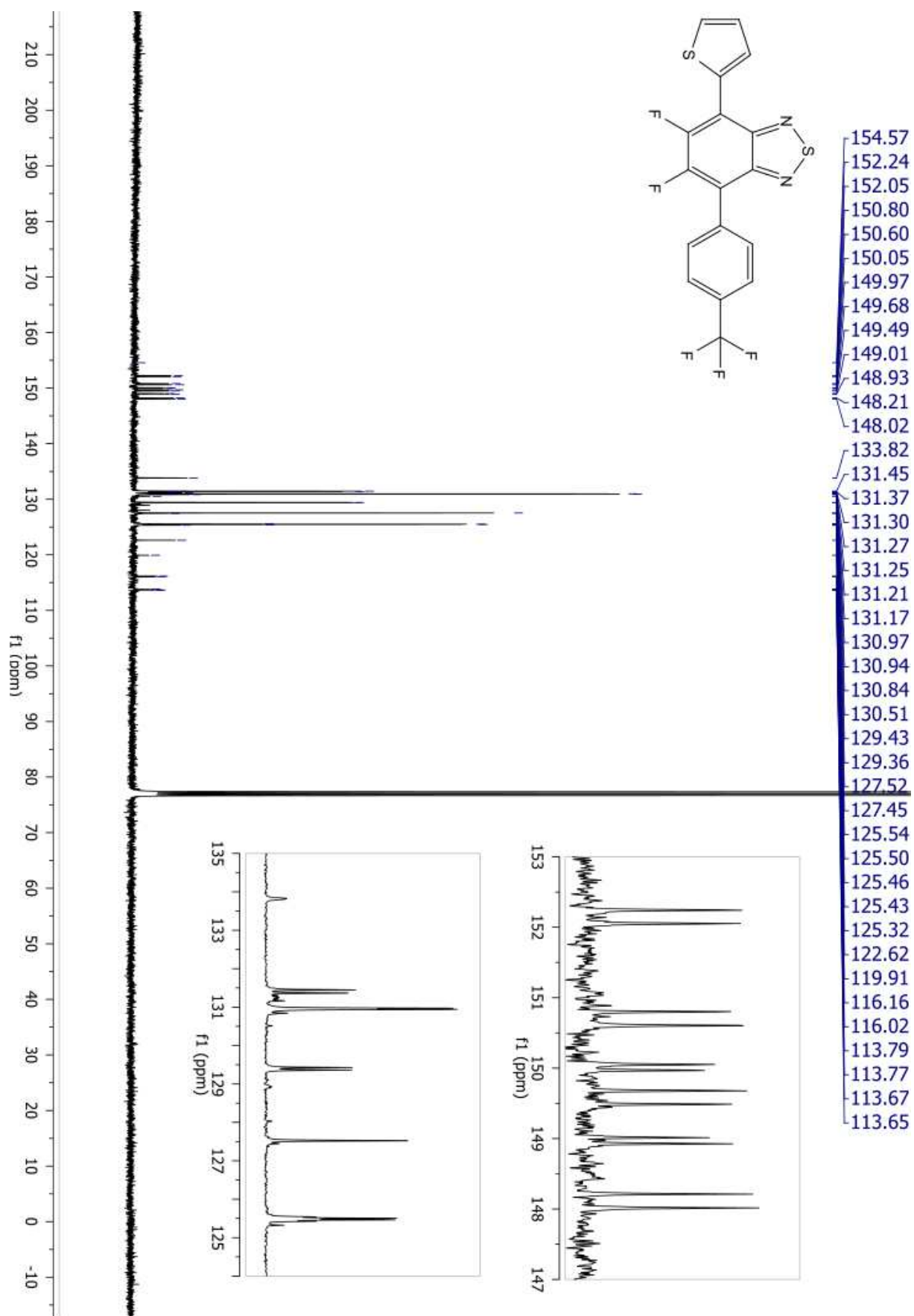
3.4. SYNTHESIS OF BENZOTHIADIAZOLE DERIVATIVES IN MICELLAR CONDITION



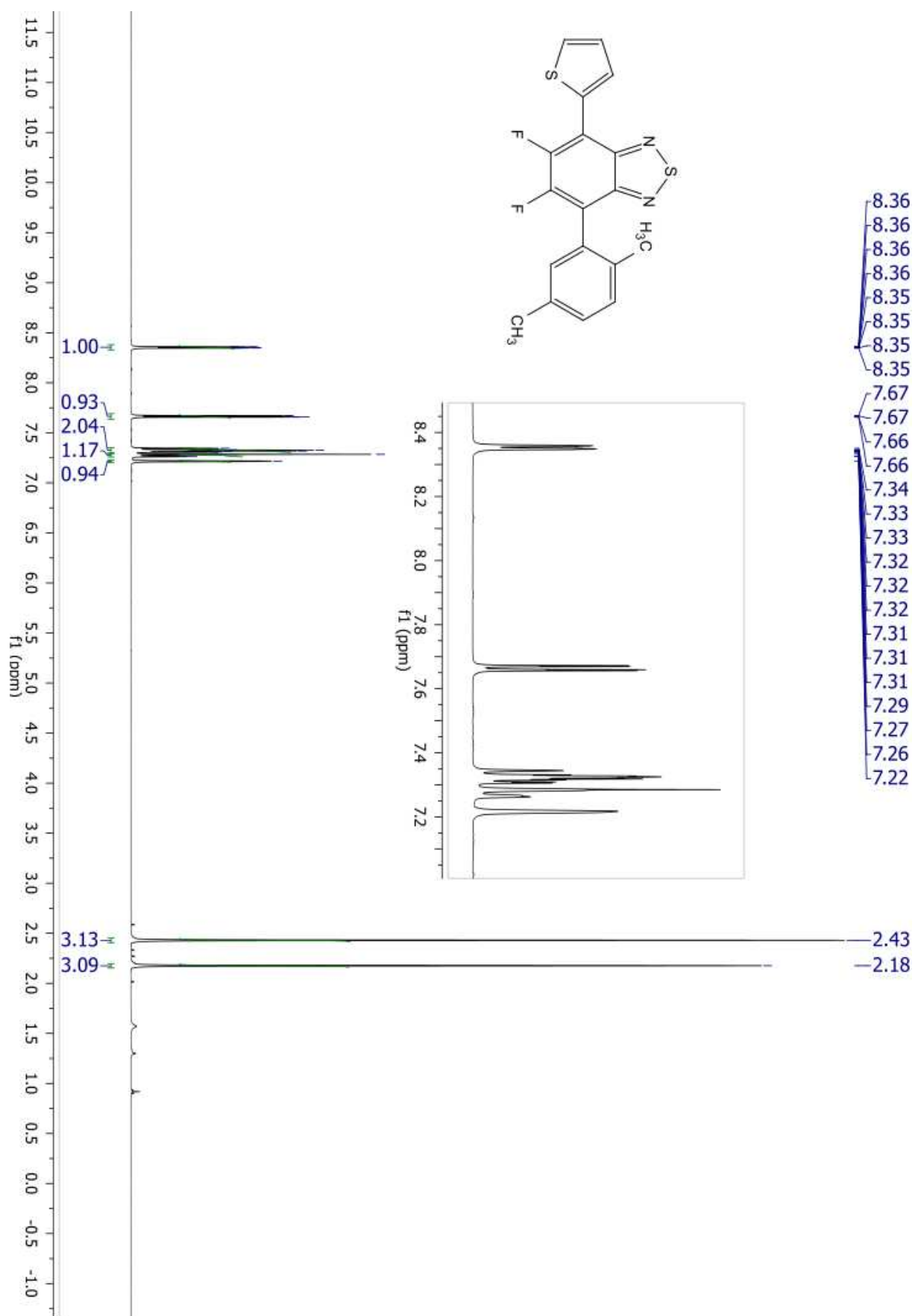


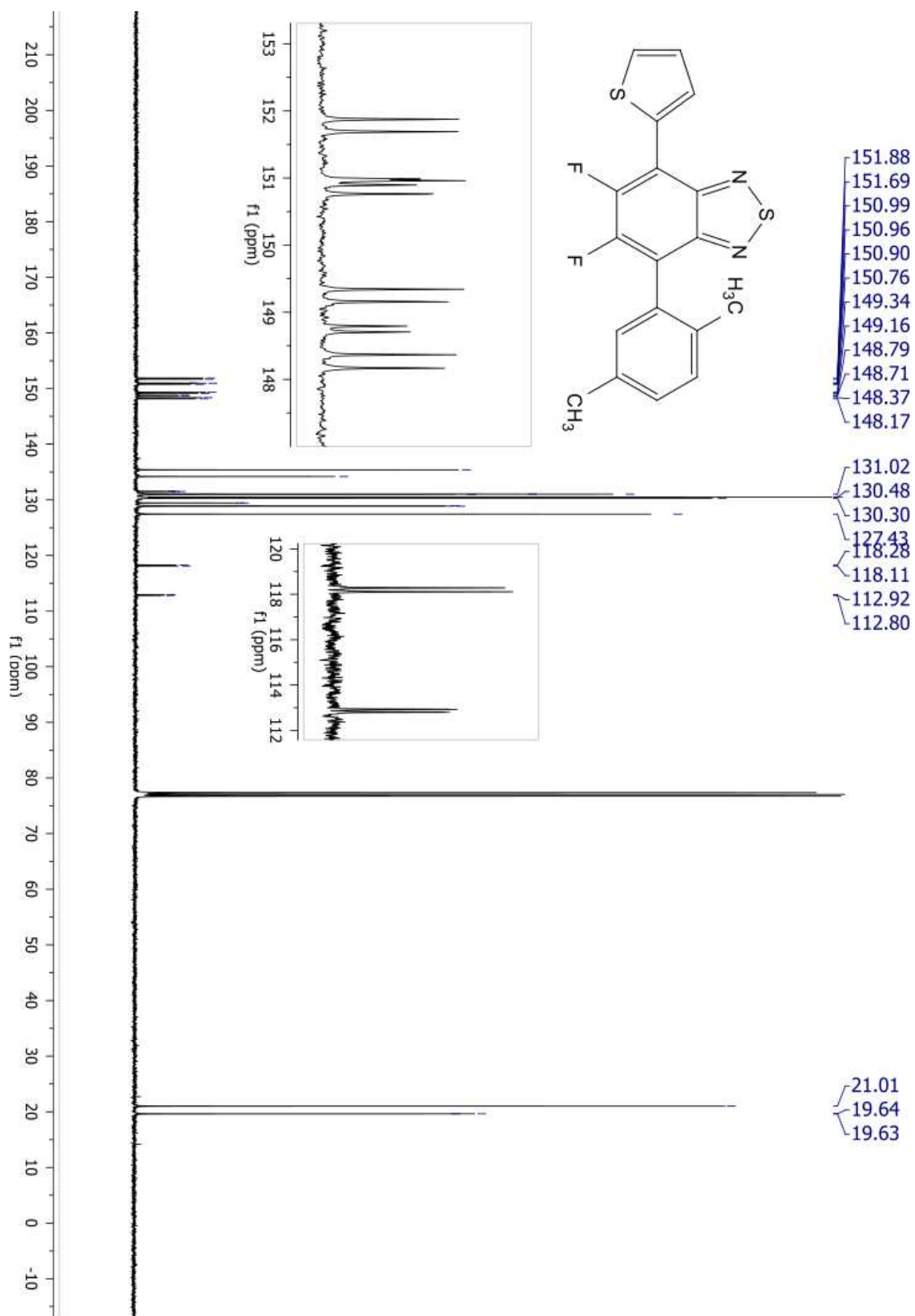
3.4. SYNTHESIS OF BENZOTHIADIAZOLE DERIVATIVES IN MICELLAR CONDITION



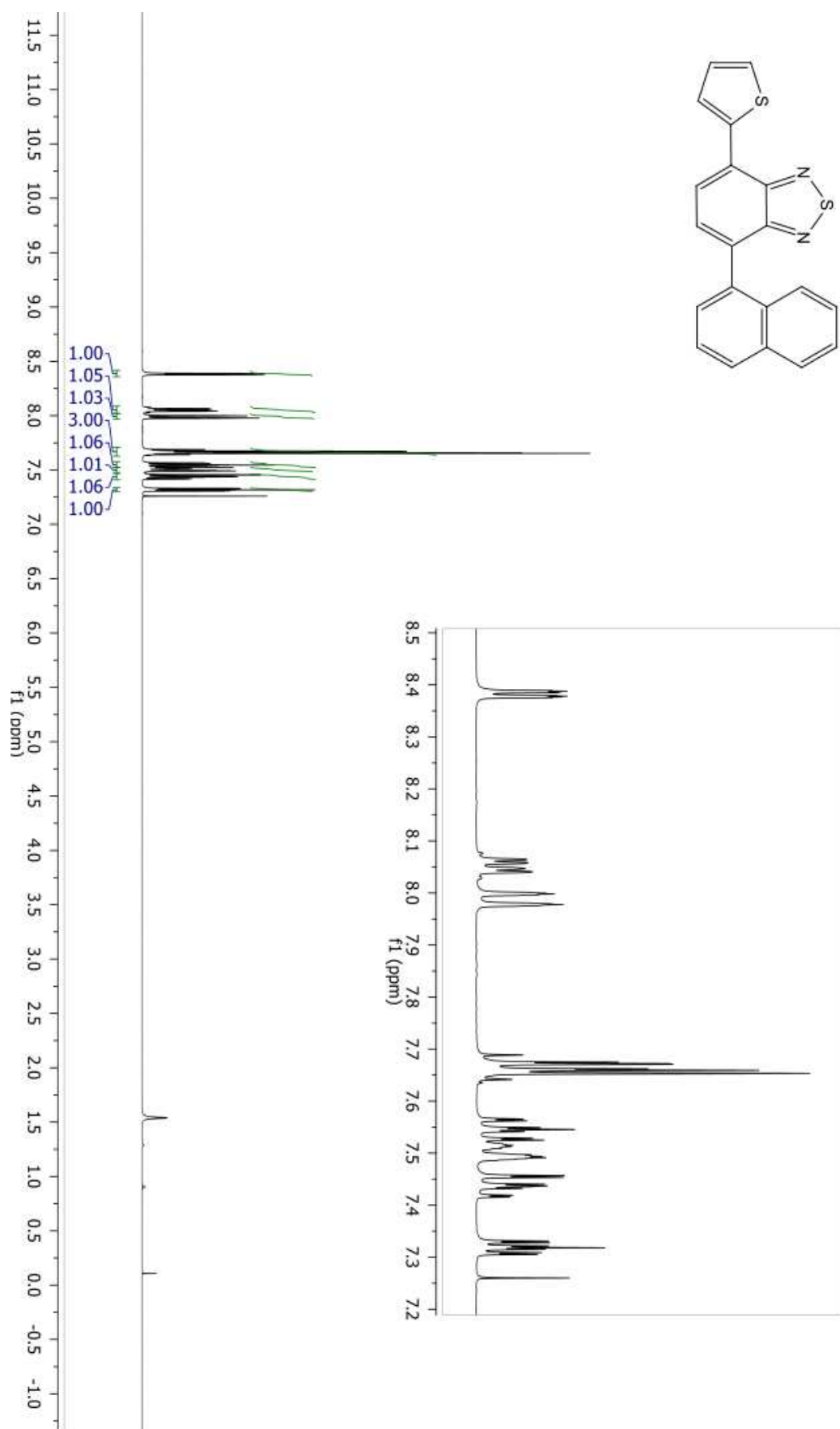


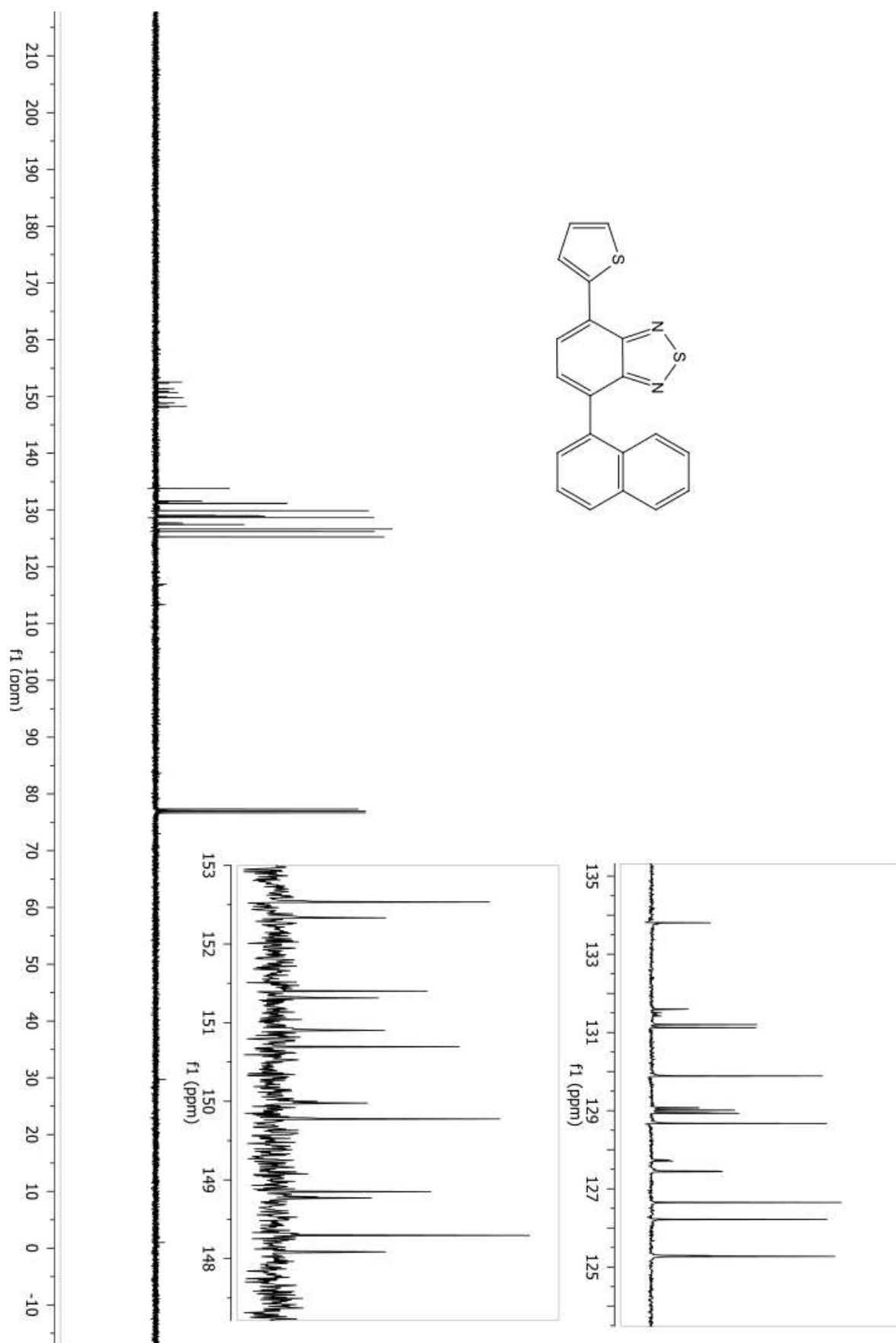
3.4. SYNTHESIS OF BENZOTHIADIAZOLE DERIVATIVES IN MICELLAR CONDITION



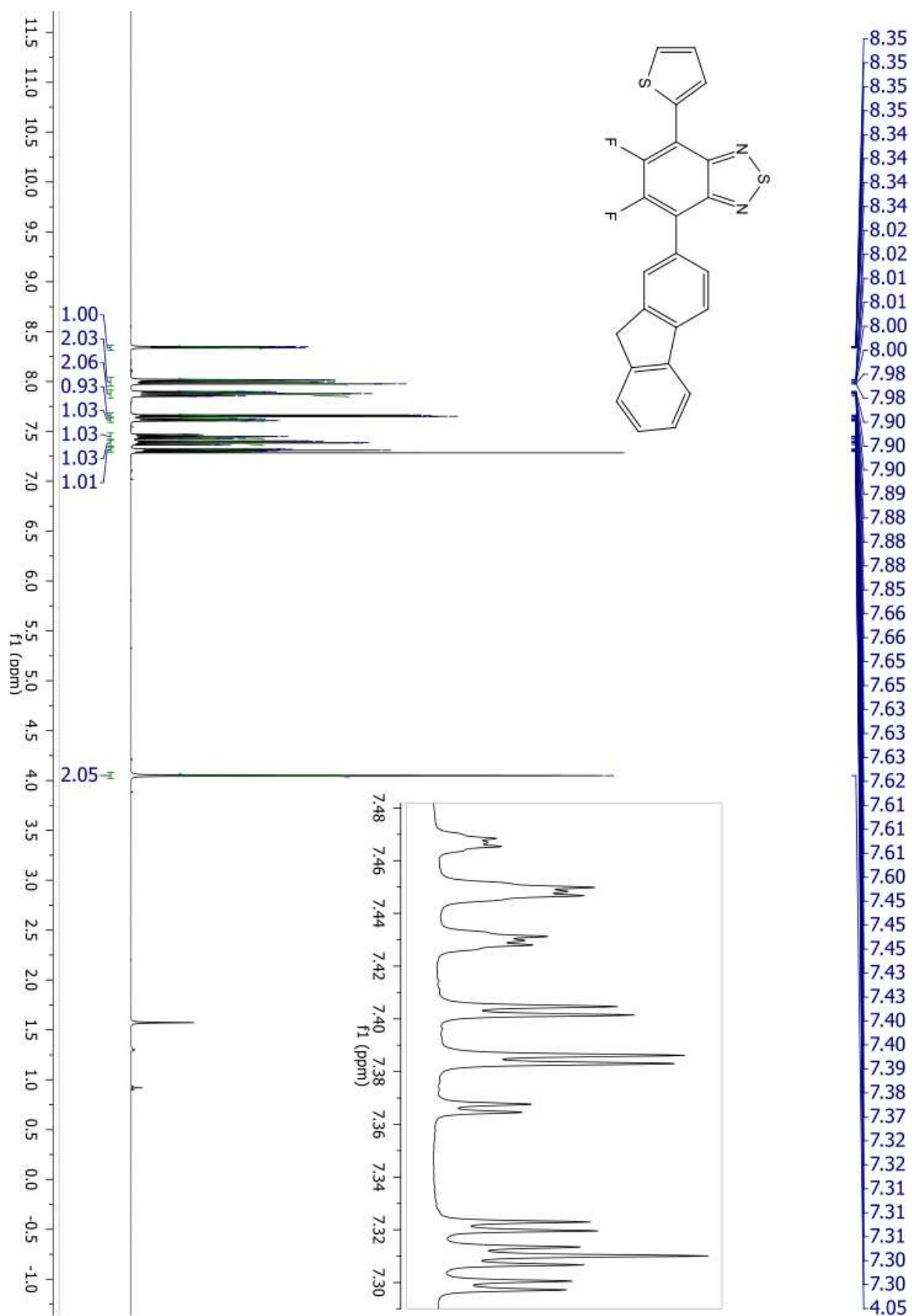


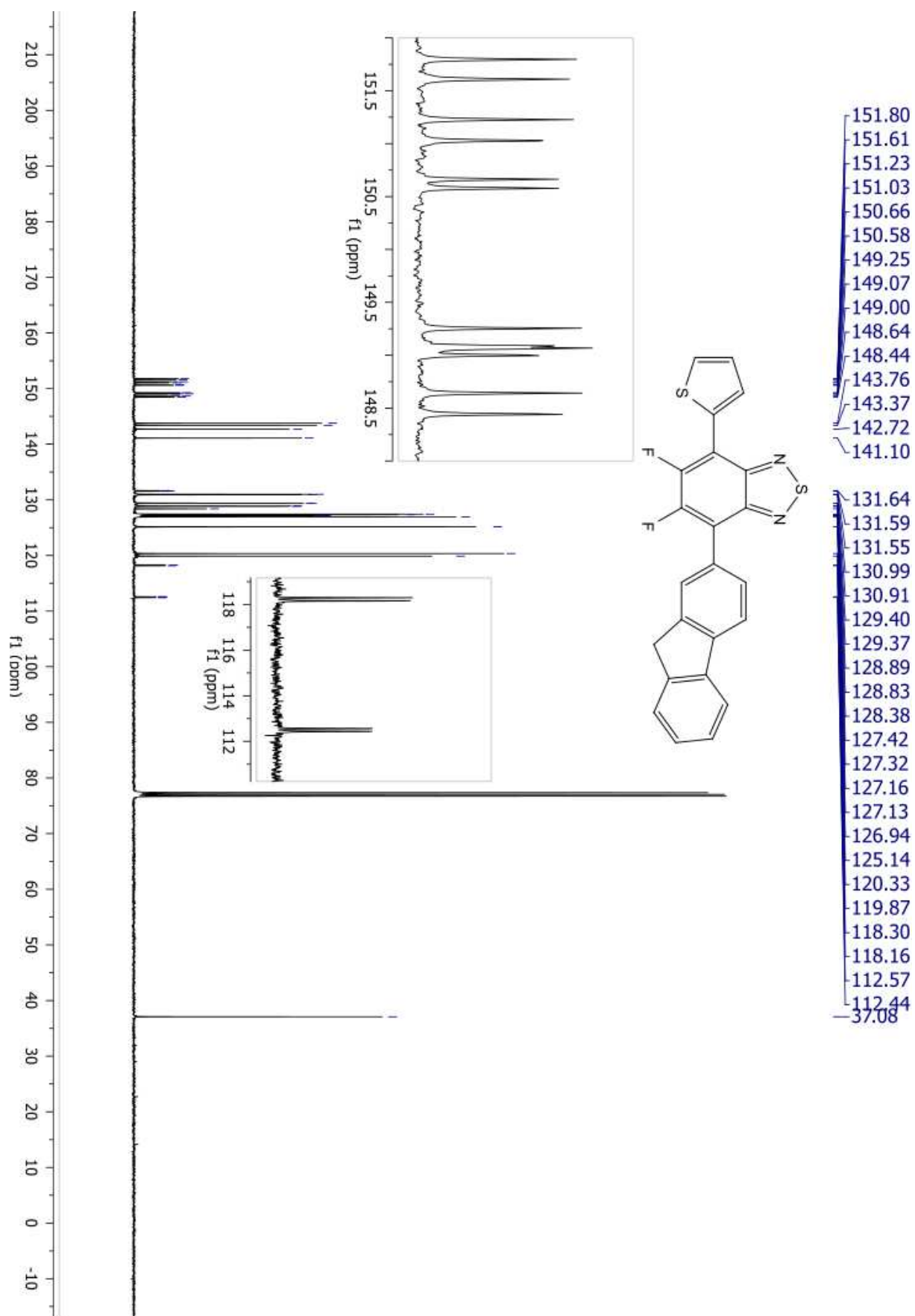
3.4. SYNTHESIS OF BENZOTHIADIAZOLE DERIVATIVES IN MICELLAR CONDITION



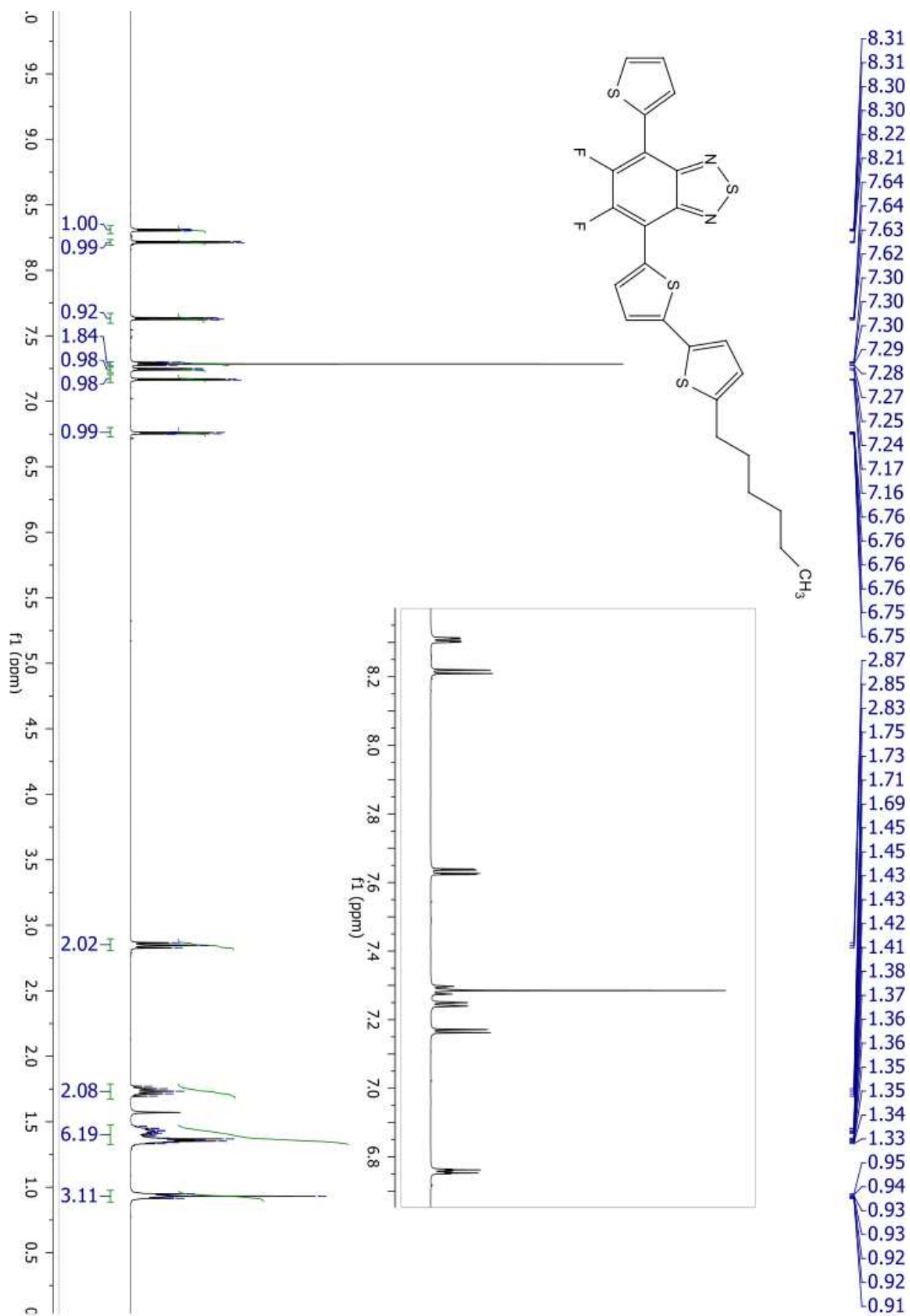


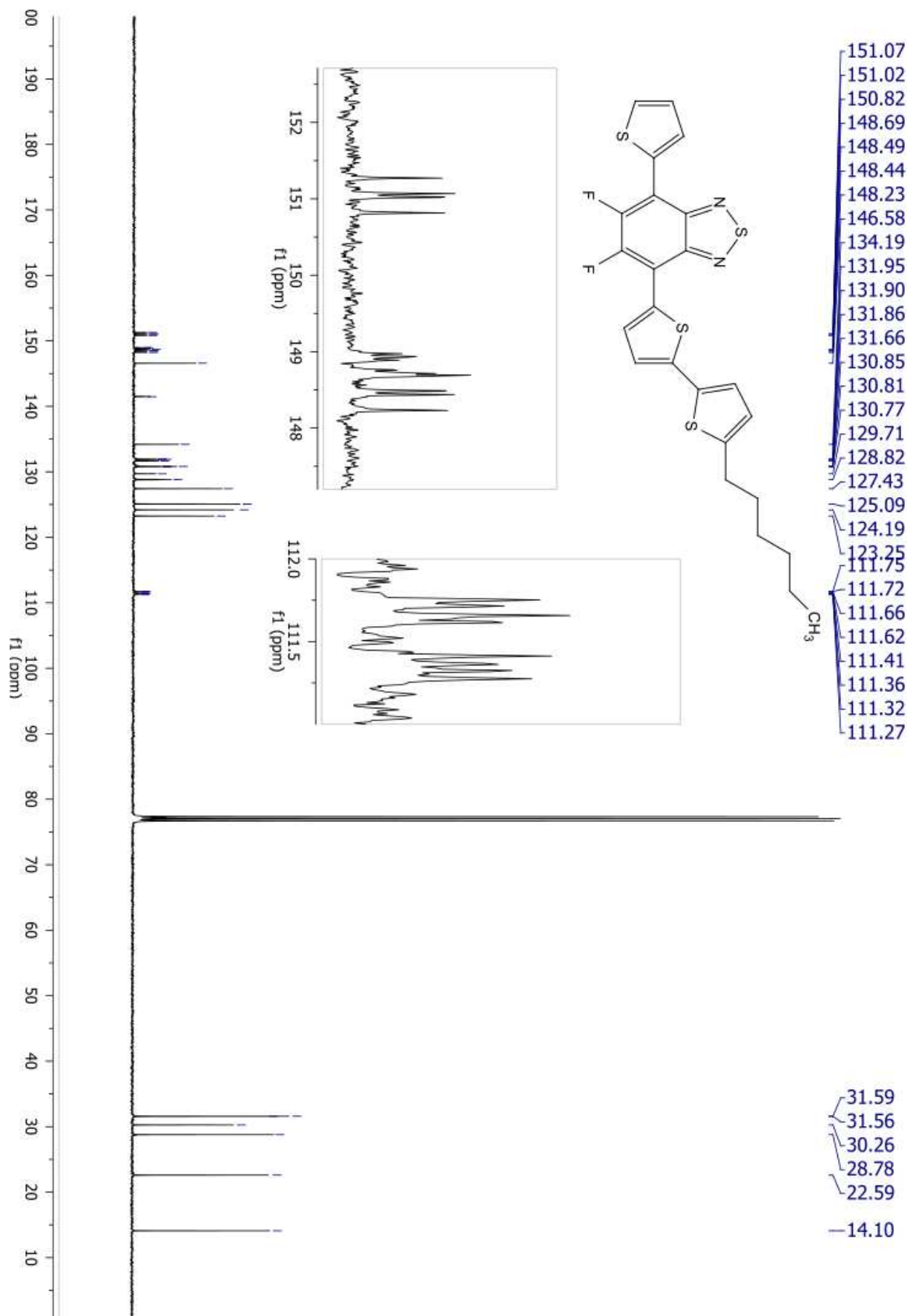
3.4. SYNTHESIS OF BENZOTHIADIAZOLE DERIVATIVES IN MICELLAR CONDITION





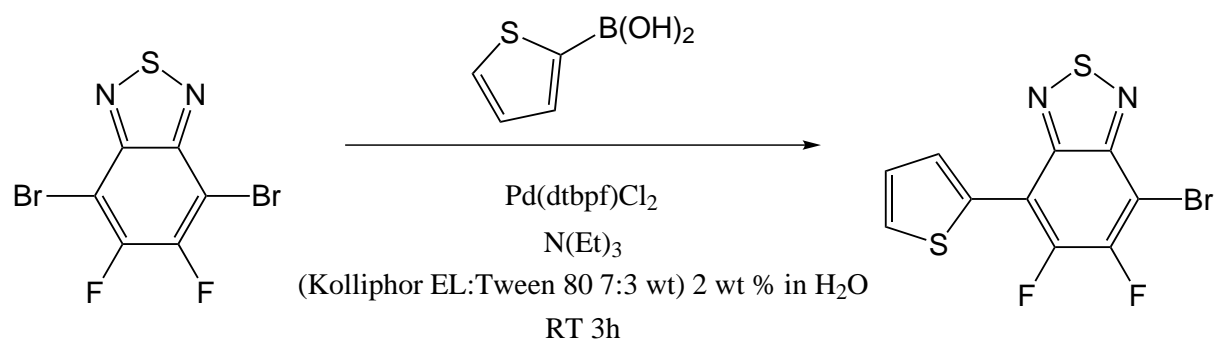
3.4. SYNTHESIS OF BENZOTHIADIAZOLE DERIVATIVES IN MICELLAR CONDITION





3.4.5.4.2 NMR spectra of unsymmetrically substituted derivatives

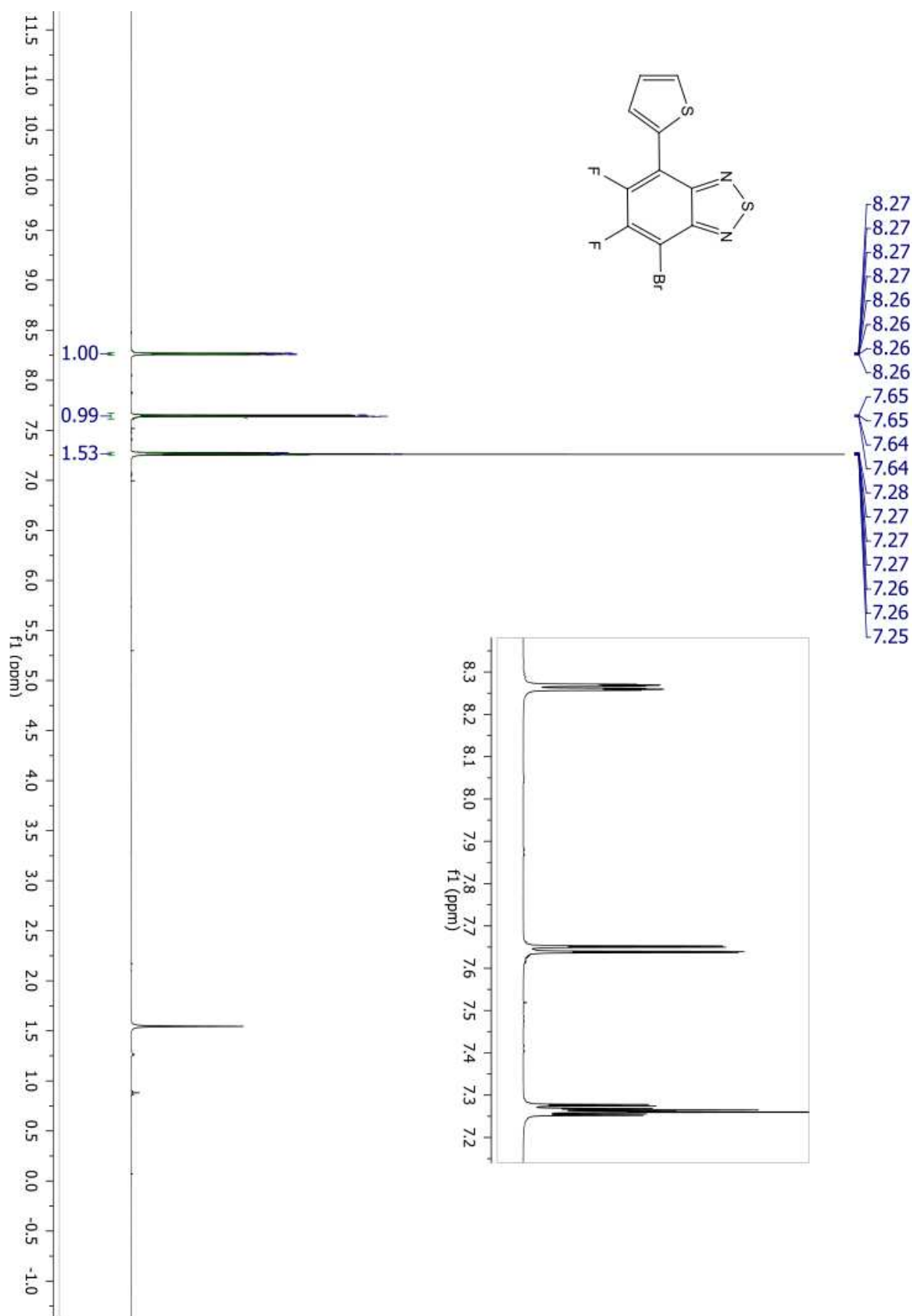
3.4.5.5 Synthesis of 4-bromo-7-(thien-2-yl)-5,6-difluoro-2,1,3- benzothiadiazole (TBF)



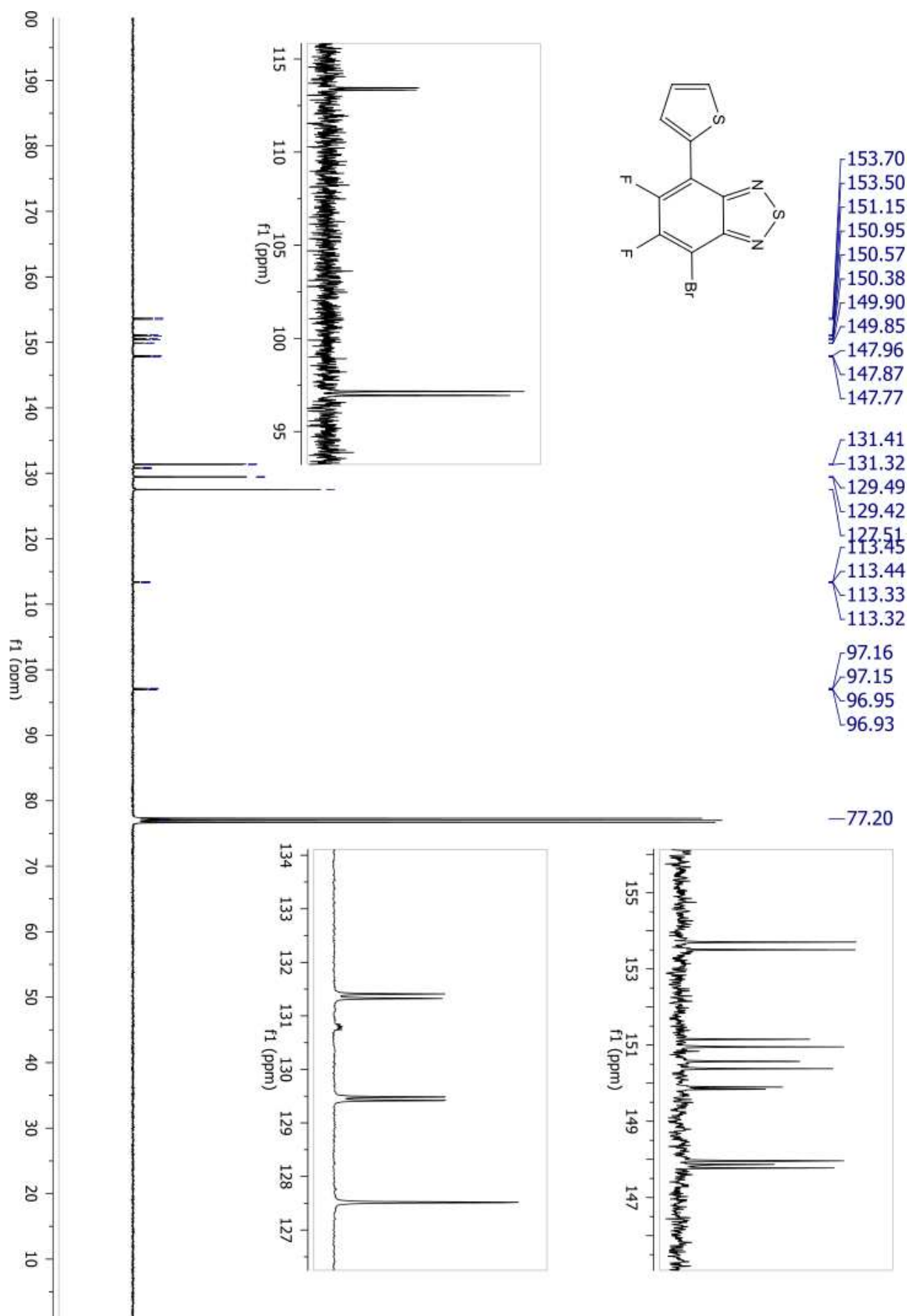
DBBF (330 mg, 1.0 mmol) and 3-thienylboronic acid (192 mg, 1.5 mmol) are weighted in the vial, then 2 mL of 10% Kolliphor EL dispersion in water is added. The mixture is stirred, then N(Et)₃ (303 mg, 3.0 mmol) is added. The mixture is allowed to homogenize for 5 minutes before addition of Pd(dtbpf)Cl₂ (13.2 mg, 0.02 mmol). After 12 h, the reaction is diluted with 10 mL of water and filtered. The crude precipitate is purified by column chromatography using heptane:toluene=7:3 as eluent. Isolated product: 187 mg (56% yield).

Anal calcd for C₁₀H₃BrF₂N₂S₂: C, 36.05; H, 0.91; N, 8.41. Found: C, 36.03; H, 0.61; N, 8.32.

¹H (CDCl₃, 400 MHz): δ 8.26 (ddd, J=3.9, 1.1, 0.7 Hz, 1H), 7.64 (dd, J=5.2, 1.1 Hz, 1H), 7.27 (ddd, J=5.2, 3.9, 1.4 Hz, 1H). ¹³C (CDCl₃, 400 MHz): δ 152.4 (dd, J=256.5, 20.3 Hz), 149.1 (dd, J=262.3, 19.0 Hz), 149.9 (d, J=5.1 Hz), 147.9, 131.4 (d, J=8.7 Hz), 130.8 (dd, J=5.8, 3.6 Hz), 129.5 (d, J=6.6 Hz), 127.5, 113.4 (dd, J=12.3 Hz, 1.4 Hz), 97.1 (dd, J=21.8, 1.4 Hz).



3.4. SYNTHESIS OF BENZOTHIADIAZOLE DERIVATIVES IN MICELLAR CONDITION



3.4.6 Appendix

3.4.6.1 Details on The Gc-MS response factor calibration

We quantified the crude product composition in terms of DBBF, TBF and DTBF by gas chromatography coupled with mass spectroscopy (GC-MS). We estimated the reaction mixture composition through area normalization based on response factors method. In order to obtain the relative response factors (f) of the different compounds, we prepared four standard solutions at known concentration of the three pure compounds in dichloromethane in a volumetric flask. Each standard solution was analyzed three times by GC-MS. Averaged areas of each peak A_x were plotted as function of the concentration. Slopes of the linear fitting $S_x = \frac{S_x}{W_x}$ were used to calculate the response factor of compound x using the formula $f_x = f_s \frac{A_s W_x}{A_x W_s} = f_s S_s \frac{1}{S_x}$

where the s labels the chosen standard. We decided to use DTBF as standard, thus $f_s = f_{DTBF} = 1.00 \pm 0.01$ and using the formula, we found $f_s = f_{TBF} = 3.1 \pm 0.1$ $f_s = f_{DBBF} = 1.03 \pm 0.03$. The weight percentage (*Weight%*a) and the mole percentage ($n/n\%$) of each component in reactions were calculated with the following formulas:

$$Weight\%_x = \left(\frac{f_x A_x^{sample}}{f_{DBBF} A_{DBBF}^{sample} + f_{TBF} A_{TBF}^{sample} + f_{DTBF} A_{DTBF}^{sample}} \right) * 100$$

$$\frac{Weight\%_x}{MW_x} / \left[\frac{Weight\%_{DBBF}}{MW_{DBBF}} + \frac{Weight\%_{TBF}}{MW_{TBF}} + \frac{Weight\%_{DTBF}}{MW} \right] * 100$$

where A_x^{sample} is compound x peak area in sample and MW_x is the compound x molecular weight.

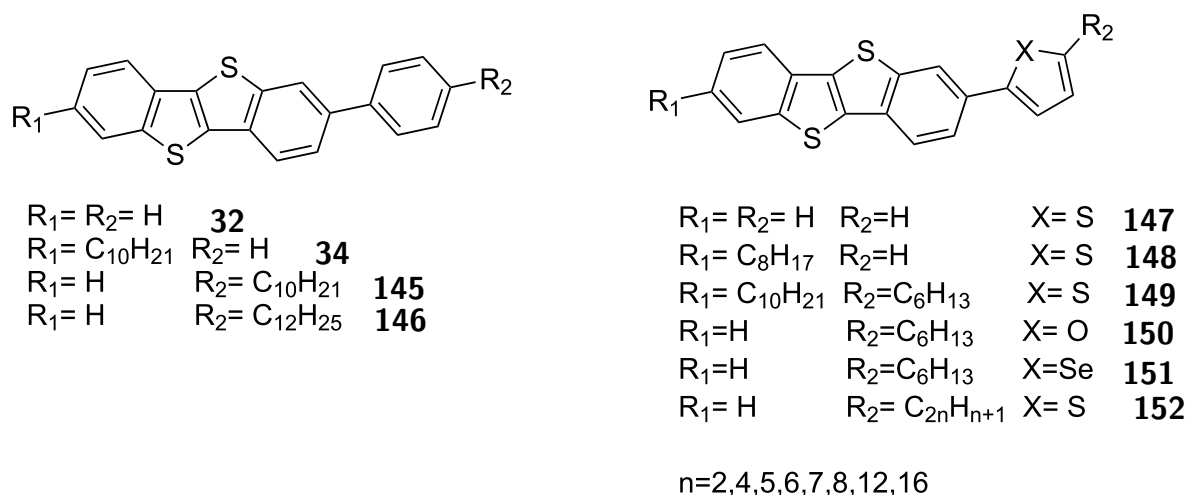
3.4.6.2 Theoretical details

All ab initio simulations based on density functional theory (DFT) have been performed by using the ORCA suite of programs¹¹¹ in a localized-basis-set framework. In detail, the Kohn–Sham orbitals have been expanded on a def2-TZVPP Gaussian type basis set.^{112, 113} The corresponding def2/J basis has been also used as an auxiliary basis set for Coulomb fitting in a resolution-of-identity/chain-of-spheres (RIJCOSX) framework.¹¹⁴ Molecular geometries have been fully optimized and their properties investigated by using the B3LYP functional.¹¹⁵ In order to simulate molecular properties inside and outside the micellar environment, the SMD continuum solvation model has been used to solvate the investigated molecules in toluene and water, respectively.^{116, 117}

3.5 Synthesis of 2(,7)-aryl-[1]benzothieno[3,2-b][1]-benzothiophene (BTBT) derivatives in micellar condition

3.5.1 Introduction

[1]Benzothieno[3,2-b]benzothiophene (BTBT) derivatives have gained a considerable interest as active, p-dopable molecular materials in the preparation of OFETs. The reasons of BTBT success were well explained in the introduction of chapter 1. In this section i want focus on arylated BTBT derivatives in order to improve molecular packing and tune HOMO and LUMO levels. BTBT's conjugated system was extended with a wide variety of aryl and heteroaryl groups¹¹⁸⁻¹²⁶ (see scheme 3.16) Generally, such π -extended derivatives are very poorly soluble thus requiring functionalization with side chains.

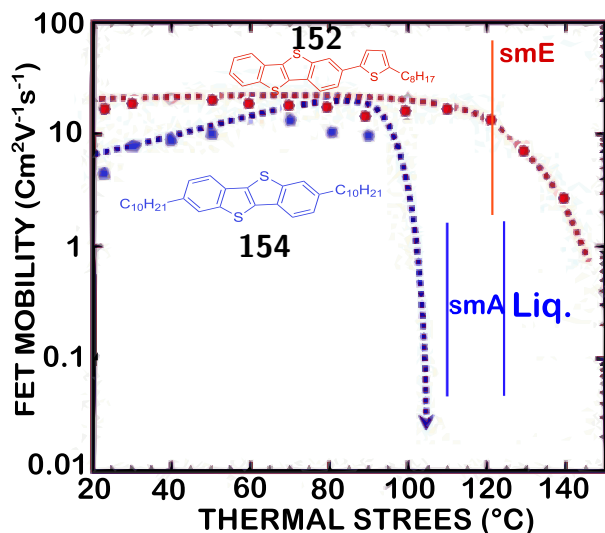


Scheme 3.16 Selection of arylated BTBT derivatives in the literature

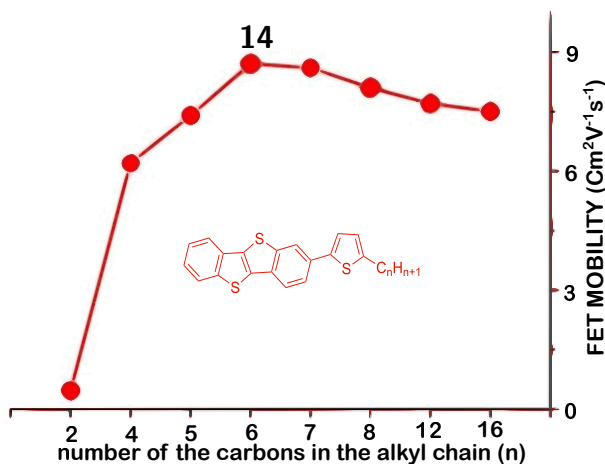
Arylated-BTBT compounds show improved mobility in OFET as they offer highly ordered thin film morphology, thermal stability, chemical and morphological as well.¹²⁷ Already mentioned, the presence of the alkyl chains improves solubility alongside with the introduction of a favorable morphology. However, dialkyl substitution often causes low thermal stability of polycrystalline thin films because the chemical modification with long alkyl chains reduce the melting point at the same time: for example BTBT has a melting point around 215°C against 2,7-dioctyl-[1]benzothieno[3,2-b]benzothiophene (diC8-BTBT, **153**, figure 3.8) melted at around 100°C¹²⁸, which is not high enough for the thermal processes required in device fabrication. Therefore, this chemical modification cannot solve the dilemma between the solubility and thermal stability in the soluble OFET materials. diC8-BTBT exhibits a liquid-like smectic mesophase of SmA,¹²⁹ which is responsible for the low thermal durability. This problem could be solved if the OFET materials exhibit any highly ordered smectic mesophase: because the highly ordered smectic mesophases exhibit a solid-like nature, their crystalline films can stay in film form when heated at their temperature range and go back to the crystal state when cooled down to the crystallization temperature; this gives the crystalline film high thermal durability. For example 2-(5-octyl-2-thienyl)-[1]benzothieno[3,2-b][1]benzothiophene (BTBT-Th-C8, compound **152** $n=8$, scheme 3.16) exhibited a highly ordered liquid crystal phase of SmE

phase at the temperature range from 131 °C to 180 °C next to the crystal phase.¹³⁰ Hanna and coworkers prepared molecularly flat and uniform thin films of BTBT-Th-C8 by spin-coating of its solution at the temperatures for the SmE phase. In addition, the thermal stability of polycrystalline thin films was very much improved up to 180 °C. BTBT-Th-C8 crystalline films can maintain their film form and never melt into a droplet when heated at 150 °C. Figure 3.8 shows the FET mobility in bottom-gate top-contact FETs fabricated with 2,7-didecyl-[1]benzothieno[3,2-b]benzothiophene (diC10-BTBT, **154**, figure 3.8) and BTBT-Th-C8, which exhibit SmA and SmE phases, respectively, after being subjected to thermal stress at a given temperature for 5 min. The FET fabricated with BTBT-Th-C8 can be operated well even after undergoing thermal stress at 150 °C for 5 min, whereas the FET from diC10-BTBT is substantially degraded because the diC10-BTBT melts (see figure 3.8a).¹³¹ Wang et al. made an optimization of the carbon chain length for the compounds series of 2-(5-alkylthien-2-yl)[1]benzothieno[3,2-b][1]benzothiophene (series of which also belongs BTBT-Th-C8, **152**). They described the synthesis and characterization of compounds with a carbons chains of 2,4,5,6,7,8,12 and 16 carbon (see figure 3.8b). All of the compounds with $n \geq 4$ show mesomorphism and display smectic A, smectic B ($n = 4$), or smectic E ($n > 4$) phases and then crystalline phases. Alkyl chain length has a noticeable influence on the microstructures of vacuum-deposited films and therefore on the performance of the organic thin-film transistors (OTFTs). All molecules except for 2-(thiophen-2-yl)[1]benzothieno[3,2-b][1]benzothiophene (**147**) and 2-(5-ethylthiophen-2-yl)[1]-benzothieno[3,2-b][1]benzothiophene (**152**, $n = 2$) feature OTFT mobilities above $5 \text{ cm}^2\text{V}^{-1}\text{s}^{-1}$. 2-(5-Hexylthiophen-2-yl)[1]benzothieno-[3,2-b][1]benzothiophene (BTBT-Th-C6, **155**, figure 3.8) shows the greatest OTFT performance with reliable hole mobilities (μ) up to $10.5 \text{ cm}^2\text{V}^{-1}\text{s}^{-1}$ because they form highly ordered and homogeneous films with diminished grain boundaries (see figure 3.8c).¹²³ In another work of the same authors they study the influence of the change of the chalcogen atoms on the heterocycle coupled with the BTBT scaffold. They replace Sulfur with Selenium (Se, compound **151**) and Oxygen (O, **150**), but **155** remain the best OFET materials in terms of hole mobility, the other compounds exhibited mobilities lower than $1 \text{ cm}^2\text{V}^{-1}\text{s}^{-1}$ except for **151** that exhibited hole mobility of $4.68 \text{ cm}^2\text{V}^{-1}\text{s}^{-1}$.¹²² 2-decyl-7-phenyl-[1]benzothieno[3,2-b][1]benzothiophene (**34**, C10-BTBT-Ph, figure 3.8) is another promising BTBT liquid crystal compounds. This material provides uniform and molecularly flat polycrystalline thin films reproducibly, deposited by spin coating, when SmE precursor thin films are crystallized, and also exhibits high durability of films up to 200 °C. In addition, the mobility of FETs is dramatically enhanced by about one order of magnitude (over $10 \text{ cm}^2\text{V}^{-1}\text{s}^{-1}$) after thermal annealing at 120 °C in bottom-gate-bottom-contact FETs (see figure 3.8c).¹¹⁸ Full X-ray crystal structure analysis of C10-BTBT-Ph were reported like flake-like single-domain crystals¹³² and also crystal structure in thin-film on polyimide gate insulator.¹³³ A study of alkyl chain length in C10-BTBT-Ph related compound are reported by Hasegawa et al.¹²⁶ and others various studies on OFET conduction.^{134, 135}

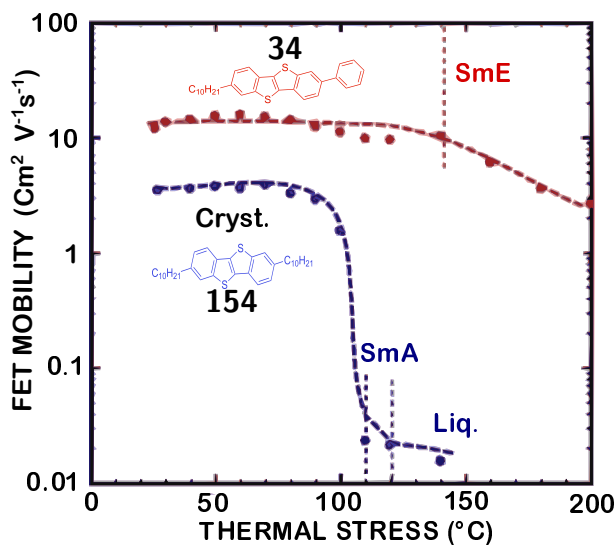
3.5. SYNTHESIS OF 2,(7)-ARYL-[1]BENZOTHIENO[3,2-B][1]BENZOTHIOPHENE (BTBT) DERIVATIVES IN MICELLAR CONDITION



(a) Comparison between between mobility in bottom-gate top-contact FETs fabricated with **152** $n=8$ and **154** in thermal stress study reported in literature¹³⁰



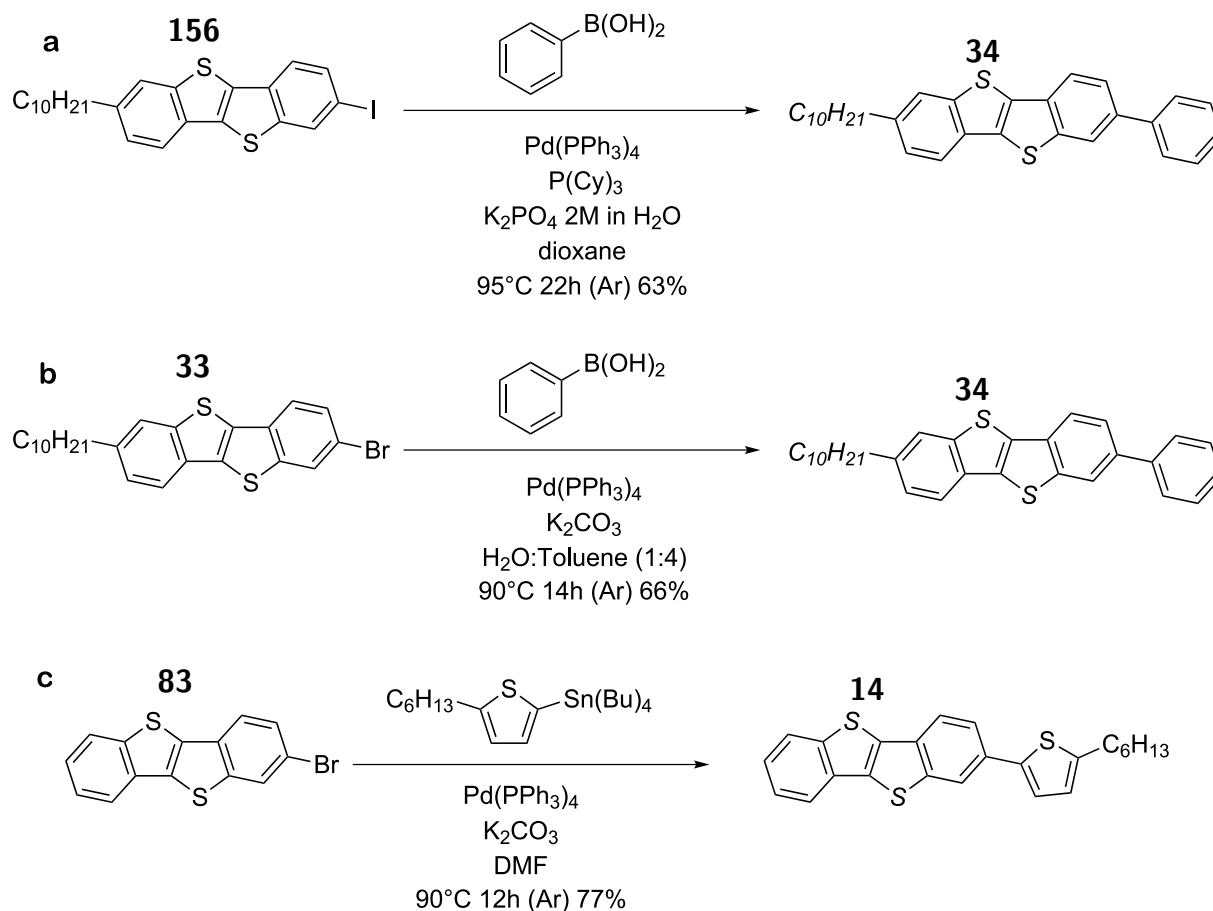
(b) study of carbon chain length influence in FETs mobility reported in literature¹²³



(c) Comparison between between mobility in bottom-gate top-contact FETs fabricated with **34** $n=8$ and **154** in thermal stress study reported in literature¹¹⁸

Arylated-BTBT compounds are prepared with Stille and Suzuki-Miyaura cross coupling reaction in organic solvent. For examples scheme 3.17 shows the last synthetic step reported in literature for compounds **14**¹²³ and **34**.^{118, 126, 136} For Compound **34** are reported two different routes (**a** and **b**), both are a SM coupling. Phenylboronic acid is coupled with 2-decyl-7-iodo-[1]benzothieno[3,2-b][1]benzothiophene(**156**) in the route **a**, instead in route **b** is coupled with 2-decyl-7-bromo-[1]benzothieno[3,2-b][1]benzothiophene(**33**), despite the use of the more reactive iodide respect the bromide, the moderate yields are comparable, around 65%. The preparation of compound **156** is a 4 step synthesis from 2-decyl-[1]benzothieno[3,2-b][1]benzothiophene (**157**) with a total yield of 22% and includes two chromatographic columns while the preparation of compound (**33**) is only 1 synthetic step with a yield of 45%. We can affirm that the route b is a better synthesis, but anyway includes the use of a large amount organic solvent, moderate yield, long reaction time (14h), argon atmosphere, degassed solvents and moderate high temperature (90°C). Scheme 3.17 shows also the last step for the preparation of compound **14**: a Stille coupling between 2-bromo-[1]benzothieno[3,2-b][1]benzothiophene(**83**) and 2-(Tributylstannyl)thiophene with a yield of 77%. The synthesis includes a chromatographic column, long reaction time (12h), argon atmosphere, degassed solvents, moderate high temperature (90°C) and the use and production of high toxic tin compounds. Similar conclusion can be done analyzing the synthesis reported also for the other compounds reported in scheme 3.16. Micellar synthesis has already demonstrated strong potential to improve sustainability of OS materials as shows in the previous section (3.3 and 3.4). In the chapter 2 (section 2.4) is described another alternative synthesis for **155** with direct arylation (DA) protocol, DA is a more sustainable cross-coupling but the yield is low and chromatographic purification are required, so further optimizations are required. In this section we show the development of two different SM micellar-catalyzed approach in order to increase the scalability and sustainability of the synthesis of the promising arylated-BTBT.

3.5. SYNTHESIS OF 2,(7)-ARYL-[1]BENZOTHIENO[3,2-B][1]BENZOTHIOPHENE (BTBT) DERIVATIVES IN MICELLAR CONDITION



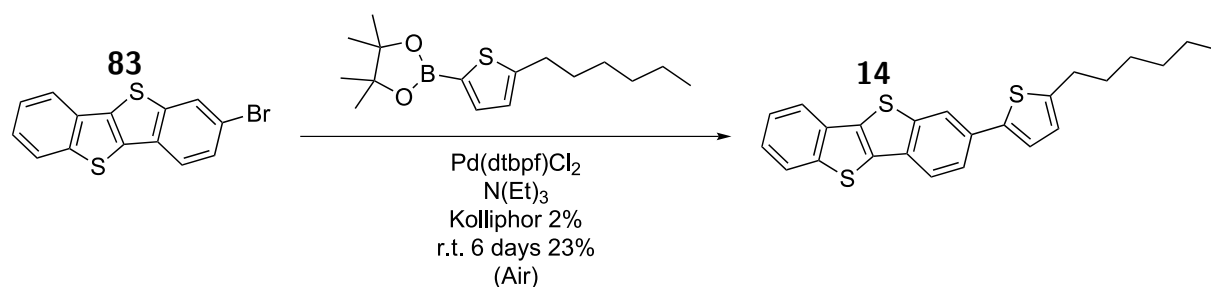
Scheme 3.17 synthesis reported in literature for compounds **34** and **14** a) synthesis of compound **34** reported in references^{118, 136} stoichiometry = 2-octyl-7-iodo-[1]benzothieno[3,2-b]benzothiophene **156** 1 eq, phenylboronic acid 2 eq, palladium tetrakis 0.05 eq., tricyclohexylphosphine 0.1 eq.; solvents and concentration = dioxane: water (18:1) and 0.05 M is the concentration of the iodide. b) synthesis of compound **34** reported in reference,¹²⁶ stoichiometry = 2-octyl-7-bromo-[1]benzothieno[3,2-b]benzothiophene **33** 1 eq., phenylboronic acid 1.5 eq, K₂CO₃ 3 eq., palladium tetrakis 0.05 eq.; solvents and concentration = toluene : water (4:1) and 0.05 M is the concentration of the bromide. c) synthesis of compound **14** reported in reference¹²³ stoichiometry = 2-bromo-[1]benzothieno[3,2-b]benzothiophene **83** 1 eq, 2-hexyl-5-tributylstannylthiophene 1.1 eq., palladium tetrakis 0.01 eq.; solvents and concentration = dimethylformamide and 0.10 M of the bromide.

3.5.2 Results and discussion

3.5.2.1 2,(7)-aryl-[1]benzothieno[3,2-b]benzothiophene's synthesis in emulsion condition

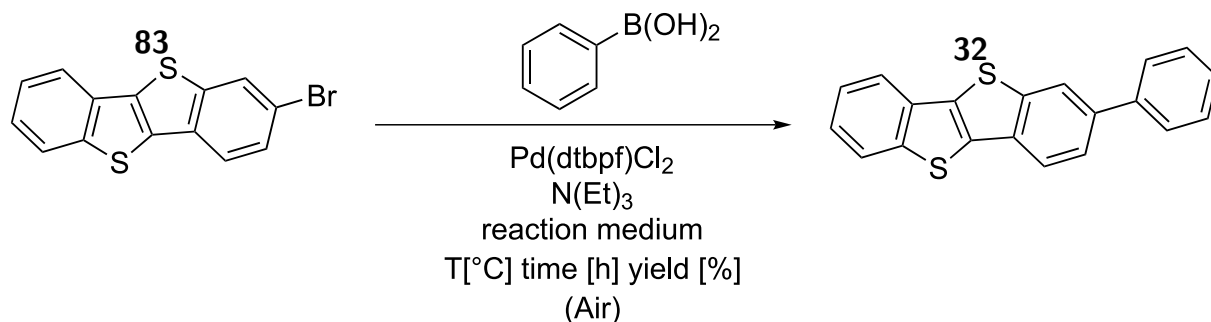
Aiming at developing sustainable approaches to some of the aforementioned derivatives, our first attempt was the synthesis of in 2% Kolliphor solution in water, with BTBT-Br (**83** (1 eq.)), Phenylboronic acid (1.5 eq.), N(Et)₃ (3 eq.) like base and Pd(dtbpf)Cl₂ like catalyst (2% in mol respect the bromide) at room temperature for 6 days. The reaction's yield is only 23% and the conversion is uncomplete. The increase in the temperature to 45°C doesn't give any improvement. As standard condition did not work well we decided to make an optimization study for BTBT derivatives micellar SM coupling.

We focused on a simpler model reaction (Table 3.7), the phenylation of compound **83**. Table 3.7 summarizes the optimization, more and more experts about the micellar OS



Scheme 3.18 First attempt of synthesis of compound **14** under standard micellar conditions. stoichiometry = 2-bromo-[1]benzothieno[3,2-b]benzothiophene **83** 1 eq., 5-Hexyl-2-thiopheneboronic acid pinacol ester 1.5 eq, Pd(dtbbpf)Cl_2 0.02 eq, N(Et)_3 3 eq. reaction medium and concentration = 2 wt% Kolliphor EL solution in Water and 0.50 M of the bromide

synthesis, we started with co-solvent approach in order to tune the micelle's HLB. as well as improve dispersability of the highly crystalline BTBTs. Like in the work on latent pigment (reported in section 3.3.4) we used a Kolliphor 2% solution in water and Co-solvent, 10% in volume respect to the Kolliphor solution. We tested Kolliphor 2%/THF micellar solution and the Kolliphor 2%/Toluene emulsion. We observed the same behaviour of the work reported in section 3.3.3 and 3.3.4. The Kolliphor 2%/Toluene emulsion provide a complete conversion and 90% yield, main byproducts are due to debromination and regioisomer formed by coupling with impurities of the reagent **83**.

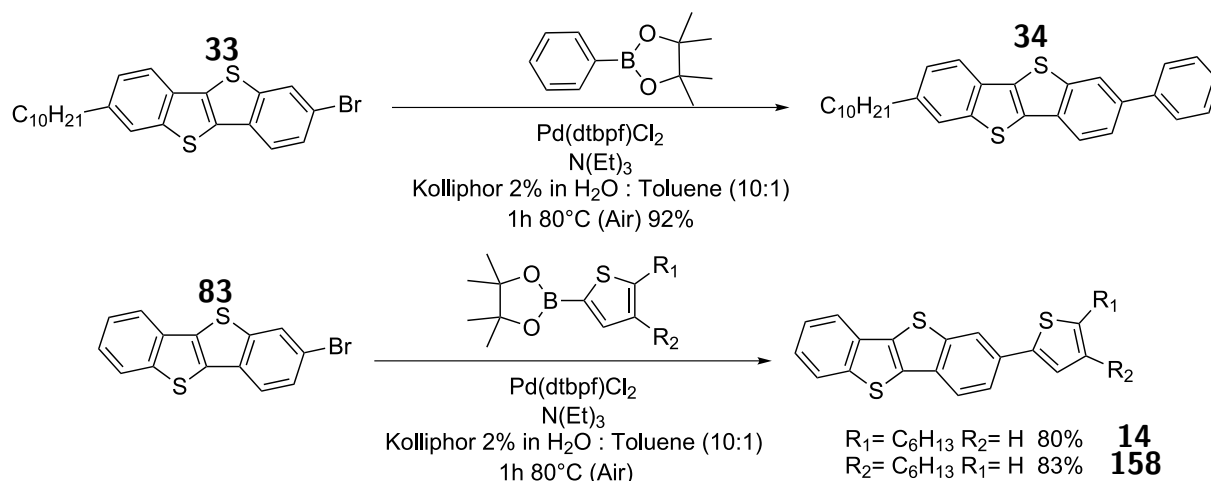


Entry	Reaction medium	Temperature	Time (h)	yield (%)
1	Kolliphor 2%	r.t.	6	26
2	Kolliphor 2%:THF (10:1)	r.t.	6	50
3	Kolliphor 2%:Toluene (10:1)	80°C	1	90

Table 3.7 Phenylation of compound **83** as model reaction for the optimization of the cosolvent approach. stoichiometry = 2-bromo-[1]benzothieno[3,2-b]benzothiophene **83** 1 eq., Phenylboronic acid 1.5 eq, Pd(dtbbpf)Cl_2 0.02 eq, N(Et)_3 3 eq. concentration = 0.50 M of the bromide

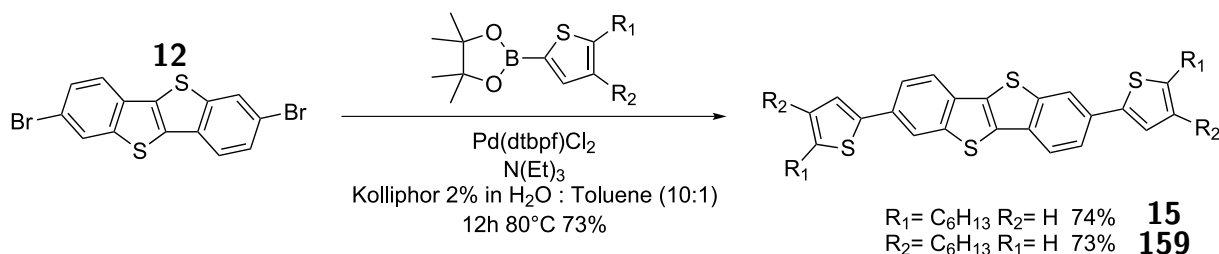
As it is shown in 3.19 we extended such optimized conditions to the synthesis of compound **34**, prepared by phenylation of compound **33**. In only one hour we could obtain the product without chromatographic purification and under air atmosphere with high yield (92%). After that we tried our conditions with the more problematic 2-thienylboronic acid aiming at the preparation of compound **14** (BTBT-Th-C6). We synthesized also a regioisomer of compound **14**, the compound **158**, with similar yield and simple purification. Compounds **14** and **158** are under devices characterization phase in order to study the influence of the alkyl chain position on OFET performances.

3.5. SYNTHESIS OF 2,(7)-ARYL-[1]BENZOTHIENO[3,2-B][1]BENZOTHIOPHENE (BTBT) DERIVATIVES IN MICELLAR CONDITION



Scheme 3.19 Synthesis of compounds **34**, **14** and **158** under emulsion conditions. stoichiometry = BTBT's bromide (**33**,**83**) 1 eq., arylboronic acid 1.5 eq, Pd(dtbpf)Cl₂ 0.02 eq, N(Et)₃ 3 eq. reaction medium and concentration = Kolliphor 2% in Water :Toluene (10:1)and 0.50 M of the bromide

We extended the reaction's scope to symmetrical bromide **12**, more problematic due higher crystallinity and extremely poor solubility. Even though the reaction time was extended from 1 h to 12 h but we succeeded in the isolation of the compounds **15** and **159** without chromatographic purification, with a extractive recrystallization in boiling methanol with a good yield, around 80%.**14** derivative was determined by GC-MS analysis and NMR spectroscopy to be the main impurity.



Scheme 3.20 Synthesis of compounds **15** and **159** under emulsion conditions. stoichiometry = 2,7-dibromo-[1]benzothieno[3,2-b]benzothiophene **12** 1 eq., thienylboronic acid pinacol ester 3.0 eq, Pd(dtbpf)Cl₂ 0.04 eq, N(Et)₃ 6 eq. reaction medium and concentration = Kolliphor 2% in Water :Toluene (10:1)and 0.50 M of the bromide

Co-solvent approach is thus efficient strategy to increase the yields of OS synthesis reactions catalyzed by Kolliphor® EL, in particular the kolliphor emulsion 2% / Toluene proved to be the most efficient. The amount of toluene used in these reactions is very low when compared to the amounts of toluene used in the SM reactions reported in literature for SM standard biphasic condition. For example, for the synthesis of compound **34** we employed 0,2 ml of Toluene for 1mmol of isolated product instead of 24 mL/g as in the standard approach¹²⁶, we thus saved around the 99% of toluene. Despite the excellent data provided by the co-solvent approach, it requires the use of an organic solvent that should preferentially be avoided in the event of industrial scaling up. We develop a third strategy, the development of designer π -surfactants not requiring the use of cosolvent (see section 3.5.2.3).

3.5.2.2 Kolliphor® EL-catalyzed Buchwald–Hartwig amination on [1]benzothieno[3,2-b][1]benzothiophene derivatives

In order to prove the scope of our Buchwald–Hartwig amination in micellar/emulsion condition exposed in the section 3.3.4 we test the reactivity of BTBT bromide **37** under such condition, a second reason of interest for this kind of compound, N-BTBT-arylated structures, is that they are reported from different patent like promising OS materials.^{137–141} Figure 3.9 shows the structures reported the patents.

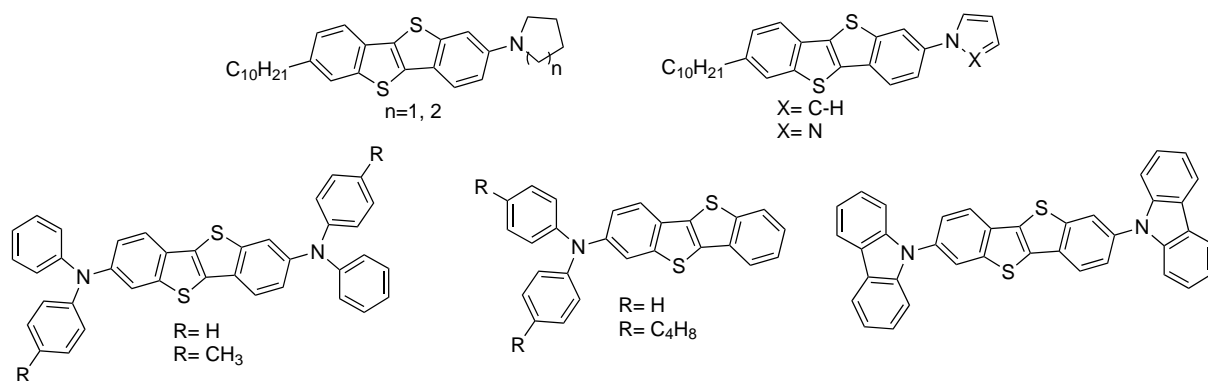
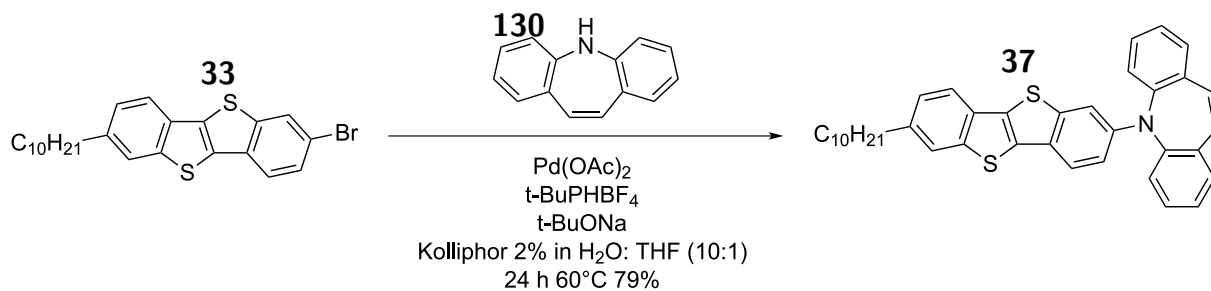


Figure 3.9 N-BTBT-arylated structures reported in patents.^{137–141}

We decided to try the BHA reaction between the bromide **33** and dibenzoazepine **130** and we could isolate the compound **37** with a yield of 79%, using a Kolliphor 2% solution in water and THF as co-solvent (10:1 volume ratio), with mild heating (60°C) under air atmosphere, according to our previous experience with naphthalene monoimide derivatives.



Scheme 3.21 Synthesis of 5-(7-decylbenzo[b]benzo[4,5]thieno[2,3-d]thiophen-2-yl)-5H-dibenzo[b,f]azepine **37** by BHA under micellar Conditions. stoichiometry = 2-decyl-7-bromo-[1]benzothieno[3,2-b]benzothiophene **33** 1 eq., dibenzoazepine **130** 1.0 eq, Pd(OAc)₂ 0.03 eq, tBuPHBF₄ 0.06 eq, tBuONa 1.5 eq. reaction medium and concentration = Kolliphor 2% in Water :Toluene (10:1) and 0.50 M of the bromide

3.5.2.3 Designer π -surfactant for BTBT's derivatives synthesis

The main problem in a standard micellar approach for BTBT derivatives SM reaction is that the surfactant isn't able to disperse efficiently the bromides, due the strong π - π interaction between the BTBT cores and a lack of specific interactions between surfactant and bromide. We decided to develop a new surfactant class for the micellar synthesis of highly crystallin/insoluble OS precursor. In order to add some specific interaction between

3.5. SYNTHESIS OF 2(,7)-ARYL-[1]BENZOTHIENO[3,2-B][1]BENZOTHIOPHENE (BTBT) DERIVATIVES IN MICELLAR CONDITION

the surfactant and the reagents, we added a π conjugated moiety. Figure 3.10 shows the general structure and “mechanism” of interaction of our designer surfactant. For the synthesis of our designer surfactant (designer π -surfactant) we adapted the design guidelines developed by Lipshutz group (TPGS-750M and Nok see section 3.1.4). Indeed we exploited PEG chain as hydrophilic group, long carbon chain as hydrophobic group and a succinic bridge as linker between the two groups.

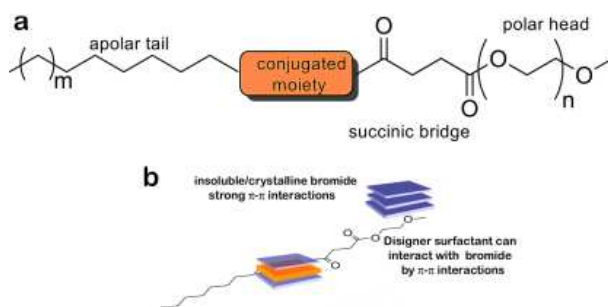


Figure 3.10 a) General structure of designer π -surfactant b) supposed mechanism of specific interaction of designer π -surfactant and conjugated bromides

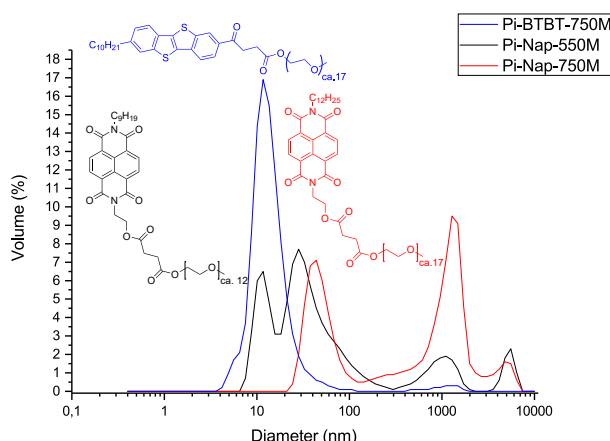
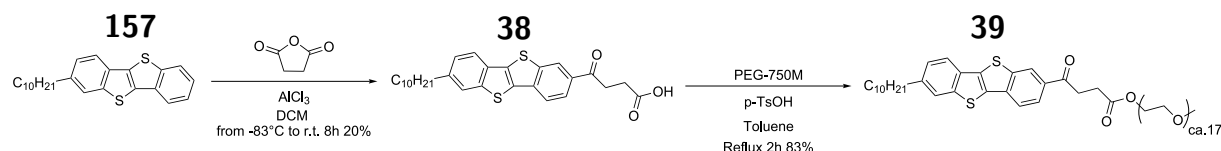


Figure 3.11 DLS analysis of designer π -surfactants 2% dispersion in water. The Pi-BTBT-750M analysis is reported in blu, the curve exhibits a maximum around 12 nm compatible with a micelle structures. The Pi-Nap-550M analysis is reported in black, the curve exhibits four relative maximum. The maximum at 12 nm is compatible with a micelle structures the others (28 nm , 1.0 μm and 5.6 μm) are correlable with bigger complex supramolecular aggregates. The Pi-BTBT-750M analysis is reported in red, the curve exhibits two relative maximum both correlable with complex supramolecular aggregates (43 nm and 1.2 μm)

3.5.2.3.1 Pi-BTBT-750M synthesis and testing Our first choice for the conjugated moiety was a BTBT core, firstly because we thought that inserting a BTBT portion in our surfactant would probably lead to a π -interaction with BTBT-bromide and secondly because we already developed conditions for acylating BTBT with a succinic portion (see. section 2.3.2.2). Scheme 3.22 shows the synthesis of Pi-BTBT-750M (compound **39**). The synthesis reported in the scheme start from the alkylated compound **157**, the condition for the alkylation of BTBT’s scaffold were described in the first chapter (see section 2.3.1), the chain is introduce in position 2 of BTBT scaffold with a Friedel-Crafts acylation followed by carbonyl group’s reduction to methylene group. In order to acylate the 7 position of compound **157**, we used the conditions developed for the synthesis

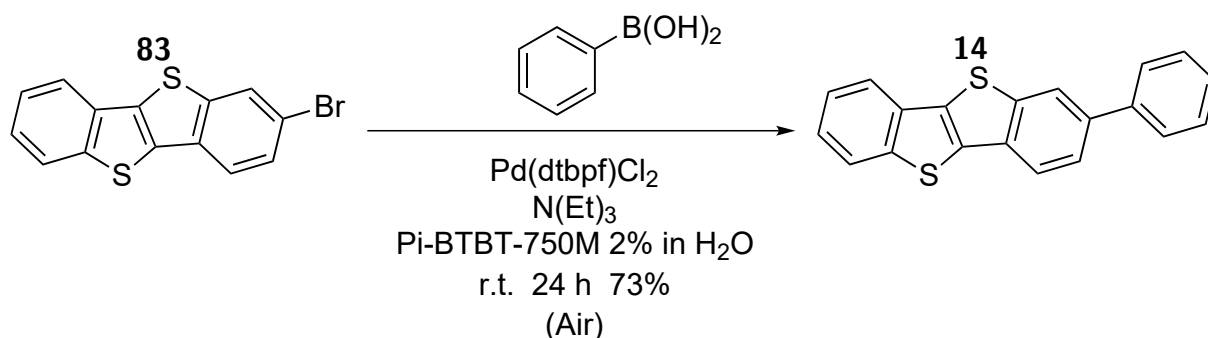
of compound **160**: succinic anhydride in the presence of aluminium chloride (AlCl_3) in dichloromethane at low temperature to maximize the regioselectivity of the aromatic electrophilic substitution in order to obtain compound **38**. The reaction yield is low because the purification of **38** from its regioisomer, that was formed during the reaction, is troublesome. The last step is Fischer esterification between the alcohol PEG-750M and the carboxylic acid **38** catalyzed by p-toluenesulfonic acid (p-TsOH). Pi-BTBT-750M (**39**) was obtained in good yield (83%) but with a little impurity of PEGchain (see NMR spectrum in the experimental parts 3.5.3), not a serious problem for our purposes as PEG impurities are a common component of most ethoxylated surfactants.



Scheme 3.22 Synthesis of Pi-BTBT-750M

DLS characterization of Pi-BTBT-750M 2 wt % solution in deionized water 3.11 confirms the capability of such surfactant to form micelles with an average hydrodynamic diameter of 12 nm and bigger complex supramolecular aggregates.

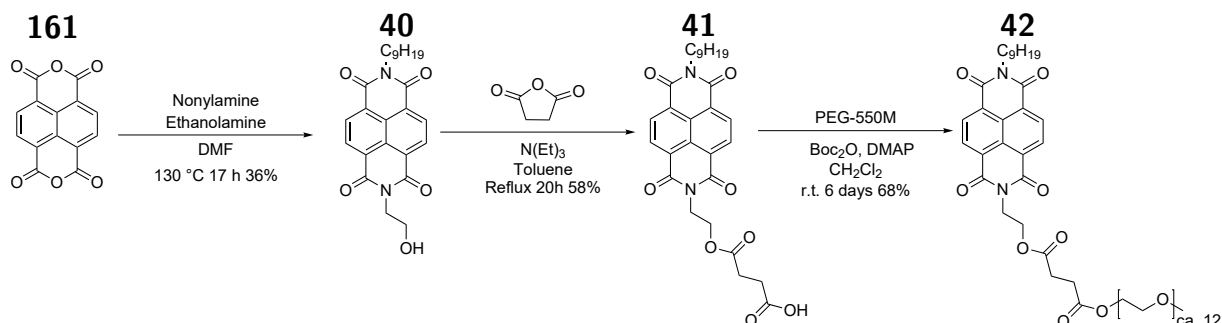
We tested Pi-BTBT-750M on the model reaction in the same conditions employed in the optimization of the emulsion condition (scheme 3.23): with BTBT-Br (**83**, 1 eq.), Phenylboronic acid (1.5 eq.), $\text{N}(\text{Et})_3$ (3 eq.) and $\text{Pd}(\text{dtbpf})\text{Cl}_2$ as the catalyst (2 % in mol with respect to the bromide) at room temperature for 1 day. The comparison of the yield of this experiment with the same reaction carried out in Kolliphor 2% water solution (Entry 1, table 3.7) it's possible to affirm that Pi-BTBT-750M is a more effective surfactant nanoreactor for the phenylation reaction of compound **83**, probably thanks to the specific π - π interactions between the surfactant and the reagent **83** which are instead absent with Kolliphor. The reaction was slower with respect to the reaction in Kolliphor 2%:toluene emulsion, also because we carried the reaction at room temperature as opposed to 80°C of the emulsion condition. The conversion wasn't complete but this could be related to poisoning of the catalyst as we performed the reaction under standard lab. conditions and there are no reasons to believe that Pi-BTBT-750M could behave as Kolliphor EL in the presence of O_2 .



Scheme 3.23 Phenylation of compound **83** in Pi-BTBT-750M 2 wt% stoichiometry = 2-bromo-[1]benzothieno[3,2-b]benzothiophene **83** 1 eq., Phenylboronic acid 1.5 eq, $\text{Pd}(\text{dtbpf})\text{Cl}_2$ 0.02 eq, $\text{N}(\text{Et})_3$ 3 eq. reaction medium and concentration = Pi-BTBT-750M 2 wt% in water and 0.50 M of the bromide

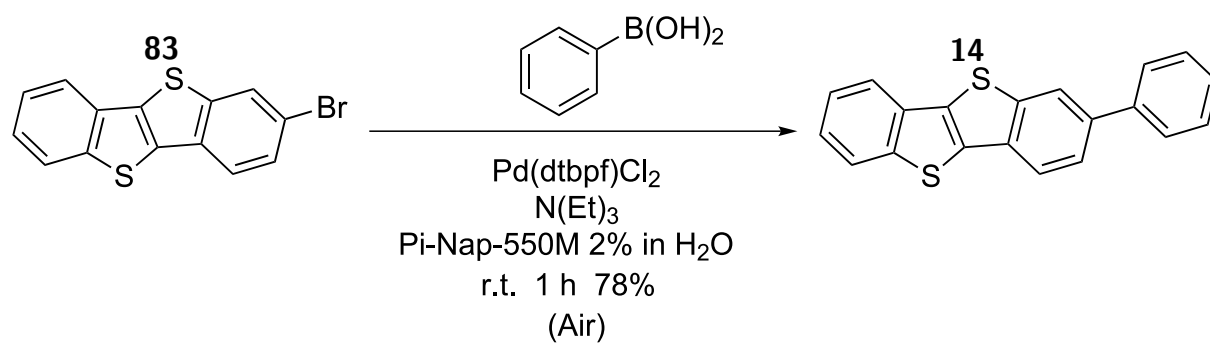
3.5. SYNTHESIS OF 2(,7)-ARYL-[1]BENZOTHIENO[3,2-B][1]BENZOTHIOPHENE (BTBT) DERIVATIVES IN MICELLAR CONDITION

3.5.2.3.2 Pi-Nap-550M synthesis and testing Once verified that the introduction of a conjugated portion inside the surfactant structure leads to an effective increase in the efficiency of the micellar catalysis for micellar SM coupling on BTBT derivatives, we develop improved surfactants, The key is to improve the interaction's strength between the reagents and our designer π -surfactant. It's well know in the literature that aromatic donor–acceptor interactions are very usefull supramolecular tools in defining π -stacked aggregates. Indeed a great number of research groups have successfully used alternating electron-rich and electron-deficient aromatic stacking as a supramolecular design principle to create a wide variety of architectures and assemblies.^{142–148} BTBT derivatives are electron-rich compounds likely to interact with an electron-deficient aromatic compound, We chose an NDI (1,4,5,8-naphthalene-tetracarboxylic diimide) scaffold as electron-deficient conjugated moiety. Scheme 3.24 shows the synthesis of our second designer π -surfactant called Pi-Nap-550M. The synthesis starts from naphthalenetetracarboxylic dianhydride (**161**), which is reacted with nonylamine and ethanolamine in order to obtain the asymmetric NDI **40**, the two symmetric NDIs that were obtained as byproduct were separate thanks to the respective different solubilities, leading to a moderate yield of 36%. In the second step the alcohol **40** was reacted with succinic anhydride in presence of triethylamine in order to obtain the carboxylic acid **41** with moderate yield (58%). The last step is a Steglich-like esterification, where Boc_2O was used in order to activate the carboxylic acid **41** and reacted with PEG-550M to afford Pi-Nap-550M. DLS characterization of Pi-Nap-550M 2 wt % solution in deionized water 3.11 confirms that our surfactant forms micelles with an avarage size of 12 nm and bigger complex supramolecular aggregates.



Scheme 3.24 Synthesis of Pi-Nap-550M

We tested Pi-Nap-550M on the model reaction in the same conditons employed in the optimization of the emulsion condition (scheme 3.23): with BTBT-Br (**83**, 1 eq. , Phenylboronic acid (1.5 eq.) , $\text{N}(\text{Et})_3$ (3 eq.) and $\text{Pd}(\text{dtbpf})\text{Cl}_2$ as the catalyst (with 2 % in mol respect the bromide) at room temperature for 1 h. The reaction's mixture apperance was very different from the other micellar reaction. Indeed, instead of the familiar grey color associated with clusters of $\text{Pd}(0)$, the suspension was blue and the reaction was strongly exothermic (see figure 3.12) . The reaction was extremely fast with respect to the reaction Kolliphor-catalyzed and probably fast at least as much as under the emulsion condition reaction, despite the much lower temperature, after 1 h the conversion was complete as confirmed by TLC and GC-MS analyses.



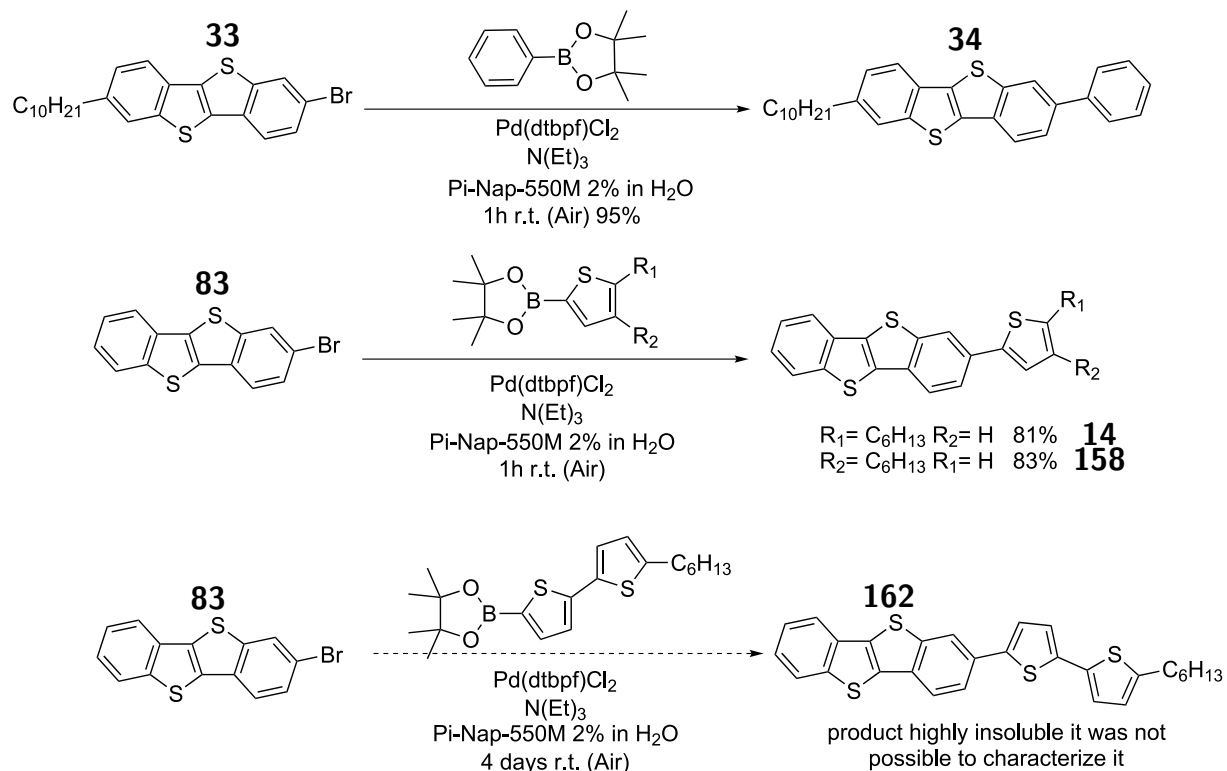
Scheme 3.25 Phenylation of compound **83** in Pi-Nap-550M 2 wt% in water solution. stoichiometry = 2-bromo-[1]benzothieno[3,2-b]benzothiophene **83** 1 eq., Phenylboronic acid 1.5 eq, Pd(dtbbpf)Cl_2 0.02 eq, N(Et)_3 3 eq. reaction medium and concentration = Pi-Nap-550M 2 wt% in water and 0.50 M of the bromide



(a) Pi-Nap-550M-catalyzed reaction (b) Kolliphor-catalyzed reaction

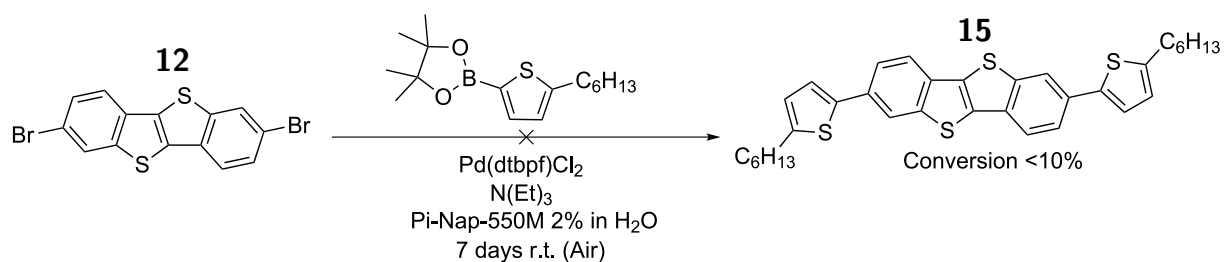
Figure 3.12 Reaction's mixture picture of the model reaction. phenylation of compound **83**

3.5. SYNTHESIS OF 2,(7)-ARYL-[1]BENZOTHIENO[3,2-B][1]BENZOTHIOPHENE (BTBT) DERIVATIVES IN MICELLAR CONDITION



Scheme 3.26 Synthesis of compounds **34**, **14**, **158** and **162** in Pi-Nap-550M 2 wt% water solution. stoichiometry = BTBT's bromide (**33**,**83**) 1 eq., arylboronic acid 1.5 eq, Pd(dtbpf)Cl₂ 0.02 eq, N(Et)₃ 3 eq. reaction medium and concentration = Pi-Nap-550M 2% in Water :Toluene (10:1)and 0.50 M of the bromide

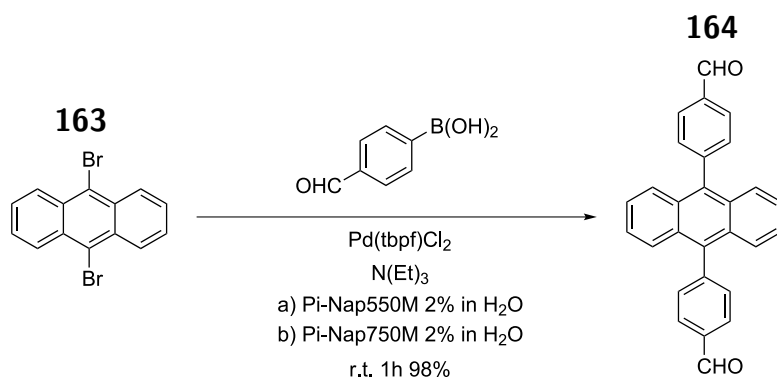
In order to widen the reaction's scope and better compare with the emulsion conditions, we synthesized the compounds **34**,**14** and **158**. We keep all the other conditions fixed (1:3:6:0.02 for bromide :boronic acid (pinacol ester):N(Et)₃:catalyst respectively) and we carried the reaction in a Pi-Nap-550M 2% solution in deionized water at room temperature (see scheme 3.26). Despite room temperature we managed to isolate products with comparable yields at the same reaction time and with the same simple purification of the respective reaction reported in scheme 3.19. The blue color and heating of reaction's mixture was observed in all of the cases reported in scheme 3.26 except for the attempt at synthesizing of **162**, where the heating was less intense. It was not possible to characterize, by NMR, the product **162** because of its very poor solubility in organic solvents, even at high temperature.



Scheme 3.27 Attempt at synthesis of compound **15** in Pi-Nap-550M 2 wt% water solution. stoichiometry = 2,7-dibromo-[1]benzothieno[3,2-b][1]benzothiophene **12** 1 eq., 5-Hexyl-2-thienylboronic acid pinacol ester 3.0 eq, Pd(dtbpf)Cl₂ 0.04 eq, N(Et)₃ 6 eq. reaction medium and concentration = Pi-Nap-550M 2 wt% water solution and 0.50 M of the bromide

We also tried to synthesize the symmetric compound **15** using Pi-Nap-550M, we mostly recovered the unreacted, and essentially insoluble, dibromide **12**. Pi-Nap-550M is not able to disperse efficiently the compound **12** at room temperature. The NMR spectrum of crude product confirms that the compound **15** was formed only in traces.

3.5.2.3.3 Pi-Nap-750M synthesis and testing Pi-Nap-550M shows very peculiar behaviour in the catalysis of SM coupling of BTBT derivatives and also was tested with other reactions that involved strongly conjugated π -material like 9,10-Dibromoanthracene (see scheme 3.28) and also with this substrate confirms its efficiency and our hypothesis of donor-acceptor aromatic interactions. The reaction behaves in the same way: very fast, exothermic and with a characteristic blue appearance

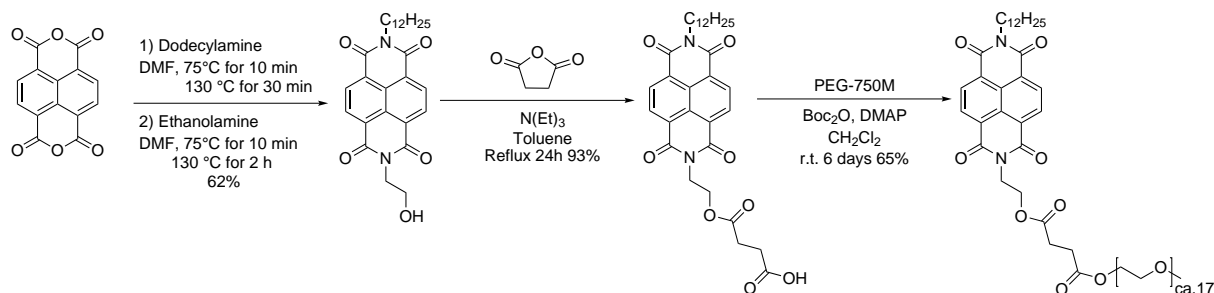


Scheme 3.28 9,10-Dibromoanthracene phenylation in micellar condition in Pi-Nap-550M and Pi-Nap-750M 2 wt% in water. stoichiometry = 9,10-Dibromoanthracene **163** 1 eq., 4-formylphenylboronic acid 3 eq., Pd(dtbbpf)Cl₂ 0.02 eq, N(Et)₃ 6 eq. reaction medium and concentration = Pi-Nap-550M 2 wt% in water for condition a, Pi-Nap-750M 2 wt% in water for condition b and 0.50 M of the bromide.

Pi-Nap-750M proved to be a very promising designer surfactant, yet limitations also became apparent. First of all the derivative is very poorly water soluble (possessing a HLB number of 10.5). Also, the complex aggregation behaviour shown in the DLS spectra makes comparison with kolliphor more troublesome. We thus designed derivative Pi-Nap-750M having two improved features: a longer PEG chain and a C₁₂ instead of a C₉ saturate chain.

Scheme 3.29 shows the Pi-Nap-750M synthesis, the first step conditions were optimized the two different amine (dodecylamine and ethanolamine) were added in two different steps and also the temperature was gradually raised during the reaction with beneficial suppression of symmetric byproducts. The second and third steps were done in the same condition of the related precursors but yield was higher in both steps. For the third step a non-chromatographic method for the purification of compound **44** has already been found, which consists in the removal with Soxhlet apparatus with heptane and isopropyl methyl ether, this led to a cleaner product respect to the chromatographic purified compound and a considerable reduction in the amount of organic solvent. In scheme 3.28 is shown a comparison between the two designer π -surfactants (Pi-Nap-550M and Pi-Nap-750M), the two surfactants both lead to high yields of reactions in a short time at room temperature, confirming the efficiency of the NDI core in catalyzing the SM reactions under micellar conditions on strongly π -conjugated 9,10-Dibromoanthracene.

3.5. SYNTHESIS OF 2(,7)-ARYL-[1]BENZOTHIENO[3,2-B][1]BENZOTHIOPHENE (BTBT) DERIVATIVES IN MICELLAR CONDITION



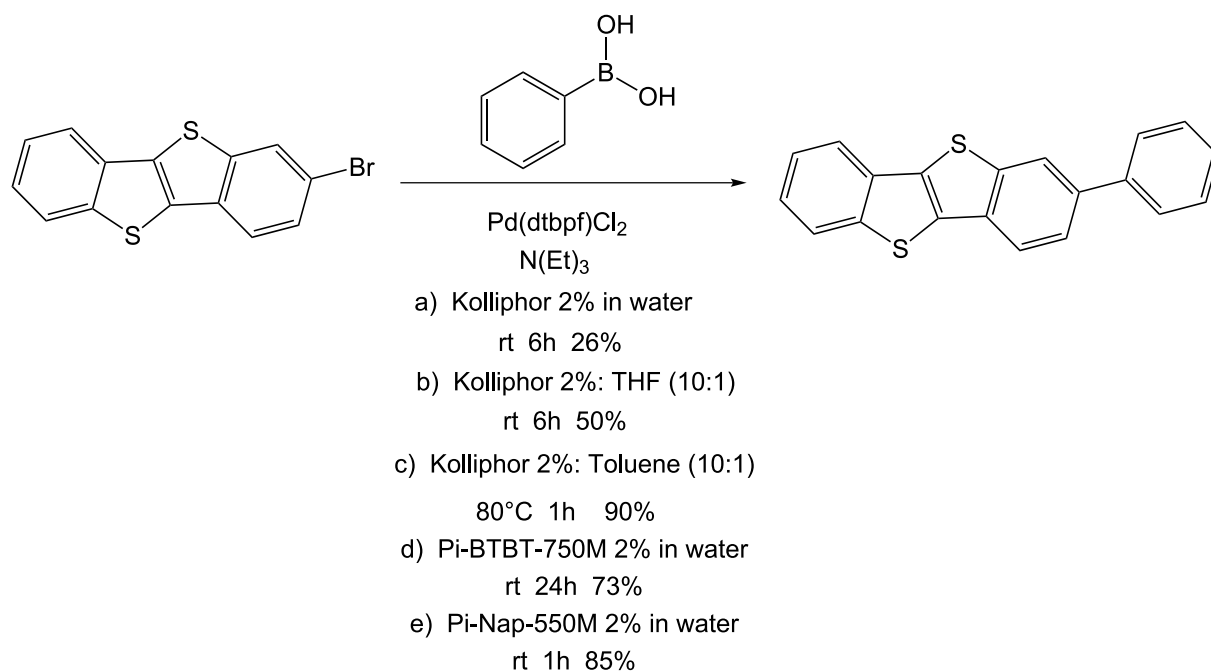
Scheme 3.29 Synthesis of Pi-Nap-750M

3.5.3 Conclusion

We developed two different micellar approaches for the SM coupling reaction on [1]benzothieno[3,2-b]benzothiophene derivatives. The first approach was in line with our previous experience and required the use of cosolvent (see section 3.3.3 and 3.3.4), indeed the use of a small amount of co-solvent to a Kolliphor 2% solution in water leads to an improvement in reaction's conversion, rate and yield under air atmosphere. In particular the emulsion system Kolliphor 2%:Toluene is the best reaction medium tested. The second approach developed is based on an original idea: the synthesis of new surfactants designed to provide a specific interactions with highly conjugated aromatic systems. We designed and synthesized three different designer π -surfactant. We tested two different aromatic moiety: BTBT and NDI scaffold. For SM reaction on [1]benzothieno[3,2-b]benzothiophene bromides the NDI scaffold turned out to be the best choice. Our hypothesis to explain better performance of Pi-Nap-550M over Pi-BTBT-750M, is the stronger π - π interaction of the latter with the [1]benzothieno[3,2-b]benzothiophene bromides. This hypothesis is under further investigation. It is also possible that the blue color of the reaction's mixture containing Pi-Nap-550M could be related with the formation of complex with Pd(0) of the NDI-core. We have already verified that the color change is observed when the catalyst, the triethylamine and the surfactant are dissolve together in water, in absence of any counterpart. The formation of such complex could assist the oxidative insertion of Palladium on the electron rich BTBT bromide. Both approach lead to greener synthesis of 2(,7)-arylated-[1]benzothieno[3,2-b]benzothiophene derivatives with respect the syntheses reported in literature. For example the SM reaction step for the synthesis of the very promising compound **34** have a E-factor of 74.17, excluding purification, for the literature reported synthesis¹²⁶ instead of 6.89 for the emulsion SM reaction and of 7.02 for the designer Pi-Nap-550M-catalyzed reaction. Furthermore, we purified our crude derivatives with a simple silica filtration instead of the columns described in the literature, thus further contributing to the sustainability of the method.

3.5.4 Experimental part

3.5.4.1 Synthesis of 2-phenyl-[1]benzothieno[3,2-b][1]benzothiophene (32)

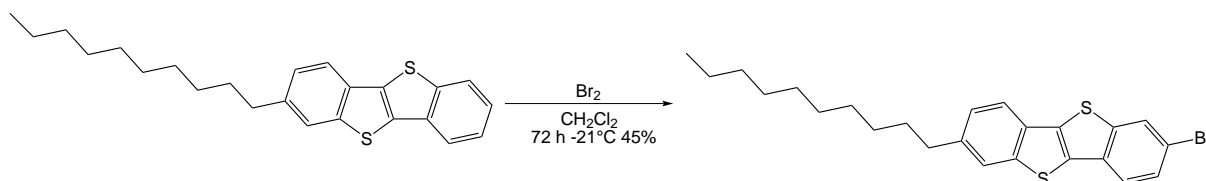


2-Bromo-[1]benzothieno[3,2-b][1]benzothiophene (1.00 mmol), phenylboronic acid (1.50 mmol) and Pd(dtbpf)Cl₂ (0.02 mmol) are weighted in the vessel, then reaction's medium (1 mL) was added. The mixture is allowed to homogenize for 5 minutes before addition of and triethylamine (3 mmol). Reaction was stirred for time required(see the scheme for the times) at room temperature (exceptet for condition C, where the reaction's temperature was 80°C). The mixture was diluted with 20 mL of dichloromethane and filtered through a pad of silica with a mixture of dichloromethane and ethyl acetate (4:1 ,100 mL). The filtrated was evaporated under reduced pressure and purified by crystallization in toluene to afford 2-phenyl-[1]benzothieno[3,2-b][1]benzothiophene as white solid (a 26% ; b 50%; c 90%; d 73%; e 85%).

H NMR (400 MHz, CDCl₃) d 8.13 (d, J 1.1 Hz, 1H), 7.99 – 7.87 (m, 3H), 7.75 – 7.66 (m, 3H), 7.53 – 7.35 (m, 5H). ¹³C NMR (101 MHz, CDCl₃) d 143.23, 142.50, 140.89, 138.57, 133.89, 133.38, 133.30, 132.34, 129.09, 127.64, 127.50, 125.19, 125.09, 124.68, 124.21, 122.52, 121.93, 121.75.

3.5. SYNTHESIS OF 2(,7)-ARYL-[1]BENZOTHIENO[3,2-B][1]BENZOTHIOPHENE
(BTBT) DERIVATIVES IN MICELLAR CONDITION

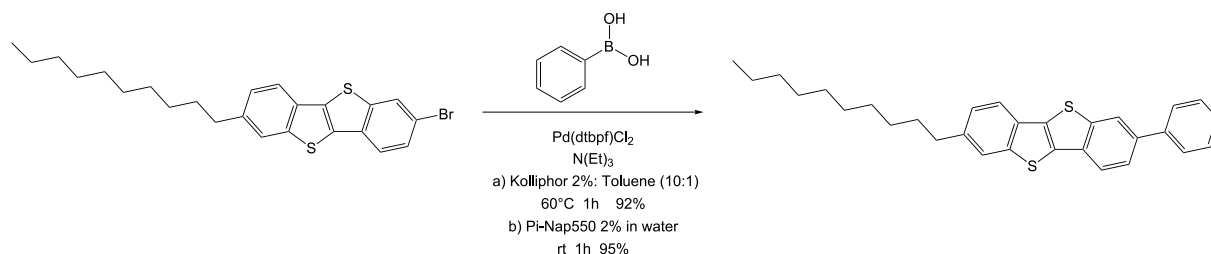
3.5.4.2 Synthesis of 2-decyl-7-bromo-[1]benzothieno[3,2-b][1]benzothiophene
(33)



To a solution of 2-decyl-[1]benzothieno[3,2-b]benzothiophene (5.000 g, 13.14 mmol) in dichloromethane (130 mL) was added a solution of bromine (2.106 g, 13.16 mmol) in dichloromethane (20 mL) using a dropping funnel at -21°C. The solution was stirred for 6 h at the same temperature. The contents were stored at -21°C for 64 h in freezer to form white precipitate. White solid was filtered, and crystallized in heptane to afford 2-decyl-7-bromo-[1]benzothieno[3,2-b][1]benzothiophene as white solid (2.721 g, 5.92 mmol, 45%).

(ppm) 8.04 (d, J = 1.7 Hz, 1H, ArH), 7.77 (d, J = 8.1 Hz, 1H, ArH), 7.71 (s, 1H, ArH), 7.71 (d, J = 8.4 Hz, 1H, ArH), 7.55 (dd, J = 1.7 Hz, 8.4 Hz, 1H, ArH), 7.28 (d, J = 8.1 Hz, 1H, ArH), 2.76 (t, J = 7.7 Hz, 2H, ArCH 2), 1.69 (tt, J = 7.7 Hz, 7.7 Hz, 2H, ArCH 2 C H 2), 1.34 - 1.26 (m, 14H, C H 2), 0.87 (t, J = 7.0 Hz, 3H, CH 3).

3.5.4.3 Synthesis of 2-decyl-7-phenyl-[1]benzothieno[3,2-b][1]benzothiophene (34)



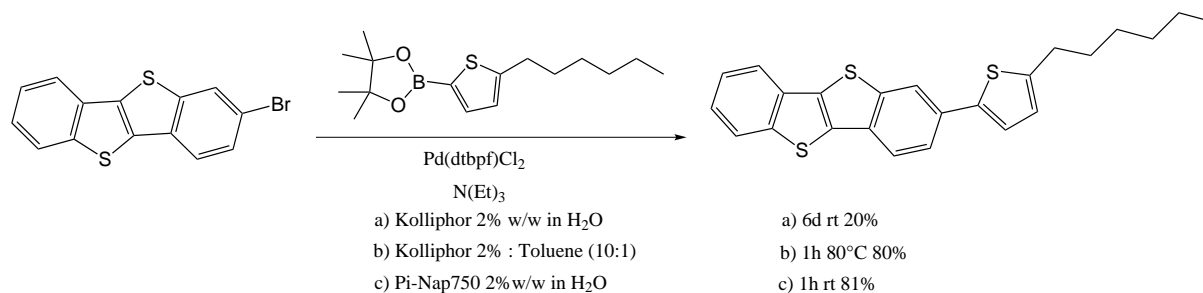
a) 2-Decyl-7-bromo-[1]benzothieno[3,2-b][1]benzothiophene (667 mg, 1.50 mmol), phenylboronic acid (264 mg, 2.16 mmol) and Pd(dtbpf)Cl_2 (20.5 mg, 0.0315 mmol) were weighted in the vessel, then Kolliphor 2%:Toluene emulsion (3.0 mL) is added. The mixture is allowed to homogenize for 5 minutes before addition of triethylamine (455 mg, 4.50 mmol). Reaction was stirred for 1h at 60°C. Reaction mixture was diluted with 50 mL of dichloromethane and filtered through a pad of silica with a mixture of dichloromethane and ethyl acetate (4:1 , around 200 ml). The filtrate was evaporated under reduced pressure to give crude product. The crude product was washed with methanol (3 x 20 mL) and purified by crystallization in toluene to afford 2-decyl-7-phenyl-[1]benzothieno[3,2-b][1]benzothiophene was obtained as white solid (634 mg , 1.38 mmol, 92%).

b) 2-Decyl-7-bromo-[1]benzothieno[3,2-b][1]benzothiophene (180 mg, 0.404 mmol), phenylboronic acid (91.2 mg, 0.746 mmol) and Pd(dtbpf)Cl_2 (7.5 mg, 0.011 mmol) were weighted in the vessel, then Pi-Nap-750 2% w/w solution in water (0.8 mL) was added. The mixture is allowed to homogenize for 5 minutes before addition of triethylamine (132 mg, 1.30 mmol). Reaction was stirred for 1h at room temperature. Reaction mixture was diluted with 10 mL of dichloromethane with a mixture of dichloromethane and ethyl acetate (4:1 , 50 mL). The filtrate was evaporated under reduced pressure to give crude product. The crude product was washed with methanol (3 x 10 mL) and purified by crystallization in toluene to afford 2-decyl-7-phenyl-[1]benzothieno[3,2-b][1]benzothiophene was obtained as white solid (175mg , 3.81 mmol, 95%).

$^1\text{H NMR}$ (500 MHz, CDCl_3): δ 8.12 (d, $J = 1.4$ Hz, 1H), 7.92 (d, $J = 8.3$ Hz, 1H, ArH), 7.79 (d, $J = 8.1$ Hz, 1H), 7.72 (s, 1H), 7.69 (m, 3H), 7.49 (dd, $J = 7.5$ Hz, 7.5 Hz, 2H), 7.38 (dd, $J = 7.5$ Hz, 7.5 Hz, 1H), 7.29 (d, $J = 8.1$ Hz, 1H), 2.77 (t, $J = 7.7$ Hz, 2H), 1.70 (tt, $J = 7.7$ Hz, 7.7 Hz, 2H) 1.36 - 1.25 (m, 14 H), 0.88 (t, $J = 7.0$ Hz, 3H)

3.5. SYNTHESIS OF 2(,7)-ARYL-[1]BENZOTHIENO[3,2-B][1]BENZOTHIOPHENE (BTBT) DERIVATIVES IN MICELLAR CONDITION

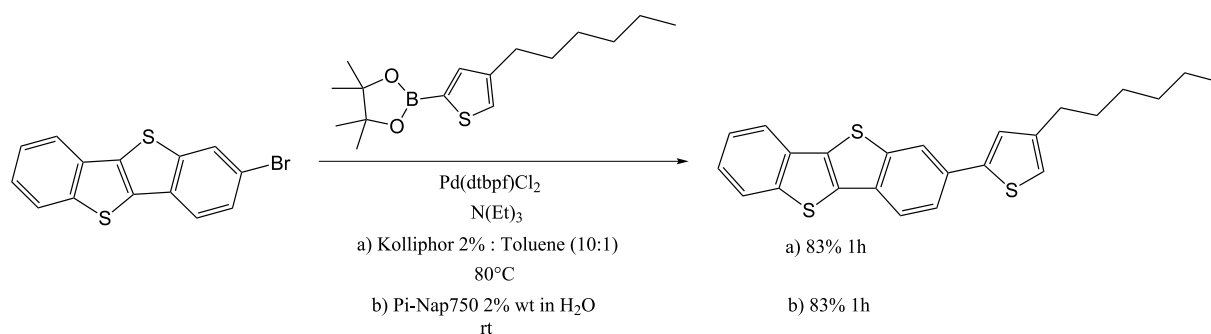
3.5.4.4 Synthesis of 2-(5-hexyl-2-thienyl)-[1]benzothieno[3,2-b][1]benzothiophene(14)



2-Bromo-benzo[b]benzo[4,5]thieno[2,3-d]thiophene (1.00 mmol), 5-Hexyl-2-thiopheneboronic acid pinacol ester (1.50 mmol) and Pd(dtbpf)Cl₂ (0.02 mmol) were weighted in the vessel, then 2mL of reaction's medium were added. The mixture is stirred for 5 minutes, then triethylamine (3.00 mmol) is added. The Reaction was stirred for time required (see the scheme for the times) at room temperature (except for condition b, where the reaction's temperature was 80°C). The mixture was diluted with 20 ml of dichloromethane. The solution was washed with brine (3 x 5 ml), and dried over magnesium sulfate. The solution was filtered through a pad of silica then the dichloromethane was removed under reduce pressure. The solid was dispersed in methanol (100 mL) and sonicated for 20 min. The solid was filtered. The crude product was crystallized in toluene to obtain 2-(5-hexyl-2-thienyl)-[1]benzothieno[3,2-b][1]benzothiophene as white crystallin solid (a 20%; b 80%; c 81%).

¹H NMR (500 MHz, CDCl₃) δ 8.08 (d, J = 1.3 Hz, 1H), 7.90 (dd, J = 20.4, 7.9 Hz, 2H), 7.83 (d, J = 8.3 Hz, 1H), 7.66 (dd, J = 8.3, 1.6 Hz, 1H), 7.44 (ddd, J = 15.2, 10.9, 3.9 Hz, 2H), 7.22 (d, J = 3.5 Hz, 1H), 6.79 (d, J = 3.5 Hz, 1H), 2.85 (t, J = 7.6 Hz, 2H), 1.78 – 1.67 (m, 2H), 1.37 (tt, J = 7.0, 5.3 Hz, 6H), 0.91 (t, J = 7.0 Hz, 3H). ¹³C NMR (126 MHz, CDCl₃) δ 147.10, 143.97, 143.13, 142.04, 134.37, 134.20, 133.99, 132.89, 132.72, 126.11, 125.85, 125.80, 124.90, 123.98, 123.82, 122.61, 122.41, 121.26, 32.50, 32.47, 31.19, 29.67, 23.47, 14.97.

3.5.4.5 Synthesis of 2-(4-hexyl-2-thienyl)-[1]benzothieno[3,2-b][1]benzothiophene(35)

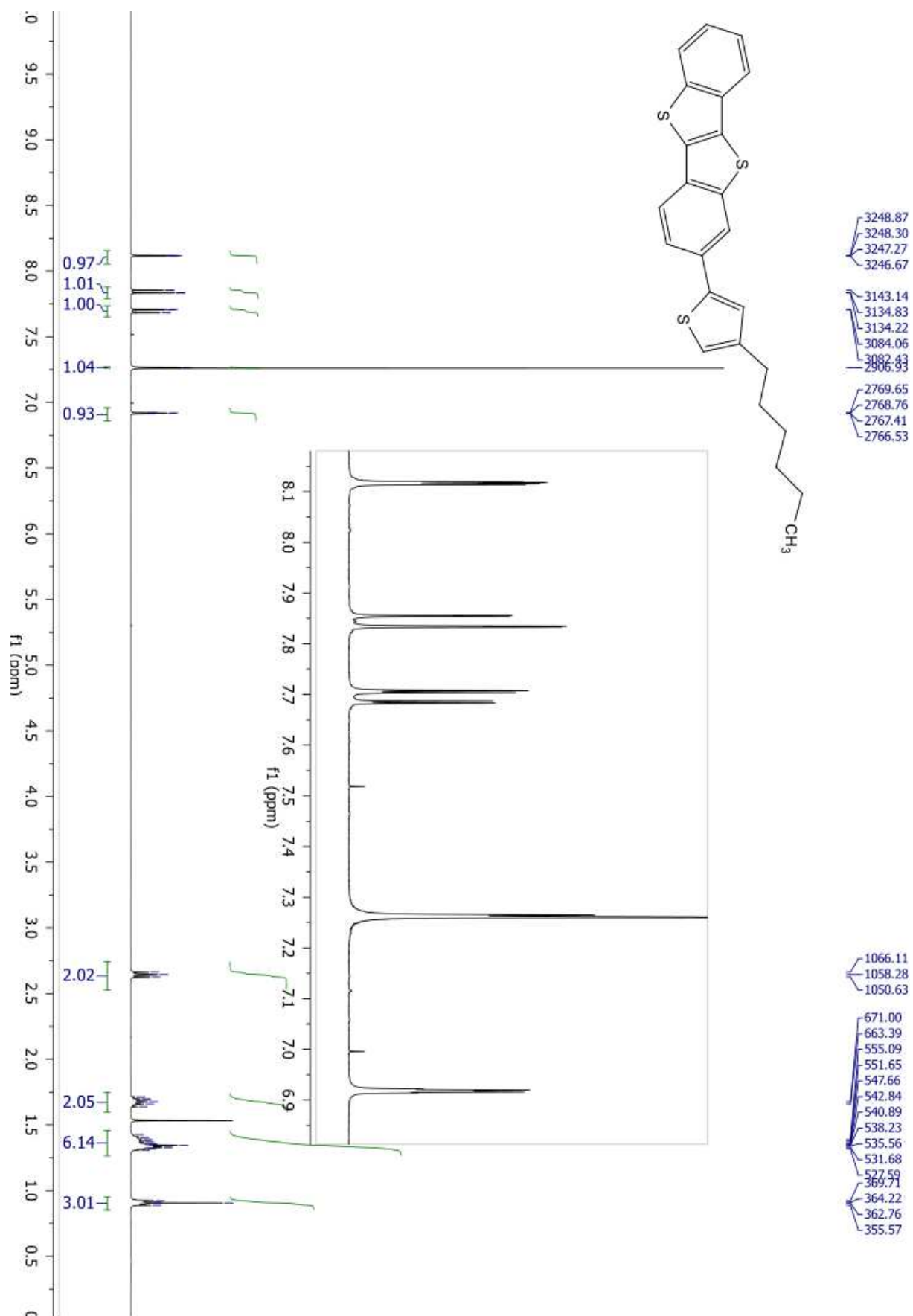


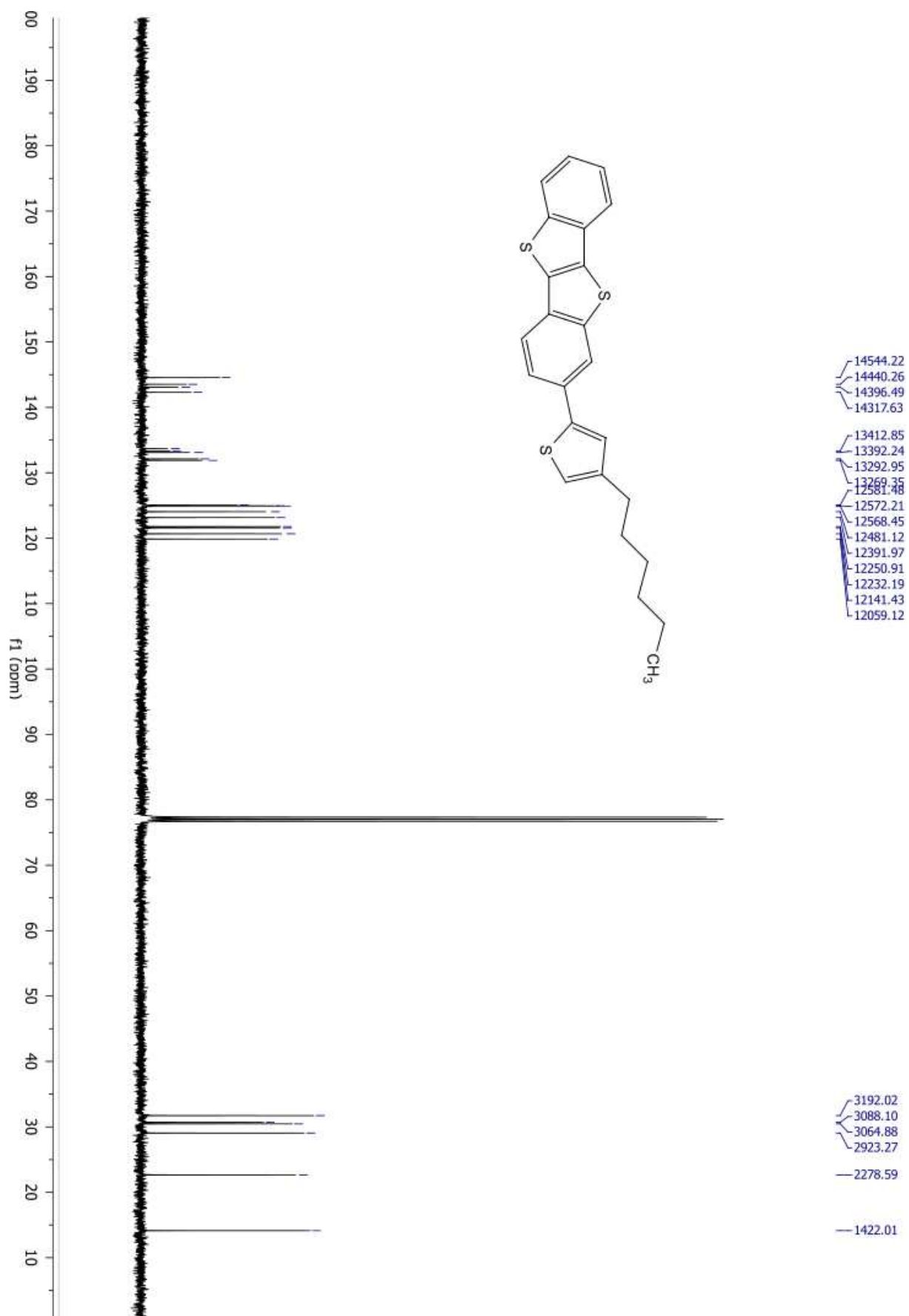
2-Bromo-benzo[b]benzo[4,5]thieno[2,3-d]thiophene (1.00 mmol), 4-Hexyl-2-thiopheneboronic acid pinacol ester (1.50 mmol) and Pd(dtbbpf)Cl₂ (0.02 mmol) were weighted in the vessel, then 2 mL of reaction's medium were added. The mixture is stirred for 5 minutes, then triethylamine (3.00 mmol) is added. The Reaction was stirred 1h at room temperature for a) condition and at 80° for b) condition. The mixture was diluted with dichloromethane (100 mL). The mixture was diluted with 20 ml of dichloromethane. The solution was washed with brine (3 x 5 ml), and dried over magnesium sulfate. The solution was filtered through a pad of silica then the dichloromethane was removed under reduce pressure. The solid was dispersed in methanol (100 mL) and sonicated for 20 min. The solid was filtered. The crude product was crystallized in toluene to obtain 2-(4-hexyl-2-thienyl)-[1]benzothieno[3,2-b][1]benzothiophene as white crystallin solid (337 mg, 0.829 mmol, 83%).

b) 2-Bromo-benzo[b]benzo[4,5]thieno[2,3-d]thiophene (323 mg, 1.01 mmol), 4-Hexyl-3-thiopheneboronic acid pinacol ester (445 mg, 1.51 mmol) and Pd(dtbbpf)Cl₂ (14.68 mg, 0.02 mmol) were weighted in the vessel, then a solution of Pi-Nap750 in water (2 mL , 2% w/w) was added. The mixture is stirred, then triethylamine (306 mg, 3.0 mmol) was added. The mixture was stirred at room temperature for 1h. The mixture was diluted with 100 mL of dichloromethane. The solution was washed with brine (2 x 50 ml) and dried over magnesium sulfate. The solution was filtered through a pad of silica then the dichloromethane was removed under reduce pressure. The solid was dispersed in methanol (200 mL) and sonicated for 20 min then filtered. The solid was filtered. The impurities were removed by hot filtration in isopropanol. The isopropanol was removed under reduce pressure and the product was dry overnight under vacuum at 70°C to obtain 2-(4-hexyl-2-thienyl)-[1]benzothieno[3,2-b][1]benzothiophene as white crystallin solid (338 mg, 0.831 mmol, 83%).

¹H NMR (400 MHz, CDCl₃) δ 8.12 (dd, J = 1.6, 0.6 Hz, 1H), 7.88 – 7.79 (m, 1H), 7.70 (dd, J = 8.3, 1.6 Hz, 1H), 6.92 (dd, J = 2.2, 0.9 Hz, 1H), 2.74 – 2.53 (m, 2H), 1.68 (dt, J = 15.3, 7.3 Hz, 2H), 1.46 – 1.27 (m, 6H), 0.95 – 0.85 (m, 3H). ¹³C NMR (101 MHz, CDCl₃) δ 144.56, 143.52, 143.09, 142.30, 133.69, 133.31, 133.11, 132.12, 131.89, 125.05, 124.96, 124.92, 124.05, 123.16, 121.76, 121.58, 120.67, 119.86, 31.73, 30.69, 30.46, 29.05, 22.65, 14.13.

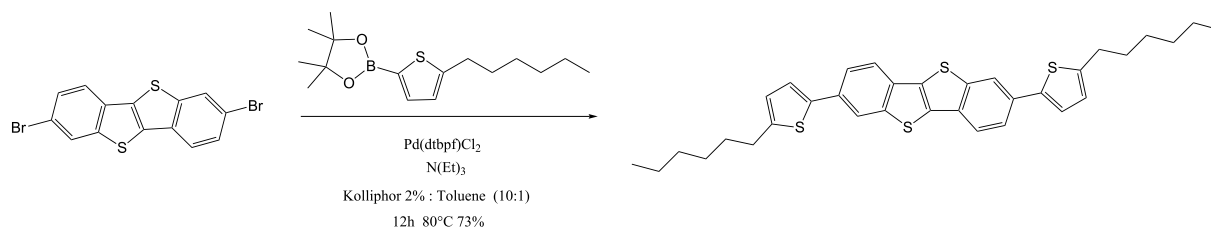
3.5. SYNTHESIS OF 2(,7)-ARYL-[1]BENZOTHIENO[3,2-B][1]BENZOTHIOPHENE (BTBT) DERIVATIVES IN MICELLAR CONDITION





3.5. SYNTHESIS OF 2(,7)-ARYL-[1]BENZOTHIENO[3,2-B][1]BENZOTHIOPHENE
(BTBT) DERIVATIVES IN MICELLAR CONDITION

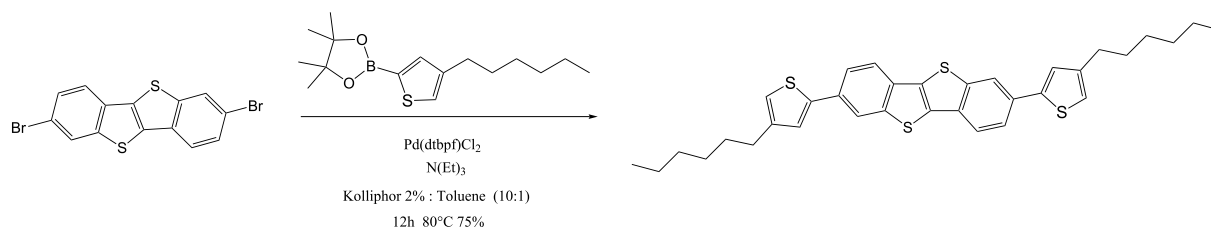
3.5.4.6 Synthesis of 2,7-di-(5-hexyl-2-thienyl)-[1]benzothieno[3,2-b][1]benzothiophene (15)



2,7-Dibromo-benzo[b]benzo[4,5]thieno[2,3-d]thiophene (199 mg, 0.500 mmol), 5-Hexyl-2-thiopheneboronic acid pinacol ester (441 mg, 1.50 mmol) and Pd(dtbpf)Cl₂ (14.70 mg, 0.02 mmol) were weighted in the vessel, then Kolliphor 2%:Toluene (10:1) emulsion (1 mL) was added. The mixture is stirred, then triethylamine (303 mg, 2.99 mmol) is added. The mixture was stirred at 80°C for 12h. The suspension was diluted with methanol and filtered. The solid was washed with methanol and dichloromethane. The solid purified with extractive crystallization in chloroform to afford 2,7-di-(5-hexyl-2-thienyl)-[1]benzothieno[3,2-b][1]benzothiophene as white crystallin solid (213 mg, 0.372 mmol, 73 % yield).

¹H NMR (400 MHz, CDCl₃) δ 8.07 (dd, J = 1.6, 0.6 Hz, 1H), 7.83 (dd, J = 8.3, 0.6 Hz, 1H), 7.67 (dd, J = 8.3, 1.6 Hz, 1H), 7.23 (d, J = 3.6 Hz, 1H), 6.79 (dt, J = 3.6, 0.9 Hz, 1H), 2.85 (t, J = 7.7 Hz, 2H), 1.73 (dt, J = 15.4, 7.5 Hz, 2H), 1.37 (tt, J = 7.2, 5.5 Hz, 6H), 0.95 – 0.86 (m, 3H). ¹³C NMR (101 MHz, CDCl₃) δ 146.23, 143.75, 141.16, 137.51, 131.97, 131.85, 125.24, 123.09, 122.99, 121.66, 120.35, 31.61, 31.58, 30.31, 28.78, 22.58, 14.08.

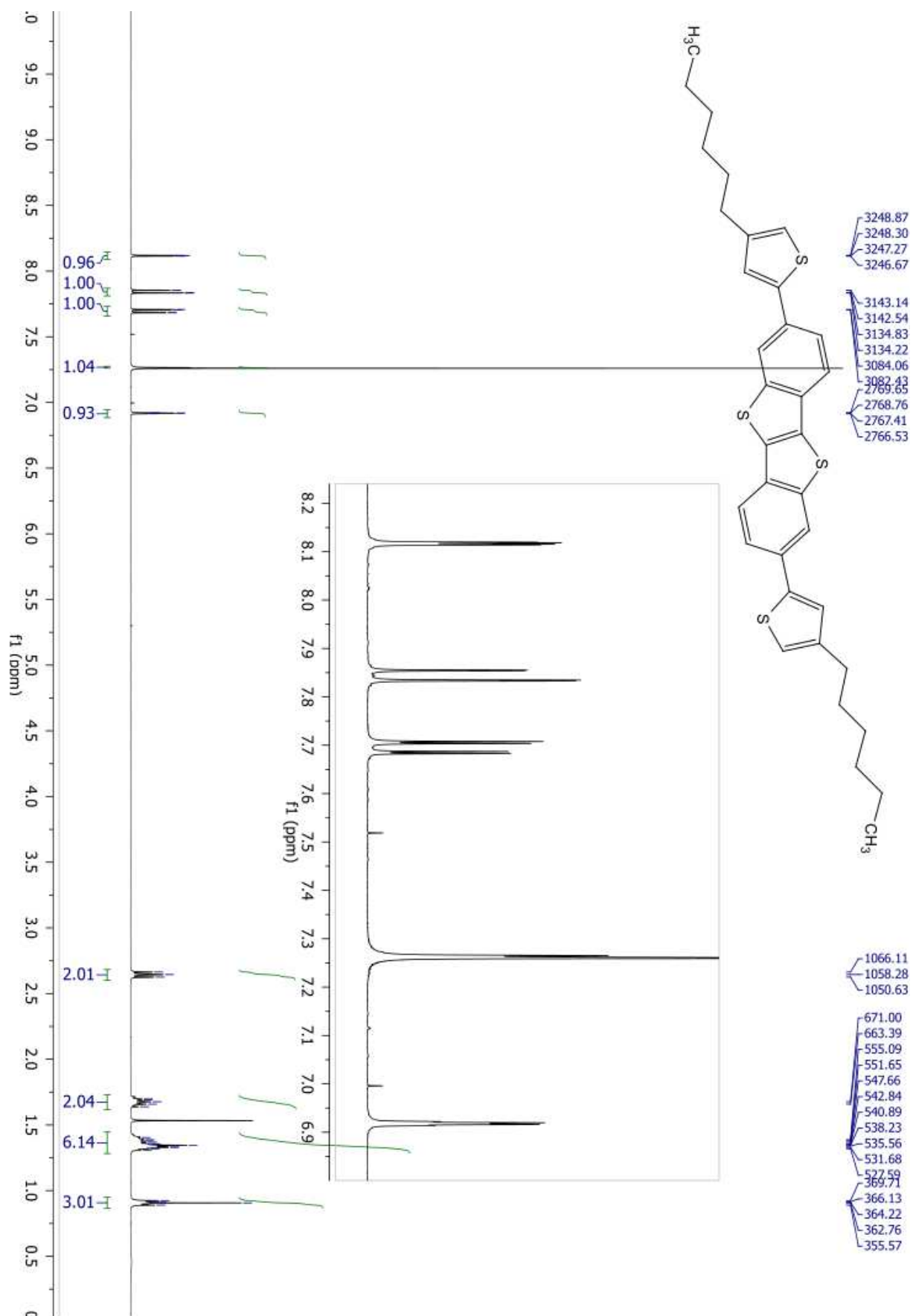
3.5.4.7 Synthesis of 2,7-di-(4-hexyl-2-thienyl)-[1]benzothieno[3,2-b][1]benzothiophene (36)

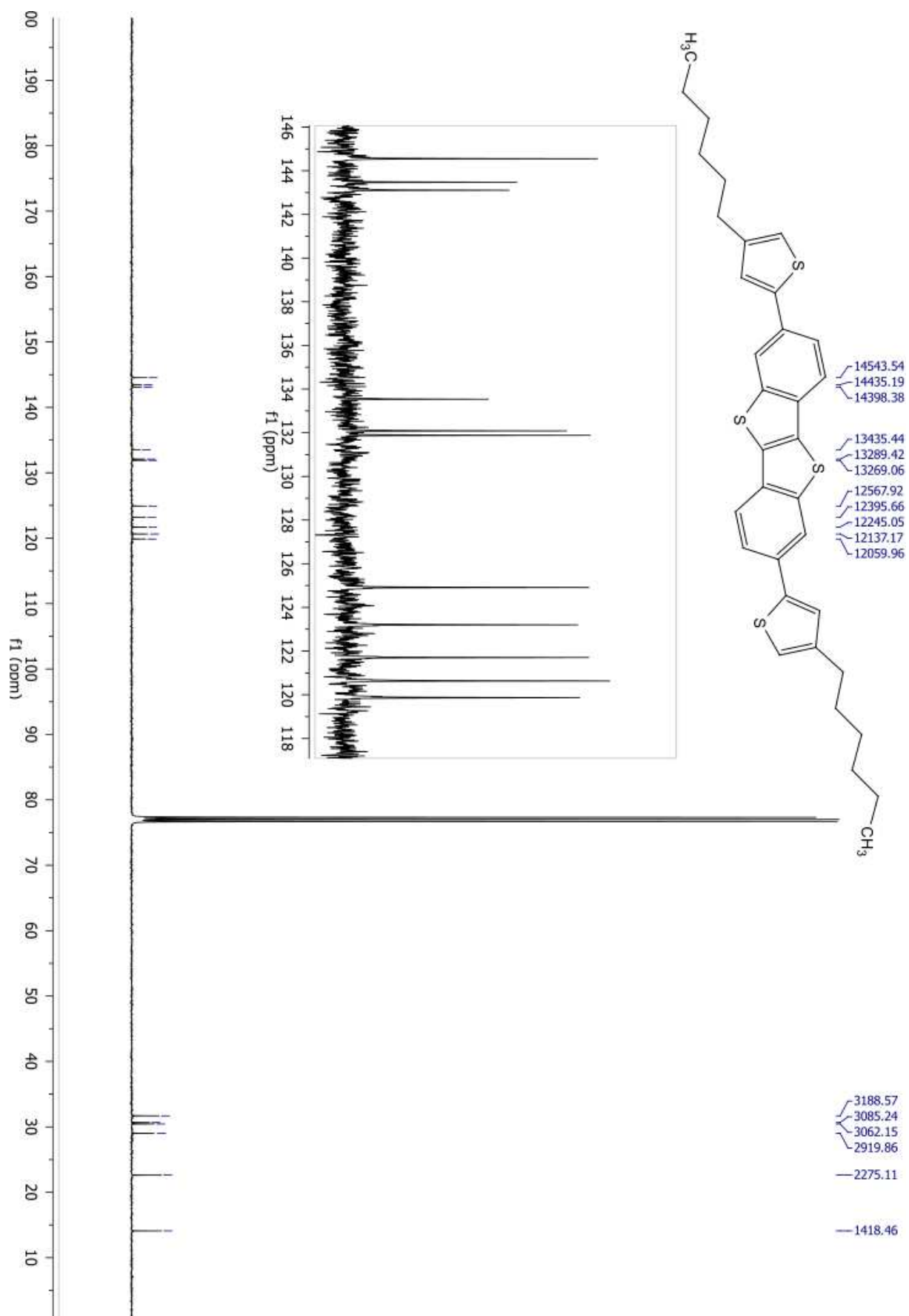


2,7-Dibromo-benzo[b]benzo[4,5]thieno[2,3-d]thiophene (199 mg, 0.500 mmol), 4-Hexyl-2-thiopheneboronic acid pinacol ester (440 mg, 1.50 mmol) and Pd(dtbpf)Cl_2 (16.02 mg, 0.02 mmol) were weighed in the vessel, then Kolliphor 2%:Toluene (10:1) emulsion (1 mL) was added. The mixture is stirred, then triethylamine (307 mg, 3.03 mmol) was added. The mixture was stirred at 80°C for 12h. The suspension was diluted with methanol and filtered. The solid was washed with methanol and dichloromethane. The solid was purified with extractive crystallization in chloroform to afford 2,7-di-(4-hexyl-2-thienyl)-[1]benzothieno[3,2-b][1]benzothiophene as white crystallin solid (210 mg, 0.367 mmol, 75 % yield).

$^1\text{H NMR}$ (400 MHz, CDCl_3) δ 8.12 (dd, $J = 1.6, 0.6$ Hz, 1H), 7.84 (dd, $J = 8.3, 0.6$ Hz, 1H), 7.70 (dd, $J = 8.3, 1.6$ Hz, 1H), 7.26 (d, $J = 1.5$ Hz, 1H), 6.92 (dd, $J = 2.2, 0.9$ Hz, 1H), 2.68 – 2.60 (m, 2H), 1.73 – 1.62 (m, 2H), 1.45 – 1.28 (m, 6H), 0.95 – 0.86 (m, 3H). $^{13}\text{C NMR}$ (101 MHz, CDCl_3) δ 144.55, 143.47, 143.11, 133.54, 132.08, 131.88, 124.91, 123.20, 121.70, 120.63, 119.87, 31.69, 30.66, 30.44, 29.02, 22.61, 14.10.

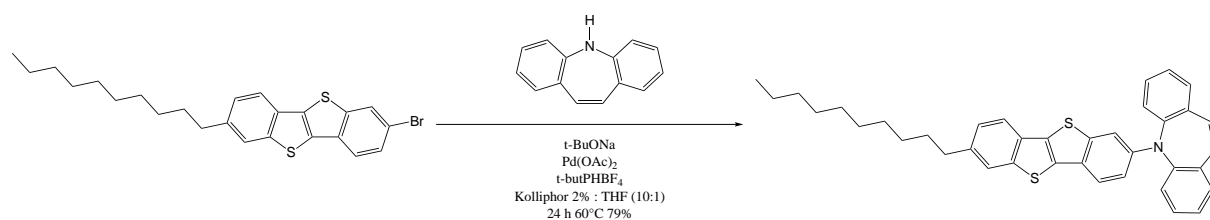
3.5. SYNTHESIS OF 2,(7)-ARYL-[1]BENZOTHIENO[3,2-B][1]BENZOTHIOPHENE (BTBT) DERIVATIVES IN MICELLAR CONDITION





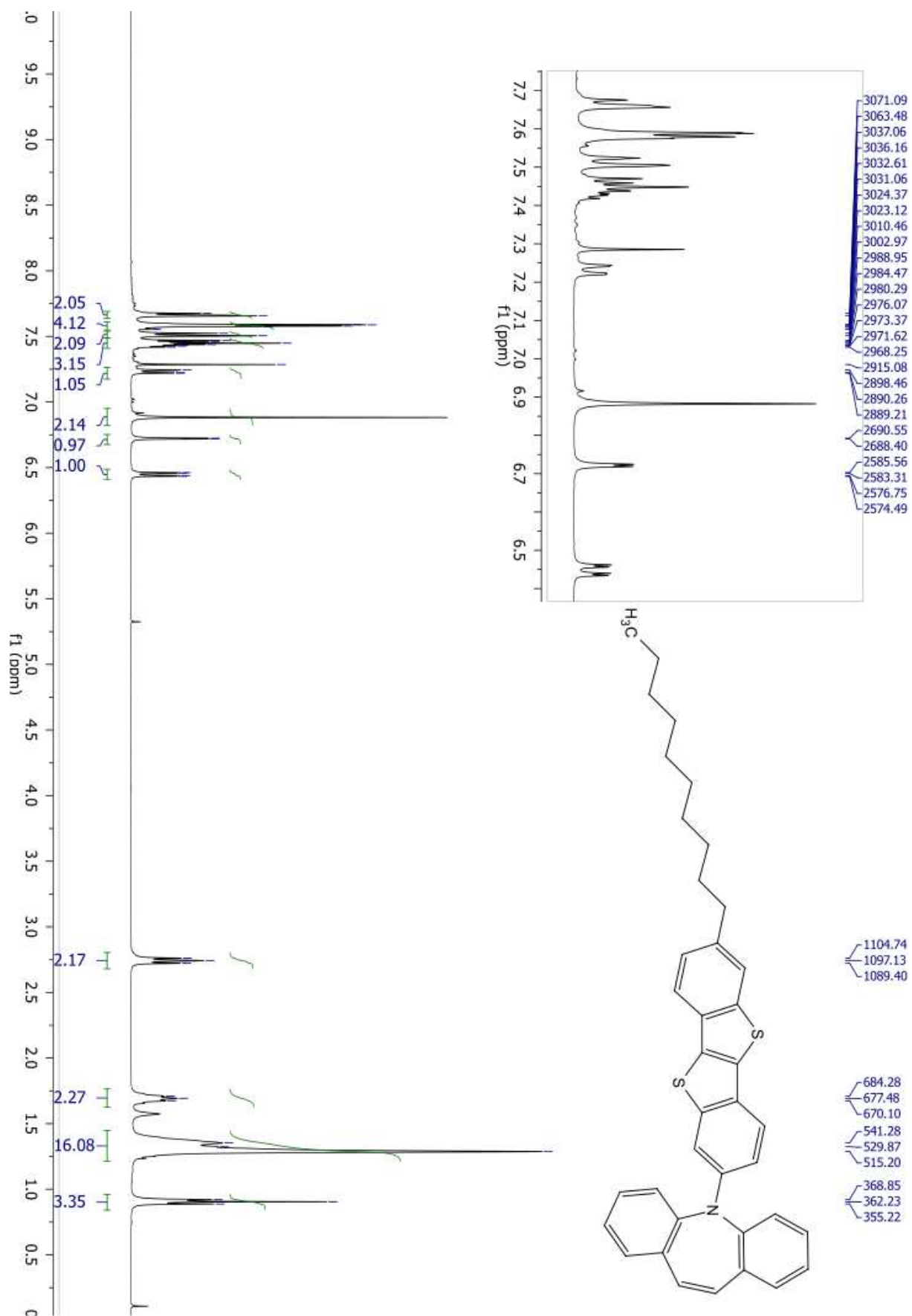
3.5. SYNTHESIS OF 2(,7)-ARYL-[1]BENZOTHIENO[3,2-B][1]BENZOTHIOPHENE (BTBT) DERIVATIVES IN MICELLAR CONDITION

3.5.4.8 Synthesis of 5-(7-decylbenzo[b]benzo[4,5]thieno[2,3-d]thiophen-2-yl)-5H-dibenzo[b,f]azepine (37)

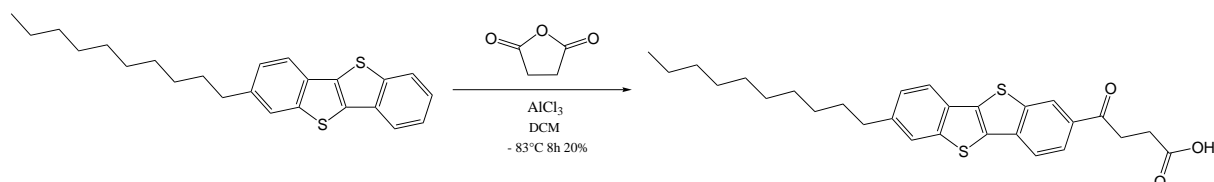


7-Decyl-2-bromo-benzo[b]benzo[4,5]thieno[2,3-d]thiophene (230 mg, 0.500 mmol) and dibenzoazepine (98 mg, 0.51 mmol) were weighted in the vessel, then 1 mL of Kolliphor 10%: THF solution in water is added. The mixture is stirred, then t-BuONa (73 mg, 0.75 mmol) was added. The mixture is allowed to homogenize for 5 minutes before addition of Pd(OAc)₂ (3.36 mg, 0.0150 mmol) and tBuPHBF₄(8.81 mg, 0.0304 mmol). After 24 h, the reaction is diluted with 10 mL of methanol and filtered. Solid was dissolved in dichloromethane and filtered through a pad of silica. dichloromethane was removed under reduce pressure. Crude product was crystallized in isopropanol to afford 5-(7-decylbenzo[b]benzo[4,5]thieno[2,3-d]thiophen-2-yl)-5H-dibenzo[b,f]azepine(226 mg, 0.395 mmol, 79%).

¹H NMR (400 MHz, CDCl₃) δ 7.67 (d, J = 7.6 Hz, 2H), 7.61 – 7.55 (m, 4H), 7.51 (d, J = 7.5 Hz, 2H), 7.49 – 7.41 (m, 3H), 7.26 – 7.17 (m, 1H), 6.90 (d, J = 13.5 Hz, 2H), 6.72 (d, J = 2.2 Hz, 1H), 6.45 (dd, J = 8.8, 2.3 Hz, 1H), 2.80 – 2.68 (m, 2H), 1.68 (dd, J = 14.7, 7.3 Hz, 2H), 1.45 – 1.21 (m, 15H), 0.90 (t, J = 6.8 Hz, 3H).¹³C NMR (101 MHz, CDCl₃) δ 147.11, 143.89, 142.95, 141.86, 139.22, 136.44, 132.65, 131.45, 130.61, 130.58, 130.45, 129.98, 127.39, 125.65, 125.30, 123.21, 121.12, 120.52, 111.25, 105.82, 36.09, 31.91, 31.77, 29.63, 29.61, 29.54, 29.34, 22.70, 14.13.



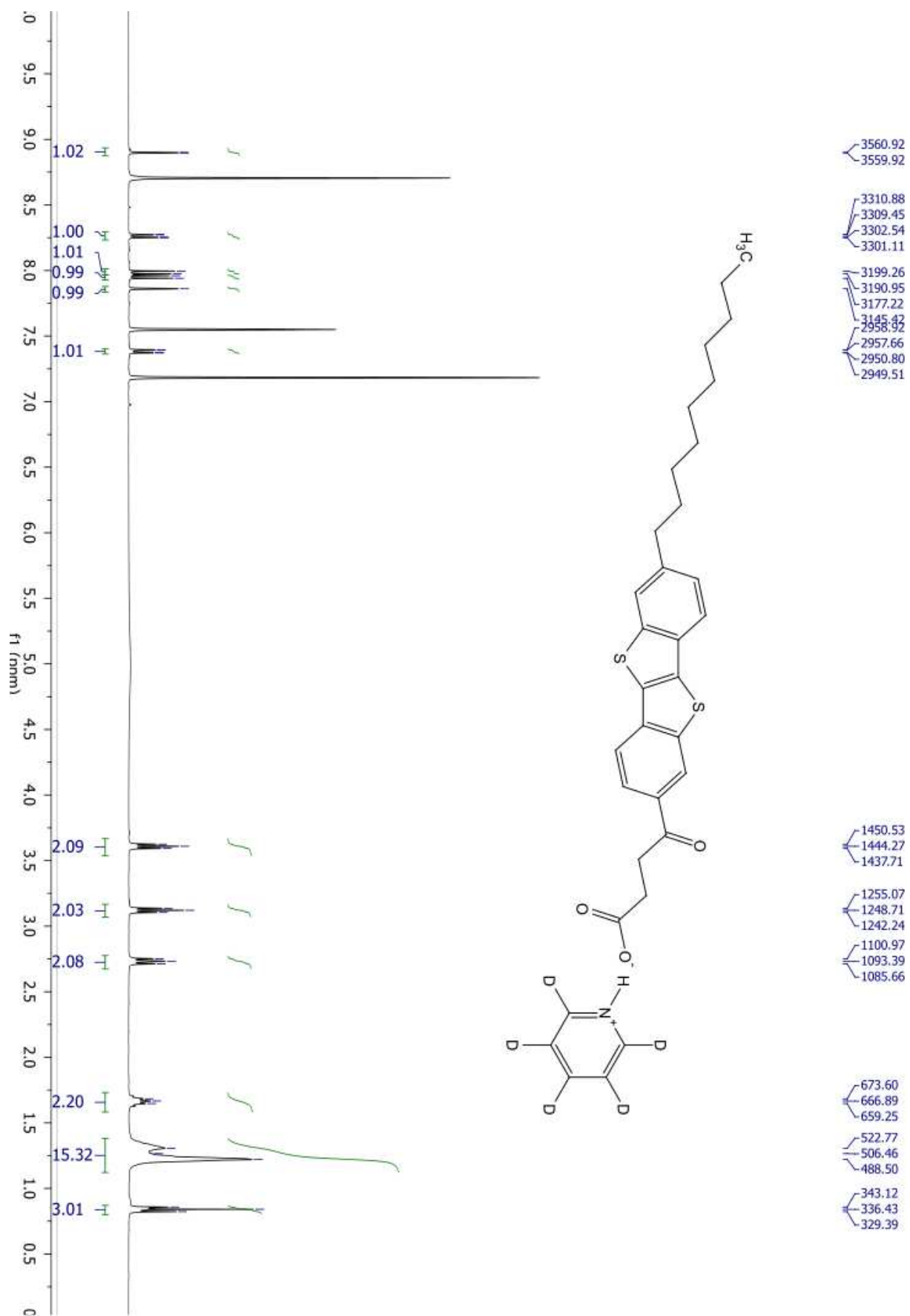
3.5.4.9 Synthesis of 4-(7-decylbenzo[b]benzo[4,5]thieno[2,3-d]thiophen-2-yl)-4-oxobutanoic acid (38)

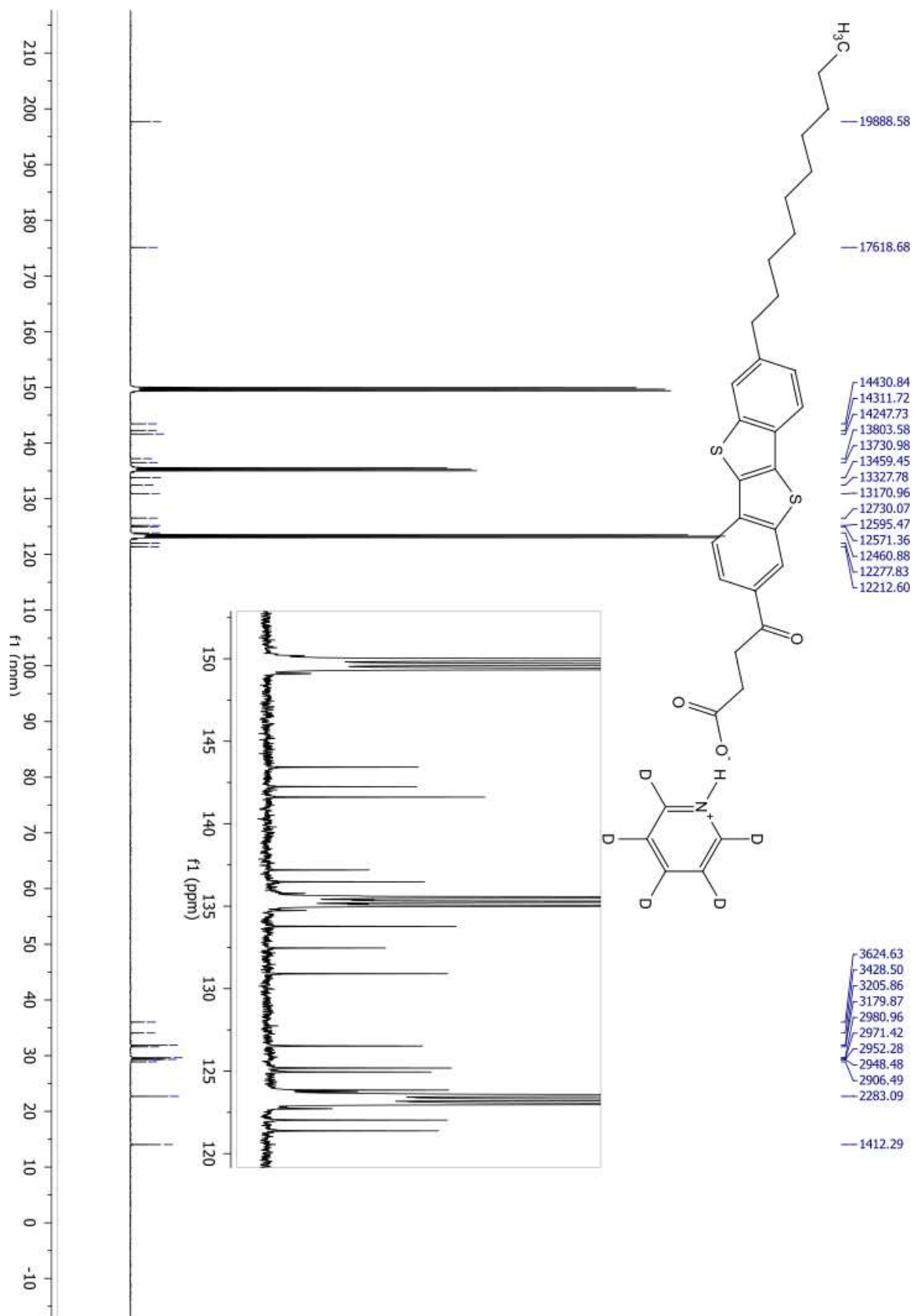


2-Octyl-[1]benzothieno[3,2-b][1]benzothiophene (1.004 g, 2.63 mmol) was dissolved in dry dichloromethane (50 mL), under nitrogen, followed by the addition of aluminum chloride (0.958 g, 65.68 mmol) at -10 °C. The solution was cooled to -83 °C and succinic anhydride (0.267 g, 2.63 mmol) was added dropwise, and the mixture was stirred for 1 h at the same temperature. The reaction mixture was allowed to stand without cooling and stirred for 8 h. The reaction mixture was cooled to 0 °C, quenched with ice water (25 mL), and diluted with methanol (75 mL) to give two separate phases. The organic phase was washed with water (2 x 50 mL) and brine (1 x 50 mL). To the aqueous phase was added hydrochloric acid solution (25 mL, 1M) and was extracted with dichloromethane (3 x 25 mL). All organic phase were mixed together. Dichloromethane was removed to give crude product. Crude product was purified with crystallization in toluene to give 4-(7-decylbenzo[b]benzo[4,5]thieno[2,3-d]thiophen-2-yl)-4-oxobutanoic acid (0.250 g, 0.52 mmol, 20%) as yellow solid.

¹H NMR (400 MHz, Pyr) δ 8.90 (d, J = 1.0 Hz, 1H), 8.26 (dd, J = 8.3, 1.4 Hz, 1H), 7.99 (d, J = 8.3 Hz, 1H), 7.95 (d, J = 8.1 Hz, 1H), 7.86 (s, 1H), 7.38 (dd, J = 8.1, 1.3 Hz, 1H), 3.61 (t, J = 6.4 Hz, 2H), 3.12 (t, J = 6.4 Hz, 2H), 2.78 – 2.67 (m, 2H), 1.73 – 1.58 (m, 2H), 1.38 – 1.12 (m, 15H), 0.84 (t, J = 6.9 Hz, 3H). ¹³C NMR (101 MHz, Pyr) δ 197.67, 175.11, 143.43, 142.25, 141.61, 137.20, 136.47, 133.77, 132.47, 130.91, 126.53, 125.19, 124.95, 123.85, 122.03, 121.38, 36.03, 34.08, 31.86, 31.61, 29.63, 29.53, 29.34, 29.31, 28.89, 22.69, 14.04.

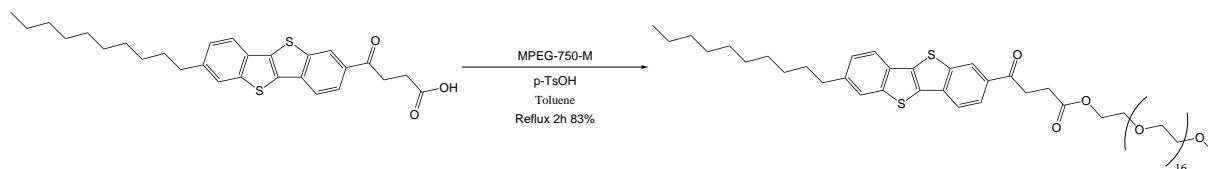
3.5. SYNTHESIS OF 2(,7)-ARYL-[1]BENZOTHIENO[3,2-B][1]BENZOTHIOPHENE (BTBT) DERIVATIVES IN MICELLAR CONDITION





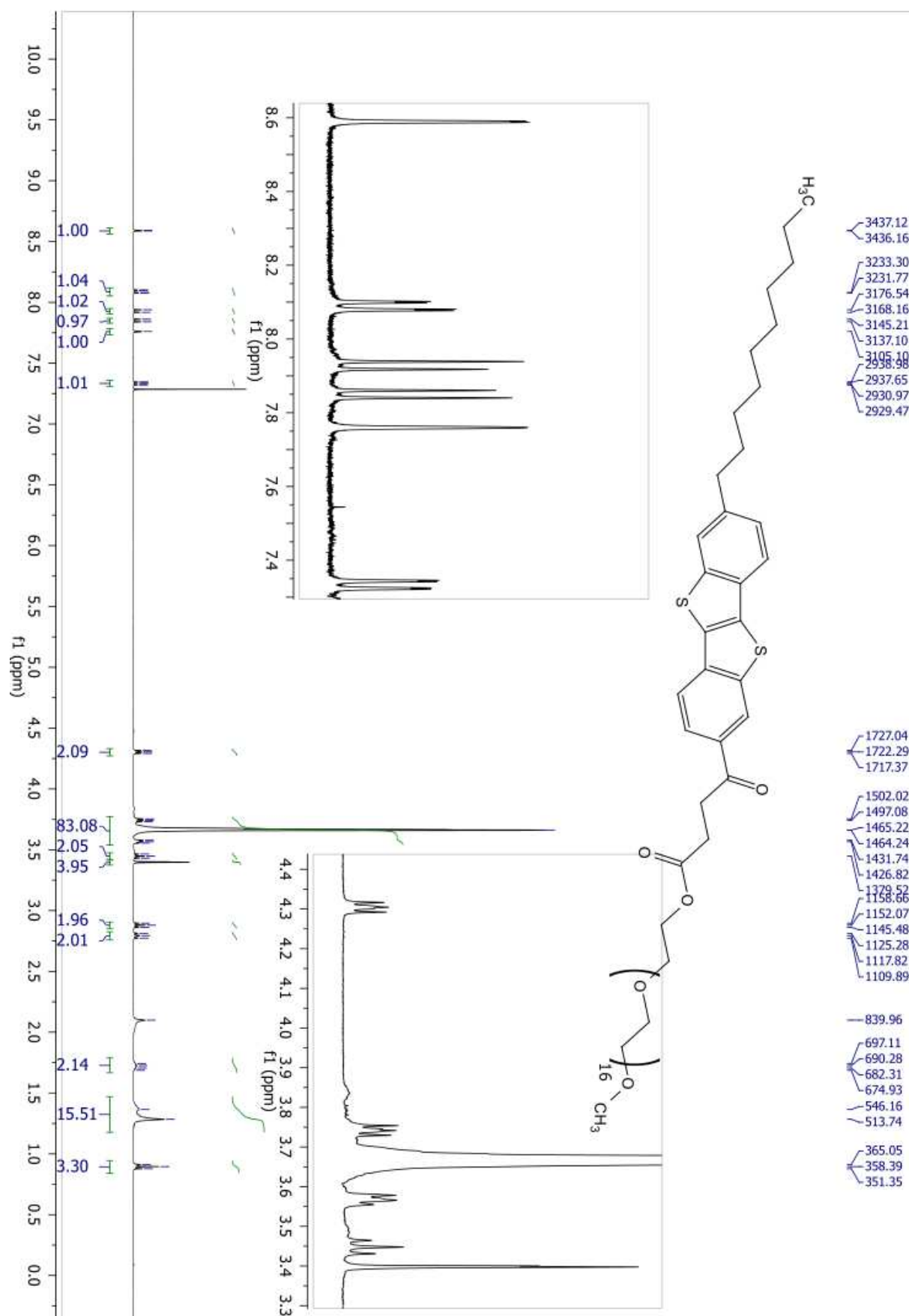
3.5. SYNTHESIS OF 2(,7)-ARYL-[1]BENZOTHIENO[3,2-B][1]BENZOTHIOPHENE
(BTBT) DERIVATIVES IN MICELLAR CONDITION

3.5.4.10 Synthesis of Pi-BTBT-750M (39)

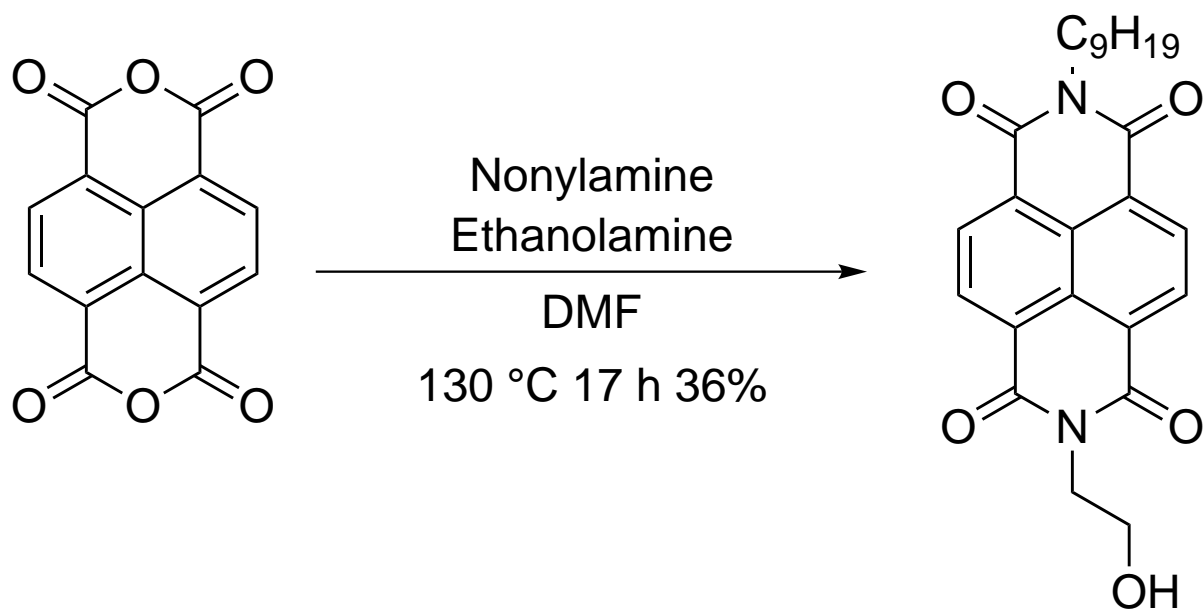


4-(7-Decylbenzo[b]benzo[4,5]thieno[2,3-d]thiophen-2-yl)-4-oxobutanoic acid (0.200 g, 0.42 mmol), MPEG-750-M (0.474 g, 0.63 mmol), and p-TsOH (50 mg, 0.29 mmol), were added into a 25 mL round-bottom flask. Toluene (10 mL) was added via syringe, and then the mixture was refluxed using a Dean-Stark trap for 2h. After cooling to rt, the mixture was poured into saturated aqueous NaHCO₃ and extracted with DCM. The combined organic extracts were washed with saturated aqueous NaHCO₃ (3 × 50 mL), brine (2 × 80 mL), dried over anhydrous magnesium sulfate and concentrated under reduced pressure to afford a pale-yellow, viscous liquid. The oil was poured on top of a silica gel bed, and then first eluted with 50% v/v EtOAc/hexane to remove an impurity, followed by 10% MeOH/DCM to obtain the product. Concentration under vacuum followed by storage under high vacuum overnight afforded 2,5,8,11,14,17,20,23,26,29,32,35,38,41,44,47,50-heptadecaaxadopentacontan-52-yl 4-(7-decylbenzo[b]benzo[4,5]thieno[2,3-d]thiophen-2-yl)-4-oxobutanoate as an off-yellow waxy solid (0.430g, 3.50 mmol, 83%)

¹H NMR (400 MHz, CDCl₃) δ 8.59 (d, J = 1.0 Hz, 1H), 8.09 (dd, J = 8.4, 1.5 Hz, 1H), 7.93 (d, J = 8.4 Hz, 1H), 7.85 (d, J = 8.1 Hz, 1H), 7.76 (s, 1H), 7.33 (dd, J = 8.1, 1.4 Hz, 1H), 4.33 – 4.27 (m, 2H), 3.77 – 3.54 (m, 81H), 3.45 (t, J = 6.7 Hz, 2H), 3.40 (d, J = 1.0 Hz, 4H), 2.88 (t, J = 6.6 Hz, 2H), 2.83 – 2.76 (m, 2H), 2.10 (broad, 5H), 1.71 (dd, J = 15.1, 7.1 Hz, 2H), 1.32 (d, J = 32.4 Hz, 15H), 0.90 (t, J = 6.9 Hz, 3H). ¹³C NMR (101 MHz, CDCl₃) δ 197.06, 172.91, 143.23, 142.06, 141.49, 137.22, 136.72, 132.84, 132.17, 130.67, 126.24, 124.61, 123.46, 121.79, 121.24, 71.95, 70.58, 70.53, 69.13, 63.89, 59.04, 36.19, 33.50, 31.90, 31.62, 29.61, 29.58, 29.51, 29.33, 29.30, 28.35, 22.68, 14.12.



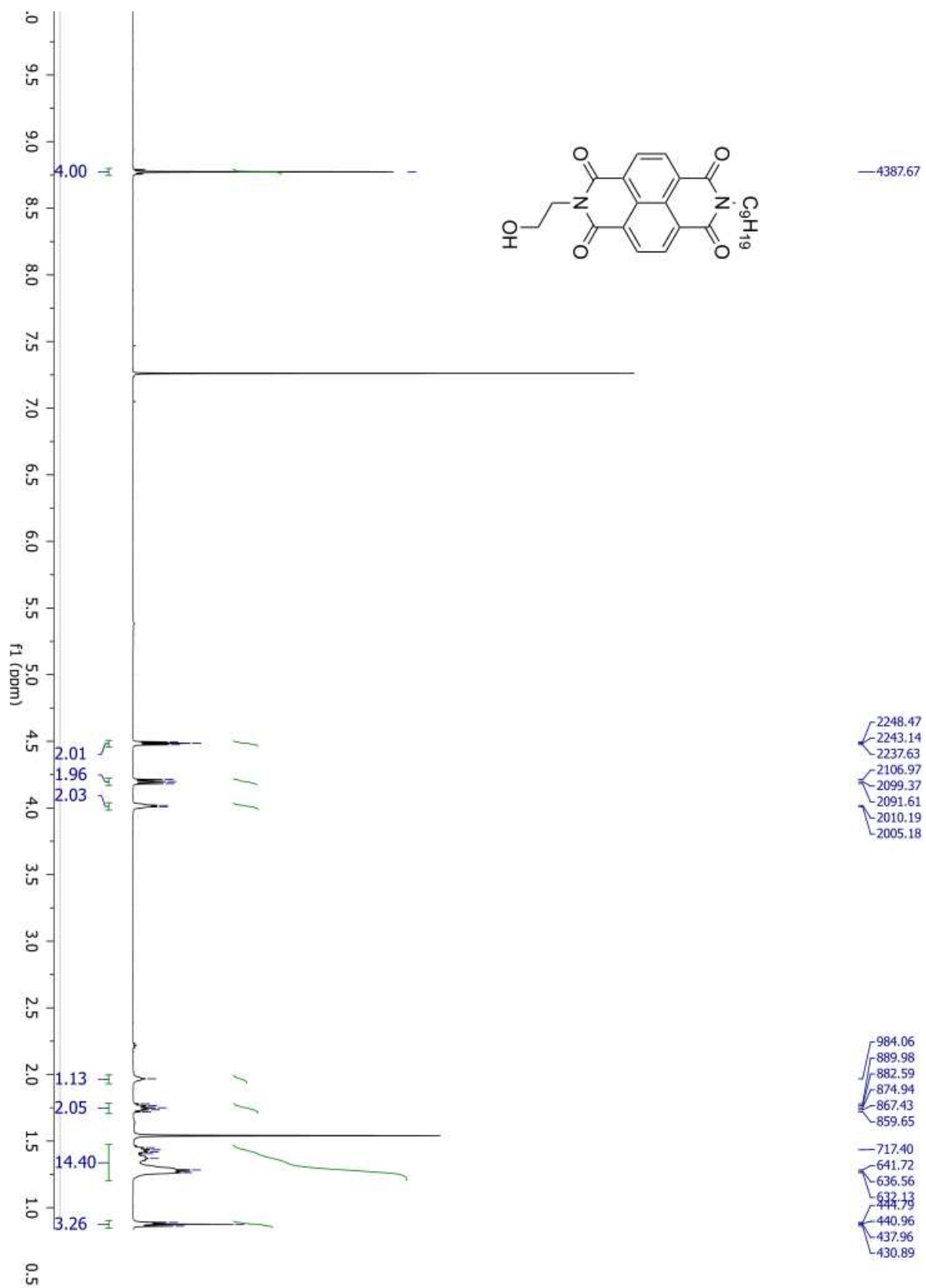
3.5.4.11 Synthesis of 2-(2-hydroxyethyl)-7-nonylbenzo[lmn][3,8]phenanthroline-1,3,6,8(2H,7H)-tetraone (40)

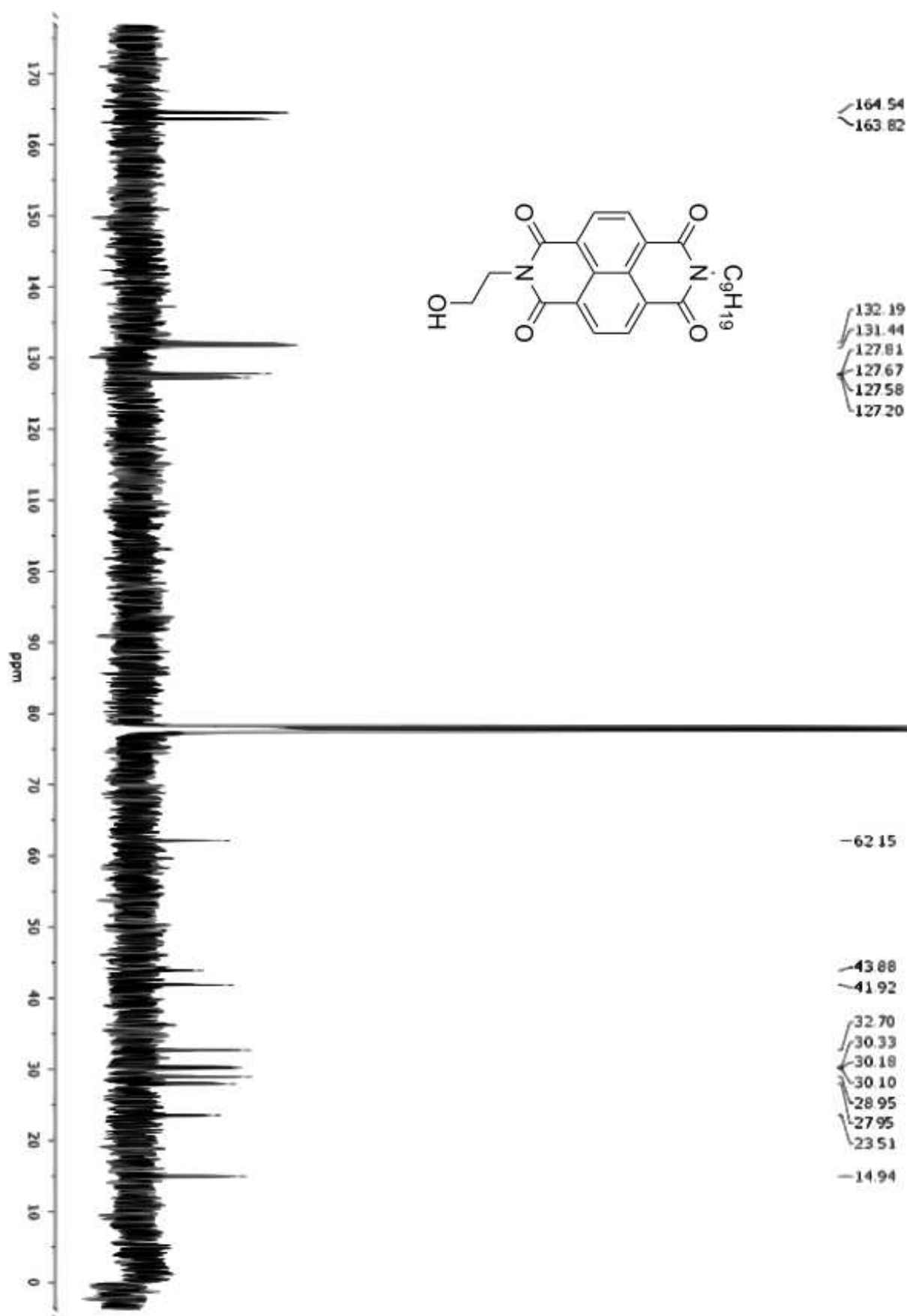


In a two neck flask, under N_2 , a solution of 1,4,5,8-tetracarboxylic dianhydride (10.000 g, 37.288 mmol) in 100 mL of dry DMF was prepared, stirring the mixture at 130°C for 30 minutes. A solution of nonylamine (5.329 g, 37.20 mmol) and ethanolamine (2.273 g, 37.21 mmol) in 15 mL of dry DMF was added slowly by syringe. The reaction mixture was stirred for 15 h at 130°C. The reaction was cooled down to room temperature and 200 mL of water were added to obtain a precipitate. The precipitate was recovered by filtration and washed with a mixture of water and ethanol (1:1). The solid was dried under vacuum at 105°C for 12 h. The solid was recrystallized in chloroform with extractive crystallization to afford 2-(2-hydroxyethyl)-7-nonylbenzo[lmn][3,8]phenanthroline-1,3,6,8(2H,7H)-tetraone as crystalline pink solid (5.898 g, 13.51 mmol, 36%).

1H NMR (500 MHz, $CDCl_3$) δ [ppm]: 8.77 (s, 4H), 4.48 (t, $J = 5.4$ Hz, 2H), 4.22 – 4.18 (m, 2H), 4.01 (s, 2H), 1.97 (s, 1H), 1.78 – 1.72 (m, 2H), 1.57 – 1.23 (m, 14H), 0.88 (dd, $J = 8.5, 5.4$ Hz, 3H). ^{13}C NMR (126 MHz, $CDCl_3$) δ [ppm]: 164.54, 163.82, 132.19, 131.44, 127.81, 127.67, 127.58, 127.20, 62.15, 43.88, 41.92, 32.70, 30.33, 30.18, 30.10, 28.95, 27.95, 23.51, 14.94.

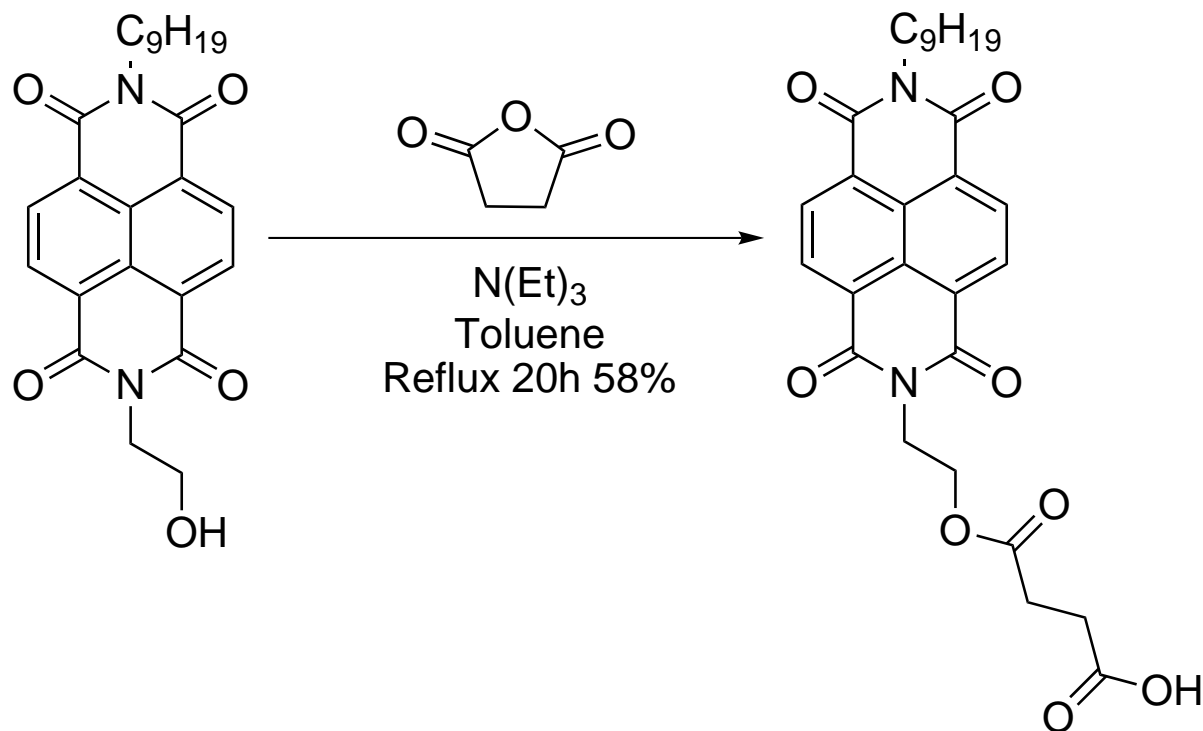
3.5. SYNTHESIS OF 2(,7)-ARYL-[1]BENZOTHIENO[3,2-B][1]BENZOTHIOPHENE (BTBT) DERIVATIVES IN MICELLAR CONDITION





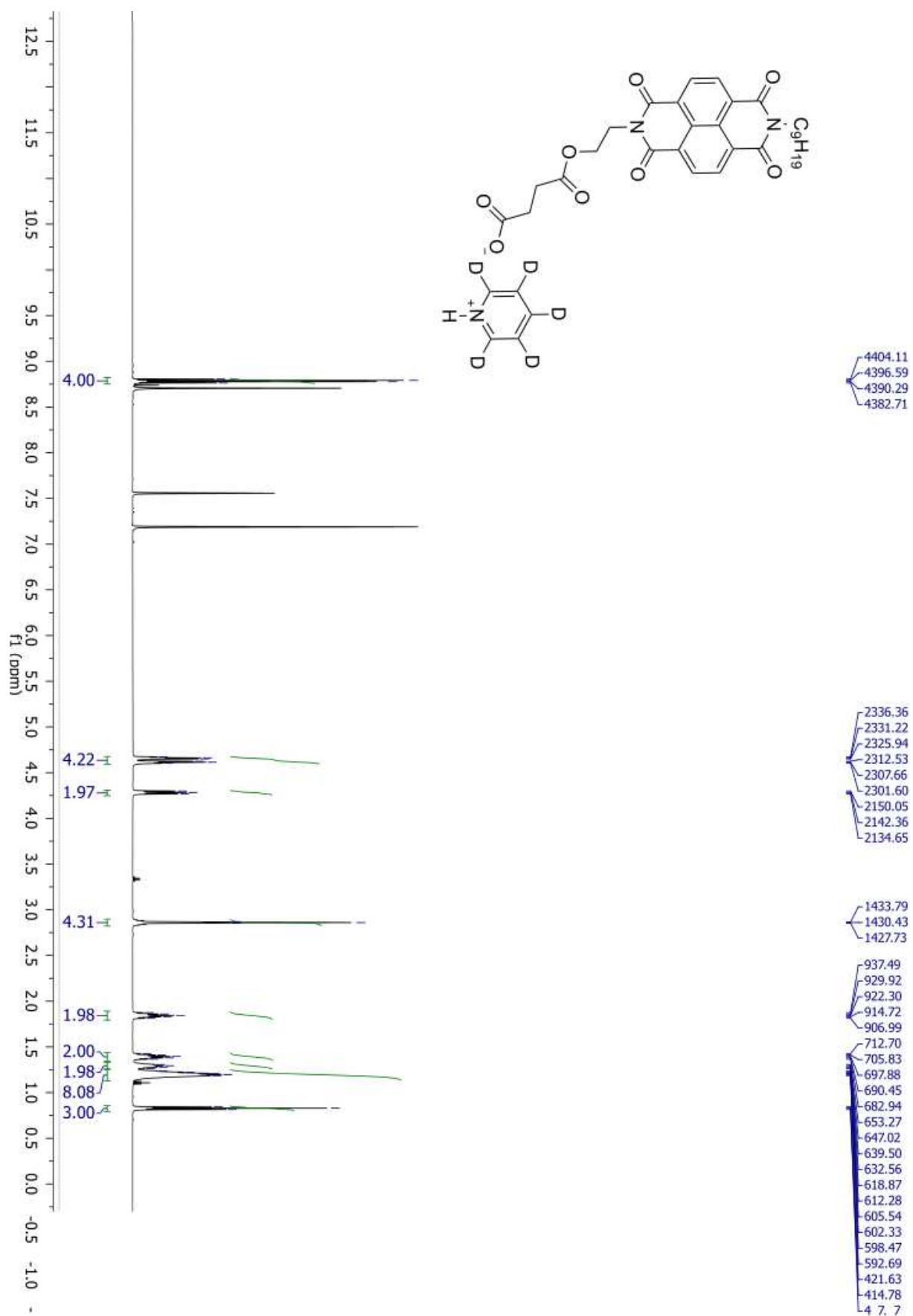
3.5. SYNTHESIS OF 2(,7)-ARYL-[1]BENZOTHIENO[3,2-B][1]BENZOTHIOPHENE
(BTBT) DERIVATIVES IN MICELLAR CONDITION

3.5.4.12 Synthesis of 4-(2-(7-nonyl-1,3,6,8-tetraoxo-7,8-dihydrobenzo[lmn]-
[3,8]phenanthrolin-2(1H,3H,6H)-yl)ethoxy)-4-oxobutanoic acid (41)

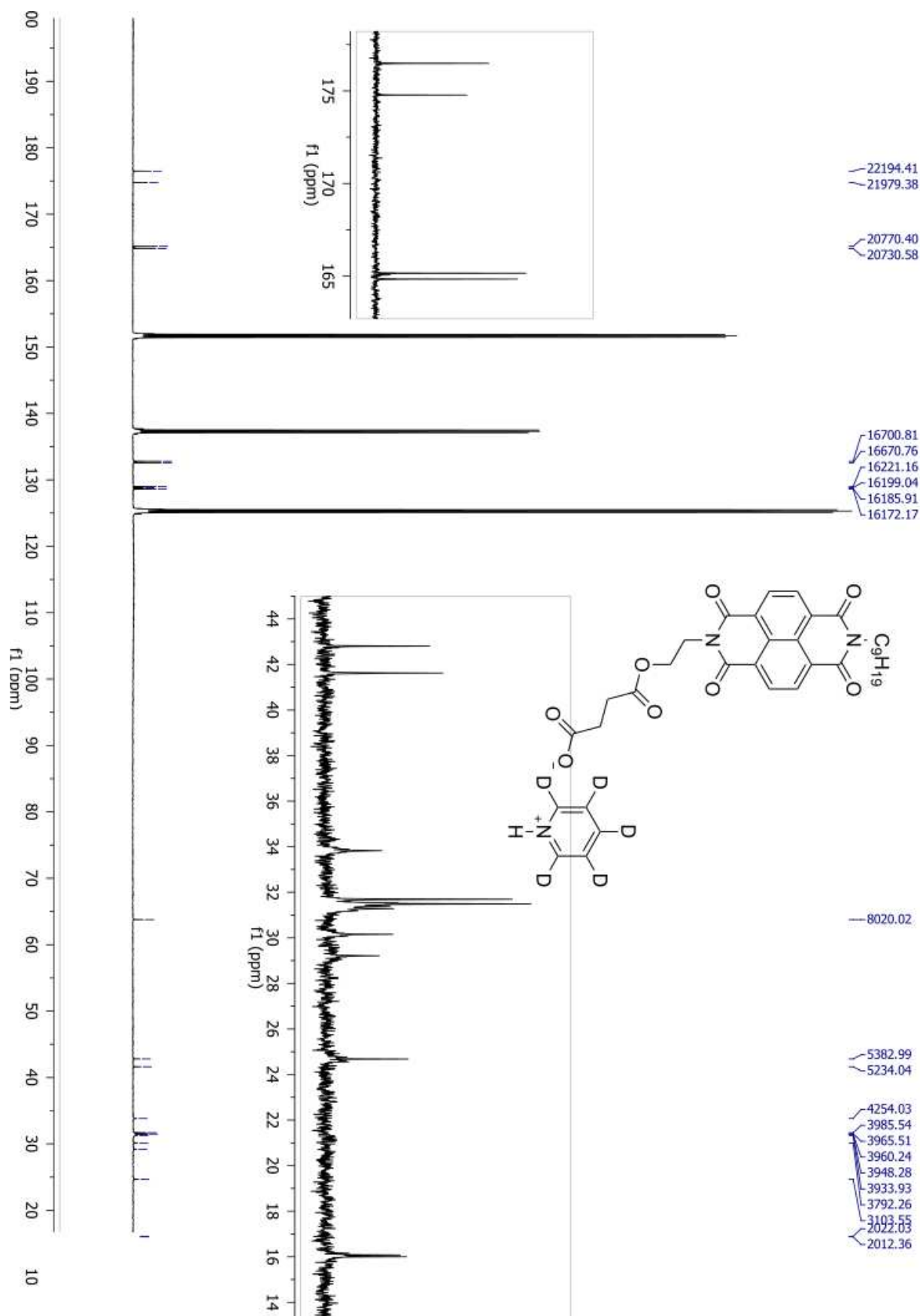


In a two neck flask, under N_2 , were added 2-(2-hydroxyethyl)-7-nonylbenzo[lmn][3,8]phenanthroline-1,3,6,8(2H,7H)-tetraone (3.509 g, 8.039 mmol) and succinic anhydride (1.215 g, 12.14 mmol). Dry dichloromethane (35 mL) and $N(Et)_3$ (0.203 g, 2.01 mmol) were added by syringe. The reaction mixture was stirred at reflux for 20 h. The reaction was let cooled down to room temperature. The solvents were evaporated under reduce pressure to afford crude product. The crude product was purified by crystallization in acetic acid and hot filtration in toluene in order to remove the insoluble impurities. Toluene was removed under reduce pressure to afford 4-(2-(7-nonyl-1,3,6,8-tetraoxo-7,8-dihydrobenzo[lmn][3,8]phenanthrolin-2(1H,3H,6H)-yl)ethoxy)-4-oxobutanoic acid as crystalline white solid (4.318 g, 8.047 mmol, 58%).

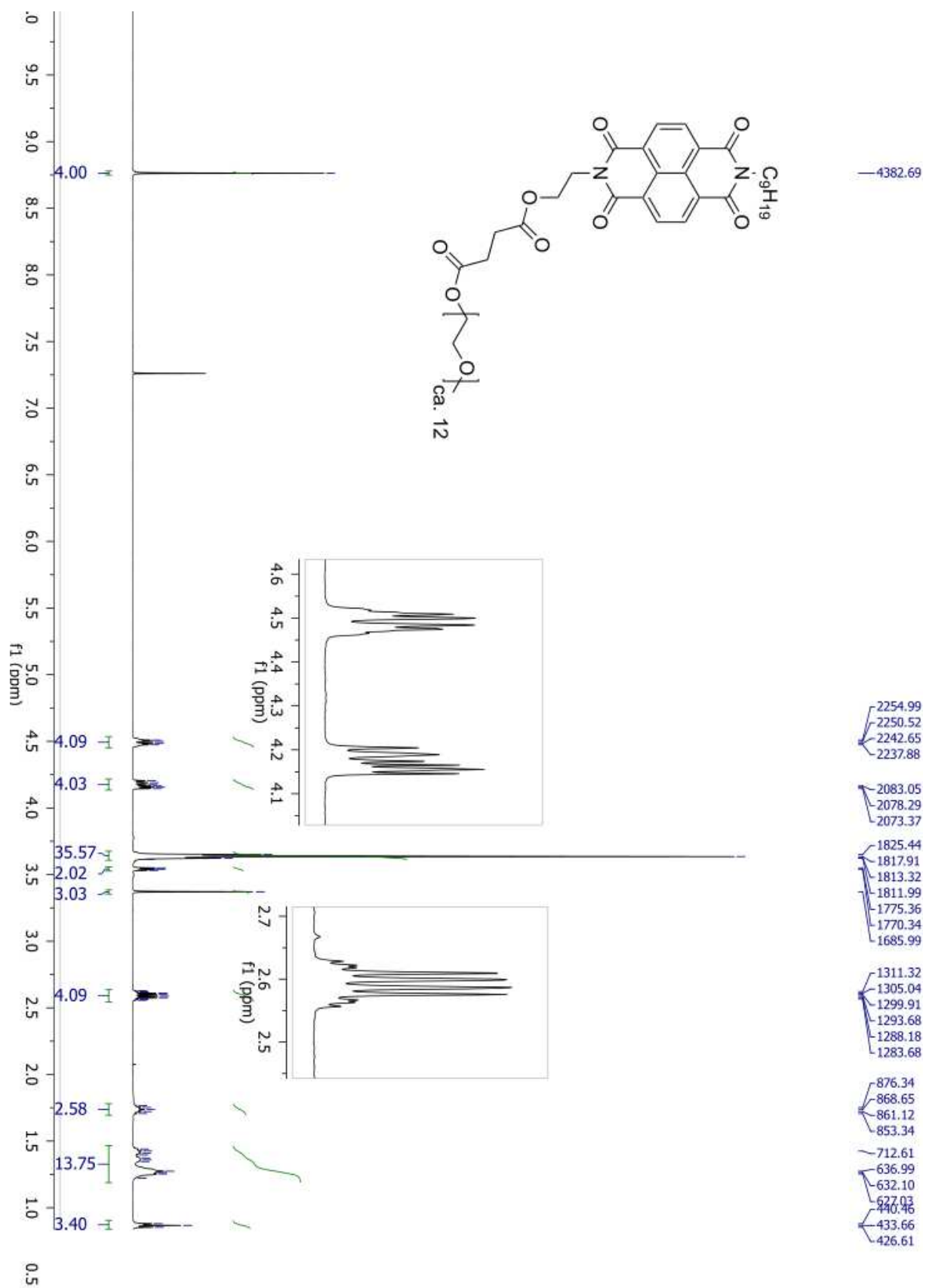
1H NMR (500 MHz, Pyr) δ 8.78 (q, $J = 7.5$ Hz, 4H), 4.64 (dt, $J = 24.3, 5.6$ Hz, 4H), 4.31 – 4.25 (m, 2H), 2.86 (t, $J = 3.0$ Hz, 4H), 1.89 – 1.79 (m, 2H), 1.44 – 1.35 (m, 2H), 1.29 (dd, $J = 14.1, 6.6$ Hz, 2H), 1.25 – 1.13 (m, 8H), 0.83 (t, $J = 7.0$ Hz, 3H). ^{13}C NMR (126 MHz, Pyr) δ 176.49, 174.78, 165.16, 164.85, 132.80, 132.56, 128.99, 128.81, 128.71, 128.60, 63.77, 42.80, 41.62, 33.83, 31.69, 31.53, 31.49, 31.40, 31.28, 30.16, 29.21, 24.68, 16.08, 16.00.

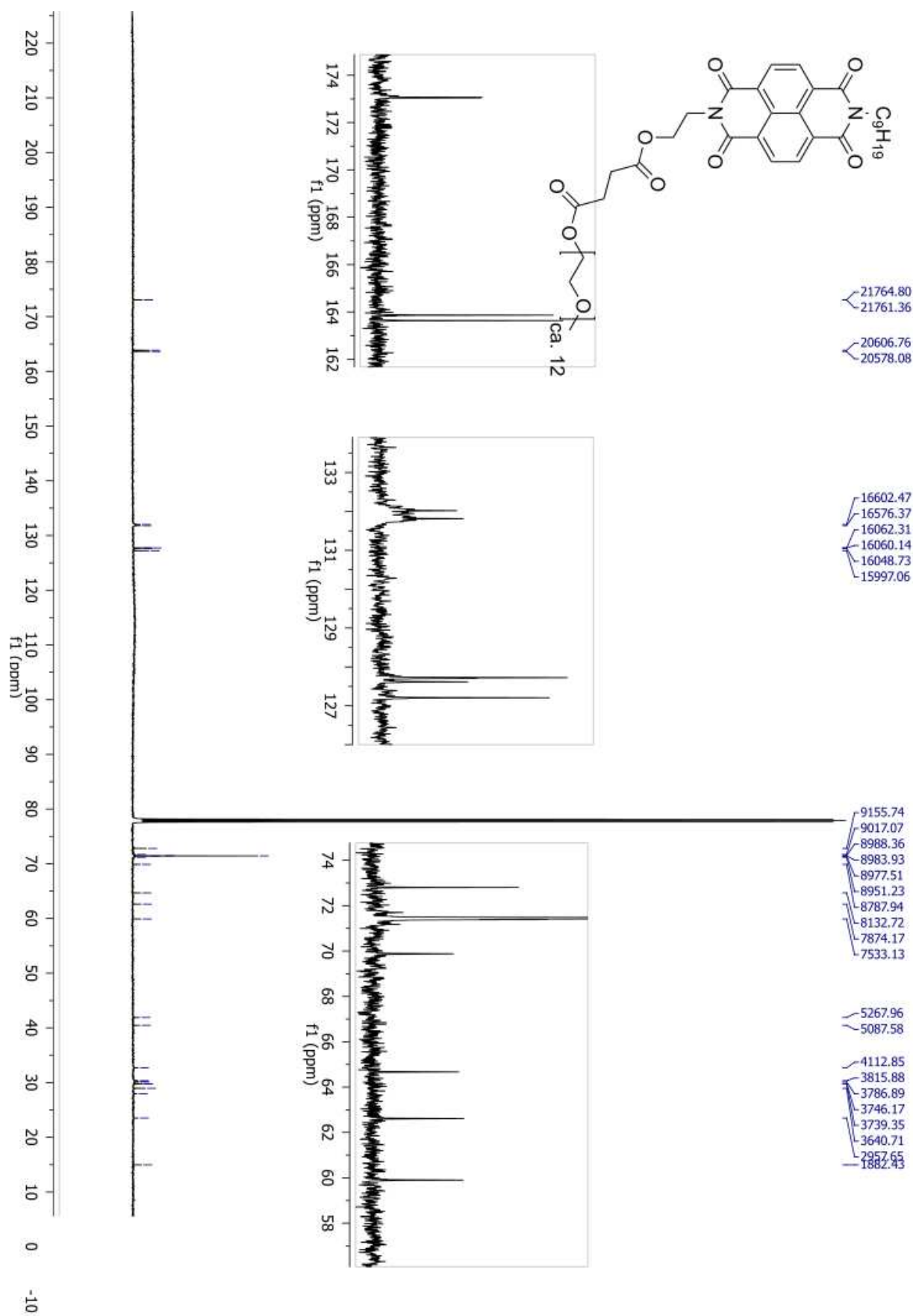


3.5. SYNTHESIS OF 2,(7)-ARYL-[1]BENZOTHIENO[3,2-B][1]BENZOTHIOPHENE (BTBT) DERIVATIVES IN MICELLAR CONDITION



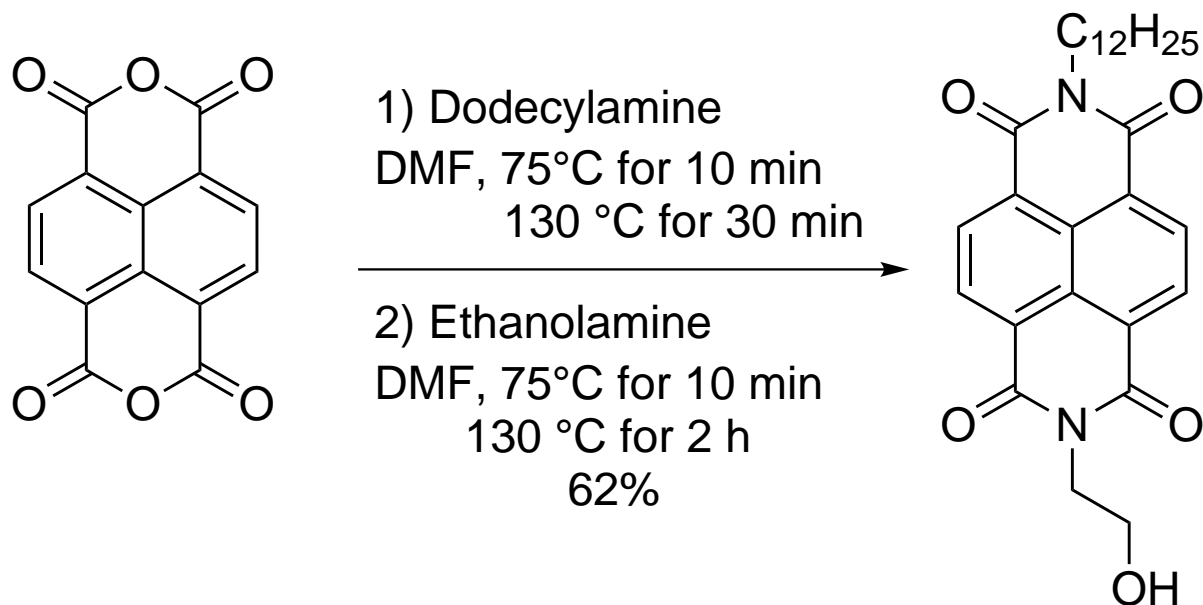
3.5. SYNTHESIS OF 2(,7)-ARYL-[1]BENZOTHIENO[3,2-B][1]BENZOTHIOPHENE (BTBT) DERIVATIVES IN MICELLAR CONDITION





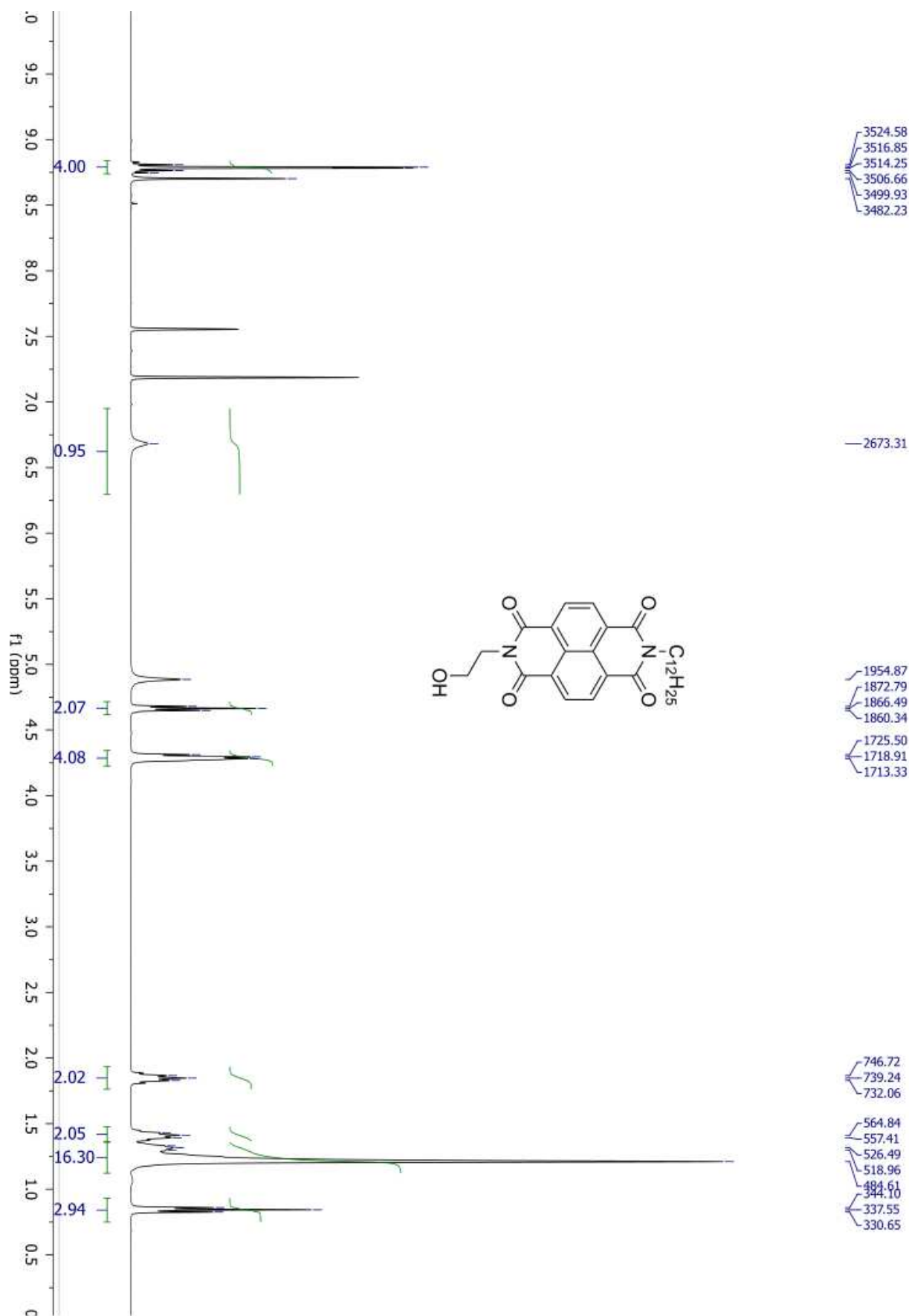
3.5. SYNTHESIS OF 2(,7)-ARYL-[1]BENZOTHIENO[3,2-B][1]BENZOTHIOPHENE
(BTBT) DERIVATIVES IN MICELLAR CONDITION

3.5.4.14 Synthesis of 2-dodecyl-7-(2-hydroxyethyl)benzo[*lmn*][3,8]phenanthroline-1,3,6,8(2H,7H)-tetraone (43)

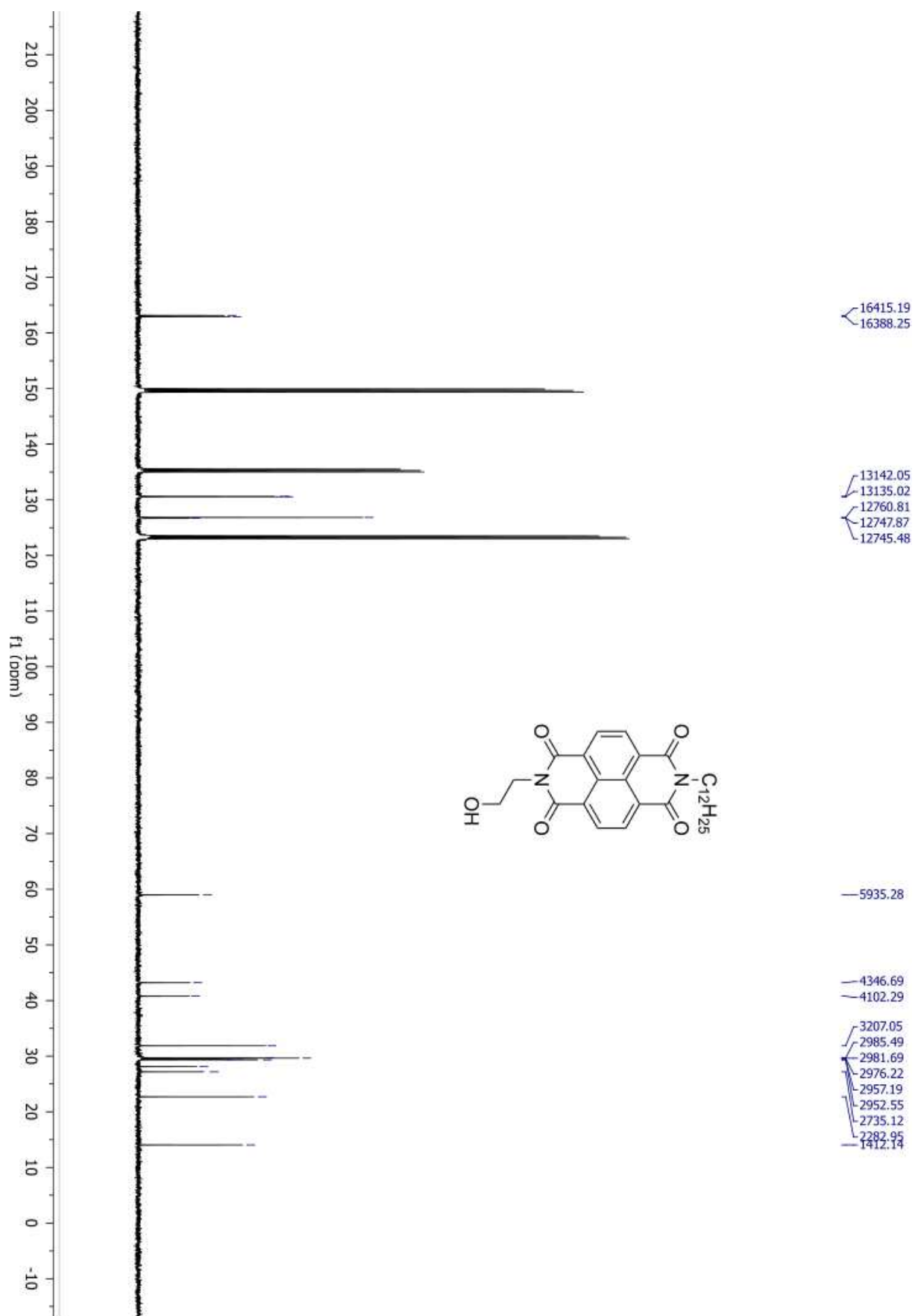


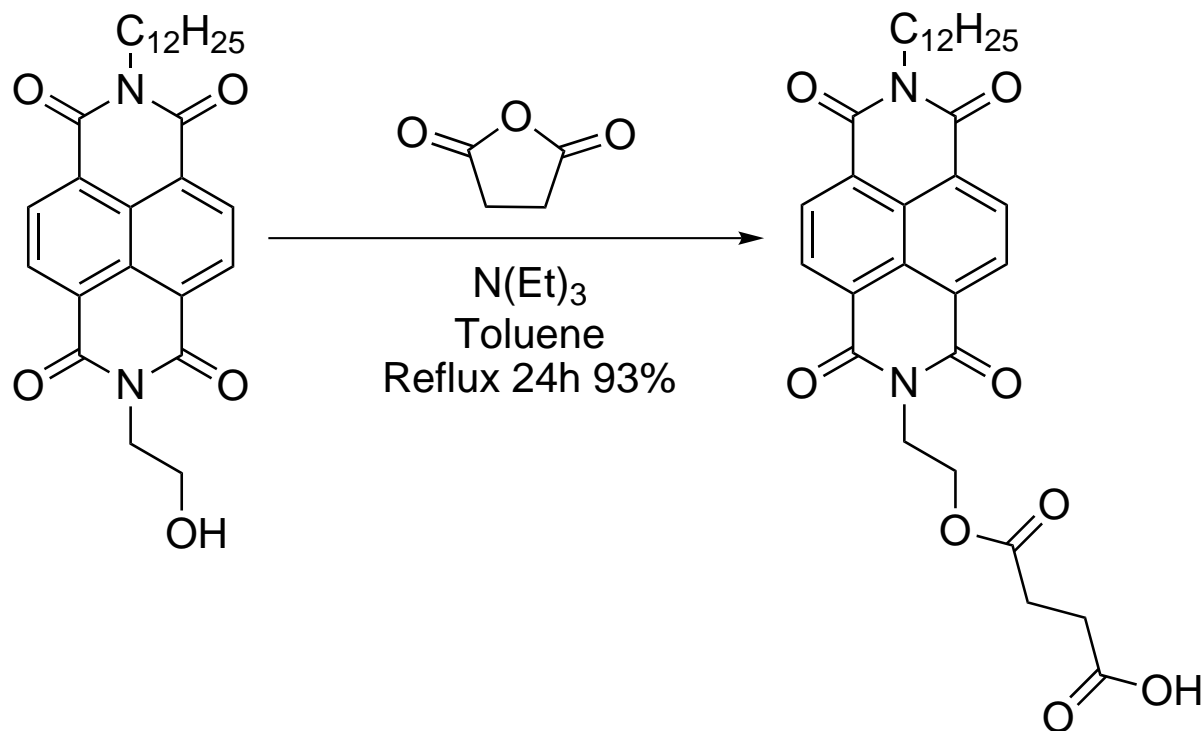
In a two neck flask, under N₂, a solution of 1,4,5,8-tetracarboxylic dianhydride (30.000 g, 111.80 mmol) and dodecylamine (20.730 g, 111.80 mmol) in 200 mL of dry DMF, stirring the mixture at 75°C for 10 minutes then the reaction mixture was stirred at 130°C for 30 minutes. The reaction was cooled down to 75°C and ethanolamine was added by syringe (6.832, 111.80 mmol). The reaction mixture was stirred at the same temperature for 10 minutes then at 130°C for 2 h. The reaction was cooled down and 500 mL of water were added in order to obtain a precipitate. The solid was recovered by filtration and washed with a mixture of ethanol and water (1:1). The solid was dried under vacuum at 105°C for 12 h. The solid was extracted with soxhlet apparatus with chloroform. The chloroform solution was cooled down to room temperature and the formation of a precipitate was observed. The precipitate was recovered by filtration and purified with crystallization in chloroform to afford 2-dodecyl-7-(2-hydroxyethyl)benzo[*lmn*][3,8]phenanthroline-1,3,6,8(2H,7H)-tetraone as pink solid (33.303 g, 69.32 mmol, 62%).

¹H NMR (Pyr-d₅, 400 MHz) 8.81-8.77 (m, 4H), 6.68 (br, 1H) 4.66 (t, J = 6.3, 2H), 4.31-4.28 (m, 4H), 1.88- 1.81 (m, 2H), 1.45-1.37 (m, 2H), 1.33-1.21 (m, 16H), 0.84 (t, J = 6.7 Hz, 3H). ¹³C NMR (Pyr-d₅, 100 MHz) 163.1, 162.9, 130.6, 130.5, 126.8, 126.7, 126.68, 59.00, 43.2, 40.8, 31.9, 29.8, 29.6, 29.6, 29.4, 29.4, 28.1, 27.2, 22.7, 14.0.



3.5. SYNTHESIS OF 2(,7)-ARYL-[1]BENZOTHIENO[3,2-B][1]BENZOTHIOPHENE (BTBT) DERIVATIVES IN MICELLAR CONDITION

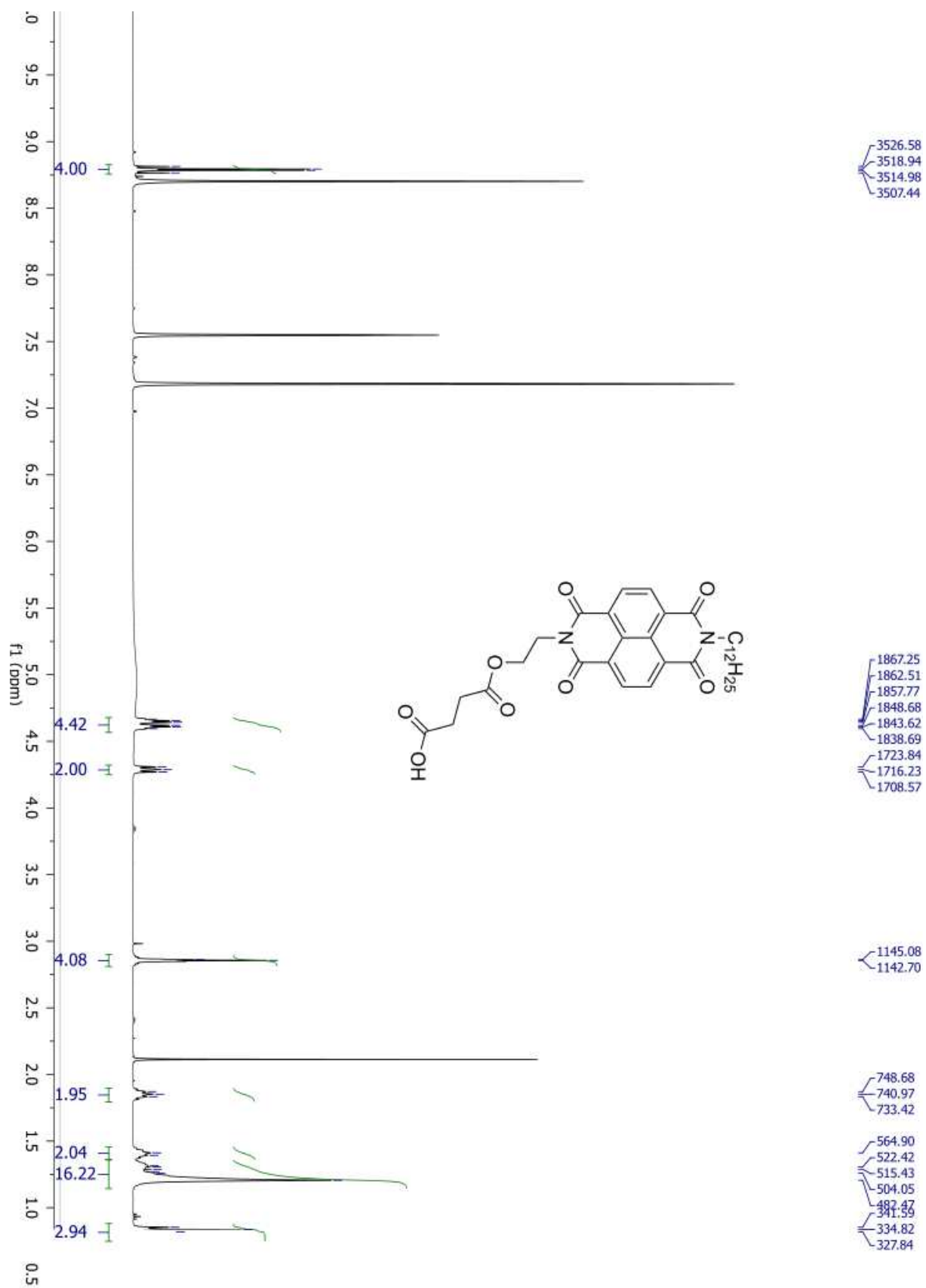


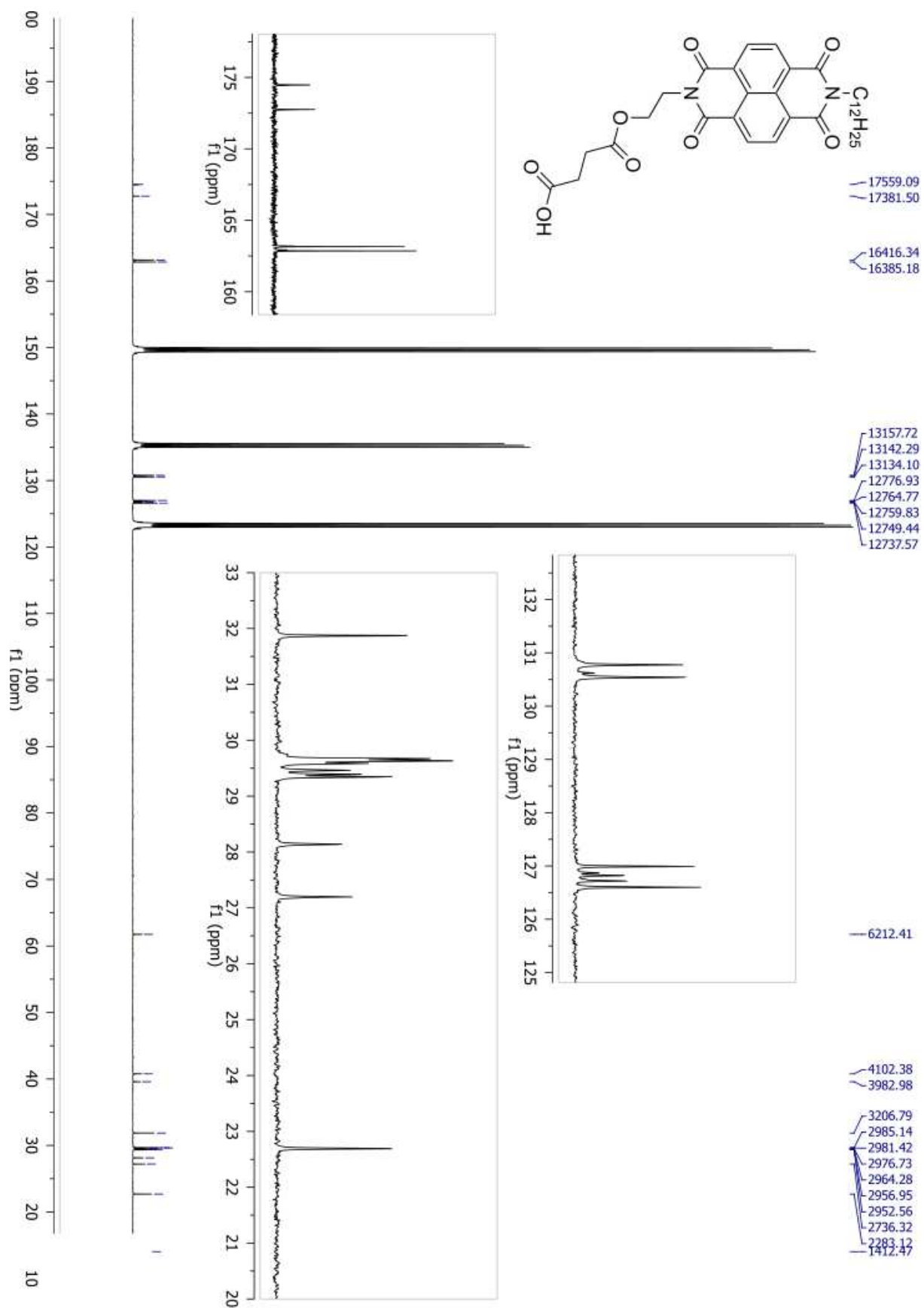
3.5.4.15 Synthesis of 2-dodecyl-7-(2-hydroxyethyl)benzo[*lmn*][3,8]phenanthroline-1,3,6,8(2H,7H)-tetraone (43)

In a two neck flask, under N_2 , were added 2-dodecyl-7-(2-hydroxyethyl)benzo[*lmn*][3,8]-phenanthroline-1,3,6,8(2H,7H)-tetraone (10.0 g, 20.9 mmol) and succinic anhydride (3.00 g, 30.0 mmol) and were dissolved in 120 mL of toluene. N(ET)_3 (212 mg, 2.10 mmol) were added by syringe. The reaction mixture was stirred at reflux for 24 h. The reaction was cooled down to room temperature and the formation of a precipitate was observed. The solid was recovered by filtration and crystallized in 60 mL of acetic acid to afford 2-dodecyl-7-(2-hydroxyethyl)benzo[*lmn*][3,8]phenanthroline-1,3,6,8(2H,7H)-tetraone as yellow solid (11.350 g, 19.437 mmol, 93%).

$^1\text{H NMR}$ (Pyr- d_5 , 400 MHz) 8.8-8.77 (m, 4H), 4.65-4.61 (m, 4H), 4.31-4.27 (m, 2H), 2.87-2.86 (m, 4H), 1.89-1.81 (m, 2H), 1.43-1.21 (m, 18H), 0.84 (t, $J = 6.9$ Hz, 3H). $^{13}\text{C NMR}$ (Pyr- d_5 , 100 MHz) 174.5, 172.8, 163.2, 162.8, 130.8, 130.5, 127.0, 126.8, 126.7, 126.7, 61.7, 40.8, 39.6, 31.9, 29.6, 29.5, 29.3, 28.1, 27.2, 22.7, 14.0. $^{13}\text{C NMR}$ (101 MHz, Pyr) δ 174.52, 172.76, 163.16, 162.85, 130.78, 130.62, 130.54, 126.99, 126.87, 126.82, 126.72, 126.60, 61.75, 40.77, 39.59, 31.87, 29.67, 29.63, 29.59, 29.46, 29.39, 29.35, 28.14, 27.20, 22.69, 14.04.

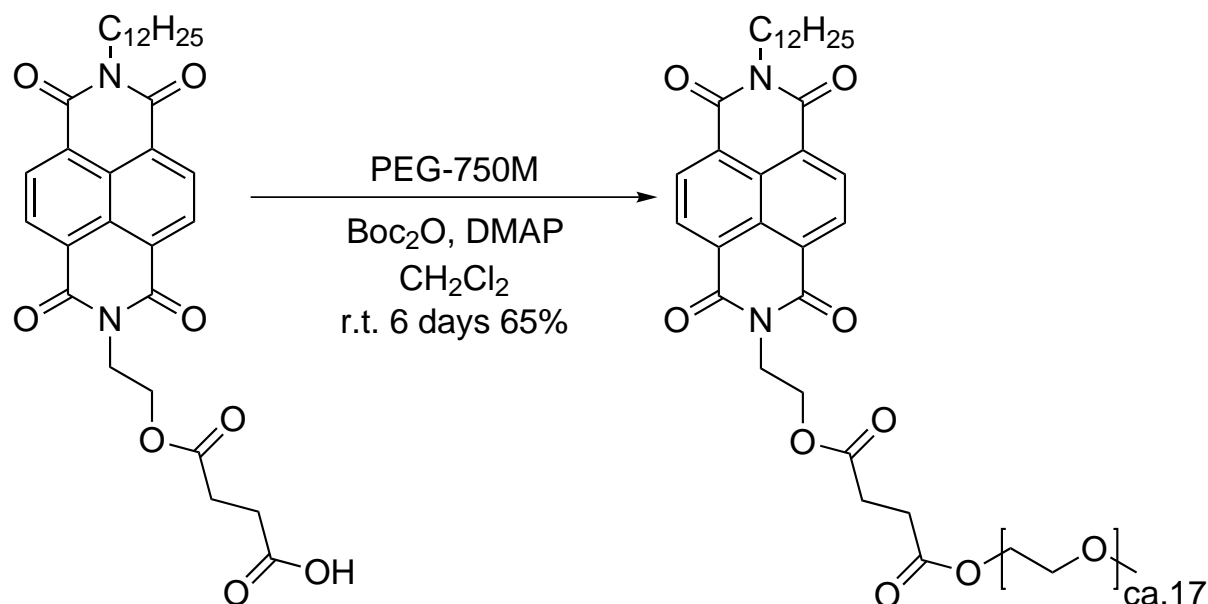
3.5. SYNTHESIS OF 2(,7)-ARYL-[1]BENZOTHIENO[3,2-B][1]BENZOTHIOPHENE (BTBT) DERIVATIVES IN MICELLAR CONDITION





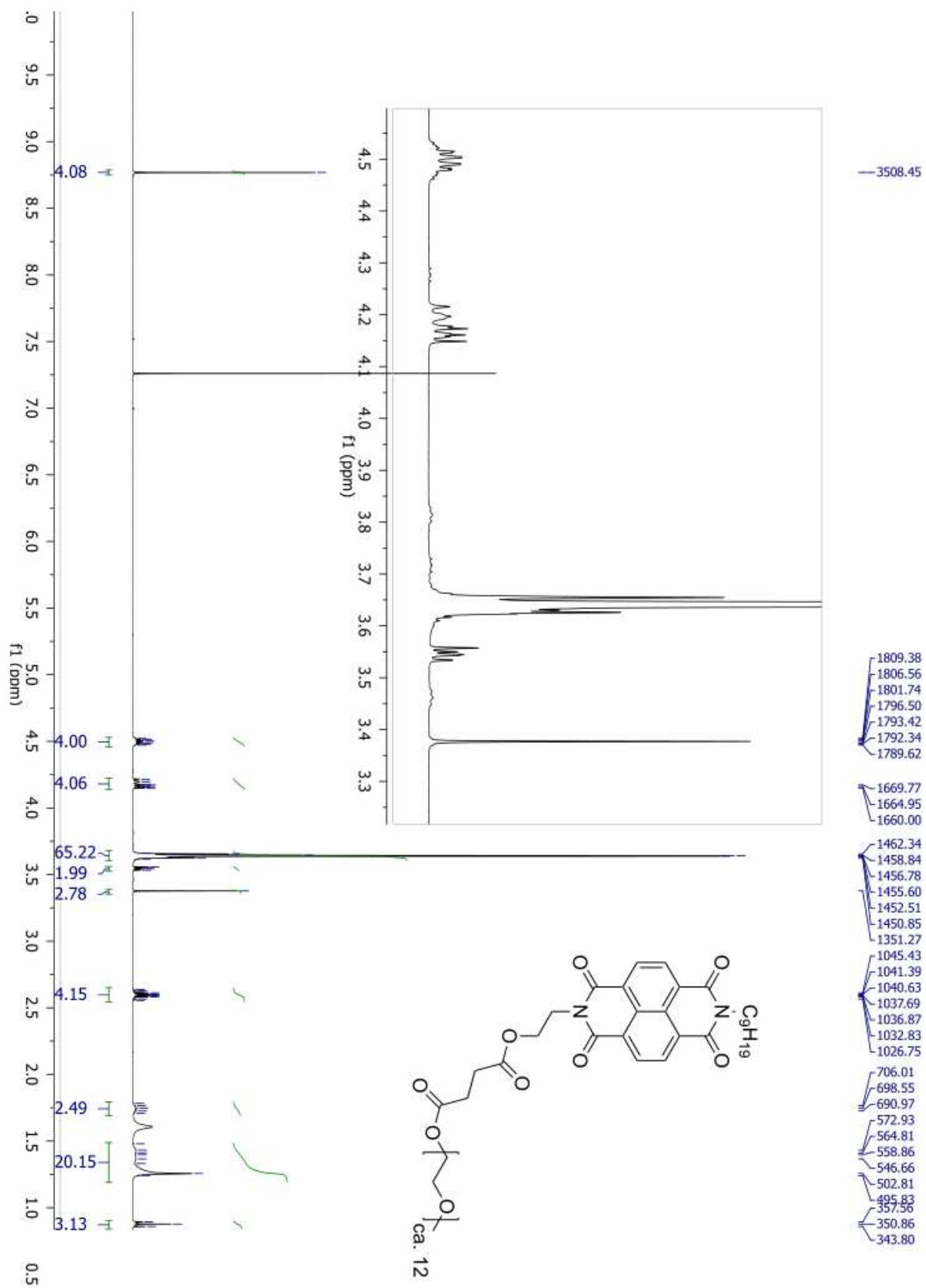
3.5. SYNTHESIS OF 2(,7)-ARYL-[1]BENZOTHIENO[3,2-B][1]BENZOTHIOPHENE
(BTBT) DERIVATIVES IN MICELLAR CONDITION

3.5.4.16 Synthesis of Pi-Nap-750M (44)

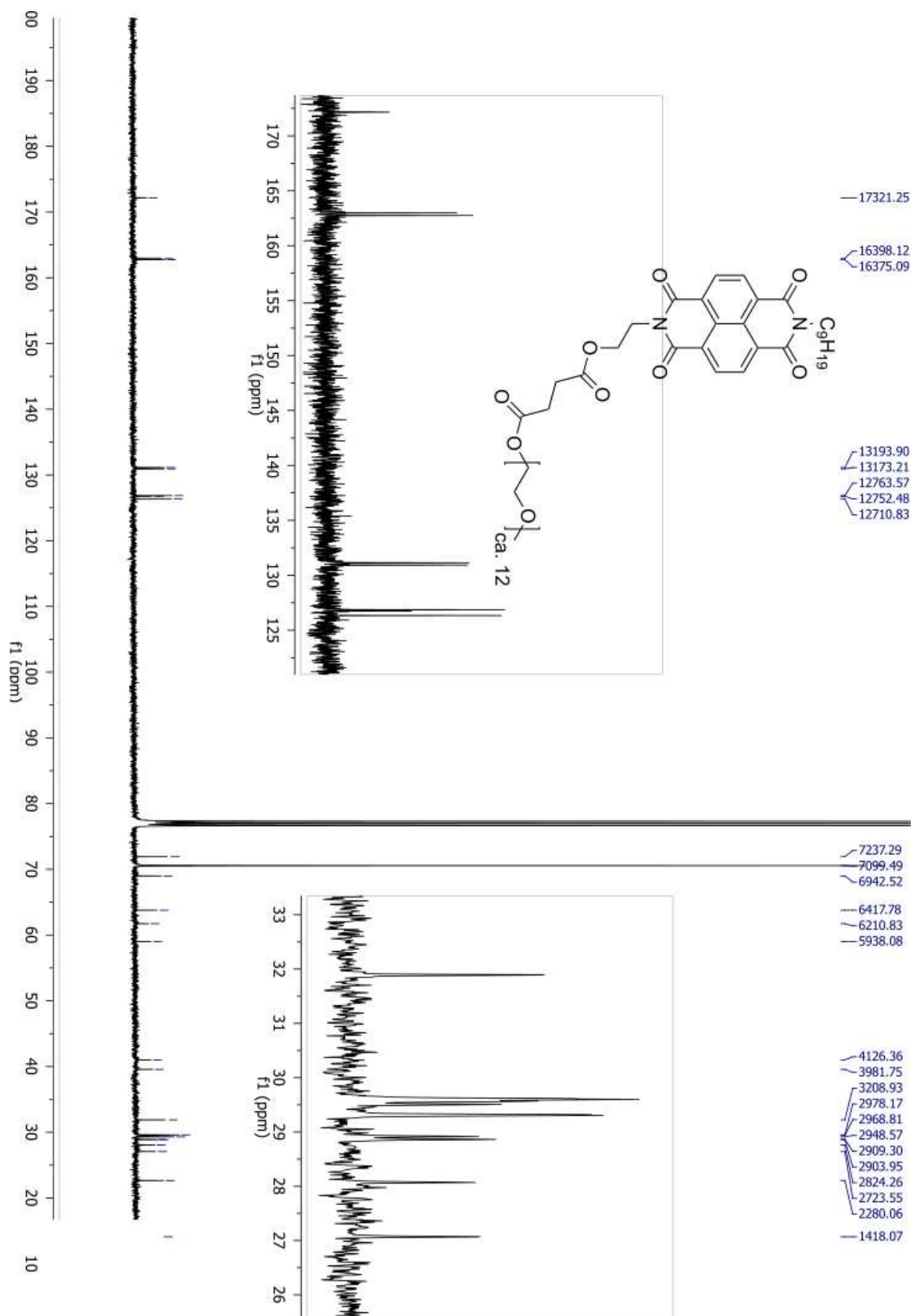


In a two neck flask, 2-dodecyl-7-(2-hydroxyethyl)benzo[lmn][3,8]phenanthroline-1,3,6,8-(2H,7H)-tetraone (8.500 g, 4.70 mmol), DMAP (183 mg, 1.50 mmol), and mPEG-750 (11.30 g, 15.07 mmol) were weighed. Dry dichloromethane (150 mL) and a solution of di-tert-butyl dicarbonate 2M in THF (8.63 mL, 17.2 mmol) were added by syringe. The reaction mixture was stirred at room temperature for 6 days. Solvents and volatile compounds were removed under reduce pressure to obtain crude product. The crude product was washed with 100 mL of diethyl ether. The crude product was purified by column chromatography on silica using a mixture of ethylacetate and ethanol (7:3 → 1:1) in gradient elution. Pi-Nap-750M was obtained as waxy solid (4.288 g, 3.196 mmol, 65%).

^1H NMR (CDCl_3 , 400 MHz) 8.77 (s, 4H), 4.53-4.46 (m, 4H) 4.21-4.16 (m, 4H), 3.66-3.62 (m, 63H) 3.57-3.53 (m, 2H) 3.38 (s, 3H) 2.64-2.56 (m, 4H), 1.78-1.71 (m, 2H), 1.43-1.20 (m, 18H) 0.88 (t, $J = 6.9$ Hz, 3H). ^{13}C NMR (CDCl_3 , 100 MHz) 172.1, 163.0, 162.8, 131.1, 130.9, 126.9, 126.8, 126.7, 126.3, 71.9, 70.6, 69.0, 63.8, 61.7, 59.0, 41.0, 39.6, 31.9, 29.6, 29.6, 29.5, 29.3, 28.9, 28.9, 28.0, 27.0, 22.6, 14.1.



3.5. SYNTHESIS OF 2(,7)-ARYL-[1]BENZOTHIENO[3,2-B][1]BENZOTHIOPHENE (BTBT) DERIVATIVES IN MICELLAR CONDITION



3.6 General conclusion and future development

We started our work of develop of SM micellar synthesis protocol with the choice of a surfactant, we chosen use a large-scale, commercially available surfactant, called Kolliphor® EL. We made a lot of examples on model small molecules and the conclusions were that Kolliphor® EL-catalyzed reaction were comparable in terms of yield with TPGS-750-catalyzed reaction but with the advantage of oxygen insensitivity, We observed that often the simple extension of the micellar conditions developed on model small molecules does not lead to the desired results, in this chapter several are the examples. The use of micellar catalysis for OS material in not trivial indeed organic semiconductors are usually heavily functionalized molecules, highly crystalline and these lead to low conversion, consequently long purification steps and low yield. The major issue is that the coupling partner and the catalyst must be localized in the same micellar compartment in order to perform the coupling instead of parasitic reaction as dehalogenation and homo-coupling or incomplete conversion. In order to solve this issue micellar reactions requires a specifically devised approach where tuning of common reaction parameters (concentration, temperature time, catalyst) has to go hand in hand with the toolbox of the formulation chemist, indeed of particular relevance is the tuning of the affinity of the different reagent, intermediate and product with the micellar environments. This affinity must be finely tuning indeed if the affinity it's too low often the reagent aren't dispersed efficiently and they remain simple suspended in the reaction environment on the other hand the affinity can't be too high, or better can't be too different between the reagent and reaction's intermediates in favor of the second, if no a stable saturation of the micellar compartment where the coupling take place can happen with resulting reaction stop. Particularly indicative for this aspect are the examples of SM coupling on 4,7- dibromo-5,6-difluoro-2,1,3-benzothiadiazole reported in section 3.4. The strategies we have identified to solve this problem are the use a small amount of co-solvent and the use of a co-surfactant. Co-solvent effect has been already described in literature and was rationalized in terms of a swelling effect of the micelles's core. This results in a larger effective volume for the reactions to take place. The use of a co-solvent was found particularly beneficial with highly crystalline or poorly soluble starting materials. In our experience this explanation can be considered more truthful for system like [1]benzothieno[3,2-b][1]benzothiophene or anthracene derivatives, but we shows in several examples can not be the main reason, the most significant is that SM coupling reaction of latent pigment system, compounds design to be soluble, reported in section 3.3.3. Rather, the explanation is to be found in the affinity tuning mentioned before and throughout the chapter. The co-surfactant approach has proved to be effective in order to completely eliminate the use of organic solvent as the solvent of the reactions, indeed choosing a HLB surfactant different from the main one can adjust the HLB of the final system. the co-solvent and co-surfactant approaches are two solutions that have good chances to find real application in industrial scale if surfactants employed are large-scale, commercially available surfactants. A third strategy we identified (section 3.5.2.3), certainly more distant from an industrial application, but still very interesting is the approach of the designer π -surfactant: original surfactants design for have a specific interaction with highly conjugated aromatic system, routine compounds in OS chemistry. In the near future we will begin to study the recycling of surfactant and the use of low concentrations of palladium, fundamental aspects for the development of sustainable and scalable protocols. We have already begun to extend the protocols developed for Suzuki-Miyaura reaction to other cross-coupling reaction, in this chapter there are sev-

3.6. GENERAL CONCLUSION AND FUTURE DEVELOPMENT

eral examples of Buchwald–Hartwig amination (section 3.3.4 and 3.5.2.2), but we intend to extend the examples to other reactions as well, of particular relevance would be the development of direct arylation reactions surfactant-catalyzed. It would be particularly important from the point of view of sustainability of the synthesis, we've already some preliminary data on OS system but are out of the scope of this thesis.

Bibliography

- [1] Nisato, G., Lupo, D., and Ganz, S. *Organic and Printed Electronics*. Pan Stanford, **2016**. ISBN 978-981-4669-74-0.
- [2] Po, R., Bernardi, A., Calabrese, A., Carbonera, C., Corso, G., and Pellegrino, A. *Energy & Environmental Science* **2014**, *7*, 925. doi: 10.1039/c3ee43460e.
- [3] Po, R. and Roncali, J. *Journal of Materials Chemistry C* **2016**, *4*, 3677–3685. doi: 10.1039/C5TC03740A.
- [4] Po, R., Bianchi, G., Carbonera, C., and Pellegrino, A. *Macromolecules* **2015**, *48*, 453–461. doi: 10.1021/ma501894w.
- [5] Bianchi, G., Po, R., Sassi, M., Beverina, L., Chiaberge, S., Spera, S., and Cominetti, A. *ACS Omega* **2017**, *2*, 4347–4355. doi: 10.1021/acsomega.7b00987.
- [6] Anastas, P. T. and Kirchhoff, M. M. *Accounts of Chemical Research* **2002**, *35*, 686–694. doi: 10.1021/ar010065m.
- [7] *United States Environmental Protection Agency — US EPA*.
- [8] Clark, J. H. and Tavener, S. J. *Organic Process Research and Development* **2007**, *11*, 149–155. doi: 10.1021/op060160g.
- [9] Lipshutz2B. *ACS Sustainable Chemistry and Engineering* **2016**, *4*, 5838–5849. doi: 10.1021/acssuschemeng.6b01810.
- [10] Sheldon, R. A., Arends, I. W. C. E., and Hanefeld, U. *Green Chemistry and Catalysis*. **2007**. ISBN 9783527307159.
- [11] Sheldon, R. A. *ACS Sustainable Chemistry and Engineering* **2018**, *6*, 32–48. doi: 10.1021/acssuschemeng.7b03505.
- [12] Sheldon, R. A. *Green Chemistry* **2007**, *9*, 1273–1283. doi: 10.1039/b713736m.
- [13] Capello, C., Fischer, U., and Hungerbühler, K. *Green Chemistry* **2007**, *9*, 927–934. doi: 10.1039/b617536h.
- [14] MacMillan, D. S., Murray, J., Sneddon, H. F., Jamieson, C., and Watson, A. J. *Green Chemistry* **2012**, *14*, 3016–3019. doi: 10.1039/c2gc36378j.
- [15] Vaghi, L., Sanzone, A., Sassi, M., Pagani, S., Papagni, A., and Beverina, L. *Synthesis (Germany)* **2018**, *50*, 1621–1628. doi: 10.1055/s-0036-1591937.
- [16] Rooney, M., Mattiello, S., Stara, R., Sanzone, A., Brazzo, P., Sassi, M., and Beverina, L. *Dyes and Pigments* **2018**, *149*, 893–901. doi: 10.1016/j.dyepig.2017.11.044.
- [17] Mattiello, S., Rooney, M., Sanzone, A., Brazzo, P., Sassi, M., and Beverina, L. *Organic Letters* **2017**, *19*, 654–657. doi: 10.1021/acs.orglett.6b03817.
- [18] La Sorella, G., Strukul, G., and Scarso, A. *Green Chemistry* **2015**, *17*, 644–683. doi: 10.1039/c4gc01368a.

- [19] Lipshutz, B. H., Ghorai, S., and Cortes-Clerget, M. *Chemistry - A European Journal* **2018**, *24*, 6672–6695. doi: 10.1002/chem.201705499.
- [20] Rideout, D. C. and Breslow, R. *Journal of the American Chemical Society* **1980**, *102*, 7816–7817. doi: 10.1021/ja00546a048.
- [21] Blackmond, D. G., Armstrong, A., Coombe, V., and Wells, A. *Angewandte Chemie - International Edition* **2007**, *46*, 3798–3800. doi: 10.1002/anie.200604952.
- [22] Chanda, A. and Fokin, V. V. *Chemical Reviews* **2009**, *109*, 725–748. doi: 10.1021/cr800448q.
- [23] Dallinger, D. and Kappe, C. O. *Chemical reviews* **2007**, *107*, 2563–2591. doi: 10.1021/cr0509410.
- [24] J., K. A. and Florian, H. *From Enzyme Models to Model Enzymes*. Royal Society of Chemistry, Cambridge, 1st editio ed., **2009**. ISBN 978-0-85404-175-6.
- [25] Myers, D. *Physiological Research* **2006**, , 374doi: 10.1073/pnas.0703993104.
- [26] Lombardo, D., Kiselev, M. A., Magazù, S., and Calandra, P. *Advances in Condensed Matter Physics* **2015**, *2015*. doi: 10.1155/2015/151683.
- [27] Dwars, T., Paetzold, E., and Oehme, G. *Angewandte Chemie - International Edition* **2005**, *44*, 7174–7199. doi: 10.1002/anie.200501365.
- [28] Gattuso, G., Notti, A., Pappalardo, A., Pappalardo, S., Parisi, M. F., and Puntoriero, F. *Tetrahedron Letters* **2013**, *54*, 188–191. doi: 10.1016/j.tetlet.2012.10.125.
- [29] Guerin, G., Qi, F., Cambridge, G., Manners, I., and Winnik, M. a. *The journal of physical chemistry. B* **2012**, *116*, 4328–37. doi: 10.1021/jp210454z.
- [30] Friedrich, H., Frederik, P. M., De With, G., and Sommerdijk, N. A. *Angewandte Chemie - International Edition* **2010**, *49*, 7850–7858. doi: 10.1002/anie.201001493.
- [31] Gratzel, M. *Kinetics and Catalysis in Microheterogeneous Systems*. **1991**. ISBN 0-8247-8495-2.
- [32] Christian, S. D. and Scamehorn, J. F. *Solubilization in Surfactant Aggregates*. Cmc. **1995**. ISBN 9780824790998.
- [33] Kumar, A., Gupta, M. K., Kumar, M., and Saxena, D. *RSC Advances* **2013**, *3*, 1673–1678.
- [34] Varszegi, C., Ernst, M., van Laar, F., Sels, B. F., Schwab, E., and De Vos, D. E. *Angewandte Chemie* **2008**, *120*, 1499–1502.
- [35] Ganguly, N. C. and Barik, S. K. *Synthesis* **2009**, *2009*, 1393–1399.
- [36] Baxová, L., Cibulka, R., and Hampl, F. *Journal of Molecular Catalysis A: Chemical* **2007**, *277*, 53–60.
- [37] Cavarzan, A., Scarso, A., Sgarbossa, P., Michelin, R. A., and Strukul, G. *Chem-CatChem* **2010**, *2*, 1296–1302.

BIBLIOGRAPHY

- [38] Bahrami, K., Khodaei, M. M., and Abbasi, J. *Synthesis* **2012**, *44*, 316–322.
- [39] Saha, R., Ghosh, A., and Saha, B. *Chemical Engineering Science* **2013**, *99*, 23–27.
- [40] Zielinski, M. E. and Morris, K. F. *Magnetic Resonance in Chemistry* **2009**, *47*, 53–56.
- [41] Chaghi, R., De Menorval, L.-C., Charnay, C., Derrien, G., and Zajac, J. *Langmuir* **2009**, *25*, 4868–4874.
- [42] Denis, C., Laignel, B., Plusquellec, D., Le Marouille, J.-Y., and Botrel, A. *Tetrahedron letters* **1996**, *37*, 53–56.
- [43] Das, D., Roy, S., and Das, P. K. *Organic letters* **2004**, *6*, 4133–4136.
- [44] Huang, S., Voigtritter, K. R., Unger, J. B., and Lipshutz, B. H. *Synlett* **2010**, *2010*, 2041–2044.
- [45] Caminade, A.-M., Ouali, A., Keller, M., and Majoral, J.-P. *Chemical Society Reviews* **2012**, *41*, 4113–4125.
- [46] Bassetti, M., Cerichelli, G., and Floris, B. *Gazz. Chim. Ital.* **1991**, *121*, 527–532.
- [47] Peng, Y.-Y., Ding, Q.-P., Li, Z., Wang, P. G., and Cheng, J.-P. *Tetrahedron letters* **2003**, *44*, 3871–3875.
- [48] Lipshutz, B. H. and Ghorai, S. *Organic letters* **2011**, *14*, 422–425.
- [49] Li, X.-H., Meng, X.-G., Pang, Q.-H., Liu, S.-D., Li, J.-M., Du, J., and Hu, C.-W. *Journal of Molecular Catalysis A: Chemical* **2010**, *328*, 88–92.
- [50] Otto, S., Engberts, J. B., and Kwak, J. C. *Journal of the American Chemical Society* **1998**, *120*, 9517–9525.
- [51] Anderton, G. I., Bangerter, A. S., Davis, T. C., Feng, Z., Furtak, A. J., Larsen, J. O., Scroggin, T. L., and Heemstra, J. M. *Bioconjugate chemistry* **2015**, *26*, 1687–1691.
- [52] Jewett, J. C. and Bertozzi, C. R. *Chemical Society Reviews* **2010**, *39*, 1272–1279.
- [53] Kolb, H. C., Finn, M., and Sharpless, K. B. **2001**, *40*, 2004–2021. doi: 10.1002/1521-3773(20010601)40:11;2004::AID-ANIE2004;3.3.CO;2-X.
- [54] Tornøe, C. W., Christensen, C., and Meldal, M. *The Journal of organic chemistry* **2002**, *67*, 3057–3064.
- [55] Clarisse, D., Prakash, P., Geertsen, V., Miserque, F., Gravel, E., and Doris, E. *Green Chemistry* **2017**, *19*, 3112–3115.
- [56] Bollenbach, M., Wagner, P., Aquino, P. G., Bourguignon, J.-J., Bihel, F., Salomé, C., and Schmitt, M. *ChemSusChem* **2016**, *9*, 3244–3249.
- [57] Linsenmeier, A. M. and Braje, W. M. *Tetrahedron* **2015**, *71*, 6913–6919.

- [58] Klumphu, P., Desfeux, C., Zhang, Y., Handa, S., Gallou, F., and Lipshutz, B. H. *Chemical Science* **2017**, *8*, 6354–6358. doi: 10.1039/c7sc02405c.
- [59] Rühling, A., Galla, H.-J., and Glorius, F. *Chemistry - A European Journal* **2015**, *21*, 12291–12294. doi: 10.1002/chem.201502542.
- [60] Xu, S., Kim, E. H., Wei, A., and Negishi, E.-i. *Science and Technology of Advanced Materials* **2014**, *15*, 044201. doi: 10.1088/1468-6996/15/4/044201.
- [61] Kitanosono, T., Masuda, K., Xu, P., and Kobayashi, S. *Chemical Reviews* **2018**, *118*, 679–746. doi: 10.1021/acs.chemrev.7b00417.
- [62] Brals, J., Smith, J. D., Ibrahim, F., Gallou, F., and Handa, S. *ACS Catalysis* **2017**, *7*, 7245–7250. doi: 10.1021/acscatal.7b02663.
- [63] Lipshutz, B. H., Ghorai, S., Abela, A. R., Moser, R., Nishikata, T., Duplais, C., Krasovskiy, A., Gaston, R. D., and Gadwood, R. C. *Journal of Organic Chemistry* **2011**, *76*, 4379–4391. doi: 10.1021/jo101974u.
- [64] Warner, W. A., Sanchez, R., Dawoodian, A., Li, E., and Momand, J. **2013**, *80*, 631–637. doi: 10.1111/j.1747-0285.2012.01428.x.Identification.
- [65] Klumphu, P. and Lipshutz, B. H. *Journal of Organic Chemistry* **2014**, *79*, 888–900. doi: 10.1021/jo401744b.
- [66] Andersson, M. P., Gallou, F., Klumphu, P., Takale, B. S., and Lipshutz, B. H. *Chemistry - A European Journal* **2018**, *24*, 6778–6786. doi: 10.1002/chem.201705524.
- [67] Kondo, K., Klosterman, J. K., and Yoshizawa, M. *Chemistry - A European Journal* **2017**, *23*, 16710–16721. doi: 10.1002/chem.201702519.
- [68] Gallou, F., Isley, N. A., Ganic, A., Onken, U., and Parmentier, M. *Green Chemistry* **2015**, *18*, 14–19. doi: 10.1039/c5gc02371h.
- [69] Petros, R. A. and Desimone, J. M. *Nature Reviews Drug Discovery* **2010**, *9*, 615–627. doi: 10.1038/nrd2591.
- [70] Mattiello, S., Monguzzi, A., Pedrini, J., Sassi, M., Villa, C., Torrente, Y., Marotta, R., Meinardi, F., and Beverina, L. *Advanced Functional Materials* **2016**, *26*, 8447–8454. doi: 10.1002/adfm.201603303.
- [71] Zambounis, J. and Iqbal, A. *Society* **1992**, , 4436–4437doi: 10.1038/40532.
- [72] Barra, M., Girolamo, F. D., Chiarella, F., Salluzzo, M., Chen, Z., Facchetti, A., Anderson, L., and Cassinese, A. *The Journal of Physical Chemistry C* **2010**, *114*, 20387–20393.
- [73] Wolfe, J. P., Wagaw, S., Marcoux, J.-F., and Buchwald, S. L. *Accounts of Chemical Research* **1998**, *31*, 805–818.
- [74] Hartwig, J. F. *Accounts of chemical research* **1998**, *31*, 852–860.
- [75] Hartwig, J. F. *Angewandte Chemie International Edition* **1998**, *37*, 2046–2067.

BIBLIOGRAPHY

- [76] Prim, D., Campagne, J.-M., Joseph, D., and Andrioletti, B. *Tetrahedron* **2002**, *58*, 2041–2076.
- [77] Schlummer, B. and Scholz, U. *Advanced Synthesis & Catalysis* **2004**, *346*, 1599–1626.
- [78] Hartwig, J. F. *Synlett* **2006**, *2006*, 1283–1294.
- [79] Surry, D. S. and Buchwald, S. L. *Angewandte Chemie International Edition* **2008**, *47*, 6338–6361.
- [80] Hartwig, J. F. *Accounts of chemical research* **2008**, *41*, 1534–1544.
- [81] Surry, D. S. and Buchwald, S. L. *Chemical Science* **2011**, *2*, 27–50.
- [82] Shirota, Y. and Kageyama, H. *Chemical reviews* **2007**, *107*, 953–1010.
- [83] Albrecht, K., Matsuoka, K., Fujita, K., and Yamamoto, K. *Angewandte Chemie International Edition* **2015**, *54*, 5677–5682.
- [84] Tanimoto, S., Suzuki, T., Nakanotani, H., and Adachi, C. *Chemistry Letters* **2016**, *45*, 770–772.
- [85] Kim, O. Y., Kim, B. S., and Lee, J. Y. *Synthetic Metals* **2015**, *201*, 49–53.
- [86] Cha, J.-R., Lee, C. W., Lee, J. Y., and Gong, M.-S. *Dyes and Pigments* **2016**, *134*, 562–568.
- [87] Godumala, M., Choi, S., Cho, M. J., and Choi, D. H. *Journal of Materials Chemistry C* **2016**, *4*, 11355–11381.
- [88] Wex, B. and Kaafarani, B. R. *Journal of Materials Chemistry C* **2017**, *5*, 8622–8653.
- [89] McClenaghan, N. D., Passalacqua, R., Loiseau, F., Campagna, S., Verheyde, B., Hameurlaine, A., and Dehaen, W. *Journal of the American Chemical Society* **2003**, *125*, 5356–5365.
- [90] Kwon, J. K., Cho, J. H., Ryu, Y.-S., Oh, S. H., and Yum, E. K. *Tetrahedron* **2011**, *67*, 4820–4825.
- [91] Börger, C., Kataeva, O., and Knölker, H.-J. *Organic & biomolecular chemistry* **2012**, *10*, 7269–7273.
- [92] Yoo, W.-J., Tsukamoto, T., and Kobayashi, S. *Organic letters* **2015**, *17*, 3640–3642.
- [93] Zhao, X., She, Y., Fang, K., and Li, G. *The Journal of organic chemistry* **2017**, *82*, 1024–1033.
- [94] Rull, S. G., Blandez, J. F., Fructos, M. R., Belderrain, T. R., and Nicasio, M. C. *Advanced Synthesis & Catalysis* **2015**, *357*, 907–911.
- [95] Minami, Y., Komiyama, T., Shimizu, K., Uno, S.-i., Hiyama, T., Goto, O., and Ikehira, H. *Synlett* **2017**, *28*, 2407–2410.

- [96] Vaccaro, G., Bianchi, A., Mauri, M., Bonetti, S., Meinardi, F., Sanguineti, A., Simonutti, R., and Beverina, L. *Chemical Communications* **2013**, *49*, 8474–8476.
- [97] Lipshutz, B. H., Chung, D. W., and Rich, B. *Advanced synthesis & catalysis* **2009**, *351*, 1717–1721.
- [98] Wagner, P., Bollenbach, M., Doebelin, C., Bihel, F., Bourguignon, J.-J., Salome, C., and Schmitt, M. *Green Chemistry* **2014**, *16*, 4170–4178.
- [99] You, J., Dou, L., Yoshimura, K., Kato, T., Ohya, K., Moriarty, T., Emery, K., Chen, C.-C., Gao, J., Li, G., *et al.* *Nature communications* **2013**, *4*, 1446.
- [100] Hong, J., Sung, M. J., Cha, H., Park, C. E., Durrant, J. R., An, T. K., Kim, Y.-H., and Kwon, S.-K. *ACS applied materials & interfaces* **2018**, *10*, 36037–36046.
- [101] Uddin, M. A., Lee, T. H., Xu, S., Park, S. Y., Kim, T., Song, S., Nguyen, T. L., Ko, S.-j., Hwang, S., Kim, J. Y., *et al.* *Chemistry of Materials* **2015**, *27*, 5997–6007.
- [102] Li, W., Deng, W., Wu, K., Xie, G., Yang, C., Wu, H., and Cao, Y. *Journal of Materials Chemistry C* **2016**, *4*, 1972–1978.
- [103] Fan, B., Sun, C., Jiang, X. F., Zhang, G., Chen, Z., Ying, L., Huang, F., and Cao, Y. *Advanced Functional Materials* **2016**, *26*, 6479–6488. doi: 10.1002/adfm.201601625.
- [104] Heuvel, R., van Franeker, J. J., and Janssen, R. A. *Macromolecular Chemistry and Physics* **2017**, *218*, 1–11. doi: 10.1002/macp.201600502.
- [105] Uddin, M. A., Lee, T. H., Xu, S., Park, S. Y., Kim, T., Song, S., Nguyen, T. L., Ko, S. J., Hwang, S., Kim, J. Y., and Woo, H. Y. *Chemistry of Materials* **2015**, *27*, 5997–6007. doi: 10.1021/acs.chemmater.5b02251.
- [106] Li, G., Kang, C., Gong, X., Zhang, J., Li, C., Chen, Y., Dong, H., Hu, W., Li, F., and Bo, Z. *Macromolecules* **2014**, *47*, 4645–4652. doi: 10.1021/ma500417r.
- [107] Zhang, J., Chen, W., Rojas, A. J., Jucov, E. V., Timofeeva, T. V., Parker, T. C., Barlow, S., and Marder, S. R. *Journal of the American Chemical Society* **2013**, *135*, 16376–16379. doi: 10.1021/ja4095878.
- [108] Cox, P. A., Leach, A. G., Campbell, A. D., and Lloyd-Jones, G. C. *Journal of the American Chemical Society* **2016**, *138*, 9145–9157. doi: 10.1021/jacs.6b03283.
- [109] Gabriel, C. M., Lee, N. R., Bigorne, F., Klumphu, P., Parmentier, M., Gallou, F., and Lipshutz, B. H. *Organic Letters* **2017**, *19*, 194–197. doi: 10.1021/acs.orglett.6b03468.
- [110] Mollet, H. and Grubenmann, A. *Formulation Technology: Emulsions, Suspensions, Solid Forms*, vol. 21. **2008**. ISBN 3527612939.
- [111] Neese, F. *Wiley Interdisciplinary Reviews: Computational Molecular Science* **2012**, *2*, 73–78. doi: 10.1002/wcms.81.
- [112] Schäfer, A., Horn, H., and Ahlrichs, R. *The Journal of Chemical Physics* **1992**, *97*, 2571–2577. doi: 10.1063/1.463096.

BIBLIOGRAPHY

- [113] Weigend, F. and Ahlrichs, R. *Phys. Chem. Chem. Phys.* **2005**, *7*, 3297–3305. doi: 10.1039/b508541a.
- [114] Weigend, F. *Physical Chemistry Chemical Physics* **2006**, *8*, 1057–1065. doi: 10.1039/b515623h.
- [115] Becke, A. D. *The Journal of Chemical Physics* **1993**, *98*, 1372–1377. doi: 10.1063/1.464304.
- [116] Marenich, A. V., Cramer, C. J., and Truhlar, D. G. *Journal of Physical Chemistry B* **2009**, *113*, 6378–6396. doi: 10.1021/jp810292n.
- [117] Barone, V. and Cossi, M. *J. Phys. Chem. A* **2001**, *102*, 1995–2001. doi: 10.1021/jp9716997.
- [118] Iino, H., Usui, T., and Hanna, J.-i. *Nature Communications* **2015**, *6*, 6828. doi: 10.1038/ncomms7828.
- [119] Reddy, M. R., Kim, H., Kim, C., and Seo, S. Y. *Synthetic Metals* **2018**, *235*, 153–159. doi: 10.1016/j.synthmet.2017.12.012.
- [120] Ullah, M., Wawrzinek, R., Nagiri, R. C. R., Lo, S.-C., and Namdas, E. B. *Advanced Optical Materials* **2017**, *5*, 1600973. doi: 10.1002/adom.201600973.
- [121] He, Y., Sezen, M., Zhang, D., Li, A., Yan, L., Yu, H., He, C., Goto, O., Loo, Y. L., and Meng, H. *Advanced Electronic Materials* **2016**, *2*, 1–7. doi: 10.1002/aelm.201600179.
- [122] He, K., Li, W., Tian, H., Zhang, J., Yan, D., Geng, Y., and Wang, F. *Organic Electronics* **2018**, *57*, 359–366. doi: 10.1016/j.orgel.2018.03.015.
- [123] He, K., Li, W., Tian, H., Zhang, J., Yan, D., Geng, Y., and Wang, F. *ACS Applied Materials & Interfaces* **2017**, , acsami.7b10675doi: 10.1021/acsami.7b10675.
- [124] He, Y., Xu, W., Murtaza, I., Zhang, D., He, C., Zhu, Y., and Meng, H. *RSC Advances* **2016**, *6*, 95149–95155. doi: 10.1039/c6ra22999a.
- [125] Takimiya, K., Ebata, H., Sakamoto, K., Izawa, T., Otsubo, T., and Kunugi, Y. *Journal of the American Chemical Society* **2006**, *128*, 12604–12605. doi: 10.1021/ja064052l.
- [126] Inoue, S., Minemawari, H., Tsutsumi, J., Chikamatsu, M., Yamada, T., Horiuchi, S., Tanaka, M., Kumai, R., Yoneya, M., and Hasegawa, T. *Chemistry of Materials* **2015**, *27*, 3809–3812. doi: 10.1021/acs.chemmater.5b00810.
- [127] Lino, H., Usui, T., Kobori, T., and Hanna, J.-I. *SID Symposium Digest of Technical Papers* **2012**, *43*, 497–500. doi: 10.1002/j.2168-0159.2012.tb05826.x.
- [128] Kosata, B., Kozmik;Vaclav, Svoboda;jiri, Novotna;Vladimira, Vanek;Premysl, and Glogarova;milada. *Liquid Crystals* **2003**, *30*, 603–610. doi: 10.1080/0267829031000097484.

- [129] Kim, A., Jang, K. S., Kim, J., Won, J. C., Yi, M. H., Kim, H., Yoon, D. K., Shin, T. J., Lee, M. H., Ka, J. W., and Kim, Y. H. *Advanced Materials* **2013**, *25*, 6219–6225. doi: 10.1002/adma.201302719.
- [130] Iino, H., Kobori, T., and Hanna, J. I. *Journal of Non-Crystalline Solids* **2012**, *358*, 2516–2519. doi: 10.1016/j.jnoncrysol.2012.03.021.
- [131] Iino, H., Kobori, T., and Hanna, J.-i. **2012**, *02*, 6–11.
- [132] Minemawari, H., Tsutsumi, J., Inoue, S., Yamada, T., Kumai, R., and Hasegawa, T. *Applied Physics Express* **2014**, *7*, 091601. doi: 10.7567/APEX.7.091601.
- [133] Kim, S., Kim, A., Jang, K.-S., Yoo, S., Ka, J.-W., Kim, J., Yi, M. H., Won, J. C., Hong, S.-K., and Kim, Y. H. **2016**, doi: 10.1016/j.synthmet.2016.06.021.
- [134] Kunii, M., Iino, H., and Hanna, J. *Applied Physics Letters* **2017**, *110*, 1–5. doi: 10.1063/1.4985628.
- [135] Minemawari, H., Tanaka, M., Tsuzuki, S., Inoue, S., Yamada, T., Kumai, R., Shimoi, Y., and Hasegawa, T. *Chemistry of Materials* **2017**, *29*, 1245–1254. doi: 10.1021/acs.chemmater.6b04628.
- [136] Hanna;Junichi, Hiroaki, I., Yasuyuki, W., Junichiro, K., Maki;Hiroshi, Atsuhisa;Miyawaki, and Sakura;Yoshinobu. *EP 2 966 701 A1*, **2014**.
- [137] OSHIMA, K., KURATA, T., KUWABARA, H., and IKEDA, M. *HETEROCYCLIC COMPOUND AND ITS APPLICATION JP5334165 (B2)*, **2015**.
- [138] GAO, W., HENRY, H., DIEV, V., and WU, W. *ELECTROACTIVE MATERIALS WO2016069321 (A2)*, **2014**.
- [139] SATAKE, M. *NOVEL COMPOUND AND DYE-SENSITIZED PHOTOELECTRIC CONVERSION ELEMENT USING THE SAME JP2016196422 (A)*, **2015**.
- [140] TAKI, M. and KAJIWARA, K. *RING-FUSED THIOPHENE COMPOUND AND OIL DROPLET DYE USING SAME WO2018159848 (A1)*, **2017**.
- [141] CHIHAYA, A., KUWABARA, H., and YUI, T. *LIGHT-EMITTING ELEMENT JP2009246139 (A)*, **2008**.
- [142] Etheridge, F. S., Fernando, R., Golen, J. A., Rheingold, A. L., and Sauve, G. *RSC Advances* **2015**, *5*, 46534–46539. doi: 10.1039/c5ra05920h.
- [143] Bhosale, S. V., Jani, C. H., and Langford, S. J. *Chemical Society Reviews* **2008**, *37*, 331–342. doi: 10.1039/b615857a.
- [144] Dehkordi, M. E., Luxami, V., and Pantos, G. D. *The Journal of Organic Chemistry* **2018**, , acs.joc.8b01629doi: 10.1021/acs.joc.8b01629.
- [145] Reczek, J. J. and Iverson, B. L. *Macromolecules* **2006**, *39*, 5601–5603. doi: 10.1021/ma0611669.
- [146] Reczek, J. J., Villazor, K. R., Lynch, V., Swager, T. M., and Iverson, B. L. **2006**, , 7560–7563.

BIBLIOGRAPHY

- [147] Petitjean, A., Cuccia, L. A., Schmutz, M., and Lehn, J. M. *Journal of Organic Chemistry* **2008**, *73*, 2481–2495. doi: 10.1021/jo702495u.
- [148] Lehn, J. M. *Australian Journal of Chemistry* **2010**, *63*, 611–623. doi: 10.1071/CH10035.

Chapter 4

Green approaches to the preparation of organic polymeric semiconductors

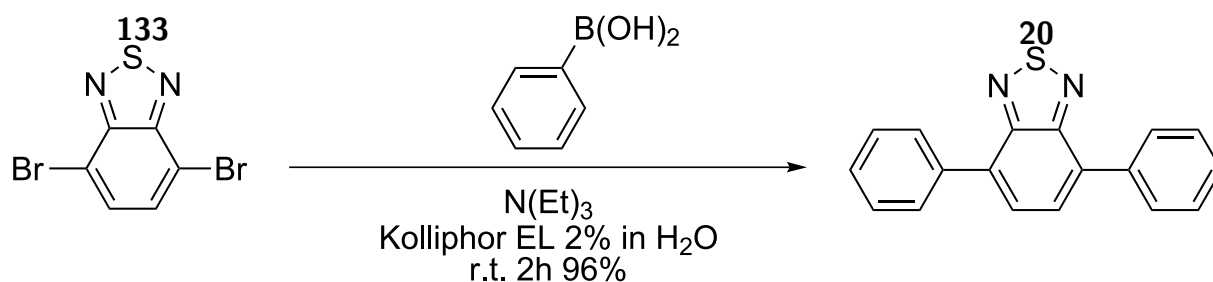
4.1 Introduction

In chapter 3 the topic of the sustainability of the synthesis of organic semiconductors was widely discussed, in particular we focused on the development of the synthesis of OS small molecules in micellar conditions. In this chapter, instead, we will focus on the synthesis of OS polymeric systems. Most polymerization methods used for conjugated polymer synthesis are conventional transition-metal-catalyzed polycondensations such as Stille,¹ Suzuki,² and Kumada³⁴ polycondensations. Nevertheless, each of these methods has its own shortcomings. For example, the in situ preparation of monomers without purification (Kumada), the use of organo-metallic monomers resulting in highly toxic side products⁵ (Stille), or the need for cryogenic temperatures or catalytic protocols for monomer functionalization (Stille and Suzuki) are environmentally problematic. One of the most promising methods to build up conjugated polymers in a more atom-economic fashion is the direct C–H arylation polycondensation (DAP).^{6, 7} Direct arylation reaction has already been introduced in the section 2.4.1 of this thesis. In the chapter 4.3. In particular, there are two approaches that we have used in order to develop new scalable and sustainable synthesis for OS semiconductor polymers: the application of the Kolliphor® EL-catalyzed condition also for the synthesis of polymeric materials and the development of the synthesis of a new soluble polymers by direct arylation. In section 4.2 it is reported the optimization of Poly[(9,9-dioctylfluorenyl-2,7-diyl)-alt-(benzo[2,1,3]thiadiazol-4,7-diyl)] (F8BT) synthesis in micellar and emulsion conditions with an in-depth chemical characterization of the obtained materials. In section 4.3 is reported a study of optimization of the polymerization conditions with the aim of regulating the molecular weights of a new OFET n-material that we are developing. A part of this work in this chapter was developed at the Technische Universität Chemnitz in collaboration with Prof. Dr. Michael Sommer and his research group.

4.2 F8BT synthesis in emulsion/micellar conditions

4.2.1 Why F8BT?

Having successfully developed Kolliphor® EL-catalyzed conditions for the synthesis of molecular materials (chapter 3), we decided to extend the micellar approach also to synthesis of OS polymer materials. The first macromolecular system chosen is the commercial polymer F8BT. The reasons for F8BT choice are several: F8BT is a well-known commercial p-material used in different OS application, several synthesis of this polymer are already reported in literature including micellar/emulsion condition⁸⁻¹¹ and finally we have shown the excellent reactivity of 4,7-dibromobenzo[c]-1,2,5-thiadiazole (**133**) in micellar condition (see scheme 4.1), and we expected that phenylboronic acid reactivity wasn't so different from 9,9-Dioctyl-9H-fluorene-2,7-diboronic acid bis(pinacol) ester (**166**) reactivity.

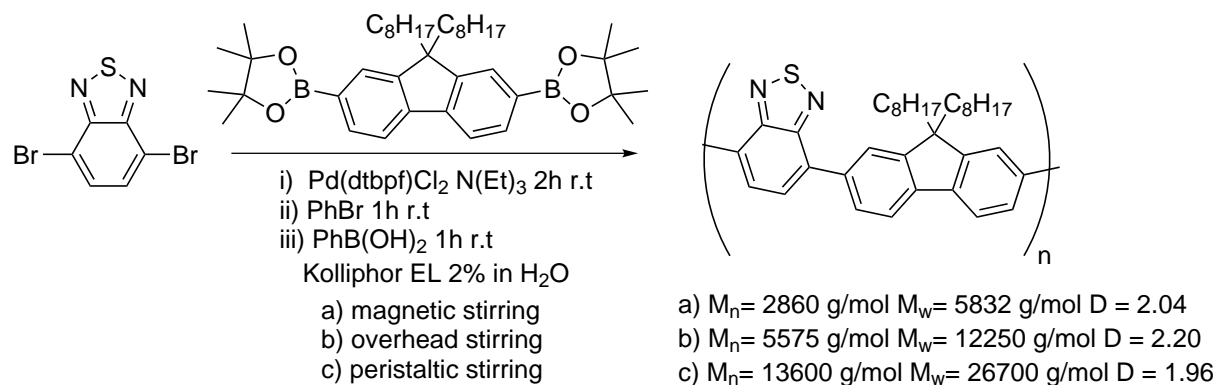


Scheme 4.1 SM reactions carried out on **133** in Kolliphor EL-catalyzed conditions

4.2.2 Results and discussion

For the first trial we used the same condition developed for the synthesis of compound **20**: solution of kolliphor EL at 2% in water as the reaction medium, Pd(dtbpf)Cl₂ as the catalyst, NEt₃ as base, at room temperature for 2 hours under air with a molar ratio of 1:1 between 9,9-dioctyl-9H-fluorene-2,7-diboronic acid bis(pinacol) ester (compound **166**) and 4,7-Dibromobenzo[c]-1,2,5-thiadiazole (compound **133**) (Condition **a** in scheme 4.2). Polymer were terminated by using bromobenzene and phenylboronic acid successively, and the solids were collected by filtration after precipitating the mixture in methanol and were purified by Soxhlet extraction using methanol, acetone, and petroleum ether successively to remove the small-molecular-weight fraction.

4.2. F8BT SYNTHESIS IN EMULSION/MICELLAR CONDITIONS

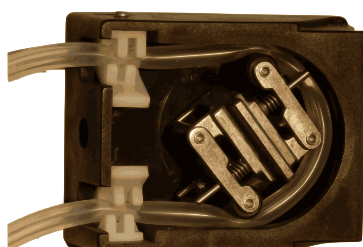


Scheme 4.2 F8BT polymerization in Kolliphor EL-micellar solution conditions with different stirring methods. **133**(1 eq.), **166**(1 eq.), Pd(dtbbpf)Cl₂ (0.02 eq.) , N(Et)₃ (6 eq.) , bromobenzene (PhBr)(10 eq.) and phenylboronic acid (10 eq.)

Number average molecular weight (M_n), weight average molecular weight (M_w), and polydispersity (D) of F8BT were respectively 2.9 Kg/mol , 5,8 Kg/mol and 2.04 as estimated by gel permeation chromatography (GPC) analysis using THF as the eluent and linear polystyrene as the standard. The obtained F8BT has M_n and M_w sensibly lower compared with reported values under similar emulsion condition. For example Behrendt et al.,⁹ reported a M_n= 9.4 kDa, M_w= 21,6 KDa and PDI= 2,3 for a polymerization carried out in emulsion of sodium dodecyl sulfate (SDS) in water at 0.25 wt % and toluene (20 : 1) at room temperature with the same monomers in the same monomers ratio. The problem highlighted is that as the reaction goes on and the polymeric chains grow, the stirring becomes less and less efficient. The most part of the material was deposited on the magnetic bar as sticky solid. With the aim of further increasing the polymer length in our conditions we tried to use more efficient stirring methods: overhead stirring and peristaltics stirring. The overhead stirring contemplates the use of a dedicated apparatus, an example is shown in figure 4.1a , overhead stirrers have motor-powered stirring tools immersed in the reaction's vessel. Peristaltics stirring contemplates the use of a peristaltic pump, a type of positive displacement pump used for pumping a variety of fluids. The fluid is contained within a flexible tube fitted inside a circular pump casing. A rotor with a number of "rollers", "shoes", "wipers", or "lobes" attached to the external circumference of the rotor compresses the flexible tube. As the rotor turns, the part of the tube under compression is pinched closed thus forcing the fluid to be pumped to move through the tube. Additionally, as the tube opens to its natural state after the passing of the cam ("restitution" or "resilience") fluid flow is induced to the pump (see figure 4.1b), so the reaction's mixture was charged in the pump's tube and the tube itself was used like reactor.



(a)

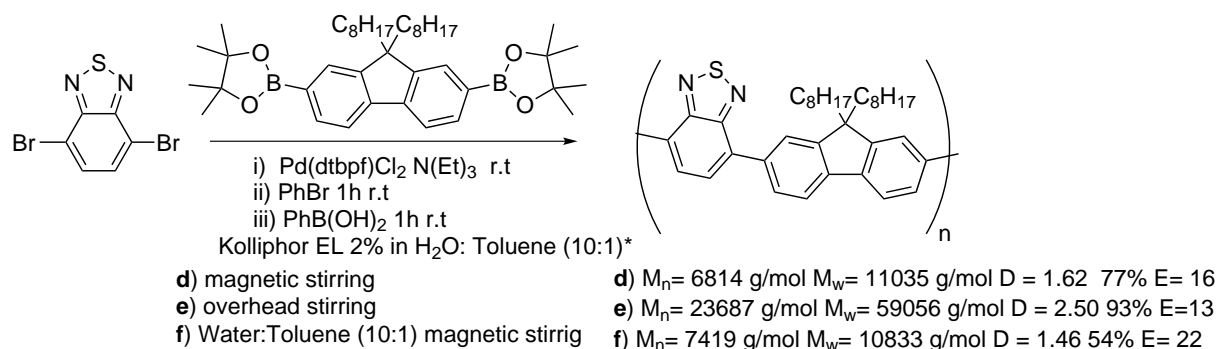


(b)

Figure 4.1 Different stirring methods employed : a) Overhead stirrer and b) peristaltic pump

The polymer size distribution was strongly influenced by the stirring mode and geometry of the reactor, as it can be seen by the values reported in scheme 4.2 for the conditions **a**, **b** and **c**. We tried also the co-solvent approach, we have chosen toluene as a co-solvent because it has often proved to be an efficient co-solvent in our previous works and is also used as such in other literature works for this polymerization.^{9, 11} We tested the familiar emulsion Kolliphor El 2 wt% in water : toluene (10:1 by volume). As expected the co-solvent approach lead to an increase of the molecular weights of the resulted polymers, M_n , M_w and D for the F8BT obtained with a solution of kolliphor EL at 2% in water as reaction medium are 5.6 kg/mol , 12.3 kg/mol and 2.20 with overhead stirring (condition **b** in scheme 4.2) against the values of 23.7 kg/mol, 59.1 kg/mol and 2.50 for the reaction carried in the emulsion system (condition **e** in scheme 4.3) with the same stirring system. We didn't tried the peristaltic stirring with the emulsion as reaction's medium due to the incompatibility of the tube's material with the emulsion system.

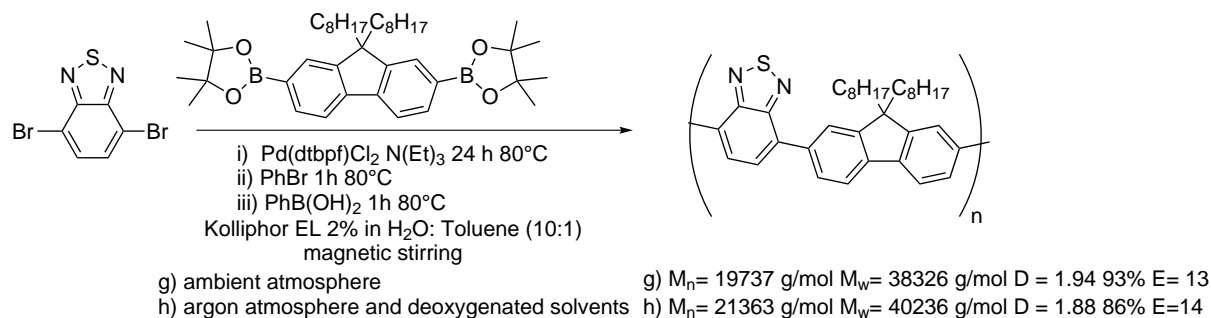
4.2. F8BT SYNTHESIS IN EMULSION/MICELLAR CONDITIONS



Scheme 4.3 F8BT polymerization in Kolliphor-stabilized and Kolliphor-free emulsion conditions, with different stirring methods. **133**(1 eq.), **166**(1 eq.), Pd(dtbbpf)Cl₂ (0.02 eq.), N(Et)₃ (6 eq.), bromobenzene (PhBr)(10 eq.) and phenylboronic acid (10 eq.)

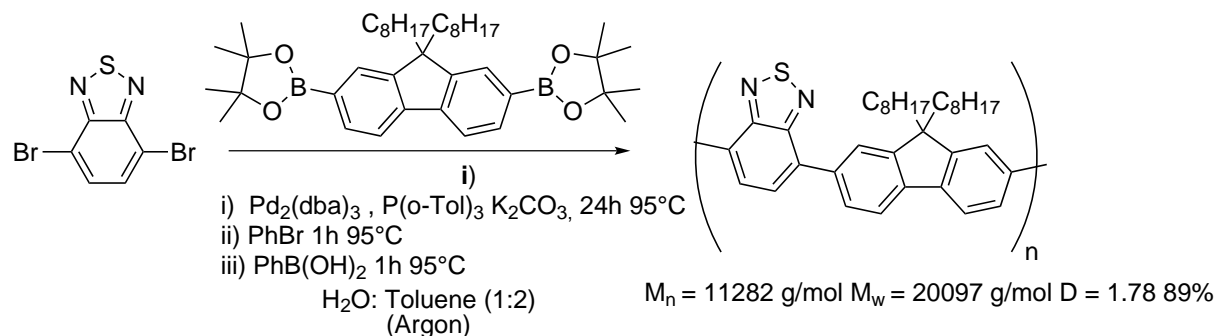
In order to evaluate the Kolliphor EL effect on the polymerization we performed control experiments in condition **f** of the scheme 4.3 using an emulsion of water and toluene in the same volume ratio as the Kolliphor-stabilized emulsion (10:1). The obtained F8BT has a comparable molecular weight distribution (M_n= 7.4 kg/mol, M_w= 10.8 kg/mol and D= 1.46) with the F8BT obtained in condition **d** but the polymerization yield was 54% against the 77% obtained with the Kolliphor-stabilized emulsion. The lower yield is correlated with the catalyst's oxygen poisoning that is faster in the absence of the oxygen-barrier effect of the Kolliphor EL. We tried to evaluate also the temperature effects, indeed we carried out the reaction with the Kolliphor EL 2% in water : Toluene emulsion system as reaction medium at 80°C, and in order to evaluate the oxygen-barrier effect of the Kolliphor EL at 80°C we carried out two twin reactions, one under environmental conditions and one with degassed solvents and under argon atmosphere (scheme 4.4). The temperature has a strong influence on the molecular weight distribution of the F8BT obtained, for example under ambient atmosphere at 80°C we obtained values of M_n= 19.4 kg/mol, M_w= 38.3 kg/mol and D= 1.94 and a polymerization yield of 93% (condition **g** scheme 4.4) against M_n= 6.8 kg/mol, M_w= 11.0 kg/mol and D= 1.62 and a polymerization yield of 77% (condition **d** scheme 4.3) for the reaction carried out at room temperature under otherwise identical conditions. The influence of the presence of oxygen in the reaction environment is less marked in fact in terms of M_n, M_w and D the two polymers obtained in twin reactions are comparable (see condition **g** and **h** in scheme 4.4), even though the reaction carried out in the atmosphere of argon and with degassed solvents has higher values, a symptom that the presence of oxygen in some way affects the polymerization.

CHAPTER 4. GREEN APPROACHES TO THE PREPARATION OF ORGANIC POLYMERIC SEMICONDUCTORS



Scheme 4.4 F8BT polymerization in Kolliphor-stabilized emulsion conditions, in presence or absence of oxygen. **133**(1 eq.), **166**(1 eq.), Pd(dtbpf)Cl₂ (0.02 eq.) , N(Et)₃ (6 eq.) , bromobenzene (PhBr)(10 eq.) and phenylboronic acid (10 eq.)

We did a polymer's end groups study by NMR spectroscopy, thanks a collaboration with Dr. Hartmut Komber of the Leibniz Institute of Polymer Research Dresden (IPF). The ¹H-NMR measurement of the F8BT samples were done in deuterated 1,1,2,2-Tetrachloroethane-*d*₂ (C₂D₂Cl₄), at room temperature the signal peaks are very broad due the aggregation of the polymer chain and was not possible make an accurate study of the polymer's end groups of the terminals chain but fortunately its possible obtain better resolution and less noise with high temperature measurement (120°C) (see figure 4.5 in Appendix 4.2.2 for a comparison between the spectra aquired at 25°C. vs 120°C). In order to have a comparison for the nature of polymer's end groups, we prepared a F8BT samples in standard SM biphasic condition (see scheme 4.5) and we added also the F8BT obtained in this condition to the NMR study.



Scheme 4.5 F8BT polymerization in standard SM biphasic conditions

From high resolution NMR spectra is possible obtain several information. Figure 4.2 shows an exemplary spectrum of the studies done, the spectrum reported belong to F8BT sample obtained in condition **d** of the figure 4.3, it was chosen like example because all polymer's end groups that we can recognize are observable . It is possible to see the principal polymers protons assignment (signals labeled in black: 1^p, 3^p, 4^p, 9^p and aliphatic protons) that are well visible in the range from 0 to 10 ppm, for the assignment was done 2D-NMR study reported in Appendix 4.2.2 figure 4.7 . For the samples obtained in Kolliphor-catalyzed condition is possible observe a signal at 3.67 ppm due a residue of the surfactant mixture (the assignment was done with comparison of the Kolliphor EL in CD₂Cl₄ at 120°C, see figure 4.6 in Appendix 4.2.2) , this is evidence that standard purification was not able to remove completely all surfactant components. The range 7.87-6.84

4.2. F8BT SYNTHESIS IN EMULSION/MICELLAR CONDITIONS

ppm is very informative range, indeed is it possible to find the terminal chain signals, in the figure are reported the structure and the assignment based on reported work where similar study were done on polyfluorene.¹² Hydrogen termination at the fluorene end (F8-H) was observed, obviously as a result of deborylation. This side reaction, which is more commonly observed with electron-rich boronic ester-functionalized substrates,^{13, 14} Hydroxyl termination of the fluorene end (F8-OH) was observed, we assumed that introduction of oxygen leads to Pd–O₂ intermediates^{15, 16} and finally to F8-OH. Phenyl termination at the fluorene end (F8-Ph) was observed only in this samples, result of the polymerization's termination with bromobenzene and finally is possible observe the pinacol ester termination at the fluorene end (F8-B(pinacol)), simply unreacted functionality.

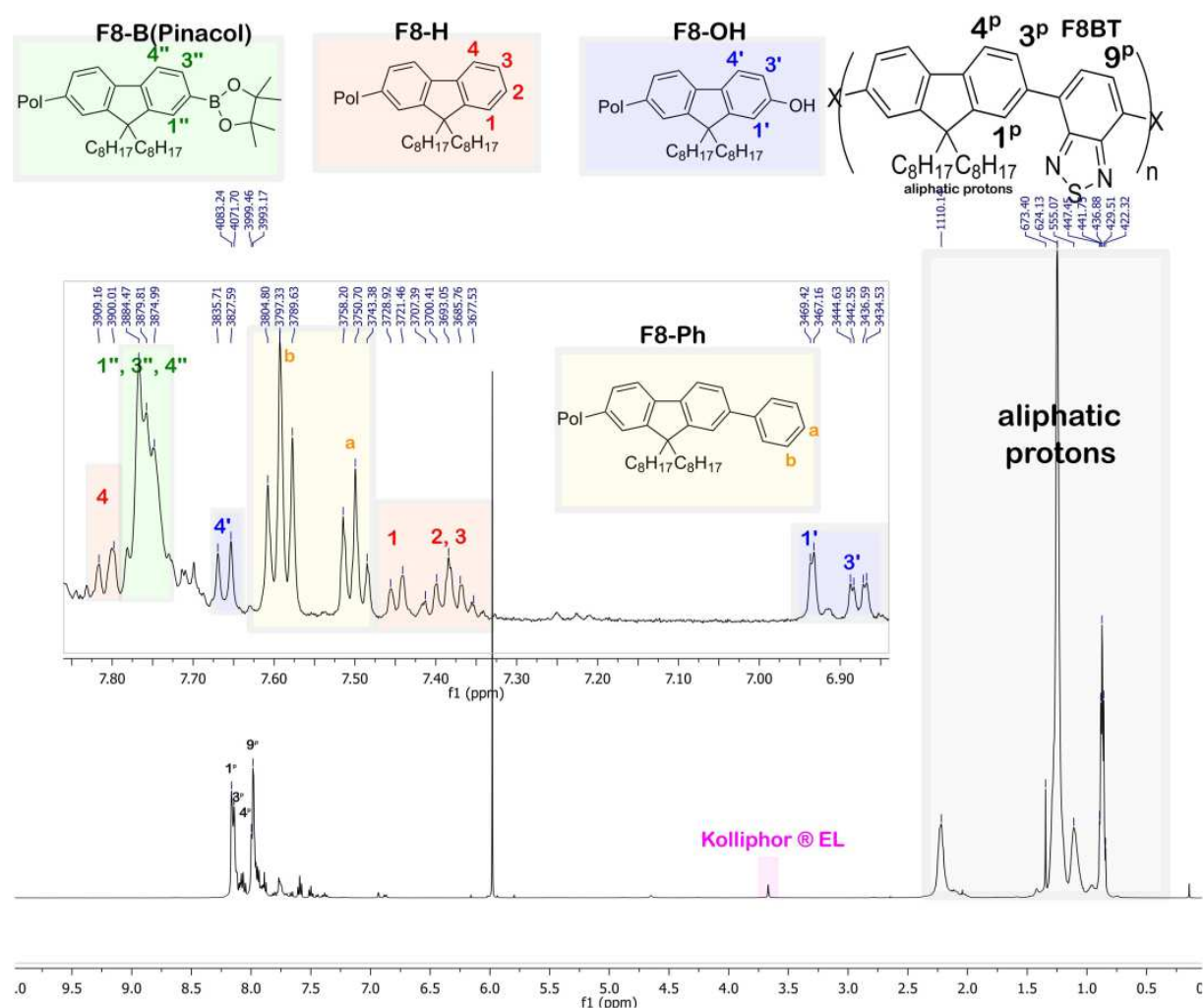


Figure 4.2 Exemplary spectrum of high resolution ¹H-NMR spectra of F8BT materials obtained at 120°C in C₂D₂Cl₂

The results of the polymer's end groups study are summarized in table 4.1. Using the integrals of end group's signals it is possible to calculate the ratio percentage of the different polymer's end group (for details see figure 4.4 in Appendix). By comparison of the ratio percentage of the polymer's end groups it is possible to affirm that deborylation is a major termination mechanism at 80°C while it becomes a minority process at room temperature (30°C). Analyzing entry 1 we can affirm that at room temperature the polymer chains stop growing for kinetic problems indeed the major polymer's end

groups are F8-Ph and F8-B(pinacol) in according with the strong influence of the stirring mode. Analyzing entry 2 we have another evidence that the polymerization yield was sensibly lower in this Kolliphor-free condition under ambient atmosphere because catalyst Oxygen-poisoning, indeed the major polymer's end groups is F8-B(pinacol) and F8-Ph was not observed, symptom of complete deactivation of the catalyst. This evidence confirms good Kolliphor-Oxygen barrier effects also in emulsion condition but not a full barrier because a minor part of F8-OH is observed for entries 1,2,3 and also in Entry 4 when the reaction is performed under argon atmosphere a 5% of F8-OH was observed. Under this condition probably the oxygen presence is due non-optimal deoxygenation of the surfactant used in the formation of the emulsion with degassed water and toluene. Indeed the same water and toluene were used to perform the biphasic reaction of entry 5 where the F8-OH was not observed. Under second hypothesis is a minor affinity to oxygen of the different catalyst system employed in these condition. A method to suppress the formation of F8-OH terminals is under investigation, in fact this type of terminations can interfere with the electroluminescence of the material, thus negatively affecting the performance of the same in OLED devices. There are two possible solutions that we are studying, the development of a protocol for a more efficient deoxygenation of the surfactant, for example by directly deoxygenating a solution of Kolliphor in water or in toluene rather than doing it separately for the three components or more scalable solution is a final derivatization of the hydroxyl groups with for examples trimethylsilyl group (TMS). Also the F8-B(pinacol) must be suppressed for the same reason,¹⁷ but in this case probably the solutions are: adding fresh catalyst with the terminators compounds, better tuning of the reaction's time or a final heating of the reaction mixture in order to promote the deboration reaction.

En.	Condition/ scheme	Temp. [°C]	Reaction medium	Atm.	F8- OH [%]	F8-H [%]	F8- Ph [%]	F8- B(pin.) [%]
1	d / scheme 4.3	30	Koll. EL 2% in H ₂ O: Toluene (10:1)	Air	12	13	38	38
2	f / scheme 4.3	30	H ₂ O: Toluene (10:1)	Air	14	9	0	76
3	g / scheme 4.4	80	Koll. EL 2% in H ₂ O: Toluene (10:1)	Air	12	47	0	41
4	h / scheme 4.4	80	Koll. EL 2% in H ₂ O: Toluene (10:1)	Ar	5	65	0	30
5	i / scheme 4.5	95	H ₂ O: Toluene (1:2)	Ar	0	60	0	40

Table 4.1 Polymer's end groups relative distribution

4.2.3 Conclusion

Apart from the problems of effective polymer termination yet to be optimized in order to obtain high quality F8BT, in terms of molecular weight distribution our results are comparable with others reported F8BT's values. Figure 4.3 summarizes recent reported synthesis with the respective F8BT's M_n , M_w , D reported values and estimated E factor. For the calculation of this last factor the purification step was excluded due to lack of data on volumes of the solvents used. Very interesting is the comparison with the other reported emulsion condition (figure 4.3 b and d), also in this condition was employed commercial surfactants (SDS, Triton X-102) in water solution emulsified with aromatic solvents (Toluene and Xylene), from this points of view these conditions are very similar with the Kolliphor-catalyzed conditions here reported, but these conditions are hardly scalable for F8BT synthesis, the principal difference is the nominal concentration of the monomers, in reported synthesis the concentrations are from 30 (for condition d in figure 4.3) to 100 (for condition b in figure 4.3) times lower than our working nominal concentration (0.5 M), this difference is reflected by the high difference of E factor. For our conditions, it must also be considered that about 50% of the E factor is due to the large excess of polymerization terminators employed (10 eq.), which will certainly be optimized in the future, as shown by the NMR study is not efficient.

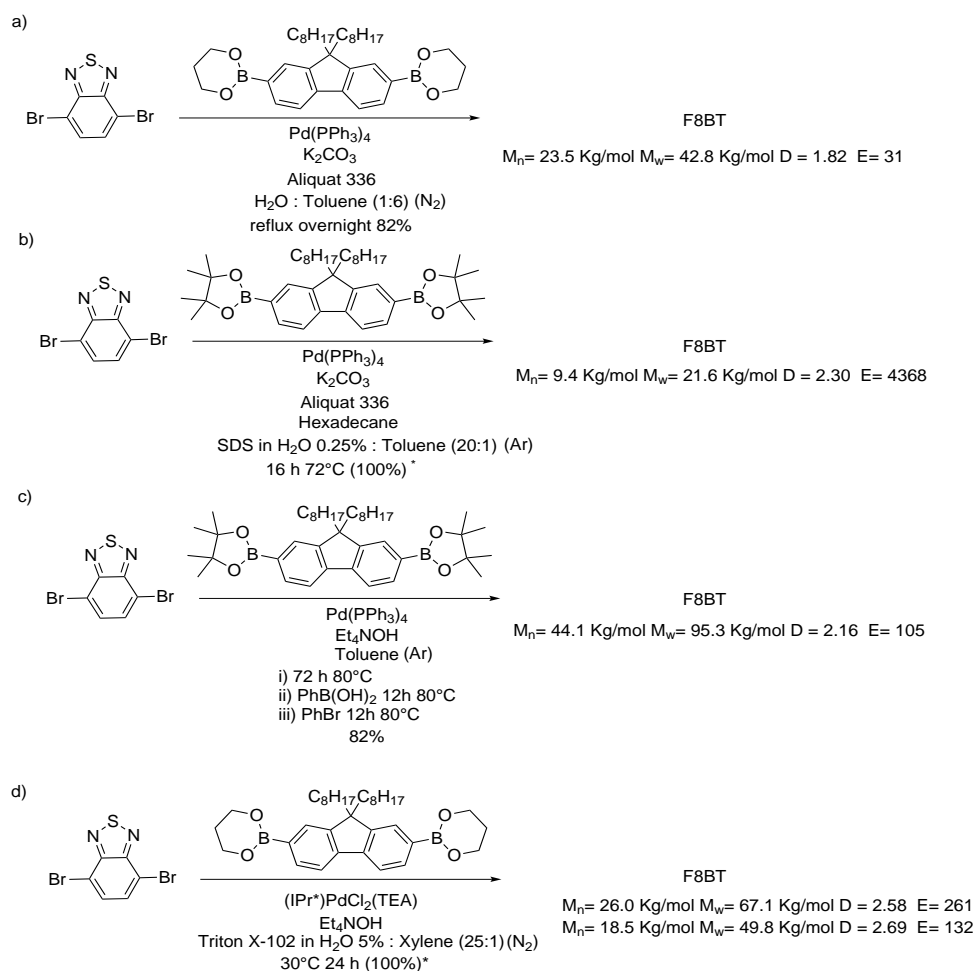
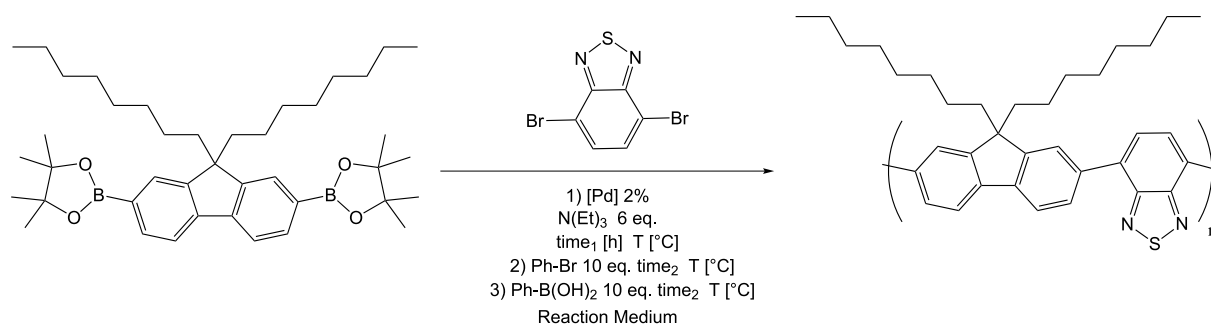


Figure 4.3 F8BT reported synthesis : a⁸, b,⁹c¹⁰ and d¹¹ * the polymerization's yield is not reported in the referent article, for the estimation of the factor E , the reaction was considered quantitative

4.2.4 Experimental part

F8BT polymerization procedure



Procedure for conditions: **a,d,f,g,h** and **i**

9,9-Dioctyl-9H-fluorene-2,7-diboronic acid bis(pinacol) ester (0.15 mmol), 4,7-Dibromobenzo[c]-1,2,5-thiadiazole (0.15 mmol), Pd(dtbpf)Cl₂ (or other precatalyst see the table) (0.003 mmol) were weighed directly in the reaction's vessel equipped with stirring bar. Reaction medium was added by syringe (0.3 mL) (after 3 vacuum/Argon cycle was syringed under argon atmosphere if the condition required argon atmosphere) and the reaction's mixture was stirred for 5 minutes before the adding of N(Et)₃ (0.9 mmol). The reaction was stirred for determined time *time*₁ (see table) at determined temperature (see table), then bromobenzene (1.5 mmol) and phenylboronic acid (1.5 mmol) were added subsequently (let reacted for time *time*₂ each one). The reaction was cooled to room temperature and the reaction mixture was diluted in 10 mL of dichloromethane and the crude polymer was precipitated in methanol (50 mL), the orange/yellow solid was filtered directly in Soxhlet extraction thimbles and purified by extraction with: Methanol, Acetone, Petroleum Ether and finally the polymer was recovered with dichloromethane. Dichloromethane was removed by evaporation and the polymer was dried in oven under vacuum for 12h at 50°C.

For condition **h** and **i**, that required deoxygenated conditions, solvents and liquid reagents were deoxygenated in the following way: Toluene was thoroughly degassed for 30 min by bubbling Argon gas through the solution, while being stirred; Water was thoroughly degassed for 60 min by bubbling Argon gas through the solution, while being stirred at reflux temperature; N(Et)₃ was degassed with the Freeze-Pump-Thaw Degassing method and Kolliphor EL was degassed with 4 cycle of vacuum/Argon.

4.2. F8BT SYNTHESIS IN EMULSION/MICELLAR CONDITIONS

En.	Condition/ scheme	[Pd]	Reaction medium / Atm.	T. [°C]	time <i>time</i> ₁ / <i>time</i> ₂ [h]	Yield [%]
1	a / scheme 4.3	Pd(dtbbpf)Cl ₂	Koll. EL 2% in H ₂ O/ Air	30	90/3	52
2	d / scheme 4.3	Pd(dtbbpf)Cl ₂	Koll. EL 2% in H ₂ O: Toluene (10:1)/ Air	30	90/3	77
3	f / scheme 4.3	Pd(dtbbpf)Cl ₂	H ₂ O: Toluene (10:1)/ Air	30	90/3	54
4	g / scheme 4.4	Pd(dtbbpf)Cl ₂	Koll. EL 2% in H ₂ O: Toluene (10:1)/ Air	80	24/1	93
5	h / scheme 4.4	Pd(dtbbpf)Cl ₂	Koll. EL 2% in H ₂ O: Toluene (10:1)/ Argon	80	24/1	86
6	i / scheme 4.5	Pd ₂ (dba) ₃ (0,01 eq) P(o-Tol) ₃ (0.04 eq)	H ₂ O: Toluene (1:2)/ Argon	95	24/1	89

Table 4.2

Procedure for conditions: **b** and **e**

9,9-Dioctyl-9H-fluorene-2,7-diboronic acid bis(pinacol) ester (1.5 mmol), 4,7-Dibromobenzo[c]-1,2,5-thiadiazole (1.5 mmol), Pd(dtbbpf)Cl₂ (0.03 mmol) were weighed directly in two necked flask equipped with overhead stirrer. Reaction medium was added (3 mL) and the reaction's mixture was stirred for 5 minutes before the adding of N(Et)₃ (g). The reaction was stirred for 6 h at room temperature, then bromobenzene (15 mmol) and phenylboronic acid (15 mmol) were added subsequently and let reacted for 1 h. The reaction mixture was diluted in 100 mL of dichloromethane and the crude polymer was precipitated in methanol (200 mL), the orange/yellow solid was filtered directly in Soxhlet extraction thimbles and purified by extraction with: Methanol, Acetone, Petroleum Ether and finally the polymer was recovered with dichloromethane. Dichloromethane was removed by evaporation and the polymer was dried in oven under vacuum for 12h at 50°C.

Procedure for condition **c**

CHAPTER 4. GREEN APPROACHES TO THE PREPARATION OF ORGANIC POLYMERIC SEMICONDUCTORS

9,9-Dioctyl-9H-fluorene-2,7-diboronic acid bis(pinacol) ester (1.5 mmol), 4,7-Dibromo-benzo[c]-1,2,5-thiadiazole (1.5 mmol), Pd(dtbpf)Cl₂ (0.03 mmol) were weighed and after grinding in a mortar were added directly in the tube of the peristaltic pump with 3 mL of a solution of Kolliphor® EL 2 wt% in water. The reaction was stirred for 15 min with the peristaltic pump, then N(Et)₃ (9 mmol) were syringed directly in the tube. The reaction was stirred for 6 h at room temperature, then bromobenzene (15 mmol) and phenylboronic acid (15 mmol) were added subsequently and let reacted for 1 h. The reaction mixture was diluted in 100 mL of toluene and the crude polymer was precipitated in methanol (200 mL), the orange/yellow solid was filtered directly in Soxhlet extraction thimbles and purified by extraction with: Methanol, Acetone, Petroleum Ether and finally the polymer was recovered with dichloromethane. Dichloromethane was removed by evaporation and the polymer was dried in oven under vacuum for 12h at 50°C.

4.2.5 Appendix

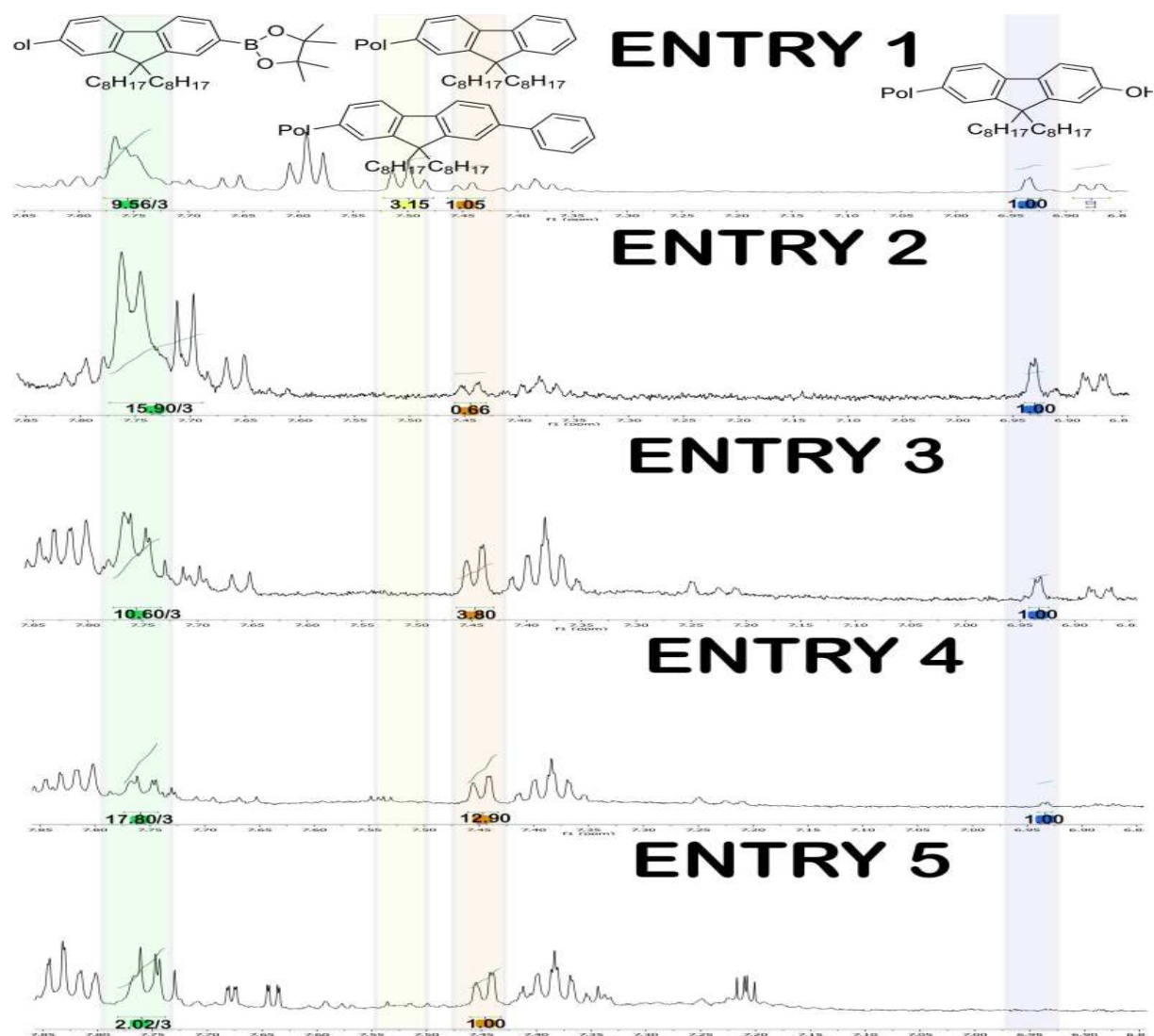


Figure 4.4 F8BT High temperature NMR spectra in $C_2D_2Cl_4$ (condition **d,f,g,h** and **i**), range 7.86-6.84 ppm. For the relative quantification of the polymer's end group the integrals of reference signals have been chosen, peak integrating 1H and well resolved by the others signals except for the termination F8-B (pinacol.) where all three peaks have been integrated together (3H) due low resolution .

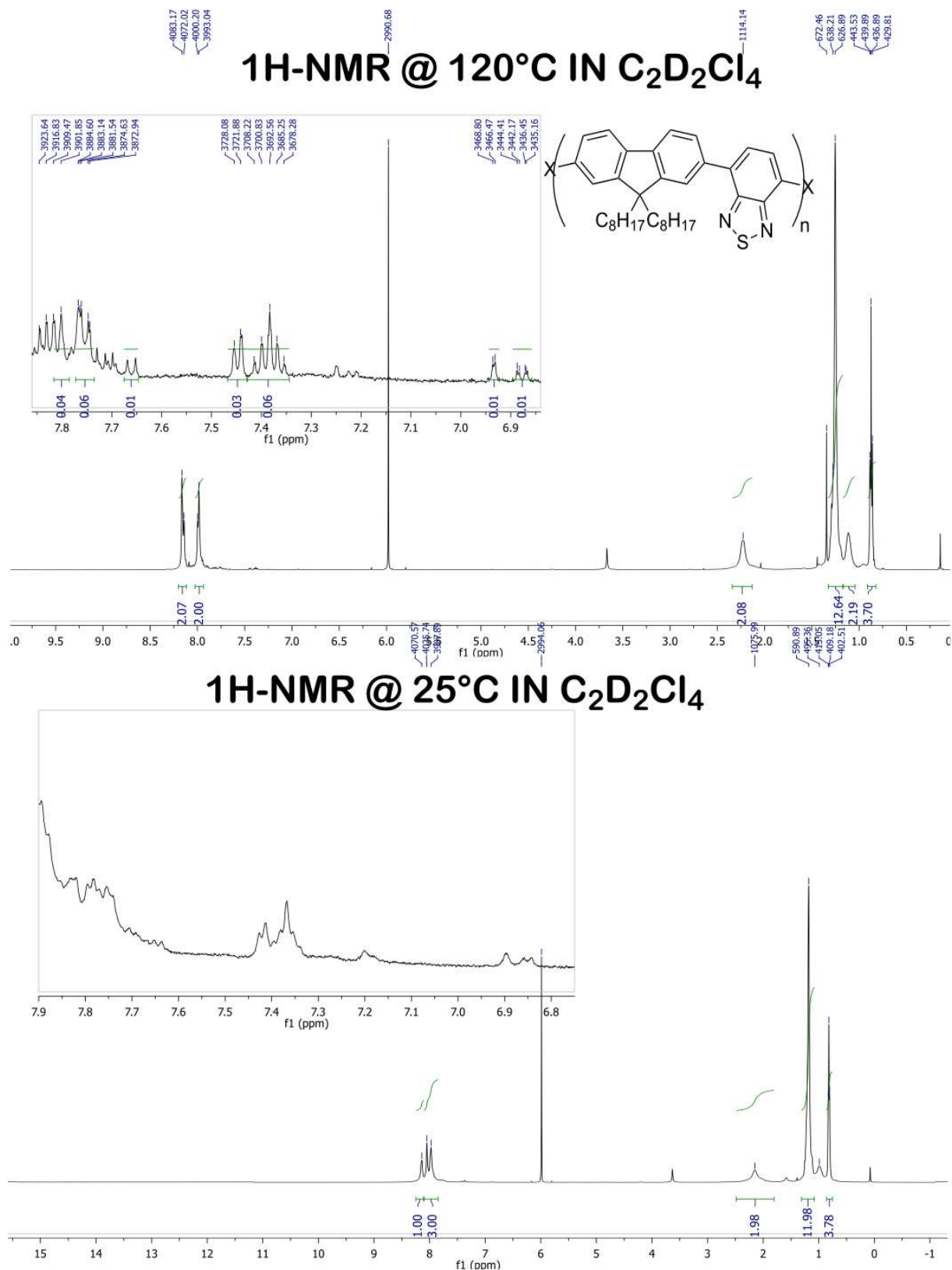


Figure 4.5 Comparison between NMR acquired spectra at room temperature and 120°C of a F8BT samples in $\text{C}_2\text{D}_2\text{Cl}_4$ $^1\text{H-NMR}$ (500 MHz, $\text{C}_2\text{D}_2\text{Cl}_4$, 393 K) δ 8.20-8.12 (m, 2H), 8.04-7.96 (m, 2H), 2.23 (broad, 2H), 1.33-1.05 (m, 14H), 0.92-0.84 (m, 3H). $^1\text{H-NMR}$ (500 MHz, $\text{C}_2\text{D}_2\text{Cl}_4$, 298 K) δ 8.22-8.10 (broad, 1H), 8.1-7.86 (m, 3H), 2.15 (broad, 2H), 1.30-0.90 (m, 14H), 1.33-1.03 (m, 14H), 0.82 (t, $J = 6.3$ Hz, 3H).

4.2. F8BT SYNTHESIS IN EMULSION/MICELLAR CONDITIONS

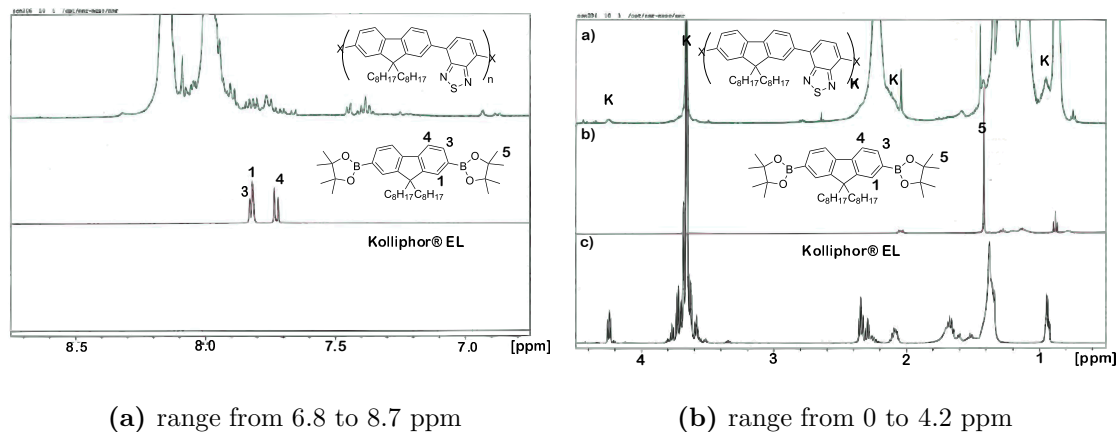


Figure 4.6 Comparison between NMR spectra of: F8BT, 9,9-Dioctyl-9H-fluorene-2,7-diboronic acid bis(pinacol) ester and Kolliphor® EL in $C_2D_2Cl_4$ at $120^\circ C$

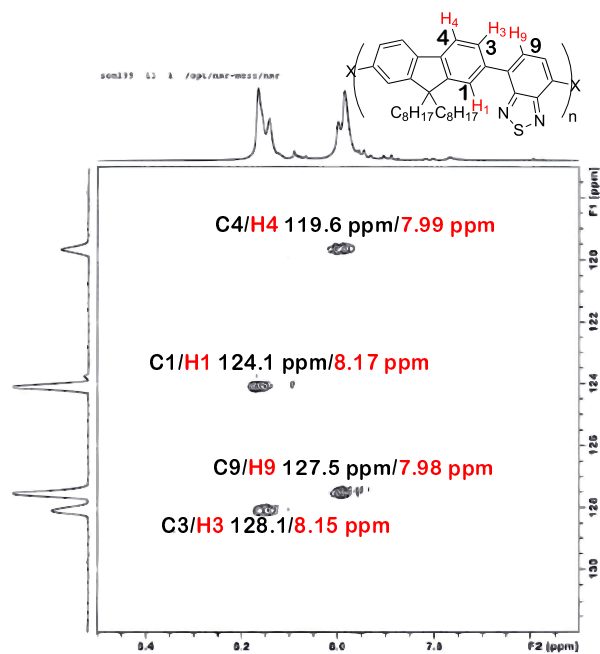


Figure 4.7 F8BT NMR-2D ($^1H,^{13}C$) at $120^\circ C$ in $C_2D_2Cl_4$

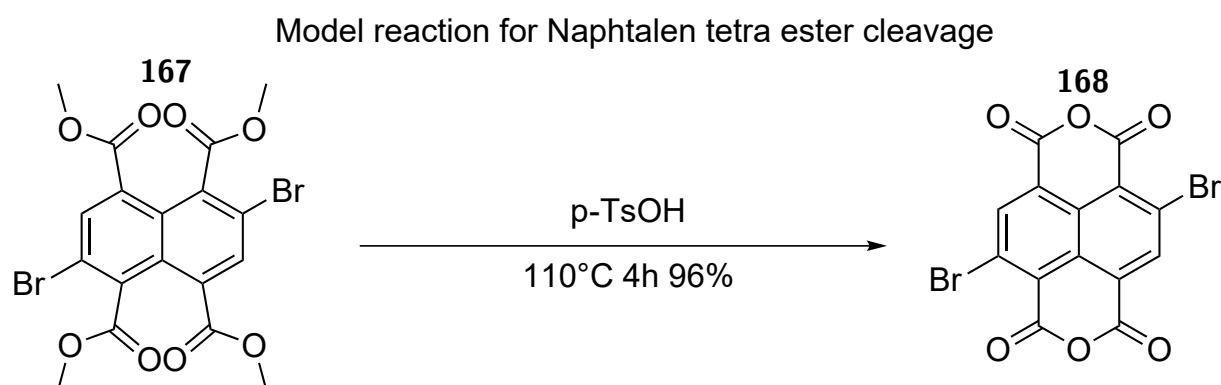
4.3 Development of direct arylation polycondensation condition for innovative NDA-based materials for OFTF applications

4.3.1 Latent pigment approach a clever solution for OS polymers

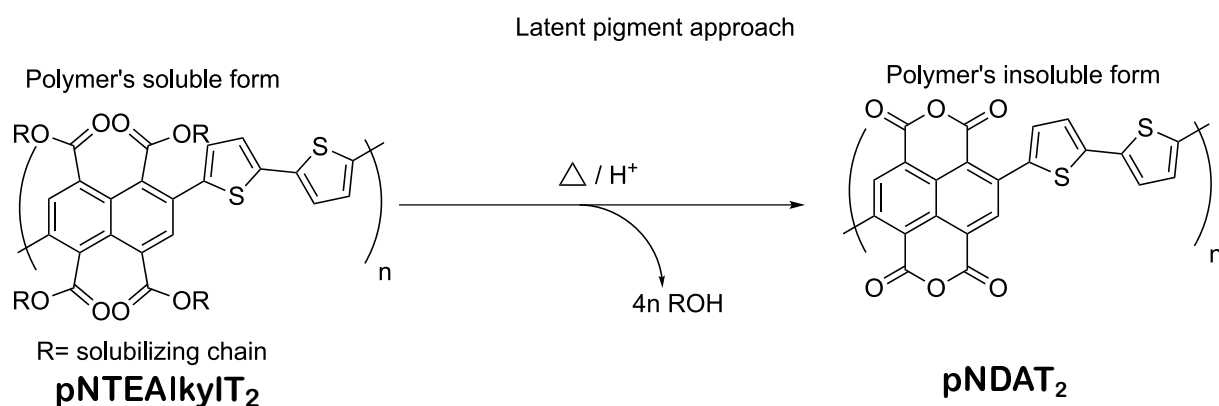
Solution-based techniques are widely used to deposit organic thin films mainly because of the facility of obtaining large-area films by printing techniques. On the lab scale the spin coating is the most convenient technique for the active layer deposition on small surface area, the reason of its success are simplicity of the method. Usually a small amount of coating material is applied on the center of the substrate, then the substrate is rotated at high speed in order to spread the coating material by centrifugal force. However spin coating is characterized by very high wastes of ink (in the 90% range) and is not scalable to a R2R process. Scalable printing/coating techniques like slot-die coating,¹⁸ flexographic printing,¹⁹ or gravure printing,²⁰ are the solution-processed techniques used at industrial scale. R2R compatible printing techniques require ink formulation with relatively higher viscosities.^{21, 22} This means high concentrations must be exploited. The simplest way to increase the solubility of a polymer is to increase the number, length and branching degree of the alkyl side chain.^{23, 24} In general a trade-off between the polymer's core part and side chains part must be found. Indeed in order to maintain good device performance of OS polymer must be limited the amount of electrically insulating moieties and to keep a good morphology, and ultimately to avoid interfering with the charge-transport properties.²⁵ The solution viscosity is also proportional to the molecular weight of the polymer. The molecular weight must be high enough, but beyond a critical threshold, at sufficiently high concentrations the chains begin to entangle and the rheology of the solution becomes difficult to control. Under these premises, the best compromise between the polymer structure, polymer concentration and molecular weight must be carefully identified for a good and scalable processability of the polymeric material. Regarding to the transport properties of polymers materials, dense molecular packing is also an important factor for efficient charge transport in PFET applications.^{26, 27} From the perspective of molecular packing engineering, the π - π stacking distance, degree of crystallinity, and quality of the crystalline domains are widely studied in conjugated polymers.²⁸ These research trends of more aggregation and denser crystalline packing inevitably required very rigid backbone structures with a limited ratio of side chain, which would limit the solubility of polymeric semiconductors.²⁷ Another problem linked with the presence of the alkyl chains in the polymer structure is the chemical stability of the materials, the general trends seem to be that monomers fused systems are more stable while those with side chains especially those attached in quaternary positions or at hetero atoms promote degradation. The side chains are often the preferred first point of attack of reactive oxygen species, ultimately resulting in the degradation of the conjugated structure.²⁹⁻³¹ A clever alternative strategy to overcome all the limit presented above consists in the latent pigment approach: putting thermo/acid-cleavable side chains on the polymer. The flexible alkyl chains allow the dissolution and the processing of the material, but once the active layer is formed a thermal/acid treatment can be applied to remove the chains.³² In this section we report the development of an innovative OS copolymer materials (pNTAT₂) based on co-monomers : 1,4,5,8-naphthalenetetracarboxylic dianhydride (NDA) and bithiophene (T₂), shown

4.3. DEVELOPMENT OF DIRECT ARYLATION POLYCONDENSATION CONDITION FOR INNOVATIVE NDA-BASED MATERIALS FOR OTFT APPLICATIONS

in scheme 4.7. NDA derivatives were not previously considered like active materials for OTFT, despite having a structure very similar to NDI-based materials: indeed both NDA and NDI present a naphthalene core system conjugated to electron withdrawing groups in planar geometry, respectively anhydrides and amides. The reasons for this lack are due to the insolubility of the NDA derivatives which makes them hardly suitable as monomers in a polymerization reactions. We aimed at developing a copolymers family based on NDA by the latent pigment approach. The easy accessibility of the polymer and thereby of the constituting monomers, is a further key element that must be considered in the design of a new OS polymeric material. For this reason we optimized the monomer synthesis and polymerization reactions for the soluble polymer precursor (pNTEAlkyIT₂, see scheme 4.7) of the NDA-based copolymer. The reaction that we have decided to exploit to convert a potentially very soluble and processable structure into the insoluble and highly stable NDA is shown in the scheme 4.6. The reaction has been developed within the research group for other purposes, but we thought it can be used for our purposes, indeed replace the methyl group of compound **167** with a longer chain is possible to obtain highly soluble co-monomer suitable for the synthesis of soluble precursor polymer pNTEAlkyIT₂. Keeping in mind that another important factor to consider in the development of new material OS is the sustainability and scalability of the synthesis, we are engaged in the study of optimization of the co-polymerization conditions by direct arylation condensation.



Scheme 4.6 Model reaction for Naphtalene tetra ester derivative cleavage

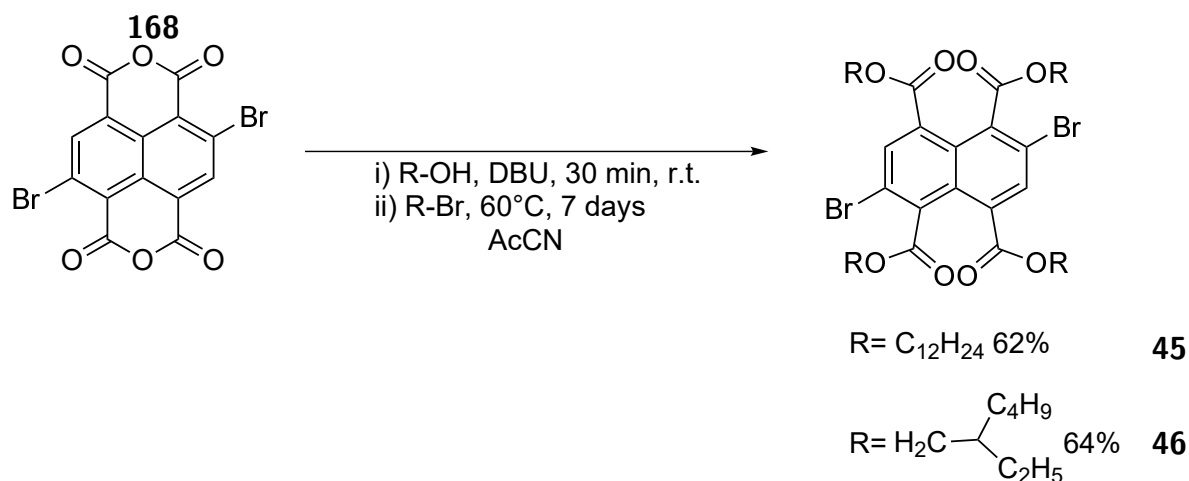


Scheme 4.7 Latent pigment approach

4.3.2 Results and discussion

4.3.2.1 Monomers synthesis and preliminary data

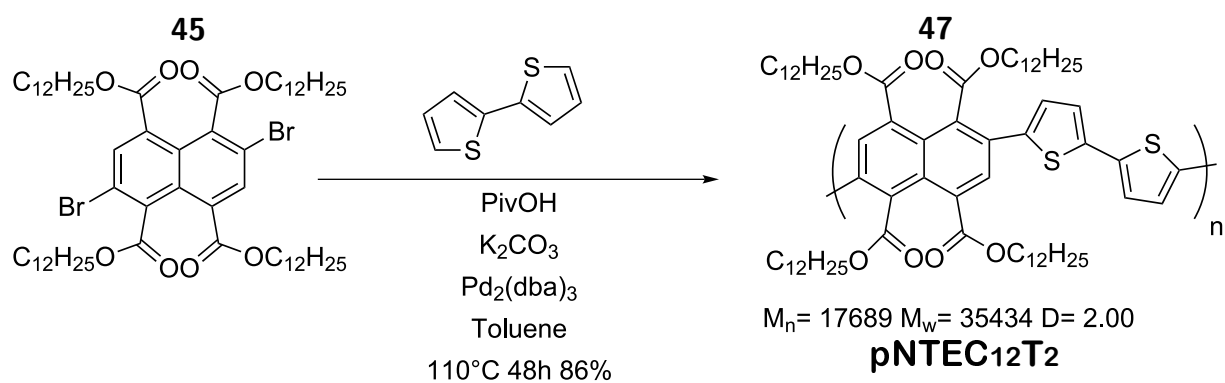
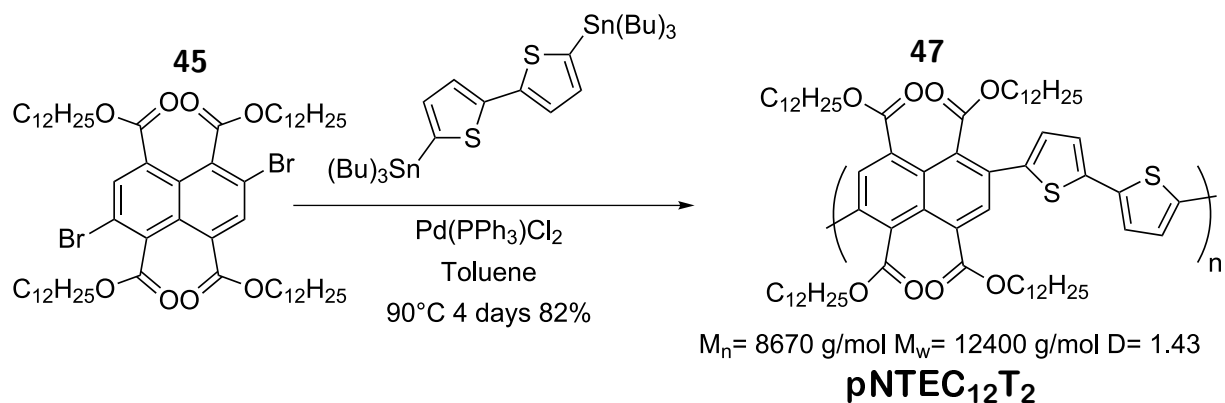
In order to start our study we decided to synthesize different naphthalene's monomers, with different alkyl chain, in particular we focused on the synthesis of a derivative with a long carbon chains, dodecanoyl groups (**45**) and a derivative with a branched chains, 2-ethyl-hexyl groups (**46**). Scheme 4.8 shows the synthesis of compounds **45** and **46**, is only a synthetic step that start from the commercial 2,6-dibromonaphthalene-1,4,5,8-tetracarboxylic dianhydride (**168**, NDABr₂) that was reacted with an alcohol: lauryl alcohol for compound **45** and 2-ethylhexanol for **46** for the initial double esterification of the dianhydride **168** to give the not isolated diester-dicarboxylic acid intermediates that was deprotonated by DBU and finally O-alkylated by nucleophilic substitution on the corresponding alkyl-bromide: 1-bromo-dodecane for compound **45** and 1-bromo-2-ethylhexane for compound **46**; to give the naphthalene tetra ester derivatives **45** and **46**.



Scheme 4.8 Syntheses monomers **45** and **46**

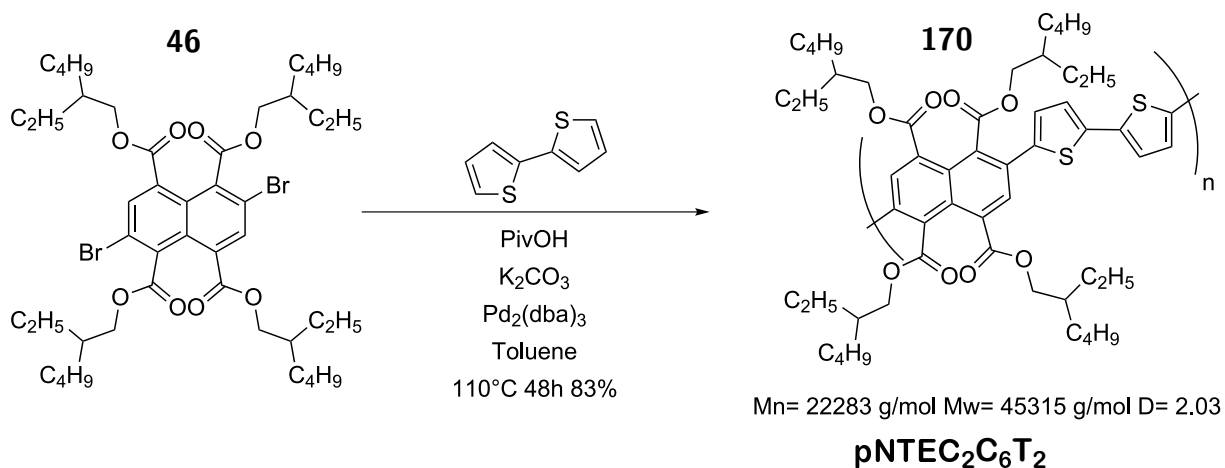
We tried the copolymerization with 2,2'-bithiophene by Stille and Direct arylation polycondensations. As the first attempt to obtain pNTEC₁₂T₂ we used Stille polycondensation in order to have a comparison for the development of a greener direct arylation protocol. As it is possible to see in the scheme 4.9 a copolymerization conditions are monomer **45** was reacted with 5,5'-Bis(tributylstannyl)-2,2'-bithiophene in Toluene at 90°C for 4 days to afford poly{tetradecyl 2-([2,2'-bithiophen]-5-yl)naphthalene-1,4,5,8-tetracarboxylate} (**47**, pNTEC₁₂T₂) with values M_n and M_w of 8.8 Kg/mol, 12.4 Kg/mol, if we take into account that the monomeric unit weighs 1141.73 g / mol, the obtained pNTEC₁₂T₂ was formed by chains averagely long only 8 monomeric units. Luckily, with direct arylation protocols (scheme 4.9): by reacting monomer **45** with 2,2'-bithiophene, in Toluene at 110°C for 2 days, we could obtain pNTEC₁₂T₂ with values around double M_n value and triple M_w value respect the Stille protocols (M_n = 17.7 Kg/mol, M_w = 35.4 Kg/mol).

4.3. DEVELOPMENT OF DIRECT ARYLATION POLYCONDENSATION CONDITION FOR INNOVATIVE NDA-BASED MATERIALS FOR OFTF APPLICATIONS



Scheme 4.9 Preparation of copolymer pNTEC₁₂T₂

DAP turns out to be the most efficient polymerization protocol for this type of copolymer, so we have moved on to the synthesis of the copolymer poly{tetrakis(2-ethylhexyl) 2-([2,2'-bithiophen]-5-yl)naphthalene-1,4,5,8-tetracarboxylate} (**169**, pNTEC₂C₆T₂), in the same DAP condition used for the synthesis of copolymer pNTEC₁₂T₂. As expected the copolymerization of the monomer **46** has led to comparable yield but better results in terms of length of the polymer chains with respect to pNTEC₁₂T₂, in fact the four branched chains impart greater solubility to the polymer allowing further growth (scheme 4.10).



CHAPTER 4. GREEN APPROACHES TO THE PREPARATION OF ORGANIC POLYMERIC SEMICONDUCTORS

The polymers **46** and pNTEC₁₂T₂ obtained by DAP were characterized by cyclic voltammetry (CV). For both of them, it is possible to observe reversible oxidation processes centered at 0.08eV and 0.09eV (respectively) vs Fc/Fc⁺, underlining that **46** has an electrochemical HOMO level of -4.86eV, meanwhile pNTEC₁₂T₂ -4.66eV. Surprisingly, according to this data, the pNTE copolymers are p-type materials, against our expectation, is probably that ester groups are extremely twisted compared to the monomer's main plane, therefore electric properties are similar to pristine naphthalene.

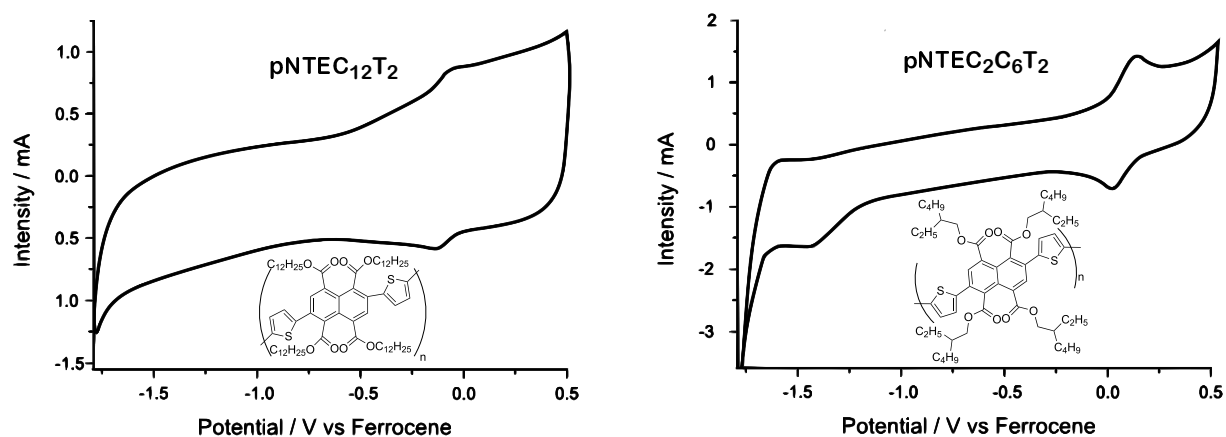


Figure 4.8 Cyclic voltammograms of pNTEC₁₂T₂ (left) and pNTEC₂C₆T₂ (right). Measures are made between 0.5 and 1.6V vs ferrocene. WE:glassy carbon, Reference electrode Ag/AgCl and auxiliary electrode Pd, using TBAPF₆/DCM 0.1 M solution as electrolyte. It is possible to notice that they are p-type polymers.

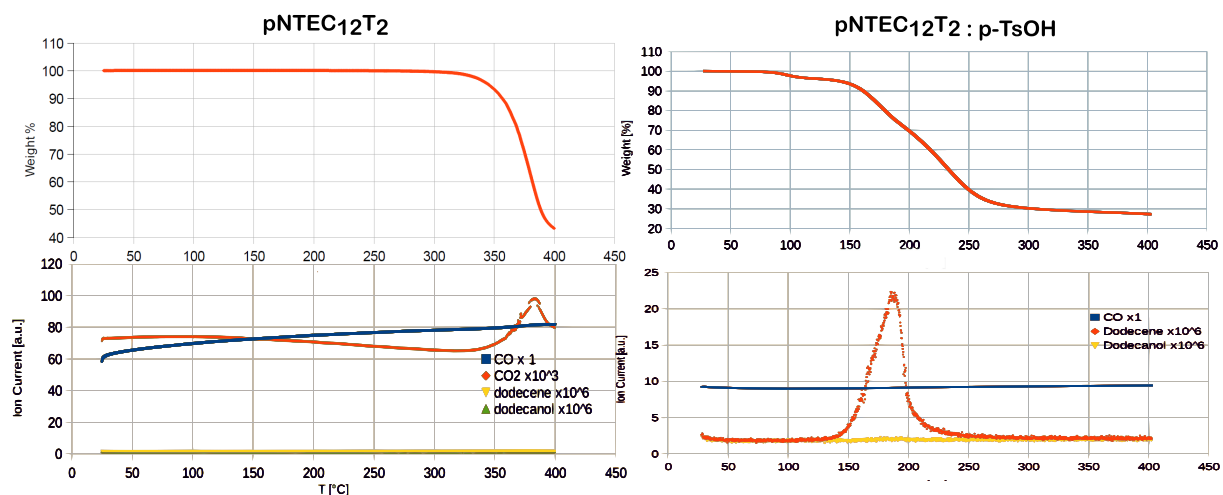


Figure 4.9 TGA-MS analysis of polymer pNTEC₁₂T₂ (on the left) and TGA-MS analysis of the blend pNTEC₁₂T₂:pTsOH (on the right)

In order to verify if pNTE copolymers could be used as a latent pigment, we have performed a TGA-MS analysis on a pNTEC₁₂T₂ sample under N₂ at a heating rate of 5°C/s from room temperature up to 400°C, monitoring the weight loss over time (see figure 4.9). It is possible to notice that the cleavage reaction starts at around 300°C and almost no mass is lost under 300°C temperature. The gasses emitted are CO and CO₂ no signs of dodecene and dodecanol are found, probably because at so high temperature dodecene and dodecanol degrade immediately a carbon's oxides or they are not detectable. In

4.3. DEVELOPMENT OF DIRECT ARYLATION POLYCONDENSATION CONDITION FOR INNOVATIVE NDA-BASED MATERIALS FOR OFTF APPLICATIONS

order to study if it is possible to catalyzed the cleavage reaction with acid catalyst, we repeated the experiment with a blend of p-Toluenesulfonic acid and pNTEC₁₂T₂. As it is possible to see in figure 4.9 the cleavage reaction starts at low temperature, around 150°C. This time from MS chromatogram it is clearly visible the dodecene peak, product of the catalyzed acid reaction of dodecanol dehydration.

We investigated the structure of the polymer obtained after the thermal/acid cleavage by FT-IR spectroscopy, the spectra are shown in figure 4.9, in blue is reported the monomer **168**'s spectra is possible to note the two characteristic carbonyl signals due to symmetrical (1780 cm⁻¹) and asymmetric (1730 cm⁻¹) C = O stretching of the anhydrides between 1700-1800 cm⁻¹, in red is reported the pNTEC₁₂T₂'s spectra, in the same region is possible to see only one C=O signals due to the carbonyl stretching of the ester, in yellow and in green are reported the spectra of the resulting polymer after the only thermal treatment (yellow) and the thermal/acid treatment in green is possible to note that the characteristic peaks of the anhydride reappear, confirming the structure of the resulting polymer pNDAT₂. Figure 4.11 shows: on the left the pNTEC₁₂T₂: p-TsOH blend; in the center the same sample after the cleavage treatment (180°C) and on the right a samples of pure pNTEC₁₂T₂ treated at higher temperatures (400°C). The co-polymer changed from a brown opaque to a violet shiny color, and sample consistence changed from soft and sticky to hard and brittle,

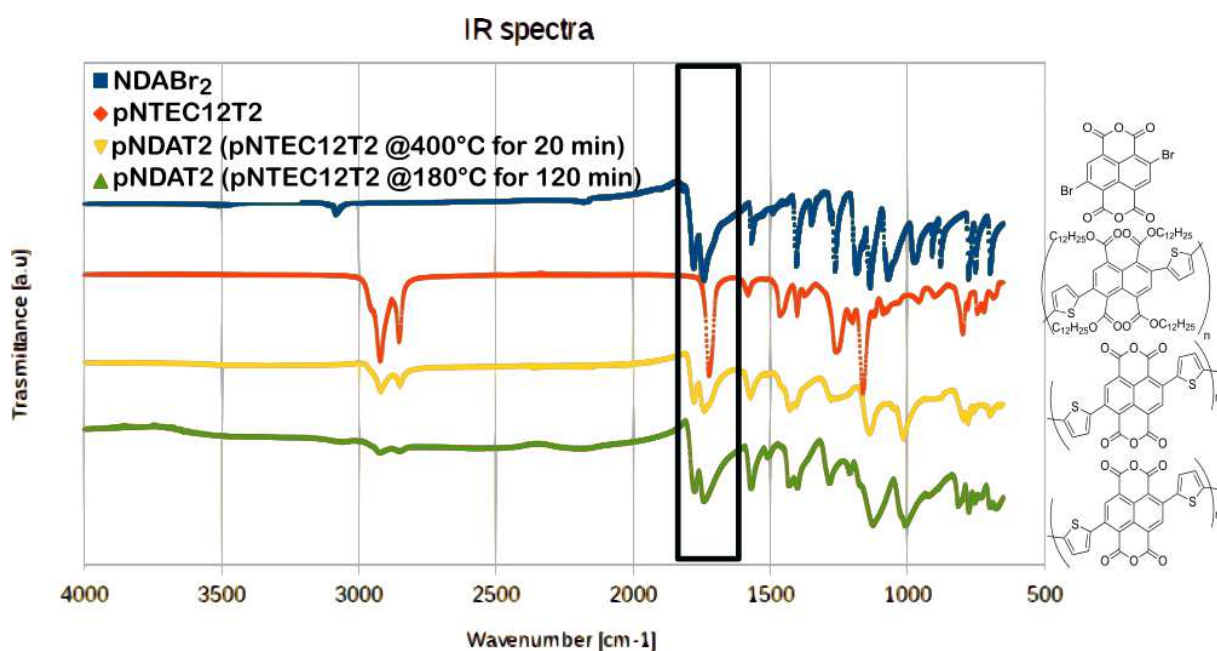


Figure 4.10 FT-IR investigation on polymer structure obtained by thermal/acid cleavage of the precursor polymer pNTEC₁₂



Figure 4.11 On the left: pNTEC₁₂T₂ before thermal treatment; in the center: pNTEC₁₂T₂ after thermal treatment with p-toluene sulfonic acid at 180°C, under N₂ for 2h; on the right: pNTEC₁₂T₂ after thermal treatment at 400°C, under N₂ for 20 minutes

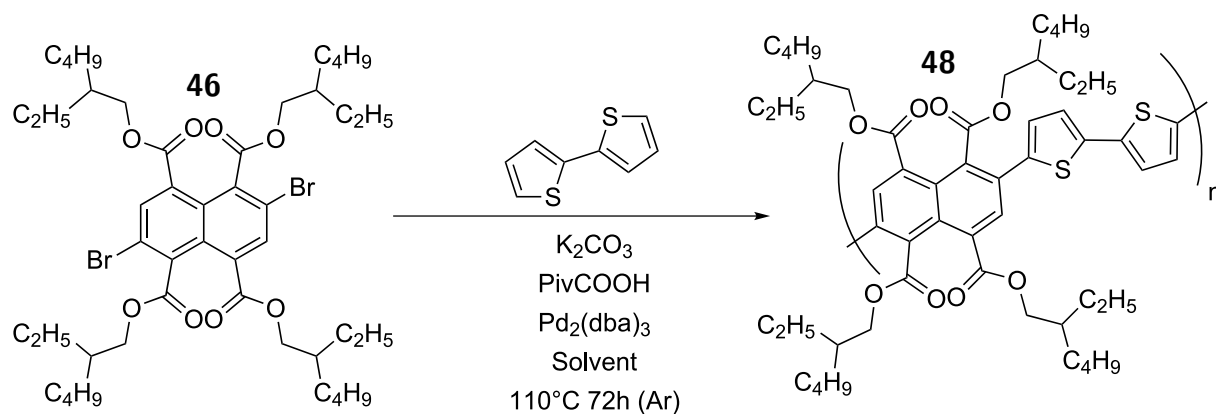
Encouraged by these first results we have moved on to the optimization of pNDAT₂ copolymerization to have more processable polymers and useful tools for the tuning of the polymer molecular weight. The optimization of copolymerization was done on the polymer **46** indeed we expected that the branched chains would allow us to achieve high molecular weights and high film-forming properties of the material. Compared with linear side chains, branched side chains have attracted more attention from researchers as they can provide better solubility for polymers.^{33–36]}

4.3.2.2 Optimization of the polymerization conditions

Influence of the solvent

The solvent for direct arylation polycondensation (DAP) is of crucial importance. When conjugated polymers exhibiting reduced solubility, the choice of solvent influences the maximum molecular weight that can be achieved, indeed polymer's precipitation is the main mechanism of termination, aromatic solvents have proved to be very useful in DAP. However, unintentional activation of C–H bonds present in aromatic solvents under DAP conditions leads to in situ solvent termination which competes with step growth.³⁷ pNTEC₂C₆T₂ was designed in order to be highly soluble in fact, the presence of four ethylhexyl chains gives high solubility to the naphthalene core in aromatic solvent like Toluene. In literature is reported a study of solvent quality of several aromatic solvents for the DAP of defect-free naphthalene diimide (NDI)-based copolymers of different solubility. The authors correlate C–H reactivity of the solvent with copolymerization behavior and MW and conclude that solvent's C–H reactivity is strongly reduced with increasing degree of substitution for both chlorine and methyl substituents. Mesitylene is largely C–H unreactive and, thus, albeit being a moderate solvent, enables very high molecular weights at elevated temperature for NDI copolymers with limited solubility.³⁸ Given the structural analogy between pNTEC₂C₆T₂ and (NDI)-based copolymers, we decided to test Mesitylene for pNTEC₂C₆T₂ copolymerization.

4.3. DEVELOPMENT OF DIRECT ARYLATION POLYCONDENSATION CONDITION FOR INNOVATIVE NDA-BASED MATERIALS FOR OFTF APPLICATIONS



Entry	Solvent	Yield / solvent (%)	M_n (g/mol)	M_w (g/mol)	D
1	Mesitylene	73/ CHCl ₃	34013	82120	2.38
2	Toluene	65 / ETP	16606	23760	1.43

Table 4.3 Solvent optimization for DAP of copolymer pNTEC₂C₆T₂ (**170**)

Table 4.3 shows a comparison between two pNTEC₂C₆T₂ copolymerization carried out under identical condition apart from the nature of the solvent. Comparing M_n , M_w and D of the two copolymers it is clear that Mesitylene is more effective solvent for polymerization rather than Toluene, It is interesting to note that the reaction mixture turned into a gel after 72h at 110 ° C due to the precipitation of the copolymer, a symptom that the solubility of the polymer had become the main termination mechanism of the polymerization rather than the solvent termination. Copolymer's high-molecular-weight fraction formed in Mesitylene were insoluble in petroleum ether unlike the one prepared in Toluene.

Influence of the temperature and monomers concentration

In order to obtain even higher molecular mass values we have considered two different strategies to increase the solubility of the growing polymer chains in Mesitylene: increase the reaction temperature or decrease the concentration of the monomers in order to work in a more diluted environment. In entry 2 of the table 4.4 is reported a copolymerization at 140°C, instead of 110°C, values of $M_n = 18.2$ Kg/mol, $M_w = 28.8$ Kg/mol were obtained at 140°C, values considerably lower than $M_n = 34.0$ Kg/mol, $M_w = 82.1$ Kg/mol for the reaction carried out at 110°C, symptom others termination mechanism become limiting at higher temperatures, like the debromination. In entries 3 e 4 are reported the more dilute conditions with respect to the reference entry 1, for this parameters was observed that the higher molecular mass values were obtained for monomers' initial concentration of 0.25M (entry 3), an intermediate concentration between 0.1M (entry 4) and 0.5M (entry 1). Indeed on the one hand the lower concentration of the initial monomers leads to a greater growth of the polymer, on the other an excessively diluted environment leads to slower kinetics and an increase of the solvent termination. By tuning of the monomer concentration was possible isolate high-molecular-weight ($M_n = 43.6$ Kg/mol, $M_w = 102.0$

CHAPTER 4. GREEN APPROACHES TO THE PREPARATION OF ORGANIC POLYMERIC SEMICONDUCTORS

Kg/mol pNTEC₂C₆T₂ with an excellent yield of 90% maintaining a relatively narrow molecular-weight-distribution (D= 2.30).

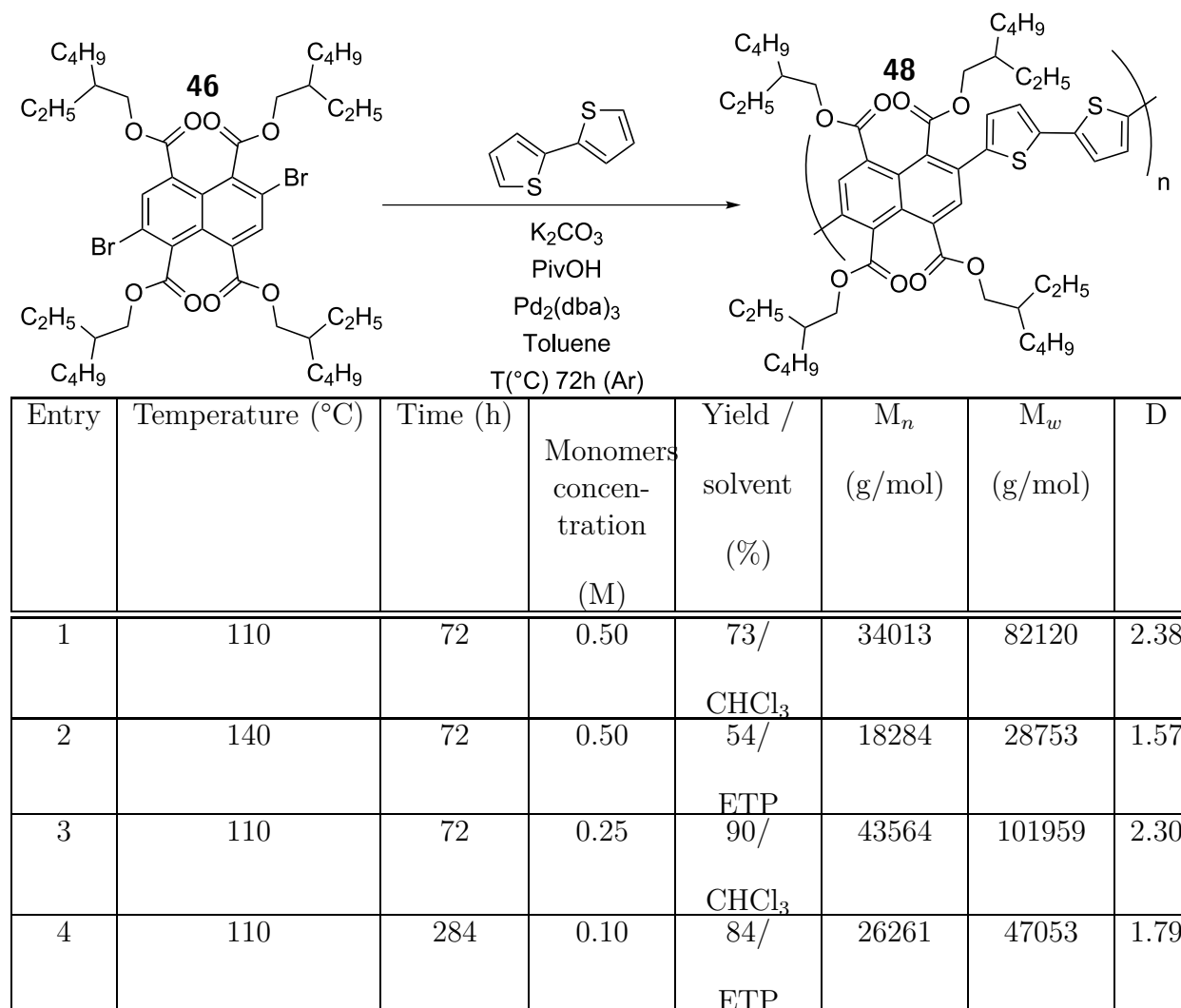


Table 4.4 Temperature optimization for DAP of copolymer pNTEC₂C₆T₂ (170)

Influence of the monomers ratio

Always inspired by a work of literature on NDI-based copolymer, another factor studied was the monomers ratio. Usually this type of empirical study is done to obtain an effective ratio between monomers equal to 1:1, because the monomers often have impurities, but in reported work it has been shown that for poly{[N,N'-bis(2-octyldodecyl)naphthalene-1,4,5,8-bis-(dicarboximide)-2,6-diyl]-alt-5,5'-(2,2'-bithiophene)} (pNDIT₂), slight excess of bromide leads to higher molecular weights respect a 1:1 ratio. This result was explained by the authors by mechanistic reasons proved by NMR polymer's end chain study.³⁹

4.3. DEVELOPMENT OF DIRECT ARYLATION POLYCONDENSATION CONDITION FOR INNOVATIVE NDA-BASED MATERIALS FOR OTTF APPLICATIONS

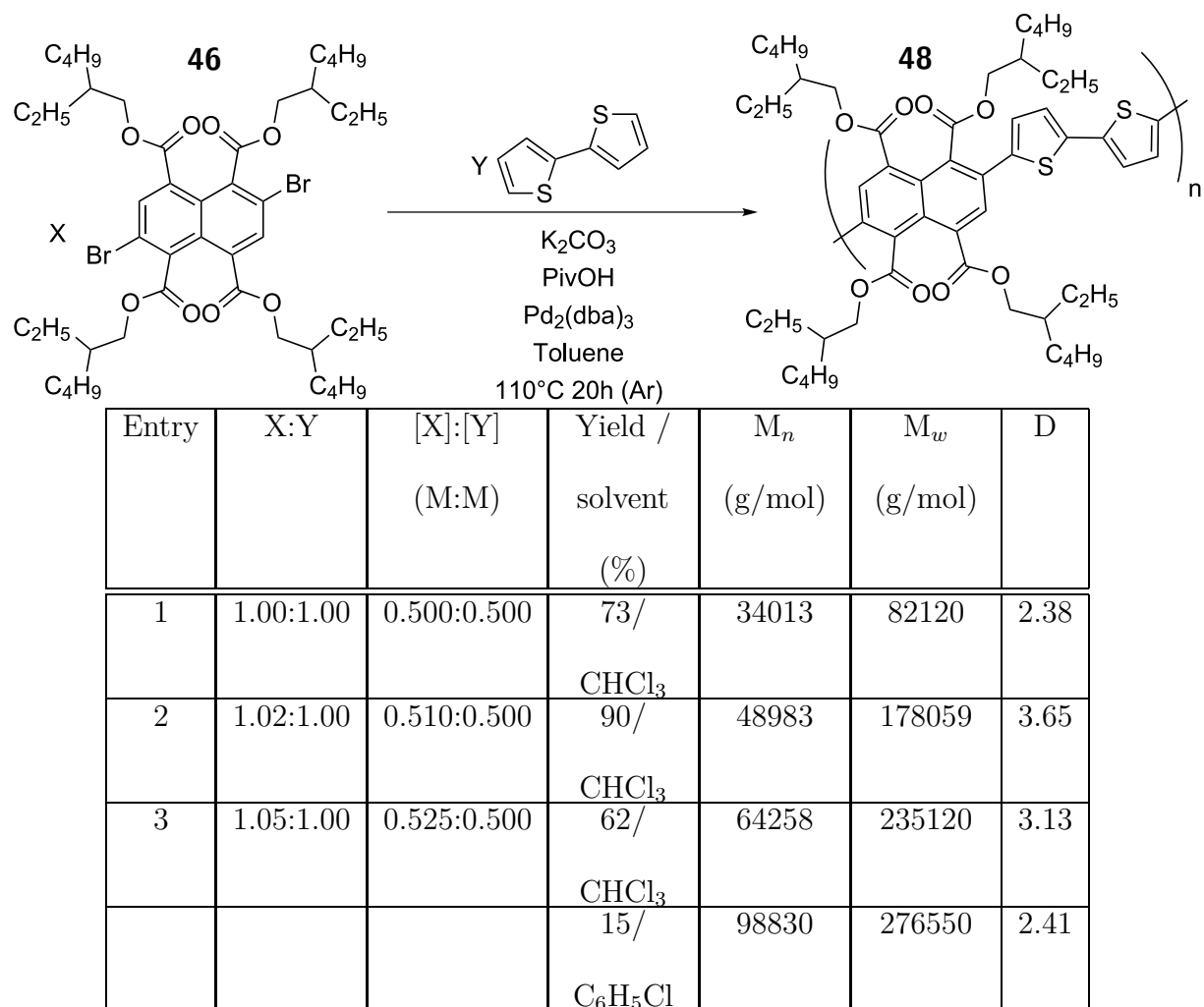


Table 4.5 Comonomers ratio optimization for DAP of copolymer pNTEC₂C₆T₂ (**170**)

Table 4.5 shows that also for the copolymerization of pNTEC₂C₆T₂ was observed this trend, indeed when 2% (Entry 1) and 5% (entry 3) molar excess of bromide were employed the polymers obtained have very high molecular-weight. For examples for the higher molecular-weight fraction obtained for the entry 3, that was extracted in chlorobenzene the values of M_n , M_w and D are 98.8 Kg/mol, 276.6 kg/mol and 2.41.

4.3.3 Conclusion

The development of ambient stable organic n-channel semiconductor molecules for thin-film transistors has experienced a tremendous impetus in the last decade to close the gap in performance in comparison to that of their p-channel counterparts. Especially naphthalene tetracarboxylic diimides (NDI) have shown to be the most valuable building blocks to achieve this challenging goal and to gain insight into the molecular structure-transistor performance relationship.⁴⁰ 1,4,5,8-Naphthalenetetracarboxylic dianhydride (NDA) derivatives were not previously considered as active materials for OTFT, despite having a structure very similar to NDI. Aiming at developing NDA-based copolymers thanks the latent pigment approach, clever alternative to the more traditional side chain functionalization. For this reason we optimized the synthesis and the co-polymerization

CHAPTER 4. GREEN APPROACHES TO THE PREPARATION OF ORGANIC POLYMERIC SEMICONDUCTORS

of NTE monomers obtaining a soluble and easily processable co-polymer from solution, precursor of an NDA-based copolymer potentially useful for highly stable OTFTs. Always keeping in mind that beyond the performance and stability of the materials it is very important to develop sustainable synthesis, for a possible scaling up at industrial level, we have developed a copolymerization by direct arylation polycondensation. The parameters investigated were the nature of the solvent, temperature, monomer's concentration and ratio. All these parameters have a great influence on the final material and so it is possible to tune the molecular weight distribution of the final copolymer changing this copolymerization's parameters. The possibility of being able to adjust the molecular weights of the co-polymer is a fundamental tool to find a good balance between performance and processability. The materials are now in OTFT characterization phase in order to evaluate the OTFT performance and also is under development an effective strategy in order to make the cleavage for the precursor copolymer at low temperatures and as fast as possible, in order to make the latent pigment approach compatible with plastic substrates. The figure 4.12 shows a free-standing film obtained by accidental evaporation of the solvent of a pNTEC₂C₆T₂ solution, has been reported as evidence of the excellent film-forming properties of the material.

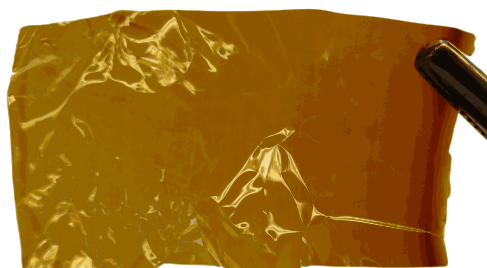
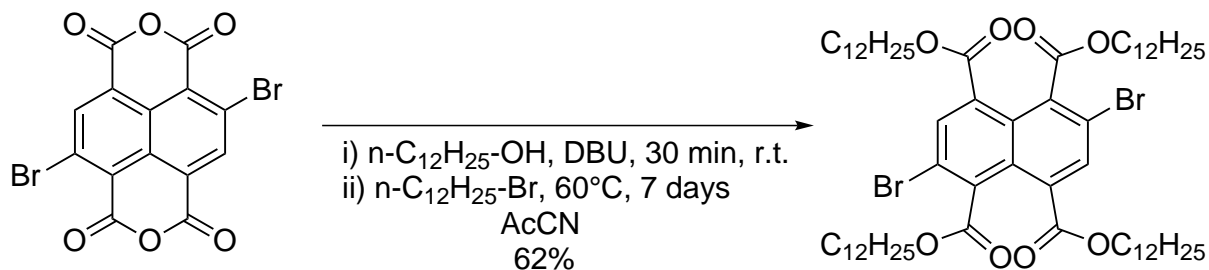


Figure 4.12

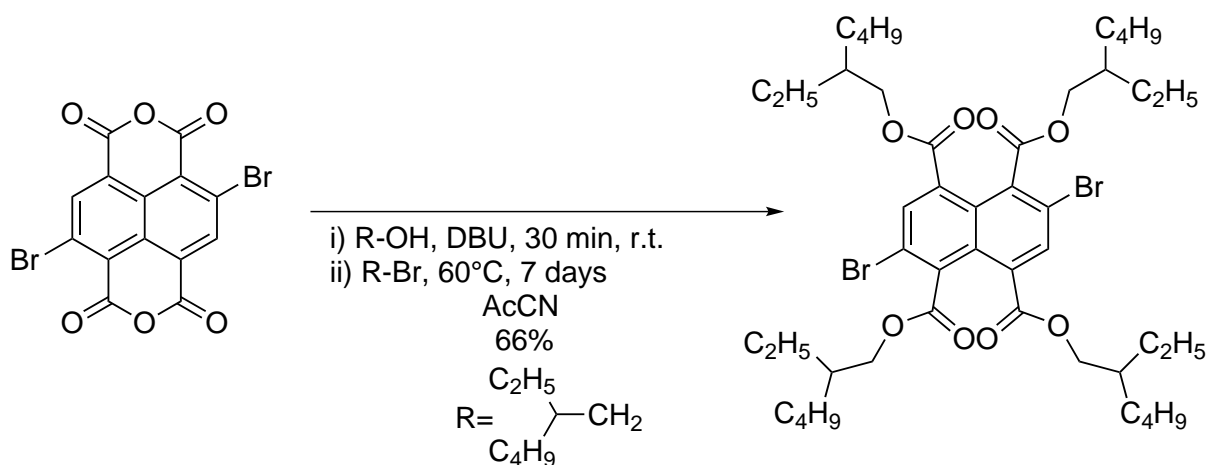
4.3.4 Experimental part

4.3.4.1 Synthesis of tetradodecyl 2,6-dibromonaphthalene-1,4,5,8-tetracarboxylate (45)



In a two neck flask, under N₂, a mixture of 2,6-dibromonaphthalene-1,4,5,8-tetracarboxylic dianhydride (6.164g, 14.47 mmol) and dodecanol (6.725g, 36.08) in 40mL of dry acetonitrile was prepared. DBU (5.434g, 35.694mmol) were added under stirring. After 30min 1-bromododecane (8.774g, 35.199mmol) is added and the solution was heated at 60°C for 2 days. After cooling down the reaction, the solvent is evaporated, petroleum ether is added and the solid particulate (DBU salt) is filtered away. Petroleum ether was evaporated under reduce pressure and crude product was obtained. The crude product is purified by column chromatography using n-heptane : toluene 1:1 as eluent. After purification tetradodecyl 2,6-dibromonaphthalene-1,4,5,8-tetracarboxylate was obtained as a white solid (9.932g , 8.751mmol, 62%). ¹H NMR (500MHz, CDCl₃) δ [ppm]: 8.05 (s, 2H), 4.29 (t, J=6.8Hz, 8H), 1.81-1.75 (m, 4H), 1.47-1.26 (m, 72H), 0.88 (t, J=6.8, 12H).

4.3.4.2 Synthesis of tetrakis(2-ethylhexyl) 2,6-dibromonaphthalene-1,4,5,8-tetracarboxylate (46)



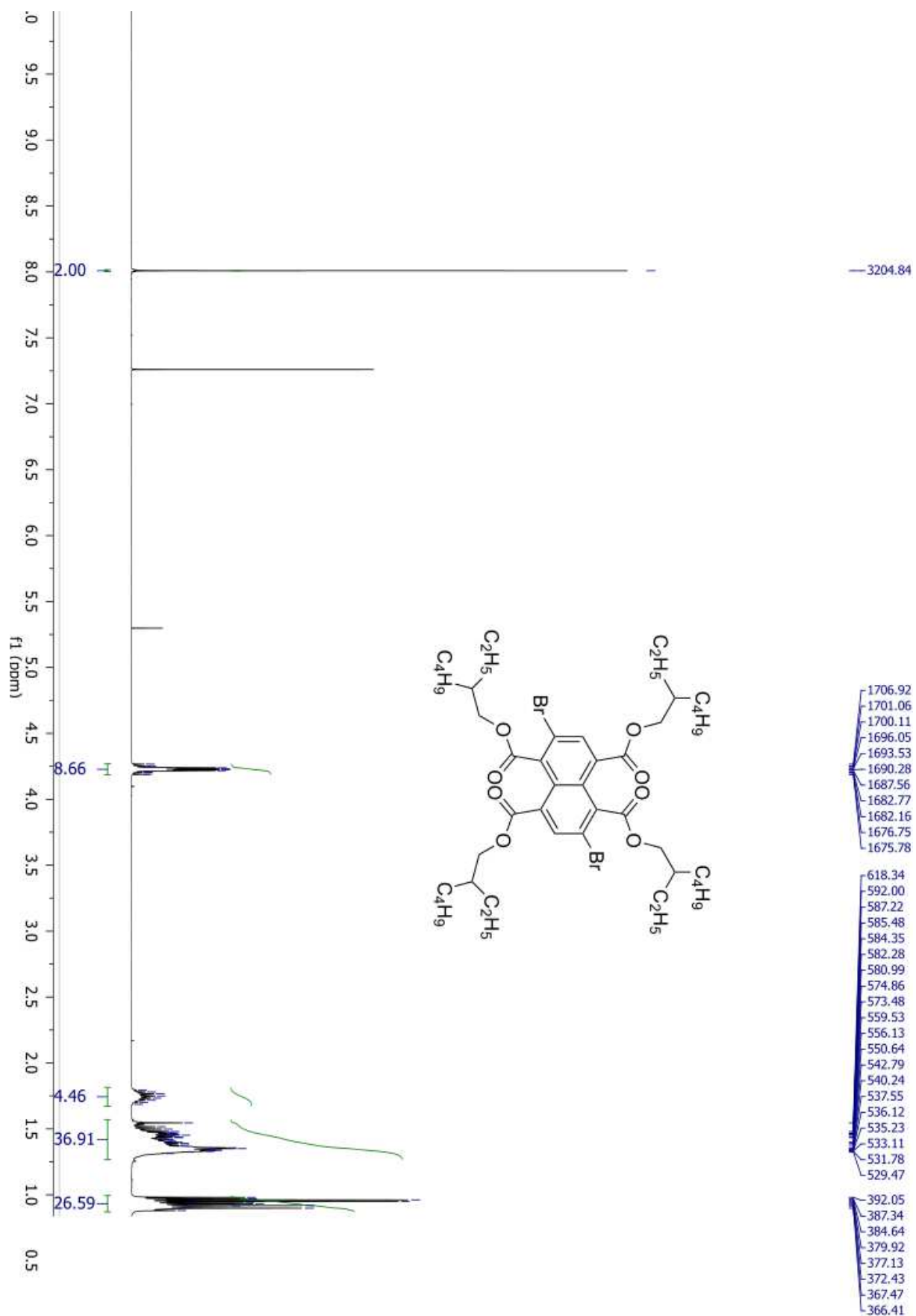
In a two neck 100mL flask, a mixture of 2,6-dibromonaphthalene-1,4,5,8-tetracarboxylic dianhydride (4.000 g, 9.390 mmol) and 2-ethylhexan-1-ol (3.057 g, 23.48 mmol) was prepared. Acetonitrile anhydrous (40 mL) and DBU (3.574g, 23.48 mmol) were added under

CHAPTER 4. GREEN APPROACHES TO THE PREPARATION OF ORGANIC POLYMERIC SEMICONDUCTORS

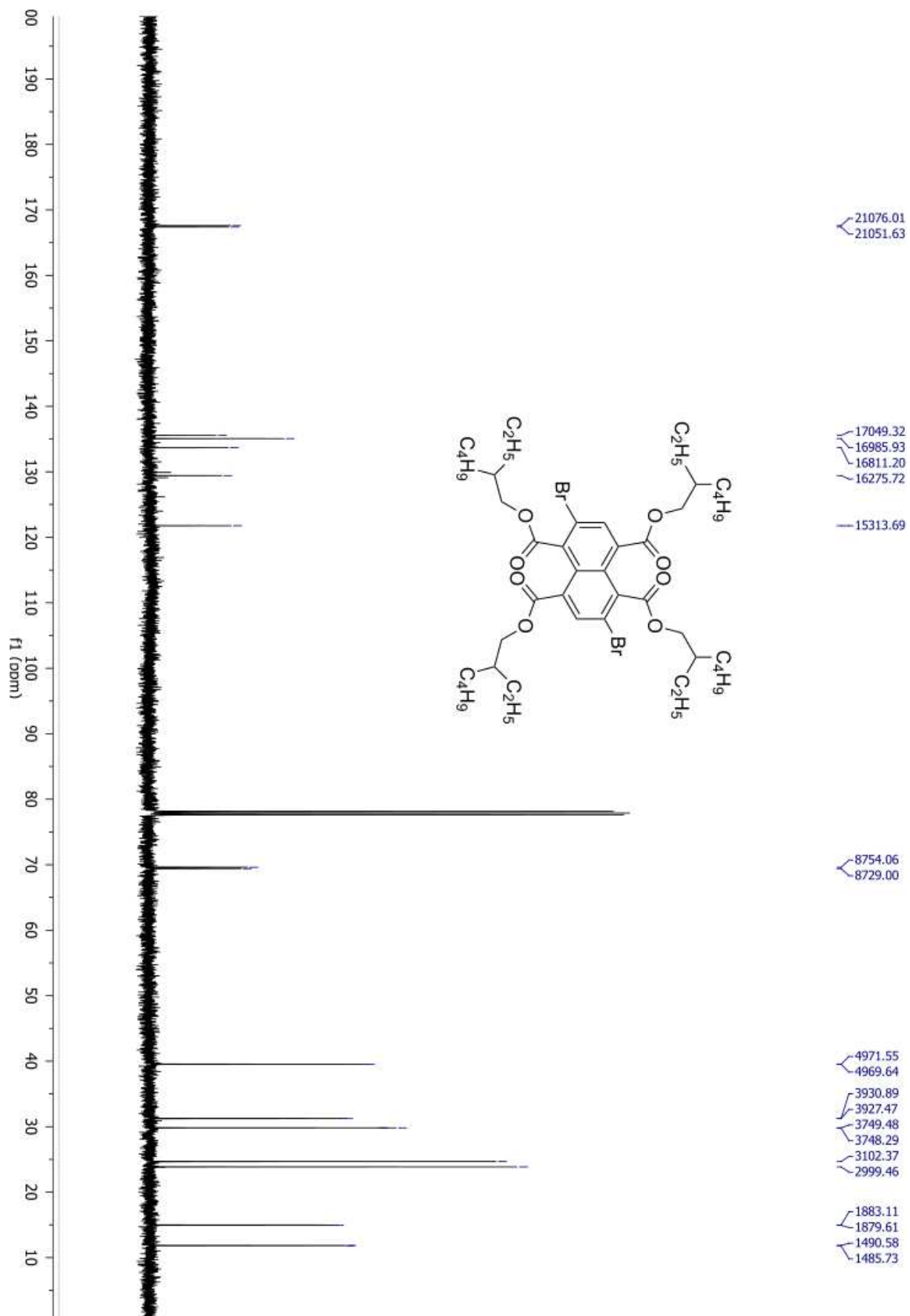
stirring. After 30 min 3-(bromomethyl)heptane (4.534 g, 23.48 mmol) was added and the solution is heated at 60°C for 7 days. Then reaction is stopped and it is cooled down at room temperature. After cooling down the reaction, the solvent is evaporated, petroleum ether is added and the solid particulate (DBU salt) is filtered away. Petroleum ether was evaporated under reduce pressure. Crude product was purified by chromatographic columns on silica using a mixture of heptane and toluene (7:3 → 3:7) in gradient elution product was obtained in pure form as a clear oil (5.645g, 6.197 mmol, 66% yield).

¹H NMR (500MHz, CDCl₃) δ [ppm]: 8.01(s, 2H), 4.26-4.20 (m, 8H), 1.79-1.71 (m, 4H), 1.56-1.30 (m, 32H), 0.98-0.96 (m, 24H) ¹³C NMR (126 MHz, CDCl₃) δ 167.59, 167.40, 135.57, 135.07, 133.68, 129.42, 121.77, 69.61, 69.41, 39.53, 39.52, 31.26, 31.23, 29.82, 29.81, 24.67, 23.85, 14.97, 14.95, 11.85, 11.81.

4.3. DEVELOPMENT OF DIRECT ARYLATION POLYCONDENSATION CONDITION FOR INNOVATIVE NDA-BASED MATERIALS FOR OFTF APPLICATIONS



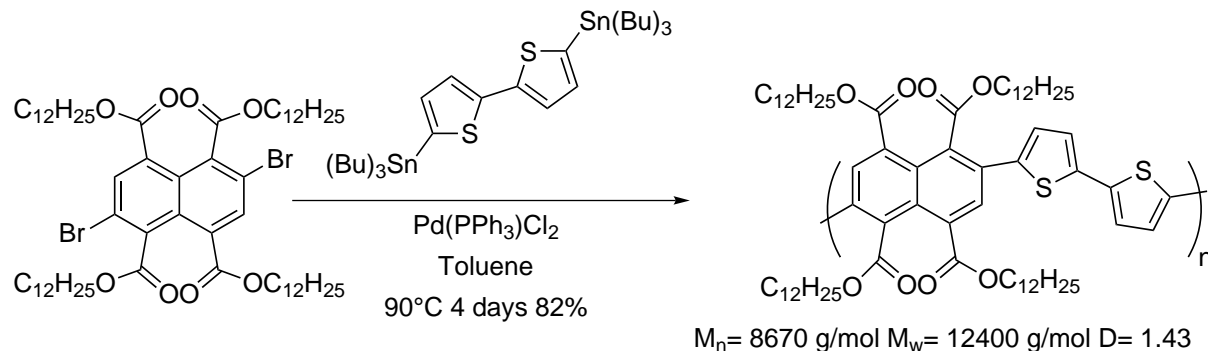
CHAPTER 4. GREEN APPROACHES TO THE PREPARATION OF ORGANIC POLYMERIC SEMICONDUCTORS



4.3. DEVELOPMENT OF DIRECT ARYLATION POLYCONDENSATION CONDITION FOR INNOVATIVE NDA-BASED MATERIALS FOR OFTF APPLICATIONS

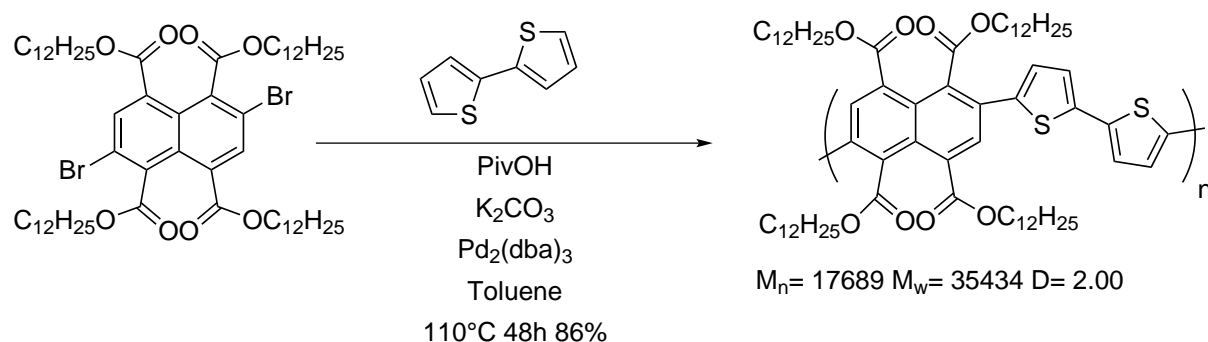
4.3.4.3 Synthesis of Copolymer Poly[tetrakis(2-dodecyl-2-([2,2'-bithiophen]-5-yl)naphthalene-1,4,5,8-tetracarboxylate) (47)

Stille polycondensation



In a two neck 50mL flask, a mixture of tetradodecyl 2,6-dibromonaphthalene-1,4,5,8-tetracarboxylate (0.499g, 0.440 mmol), 5,5'-bis(tributylstannyl)-2,2'-bithiophene (0.327g, 0.439 mmol) and $\text{Pd}(\text{PPh}_3)\text{Cl}_2$ (16.7 mg, 0.024 mmol) was prepared. Under N_2 , 23mL of toluene anhydrous and of bithiophene are added. The flask is left under stirring, under N_2 at 90°C for 4 days. The flask is cooled at room temperature and a solution of 4.6g of KF in 10mL water is added under stirring. After 2h, 150mL of dichloromethane are added and the organic phase is washed 3 times with 100mL of brine and it is dried over anhydrous Na_2SO_4 . Solvent is evaporated under reduced pressure, the product is then dissolved in 5mL dichloromethane and it is poured drop wise in MeOH. The orange sticky solid is filtered and it is continuously extracted, using MeOH, acetone, petroleum ether. Petroleum ether are then evaporated under reduced pressure to afford pNTEC₁₂T₂ (0.402 g, Yield 49%, $M_n = 8670 \text{ g/mol}$ and $M_w = 12400 \text{ g/mol}$ $D = 1.43$)

Direct arylation polycondensation



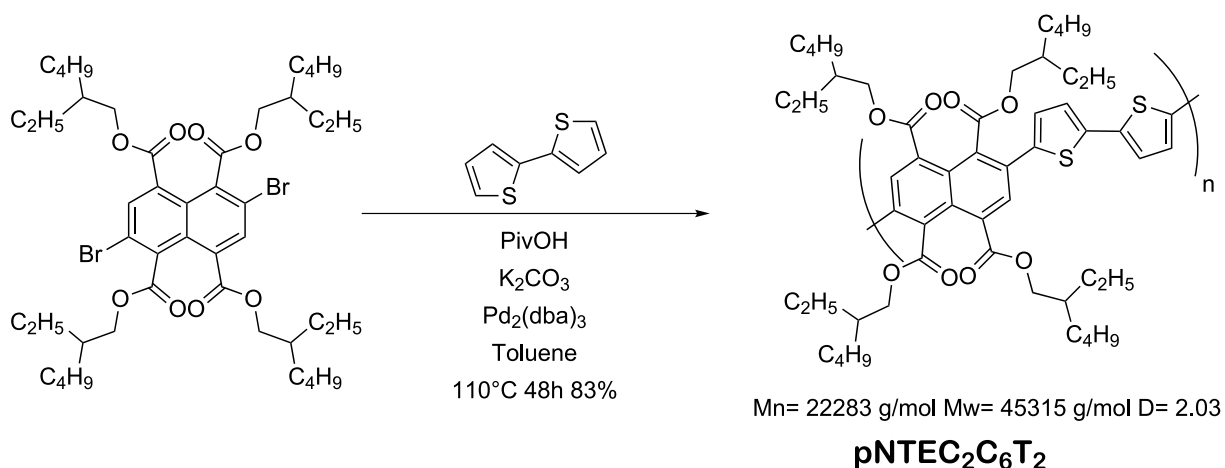
In a Schlenk tube, a mixture of tetradodecyl 2,6-dibromonaphthalene-1,4,5,8-tetracarboxylate (3.310 g, 2.916 mmol), bithiophene (0.503 g, 3.024 mmol), K_2CO_3 , pivalic

CHAPTER 4. GREEN APPROACHES TO THE PREPARATION OF ORGANIC POLYMERIC SEMICONDUCTORS

acid (0.310 g, 3.04 mmol) and $\text{Pd}_2(\text{dba})_3$ (27.6 mg, 0.0301 mmol) is prepared inside N_2 glove box. Then 6mL of toluene anhydrous are added. The reaction is left 48h under stirring at 110°C . The product is filtered and continuously extracted with MeOH, acetone and petroleum ether. Petroleum ether was evaporated under reduced pressure and the brown sticky polymer's film is washed with acetone and triturated with MeOH, After solvent removal a thick brown-orange polymeric film was obtained (2.858g, 86% Yield, $M_n = 17689$ g/mol, $M_w = 35434$ g/mol $D = 2.00$).

4.3.4.4 Synthesis of Copolymer Poly[tetrakis(2-dodecyl-2-([2,2'-bithiophen]-5-yl)naphtalene-1,4,5,8-tetracarboxylate) (48)

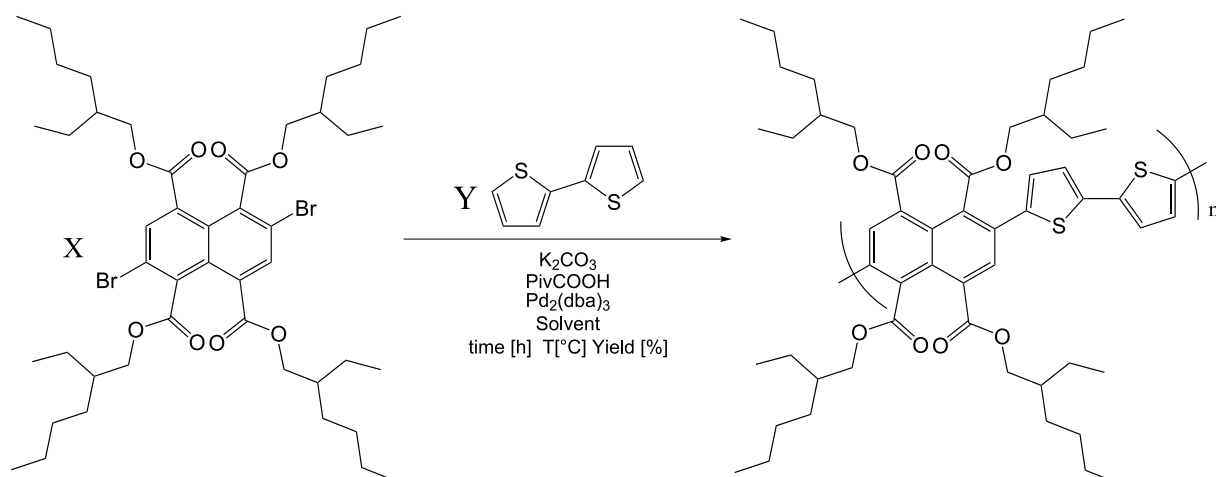
Standard reaction



In a pressure tube tetrakis(2-ethylhexyl) 2,6-dibromonaphthalene-1,4,5,8-tetracarboxylate (3.310 g, 2.916 mmol), bithiophene (0.219g, 1.32 mmol), potassium carbonate (0.846 g 3.95 mmol), pivalic acid (0.135g, 1.32 mmol) and $\text{Pd}_2(\text{dba})_3$ (12.06 mg, 0.013174 mmol) are inserted, then the tube is put inside N_2 glove box where 2mL toluene are added. After 10 min $\text{Pd}_2(\text{dba})_3$ is inserted and the tube is sealed. Solution is heated at 100°C for 1h, under stirring, then is heated at 110°C for 19h. Then the solution is cooled down to room temperature and products are dissolved in 20mL DCM. Such solution is added drop wise in 200mL MeOH, the precipitate is filtered and then continuously extracted with MeOH, acetone and petroleum ether. Petroleum ether is evaporated under reduced pressure, then the residue is triturated in MeOH, is filtered and it is dried in oven under vacuum. pNTEC₂C₆T₂ was obtain like brown solid (0.995 g, 1.10 mmol, Yield 83%, $M_n = 22293$ g/mol, $M_w = 45315$ g/mol, $D = 2.03$).

Optimization reaction

4.3. DEVELOPMENT OF DIRECT ARYLATION POLYCONDENSATION CONDITION FOR INNOVATIVE NDA-BASED MATERIALS FOR OFTF APPLICATIONS



Entry/ table	Solvent	Temp. [°C]	X:Y	time [h]	PE Fraction Yield	CHCl ₃	C ₆ H ₅ Cl	Mn [kDa]	Mw [kDa]	D
						Fraction Yield	Fraction Yield			
1/Table4.3	Mes	110	1 : 1	72	12%	73%	0	34	82	2.4
2/Table4.3	Tol	110	1 : 1	72	65%	1%	0	17	24	1.4
2/Table4.4	Mes	140	1 : 1	72	54%	1%	0	18	29	1.6
3/Table4.4	Mes	110	0.5 : 0.5	72	9%	90%	0	44	102	2.3
4/Table4.4	Mes	110	0.2 : 0.2	284	84%	0%	0	26	47	1.8
2/Table4.5	Mes	110	1.02 : 1	20	3%	90%	0	49	178	3.7
3/Table4.5	Mes	110	1.05 : 1	20	8%	62%	15%	64	235	3.1
								99	277	2.4

Table 4.6

In a reaction vessel tetrakis(2-ethylhexyl) 2,6-dibromonaphthalene-1,4,5,8-tetracarboxylate (X * 0.155 mmol), bithiophene (Y* 0.155 mmol), potassium carbonate (0.465 mmol), pivalic acid (0.155 mmol) and Pd₂(dba)₃ (0.0031 mmol) are directly weighed. Under Argon atmosphere, degassed solvent was added (0.32 mL). The reaction was stirred for the time at temperature indicated in table. The reaction was cooled to room temperature and the reaction mixture was diluted in 10 mL of dichloromethane and the crude polymer was precipitated in methanol (50 mL), the orange solid was filtered directly in Soxhlet extraction thimbles and purified by extraction with different solvents (methanol, acetone, petroleum ether, chloroform and chlorobenzene) depending by the molecular weight. The analyzed polymer fraction was recovered in different solvent and finally the last used solvent was removed by evaporation and the polymer was dried in oven under vacuum for 12h at 50°C.

¹H NMR (600 MHz, CDCl₃) δ 7.92 (s, 2H), 7.10 (d, J = 3.1 Hz, 2H), 6.96 (d, J = 3.1 Hz, 2H), 4.23 – 4.13 (m, 4H), 3.99 – 3.88 (m, 4H), 1.74 (m, 2H), 1.48 – 1.24 (m, 20H), 1.17 – 1.06 (m, 16H), 0.91 (t, J = 7.4 Hz, 6H), 0.85 (t, J = 6.9 Hz, 6H), 0.76 (t, J = 6.7 Hz, 6H), 0.72 (t, J = 7.4 Hz, 6H).

Bibliography

- [1] Carsten, B., He, F., Son, H. J., Xu, T., and Yu, L. **2011**, , 1493–1528.
- [2] Sakamoto, J., Rehahn, M., Wegner, G., and Schlüter, A. D. *Macromolecular Rapid Communications* **2009**, *30*, 653–687. doi: 10.1002/marc.200900063.
- [3] Osaka, I. and McCullough, R. D. *Accounts of Chemical Research* **2008**, *41*, 1202–1214. doi: 10.1021/ar800130s.
- [4] Kiriya, A., Senkovskyy, V., and Sommer, M. *Macromolecular Rapid Communications* **2011**, *32*, 1503–1517. doi: 10.1002/marc.201100316.
- [5] Snoeij, N. J., van Iersel, A. A., Penninks, A. H., and Seinen, W. *Toxicology and Applied Pharmacology* **1985**, *81*, 274–286. doi: 10.1016/0041-008X(85)90164-4.
- [6] Kowalski, S., Allard, S., Zilberberg, K., Riedl, T., and Scherf, U. *Progress in Polymer Science* **2013**, *38*, 1805–1814. doi: 10.1016/j.progpolymsci.2013.04.006.
- [7] Nitti, A., Po, R., Bianchi, G., and Pasini, D. *Molecules* **2017**, *22*. doi: 10.3390/molecules22010021.
- [8] Liang, A., Zhou, X., Zhou, W., Wan, T., Wang, L., Pan, C., and Wang, L. *Macromolecular Rapid Communications* **2017**, *38*, 1–6. doi: 10.1002/marc.201600817.
- [9] Behrendt, J. M., Esquivel Guzman, J. A., Purdie, L., Willcock, H., Morrison, J. J., Foster, A. B., O'Reilly, R. K., McCairn, M. C., and Turner, M. L. *Reactive and Functional Polymers* **2016**, *107*, 69–77. doi: 10.1016/j.reactfunctpolym.2016.08.006.
- [10] Zhong, W., Liang, J., Hu, S., Jiang, X. F., Ying, L., Huang, F., Yang, W., and Cao, Y. *Macromolecules* **2016**, *49*, 5806–5816. doi: 10.1021/acs.macromol.6b00185.
- [11] Muenmart, D., Foster, A. B., Harvey, A., Chen, M.-T., Navarro, O., Promarak, V., McCairn, M. C., Behrendt, J. M., and Turner, M. L. *Macromolecules* **2014**, *47*, 6531–6539. doi: 10.1021/ma501402h.
- [12] Kappaun, S., Zeler, M., Bartl, K., Saf, R., Stelzer, F., and Slugovc, C. *Journal of Polymer Science: Part A* **2006**, *44*, 2130–2138. doi: 10.1002/pola.
- [13] Kirschbaum, T., Azumi, R., Mena-Osteritz, E., and B auerle, P. *New Journal of Chemistry* **1999**, *23*, 241–250. doi: 10.1039/a808026g.
- [14] Jayakannan, M., Van Dongen, J. L., and Janssen, R. A. *Macromolecules* **2001**, *34*, 5386–5393. doi: 10.1021/ma0100403.
- [15] Sommer, M., Komber, H., Huettner, S., Mulherin, R., Kohn, P., Greenham, N. C., and Huck, W. T. S. *Macromolecules* **2012**, *45*, 4142–4151. doi: 10.1111/j.1365-2354.2008.01034.x.
- [16] Stahl, S. S., Thorman, J. L., Nelson, R. C., Kozee, M. A., February, R. V., and Bathocuproine, S. **2001**, *6846*, 7188–7189.
- [17] Wang, C., Dong, H., Hu, W., Liu, Y., and Zhu, D. *Chemical Reviews* **2012**, *112*, 2208–2267. doi: 10.1021/cr100380z.

BIBLIOGRAPHY

- [18] Chang, J., Chi, C., Zhang, J., and Wu, J. *Advanced Materials* **2013**, *25*, 6442–6447. doi: 10.1002/adma.201301267.
- [19] Søndergaard, R. R., Hösel, M., and Krebs, F. C. *Journal of Polymer Science, Part B: Polymer Physics* **2013**, *51*, 16–34. doi: 10.1002/polb.23192.
- [20] Hambsch, M., Reuter, K., Stanel, M., Schmidt, G., Kempa, H., F??gmann, U., Hahn, U., and H??bler, A. C. *Materials Science and Engineering B: Solid-State Materials for Advanced Technology* **2010**, *170*, 93–98. doi: 10.1016/j.mseb.2010.02.035.
- [21] Krebs, F. C. *Solar Energy Materials and Solar Cells* **2009**, *93*, 394–412. doi: 10.1016/j.solmat.2008.10.004.
- [22] Voigt, M. M., MacKenzie, R. C., King, S. P., Yau, C. P., Atienzar, P., Dane, J., Keivanidis, P. E., Zadrazil, I., Bradley, D. D., and Nelson, J. *Solar Energy Materials and Solar Cells* **2012**, *105*, 77–85. doi: 10.1016/j.solmat.2012.04.025.
- [23] Facchetti, A. *Nature Reviews Neuroscience* **2010**, *23*, 733–758. doi: 10.1021/cm102419z.
- [24] Cheng, X., Noh, Y. Y., Wang, J., Tello, M., Frisch, J., Blum, R. P., Vollmer, A., Rabe, J. P., Koch, N., and Sirringhaus, H. *Advanced Functional Materials* **2009**, *19*, 2407–2415. doi: 10.1002/adfm.200900315.
- [25] Po, R., Bernardi, A., Calabrese, A., Carbonera, C., Corso, G., and Pellegrino, A. *Energy & Environmental Science* **2014**, *7*, 925. doi: 10.1039/c3ee43460e.
- [26] Zheng, Q., Chen, S., Zhang, B., Wang, L., Tang, C., and Katz, H. E. *Organic Letters* **2011**, *13*, 324–327. doi: 10.1021/ol102806x.
- [27] Zhang, X., Richter, L. J., Delongchamp, D. M., Kline, R. J., Hammond, M. R., McCulloch, I., Heeney, M., Ashraf, R. S., Smith, J. N., Anthopoulos, T. D., Schroeder, B., Geerts, Y. H., Fischer, D. A., and Toney, M. F. **2011**, , 15073–15084.
- [28] Noriega, R., Rivnay, J., Vandewal, K., Koch, F. P. V., Stingelin, N., Smith, P., Toney, M. F., and Salleo, A. *Nature Materials* **2013**, *12*, 1038–1044. doi: 10.1038/nmat3722.
- [29] Chambon, S., Manceau, M., Firon, M., Cros, S., Rivaton, A., and Gardette, J. L. *Polymer* **2008**, *49*, 3288–3294. doi: 10.1016/j.polymer.2008.04.001.
- [30] Grisorio, R., Allegretta, G., Mastroilli, P., and Suranna, G. P. *Macromolecules* **2011**, *44*, 7977–7986. doi: 10.1021/ma2015003.
- [31] Manceau, M., Gaume, J., Rivaton, A., Gardette, J. L., Monier, G., and Bideux, L. *Thin Solid Films* **2010**, *518*, 7113–7118. doi: 10.1016/j.tsf.2010.06.042.
- [32] Helgesen, M., Gevorgyan, S. A., Krebs, F. C., and Janssen, R. A. *Chemistry of Materials* **2009**, *21*, 4669–4675. doi: 10.1021/cm901937d.
- [33] Fu, B., Baltazar, J., Sankar, A. R., Chu, P. H., Zhang, S., Collard, D. M., and Reichmanis, E. *Advanced Functional Materials* **2014**, *24*, 3734–3744. doi: 10.1002/adfm.201304231.

- [34] Back, J. Y., Yu, H., Song, I., Kang, I., Ahn, H., Shin, T. J., Kwon, S. K., Oh, J. H., and Kim, Y. H. *Chemistry of Materials* **2015**, *27*, 1732–1739. doi: 10.1021/cm504545e.
- [35] Dou, J. H., Zheng, Y. Q., Lei, T., Zhang, S. D., Wang, Z., Zhang, W. B., Wang, J. Y., and Pei, J. *Advanced Functional Materials* **2014**, *24*, 6270–6278. doi: 10.1002/adfm.201401822.
- [36] Park, G. E., Shin, J., Lee, D. H., Cho, M. J., and Choi, D. H. *Journal of Polymer Science, Part A: Polymer Chemistry* **2015**, *53*, 1226–1234. doi: 10.1002/pola.27555.
- [37] Matsidik, R., Komber, H., Luzio, A., Caironi, M., and Sommer, M. *Journal of the American Chemical Society* **2015**, *137*, 6705–6711. doi: 10.1021/jacs.5b03355.
- [38] Matsidik, R., Komber, H., and Sommer, M. *ACS Macro Letters* **2015**, *4*, 1346–1350. doi: 10.1021/acsmacrolett.5b00783.
- [39] Nübling, F., Komber, H., and Sommer, M. *Macromolecules* **2017**, *50*, 1909–1918. doi: 10.1021/acs.macromol.7b00251.
- [40] Würthner, F. and Stolte, M. *Chemical Communications* **2011**, *47*, 5109–5115. doi: 10.1039/c1cc10321k.

List of acronyms

BC bottom contact

BG bottom gate

BJT Bipolar Junction Transistor

cmc critical micellar concentration

CMD concerted metalation deprotonation

cryo-TEM Transmission electron cryomicroscopy

DAP direct arylation polycondensation

DLS Dynamic Light Scattering

DSC Differential Scanning Calorimetry

FET Field Effect Transistor

GC-MS Gass Chromatography-Mass Spectroscopy

HLB Hydrophilic-Lipophilic Balance

HOMO highest occupied molecular orbital

IC Integrated Circuits

IL Ionic Liquid

LB Lagmuir-Blodgett

LCD Liquid Crystal Display

LMWG low molecular weight gelators

LUMO lowest unoccupied molecular orbitals

MOSFET Metal-oxide-semiconductor field-effect transistor

NMR Nuclear Magnetic Resonance

OLED Organic Light-Emitting Diode

OPE Organic Printed Electronics

CHAPTER 4. LIST OF ACRONYMS

- OS** Organic Semiconductor
- OSC** Organic Solar Cell
- OTFT** Organic Thin-Film Transistor
- RFID** Radio-Frequency IDentification tags
- SAM** Self assembled monolayer
- scCO₂** supercritical CO₂
- SM** Suzuki-Miyaura
- TC** top contact
- TEM** Transmission electron microscopy
- TG** top gate
- TGA** thermogravimetric analysis
- TM** Transition metals
- UC** Up-Conversion
- VOCs** Volatile Organic Compounds

List of chemicals names

AcOEt ethyl acetate

BT Benzothiadiazole

BTBT [1]benzothieno[3,2-b][1]benzothiophene

DBA 9,10-dibromoanthracene

DBBF 4,7-dibromo-5,6-difluoro-2,1,3-benzothiadiazole

DBU 1,8-diazabicyclo[5.4.0]undec-7-ene

DCE dichloroethane

DMA dimethylacetamide

DMF N,N-dimethylformamide

DPP Diketopyrrolopyrrole

DTBF 4,7-di(thiophene-2-yl)-5,6-difluoro-2,1,3-benzothiadiazole

F4-TCNQ 2,3,5,6-Tetrafluoro-7,7,8,8-tetracyanoquinodimethane

F8BT Poly[(9,9-dioctylfluorenyl-2,7-diyl)-alt-(benzo[2,1,3]thiadiazol-4,7-diyl)]

IG Isoindigo

NBS N-bromosuccinimide

NDI Naphthalenediimide

NMP N-Methyl-2-pyrrolidone

PFDT 1H,1H,2H,2H-perfluorodecanethiol

PMMA Polymethylmetacrylate

PS Polystyrene

PSS Polystyrene sulfonates

TIIG Thienoisindigo

TMP-CH2-SH 3,4,5-trimethoxybenzylthiol

CHAPTER 4. LIST OF CHEMICALS NAMES

TMP-SH 3,4,5-Trimethoxythiophenol

TMS trimethylsilyl

Tol Toluene

TTD Thienothiadiazole